GROUND IMPROVEMENT USING VACUUM PRELOADING TOGETHER WITH PREFABRICATED VERTICAL DRAINS

BY

ABDUL QUDOOS KHAN

DISSERTATION

Submitted in partial fulfillment of the requirements
for the degree of Doctor of Philosophy in Civil Engineering
in the Graduate College of the
University of Illinois at Urbana-Champaign, 2010

Urbana, Illinois

Doctoral Committee:

Professor Gholamreza Mesri, Chair
Associate Professor James H. Long
Associate Professor Scott M. Olson
Professor Stephen Marshak

ABSTRACT

The use of vacuum preloading as an alternative to or in combination with fill preloading has become widely acceptable throughout the world. A number of successful case histories of vacuum preloading using different techniques have been reported in the literature. The vacuum pressure, which is applied to the soft soil through the vertical drains, results in an isotropic increase in effective stress within the soil mass, and therefore, can be applied with full intensity in a single stage. On the other hand an equivalent fill preload is applied in stages to avoid instability and bearing capacity failure. The additional stability achieved due to application of vacuum and associated consolidation also helps in speedy construction of fill preload and thus reduces the overall duration of any preloading operation.

Despite the increasing use of vacuum as a preload and development of a number of innovative techniques for its application, the exact mechanism of vacuum preloading remains largely unknown. Field trials, laboratory studies, and actual case histories are used to support contradicting concepts about the soil behavior during vacuum or combined vacuum-fill preloading. There is no consensus among the engineers and researcher about the distribution of vacuum pressure along the vertical drains, rate and magnitude of induced settlements, interpretation of porewater pressures, nature of lateral displacements, and increase in undrained shear strength due to vacuum preloading. As a consequence, modifications to existing consolidation theories and separate design procedures have been proposed to incorporate the effects of vacuum pressure during the preloading operation.

The present study aims at evaluating the performance of vacuum preloading as compared to that of fill preloading. Data from 40 case histories and 8 laboratory studies of vacuum consolidation were collected to study different aspects of vacuum preloading as compared to those of fill preloading. Time-dependent behavior of soft soil subjected to vacuum or vacuum-fill preload, distribution of vacuum pressure with depth and time, performance of vertical drains, lateral displacements, increase in undrained shear strength, and effectiveness of different techniques of applying vacuum in the field are examined carefully to explain the soil behavior during vacuum preloading operation.

Applicability of existing consolidation theories to explain soil behavior during vacuum or vacuum-fill preloading was studied using the computer program ILLICON (based on the ILLICON theory of consolidation) by modeling the applied vacuum as an equivalent fill preload. The settlement analyses of 11 sections from 8 different case histories of vacuum, vacuum-fill, and fill preloading show that the applied vacuum can be modeled as an equivalent fill preload to predict the settlements under vacuum or vacuum-fill preload, i.e., principle of superposition can be used with confidence to predict or to back-analyze the field behavior during vacuum or vacuum-fill preloading. The porewater pressures due to a vacuum or vacuum-fill preload can also be predicted using principle of superposition by converting the positive porewater pressure response (as a result of assuming applied vacuum as an equivalent fill load) to a porewater pressure response due to vacuum by using a unique definition of excess porewater pressure and by considering the relative magnitudes of applied vacuum and fill preloads as well as the distribution of vacuum pressure with depth and time. The distribution of vacuum pressure which should be constant with depth under ideal conditions, may not develop to full intensity at different depths due to 'leakage' of vacuum from specific sublayers; therefore it is absolutely important to ascertain actual distribution of vacuum pressure with depth and time to carry out a meaningful settlement analysis. Hence, with correct interpretation of field data, the existing consolidation theories can be used as such without any modifications to fully explain and predict the soil behavior during vacuum or a combined vacuum-fill preloading operation.

The study also shows that the increase in undrained shear strength due to vacuum, vacuum-fill, and fill preloads can be predicted using the available empirical correlations developed for fill preloading. The ratio of initial vane shear strength to preconsolidation pressure, $s_{uo}(FV)/\sigma'_p$, which remains constant in the compression range, can be used to predict the increase in undrained shear strength at the end of preloading operation; however, it is important to consider the degree of consolidation achieved as a result of preloading and the distribution of vacuum pressure with depth and time to correctly access the consolidation pressure which is responsible for the increase in undrained shear strength.

Lateral displacements due to vacuum preloading can be better explained in terms of consolidation behavior of soil; however, contribution of other soil parameters cannot be ignored. Among other factors, the distribution of vacuum pressure with depth and time appears to be a major factor governing the magnitude of lateral displacements. Analysis of lateral displacement data from different case histories of vacuum consolidation shows that the lateral displacements are maximum at the ground surface and reduce with depth. Moreover, the magnitude of lateral displacements (at the boundary of treatment area) is independent of the width of treatment area as well as the depth of penetration of vertical drains; therefore, no specific relation should be expected between these parameters. An empirical method to predict lateral displacements with depth and time is also proposed in the study.

A simple procedure for design of preloading is also suggested in the present study. The proposed design procedure is based on ascertaining the increase in effective stress at a given time using the computer program ILLICON and predicting the increase in shear strength using the empirical correlation for undrained shear strength proposed by Terzaghi et al. (1996) together with a suitable method to compute factor of safety at a given time. Application of the proposed procedure to actual case histories shows that it can be used with confidence for design of preloading.

In the Name of ALLAH, The Most Beneficent, The Most Merciful

This work is dedicated to My Parents, Wife and Kids

ACKNOWLEDGEMENTS

All Praises are due to ALLAH, the Creator, Sustainer and Owner of the universe, Who was always there to guide me and enabled me to complete my research successfully.

I am indebted to the Pakistan Army and National University of Scienes and Technology, Pakistan who provided me with the opportunity to undertake my PhD studies at one of the best institution in the world. I am also thankful to the University of Illinois at Urbana-Champaign for providing an excellent research environment.

I would like to express my sincere gratitude and appreciation to my PhD adviser Professor Gholamreza Mesri for his invaluable advice, geniuine concern and insightful suggestions throughout the course of my studies and research. It was a great learning experience working under his able supervision.

I wish to thank Professor J. H. Long, Professor S. M. Olson, and Professor S. Marshak for their willingness to serve on my dissertation committee and for their useful contribution in my research work.

I would like to thank my friends and colleagues for their encouragement and support during my research and stay at Illinois. My special thanks to Manzoor Hussain, Sarfraz Ahmed, Kamran Akhtar, Addel Zafar, Kashif Muhammad, Qazi Aurangzeb, Khan Shahzada, Dr. Inayat, and Zohaib Sheikh for their support and providing a family environment. I am also grateful to Pakistan Graduate Student Association for maintaining a cordeal atmosphere and arranging social gatherings on different occasions.

The Central Illinois Mosque and Islamic Center deserves special appreciation for providing a congenial environment for fulfilling spiritual and religious obligations. I appreciate the efforts of CIMIC committee for running the Mosque affairs at the cost of their personal compfort. Special thanks to Brothers Izzuddin and Emmad Jasim for their sincere wishes and prayers.

I would also like to extend my thanks to Mr. Jason Funk for his useful discussions relating to my research and help in understanding and running the computer program ILLICON. Thanks to Geotechnical Engineering Students Organization (GESO) for arranging real useful seminars on different aspects of Geotechnical Engineering.

I gratefully acknowledge the cooperation, support, encouragement, patience and understanding of my wife, Mahwish Khan, during the course of my studies and research. I am also grateful to my children, Nawaal, Areeba, and Abdullah Yousaf for their love and patience. Special thanks to my parents for their sincere wishes and prayers which brought me all the successes in this life.

May ALLAH ALMIGHTY bless all those who helped me in my research work and obliged me with best wishes and prayers.

TABLE OF CONTENTS

Page

LIST OF TABLES

Table **Page**

LIST OF FIGURES

Figure **Page**

CHAPTER 1. INTRODUCTION

1.1 Problem Statement

Construction on soft soils involves the risk of excessive deformation that may be accompanied by a bearing capacity failure. Preloading is a commonly used method to improve geotechnical properties of such deposits in order to minimize post construction settlements and to increase undrained shear strength. To preload a soil deposit, a load (usually an embankment fill) is applied to the compressible layer which increases the total stresses and generates excess porewater pressure within the soil mass. As a consequence, the effective stress increases as the porewater pressure dissipates with time.

Kjellman (1952) proposed to use atmospheric pressure as an alternative to fill preload by sealing off the treatment area from its surrounding and subjecting it to a vacuum suction, applied through a network of horizontal and vertical drainage system (drainage blanket and vertical drains) placed within the isolated soil mass. Although Kjellman's idea was based on sound theoretical principles and was supported by field experiments (a vacuum pressure of 80kPa was maintained for 110 days in one of the four experiments), yet the method found limited practical application owing primarily to non-availability of compatible material and technology to generate and sustain vacuum pressure over a large area for a considerable length of time (Holtz and Wager 1975). In about thirty years following Kjellman's experiments, investigations on use of vacuum preloading continued in different parts of the world; however, limited success was achieved (Halton et al. 1965; Johnson et al. 1977; and Hammer 1981; etc.).

The rapid urbanization associated with huge amount of construction activities has forced the engineers and planners to utilize such lands which were once considered useless. The development of robust plastic materials, increasing cost of labor and

conventional fill materials and rising environmental concerns (Holtz and Wager 1975; Thevanayagam et al. 1994) have renewed the interest of researchers and engineers to develop the Kjellman method as a practically viable tool. Since early 1980s, the method has been studied extensively in different parts of the world and many successful applications have been reported in the literature (Choa 1989; Cognon et al. 1994; Tang and Shang 2000; Masse et al. 2001; etc.).

Although vacuum is being used increasingly in different parts of the world and new techniques, including development of more robust materials have been introduced for vacuum preloading of the soft ground; still differing opinions exist with regard to its exact mechanism. Data from laboratory studies, field trials, and actually implemented projects show a great variation in results, which are used to support the contradicting views regarding the mechanism of vacuum preloading compared to that of fill preloading. The contradicting opinions on different aspects of vacuum preloading compared to an equivalent fill preload include:

- Ter-Martirosyan and Cherkasova (1983), Woo et al. (1989), Yixiong (1996a), Mohamedelhassan and Shang (2002), Mahfouz et al. (2005) propose that the settlement and porewater pressure response due to a vacuum and an equivalent fill preload are similar under similar conditions; thus, the principle of superposition may be used to evaluate settlement and porewater pressure response under a combined vacuum-fill preloading (Mohamedelhassan and Shang 2002). On the other hand, Indraratna et al. (2004), Chai et al. (2005a, b and 2009), Rujiakiatkamjorn et al. (2007), and Qiu et al. (2007) etc., suggest that the rate of settlement is faster whereas the magnitude of settlement induced by vacuum is less than that of an equivalent fill preload.
- Chai et al. (2005a), Rujiakiatkamjorn et al (2007), Qiu et al. (2007) propose a linear reduction in vacuum intensity with depth in vertical drains, however no fixed rate (or range) of reduction with depth in vacuum intensity is proposed; instead, the reduction in vacuum intensity is worked out on case to case basis. Field measurements of porewater pressure in soil suggest no

systematic pattern of vacuum distribution with depth. In some of the case histories of vacuum preloading (Choa 1989; Yan and Chu 2003 and 2005; Chai et al. 2006 etc.) the observed reductions in porewater pressure were greater at greater depths which contradicts the concept of linear reduction in vacuum intensity with depth.

- Lateral displacements due to vacuum preloading may damage structures or services located in the vicinity of treatment area. Limited attempts have been made to explain and predict the lateral ground movements due to vacuum consolidation of an area. The methods proposed to predict lateral displacements (Chai et al. 2005a and b, Dam et al. 2007) are not very efficient in predicting the lateral displacements.
- The increase in shear strength due to vacuum preloading is considered to be more significant, especially near the ground surface (Dam et al. 2007), due to vacuum preloading as compared to that of an equivalent fill preload. There is neither enough field evidence nor any laboratory study available to support this concept. The laboratory study carried out by Mahfouz et al. (2005) shows that a similar increase in shear strength is expected due to either type of loads; whereas, Leong et al. (2000) suggests that the increase in shear strength due to fill preload is more significant than a vacuum load.
- Under fill preloading, the vertical drains may or may not be freely draining; however, vertical drains under vacuum preloading have been assumed to perform without any well resistance. It is surprising to note that such an important assumption is accepted by all without studying this aspect of vacuum preloading.
- Consolidation parameters obtained from laboratory studies also present conflicting and at times inconsistent results. For example, Mohamedelhassan and Shang (2002) and Mahfouz (2005) reported that the test results from conventional oedometer testing can be used for design of vacuum preloading. On the other hand, Chung (2009) reported that although the coefficient of consolidation obtained in laboratory using either type of

loads is the same, the rate of settlement in the field due to vacuum preloading is higher as compared to that of a fill preload. Similarly, Mohamedelhasan and Shang (2002) reported that principal of superposition can be used to predict settlements as well as porewater pressures due to a combined vacuum-fill preload; however, Bamunawita (2004) and Rujiakiatkamjorn (2005) conclude that principal of superposition can only be used for interpretation of porewater pressures but not for settlement predictions, and thus, recommended modifications to existing consolidation theories to incorporate effect of vacuum loading.

The available literature shows that much of the vacuum application is carried out without proper understanding of the mechanisms involved. Thus, there is a need to understand and explain the soil behavior under vacuum preloading compared to that of an equivalent fill preload.

1.2 Research Objectives

The focus of this study is understanding and explaining the mechanisms involved in vacuum preloading, compared to that of fill preloading by (1) analyzing case histories of vacuum preloading of soft ground and (2) evaluating the laboratory studies carried out to explain the soil behavior during vacuum preloading. The main objectives of this research are as the following:

- To evaluate the applicability of existing consolidation theories, such as ILLICON theory of consolidation, for cases of vacuum or vacuum-fill preloading by examining the time dependent settlement and porewater pressure behavior of soft soils subjected to vacuum or vacuum-fill preloading.
- To propose a suitable method for interpretation of porewater pressures under vacuum or vacuum-fill preloading if an existing consolidation theory is used to predict the settlements and porewater pressures at different times and at different depths.
- To evaluate the field performance of vertical drains under vacuum or vacuum-fill preloading to examine the commonly accepted assumption that

the vertical drains perform without well resistance under vacuum preloading.

- To evaluate the proposed distribution of vacuum pressure with depth and with time by (1) carefully examining the observed data reported in different case histories and (2) evaluating and interpreting the results reported in different laboratory studies on vacuum consolidation; and recommend a suitable vacuum pressure distribution for design of vacuum preloading or for back-analysis of vacuum preloading case histories.
- To study the lateral deformations induced by vacuum preloading and propose a method for predicting the lateral displacements with time and with depth during vacuum preloading in the field.
- To examine the increase in undrained shear strength due vacuum or vacuum-fill preloading and propose a suitable method for predicting shear strength during or at the end of preloading operation.
- To propose a method for design of preloading of soft soils using vacuum, fill or combined vacuum-fill preloads.

1.3 Scope

The study is presented in eleven chapters. A brief description of each Chapter is as following.

Chapter 1 briefly highlights the need for research and lays down the objectives of the investigation.

In Chapter 2, theory of vacuum consolidation along with a detailed description of its historical development in various parts of the world is presented. Essential components of a vacuum consolidation system, numerous techniques of applying vacuum to the soft ground, and materials and equipment used for execution of vacuum consolidation in the field are also briefly introduced in this chapter.

The study has been carried out using the computer program ILLICON developed at the University of ILLINOIS at Urbana-Champaign (Mesri et al. 1988). Chapter 3 covers the details of ILLICON procedure employed to analyze the case

histories of vacuum consolidation of soft ground. Data available in different case histories of vacuum and vacuum-fill preloading are also summarized in this chapter.

Settlement analyses of eleven sections from eight different case histories are presented in Chapters 4 to 8. Nine of the eleven sections were treated with either vacuum or combined vacuum-fill preloads; two sections treated with fill preload are also analyzed for comparing the results. Whenever required, procedures for estimating the data not reported in the literature, but required for ILLICON analysis, are also described in these chapters.

Chapter 9 summarizes the characteristics of vacuum consolidation. Distribution of vacuum pressure with depth and with time, time dependent settlement and porewater pressure response, lateral displacements, increase in undrained shear strength, and field performance of vertical drains due to vacuum or combined vacuum-fill preloading are described in detail by evaluating the available laboratory studies, field trials, and analyzed case histories of vacuum and vacuum-fill preloading. Methods to predict lateral displacements and increase in undrained shear strength along with their application to case histories are also proposed in this chapter.

The proposed procedure for design of preloading along with its application to two case histories of vacuum-fill preloading is described in Chapter 10.

Major conclusions from this study are summarized in Chapter 11.

CHAPTER 2. VACUUM CONSOLIDATION – THEORY AND PRACTICE

2.1 Introduction

Use of atmospheric pressure as an alternative to fill preloading was first proposed by Kjellman in 1952. During fill preloading, the increase in effective stress is achieved by increasing the total stress, whereas, in a vacuum preloading operation, the increase in effective stress is achieved by reduction in the porewater pressure while keeping the total stress constant. The reduction in porewater pressure is affected by isolating the soil mass from its surrounding and then subjecting it to a suction pressure. The method proposed by Kjellman was based on sound theoretical principles and was supported by field experiments (Kjellman 1952), yet it found limited application owing primarily to the non-availability of compatible material to generate and sustain vacuum pressure over a large area for a considerable length of time (Holtz and Wager 1975). The rapid urbanization, development of robust plastic materials, increasing cost of labor and conventional fill materials and rising environmental concerns associated with huge amount of construction activities, renewed interest of engineers and researchers to develop the Kjellman method as a practically viable tool (Holtz and Wager 1975; Thevanayagam et al. 1994). Since early 1980s, the method has been studied extensively in different parts of the world and many successful applications have been reported (Choa 1990; Cognon et al. 1994; Yixiong 1996b; Tang and Shang 2000; Masse et al. 2001, etc).

Theory of vacuum consolidation, its historical development, components, various techniques of applying vacuum to the ground and equipment used in a vacuum consolidation system, are briefly reviewed in this Chapter.

2.2 Principle of Vacuum Consolidation

The basic principle of vacuum consolidation can be stated as following:

The removal of atmospheric pressure from an isolated soil mass will cause a reduction in the porewater pressure. The reduction in porewater pressure, which results in an increase in effective stress, sets up a porewater pressure gradient between the soil mass and the point of application of vacuum (usually vertical drains). The process of consolidation is initiated under this porewater pressure gradient.

The intensity of atmospheric pressure is constant at a given elevation. Because atmospheric pressure is present on all surfaces, it is generally not considered in stress calculations in normal geotechnical practice. The equation for effective stress in a soil mass can be written in the form (Masse et al. 2001):

$$\sigma'_v + p_a = \sigma_v - u + p_a \tag{2.1}$$

where, at a given elevation, σ'_v is the effective vertical stress, p_a is the atmospheric pressure, σ_v is the total vertical stress and u is the porewater pressure.

If the atmospheric pressure (p_a) is removed from left hand side of Eq. 2.1, then the effective stress in the soil mass increases by an amount equal to p_a. Figure 2.1 compares the idealized distribution of stresses and porewater pressures under the application of a wide fill load (80kPa), uniform vacuum load (80kPa), and a combined vacuum-fill load (80+80=160kPa). It is assumed that all three types of load can be applied instantaneously and will remain constant with time and with depth (submerged unit weight of 6kN/m^3 is assumed) till the completion of primary compression under the respective loads. Under the action of a fill load, at time, t = 0 (Fig. 2.1b), the porewater pressure and the total vertical stress increase by an amount equal to the applied load; whereas the effective stress remains unchanged. With time, the effective vertical stress increases as the porewater pressure dissipates, and at time $t = t_p$ (time required for completion of primary compression), the porewater pressure falls back to its original hydrostatic condition, and the applied load is completely transferred to soil skeleton as an increase in effective vertical stress. For vacuum load however (Fig. 2.1c); the porewater

pressure and the effective stress remain unchanged at time, t = 0; however, the porewater pressure in the vertical drains reduces to the applied vacuum. With time, the porewater pressure in the soil decreases by the applied vacuum and consequently, the effective stress increases by the same amount. At time t = t_p, the porewater pressure in the soil mass decreases by the amount of the applied vacuum and hence the effective vertical stress increases by an amount equal to the applied vacuum. Figure 2.1d shows the combined action of a vacuum-fill load which shows that at time t=0, the porewater pressure in the soil mass increases by an amount equal to applied fill load, while the porewater pressure in the vertical drains reduces to applied vacuum. Thus, with time the porewater pressure in the soil mass starts at u_o+80kPa (at t =0) and approaches u_o-80kPa (at time t = t_p). Therefore effective vertical stress at time t = t_p increases by 160kPa. Under identical conditions, there is no difference in the porewater pressure generation and dissipation patterns due a fill, vacuum or a combined vacuum-fill preload.

2.3 Historical Development of Vacuum Consolidation

2.3.1 The Kjellman Method

Kjellman (1952), while working at Swedish Geotechnical Institute (SGI), was the first to propose use of atmospheric pressure as a temporary surcharge to affect consolidation. He theorized that as the reduction in porewater pressure results in an increase in the effective stress provided the total stress is kept constant; the consolidation process can be initiated if atmospheric pressure is removed from within an isolated soil mass. He proposed to achieve the reduction in porewater pressure by isolating a soil mass from surrounding and then subjecting it to vacuum using high capacity vacuum pumps. The area could be isolated by covering the ground surface with an air tight membrane and extending it, on the sides below the water table in the clay layer.

A series of four experiments were conducted by SGI to ascertain the feasibility of using vacuum as an alternative to fill load. A 0.3 mm thick, polyvinyl chloride (PVC) membrane was used in three of the four experiments, whereas a 1 mm thick rubber sheet welded at the joints was used in the fourth experiment. For all the tests cardboard vertical drains, with a penetration depth of 4.8m were installed in a square grid at a spacing of 0.5m. The membrane was keyed into the soft layer by digging a 1.5 to 1.7m deep side

trench around the each test site. The PVC membrane became brittle and could not last for more than 30 days. However, with the welded rubber sheet membrane, the test was continued for 110 days and a total settlement of 54cm was recorded. On the average, an under membrane vacuum pressure of 80kPa was achieved and maintained during the fourth test. Based on these tests, following procedure was proposed for the implementation of vacuum consolidation in the field (Kjellman 1952):

- Provision of a filter layer (coarse granular material) on top of the ground to be improved. If permanent fill to be used is granular then separate filter is not required.
- Installation of vertical drains at desired spacing and up to desired depth in the area to be treated.
- Isolation of the treatment area by covering the filter layer with an air-tight membrane and
    - Extending the membrane on the sides below the water table in the soft layer by digging a ditch all around if the water table within the clay is shallow, or
    - Driving sheet piles below the water table into the soft layer if the water table is deep or a permeable layer overlies the soft clay layer.
- Connecting the vacuum pump to the drainage layer through the membrane.
- Maintaining a layer of water on top of membrane to prevent leakage and aging of membrane.

The results of experiments were encouraging and it was shown that with the right materials, vacuum preloading could be used as an effective tool; however, the technique was not put into practical use primarily because of non-availability of suitable materials (Holtz and Wager 1975).

2.3.2 Application of Vacuum at Philadelphia International Airport Runway

In 1958, vacuum consolidation was used in conjunction with dewatering and sand drain stabilization to improve subsoil conditions for speedy extension of a runway at Philadelphia International airport (Halton et al. 1965). The soil profile at the site

consisted of 5 to 10 feet of recent hydraulic fill dredged from the Delaware river, over 15 to 20 feet of organic silt and clay underlain by a 40 feet thick layer of sand and gravel with traces of silt. A total of 595 non-displacement type vertical sand drains with 12 inch diameter were used over an area of 1500,000 square feet. The top of the sand drains were sealed and vacuum was applied from the bottom of compressible layer to make use of existing sand and gravel as a drainage layer. A vacuum pressure of 50kPa was to be maintained during the treatment. Concurrent with the application of vacuum, dewatering was carried out by installing deep wells (to a depth of 70 feet) at a spacing of 600 feet along the periphery of treatment area. It was also decided to remove top soil within six feet of the runway, taxiway and apron area and replace it with granular fill. The soil profile and combined arrangements for vacuum consolidation and dewatering are shown in Fig. 2.2.

Vacuum was applied for a period of 18 days. Following application of vacuum, an increase in rate of settlement was observed; however, piezometers installed in the compressible layer (depth not reported) indicated a vacuum level of 3 to 34kPa. It is difficult to comment on the effectiveness of vacuum during this project due to the following:

- A direct contact with permeable layer is typically avoided by terminating the vertical drains 0.5 to 2m short of the bottom permeable layer (Dam et al. 2006), to avoid loss of vacuum pressure. In this case, vacuum pressure was applied from bottom using existing 40 feet thick sand and gravel layer without using any sort of isolation to prevent leakage of vacuum pressure.
- It can be seen from Fig. 2.2 that only two vacuum pumps were used to distribute vacuum pressure over an area of approximately 1500,000 square feet. Moreover the spacing between sand drains was 40 to 50 feet (Fig. 2.2b), which is very large for vacuum to be effective within the soil in a short period of time (18 days in this case).
- It was mentioned earlier that the piezometers registered a vacuum pressure of 3 to 34kPa in the clay layer (the depth of piezometers and time of measurement was not reported). This shows that the vacuum pressure was

neither distributed uniformly within the compressible layer, nor it achieved the design intensity of 50kPa. Therefore, a significant improvement in settlement due vacuum load in this case is unlikely.

- Replacement of top soil with granular fill (3 to 6 feet) is also likely contributed toward the observed settlement.

Despite the above mentioned ambiguities, this was the first application of vacuum consolidation after the Kjellman's experiments, and therefore, can be regarded as a first step toward the development of vacuum consolidation method.

2.3.3 Experiments by US Army Corps of Engineers

In 1970s, US Army Corps of Engineers (USACE) carried out a study to evaluate the effectiveness of conventional techniques (including under-drainage and seepage consolidation in combination with partial vacuum) to increase the storage capacity of disposal areas by densification and to improve the engineering characteristics of dredged material (Johnson et al. 1977). The study concluded that conventional techniques could be effectively used to treat the dredged material. Use of vacuum in combination with under-drainage and seepage consolidation were identified as potentially useful techniques to densify the dredged material. Following this study, field experiments were conducted to evaluate the effectiveness of four techniques, including gravity under-drainage, partial vacuum with under-drainage, seepage consolidation and seepage consolidation with partial vacuum in under-drainage layer (Hammer 1981).

The test site was located in an existing dredged material disposal area near Mobile, Alabama. Five test pits were excavated on a sand mound, each with a base area of 30ft x 30ft and side slopes of 1V:2H. One section was used for each of the consolidation techniques, whereas the fifth section, which was not treated, served as a control section. The layout of test site with bottom elevation is shown in Fig. 2.3. To ensure that water does not flow out of the treatment area, each excavation was lined with two layers of polypropylene plastic sheet. Two feet thick layer of sand was laid in each excavation to serve as under-drainage layer. For vacuum test sections (sections 2 and 3), this layer was also used to develop vacuum pressure in the dredged slurry. A collector system, comprising of slotted PVC pipes was then laid (for vacuum test sections only) in

small trenches excavated in the drainage layer. The collector system was connected to a main solid PVC pipe near the inside toe of the test section slope. The main pipe was passed through the slope and connected to vacuum pump on outside of the slope as shown in Fig. 2.4. Instrumentation to monitor settlement and porewater pressure was placed after installation of the vacuum system. Dredged material was then pumped into the excavation in layers to a height of ±6.5ft (Hammer 1981).

Treatment began in November 1976 and continued for two years. After first year of treatment, a second lift of dredged material was added after placing a 1ft thick sand layer on top of the first lift. For test section 2 (vacuum in combination with seepage consolidation), the intermediate sand layer was connected to the under-drainage layer by using four 8inch diameter sand columns. Test section 3 (vacuum in combination with under drainage) cracked extensively as a result of surface desication, with some cracks propagating to the under-drainage layer. These cracks were filled with sand and used as a connection between the intermediate sand layer and under-drainage layer. The connection arrangements between under-drainage layer and intermediate sand layer in test sections 2 and 3 are shown in Fig. 2.5.

Figure 2.6 shows the average vacuum pressure in the under-drainage layer for test sections 2 and 3 and settlement response for all the five test sections. It can be seen that vacuum pressure developed relatively quickly to 10.5psi (72kPa); however it immediately dropped to 8psi (55kPa). Vacuum pressure remained somewhat stable for approximately one month and then experienced a continuous drop till the end of treatment period. By the end of treatment period, a vacuum intensity of only 2psi (14kPa) could be maintained. Hammer (1981) attributed the loss of vacuum intensity partly to the surface drying and mainly to the leakages at connections and efficiency of vacuum pumps. Hammer (1981) also reported that a maximum of 1psi (7kPa) vacuum pressure was observed in the intermediate sand layer, which indicates that the vacuum could not be transferred to the intermediate sand layer. It is also interesting to note that the vacuum pressure in under-drainage layer was around 50kPa in Test Section 2 and 40kPa in Test Section 3. Therefore, a significant vacuum pressure should have been transmitted through the vertical sand connectors to the intermediate sand layer. It is possible that beside

leakages in the system, clogging of under-drainage layer due clay particles may also be a possible cause of reducing the efficiency of vacuum system. It is probably because of this reason that vacuum could not be transmitted to intermediate sand layer despite establishing elaborate connections between the under-drainage layer and the intermediate sand layer. The decrease in vacuum pressure in the under-drainage layer with time supports the idea of clogging of sand by clay particles from the dredged material.

Despite the inability to maintain a high vacuum pressure in the under-drainage layer, the observed settlements (Fig 2.6b) show that vacuum with under-drainage was the most efficient of all the techniques.

The field experiments by US Army Corps of Engineers established the efficacy of vacuum consolidation method; however, it was not further developed/studied in the US until mid 1990s.

2.3.4 Development of Vacuum Consolidation Method in China

In early 1980s, Tianjin Port Engineering Institute (TPEI), formerly known as First Navigation Bureau, in China, extensively studied vacuum consolidation. By this time, the efficacy of the method had already been established; however, the method was not used regularly on a large scale because of the technological aspects. In 1980, TPEI started field trials to address the technological issues (including sealing membranes and vacuum equipment) associated with the practical application of vacuum consolidation method (Yixiong, 1996a). Within two years, TPEI successfully developed the method and applied it to improve reclaimed land (480,000m^2) for development of Xingang Port in China (Choa 1989 & 1990; Yixiong 1996a & b; Shang et al. 1998). A major contribution of TPEI research is the large scale implementation of vacuum consolidation projects where surface areas up to 25000 – 30000m^2 were treated using a single sealing membrane (Tang and Gao, 1989). From 1982 to 1994, the method was applied on 51 different projects to improve a total area of 2.1 million square meters (Yixiong, 1996a). Data from Yixiong (1996b) show that up to 1987, sand packed vertical drains were used; however after 1987, PVDs were used in most of the projects.

The method employed by TPEI, as shown in Fig 2.7, was essentially similar to the original method proposed by Kjellman in 1952. The field trials conducted by TPEI in

connection with development of East Pier at Xingang Port are discussed in detail in Chapter 8.

2.3.5 Development of Vacuum Consolidation Method in Other Countries

In early 1980s, several studies were conducted to evaluate the use of vacuum as an alternative to or in combination with fill preloading to carry out ground improvement works for Second Bangkok International airport. Different techniques including application of vacuum (a) directly to sand drains as described in Chapter 8 (Woo et al. 1989), (b) to an isolated area covered with a drainage blanket and PVC membrane using the Kjellman method (STS and NGI 1992; Bergado et al. 1997) and (c) to capped prefabricated vertical drains (CPVDs) where surface PVC membrane is not required (COFRA 1996) were used to improve the soft Bangkok clay. These studies (discussed in detail in Chapter 6) proved vacuum preloading as an acceptable and practically viable alternative for the conventional fill preloading.

During late 1980s and in early 1990s, the method became widespread all over the world and its use was extended to various applications. Several innovations were made and new techniques are being developed to make the method more efficient and economical. During a dredged material stabilization project in Belgium for railway track development, submersible vacuum pumps were installed below the compressible layer and a naturally existing confined sand layer was used as the drainage layer. The top of the vertical drains were capped to avoid loss of vacuum (Mieghem et al. 1999). In Japan, cap-drains are being used to apply vacuum directly to the compressible layer after by-passing the top layer (Yoneya et al. 2003; Chai et al. 2008). In USA, vacuum is mostly used in port and harbor extension facilities for stabilization of hydraulic fill and disposal of dredged material (Rollings 1996; Thevanayagam, 1997). In a vacuum application of 2 years, the capacity of a confined disposal facility at Newark Bay, New Jersey was increased by 855,000m^3 (Dam et.al, 2006).

A number of laboratory studies were also carried out to understand and explain the mechanism involved in vacuum preloading of soft ground (Mohamedalhassan and Shang 2002; Rujiakiatkamjorn 2005; Mahfouz et al. 2005; Chai et al. 2005a etc.).Various

techniques of vacuum application, developed and used in different parts of the world are briefly reviewed in Section 2.5.

2.4 Components of Vacuum Consolidation System

Various vacuum consolidation systems have been developed throughout the world to efficiently transmit the vacuum pressure to the compressible layer; however, the fundamental components of all the systems are essentially similar to those described by Kjellman in 1952. Common features of the vacuum consolidation system are briefly described as under:

2.4.1 Vertical Drains

In addition to reducing the drainage path and carrying water to the drainage boundary, the vertical drains in a vacuum consolidation system serve the purpose of transmitting the vacuum pressure to the compressible layer. A system of optimally spaced vertical drains helps in distributing the vacuum pressure quickly and uniformly to the depth of compressible layer being treated. During different vacuum applications in Xingang port expansion project in China, it was observed that the average time for about 80kPa vacuum to be fully effective within the vertical drains was around 15 Days (Shang et al. 1998). This is much less than the time required for construction of an embankment (about 4.5m high) to produce an equivalent increase in total vertical stress.

Both sand drains and prefabricated vertical drains (PVDs) have been successfully used in different projects; however, due to ease of installation, PVDs are much preferred (Dam et a. 2006). DGI Menard has developed vacuum transmission pipes (VTPs) to transmit the applied vacuum to the soft ground (Masse et al. 2001). Capped prefabricated vertical drains (CPVDs) are also being used increasingly in different parts of the world (COFRA 1996; Chai et al. 2008; Saowapakpiboon et al. 2008). Different types of vertical drains used with vacuum preloading are discussed in Section 2.6.

2.4.2 Drainage/Filter Layer

If the ground surface is soft with low permeability characteristics, a 30 to 100cm thick granular layer (mostly sand) is placed over the treated area to act as a drainage layer. The purpose of this layer is to facilitate movement of water discharged by the vertical drains towards the peripheral boundary. For very soft ground, this layer also

acts as a working platform over which equipment and material is maneuvered and through which vertical drains are installed. If the ground surface consists of a permeable layer or the permanent fill to be used is granular, then a separate drainage layer is not required (Kjellman 1952; Tang and Shang 2000).

In most of the modern applications, a network of longitudinal and transverse perforated pipes, covered with a filter fabric is placed within the drainage layer (Yixiong 1996a; Dam et al. 2006). The horizontal drainage system helps in efficient distribution of vacuum and also disposes off the water toward the peripheral boundary through drainage connections through the membrane at specified locations. In Japan, drainage geotextile has also been used instead of sand mat to act as a drainage layer (Dam et al. 2006). Existing sand layer at the bottom of the compressible layer can also be used as drainage layer (Mieghem et al. 1999). A typical layout of horizontal drainage network, used in China is shown in Fig. 2.8.

2.4.3 Site Isolation

The area being treated is isolated from surrounding to avoid loss of vacuum. In order to ensure complete isolation of the site, ground surface is sealed both from the top and from the sides.

2.4.3.1 Sealing From Top

The most common practice is to cover the ground surface with a PVC membrane. The membrane is keyed into a peripheral trench at least 0.5 meter below the ground water table (Cognon et al. 1994). The trench is then filled with low permeability material to complete the sealing. PVC membranes in single or multiple layers are used to seal the ground surface (Yixiong 1996a; Chu et al. 2000; Dam et al. 2006). In membrane-less techniques, in situ low permeability soil is used as a sealing layer. This is either done by using capped prefabricated vertical drains (COFRA 1996; Yoneya et al. 2003; Chai et al. 2008) or vacuum is applied from an existing permeable layer located at the bottom of the compressible layer. The top of vertical drains is capped to avoid loss of vacuum (Halton et al. 1965; Mieghem et al. 1999). These techniques are discussed in detail in Section 2.5.

2.4.3.2 Sealing from Sides

If the compressible layer is homogenous without any seams of high permeability material like gravel/sand, sealing from top alone can effectively maintain the vacuum. However, in case of a thick desiccated crust or a high permeability layer at greater depth, an effective seal all around the site is absolutely essential to maintain the vacuum for the entire duration of preloading. During site improvement at Yaoqiang airport runway in China, a 4.5m deep slurry wall (Fig. 2.9) was constructed through the top permeable layer and terminated into the soft clay layer to avoid loss of vacuum (Tang and Shang 2000). Kjellman proposed using sheet piles as cut off; however, slurry walls are more frequently used these days (Tang and Shang 2000; Masse et al. 2001).

2.4.4 Vacuum Pump System

A vacuum pump system is needed to provide the suction to the compressible layer and discharge air and water through the system of horizontal and vertical drains. A vacuum pump is connected to the horizontal drainage system through specially designed connectors, at specified locations. Chinese experience shows that a single pump can generate and sustain a vacuum pressure of 80kPa over an area of 1000 to 1500m^2 (Yixiong 1996a; Dam et.al, 2006), whereas Menard vacuum pumping station can maintain a vacuum pressure of 75kPa over an area of 5000 to 7000m^2 (Masse et al. 2001). In case of high permeability soils, the area per pump may be reduced significantly for efficient application of vacuum. For example, the treatment area per pump was reduced to 600m^2 at a soil improvement site where the top 3m of soil consisted of silty sand (Tang and Shang 2000). A number of vacuum pumps can be connected under a single sealing membrane to cover a larger area as shown in Fig. 2.8.

Different agencies have developed their own vacuum pump systems. Much of the details are not available regarding the mechanism and working principle of these pumps, however, the available information is discussed in Section 2.6.

2.5 Technique of Applying Vacuum in the Field

The theory of vacuum consolidation remains the same; however, the technique of applying vacuum to improve the soft ground may vary. Development of membrane-less techniques to transmit vacuum directly to the compressible layer, improvement of

sludge using horizontal drains (Shinsha et al. 1991), improvement of soft seabed clay in an under-water environment (Karlsrud et al. 2007) are some examples. The use of vacuum preloading has also been extended to improve soft seabed clay in an under-water environment (Shinsha et al. 1991; Karlsrud et al. 2007). Different techniques used to apply vacuum to treat soft ground are briefly reviewed in this section.

2.5.1 Chinese Method

Plan and section of Chinese method of vacuum application is shown in Fig. 2.7. The method is essentially similar to what was originally proposed by Kjellman in 1952 with some variations. The key features (in addition to those described in section 2.3.1) of this system are as under (Yixiong 1996a; Dam et al. 2006):

- The membrane is covered with about 30cm water by constructing revetments so as to prevent leakages and aging of membranes. If vacuum is to be used in conjunction with the fill preloading, then the fill is constructed on top of the membrane.
- Plastic board type PVDs are more commonly used in China. These drains are similar to those used in conventional fill preloading.
- A network of longitudinal and transverse pipes is usually laid within the drainage blanket. The diameter of the horizontal drainage pipes vary between 50 to 100mm. These pipes are perforated and wrapped in a filter fabric.
- PVC membrane in one or several layers is used as surface cover. The peripheral trenches are filled with clay mix slurry. In situ impermeable soil can also be used in peripheral trenches.
- Jet pumps and centrifugal pumps are used together to apply vacuum and to handle air and water flowing out of the soil mass.
- Clay mixed cut-off walls (if required) are used for lateral confinement of the site.

2.5.2 Menard Vacuum Consolidation System (MVC)

Although the basic principle remains the same, DGI Menard has made several modifications to enhance the efficiency of the consolidation system (Fig. 2.10). Important modifications (to Kjellman and Chinese method) made by Menard are as under (Masse et al. 2001):

- A woven geosynthetic is placed on ground surface and then a 1 meter thick sand blanket is placed over it. The geosynthetic and sand mat provide the stability and also act as a working platform.
- Vertical transmission pipes (VTPs) with circular cross section are used to transmit vacuum to the compressible layer. The diameter of VTPs may vary; 50mm diameter VTPs were used in a sewage treatment plant project in South Korea, whereas, 34mm diameter VTPs were used in Port of Brisbane Project, Australia. Conventional PVDs have also been employed by Menard on a number of projects (Cognon et al. 1994).
- After installation of vertical drains and horizontal drainage system, a 1.5meter thick primary fill is placed over the 1m thick sand mat (already placed). The sealing membrane is then laid over this primary fill. The primary fill helps in retaining the vacuum intensity by "maintaining non-submerged action even when it settles down below the original ground water table" (Cognon et al. 1994).
- Vacuum is applied using vacuum pumps developed by Menard.

2.5.3 Vacuum Application using Capped Prefabricated Vertical Drains (CPVDs)

Ground improvement using vacuum together with CPVDs is successfully done in various parts of world including Bangkok (Saowapakpiboon et al. 2008) and Japan (Yoneya et al. 2003; Chai et al. 2008). A CPVD is a conventional prefabricated vertical drain provided with an impermeable cap (Detailed description of CPVD is given in Section 2.6). A hose is connected to the cap of CPVD, which in turn is linked with the horizontal pipe connected with the vacuum pump. Yoneya et al. (2003) suggests that a clay layer of 1 to 2m thickness is used as a sealing layer; whereas Chai et al. (2008) and

Saowapakpiboon et al. (2008) suggest that 0.5m of soft clay layer is sufficient to prevent leakage of vacuum. Schematic layout of a vacuum-CPVD system is shown in Fig. 2.11.

Chai et al. (2008) claims that this system has the advantage of avoiding high permeability soils near the surface (and at depth) and reduce the cost of constructing cut-offs around the treatment area to avoid loss of vacuum. Practical experience however shows that the efficiency of vacuum system is significantly reduced with use of CPVDs. For example, an average vacuum pressure of 60kPa or less could be transmitted to vertical drains in case histories reported by Yoneya et al. (2003), Chai et al. (2008) and Saowapakpiboon et al. (2008). The use of CPVDs also requires more intensive control to ensure that the cap of each CPVD is embedded sufficiently into the clay layer. Capping of PVDs at a depth where permeable seams are likely to be encountered also presents special investigation and implementation challenges. Analysis of a case history (Chapter 6) reported by Saowapakpiboon et al. (2008) shows that (1) in a vacuum-CPVD system, the drains perform with significantly more well resistance as compared to conventional PVDs in a PVD-membrane system, and (2) Each CPVD may perform independently at a different discharge capacity resulting in non-uniform settlements.

2.5.4 Vacuum Application using Horizontal Drains

The horizontal drain method was developed in Japan to accelerate the consolidation of recently placed hydraulic fills. In this method, horizontal drains are placed in the ground at different levels at a horizontal and vertical spacing of 0.5m to 1.5m (Shinsha et al. 1991). Special equipment is required for installation of drains at different levels in horizontal direction. The top part of compressible layer is expected to act as a sealing layer, and therefore is left untreated. Drain installation system and installation procedure used in this method (Fig. 2.12) are briefly described in the following (Shinsha et al. 1991, Shinsha 1996):

- A floating pontoon equipped with rolls of PVDs wrapped on reels, a mandrel with rollers at different levels to facilitate laying of PVDs at the desired intervals is used.
- Anchoring arrangements are required at both ends of the treatment area. Usually bulldozers and winches are used as anchors. Bulldozers act as

support during installation and facilitate movement of equipment to next installation point after each pass.

- Wire ropes, as shown in Fig. 2.12b are attached with the installation system.
- The mandrel is driven at desired depth at an angle and the pontoon is moved from one end to the other end with the help of anchor and wire system. In one pass, drains are laid simultaneously at different depths.
- The installation system is moved to the next point and the process is repeated.
- Vacuum is applied to one end of the PVDs through a hose linking PVD with vacuum pumping system.

Shinsha et al. (1991) reported a field trial and a full scale application for waste sludge stabilization. During the field trial, 2.80m thick reclaimed clay layer (submerged) was improved, leaving the upper 0.65m to act as a sealing layer (Fig 2.13a). The 50m long drains were laid at a vertical and horizontal spacing of 0.70m in 10 rows, to improve a total area of 350m^2. During 57 days of vacuum application, 75 to 80kPa vacuum pressure was maintained and the ground settled by 1.20m (Fig. 2.13b). The average water content was reduced from 200 % to 100%. Similarly, 4.5m thick waste sludge layer, (40000m^2) was improved using 200m long PVDs at 3 levels, in a square grid of 1.50m. A vacuum pressure of 80 to 90kPa was maintained which resulted in a settlement of 1.00m in 41 days. The average reduction in water content was almost 200%. The method is effective in very soft soils; however, the depth of improvement is limited owing to the limitations of equipment.

Another way of using the horizontal drain method is to place the horizontal drains at regular intervals while placing the hydraulic fill within the dikes as shown in Fig 2.14 (Jang et al. undated). Considerable time can be saved using this technique as consolidation and fill placement is carried out simultaneously. Moreover, the use of geosynthetic drainage material results in enhanced stability (Li et al. 2009). A laboratory study was carried out by Li et al. (2009) to compare the effects of using a geosynthetic drainage blanket as compared to sand drainage blanket. Table 2.1 shows the tests conducted and Fig. 2.15 shows the conceptual model and schematic diagram of

equipment used during the laboratory study. Test results for two of the tests, LYG1 (sand drainage blanket) and LYG2 (geosynthetic drainage blanket) are shown in Fig. 2.16. It can be seen from Fig. 2.16a that vacuum developed quickly to a higher value and stayed more uniform in case of LYG1; however, Figs. 2.16b shows that vacuum pressure distribution in the soil at the end of test (113days) was quite similar in both cases. Similarly the settlement response in both tests (Fig. 2.16c) is also quite similar. Li et al. (2009) has attributed the discrepancy observed in Fig. 2.16a and Fig. 2.16b to the instrument error. These test results show that geosynthetics can be effectively used for application of vacuum pressure and for discharge of water.

2.5.5 Underwater Application of Vacuum Consolidation Method

In 2000, Norwegian Geotechnical Institute (NGI) planned and implemented a full scale test to evaluate the possibility of using vacuum consolidation to improve soft sea bed clays in an under-water environment (Karlsrud et al. 2007). The site was located in the sea, at the outlet of the Drammen River. A 30 by 50m area, with a slope of 1:20 and an average water depth of 10m was selected for the improvement. Except top 20 to 40cm soil, which was very soft, black, organic and mud like, the seabed comprised of a more than 60m thick, normally consolidated silty clay deposit.

The technique used to apply the vacuum pressure to the soft seabed clay was similar to what has been discussed in Section 2.3.1 and Sections 2.5.1 to 2.5.3, and shown in Fig. 2.17. The installation technique, however, was quite different and required special equipment to successfully carry out the field trial. Salient features of the field trial and installation technique (Fig 2.17) are the following (Karlsrud et al. 2007):

- A 30cm thick sand blanket (filter layer) was placed on the seabed with the help of a barge. The barge was kept in position by anchor piles and two jack-up legs.
- A crane mounted on the barge and equipped with specially designed pull-down system and guide frame was used to install PVDs (Fig. 2.17c). The PVDs were installed at 1.5m spacing, to a depth of 15m in the compressible layer. A special cutter was also developed to cut the drains near the seabed level.

- After installation of PVDs, a 30cm thick layer of crushed gravel was placed to act as drainage layer. The gravel layer was compacted and smoothened by a long steel beam.
- A 1.2mm thick Butyl rubber membrane was used to cover the drainage layer. The membrane was extended 5m beyond the extents of drainage layer. The 40 by 60m membrane was rolled up on a 42m long, 600mm diameter steel pipe pile with heavy steel bars with pulling straps connected to the ends. The end of membrane was carefully lowered to sea bed and connected with the anchor pile. The vessel was moved to unroll the membrane from the pipe pile as shown in Fig. 2.17d.
- Divers were monitoring the membrane unrolling operation. After the membrane was unrolled and slightly stretched, sand bags were placed all around, 0.5m inside the membrane edge.
- A 200mm diameter nipple was pre-installed in the centre of the membrane for connection with the vacuum pump as shown in Fig. 2.17b.
- The treatment area was instrumented with push type electric piezometers, settlement points and flow meters.

Application of vacuum commenced on June 27, 2000. Vacuum pressure was gradually increased to 5bars (50kPa) in 5 hours, however the operation was stopped due to detection of leakages as a result of ripping of membrane at one place and bulging of membrane at three other places. The bulging of membrane was likely due to generation of gas from the organic layer. The membrane was repaired at these places and vacuum was applied again; however, significant reduction in pore pressure could not be achieved (Fig. 2.18a) and the operation was stopped in October 2000.

In September 2001, 10m wide membrane pieces were added on two sides of the membrane and steel chains were used as a load on the membrane edges to seal the area. This improved the sealing and a reduction of -60 to -70kPa was observed in all the piezometers; however, the leakages were not completely eliminated. The capacity of vacuum pump was increased by four times which resulted in lowering of pore pressure by

100kPa in the filter and over 90 and 70kPa respectively, at depths of 2m and 14m as shown in Fig. 2.18b. For a brief time (about one week), the pore pressure in the filter and at 2m depth, respectively, registered a drop of porewater pressure by 125 and 120kPa, indicating closure and subsequent reopening of one or more leakage channels.

The experiment showed that with special arrangements, the vacuum consolidation can be carried out in an underwater environment. Moreover, a greater reduction in porewater pressure is possible due available head of water.

2.5.6 Other Techniques

2.5.6.1 SILT NV Method

The method was developed by a Belgian firm SILT NV and has been used in Belgium since 1990s (Dam et al. 2006). Vacuum is applied with the help of submergible vacuum pumps using a natural drainage layer beneath the compressible layer. Large diameter sand drains are used at a greater spacing than the usual spacing of prefabricated vertical drains. For improvement of reclaimed soil for construction of a railway embankment, sand drains were used at a spacing of about 2.70meter (Meighem et al. 1999; Dam et al. 2006). The top of sand drains was capped to prevent leakage of vacuum which was applied through an existing sand layer below the compressible layer. The naturally existing sand layer was sandwiched between two clay layers which prevented leakage of vacuum. A typical cross section of this method is shown in Fig. 2.19a. It is important to note that this technique of vacuum application is somewhat similar to the one employed by US Army Corps of Engineers (Hammer 1981); however, vertical drains were not used by US Army Corps of Engineers.

SILT NV has also developed a special lay-barge equipped with plough for inserting the horizontal drains in very soft ground. The layout of vacuum consolidation using horizontal drains is shown in Fig. 2.19b. The equipment can work in a water depth of 1 to 25m (Dam et al. 2006).

2.5.6.2 Application of Vacuum Pressure Directly to Sand Drains

Woo et al. (1989) reported a field trial to improve soft Bangkok clay in which vacuum was directly applied to non-displacement type sand drains by placing filters at

two different levels; 3m and 11m. The top 1.3m of sand drains were capped and the filters were connected to vacuum pump through manifolds and pipes. Capping of sand drains could not prevent the vacuum leakage, therefore, the operation was stopped and area was covered with a plastic membrane. Detailed description of this technique is covered in Chapter 6. The trial showed that the technique could be used effectively to improve soft soils; however, this technique has not been used again.

2.5.6.3 Air Water Separation Vacuum Pump System

The Air Water Separation Vacuum Pump System, as shown in Fig. 2.20 was developed by Hazama Corporation in Japan (Dam et al. 2006). In this system, water and air discharged by the vertical and horizontal drains are first led to a supplementary air-water separation tank. From the supplementary tank, the separated water is pumped to the main separation tank. From the main tank, the separated water and air are pumped out through the vacuum driving system (separation of air and water is also carried out in main tank if required). The air-water separation tanks are laid beneath the membrane (Dam et al. 2006).

A higher vacuum intensity can be maintained using this system. The system was used during field trial related to ground improvement for construction of Monou Interchange of Sanriku Motorway in Japan. A vacuum of 80 to 95kPa was successfully maintained throughout the project duration of 172 days (Dam et al. 2006).

2.6 Technological Aspects of Equipment used in Vacuum Consolidation

As most of the firms carrying out vacuum consolidation in the field have developed their own patented products, very limited information is available on the technological aspects of various equipments used for the implementation of vacuum consolidation. The information available in the literature is briefly reviewed in this section.

2.6.1 Vertical Drains

Kjellman (1952) performed his field trials using cardboard wick drains. Since then, vacuum consolidation has been carried out successfully using several different types of vertical drains, including sand packed drains (Yee et al. 1983), non-displacement sand drains (Woo et al. 1989), large diameter sand Drains (Mieghem et al. 1999), and a range

of different types of PVDs and CPVDs. With the development of robust plastic materials, PVDs are most commonly used for vacuum preloading operations. Fortunately, there is no particular difference in the type of vertical drains used for fill or vacuum preloading; therefore, the technical specifications reported in the literature (Holtz 1987; Mesri and Lo 1991; Lo 1991; Bo et al. 2003) in connection with fill preloading are equally applicable for vacuum preloading. Typical cross sections of some commonly used prefabricated vertical drains are shown in Fig. 2.21.

The performance of vertical drains under vacuum preloading may or may not be different from the performance of vertical drains under fill preloading which is discussed in Chapter 9. Table 2.2 presents the summary of typical drain parameters used in different techniques of vacuum consolidation. PVDs developed specifically for use in vacuum preloading operation are briefly reviewed as following:

2.6.1.1 Capped Prefabricated Vertical Drains (CPVDs)

A CPVD is a conventional PVD provided with an impermeable cap at the top as shown in Fig. 2.22. The function of this cap is to by-pass the high permeability soils near the ground surface and penetrate partly into the soft soil. The cap is tightly fixed to the PVD and is connected to the vacuum line through a flexible hose. Chai et al. (2008) specifies a cap length of 190mm for a particular CPVD produced in Japan. Cortlever et al. (2006) however, suggests that the caps are fixed to the PVDs on site as per site dictates. The use of CPVD eliminates the necessity of having a sealing membrane; however, the cap of CPVD must penetrate a sufficient distance into the soft layer to completely seal the overall system. Schematic layout of Beaudrain-S system, developed by COFRA BV is shown in Fig. 2.23.

2.6.1.2 Vacuum Transmission Pipes (VTPs)

The vacuum transmission pipes (VTPs) are circular drains developed by DGI Menard for efficient transmission and distribution of vacuum (Masse et al. 2001). The diameter of VTPs may vary, i.e. 34mm diameter VTPs were used in Port of Brisbane Project in Australia (Berthier et al. 2009) whereas 50mm diameter VTPs were used to improve Pusan clay in South Korea (Masse et al. 2001). Figure 2.24 shows the cross section of the VTP. It can be seen that the VTPs consist of a collapsible and flexible

plastic tube covered with a filter fabric on the outside. This construction enables the VTPs to deform with progress of settlement, a necessary condition for PVDs.

2.6.2 Installation of Vertical Drains

As PVDs are more commonly used in the vacuum preloading operations, the installation techniques for PVDs are discussed in this section. PVDs are normally available in rolls which are attached to drill rigs and driven to desired depth with the help of a mandrel. Commonly used equipment required for installation of PVDs is as following:

2.6.2.1 Drill Rigs

A variety of drill rigs are available for the installation of PVDs. The choice of a specific drill rig depends upon a number of factors including the bearing capacity of the soil, depth of installation, type of soil and production capacity of the rig (Bo et al. 2003). For field trials in soft Bangkok clay which has a 1.5 to 2.0m thick desiccated crust, a contact pressure of 5kPa was specified for the machinery live load to avoid stability problems (Bergado et al. 2002). For very soft soils, ground may be pre-treated to enable movement of machines or persons. For example, during improvement of reclaimed land for port development in China, ground was pretreated followed by a wait period of six months before moving the equipment for drain installation. A total of 287,626 drains were installed using gantry type, crawler type, floating type and double mandrel type of drill rigs. Vibro-driving mode of installation was used to install the PVDs for this project (Yixiong 1996b). Different types of rigs used for installation of PVDs are listed in Table 2.3.

2.6.2.2 Mandrel

A mandrel is used to drive the PVD to its desired depth and to maintain the verticality of PVDs. Mandrels are available in different cross sections including rhombic, rectangular, square and circular. The choice of mandrel depends upon the stiffness of the soil it has to penetrate and availability of equipment. Usually a small size rhombic mandrel is used to minimize the soil disturbance; however, for stiffer soils rectangular mandrels with thick steel walls are more suitable (Bo et al. 2003). Cross sections of different types of mandrels are shown in Fig 2.25.

2.6.2.3 Anchor

Anchors are used to fix the PVDs at the desired depth such that the PVD does not come out of the ground when the mandrel is retrieved. Various types of anchors including steel bar anchors and metal plate anchors are in use. Anchor also helps in preventing the intrusion of soil into the mandrel when it is pushed down. Different anchoring arrangements for PVDs are shown in Fig. 2.25.

2.6.3 Vacuum Pump System

Different agencies have developed their own vacuum pumping systems capable of applying vacuum to a large area and to handle air and water flowing out of the soil. Technical information on working principles, pump capacity and power consumption etc are not available in detail, however, broader information pertaining to area covered per pump are reported in literature. Chinese method uses 48cm diameter jet pumps for application of vacuum to the soft ground. A centrifugal pump is connected in series with jet pump to handle water and air flowing out of the system (Yixiong 1996a; Dam et al. 2006). Menard uses an indigenously developed pumping unit which can handle both air and water and generate a 70 to 80kPa vacuum over an area of 5000 to 7000m^2 (Masse et al. 2001). The available information on vacuum pumping system used in various vacuum consolidation systems is given in Table 2.4.

Figure 2.26 shows the schematic diagram of a jet type of pump. A pressurized fluid is forced through the inlet and made to pass through the tapered nozzle. The passage of fluid through the nozzle results in a sudden drop in pressure and a consequent increase in pressure as it moves towards the outlet. The sudden increase in pressure generates suction in the lower chamber of the pump forcing any fluid or material in this chamber out through the exhaust along with the fluid from the jet nozzles (www.wikepedia.com). In addition to air and water coming out of the consolidating soil, a jet pump can also handle solid particles which cause pitting of the centrifugal pump blades.

2.6.4 Horizontal Drainage System

The horizontal drainage system comprises of a drainage blanket (usually sand) and a network of longitudinal and traverse pipes laid within the drainage blanket for efficient distribution of vacuum pressure and discharge of water. Usually circular pipes

with perforations and corrugations, covered with a filter fabric are used; however, PVDs have also been used successfully for horizontal drainage (Chai et al. 2006). Typical cross sections for drains used in horizontal drainage are shown in Fig. 2.27 and available technical data are in Table 2.5.

2.6.5 Sealing System

Sealing the treatment area from its surrounding is essential for effective use of vacuum as a preload. Use of impermeable membranes to cover the surface is the most common way of sealing the treatment area. The impermeable membranes are anchored into the slurry trenches, dug slightly below the water table to complete the sealing. In case of a thick crust or a high permeable layer, the isolation of treatment area in ensured by providing a sheet pile or slurry cut off (Kjellman 1952; Tang and Shang 2000; Masse et al. 2001). In situ clay layer can also be used effectively as a sealing material to prevent loss of vacuum. In this case, the provision of surface membrane or slurry cut off is not required; however, the clay layer acting as a seal is only partly treated. In cases where submersible vacuum pumps in combination with vertical drains are used, the top of vertical drains is sealed to prevent loss of vacuum. Table 2.6 summarizes the sealing arrangements used in different techniques of vacuum application. Figure 2.28 shows the membrane laying process and a completed system linked with the vacuum pumps.

2.6.6 Connectors

The air tightness of connection between the horizontal drainage system and the vacuum pump is absolutely essential for the efficient application and distribution of vacuum pressure within the drainage blanket and in the vertical drains. Very limited information is available in the literature regarding the connection arrangements between the horizontal drainage system and the vacuum pump system. A membrane-less system, where each vertical drain is directly connected to the vacuum pump is more susceptible to leakage at the joints. It is probably for this reason that despite producing 80 to 90kPa vacuum intensity at the pump, only 50 to 60kPa can be transmitted to the CPVDs (Chai et al. 2008; Saowapakpiboon et al. 2008). Connectors used by Menard and COFRA are respectively shown in Figs. 2.28 and 2.23.

2.7 Concluding Remarks

Contrary to fill preloading, where the effective stress is increased by increasing the total stress in the soil mass; the application of vacuum to an isolated compressible layer results in an increase in effective stress by reducing the porewater pressure. The use of vacuum consolidation was first proposed by Kjellman in 1952, however, the method was developed for practical applications in mid 1980s. Since then the method has gained popularity and a number of innovative techniques of applying vacuum to the soft ground have been invented throughout the world; however, all the methods are essentially based on the same basic principle proposed by Kjellman (1952). Moreover, the essential components of any vacuum consolidation system are also the same; only the technique of application is different in different methods.

Data on field trials and laboratory studies of vacuum consolidation are available in the literature which can be analysed to understand the soil behavior during vacuum consolidation; however, sufficient details regarding the technology and equipment used to apply vacuum to the soft ground are not reported in the literature.

2.8 Tables

Table 2.1: Initial conditions for different laboratory tests (after Li et al. 2009)

Test Group	Soil Sample	Test No.	Water Content (%)	Unit Weight (kN/m3)	Thickness (cm)	Drainage Blanket
1	LYG muck	LYG1	86.00	14.9	124	Sand
		LYG2	86.40	14.9	124	Geosynthetic
2	QD muck	QD1	40.33	18.2	255	Sand
		QD2	41.50	18.1	310	[1]Geosynthetic
3	QD muck	QD3	41.65	18.1	105	Sand
		QD4	41.45	18.1	112	No
[1]Perforated pipe was used as second drainage layer						

Table 2.2: Vertical drain parameters used in various techniques of vacuum application

S.No	Method	Drain Parameters					
		Type	**Section**	**[1]Discharge Capacity (m^3/yr)**	**Penetration Depth (m)**	**Typical Spacing (m)**	**Average Time for Vacuum to be Effective (Days)**
1	Chinese [Yixiong (1996a, b); Shang et al. (1998); Yan and Chu (2003, 2005) etc.]	PVD – Plastic board type	W=100mm T=3-4mm	790	25	1.0 (0.5 – 1.3)	Average 15 (1 to 58)
2	Menard [Cognon et al. (1994); Masse et al. (2001); Ihm and Masse (2002)]	PVD, VTP	D=50mm	-	40	0.8 – 1.5	4 - 14
3	Vacuum-CPVD (COFRA) [Yoneya et al. (2003); Saowapakpiboon et al. 2008]	CPVD	W=100mm T=3-7mm	-	12	0.8 – 1.0	-
4	Horizontal Drain Method (Shinsha et al. 1991)[2]	PVD	W=100mm T=3-12mm	-	6	0.7	-
5	Under water vacuum Application (NGI) [Karlsrud et al. (2007)]	PVD	W=100mm T=4mm	-	15/25[3]	2.5	-
6	Sand drain method [Woo et al. (1989); Meighem et al. (1999)]	Sand	D=12cm	-	-	-	-
7	Air-Water Separation system [Dam et al. (2007)]	PVD	W=300mm T=7mm	-	11	0.8	-
8	USACE[4] [Hammer (19810]	Sand	-	-	-	-	-

[1]Specified by manufacturer and reported in Literature; [2]IIncluded here as these drains are used for consolidation; [3]Including depth of water

[4]Sand blanket used for vacuum application; - Data not available

W = Width, T = Thickness, D = Diameter

Table 2.3: Types of rigs used for installation of PVDs at Changi East reclamation project (after Bo et al. 2003)

Description	**Type**	**Weight (ton)**	**Penetration Power (ton)**	**Height of Rig (m)**	**Maximum Penetration Depth (m)**	**Mechanism of Penetration**	**Maximum Production/Day (m/14hours)**
Cofra	O & K Excavator, RH30, RH40	70 -110	20 - 30	36 – 55.5	50.5	Hydraulic motor, multipulley system	33400
ECON	O & K Excavator, RH30, RH40 (01) Hitachi Excavator EX1100	70 – 120	20 - 30	36 – 56.1	51.5	Hydraulic motor, multipulley system	27500
YUYANG	Samsung CX800 Crane, Daewoo solar 450III Excavator, Zeppelin Crane, P & H Crane, IHI Crane	45 – 100	25 - 30	43 – 55.8	53	Hydraulic motor, multipulley system, driven chain and cable system	15300
Chosuk	Daewoo solar 450 Excavator	45	25	56	51	Hydraulic Cylinder, multipulley system	17900
Daeyang	Daewoo solar 450III Excavator	33 - 55	20 - 34	42 - 56	52	Hydraulic motor, push in roller and clamp system	15200
B + B	Excavator	-	-	31 – 47	29 – 45	Hydraulic sprocket and chain	19200
B + B	Excavator	-	-	43 - 50	41 - 48	Vibro push in	8600

Table 2.4: Vacuum pumping systems used in various techniques of vacuum application

S.No	Method	Pump Specifications				Vacuum Intensity (kPa)
		Type	Capacity	Area per Pump (m^2)	Consumption (KW)	
1	Chinese [Yixiong (1996a, b); Shang et al. (1998); Yan and Chu (2003, 2005) etc.]	Jet and Centrifugal	-	100 - 1500 600 for high k_{vo}	7.5	> 80
2	Menard [Cognon et al. (1994); Masse et al. (2001); Ihm and Masse (2002)]	MS25	-	5000 – 7000	25	70 – 80
3	Vacuum-CPVD (COFRA) [Yoneya et al. (2003); Saowapakpiboon et al. 2008]					50 – 60
4	Horizontal Drain Method (Shinsha et al. 1991)[2]	-	1500 l/m	350[1]	-	80 - 90
5	Under water vacuum Application (NGI) [Karlsrud et al. (2007)]	Venturi pump, Centrifugal type	26 m^3/hr 100 m^3/hr	1500[1]	-	50 - 80
6	Sand drain method [Woo et al. (1989); Meighem et al. (1999)]	Submersible	-	-	-	-
7	Air-Water Separation system [Dam et al. (2007)]	-	-	3750[2]	-	80 - 95
8	USACE[4] [Hammer (19810]	-	20cfm	8.5[1]	-	50 - 2

[1]Experimental setup, actual Pump capacity/coverage area may be more

[2]Test embankment- area was divided into two sections; however, actual number of pumping units are not mentioned

Table 2.5: Details of horizontal drainage system for different vacuum consolidation techniques

S.No	Method	Drainage Blanket		Horizontal Drains				Main Collector Pipe (mm)
		Thickness (m)	Material	Type	Spacing (m)		Section (mm)	
					Longitudinal	Transverse		
1	Chinese [Yixiong (1996a, b); Shang et al. (1998); Yan and Chu (2003, 2005) etc.]	0.3 – 1	Sand	Corrugated, PVC/steel, wrapped in filter fabric	3.9	30	D = 50 -100	-
2	Menard [Cognon et al. (1994); Masse et al. (2001); Ihm and Masse (2002)]	2.5	Sand	-	-	-	Circular	-
3	Vacuum-CPVD (COFRA) [Yoneya et al. (2003); Saowapakpiboon et al. 2008]	NA	NA	-	-	-	Circular	-
4	Horizontal Drain Method (Shinsha et al. 1991)[2]	NA	NA	Horizontal drains are used for consolidation				-
5	Under water vacuum Application (NGI) [Karlsrud et al. (2007)]	0.6	Sand and Gravel	Not used				-
6	Sand drain method [Woo et al. (1989); Meighem et al. (1999)]	2	Sand	In situ sand layer (2m) used as drainage blanket				
7	Air-Water Separation system [Dam et al. (2007)]	0.7	-	Board Drains, KD 300	-	-	-	-
8	USACE[4] [Hammer (19810]	0.6	Sand	PVC, slotted	2.3	NA	D = 38	100

Table 2.6: Sealing arrangements for different vacuum consolidation techniques

S. No	Method	Sealing Membrane					Peripheral Trench			Side Cut Off
		Type	Thickness (mm)	Layers	Tensile Strength (MPa)	Strain (%)	Depth	Section	Backfill Material	
1	Chinese [Yixiong (1996a, b); Shang et al. (1998); Yan and Chu (2003, 2005) etc.]	PVC	0.3 - 1	1 - 3	-	-	Below GWT	Trapezoid	Clay slurry	In situ clay mix slurry wall
2	Menard [Cognon et al. (1994); Masse et al. (2001); Ihm and Masse (2002)]	HDPE	-	1	-	-	Below GWT	Trapezoid	Polyacrylite, bentonite mix slurry	Slurry wall
3	Vacuum-CPVD (COFRA) [Yoneya et al. (2003); Saowapakpiboon et al. 2008]	In situ Clay	0.5 – 2	NA	NA	NA	NA	NA	NA	NA
4	Horizontal Drain Method (Shinsha et al. 1991)[2]	In Situ Clay	0.5	NA	NA	NA	NA	NA	NA	NA
5	Under water vacuum Application (NGI) [Karlsrud et al. (2007)]	Butyl, rubber type	1.2	1 – 2	8.5	350	NA	NA	NA	-

NA: Not applicable

-: Not available

Table 2.6: Continued

S. No	Method	Sealing Membrane					Peripheral Trench			Side Cut Off
		Type	Thickness (mm)	Layers	Tensile Strength (MPa)	Strain (%)	Depth	Section	Backfill Material	
6	Sand drain method [Woo et al. (1989); Meighem et al. (1999)]	In situ Clay & Capping Drains	0.5 – 1	NA	NA	NA	NA	NA	NA	-
7	Air-Water Separation system [Dam et al. (2007)]	-	-	2	-	-	-	-	-	-
8	USACE[4] [Hammer (19810]	In situ soil	NA	NA	NA	NA	NA	NA	NA	Plastic membrane

NA: Not applicable

-: Not available

2.9 Figures

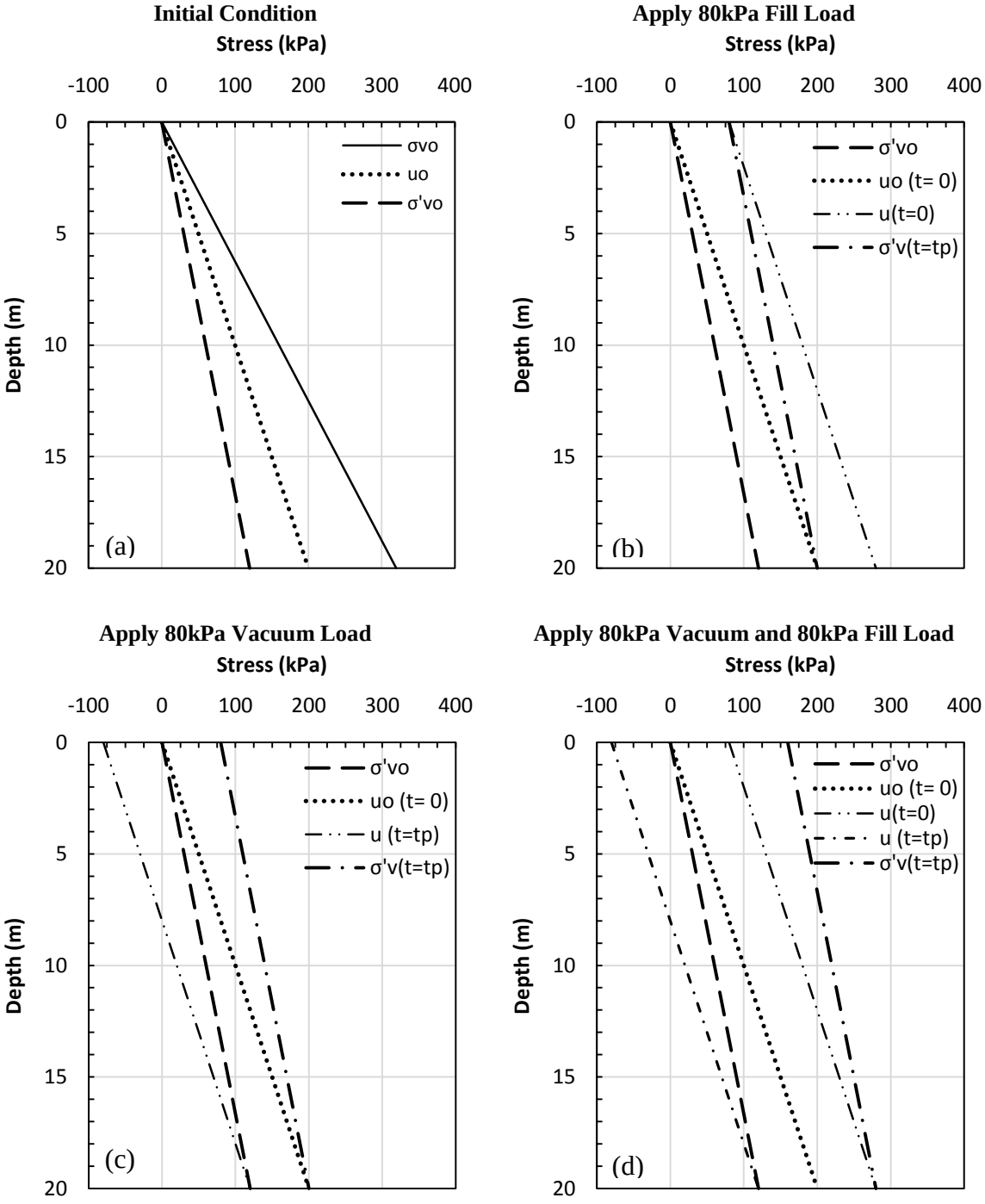

Figure 2.1: Idealized stress and porewater distribution due to (a) initial condition (b) fill preload, 80kPa, (c) vacuum preload 80kPa, and (d) combined vacuum-fill preload 160kPa (80+80); unit weight of soil = 16kN/m^3, water table at ground surface and hydrostatic porewater pressure condition.

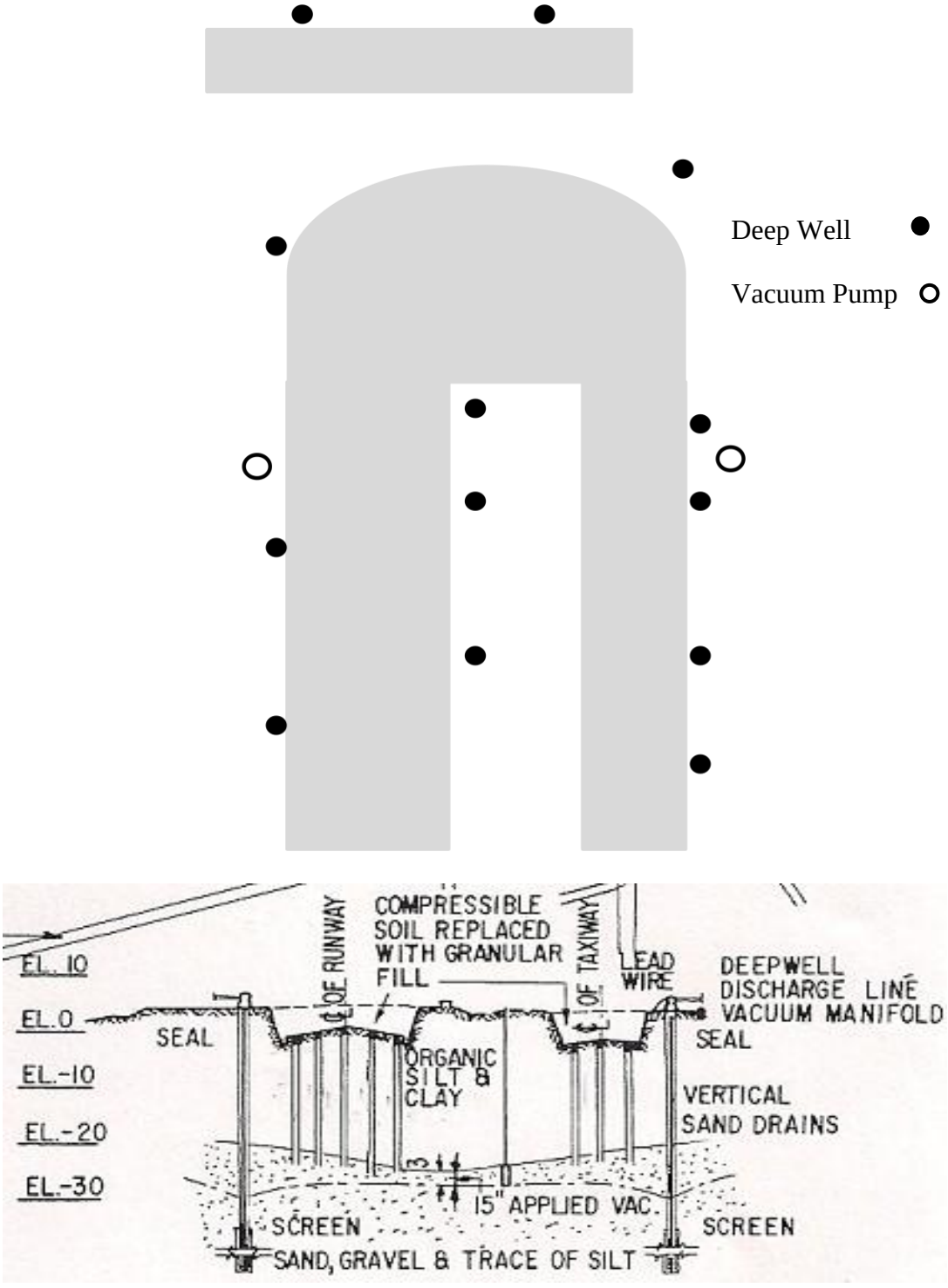

Figure 2.2: Plan and section of taxiway improved using sand drains, deep wells and vacuum pumping

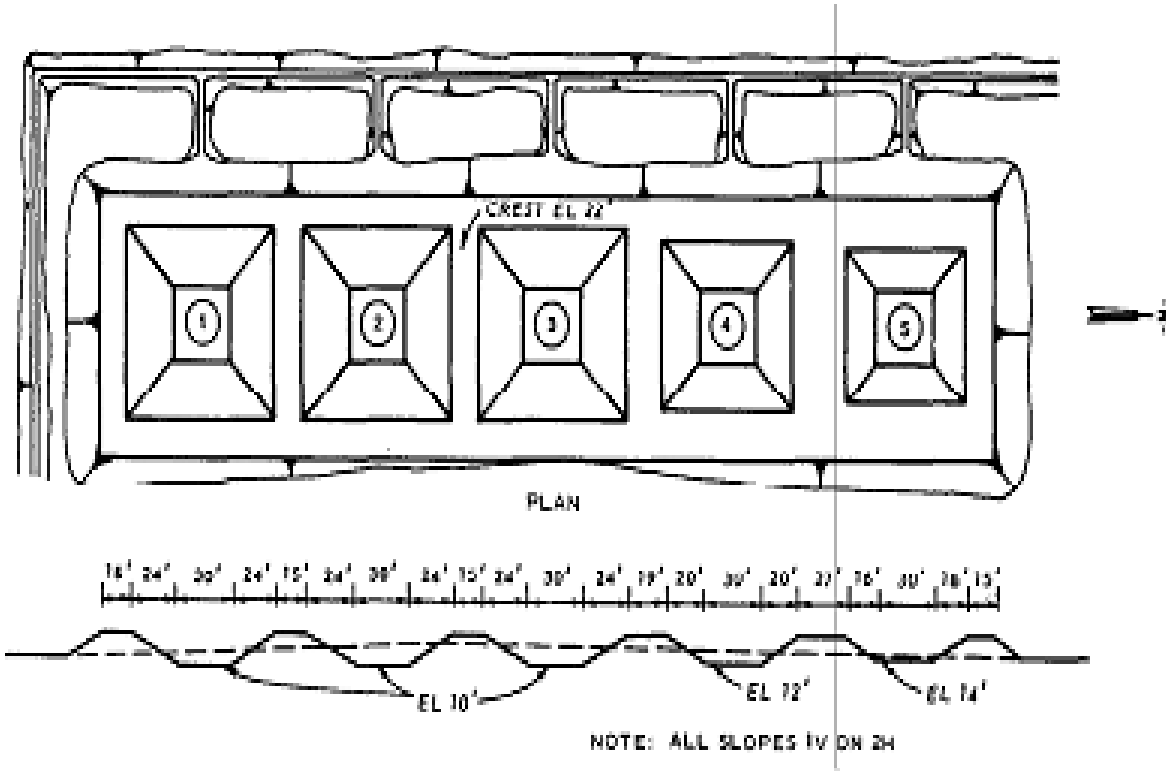

Section No	Method	Bottom Elevation (ft)
1	Seepage Consolidation	10
2	Seepage Consolidation with Vacuum	10
3	Partial Vacuum in Under-Drainage Layer	10
4	Under-Drainage	12
5	Control	14

Figure 2.3: Plan and elevation of test sections in Mobile, Alabama (after Hammer 1981)

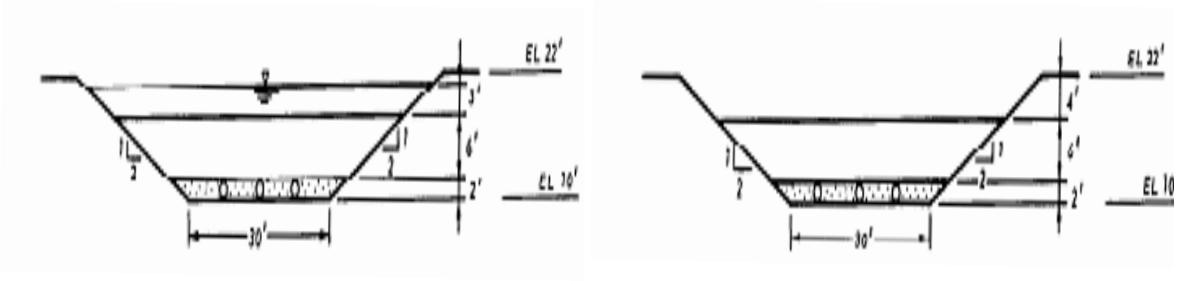

Test Section 2 Test Section 3

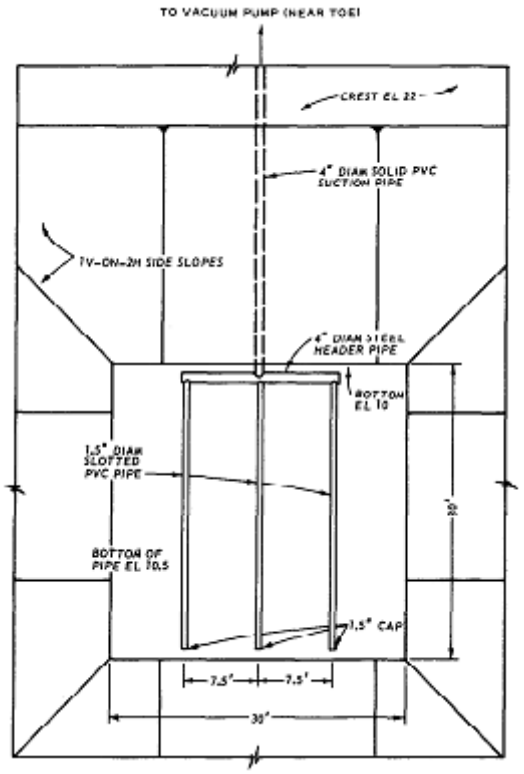

Figure 2.4: Layout of horizontal drainage used for vacuum test sections (after Hammer 1981)

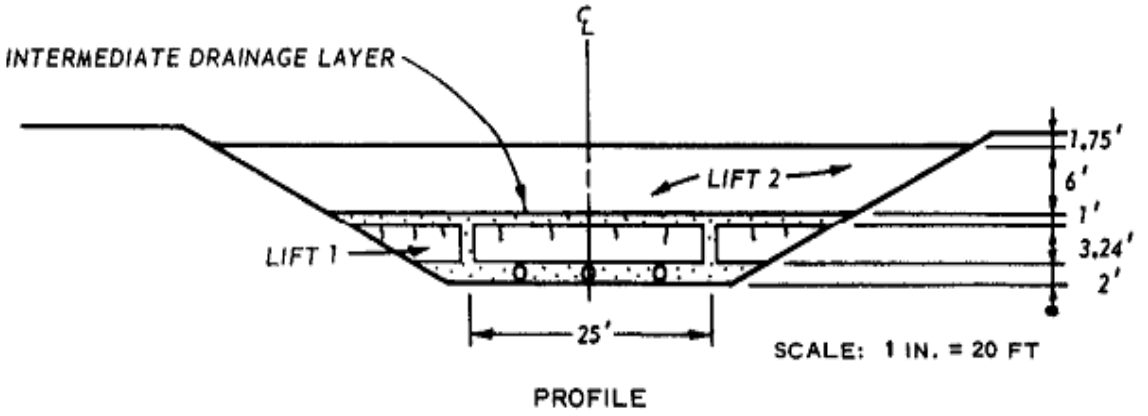

Test Section 2

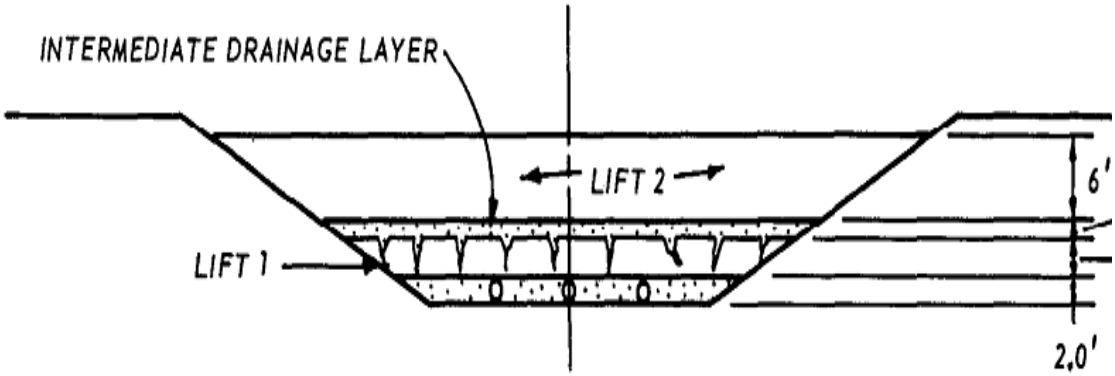

Test Section 3

Figure 2.5: Connection arrangements between under-drainage layer and intermediate layer for vacuum test sections (after Hammer 1981)

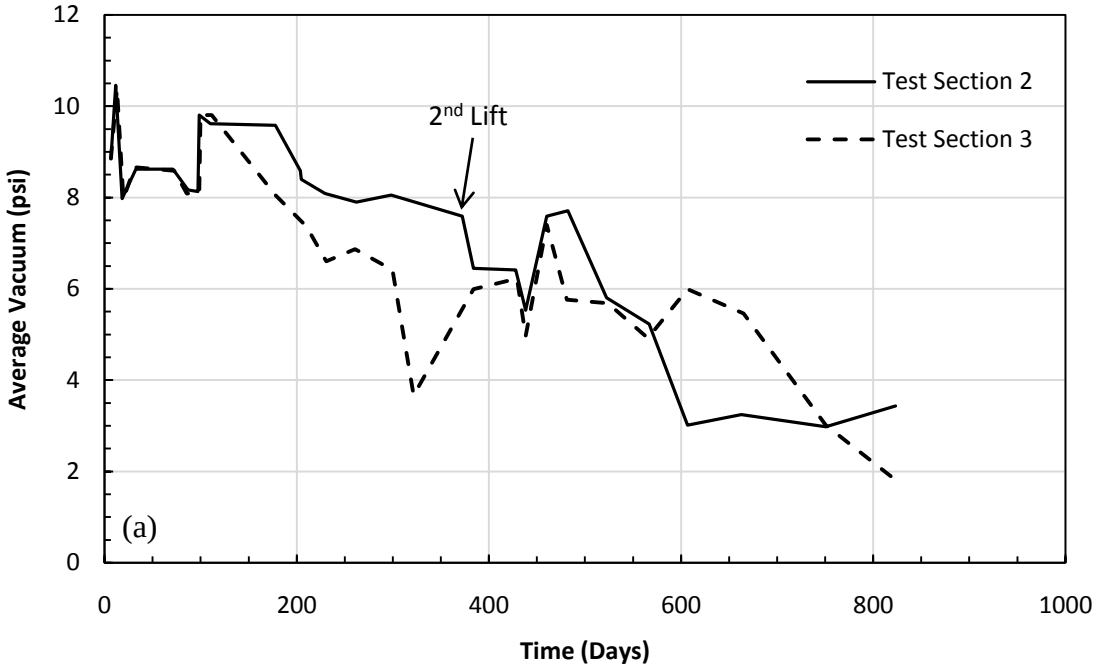

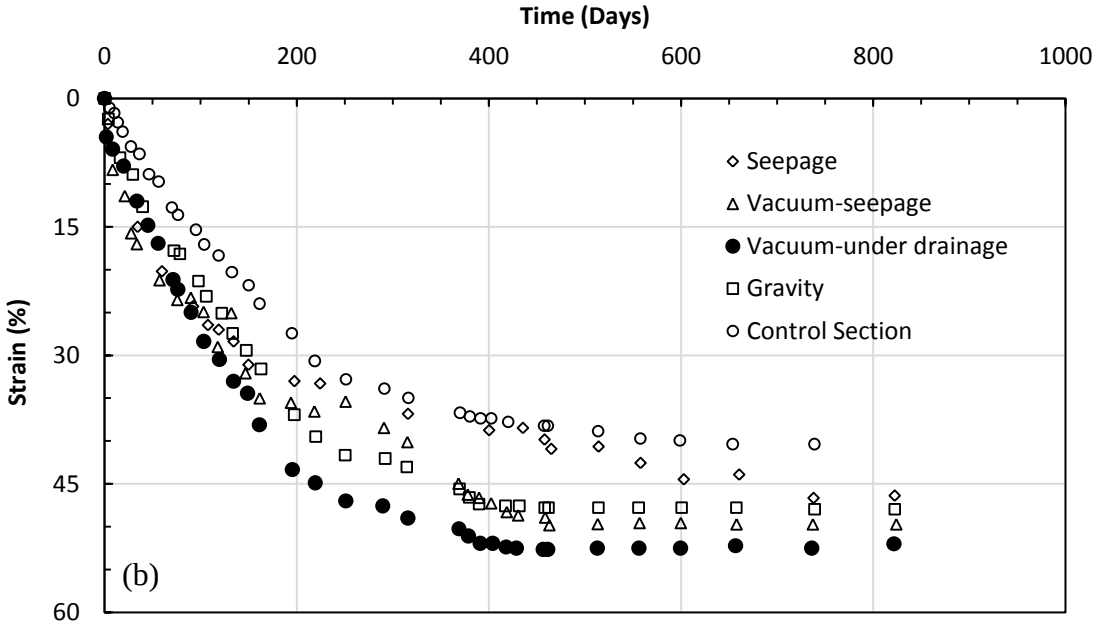

Figure 2.6: (a) Average vacuum pressure in under-drainage layers in Sections 2 and 3, (b) settlement due to different treatment methods (data from Hammer 1981)

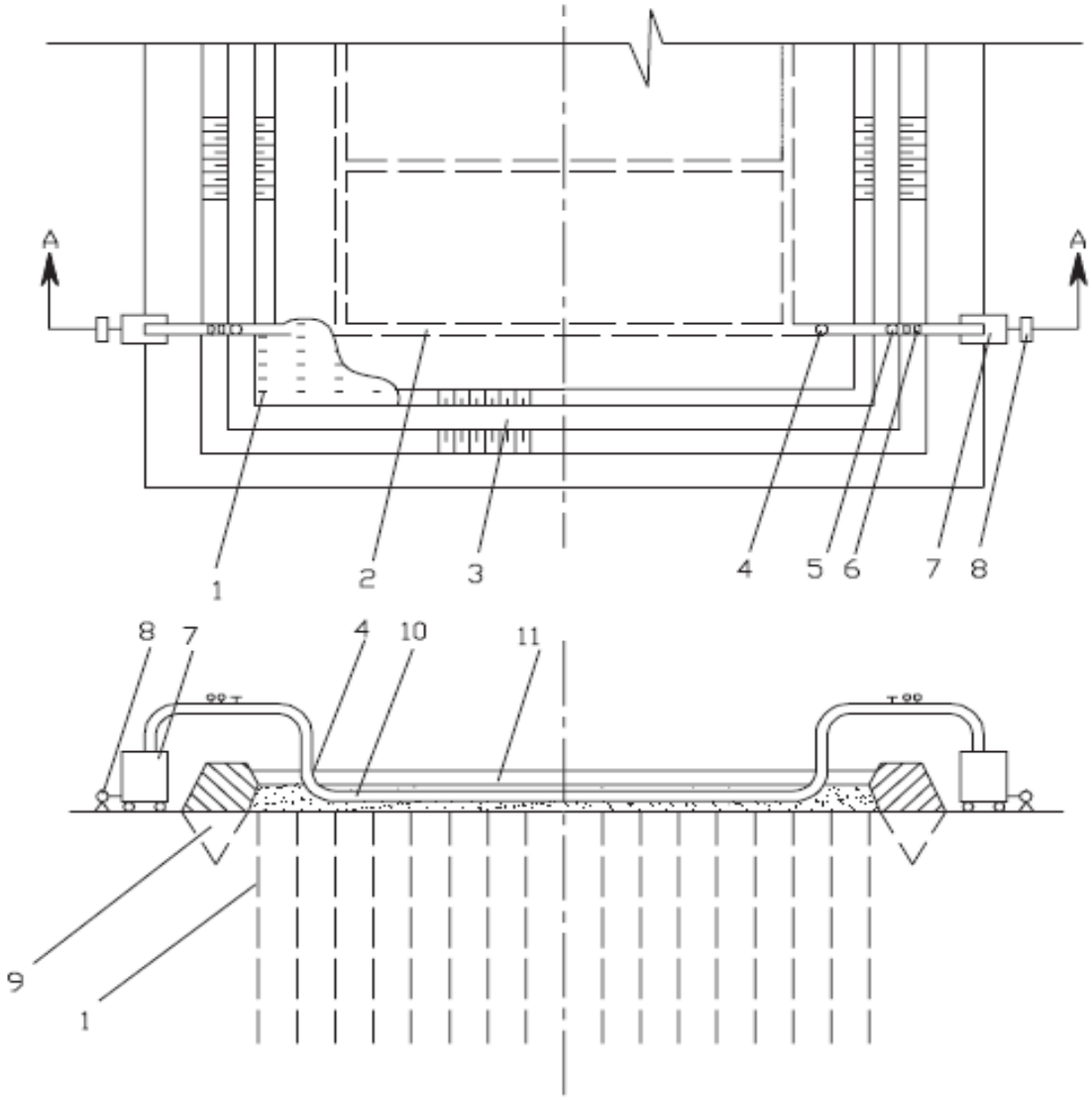

Figure 2.7: Schematic layout of vacuum consolidation system; (1) Vertical drains; (2) Filter piping; (3) Revetment; (4) Water outlet; (5) Valve; (6) Vacuum Gauge; (7) Jet pump; (8) Centrifugal pump; (9) Trench; (10) Horizontal piping; (11) Sealing membrane. (After Chu and Yan, 2005)

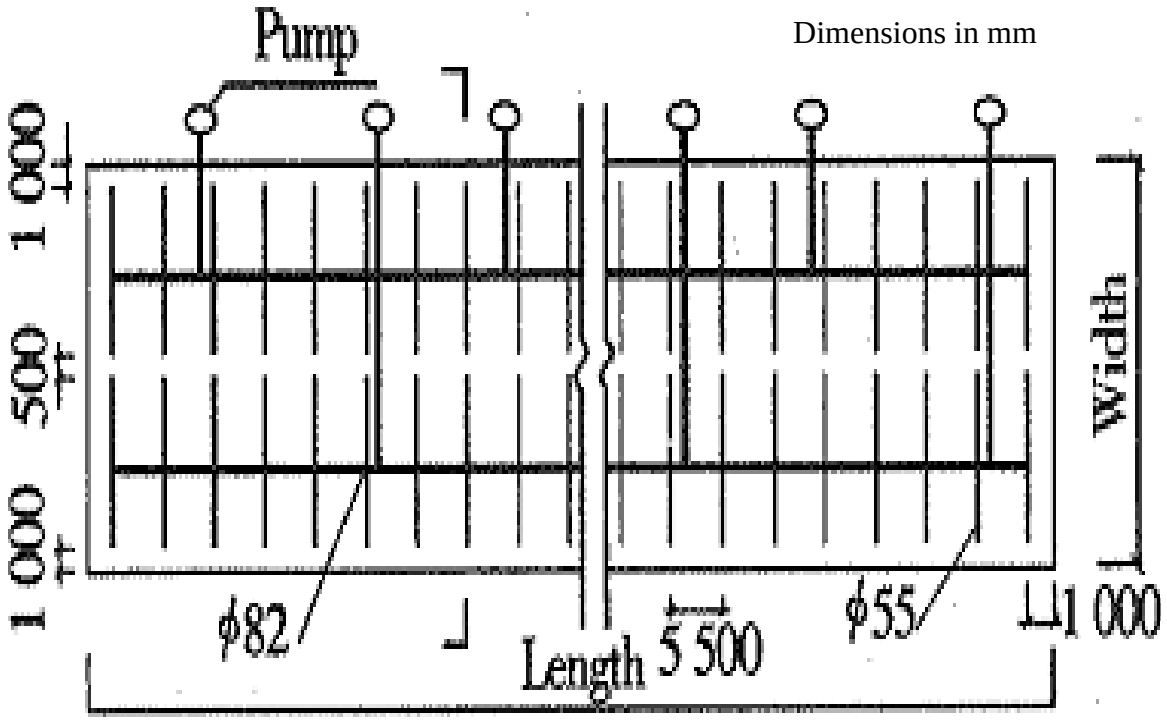

Figure 2.8: Layout of horizontal drainage network and its connection with vacuum pump (after Liu et al. 2004)

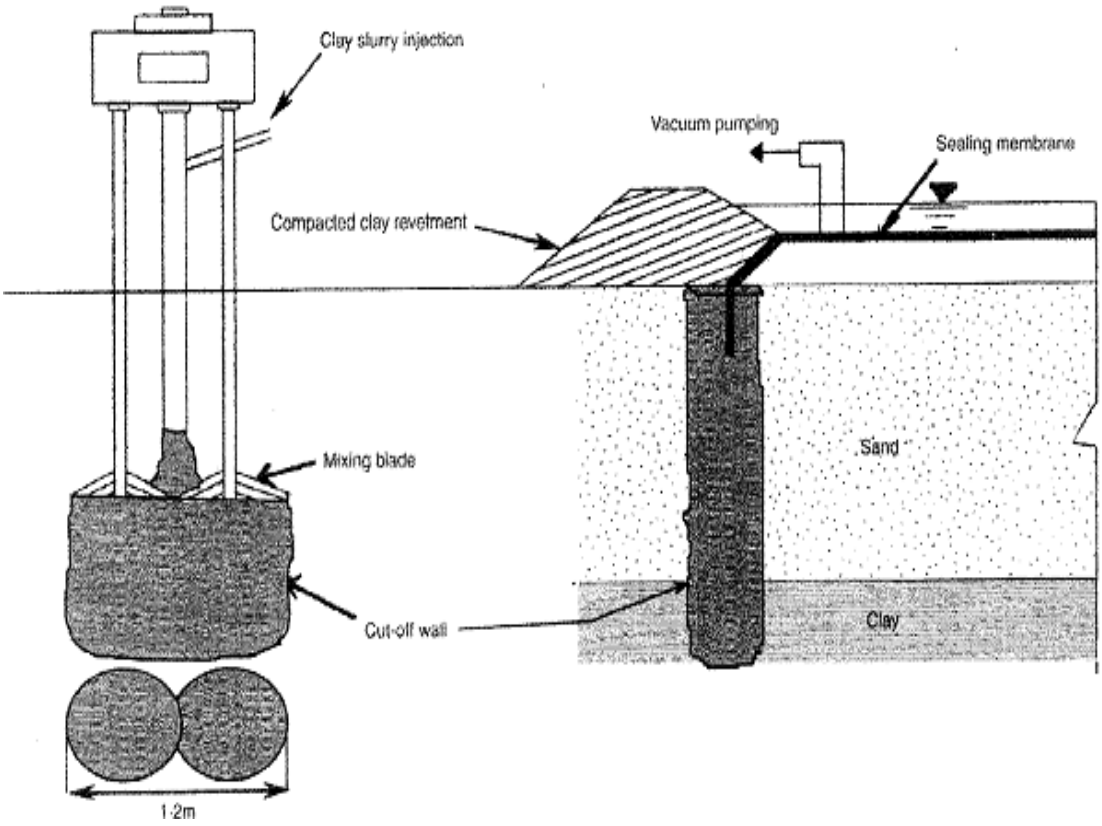

Figure 2.9: Clay-mix slurry wall constructed to prevent leakage of vacuum from a high permeability ground surface layer (Tang and Shang 2000)

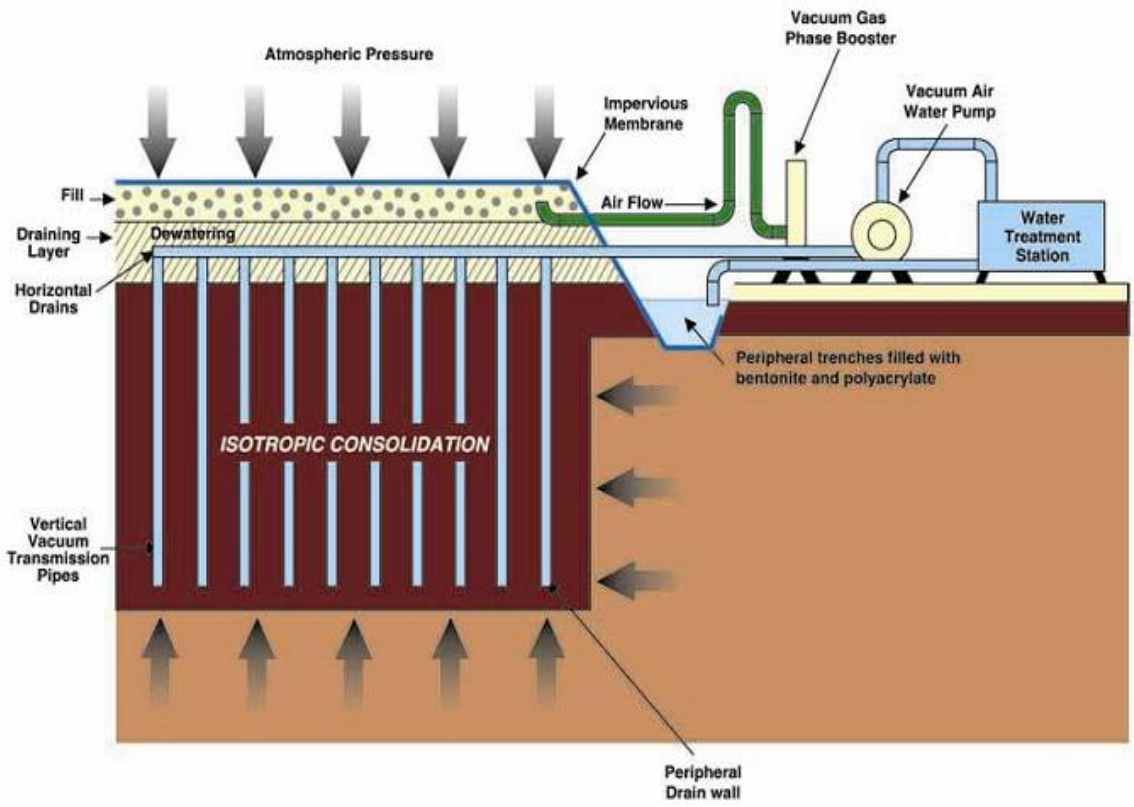

Figure 2.10: Menard method of vacuum consolidation (after Masse et al. 2001)

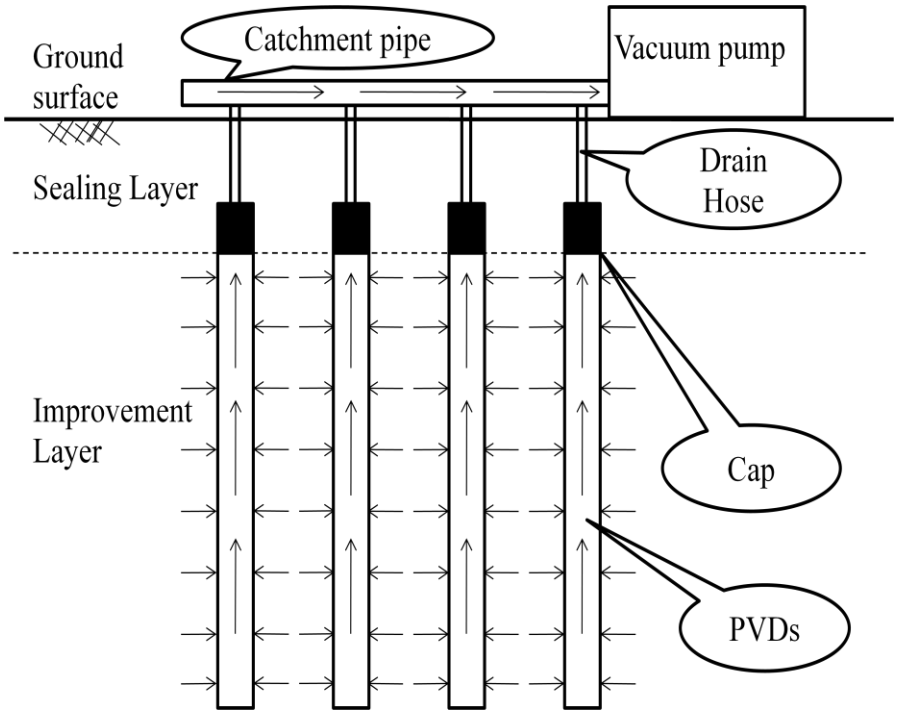

Figure 2.11: Vacuum-CPVD system (redrawn from Yoneya et al. 2003)

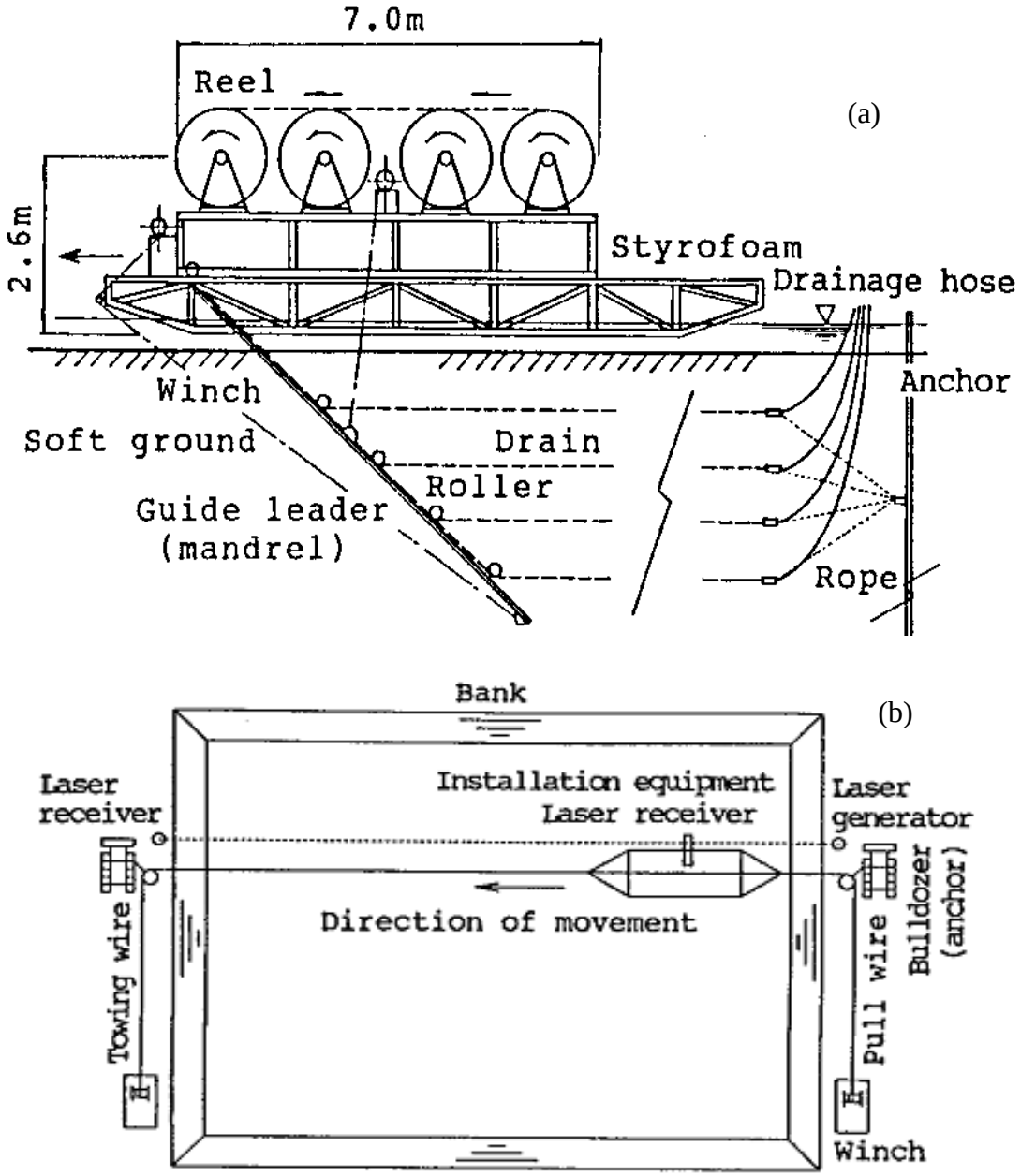

Figure 2.12: Equipment and procedure employed for installation of horizontal drains in very soft ground (after Shinsha et al. 1991)

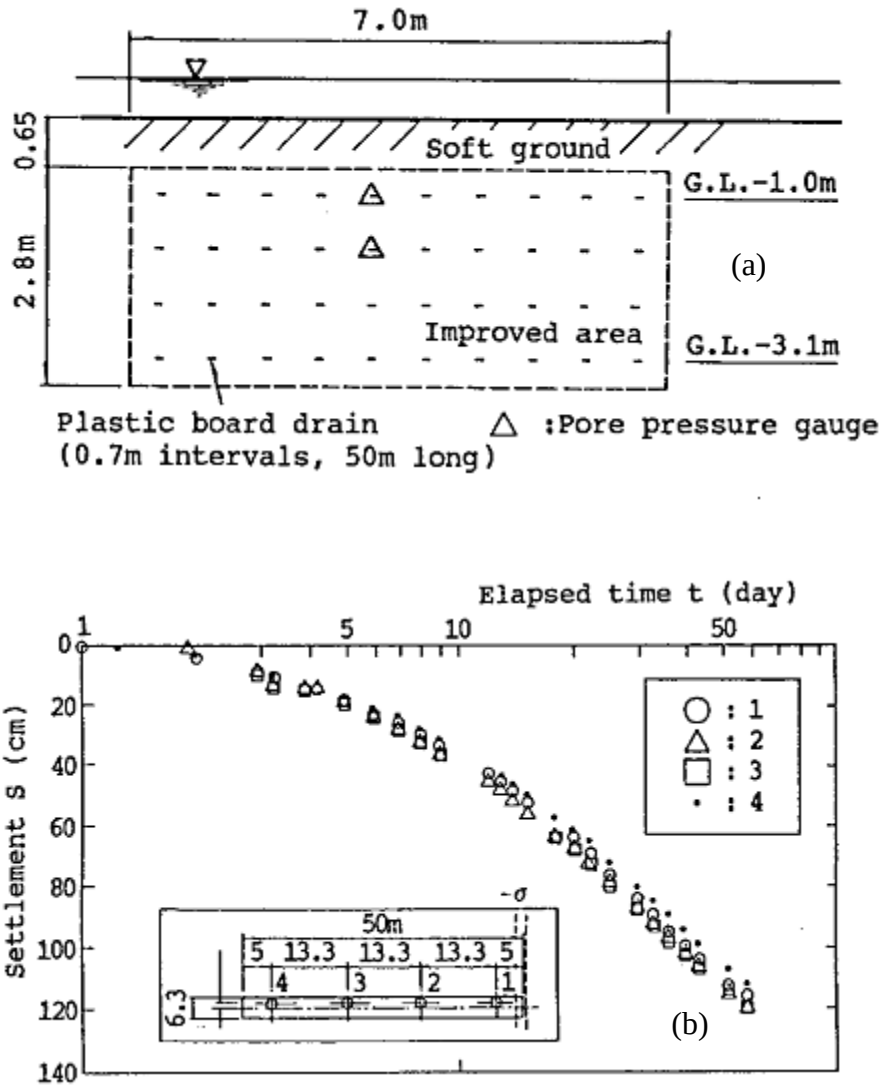

Figure 2.13: (a) Layout of horizontal drains and (b) settlement due to vacuum preloading (after Shinsha et al. 1991)

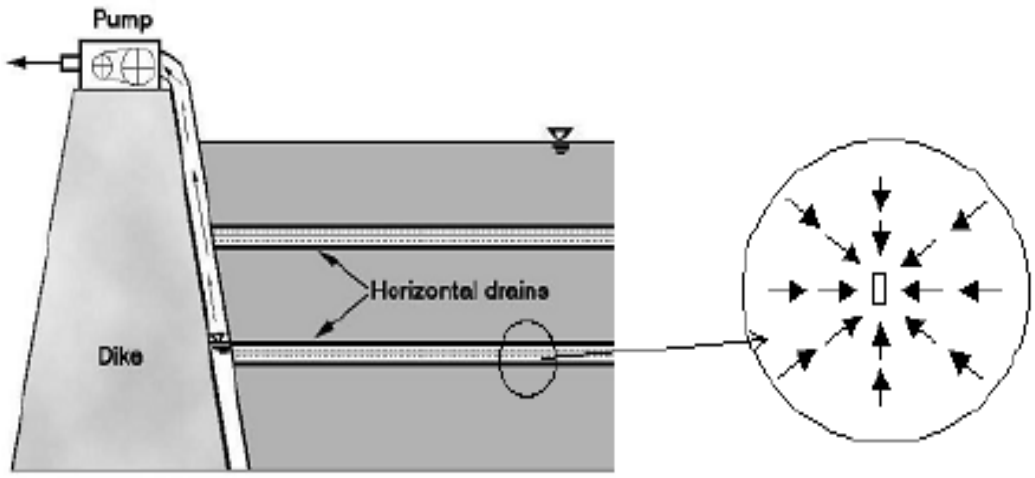

Figure 2.14: Layout of horizontal drain method (after Jang et al. undated)

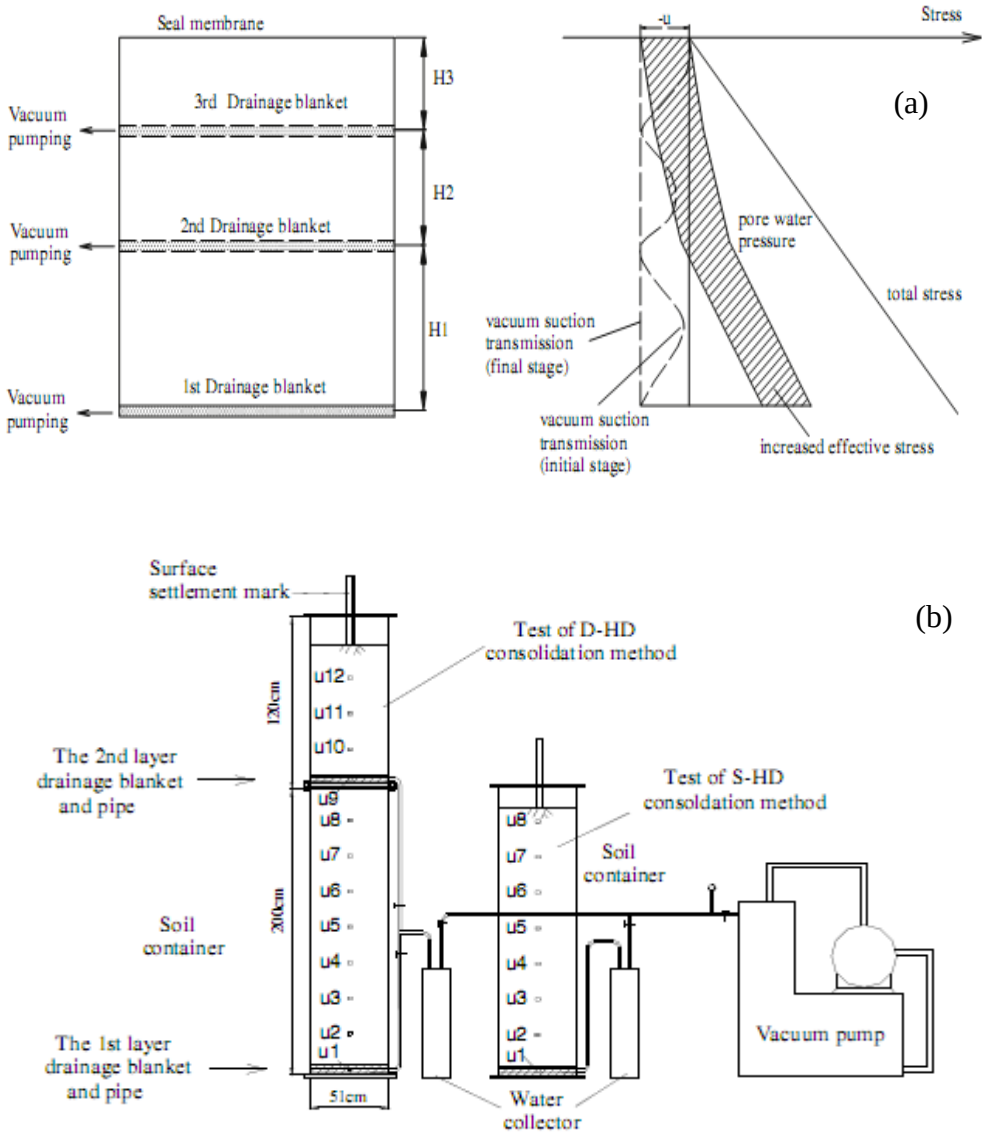

Figure 2.15: (a) Conceptual model and (b) schematic layout of laboratory equipment used to simulate horizontal drainage using vacuum (afer Li et al. 2009)

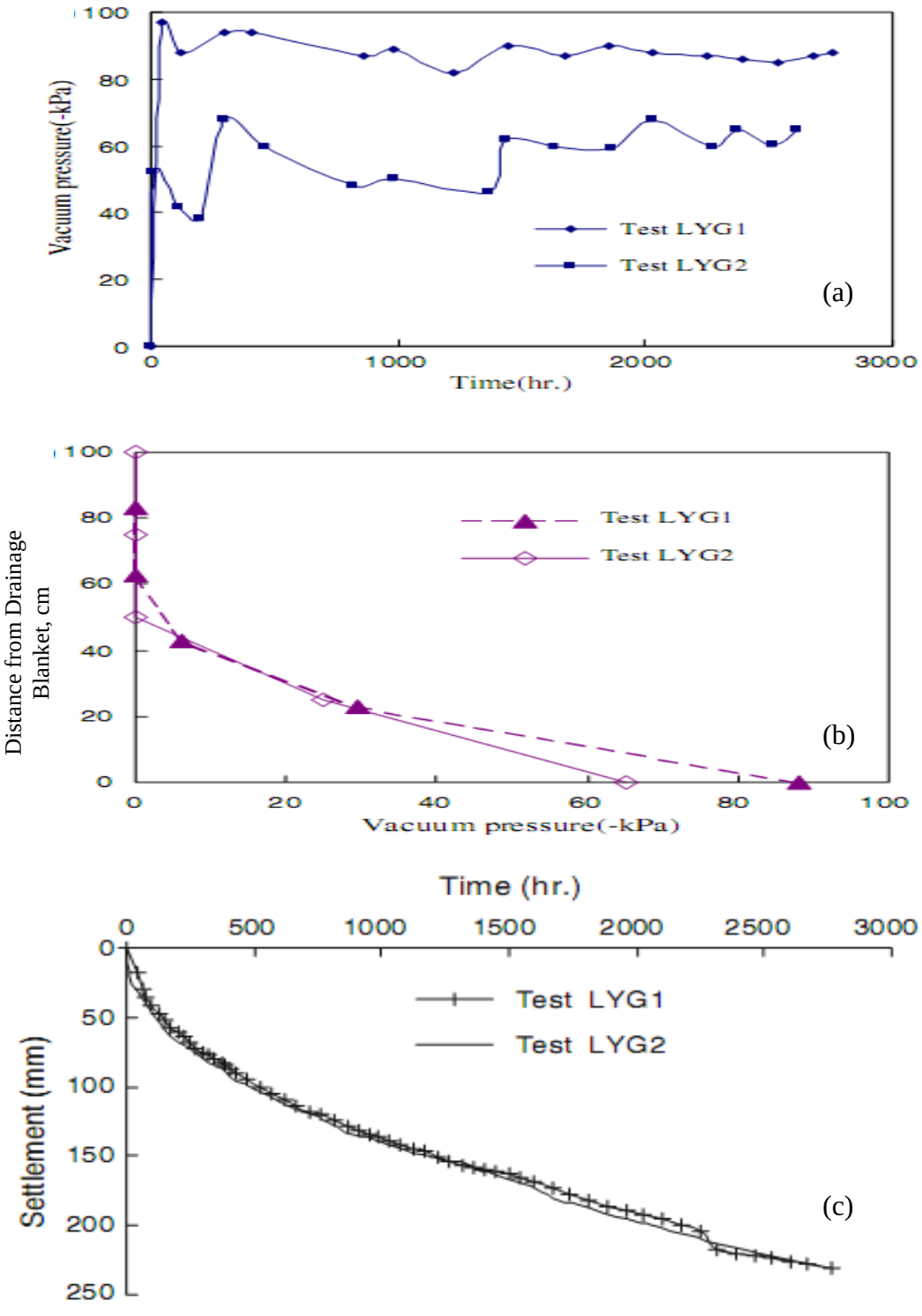

Figure 2.16: (a) Vacuum pressure in drainage layer, (b) distribution of vacuum pressure after 113 days, and (c) settlement with time (after Li et al. 2009)

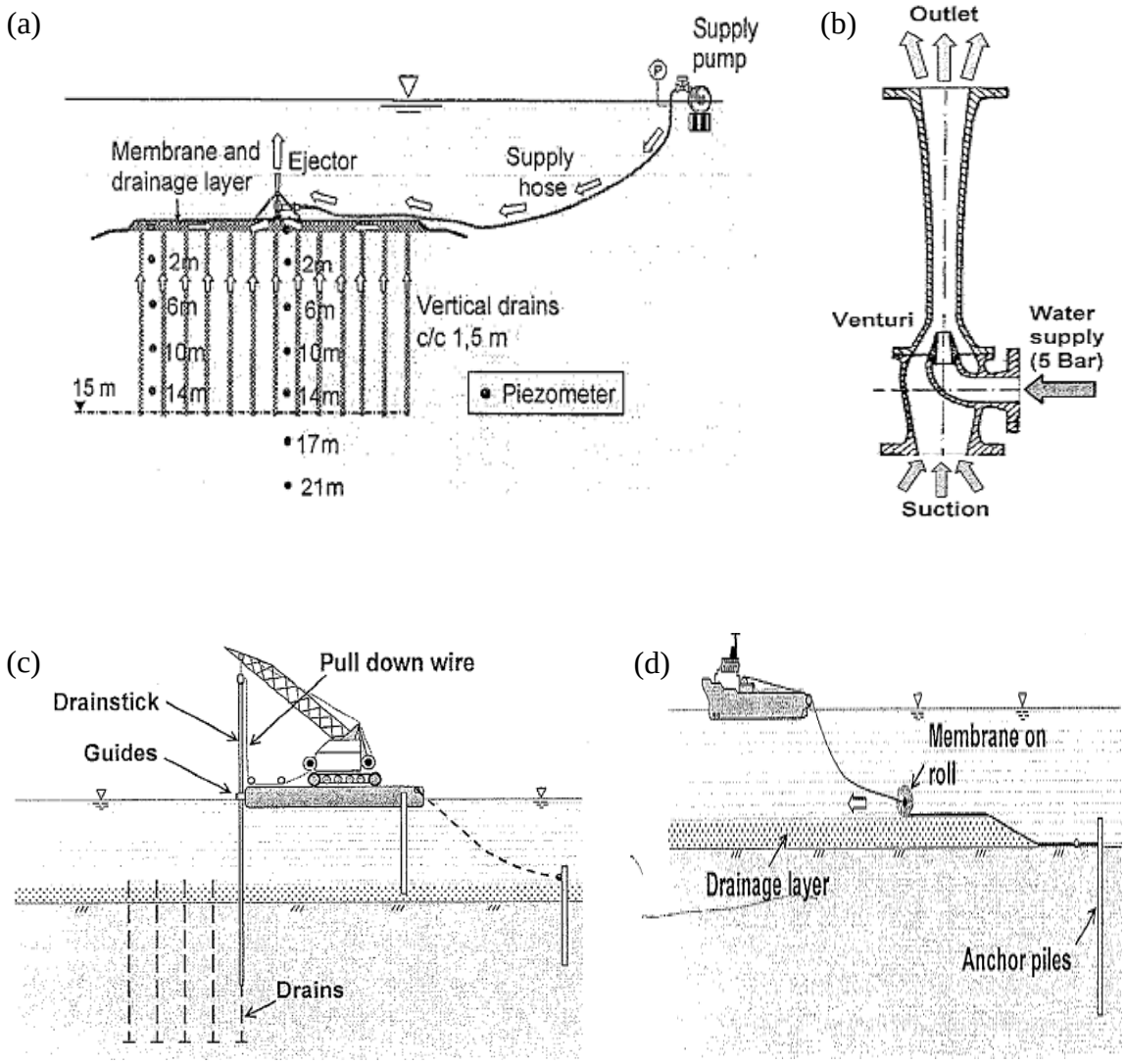

Figure 2.17: (a) Layout of under-water vacuum consolidation system, (b) connector used to connect drainage layer with vacuum pump, (c) PVD Installation, and (d) underwater installation of membrane (after Karlsrud et al. 2007)

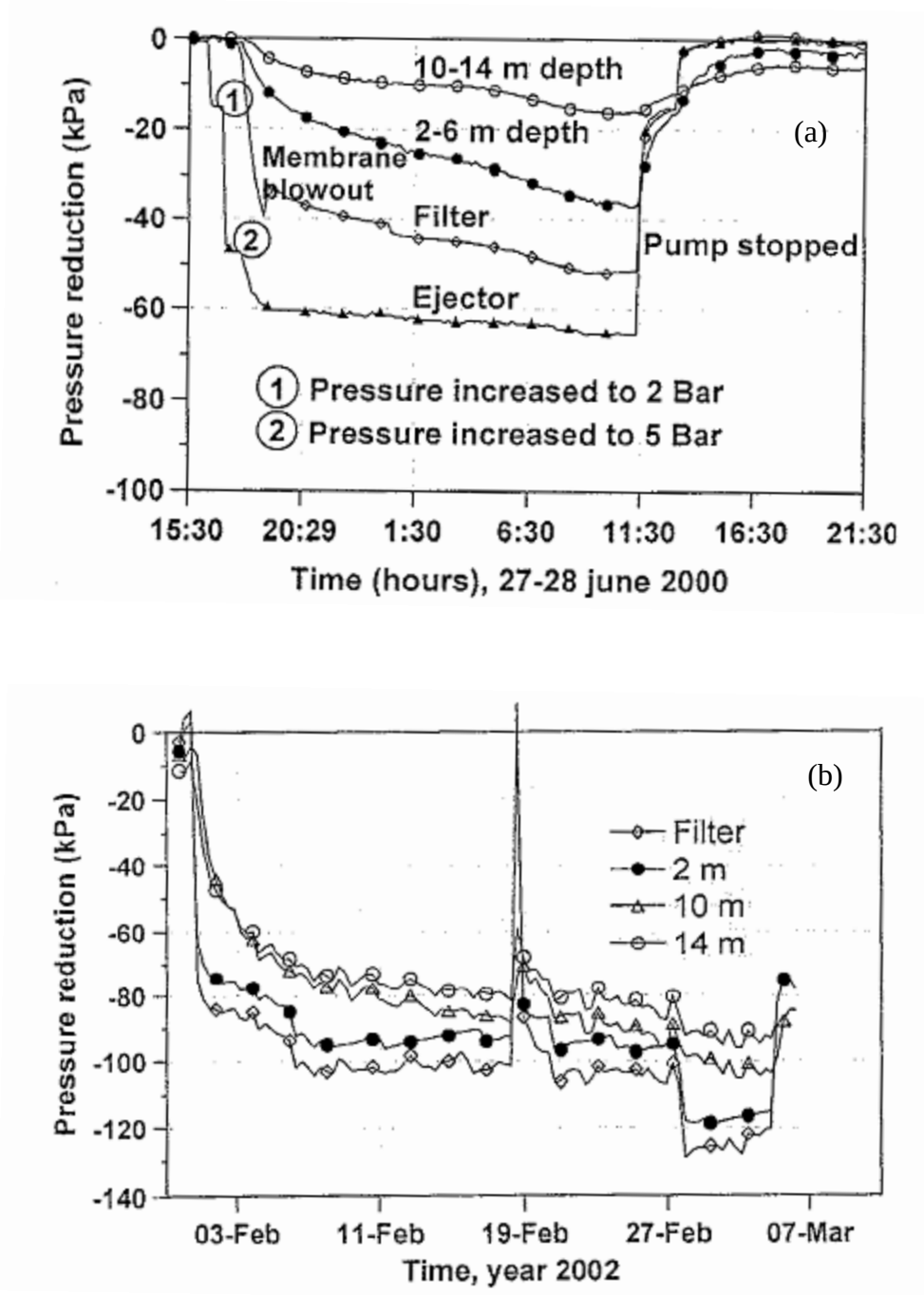

Figure 2.18: Reduction in porewater pressure (a) during first application, and (b) after extending sealing membrane and increasing pump capacity (after Karlsrud et al. 2007)

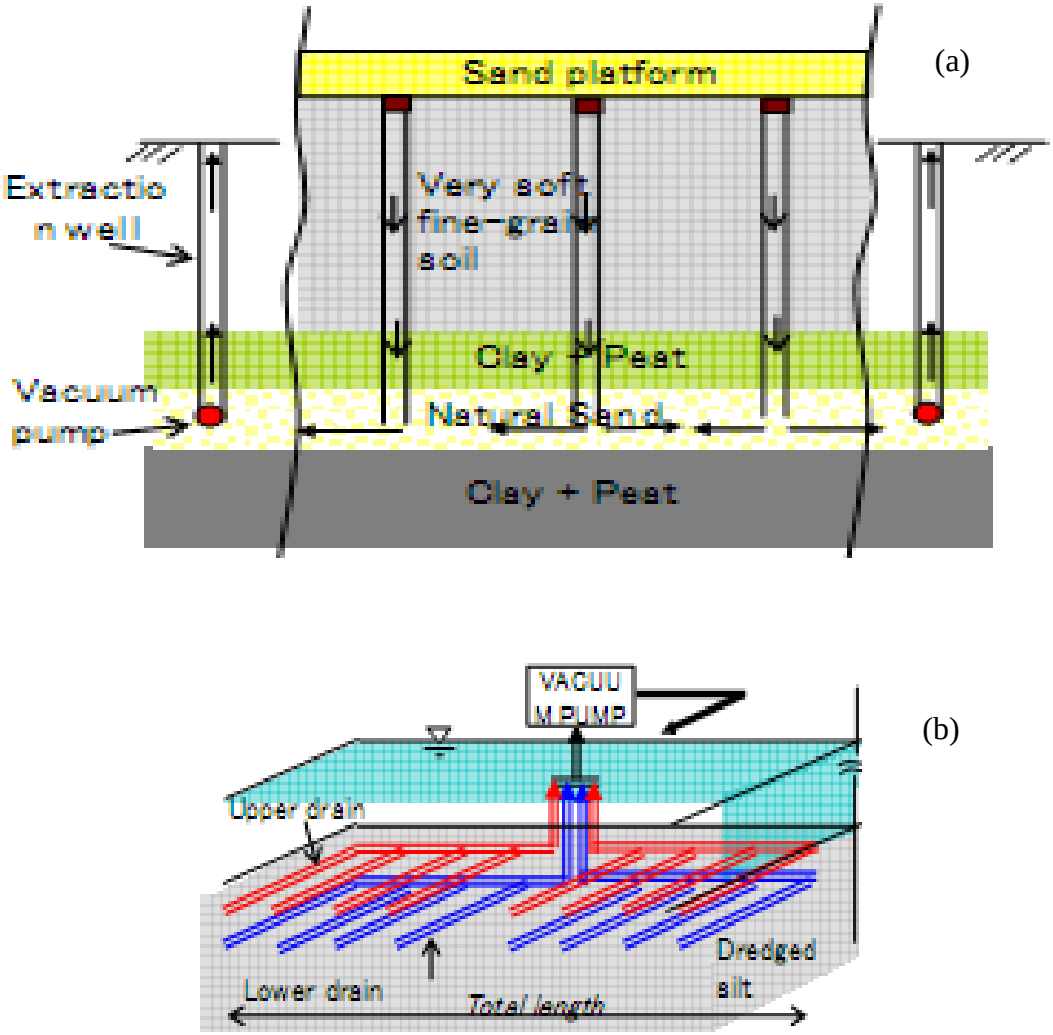

Figure 2.19: SILT NV methods for (a) application of vacuum using bottom sand as a drainage layer and (b) horizontal drain method (after Dam et al. 2006)

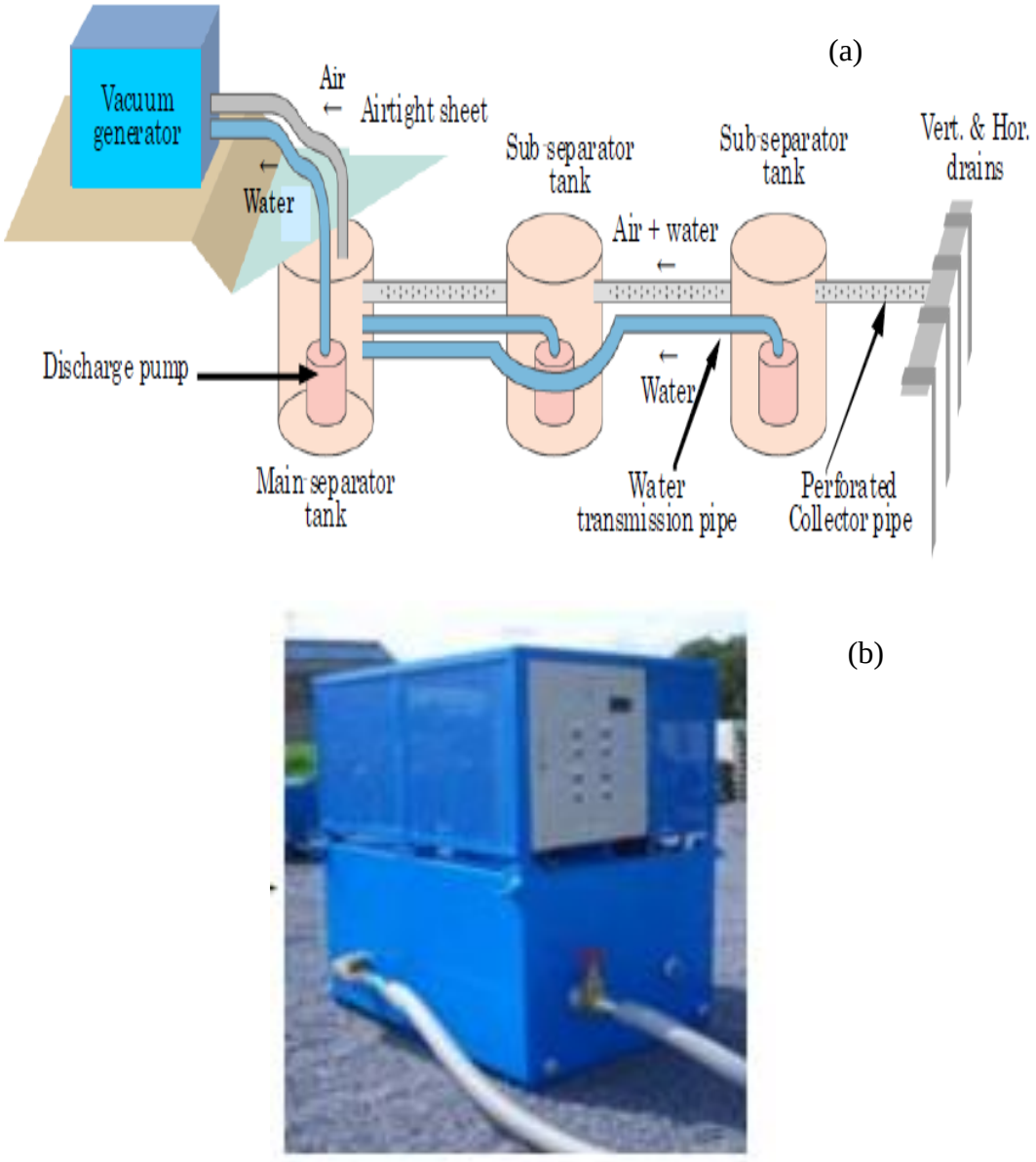

Figure 2.20: (a) Layout of Air-Water separation system for vacuum consolidation, and (b) pumping unit (after Dam et al. 2006)

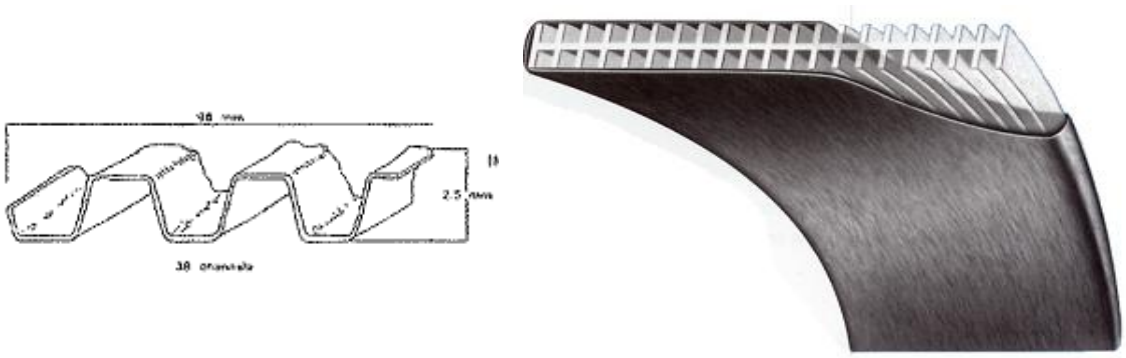

Mebra Drain

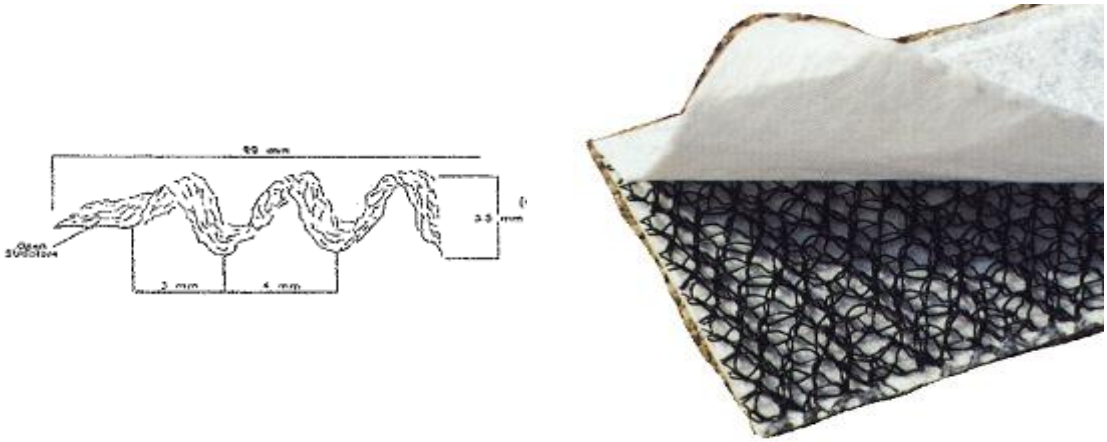

Colbond Drain

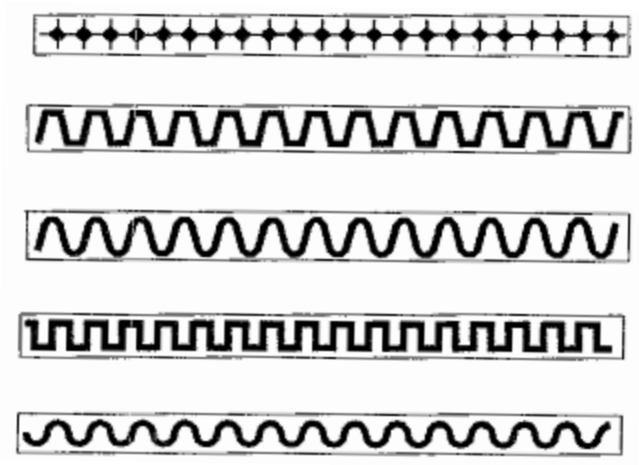

Figure 2.21: Typical sections of PVDs (after Bo et al. 2003)

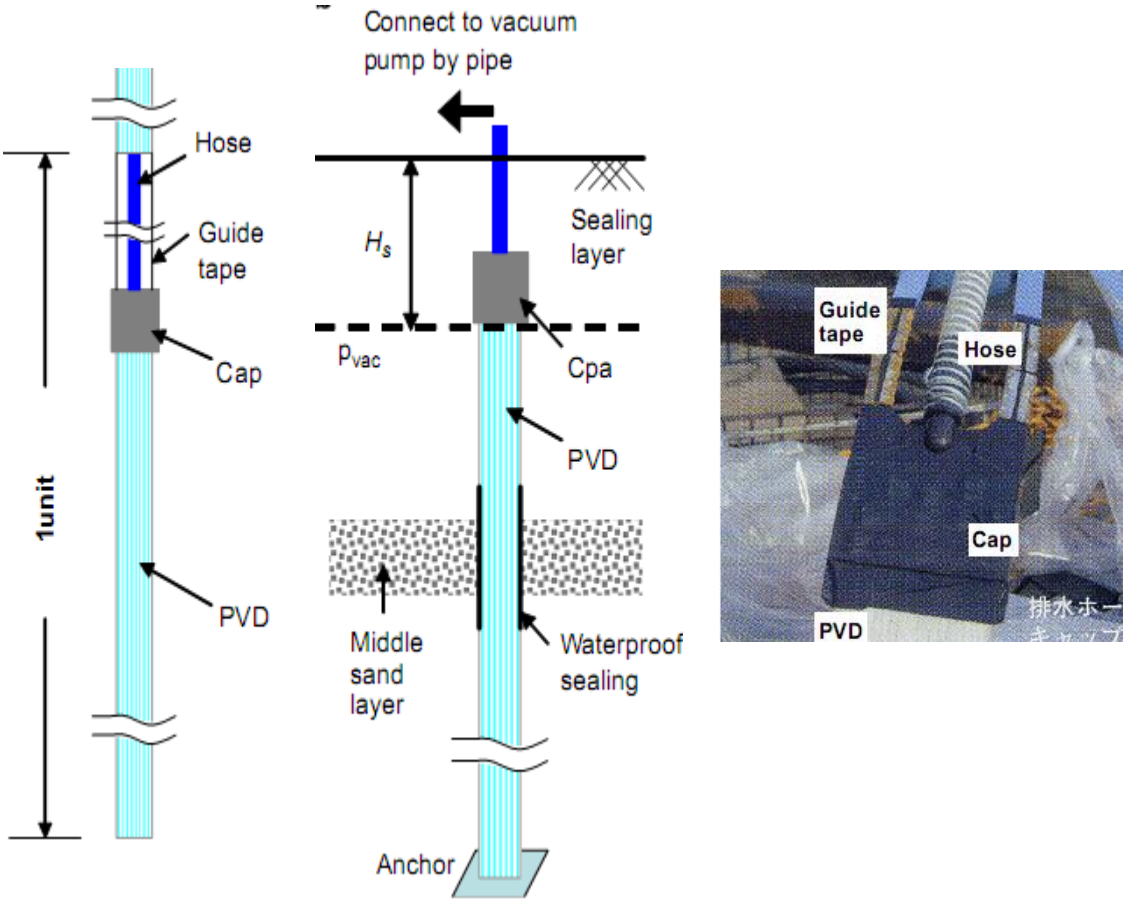

Figure 2.22: Structure of a CPVD (after Chai et al. 2008)

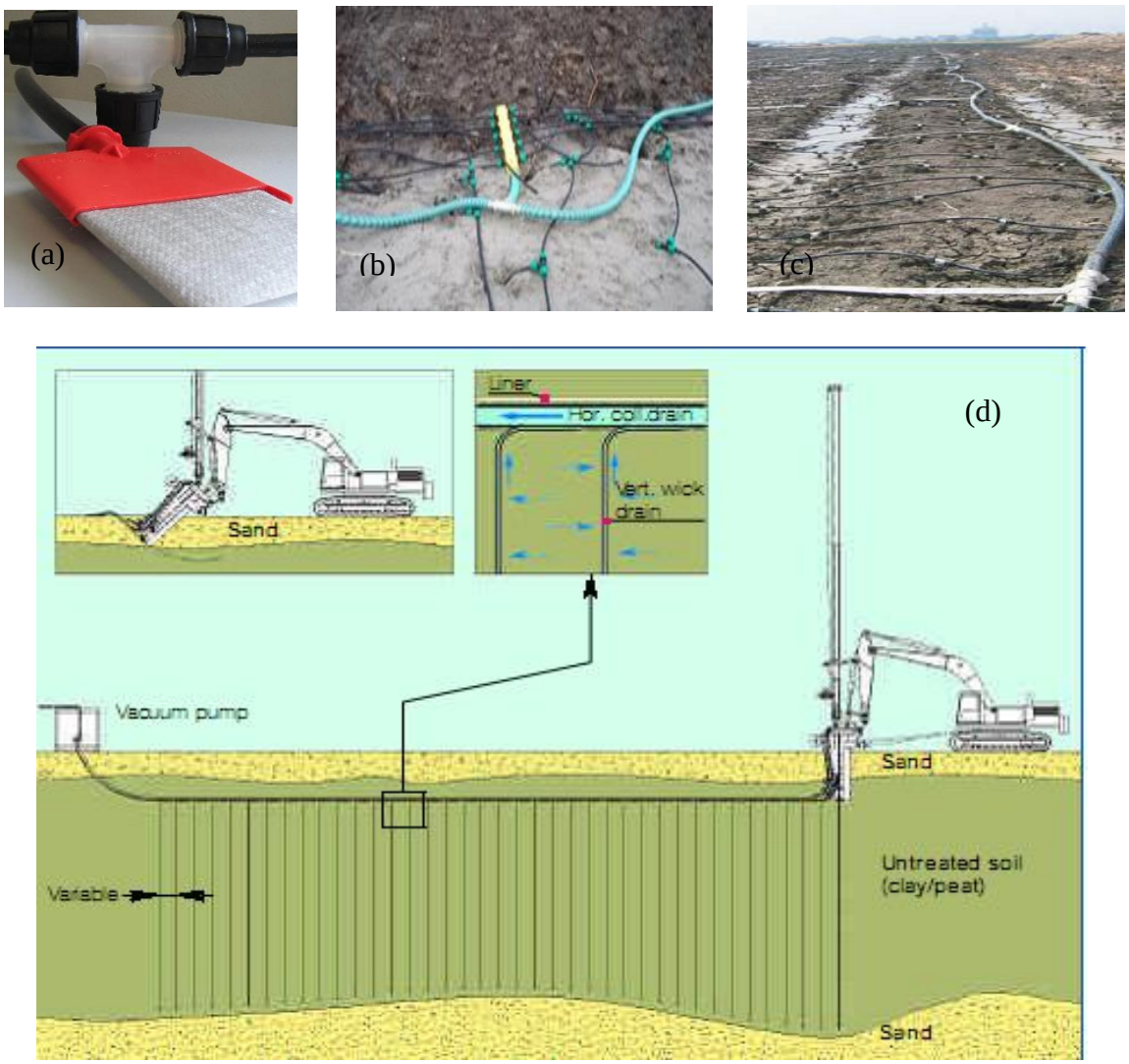

Figure 2.23: (a) CPVD and connector, (b) & (c) connection between individual CPVD and main vacuum line, and (d) layout of a completed system (www.cofrabv.com)

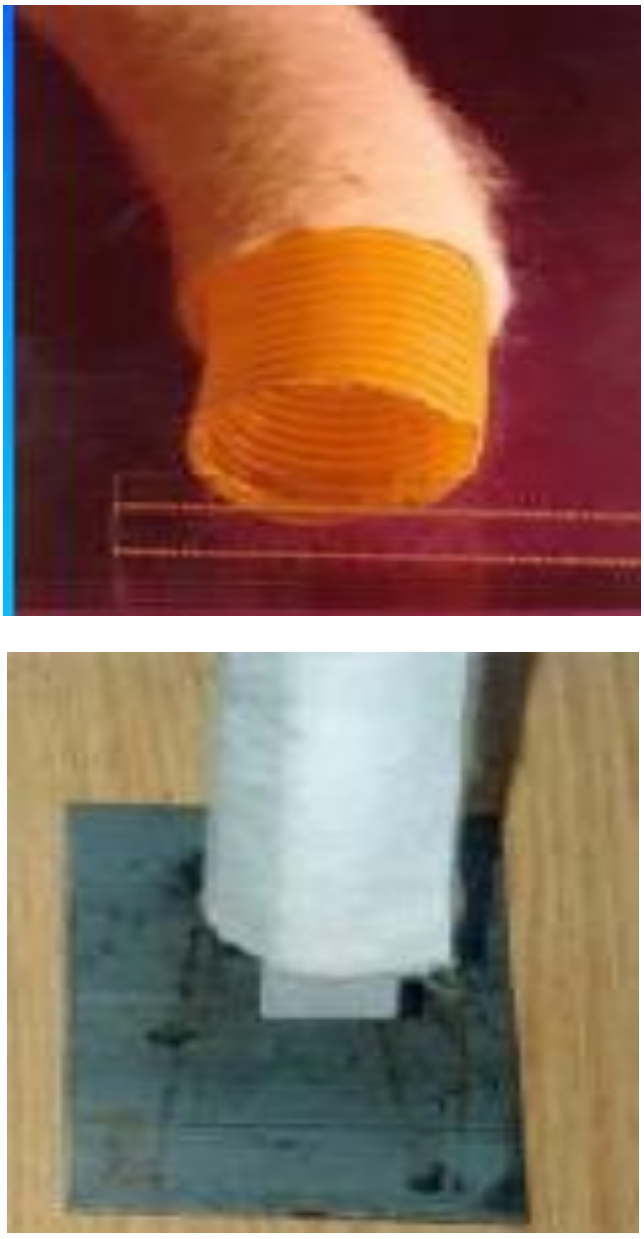

Figure 2.24: Section of VTP and anchoring arrangement (Varaksin undated)

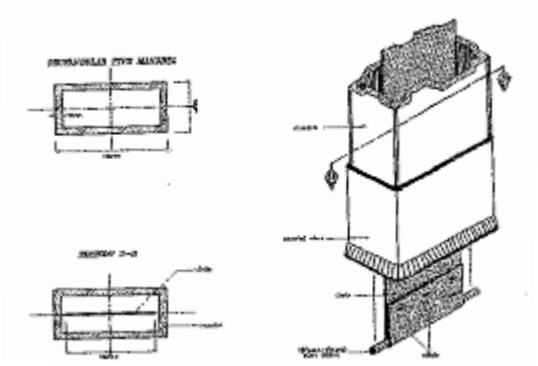

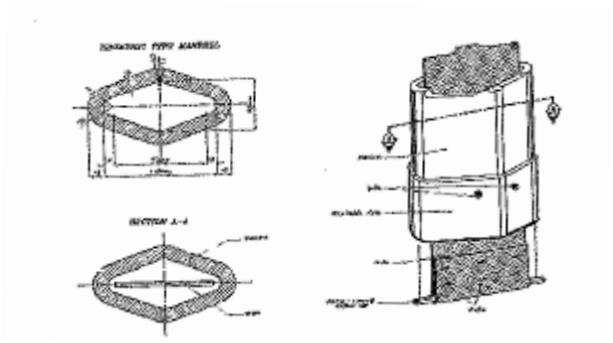

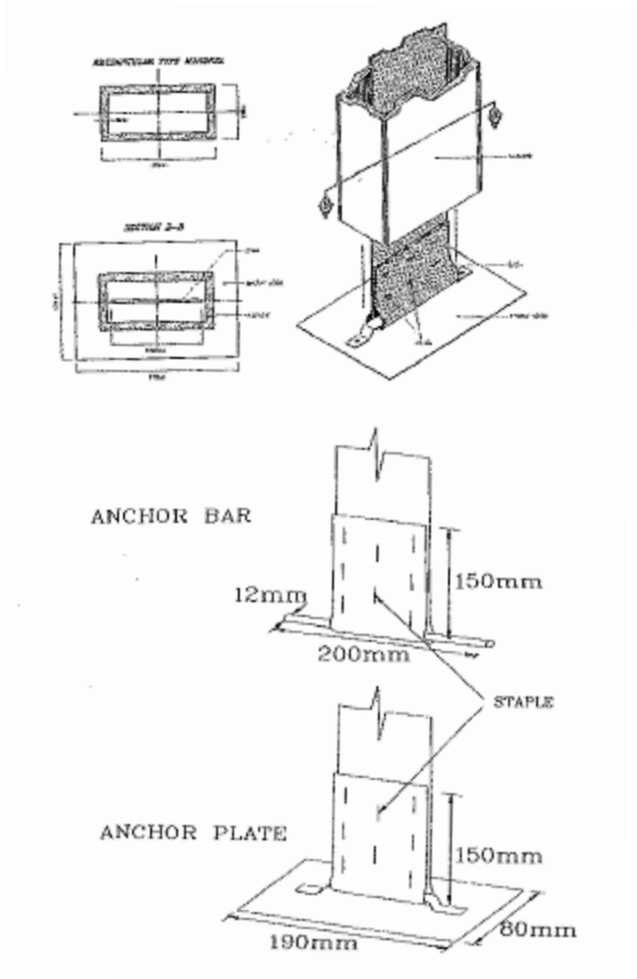

Figure 2.25: Different types of mandrels and anchors with connection details (after Bo et al. 2003) and installation of PVDs

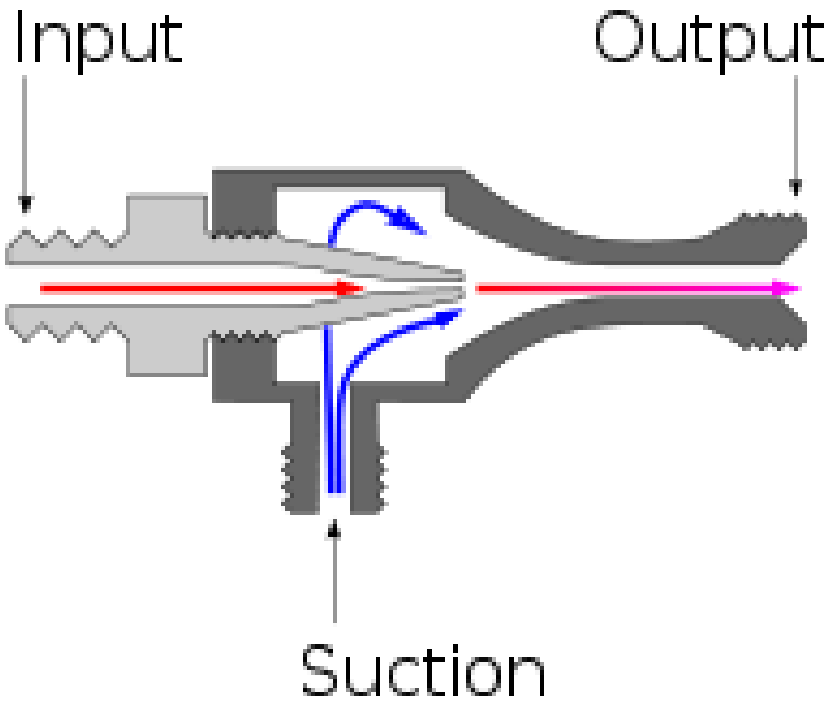

Figure 2.26: Schematic diagram of a jet type of pump (www.wikepedia.com)

Figure 2.27: Typical sections of horizontal drains used in vacuum consolidation (after Indraratna et al. 2008) and Installation technique (Varaksin 2009)

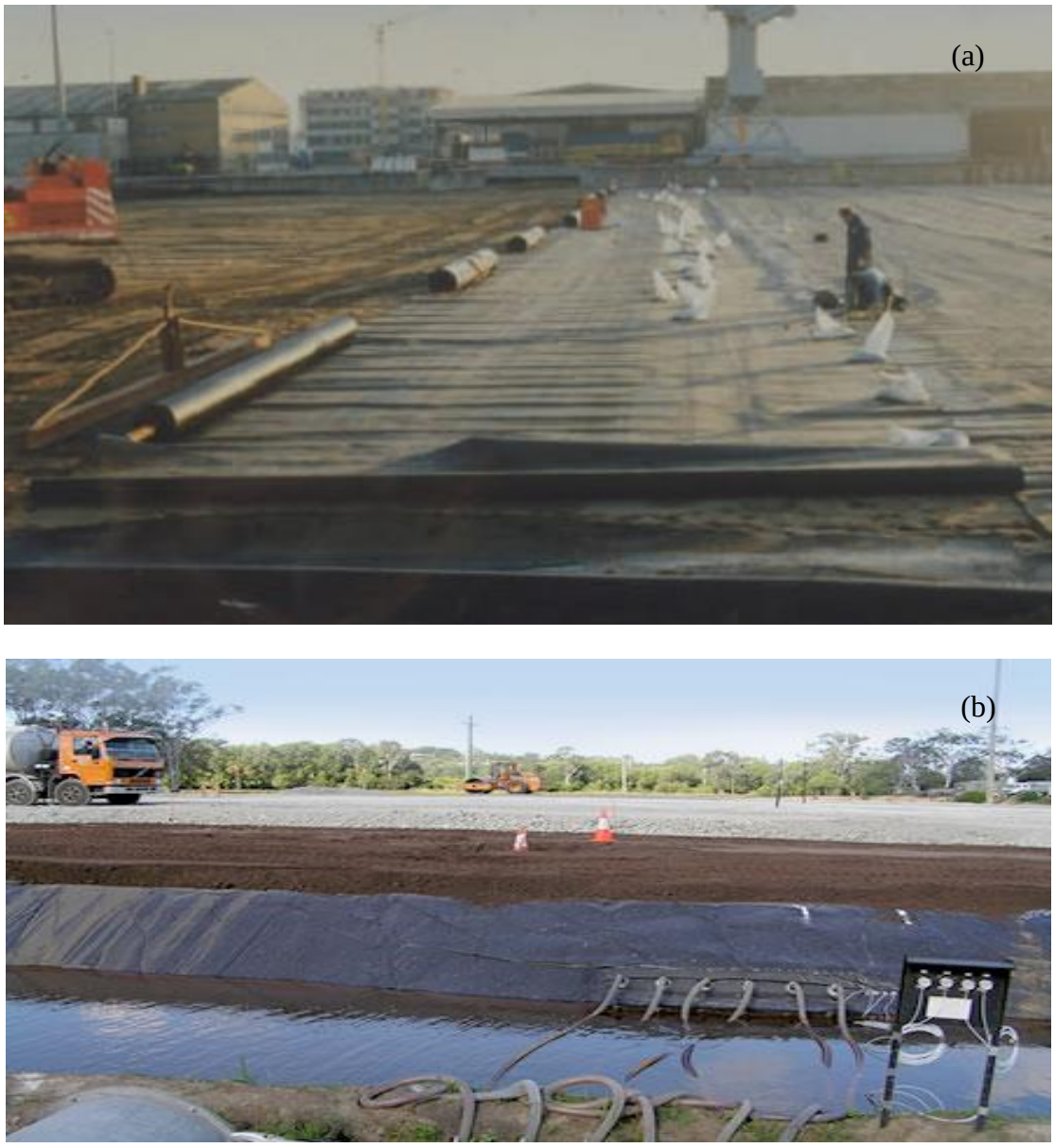

Figure 2.28: (a) Installation of vertical drains and (b) connection through membrane (after Varaksin 2009)

CHAPTER 3. METHOD FOR ANALYSIS OF VACUUM CONSOLIDATION

3.1 Introduction

Data on surface and subsurface settlements, porewater pressures, and lateral displacements, with depth and with time, and data on undrained shear strength before and after the preloading have been collected from 41 different case histories and 9 laboratory studies of vacuum or vacuum-fill preloading of soft soils as shown in Tables 3.1 to 3.3. Unfortunately, in only limited number of cases the reported data are sufficient to carry out settlement analysis, interpret porewater pressures and draw meaningful conclusions.

Data on surface and subsurface settlements and porewater pressures have been analyzed using computer program ILLICON, whereas, lateral displacements and shear strength data collected from different case histories are analyzed empirically. The methods used for settlement analysis, interpretation of porewater pressures, lateral displacements and undrained shear strength are discussed in this chapter.

3.2 Settlement Analysis and Porewater Pressure Interpretation

An review of case histories of vacuum preloading of soft ground indicates that (1) vacuum is always used together with vertical drains which are terminated short of the bottom drainage boundary, (2) vacuum and vacuum-fill preloading has been applied successfully to different types of soil including recent hydraulic fills, silt and clay deposits and waste sludge deposits from mine tailings etc., (3) typically, it takes 5 to 15 days for vacuum to fully develop to the applied intensity in the drainage system, including drainage blanket and vertical drains, and (4) there may be interruptions during application of vacuum in the field due to power failure etc. All these factors are important and should be considered for the analysis and interpretation of settlement and porewater

pressure response due to vacuum or vacuum-fill preloading. Therefore, any software used to analyze the vacuum or vacuum-fill preloading should be able to realistically model all the above conditions. The computer program ILLICON, developed at the University of Illinois at Urbana-Champaign (Mesri et al. 1988, 1994) can incorporate all the above conditions and, therefore, has been used to analyze case histories of vacuum and vacuum-fill preloading. In the following sections, the computer program ILLICON is briefly introduced:

3.3 The ILLICON Methodology

Mesri and Rokshar (1974) proposed the ILLICON theory of consolidation which takes into account the changes in compressibility and permeability of soil during the progress of consolidation by accounting for a bilinear EOP$e - log\sigma'_v$ relation with a preconsolidation pressure, and a reduction in permeability with reduction in void ratio in terms of $e - logk_v$ relationship. Subsequently, the ILLICON theory was revised to include any shape of EOP$e - log\sigma'_v$ relation, and a computer program was developed to carry out the settlement analysis and to back-analyze observed behavior of soft clay and silt deposits subjected to fill load (Mesri and Choi 1985; Choi 1982). The computer program ILLICON was further modified to include multi layer soil profile and to accommodate fully and partially penetrating vertical drains (Mesri and Lo 1987; Lo 1991). The development of computer program is covered in detail by Lo (1991); however, the key features of the program especially useful for analysis of case histories including vacuum as a preload include:

- The program can handle up to 15 layers, each having its own distinct properties including initial void ratio, initial effective vertical stress, preconsolidation pressure, $e - log\sigma'_v$ and $e - logk_v$ relations, and secondary compression index.
- Time-dependent increase and decrease in load to simulate actual loading schedule in the field can be modeled. Additionally, the program can accommodate any assumption on distribution (including elastic stress distribution) of applied load with depth and with time. This is a very significant feature as it allows to account for any leakage or stoppage in

applied vacuum and its subsequent reapplication after a certain period of time.

- The program can handle fully as well as partially penetrating vertical drains and accounts for flow in both vertical and horizontal direction within the soil when vertical drains are used. This is useful as the vertical drains used together with vacuum preloading are terminated short of the bottom drainage boundary (assuming the vacuum to be applied from the top).

The input parameters required to run computer program ILLICON are:

3.3.1 Soil Parameters

Unlike other procedures in which limited input parameters are used, ILLICON methodology requires more elaborate definition of soil parameters as an input for the analysis. The required input parameters for each layer include sublayer thickness, insitu void ratio (e_o), initial effective vertical stress (σ'_{vo}), preconsolidation pressure (σ'_p), ratio of horizontal to vertical permeability (k_h/k_v), EOP*e – log σ'$_v$* and *e – log k$_v$* relations C_r/C_c and C_α/C_c. In the present study, these parameters were either directly obtained from the reported literature for the particular case history or were computed using reported data and existing empirical correlations. For example, the compressibility characteristics were usually not reported in the literature; however, the EOP*e – log σ'$_v$* relation for any sublayer was constructed by using compression index (C_c) estimated from the insitu water content (Terzaghi et al. 1996), preconsolidation pressure estimated from undrained field vane strength, and initial and final values of effective vertical stresses. The procedure for estimating different input parameters for ILLICON analysis are discussed in detail in Chapters 4 to 8. Data on C_c and w_o used in this study in comparison to that reported by Terzaghi et al. (1996) is shown in Fig. 3.1.

3.3.2 Loading Schedule

The actual loading schedule followed in the field can be incorporated in the program by defining the increase in effective stress at a given time. The current version of ILLICON can accommodate up to 19 times on the load-time curve. It is important to note that a separate load-time relation for each sublayer is required as an input. This feature of the program enables the user to incorporate any loading condition into the

analysis which is specific to one sublayer but not relevant to other sublayers. For example, if one of the sublayers, at an intermediate depth, had some excess porewater pressures before the commencement of preloading, then an additional load ($\Delta\sigma'_v$) can be dded at time t = 0, for that particular sublayer.

3.3.3 Other Input Parameters

Other input parameters which should be clearly defined for the settlement analysis include:

- Number of sublayers considered in the analysis.
- Number of layers penetrated by vertical drains. This may be equal to or less than the number of sublayers considered in the analysis.
- Radius and permeability of vertical drains. Radius is defined in meters whereas permeability is in cm/s.
- Time for installation of vertical drains with reference to start of preloading operation, defined in days.
- Radius of influence (in meters) of vertical drains which depends upon the drain spacing and layout pattern.
- Radius of smear zone (in meters).
- Number of columns within the influence zone of vertical drains and number of columns within the smear zone. The program divides the soil column being analyzed into the desired number of sub-columns and calculates the porewater pressure at each node. Thus, the horizontal distribution of porewater pressure at a particular depth can be predicted using this feature of the program.
- Drainage boundary conditions, i.e. , freely draining or impermeable must be defined for top and bottom boundaries.
- Limit of consolidation. This is the degree of consolidation defined in percentage of primary consolidation.

3.3.4 Input and Output File Structure for Computer Program ILLICON

The current version of computer program ILLICON is a DOS based application coded using FORTRAN-77. The input to the computer program is generated by using a notepad file. The input parameters should be arranged in a specific sequence as shown in Appendix A. The input file and the executable file (program file) must be located in the same folder for the program to be executed correctly.

The desired name for output files, upper and lower limits for time increment factor and time limit for which program should be running are input into the executable file. The program stops automatically after reaching the desired degree of consolidation or time limit whichever is reached earlier.

The program generates an elaborate output by creating following notepad files:

- Output. DAT. A summary of input data is contained in this file.
- Output.CNS. This file contains information on degree of consolidation achieved at different times.
- Output.DEF. Vertical profile of settlement at different times or subsurface settlement with time at different depths can be generated using data contained in this file.
- Output.MTX. This file contains the computed results on porewater pressure, effective stress and void ratio at different times and at different depths. Porewater pressure at different depth and at different times can be generated using data from this file.
- Output.Set. This file contains the surface settlements computed at different times. The data are used to predict time rate of settlement under the defined loading schedule.

3.4 Lateral Displacements and Increase in Undrained Shear Strength

All available data on lateral displacements and undrained shear strength are examined empirically, as discussed in Chapter 9.

3.5 Stability Analysis

Stability analysis is required as a part of preloading design to safeguard against excessive deformations or a bearing capacity failure. In the present study, computer program XSTABL has been used to carryout the stability analysis during various stages of preloading.

Table 3.1: Case histories of vacuum consolidation

S.No.	Case History	Thickness of soft Layer (m)	Type of Load	Vertical Drains	Reference
1	Soil improvement for road leading to Container Terminal, China	20	Vacuum	PVDs	Yan and Chu (2003), Chu and Yan (2005)
2	Improvement of foundation soil for construction of Storage yard, China	20	Vacuum-fill	PVDs	Yan and Chu (2005), Rujiakiatkamjorn et al. (2007)
3	Field trial of vacuum preloading for soil improvement works at 2nd Bangkok International Airport, Thailand	15	Vacuum	Sand Drains	Woo et al. (1989)
4	Field trial for evaluating performance of PVDs for soil improvement works at 2nd Bangkok International Airport, Thailand	12	Fill	PVDs	Bergado et al. (1997 and 2002)
5	Field trial of vacuum-fill preloading for soil improvement works at 2nd Bangkok International Airport, Thailand	12	Vacuum-fill	PVDs	Bergado et al. (1997)
6	Improvement of Bangkok Clay using Capped prefabricated vertical drains, Bangkok, Thailand	10	Vacuum-fill	CPVDs	Zewart et al. (undated); Saowapakpiboon et al. (2008)
7	Soil improvement for road construction in Saga, Japan	10 – 12	Vacuum	PVDs	Chai et al. (2006)
8	Soil improvement works for development of East Pier Project, Port of Tianjin, China	16 – 25	Vacuum, vacuum-fill	PVDs	Choa (1989, 1990), Yixiong (1996b), Shang et al. (1998)
9	Improvement of foundation soils for embankment construction at Ballina Bypass, Australia	1 -25	Vacuum-fill, Fill	VTPs	Kelly et al. (2008), Kelly and Wong (2009), Indraratna et al. (2009)
10	Improvement of foundation soils for an oil storage station, China	20	Vacuum	PVDs	Chu et al. (2000)
11	Soil improvement for highway construction at Ambes - France	4 - 5	Vacuum-fill	PVDs	Cognon et al. (1994)
12	Soil improvement for construction of A-837 toll way – France	8 - 22	Vacuum – fill	PVDs	Spaulding and Porbaha (2004)
13	Soil improvement for construction of Sewage treatment plant at Kimhae, South Korea	Up to 40	Vacuum – fill	VTPs	Masse et al. (2001), Ihm and Masse (2002)
14	Soil improvement at Port of Brisbane – Australia	32	Vacuum-fill	VTPs	Berthier et al. (2009)

Table 3.1 (continued)

S.No.	Case History	Thickness of soft Layer (m)	Type of Load	Vertical Drains	Reference
15	Improvement of foundation soils for construction of Camau power plant - Vietnam	17	Vacuum-fill	-	Varaksin and Herve (2008)
16	Soil improvement for runway construction at Yaoqiang airport, China	12	Vacuum	PVDs	Tang and Shang (2000)
17	Improvement of high permeability soils - Port of Huanghua, China	22			
18	Pier construction at Nansha terminal, Guangzhou port - China	22	Vacuum	PVDs	Qiu et al. (2007)
19	Construction of Sea embankment, China	22	Vacuum-fill	PVDS	Liu et al. (2004)
20	Embankment construction for Highway, China	20	Vacuum-fill	PVDS	Mahfouz et al. (2007)
21	Soil improvement for construction of Zhuhai Power Station China	19	Vacuum-Fill	PVDs	Yixiong (1996b)
22	Improvement of Sea bed clay - NGI	15	Vacuum-water	PVDs	Karlsrud et al. (2007)
23	Under water vacuum consolidation of dredged silt, Belgium	6.5	Vacuum-water	PVDs (Horizontal)	Mieghem et al. (1999); Impe et al. (2001)
24	Improvement of reclaimed land using horizontal drains, Japan	3.5	Vacuum	PVDs (Horizontal)	Shinsha et al. (1991)
25	Improvement of waste sludge (soda ash) using horizontal drains, Japan	6	Vacuum	PVDs (Horizontal)	Shinsha et al. (1991)
26	Improvement of soda ash tailings, China	8	Vacuum	PVDs	Shang and Zhang (1999)
27	Soil improvement for road construction in Yamaguchi, Japan	28	Vacuum	CPVDs	Chai et al. (2008)
28	Improvement of oft soil near river bank at Kuching, Malaysia	20 – 30	Vacuum	VTPs	Yee and Wee (2001); Yee et al. (2004)
29	Soil improvement for sewage treatment plant at Jangyu, South Korea	Up to 40	Vacuum-fill	PVDs	Masse et al. (2001); Song and Kim (2004)

Table 3.1 (continued)

S.No.	Case History	Thickness of soft Layer (m)	Type of Load	Vertical Drains	Reference
30	Soil improvement for highway construction, Thailand	20 – 25	Vacuum-fill	VTPs	Yee et al. (2002)
31	Improvement of foundation soil Nanjing oil and petroleum Wharf – I, China	26	Vacuum-fill	PVDs	Yixiong (1996b)
32	Improvement of foundation soil Nanjing oil and petroleum Wharf – II, China	20	Vacuum	PVDs	Yixiong (1996b)
33	Soil improvement for sewage disposal plant at Guangzhou, China	18	Vacuum, Vacuum-fill	PVDs	Yixiong (1996b)
34	Hazama test embankment, Japan	27	Vacuum?	PVDs	Mutsomoto et al. (1998), Dam et al. (2007)
35	Sanrikuota test embankment, Japan	13	Vacuum-fill	PVDs	Dam et al. (2007)
36	Improvement of peat ground in Japan	20	Vacuum-fill	PVDs	Hayashi et al. (2004)
37	Field trial for ground improvement at Xingang port, China	23	Vacuum, fill	Packed sand drains	Ye et al. (1983)
38	Improvement of sludge using sand layer at bottom as drainage layer	10 - 12	Vacuum-fill	Sand drains	Mieghem et al. (1999)
39	Field trials of vacuum preloading, Korea	10	Vacuum	PVDs	Kim et al. (2009)
40	Field trials of vacuum preloading using CPVDs, Japan	14/13	Vacuum-fill, vacuum	CPVDs	Yoneya et al. (2003)
41	Embnakment construction Ning-Jing-Yan Expressway, Chia	40	Vacuum-fill	PVDs	Wang and Law (2007)

Table 3.2: Type of available field data from case histories of vacuum consolidation

S. No	Case History	Soil Properties				Loading		Measurements							
								Settlement		Porewater Pressure		Lateral Displacements		Shear Strength	
		Profile	Index Properties	Compressibility	Permeability	Load	Time	With Depth	With Time	With Depth	With Time	With Depth	With Time	Before	After
1	Soil improvement for road leading to Container Terminal, China	X	X	-	-	X	X	X	X	X	X	X	X	X	X
2	Improvement of foundation soil for construction of Storage yard, China	X	X	X	X	X	X	X	X	X	X	X	X	X	X
3	Field trial of vacuum preloading for soil improvement works at 2nd Bangkok International Airport, Thailand	X	X	-	-	X	X	X	X	-	-	-	-	-	-
4	Field trial for evaluating performance of PVDs for soil improvement works at 2nd Bangkok International Airport, Thailand	X	X	X	-	X	X	X	X	X	X	X	X	X	X
5	Field trial of vacuum-fill preloading for soil improvement works at 2nd Bangkok International Airport, Thailand	X	X	-	-	X	X	X	X	X	X	-	-	-	-
6	Improvement of Bangkok Clay using Capped prefabricated vertical drains, Bangkok, Thailand	X	X	X	-	X	X	-	X	-	-	-	-	-	-
7	Soil improvement for road construction in Saga, Japan	X	X	X	X	X	X	X	X	X	X	X	X	X	-

X ; Data reported; X? : Reported data is not specific, only a range is reported; - : Data not reported

Table 3.2 (continued)

S. No	Case History	Soil Properties				Loading		Measurements							
								Settlement		Porewater Pressure		Lateral Displacements		Shear Strength	
		Profile	Index Properties	Compressibility	Permeability	Load	Time	With Depth	With Time	With Depth	With Time	With Depth	With Time	Before	After
8	Soil improvement works for development of East Pier Project, Port of Tianjin, China	X	X	-	-	X	X	-	X	X	X	X	-	X	X
9	Improvement of foundation soils for embankment construction at Ballina Bypass, Australia	X	X	X	X	X	X	-	X	-	X	X	X	X	-
10	Improvement of foundation soils for an oil storage station, China	X	X	-	-	X	-	X	X	X	X	X	X	X	X
11	Soil improvement for highway construction at Ambes -France	X	X	X	-	X	-	-	X	X	X	-	-	-	-
12	Soil improvement for construction of A-837 toll way – France	-	X	X	-	X?	X?	X	X	X	X	-	-	X	-
13	Soil improvement for construction of Sewage treatment plant at Kimhae, South Korea	X	X	X	-	X?	X?	-	X	-	-	-	-	X	-
14	Soil improvement at Port of Brisbane – Australia	-	X	-	-	X?	X?	-	-	-	-	-	-	X	-
15	Improvement of foundation soils for construction of Camau power plant - Vietnam	-	X?	X	-	X?	X?	-	X	-	X	-	-	-	-
16	Soil improvement for runway construction at Yaoqiang airport, China	X	X	-	X	X	X	X?	X?	X	X	X	-	X	X
17	Improvement of high permeability soils - Port of Huanghua, China	X	X	-	-	X	X	X	X	X	X	X	X	X	X

X ; Data reported; X? : Reported data is not specific, only a range is reported; -: Data not reported

Table 3.2 (continued)

S. No	Case History	Soil Properties				Loading		Measurements							
								Settlement		Porewater Pressure		Lateral Displacements		Shear Strength	
		Profile	Index Properties	Compressibility	Permeability	Load	Time	With Depth	With Time	With Depth	With Time	With Depth	With Time	Before	After
18	Pier construction at Nansha terminal, Guangzhou port - China	X	X	X	-	-	-	X	X	X	X	X	X	-	-
19	Construction of Sea embankment, China	X	X	X	X	X	X	-	X	X	X	X	X	-	-
20	Embankment construction for Highway, China	X	X	X	X	X?	X?	-	X?	X?	X?	X?	X?	X?	-
21	Soil improvement for construction of Zhuhai Power Station China	X	X	-	-	X	X	X?	X?	-	-	X	X	X	X
22	Improvement of Sea bed clay - NGI	X	X	X?	X?	X	X	-	X	-	-	-	-	X	-
23	Under water vacuum consolidation of dredged silt, Belgium	X	-	-	-	X	X	-	X	-	-	-	-	-	X
24	Improvement of reclaimed land using horizontal drains, Japan	X	X?	-	-	X	X	-	X	-	-	-	-	-	X
25	Improvement of waste sludge (soda ash) using horizontal drains, Japan	X	X	-	-	X	X	-	X	-	-	-	-	X	X
26	Improvement of soda ash tailings, China	X	X	X	-	X	X	X	X	X	X	X	X	X	X
27	Soil improvement for road construction in Yamaguchi, Japan	X	X	X	X	X?	X?	-	X	X?	X?	X	-	X	X
28	Improvement of oft soil near river bank at Kuching, Malaysia	-	-	X	-	X	X	-	X	-	-	-	-	X	X

X ; Data reported; X? : Reported data is not specific, only a range is reported; - : Data not reported

Table 3.2 (continued)

S. No	Case History	Soil Properties				Loading		Measurements							
								Settlement		Porewater Pressure		Lateral Displacements		Shear Strength	
		Profile	Index Properties	Compressibility	Permeability	Load	Time	With Depth	With Time	With Depth	With Time	With Depth	With Time	Before	After
29	Soil improvement for sewage treatment plant at Jangyu, South Korea	X	-	-	-	X	X	-	X	X	X	X	X	-	-
30	Soil improvement for highway construction, Thailand	X	X	X	X	X	X	-	X	-	-	-	-	X	X
31	Improvement of foundation soil Nanjing oil and petroleum Wharf I, China	X	X	-	-	X	-	-	-	-	-	-	-	X	-
32	Improvement of foundation soil Nanjing oil and petroleum Wharf II, China	X	X	-	-	X?	X?	-	-	-	-	-	-	X	X
33	Soil improvement for sewage disposal plant at Guangzhou, China	X	X	-	-	X	X?	X?	-	-	-	-	-	X	X
34	Hazama test embankment, Japan	X	X	X	-	-	-	-	X	X	X	-	X	X	X
35	Sanrikuota test embankment, Japan	X	X	X	-	X	-	X	-	-	-	X	-	-	-

X ; Data reported; X? : Reported data is not specific, only a range is reported; - : Data not reported

Table 3.2 (continued)

S. No	Case History	Soil Properties				Loading		Measurements							
								Settlement		Porewater Pressure		Lateral Displacements		Shear Strength	
		Profile	Index Properties	Compressibility	Permeability	Load	Time	With Depth	With Time	With Depth	With Time	With Depth	With Time	Before	After
36	Improvement of peat ground in Japan	X	X	X	X	X	X	X	X	X	X	X	X	-	-
37	Field trial for ground improvement at Xingang port, China	X	X	-	-	X	-	-	X	-	-	-	-	X	X
38	Improvement of sludge using bottom sand as drainage layer	X	-	-	-	X?	-	X?	-	-	-	-	-	-	-
39	Field trials of vacuum preloading, Korea	X	-	-	-	X?	X?	X	X	X	X	X	X	-	-
40	Field trials of vacuum preloading using CPVDs, Japan	X	X?	-/X	-	X?	-	-	X	-	X	X	X	X	X
41	Embnakment construction Ning-Jing-Yan Expressway, Chia	X	X	X?	-	X	X	X	X	-	-	X?	X?	X	X

X ; Data reported; X? : Reported data is not specific, only a range is reported; - : Data not reported

Table 3.3: Laboratory studies on vacuum consolidation

S.No	Brief Description	Reference
1	To evaluate use of vacuum for consolidation of soft seabed clay	Harvey (1997)
2	A comparative study on increase in shear strength due to vacuum and fill preloads	Leong et al. (2000)
3	A laboratory study on consolidation behavior of soil subjected to vacuum, fill or combined vacuum-fill preload using standard oedometer	Mohamedelhassan (2002), Mohamedelhassan and Shang (2002)
4	A study of mechanism of vacuum-fill preloading using a specially manufactured triaxial cell	Mahfouz (2005)
5	A study on improvement of soft soil foundations due to vacuum preloading using a large scale oedometer together with PVD	Bamunawita (2004)
6	A study on consolidation behavior of soft clay subjected to vacuum, fill, or combined vacuum-fill preload using a large scale oedometer together with PVD	Rujiakiatkamjorn (2005)
7	A study on consolidation behavior and lateral movements due to vacuum preloading of soft soils under different drainage conditions	Chai et al. (2005a, b and 2009)
8	The study of engineering behavior of Hong Kong marine clay under vacuum preloading using a modified hydraulic cell	Chung (2009)
9	A laboratory study on vacuum consolidation during layered soil reclamation using horizontal PVDs and a geosynthetic drainage blanket	Li et al. (2009)

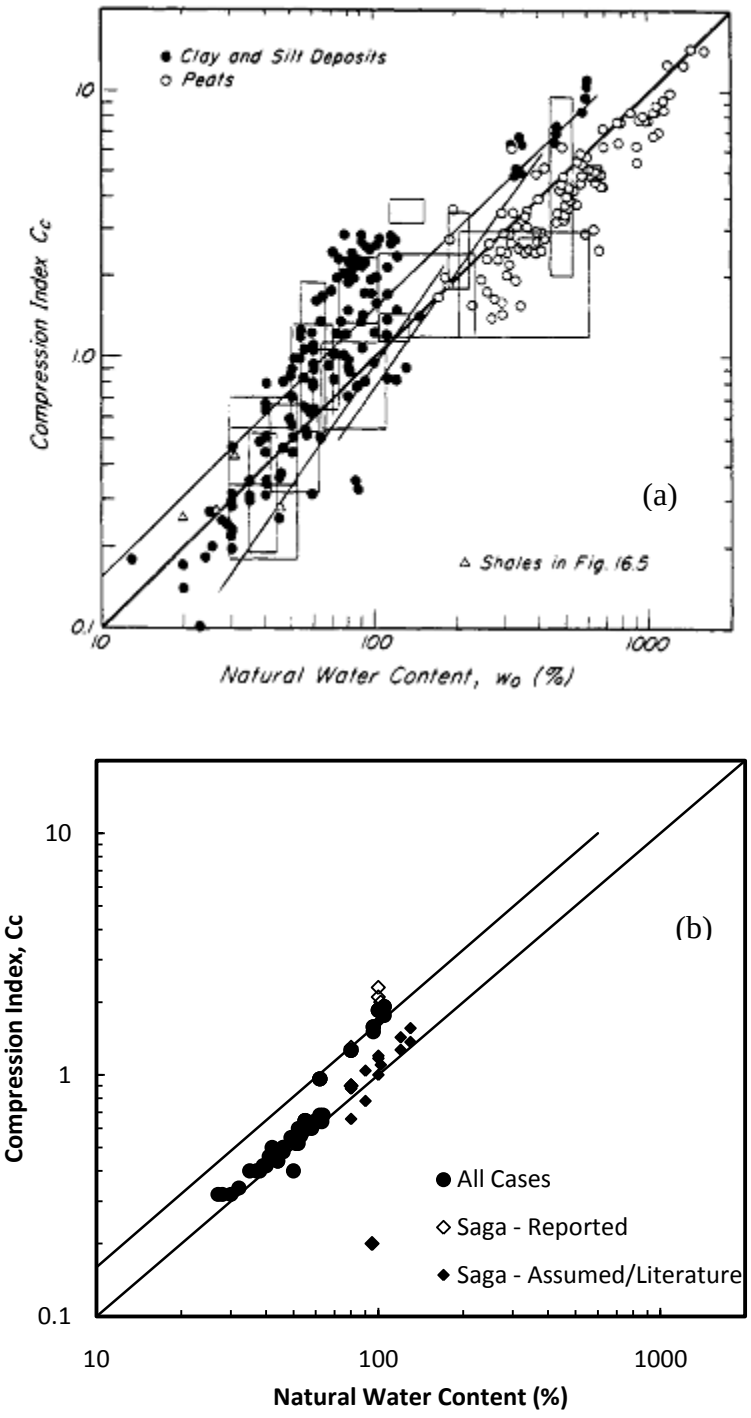

Figure 3.1: Relationship between natural water content and compression index, (a) Terzaghi et al. (1996), and (b) Used in present study

CHAPTER 4. IMPROVEMENT OF SOFT GROUND USING VACUUM PRELOADING TOGETHER WITH VERTICAL WICK DRAINS FOR A ROAD CONSTRUCTION AT TIANJIN PORT IN CHINA

4.1 Introduction

A section of road leading to container terminal at Tianjin port in China was to be constructed on a 20m thick compressible soil deposit. The treatment area was approximately 18600 square meters (51m wide and 365m long) as shown in Fig. 4.1. The top 6m of compressible layer consisted of silty clay consolidated from dredged slurry. Before the commencement of ground treatment both the reclaimed layer and the original seabed clay were undergoing primary consolidation as evidenced by porewater pressure records shown in Fig. 9 of Yan and Chu (2003). The treatment area was subdivided into two sections of approximately equal size. Both sections were treated by applying a nominal vacuum pressure of 80kPa which was maintained throughout the 90 day duration of treatment. The initial settlement (0.58m), after installation of prefabricated vertical drains and before the application of vacuum pressure, was the same in both sections; however, the observed settlements at the end of vacuum preloading operation were significantly different, with section II settling more than section I. Both sections have been analyzed using the computer program ILLICON and the predictions are compared with field observations. The subsurface data for ILLICON analyses have been extracted from Yan and Chu (2003), Chu and Yan (2005) and Chu et al. (2006). Empirical correlations have also been utilized to estimate parameters which were not reported in the literature.

4.2 Subsurface Conditions

The 20m thick compressible ground can be broadly divided into two layers; the reclaimed layer and the original seabed clay. The 6m thick reclaimed layer, consisting of silty clay consolidated from slurry, was still undergoing primary consolidation at the beginning of ground treatment. The seabed soil was further divided into four sublayers (Fig. 2 of Yan and Chu, 2003) as shown in Fig 4.2a. The vertical profiles of index properties including Atterberg limits, initial water content, void ratio, unit weight and undrained shear strength (field vane) are shown, respectively, in Figs. 4.2b, 4.2c, 4.2d and 4.2e. The properties for section I are shown by solid symbols and those for section II are shown by open symbols. It can be seen that the geotechnical properties are quiet similar for both sections. In both sections, natural moisture content in the entire soil profile is either equal to or greater than the liquid limit. The initial void ratio varies between 0.8 to 1.8 in section I and 0.6 to 1.9 in section II. Unit weights for various sublayers were calculated using weight-volume relationships. An average specific gravity of 2.70 was used for the entire deposit.

The position of ground water table was not specifically reported; however, the hydrostatic porewater pressure record (Fig. 9, Yan and Chu, 2003) suggests that the groundwater table was located at the ground surface, and the same was used in the ILLICON analyses. The porewater pressures observed at different depths at the beginning of ground improvement are shown in Fig. 4.3. The pretreatment porewater pressures, which are in excess of the hydrostatic porewater pressure indicate that the reclaimed layer as well as the original seabed clay were still undergoing primary consolidation, due to self weight and placement of dredged slurry, respectively.

Undrained shear strength (s_{uo}) measurements in the laboratory as well as in the field show that the initial shear strength was generally less than 20kPa in both sections. However, both laboratory and field tests indicated a high s_{uo} at a depth range of 5 to 6m in section II. Unconsolidated undrained compression tests in the laboratory showed a s_{uo}(UU) of 38kPa, whereas, the field vane tests indicated a s_{uo}(FV) around 40 to 50kPa at the same depth. The high s_{uo} at this depth may be attributed to the fact that the silt layer

present at this depth was the original ground surface which had experienced overconsolidation due to desiccation before placement of the dredged slurry layer.

The 20m thick compressible layer, into which PVDs were installed, was divided into 7 layers for ILLICON anlyses. A 2m thick layer of stiff clay below the tip of vertical drains was also considered in the settlement analysis to account for the settlement occurring below the penetration depth of PVDs. An average vacuum pressure of 40kPa was applied to this layer, assuming 87kPa vacuum (actual vacuum on Fig. 5 of Yan and Chu 2003) at its top decreasing to zero vacuum at its bottom. The stiff silty clay layer below the depth of 22m was assumed as an impermeable boundary for the settlement analyses. The values of initial moisture content and initial void ratio used for different sublayers in ILLICON analyses are shown with solid vertical lines for section I and dashed vertical lines for section II on Fig. 4.2b and 4.2c respectively. The average values of void ratio were directly used as input in the computer program ILLICON, whereas the moisture content values were used to estimate compression index as described in section 4.3.

4.3 EOP e - log σ'_v Relationships

The EOP e-log σ'_v relation for each sublayer was estimated based on the available data, empirical correlations, and reasonable assumptions. For constructing an EOP e-log σ'_v relationship, information on initial void ratio, initial effective vertical stress, preconsolidation pressure, recompression index and compression index, for each sublayer is required. Preconsolidation pressure (σ'_p), for different sublayers, was estimated from field vane shear strength profile togrther with empirical correlation between $s_{uo}(FV)/\sigma'_p$ and Plasticity index (Terzaghi et al. 1996). Preconsolidation pressure estimated for dredged slurry layers was found to be quite high (probably due to pretreatment excess porewater pressures) and therefore, was considered inconsistent with described state of soil (dredged clay slurry with moisture content greater than its liquid limit). Therefore, an overconsolidation ratio of 1.2 was assumed for the dredged slurry. The value of compression index (C_c) beyond σ'_p, for various sublayers, was estimated using the empirical correlation between C_c and natural water content (w_o) (Fig. 16.3,

Terzaghi et.al, 1996). A value of $C_r/C_c = 0.1$ was assumed for all sublayers. The values of compression indices and preconsolidation pressure and e-log σ'_v relations for various sublayers are shown in Fig. 4.4.

4.4 Coefficient of Permeability

The initial permeability in vertical direction was estimated using the empirical equation suggested by Mesri et.al (1994) as given below;

$$k_{vo} = 6.5*10^{-11}\left(\frac{e/CF}{A_c+1}\right)^4 \quad (4.1)$$

Holtz and Kovacs (1981) developed a chart (Fig 4.14, page 89) that can be used to identify the probable clay mineralogy of a soil deposit based on the plasticity index and liquid limit. For the present subsoil, illite was identified as the clay mineral; it has an activity ranging between 0.5 and 1.0 (Mitchell 1996). By assuming an activity (A_c) of 1, the value of clay size fraction (CF) was calculated using the reported I_p values. The value of A_c and CF were used in equation 4.1 to estimate k_{vo} for sublayers considered in the ILLICON analysis. The vertical distribution of initial permeability thus obtained was estimated for both sections and the values were examined in the light of vertical profile of initial excess porewater pressure, and considered reasonable, and were used in the analysis. The vertical distribution of k_{vo}, for both sections is shown in Fig 4.5a.

The decrease in permeability during consolidation was computed assuming a constant C_k which was determined from the empirical correlation, $C_k = 0.5e_o$ (Tavenas 1983). Permeability anisotropy was not considered in the analysis, i.e. the ratio between horizontal and vertical permeability was assumed as unity, as no data on k_h/k_v for this site was available. The vertical profile of C_k is shown in Fig. 4.5b and e-log k_v relations used in the settlement analysis are shown in Figs. 4.5c and 4.5d for section I and section II, respectively.

4.5 Prefabricated Vertical Drains (PVDs)

Table 4.1 summarizes PVD parameters used in the ILLICON analysis. It is important to note that only drain spacing and layout pattern were reported by Yan and Chu (2003). The other assumptions on PVD parameters are made considering typical Chinese vacuum consolidation system as described by Dam et.al (2006).

Mesri and Lo (1991), reported that the vertical drains perform without any significant well resistance at a discharge factor [$D=q_w/(k_h*l_m^2)$] of 5. The minimum discharge capacity corresponding to this discharge factor for the assumed section of PVDs is around $63m^3/yr$. Indraratna assumed a discharge capacity of $100m^3/yr$ (which corresponds to a discharge factor of around 8) while analyzing different projects where vacuum preloading was used in conjunction with PVDs (Indraratna et al. 2004, 2005). It is expected that increase in discharge capacity of PVDs will increase the rate of settlement up to a point where PVDs start performing without any significant well resistance. However, any further increase in discharge capacity of freely draining PVDs does not accelerate the settlement. Figure 4.6 shows the increase in settlement at a particular time (42 days in this case) with increase in discharge capacity for the assumed loading condition (Fig. 4.7a) before the application of vacuum for the case under study. It can be seen from Fig. 4.6 that the increase in discharge capacity beyond $60m^3/yr$ has a very little effect on the magnitude of settlement at 42 days, in both sections. The radius of smear zone, r_s, was defined assuming $r_s/r_m = 2.4$, where r_m is the equivalent radius of the mandrel used to install PVDs. In the ILLICON analyses, the compressibility of the smear zone was defined by a constant C_c connecting (e_o, σ'_{vo}) to (e_p, σ'_{vf}), and the permeability of the smear zone remained the same as the vertical permeability of undisturbed soil because k_h/k_v was assumed as unity. Figure 4.7 compares the ILLICON predictions with observed ground surface settlements in Sections I and II for different assumed discharge capacities. It appears from Fig. 4.7b that before application of vacuum, because of small compressibility in recompression range, PVDs performed without any significant well resistance; however, after the application of vacuum, because of high compressibility in the compression range, settlement in the field progressed at a rate which corresponds to a discharge capacity of $5m^3/yr$. or less for section I and between 9 and $11m^3/yr$ for section II. This suggests that the PVDs at this site performed with significant well resistance.

4.6 Installation of Vacuum System

The ground surface was covered with a 0.3m thick sand blanket through which PVDs were installed in a square grid at spacing of 1m to a depth of 20m. Corrugated and perforated flexible pipes with a diameter of 100mm, wrapped in a filter fabric, were

placed inside the sand blanket to link PVDs to vacuum pressure line. Three layers of thin (thickness not specified) PVC membranes were used to seal the area. Vacuum pressure was then applied using jet pumps.

The time required in carrying out the above mentioned activities and in preparation of peripheral trench was not reported. Typically, a period of 4 to 8 weeks is required for the site preparation and installation of vacuum consolidation system (Yan and Chu, 2005). A period of 7 weeks, between placement of sand blanket and first application of vacuum was assumed in the analysis. During this period a settlement of about 0.58m took place under the load of the sand blanket and equipment movement as well as dissipation of pretreatment excess porewater pressures.

4.7 Instrumentation

Both sections I and II were instrumented with settlement plates, multilevel settlement gauges, inclinometers, porewater pressure transducers and standpipe piezometers. The plan and section of various instrument locations are shown on Figs. 4.1 and 4.8 respectively.

4.8 Loading Sequence

The placement of 0.3m thick sand blanket for installation of PVDs and application of vacuum loading induced a uniform pressure of 6kPa on the ground surface. The sand blanket and PVDs were subjected to a vacuum pressure (in the sand blanket) of 87kPa for a period of 90 days. Loading schedule used in the ILLICON analysis was constructed considering the following:

- The pretreatment excess porewater pressure as shown in Fig. 4.3 was considered to be equal to a vertical stress increase at the corresponding depth. Thus it was assumed that at time t=0, an instantaneous load equal to the pretreatment excess porewater pressure was applied at respective depths for the analysis.
- The time of loading started with the placement of 0.3m thick sand blanket which was considered as a strip load of 6kPa applied uniformly over the ground surface. Although assuming a uniform pressure over a rectangular area leads to slightly smaller influence factors below depth of 10m, the

assumption of strip load is considered reasonable as section II was also subjected to a similar load which is likely to contribute to stress distribution of section I.

- The observed reduction in porewater pressure at different depths and at different times, due to application of vacuum is shown in Fig. 4.9. Although vacuum in the drainage blanket was maintained at 87kPa throughout the duration of treatment (Fig. 5; Yan and Chu, 2003); it can be seen from Fig. 4.9 that in both Sections I and II vacuum did not develop uniformly throughout the depth of compressible layer. For example, at a depth of 4m, the reduction achieved in porewater pressure at the end of vacuum preloading was 55kPa for section I and 60kPa for section II. It appears that a horizontal 'leakage' in vacuum pressure occurred in section I at several depths; the most pronounced drop in vacuum intensity is observed at a depth of 1m where the observed reduction in porewater pressure was 70kPa after 30 days and 60kPa after 90 days of vacuum application. As the vertical distribution of porewater pressure reduction gives an indirect measure of the pressure gradient under which consolidation took place, it was taken into account while constructing the loading schedule for ILLICON analysis.
- Under ideal conditions, vacuum loading is considered to act as a wide fill, i.e. vacuum load is assumed to be transmitted with full intensity, through the vertical drains, to entire treatment depth of compressible layer. The vacuum may develop in soil at different rate at different depths due to variation in permeability and compressibility of individual sublayers; however, it is expected to develop to its full (applied) intensity in all sublayers at a time corresponding to the end of primary consolidation. In this case, settlements/reductions in porewater pressure under vacuum loading were observed up to a depth of 18m, suggesting that vacuum was effective for the entire thickness of soft clay; however, Fig. 4.9 suggests that settlement progressed under different vacuum pressure at different depths, i.e., vacuum

did not develop in soil to full intensity at all depths during the preloading operation.

- Four loading options considered in settlement analysis of section I, as shown in Fig. 4.10, are as under:
    - ***Case A***. Vacuum developed uniformly in the vertical drains and subsequently in soil with full intensity (87kPa) throughout the depth of compressible layer (Fig 4.10a).
    - ***Case B***. Vacuum quickly developed in the vertical drains to 80kPa, however, with time, the vacuum intensity in soil stabilized at 60kPa as shown in Fig. 4.10b.
    - ***Case C***. Consolidation progressed under a reduced vacuum pressure of 50kPa in the compressible layer, assumed to develop uniformly throughout the depth of compressible layer (Fig 4.10c).
    - ***Case D***. Consolidation progressed under different effective vacuum pressure in the compressible layer at different depths as shown in Fig. 4.10d.
- Two loading options were considered in settlement analysis of section II, as shown in Fig. 4.11., are as under:
    - ***Case A***. Vacuum developed uniformly in the vertical drains and soil with full intensity (87kPa) throughout the depth of compressible layer (Fig 4.11a).
    - ***Case B***. Vacuum quickly developed to 70kPa and then increased to 85kPa as shown in Fig. 4.11b.
- PVDs and horizontal drainage system are installed in the ground using light weight machinery. A live load of 10kPa was assumed in the analysis to act for a duration of 2 weeks
- Vacuum load was applied 42 days after placement of the sand blanket.

4.9 Settlements

Surface settlement of 0.58m was observed in both Sections I and II, after installation of PVDs and before application of the vacuum load. This settlement is attributed to the placement of sand blanket, dissipation of the pretreatment excess porewater pressure, soil disturbance due to installation of PVDs and machinery live load. ILLICON predicts a surface settlement of 0.58m for section I which corresponds to a discharge capacity of $32m^3$/yr, and 0.56m for section II which corresponds to a discharge capacity of $100m^3$/yr. as shown in Fig. 4.6. This indicates that, PVDs performed with some well resistance in Section I even before the application of vacuum pressure. In Section II, however, PVDs performed without any significant well resistance before the application of vacuum.

For section I, Figs. 4.12 and 4.13, respectively, compare the surface and subsurface settlements predicted by ILLICON with those observed in the field, for all the loading cases considered in the analyses. It is important to note that the settlement predicted by ILLICON correspond to a discharge capacity of $32m^3$/yr. and $5m^3$/yr. before and after the application of vacuum load, respectively. The initial settlement of 0.58m and a time period of 42 days were added to each reported field observation of settlement for comparison with the ILLICON results. Similarly, the settlements predicted by ILLICON at 42 days were added to observed subsurface settlements at the corresponding depths for comparing the observed data with ILLICON predictions. Figure 4.12 shows that the observed ground surface settlements are in good agreement with the predicted settlements except for Case A loading condition, which overestimates the observed ground surface settlements and therefore, was discarded as a possible loading condition. Figure 4.13 shows that, at all depths, case C loading condition, slightly underestimates the observed subsurface settlements. Both case B and case D loading conditions are based on the assumption of changing vacuum pressure with depth and with time. The agreement in surface and subsurface settlements with the assumed loading conditions indicates the possibility of internal leakage (i.e. horizontal flow) in vacuum intensity at different depths without any noticeable drop in vacuum intensity in drainage blanket. It can also be observed that settlements observed at the depth of 15.5m exceed the predicted settlements

under all loading conditions. It is interesting to note that these settlements also exceed settlements at 13m which is not theoretically possible; hence the differences at this depth are attributed to instrument/reading error and therefore, ignored in the analyses.

Figures 4.14 and 4.15, respectively, compare the observed surface and subsurface settlements with those predicted by ILLICON for Section II for both loading conditions considered in Fig. 4.11. These figures are plotted in a similar way as described above, however, in this case, the settlements predicted by ILLICON correspond to a discharge capacity of $11m^3/yr$. It can be seen from Fig. 4.14 that a constant vacuum intensity of 87kPa (case A) overestimates the rate of observed settlements and hence was not considered reasonable. Figure 4.15 shows that subsurface settlement observations and predictions for Section II are in reasonable agreement at all depths up to 100 days (approximately 60 days after application of vacuum); however, after this time, there is a sudden increase in observed settlements which is only possible if the load was somehow increased at these depths. Theoretical upper limit up to which, vacuum can be applied is 100kPa. An analysis was carried out by increasing the vacuum pressure, after 100 days, to theoretical maximum limit of 100kPa as shown in Fig. 4.16. It can be seen that under this loading condition, ILLICON predicts a greater surface settlement whereas the observed subsurface settlements at deeper depths are still greater than those predicted by ILLICON. As there is no evidence of an increased vacuum pressure or any other externally applied load, it is possible that there is an incremental error in recording/reporting settlement observations after 60 days of vacuum application.

Figure 4.17 compares the vertical profiles of observed and predicted settlements (case B for section I and case B for section II) at different time intervals. It can be seen that there is a reasonable agreement between observed and predicted settlements in both the sections except at 90days (below 13m for Section I and Section II; due to instrument/reading error as explained earlier). This validates the assumptions made on development of vacuum pressure within the vertical drains and soil at different depths and at different times.

4.10 Porewater Pressure

Porewater pressures were interpreted using the following equation:

$$u = u_o + u_{sm} + u'' \tag{4.2}$$

where

u is the total porewater pressure at any time and at any depth;

u_o is the initial hydrostatic porewater pressure;

u_{sm} is the applied maximum vacuum pressure (negative porewater pressure); and

u'' is the positive excess porewater pressure from ILLICON analysis with possible maximum value of $u_{sm} + \Delta\sigma_v$, where u_{sm} is the absolute value of vacuum (i.e. positive load) and $\Delta\sigma_v$ is the increase in effective vertical stress (positive load).

Figure 4.18 shows a comparison of observed and predicted porewater pressures with respect to depth at different times. As in the case of settlement, the reported data have been reinterpreted considering the following;

- A period of 42 days was added to the field observations in Fig. 7 of Yan and Chu (2003), to make the observed data comparable with the ILLICON predictions which stats from the the time of placement of drainage blanket.
- The reported data (Figs. 7 and 9 of Yan and Chu; 2003) give the observed reductions in porewater pressure with time considering the pretreatment excess porewater pressure as the reference line. This cannot be justified, as part of these pretreatment excess porewater pressures dissipated as evidenced by observed settlement before the application of vacuum load. Therefore, the reference porewater pressure for the comparison of observed and predicted settlements is taken as the total porewater pressure predicted by ILLICON at 42 days (before application of vacuum) for the respective depths (which is almost hydrostatic), corresponding to a discharge capacity of $32 m^3/yr$.

A constant value of vacuum pressure (e.g. 87kPa) was used in Eq. 4.2, to interpret the total porewater pressure during the vacuum preloading. It can be seen from Fig. 4.18 that there is generally a good agreement between the observed and predicted values of porewater pressure for case B and case D loading conditions for section I and for section II. Slight differences in observed and predicted porewater pressure, especially after 30

days, can be attributed to the fact that vacuum had not developed to 87kPa by that time within the vertical drains at the corresponding depth. For case C of section I, the ILLICON predicts more than 95% dissipation of porewater pressures within 60 days of vacuum application, which is contrary to field observations, and therefore, this loading condition is not considered reasonable.

4.11 Degree of Consolidation

Yan and Chu (2003) have reported average degree of consolidation ($\bar{U}$) based on settlement and porewater pressure separately. The $\bar{U}$ based on settlement at the end of vacuum preloading was reported as 86% and 83% (Chu and Yan, 2005) for Sections I and II, respectively. The $\bar{U}$ based on surface settlements observations calculated using Asoaka method (Asoaka 1978; Mesri and Huvaj 2009), as shown in Figs. 4.19 and 4.20, was 84% and 83%, respectively, for sections I and II which is similar to the reported values. The average DOC predicted by ILLICON at the end of vacuum preloading operation was 86% and 80% for case B and case D of Section I and 87.5% for case B of Section II. It can also be seen from Figs. 4.19 and 4.20 that DOC at different depths was different, i.e. at depths of 2m and 7.5m in section I, EOP consolidation is almost completed, whereas at 9.5m and 13m depths, it is not possible to predict the EOP settlement. This confirms that the consolidation progressed under different pressures at different depths.

The average DOC based on porewater pressure data was estimated as 73% for section I and 75% for section II by Chu and Yan (2005). It has already been discussed in section 4.10, that defining pretreatment porewater pressures as reference is not considered reasonable as most of these porewater pressures had dissipated before the application of vacuum pressure. Therefore, the degree of consolidation based on reference porewater pressure as shown in Fig. 4.18 were used by Chu and Yan (2005) in Eq. 4.3 to estimate $\bar{U}$ at different depths.

$$U_{avg} = 1 - \left[\frac{\int u_{t(z)} - u_{s(z)}}{\int u_{o(z)} - u_{s(z)}} \right] \tag{4.3}$$

Tables 4.2 and 4.3, respectively, compare the reported and reinterpreted DOC at different depths and also compare the average DOC with that of ILLICON for assumed loading conditions. It can be seen that the reinterpreted DOC based on porewater pressure is 82% for section II which compares well to 83% DOC based on settlement. For section I, however, there is a significant difference in DOC based on settlement and porewater pressure which can be explained in terms of the assumed loading condition and the actual loading condition under which consolidation took place. It has already been shown from settlement analyses that, the consolidation did not progress under a uniform vacuum pressure of 80kPa as assumed by Yan and Chu (2003), and Chu and Yan (2005); therefore, the EOP settlement predicted at different depths by the Asoaka method (as shown in Fig. 4.20) reflects a settlement under reduced load intensity. It is interesting to note that the DOC based on porewater pressure predicted by ILLICON with case D loading condition is in close agreement with that calculated by Eq. 4.3 and reinforces the possibility of internal leakage in vacuum pressure at different depths without a noticeable change of vacuum intensity in the drainage blanket.

4.12 Lateral Displacements

Figure 4.21 shows the lateral displacements at different depths, plotted against the settlements at corresponding depths, observed at different times during vacuum preloading operation. It can be seen from Fig. 4.21 that the lateral displacement at any time are 15% to 40% of settlement for Section I, and 14% to 44% of the settlement for Section II. Figure 4.22 shows the mid-sublayer lateral displacements at different times, plotted against sub-layer settlements at the same times for both sections. The figure indicates that for the surface layers, the mid-layer lateral displacements generally exceed the sub-layer settlement; however, at greater depths, the mid-sublayer lateral displacements are smaller than the sub-layer settlements. The mid-sublayer lateral displacements are greater than the sub-layer settlements up to a depth of 4m for Section I and 8m for Section II. As the geotechnical properties of compressible layer were similar in both sections, the significant difference in distribution of lateral displacements can be attributed to the non-uniform distribution of vacuum pressure with depth, especially for section I, as shown in Fig. 4.23. For both Section I and Section II, at all depths, the last

measurements of of mid-sublayer lateral displacements are more or less equal to last measurements of sublayer settlement (colored markers on Fig. 4.22).

4.13 Increase in Undrained Shear Strength due to Vacuum Preloading

At the end of vacuum preloading operation, an increase in field vane shear strength was measured in both sections as shown in Fig. 4.24. It can be seen that (1) at all depths, the increase in shear strength in Section II (with higher and more uniform vacuum intensity) is more significant than in Section I, (2) the maximum increase in shear strength is observed at a depth of 5m for section I and at 2m depth for Section II (Fig. 4.24c); therefore, it is not reasonable to express increase in shear strength as a function of depth alone, and (3) the increase in shear strength appears to be influenced by the applied vacuum pressure as well as the initial shear strength. For e.g. in Section I, the shear strength increases from 15kPa to 32kPa and 30kPa to 33kPa, respectively, at depths of 5.5m and 8.5m.

4.14 Post Treatment Void Ratio

Moisture content was measured after the treatment to evaluate the performance of vacuum precompression. Post treatment moisture content profile is reported in Fig. 11 of Yan and Chu (2003). The moisture content was used to back calculate the end of treatment void ratio by assuming a 100% degree of saturation and the results are compared to the void ratio predicted by ILLICON at a time corresponding to end of vacuum loading (Fig. 4.25). Figure 4.25 shows a reasonable agreement between the measured and the predicted void ratios at all depths for both sections. The concept of taking into account vacuum losses is reinforced by the agreement between prediction and measurement of end-of-treatment void ratios.

4.15 Concluding Remarks

The analysis of this case history shows that:

- Pre-vacuum activities such as placement of sand blanket, installation of PVDs, and ground surface movement of equipment, etc. May result in excess porewater pressures and settlements that should be taken into account in comparing the field measurements and predictions. Reinterpretation of porewater pressures by accounting for the dissipation affected before the

application of vacuum resulted in agreement between the degree of consolidation based on settlement and porewater pressures.

- There is good agreement between the observed and predicted surface as well as subsurface settlementsas a function of time. As the predictions were made considering vacuum pressure similar to fill load, this indicates that vacuum pressure can be modeled as an embankment load, and thus existing theories of consolidation can be used to predict settlement due to vacuum preloading.
- With a unique definition of excess porewater pressure, the porewater pressure response due to vacuum preloading can be interpreted by using a porewater pressure response generated by a fill load.
- Under ideal conditions, vacuum pressure develops uniformly in the drainage system (drainage blanket and vertical drains); however, due to stratigraphic variations, vacuum may be transferred to different sublayers at different rate. However, porewater pressures at all depths are expected to reduce by the amount of the applied vacuum by the end of primary consolidation.
- Due to internal leakages, vacuum pressure may develop to different intensities at different depths. This implies that consolidation may progress under different vacuum pressures at different depths. For the back-analysis of case histories including porewater pressure observations, the consolidation pressure at different depths can be reasonably estimated using the observed reductions in porewater pressure.
- The agreement between measured and predicted post treatment void ratios for loading conditions that accounts for a leakage in vacuum pressure confirms that the consolidation may progress to different final vacuum intensities at different depths.
- The PVDs in this case performed with significant well resistance; therefore, the possibility of well resistance should be taken into account during vacuum preloading.

- Lateral displacements due to vacuum preloading are maximum at ground surface and reduce with depth. The lateral displacements at any depth can be expressed in terms of respective settlements. In this case, the lateral displacements were generally between 14 to 44 percent of the settlements. Among other factors, the vacuum intensity is the major factor governing lateral displacement at different depths.
- The increase in undrained shear strength appears to be independent of depth, instead it depends upon the initial undrained shear strength, preconsolidation pressure as well as the applied vacuum pressure (consolidation pressure).

4.16 Tables

Table 4.1: PVD parameters used in ILLICON analysis

<table>
<tr><td>Spacing, square grid (m)</td><td colspan="2">1.0</td><td rowspan="2">Yan and Chu (2003)</td></tr>
<tr><td>Penetration Depth, l_m (m)</td><td colspan="2">20</td></tr>
<tr><td>Section (mm)</td><td colspan="2">100 * 3</td><td rowspan="5">Assumed</td></tr>
<tr><td rowspan="2">Discharge Capacity, q_w (m^3/year)</td><td>Section I</td><td>Section II</td></tr>
<tr><td>5 - 100</td><td>9 -100</td></tr>
<tr><td>Dimension of Mandrel (mm)</td><td colspan="2">120 * 50</td></tr>
<tr><td>r_s/r_m</td><td colspan="2">2.4</td></tr>
<tr><td>Time for Installation of drains (Days)</td><td colspan="2">10 days</td></tr>
<tr><td colspan="4">r_s = radius of smear zone
r_m = radius of mandrel</td></tr>
</table>

Table 4.2: Degree of consolidation based on porewater pressure for Section I, estimated by Eq. 4.3 and predicted by ILLICON.

Depth (m)	u_{oz}(kPa)		DOC (%)					
			30 Days		60 Days		90 Days	
	Reported	Reinterpreted	Reported	Reinterpreted	Reported	Reinterpreted	Reported	Reinterpreted
1	18	16	71.4	68.0	67.3	64.1	63.3	60.2
4	63	45	13.6	15.2	32.5	36.4	53.9	60.3
6	88	62	71.3	86.5	69.9	84.8	65.7	79.8
8.5	92	86	90.8	89.8	92.0	90.9	94.3	93.2
11	111	111	96.9	89.2	96.3	88.6	98.8	90.9
14.5	155	146	37.8	38.6	68.9	70.5	73.3	75.0
18	200	186	53.5	57.5	72.0	77.4	78.0	83.9
Average - Observed			62.2	63.5	71.3	73.2	**75.3**	**77.6**
Average - ILLICON (Case B)			61.2		75.4		**87.6**	
Average - ILLICON (Case D)			47.5		66.7		**79.8**	

Table 4.3: Degree of consolidation based on porewater pressure for Section II, estimated by Eq. 4.3 and predicted by ILLICON.

Depth (m)	**u_{oz}(kPa)**		**DOC (%)**					
			30 Days		**60 Days**		**90 Days**	
	Reported	**Reinterpreted**	**Reported**	**Reinterpreted**	**Reported**	**Reinterpreted**	**Reported**	**Reinterpreted**
1	20	19	75.0	70.8	76.0	71.7	83.0	78.3
4	62	42	28.4	32.6	44.1	50.6	58.8	67.4
6	66	60	81.4	80.5	87.2	86.2	94.2	93.1
8.5	86	85	79.0	73.6	88.9	82.8	88.9	82.8
11	115	110	83.5	81.6	85.9	83.9	92.9	90.8
14.5	183	146	22.0	29.5	55.9	75.0	57.6	77.3
18	197	180	59.8	66.7	74.2	82.8	76.3	85.1
Average - Observed			61.3	62.2	73.2	76.1	**78.8**	**82.1**
Average - ILLICON (Case B)			59		75.5		**87.5**	

4.17 Figures

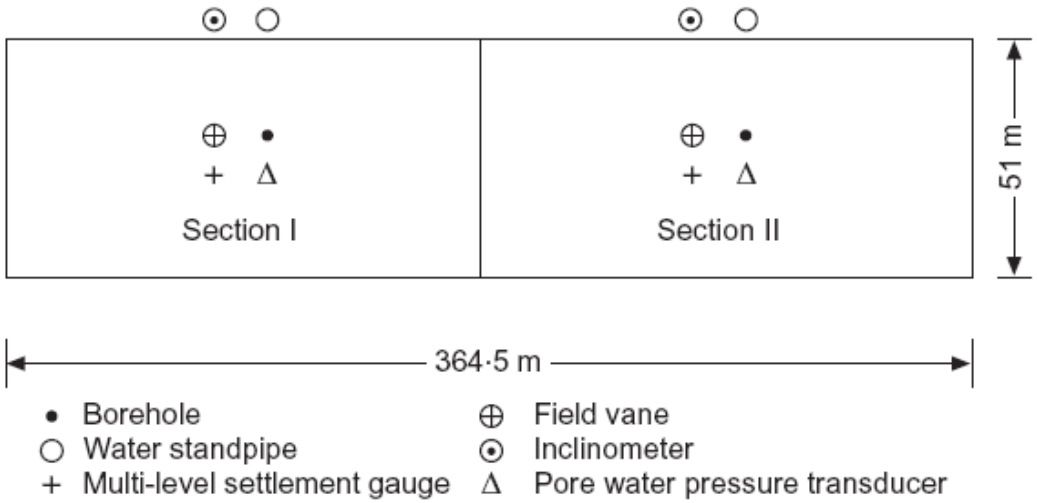

Figure 4.1: Plan of treatment area with location of various instruments (after Yan and Chu; 2003)

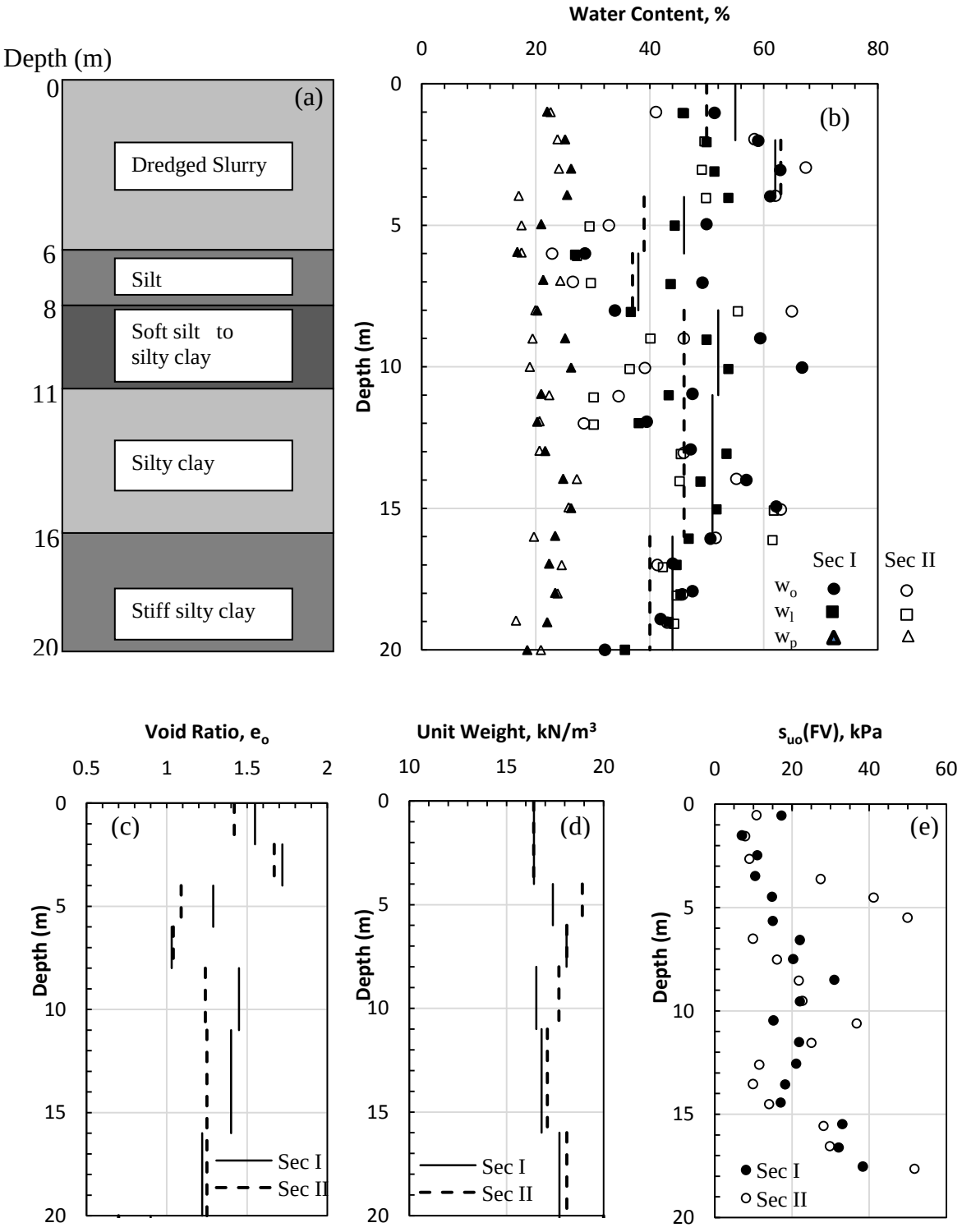

Figure 4.2: Soil profile and geotechnical properties (data from Yan and Chu 2003)

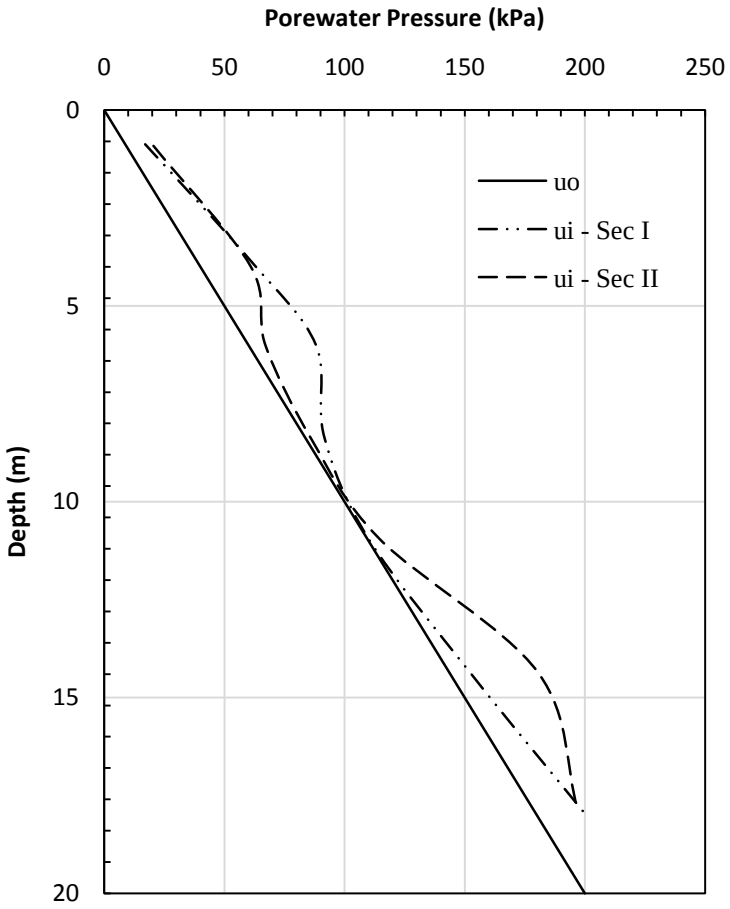

Figure 4.3: Pretreatment porewater pressure profile for Section I and Section II (data from Yan and Chu 2003)

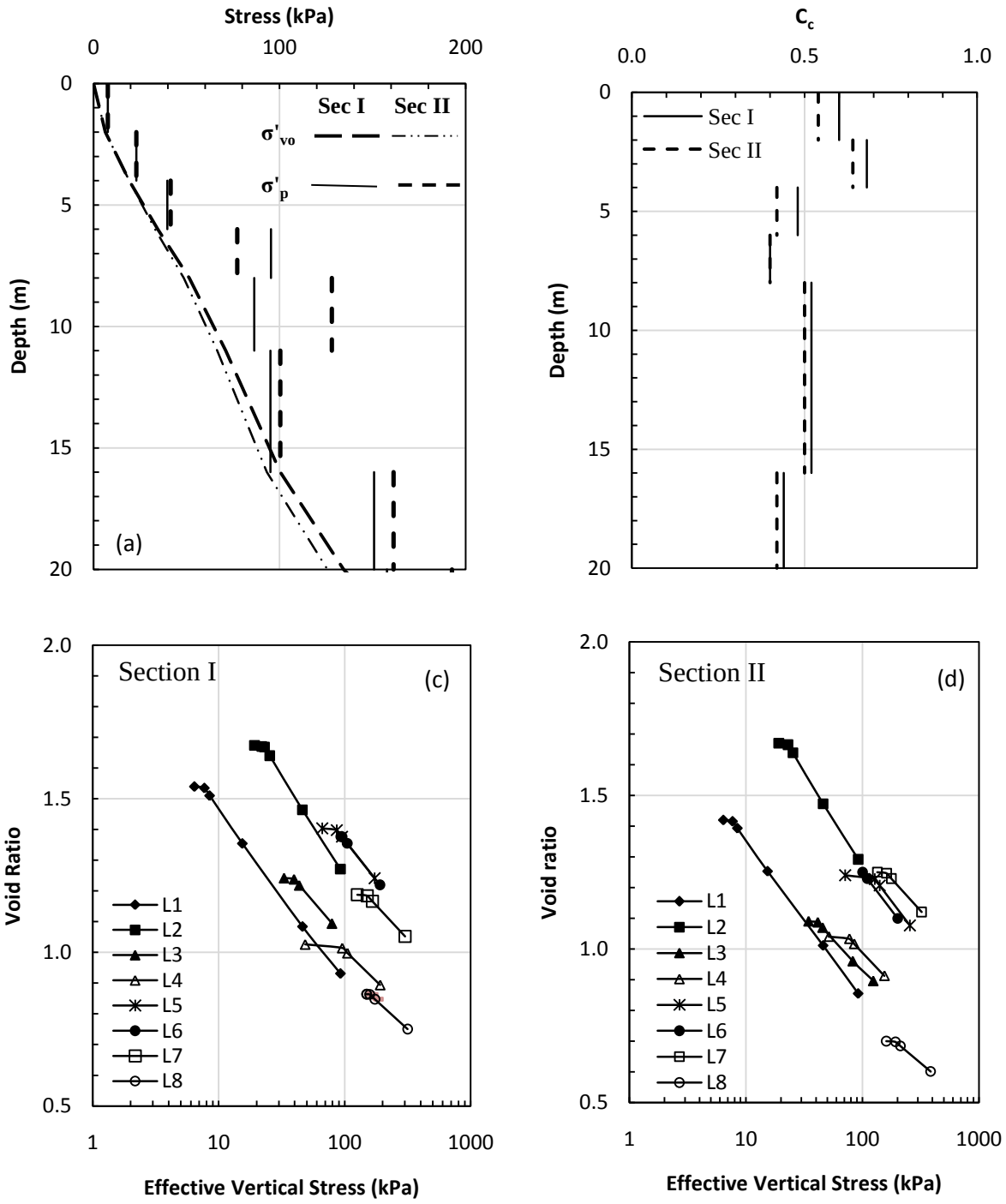

Figure 4.4: (a) Initial effective vertical stress and preconsolidation pressure, (b) Compression index, (c) and (d) EOP e-log σ'_v relations for sublayers of Section I and Section II, respectively

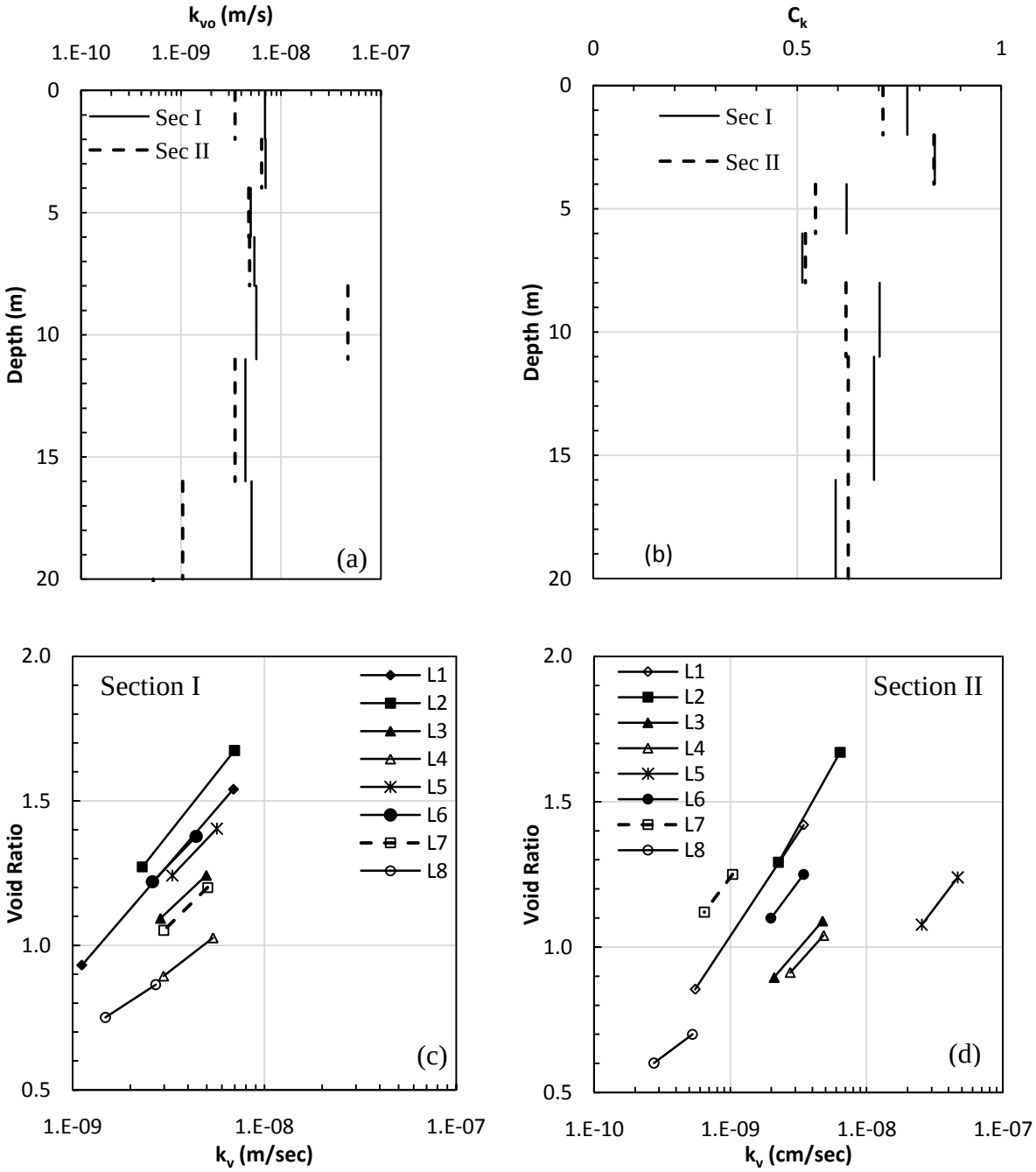

Figure 4.5: Vertical distribution of (a) Initial permeability, (b) C_k, (c) and (d) e-log k_v relations for sublayers of Section I and Section II, respectively

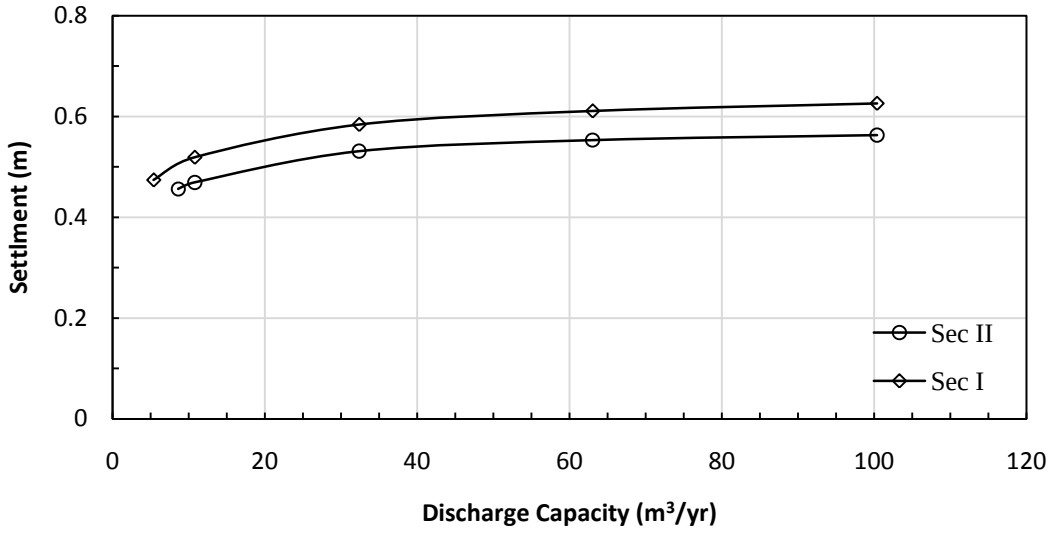

Figure 4.6: Variation in settlement at 42 days with discharge capacity of PVDs for Sections I and II

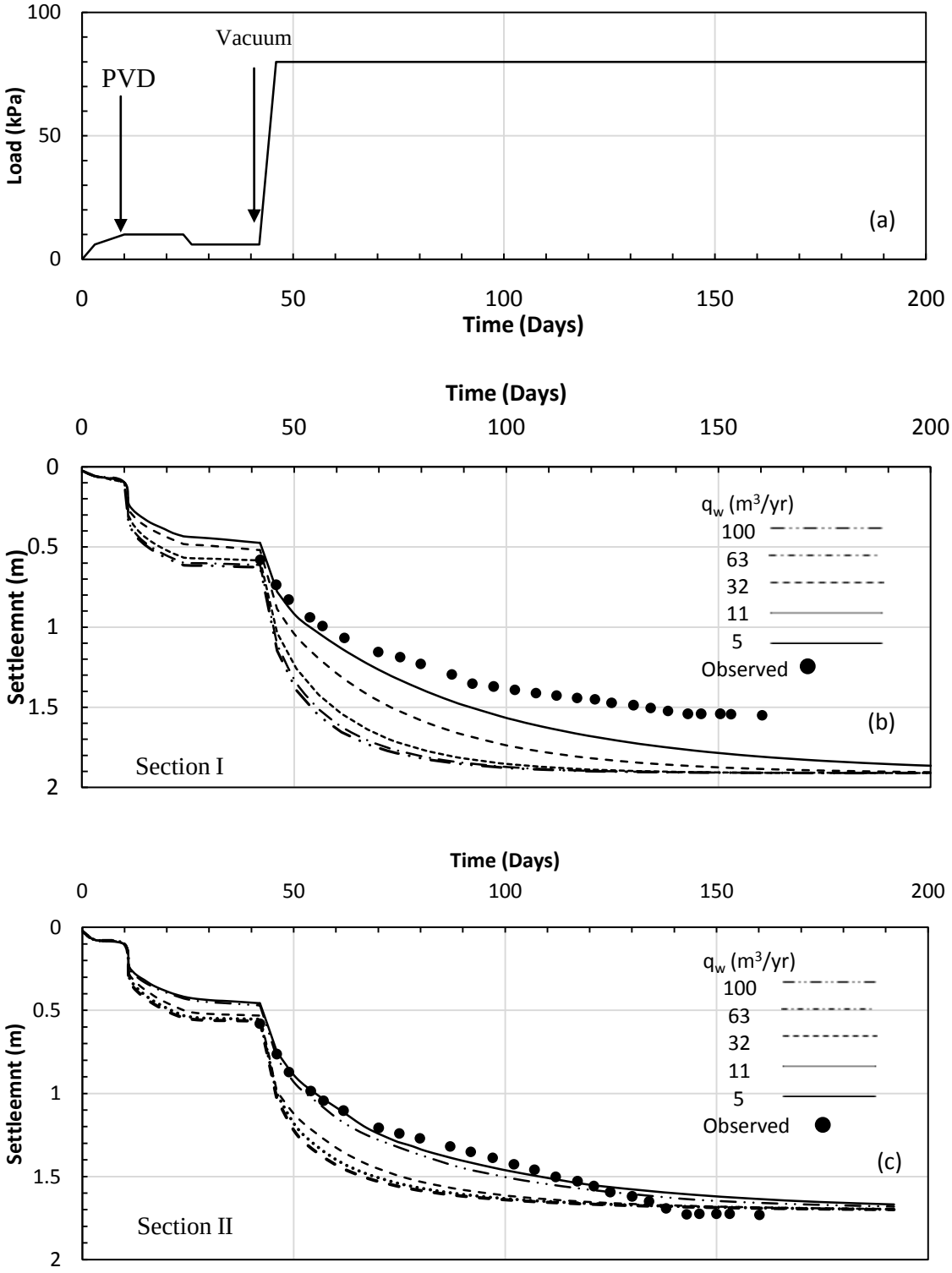

Figure 4.7: (a) Loading schedule, (b) and (c) effect of discharge capacity on rate of settlement for Section I and Section II

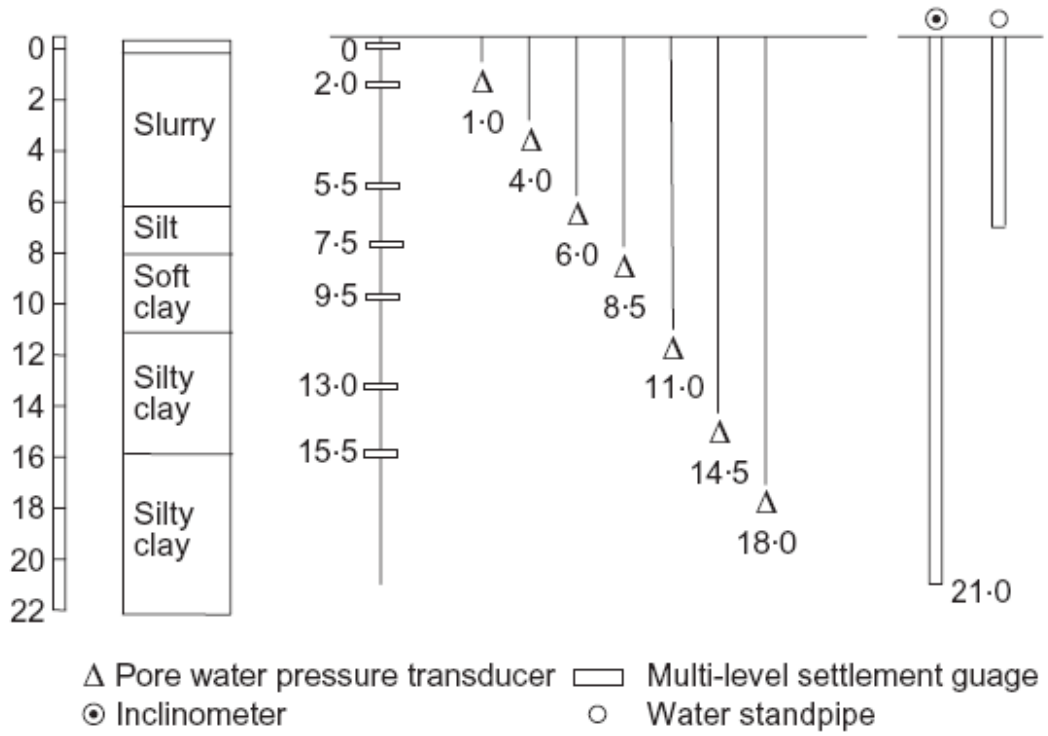

Figure 4.8: Location of various instruments at different depths (after Yan and Chu 2003)

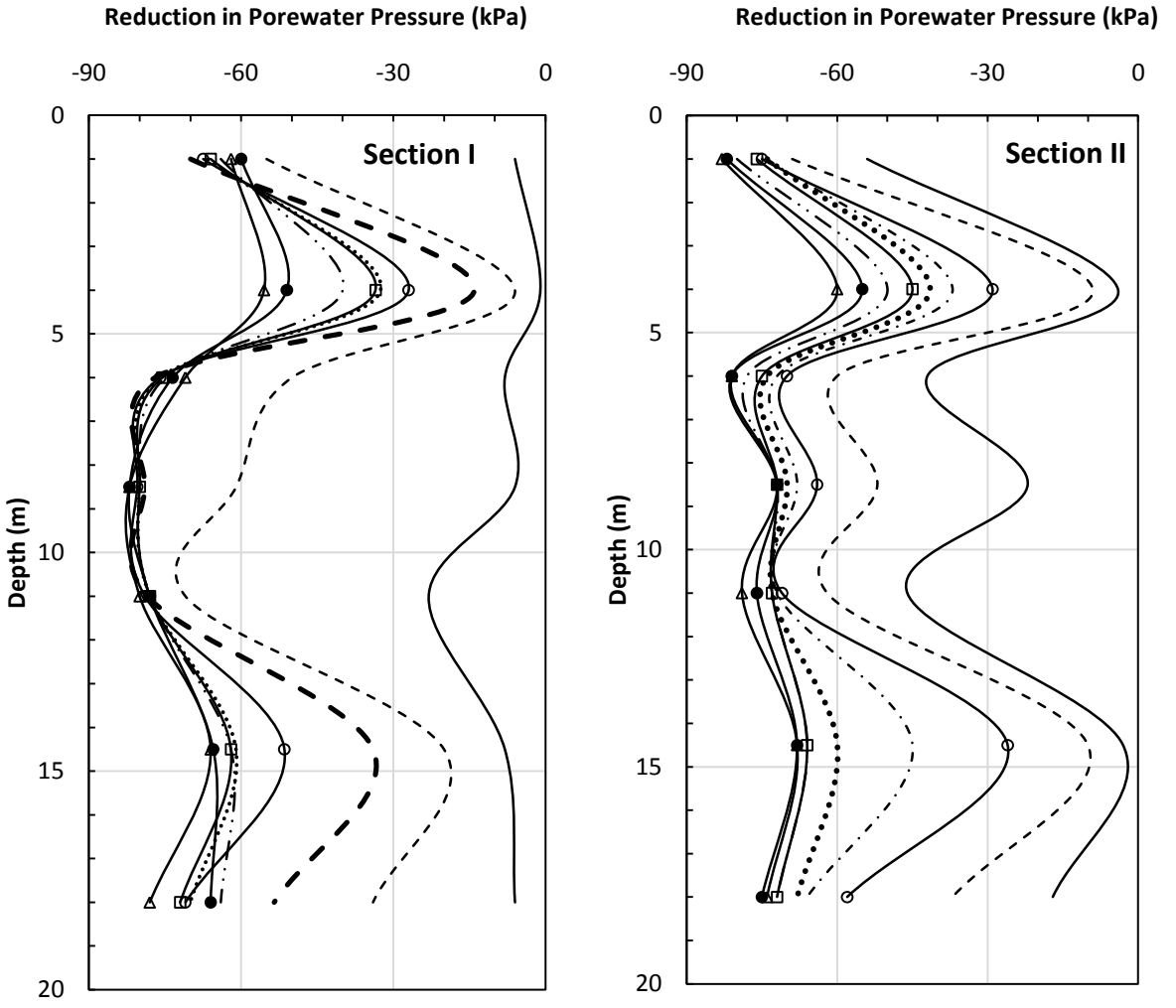

Elapsed Time (Days)	Porewater Pressure Reduction (kPa)	Elapsed Time (Days)	Porewater Pressure Reduction (kPa)
10		60	
20		70	
30		80	
40		90	
50			

Figure 4.9: Vertical distribution of observed reduction in porewater (data from Yan and Chu 2003)

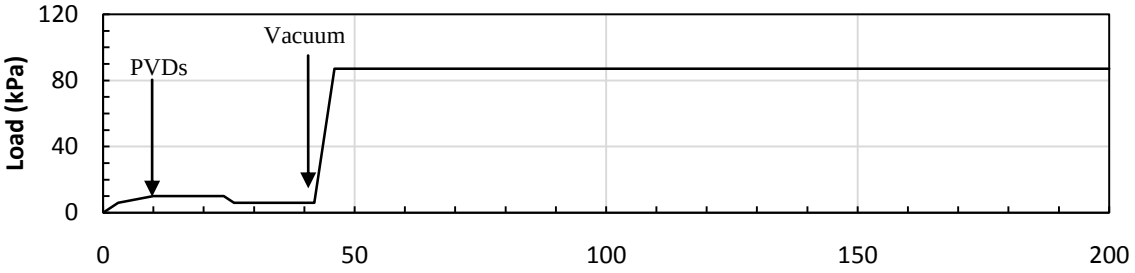

(a) Uniform vacuum intensity in drainage layer and all along the depth of PVDs

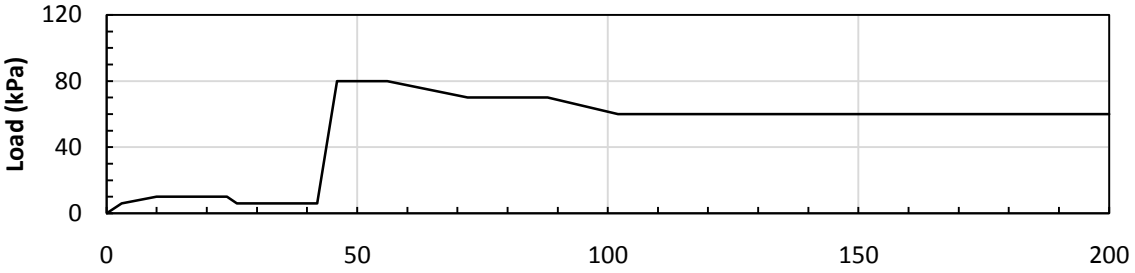

(b) Vacuum quickly reached to 80kPa and then gradually decreased to 60kPa. Uniform vacuum intensity in drainage layer and all along the depth of PVDs

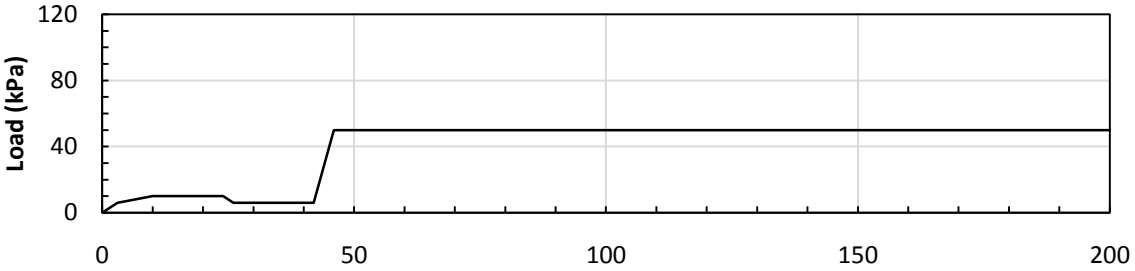

(c) Consolidation progressed under an effective vacuum pressure of 50kPa. Uniform vacuum intensity in drainage layer and all along the depth of PVDs

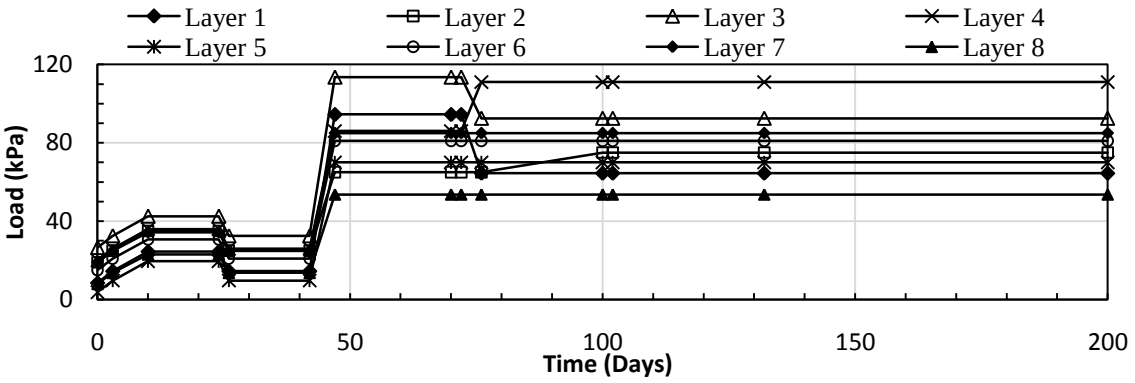

(d) Vacuum developed in different sublayers independent of each other

Figure 4.10: Assumed loading conditions for settlement analysis of Section I

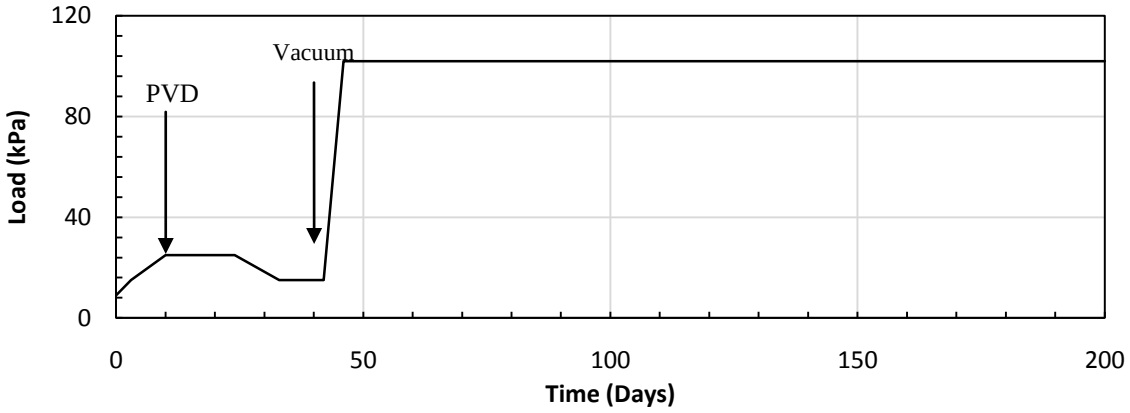

(a) Uniform vacuum intensity in drainage layer and all along the depth of PVDs

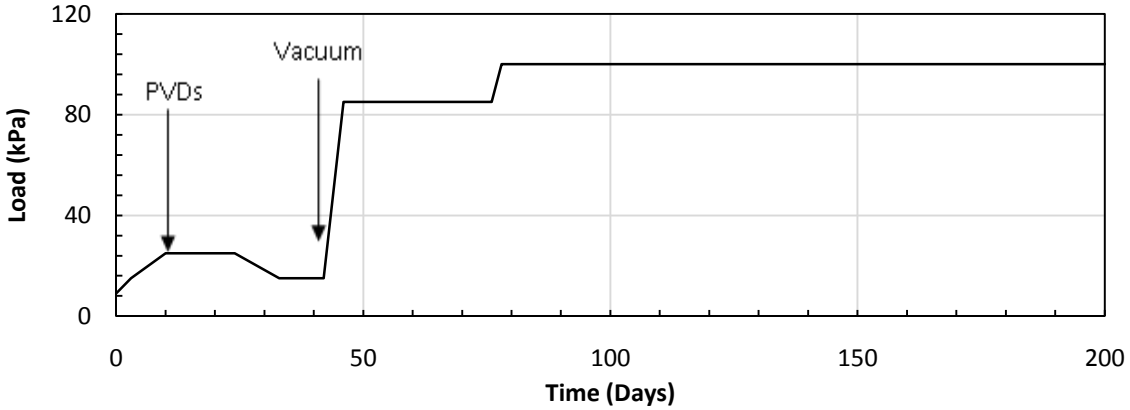

(b) Vacuum gradually developed to full intensity

Figure 4.11: Assumed loading conditions for settlement analysis of Section II

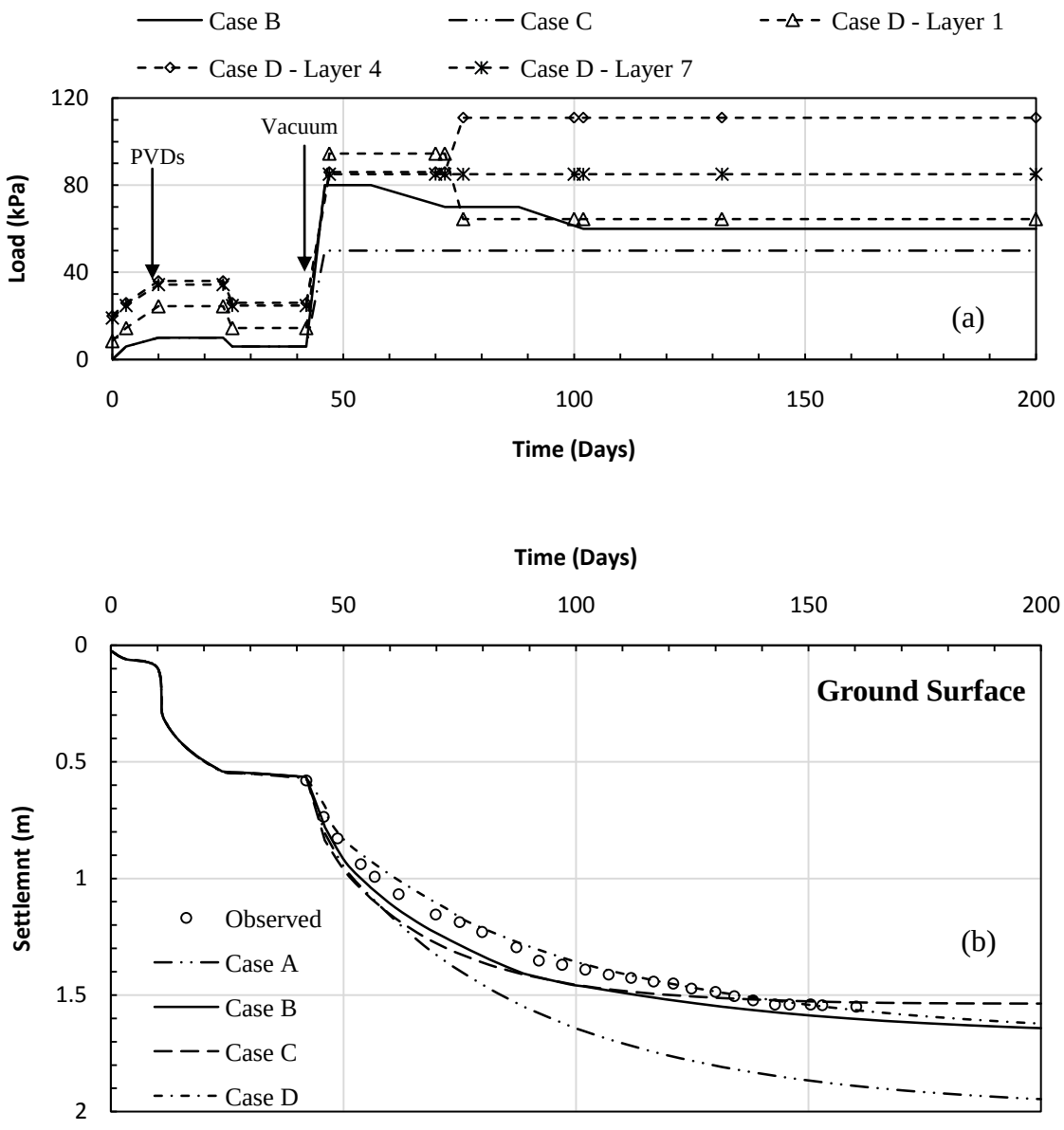

Figure 4.12: Comparison of observed and predicted ground surface settlements for assumed loading conditions in Section I

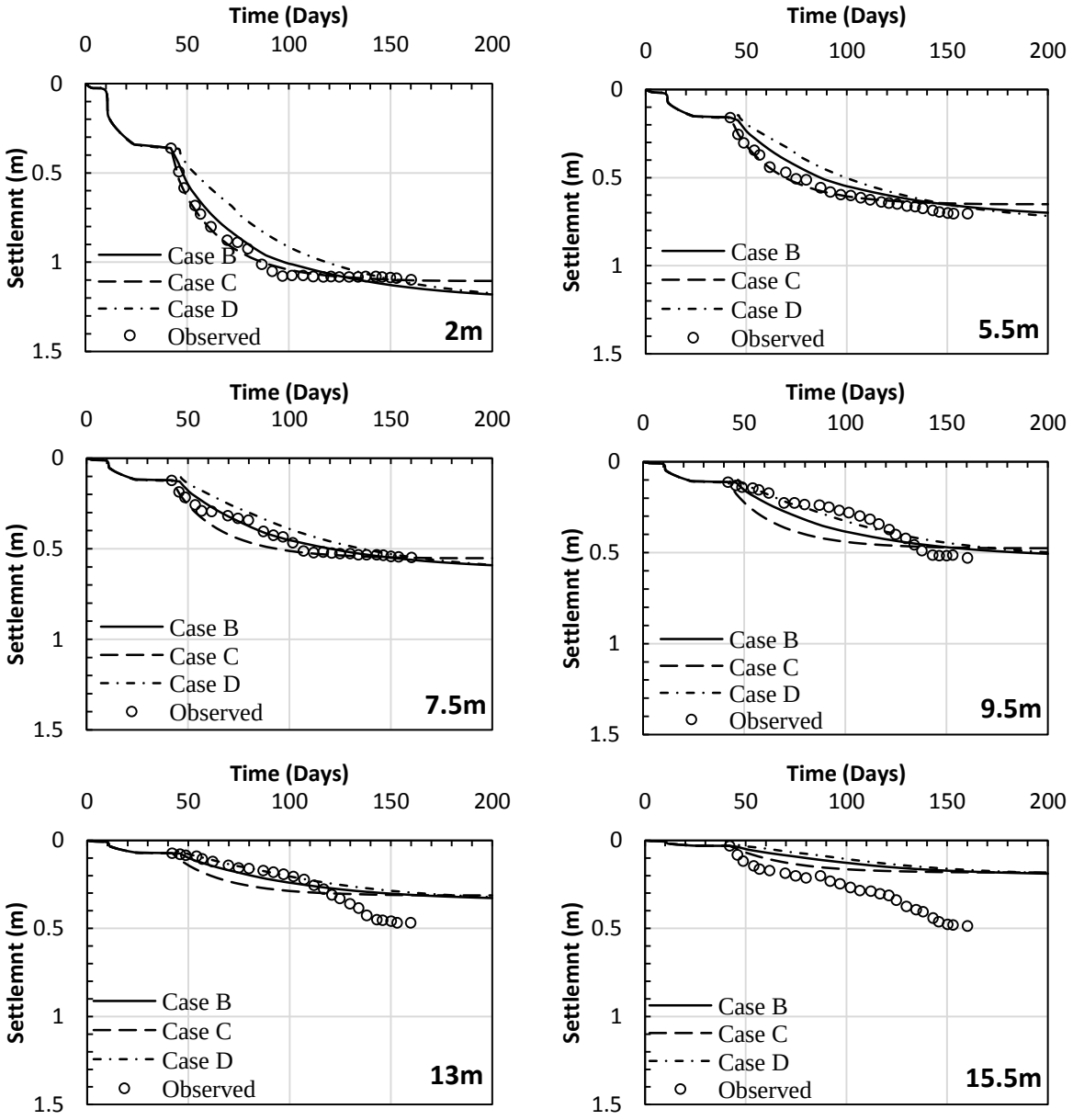

Figure 4.13: Comparison of observed and predicted subsurface settlements for assumed loading conditions in Section I

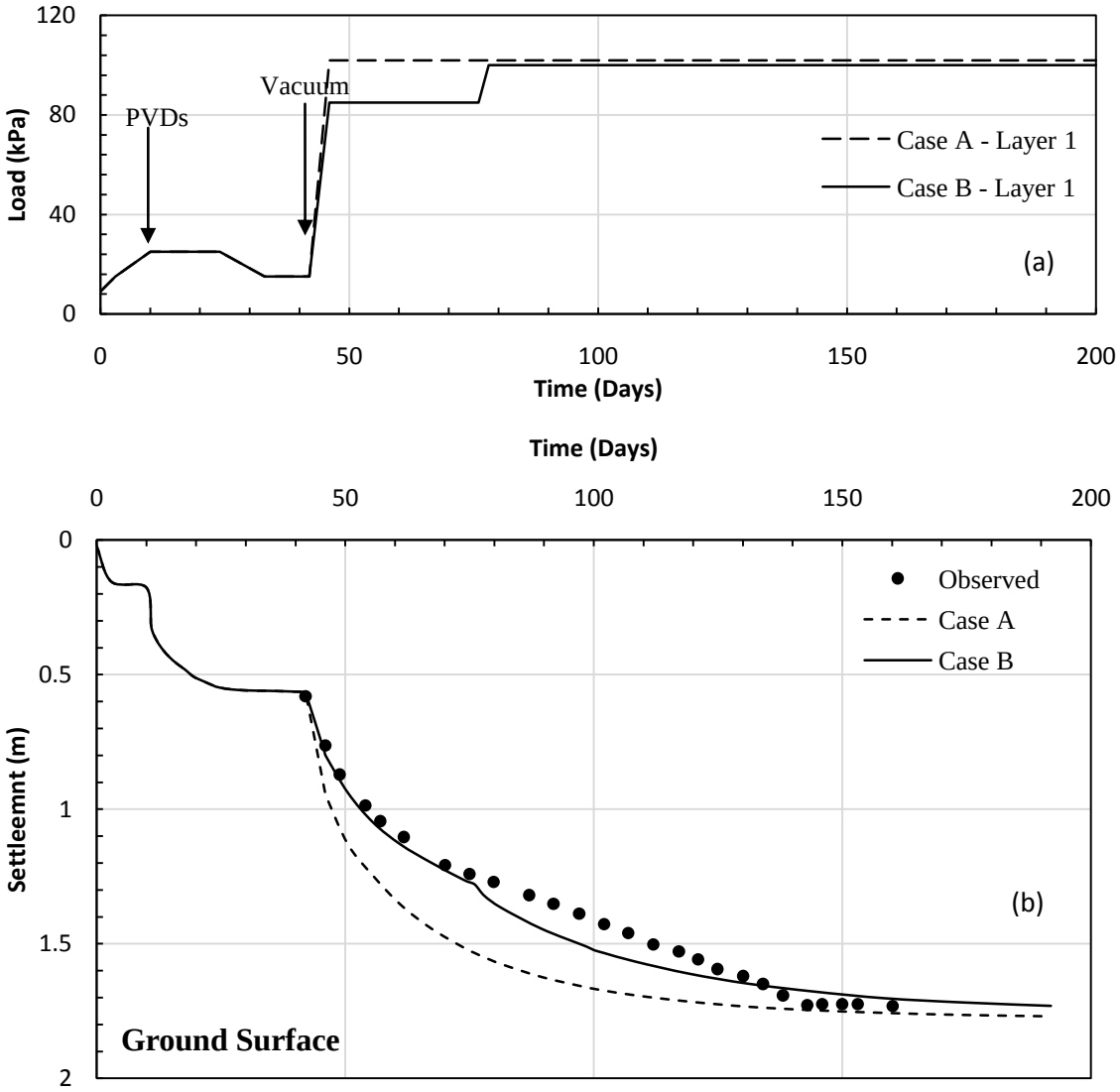

Figure 4.14: Comparison of observed and predicted ground surface settlements for assumed loading conditions in Section II

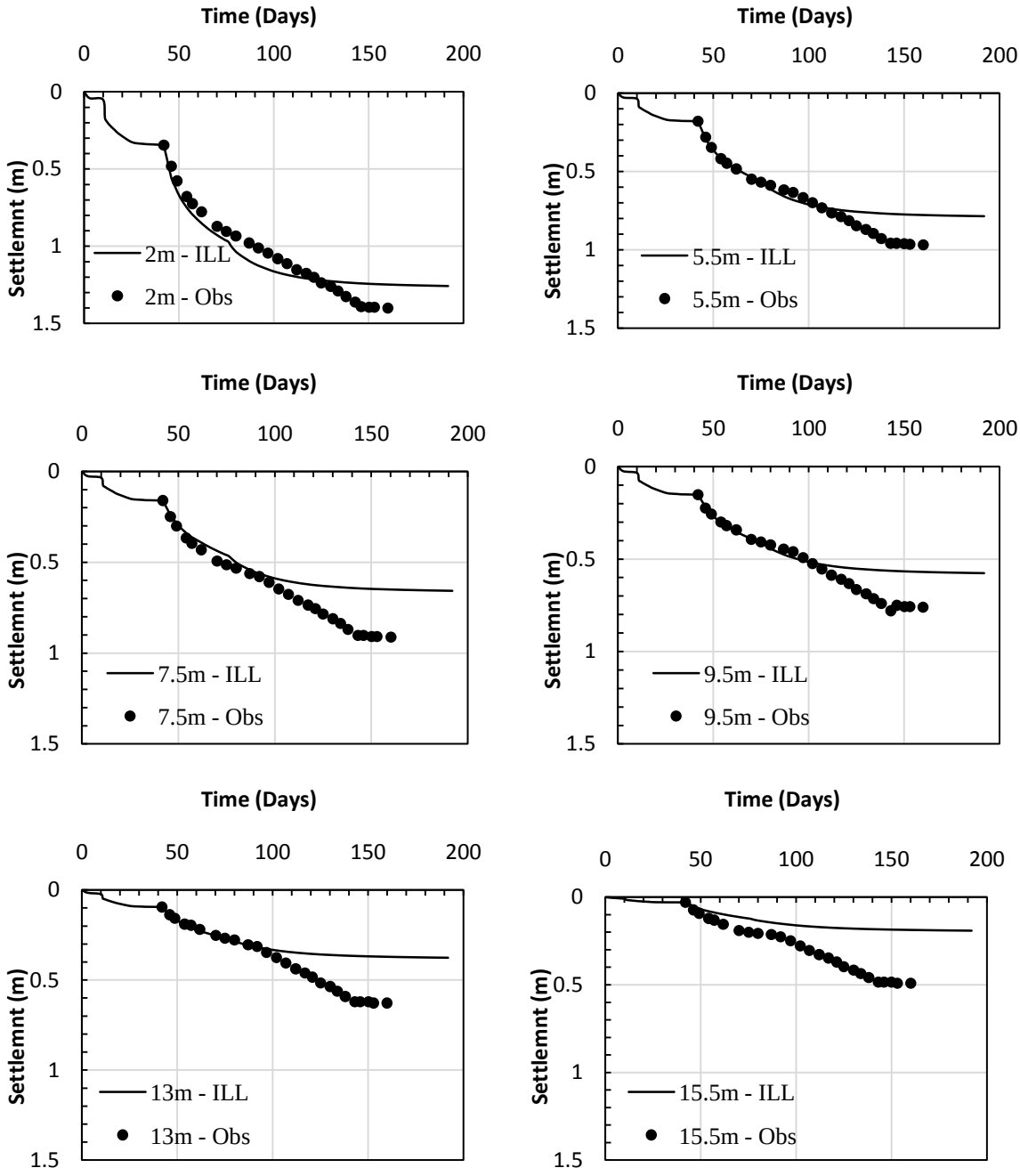

Figure 4.15: Comparison of observed and predicted subsurface settlements for case B loading condition in Section II

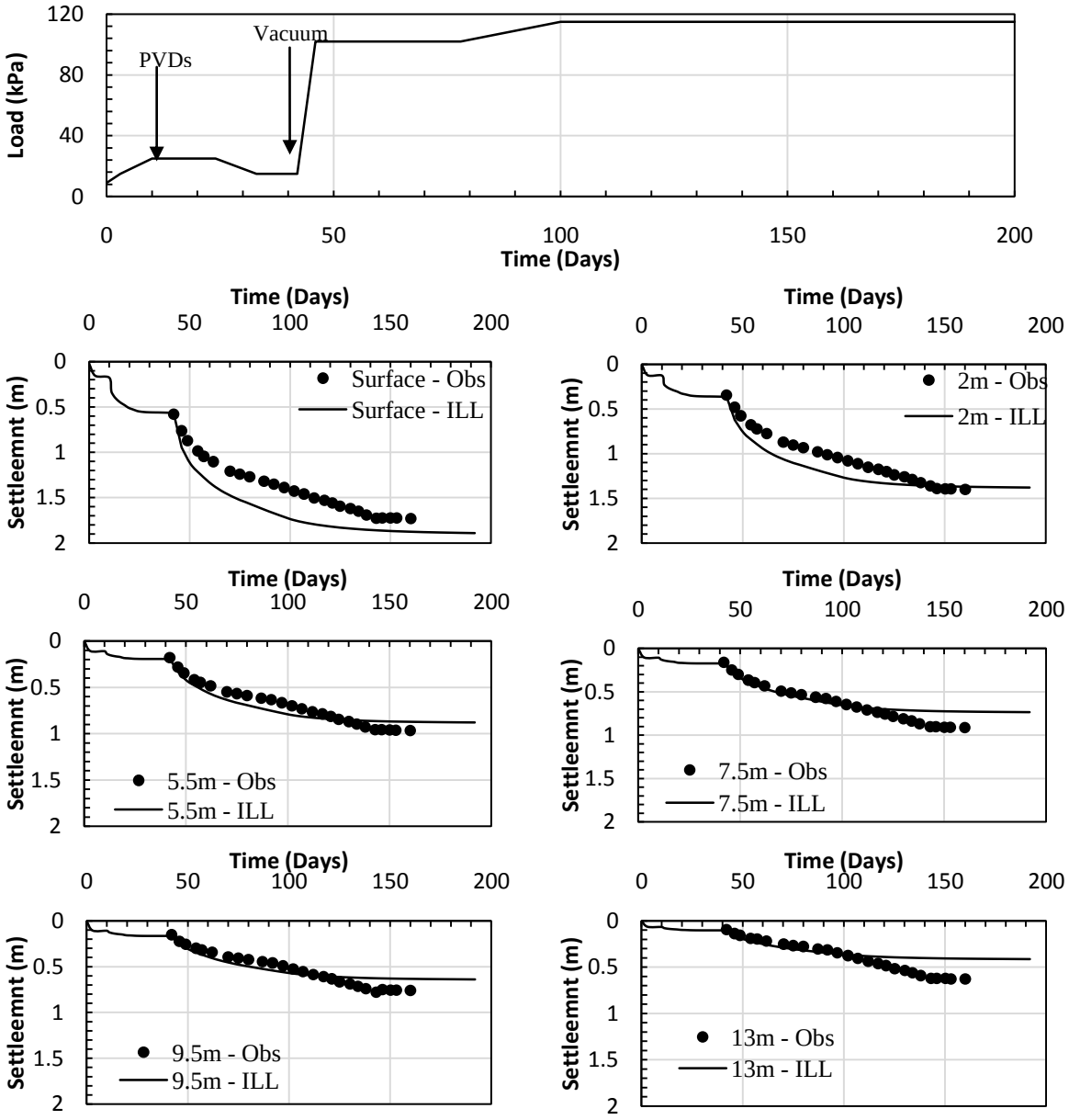

Figure 4.16: Comparison of observed and predicted settlements for different depths of section II with vacuum intensity increased to 100kPa after 100 days (60 days of vacuum application)

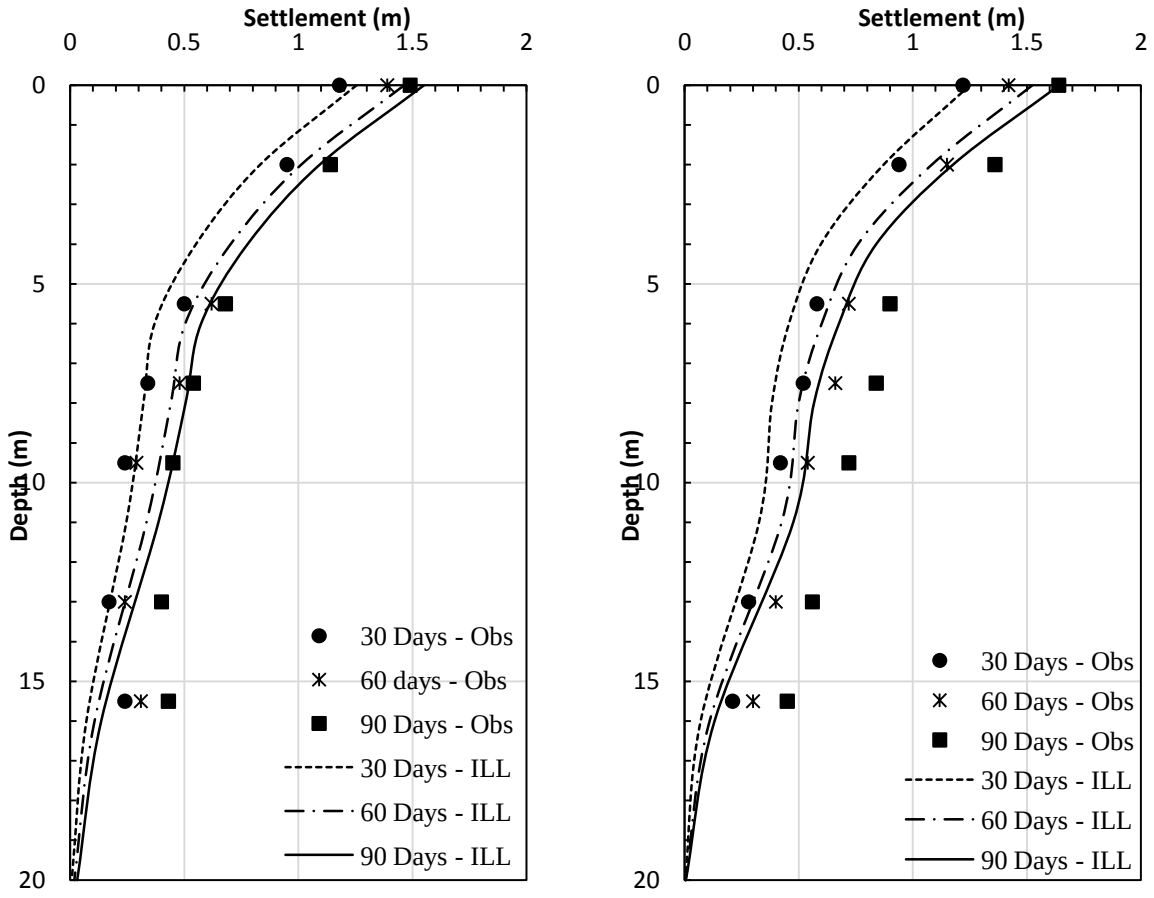

(a) Case B – section I

(b) Case B – section II

Figure 4.17: Observed and predicted settlements at different times and at different depths (a) Section I, and (b) Section II

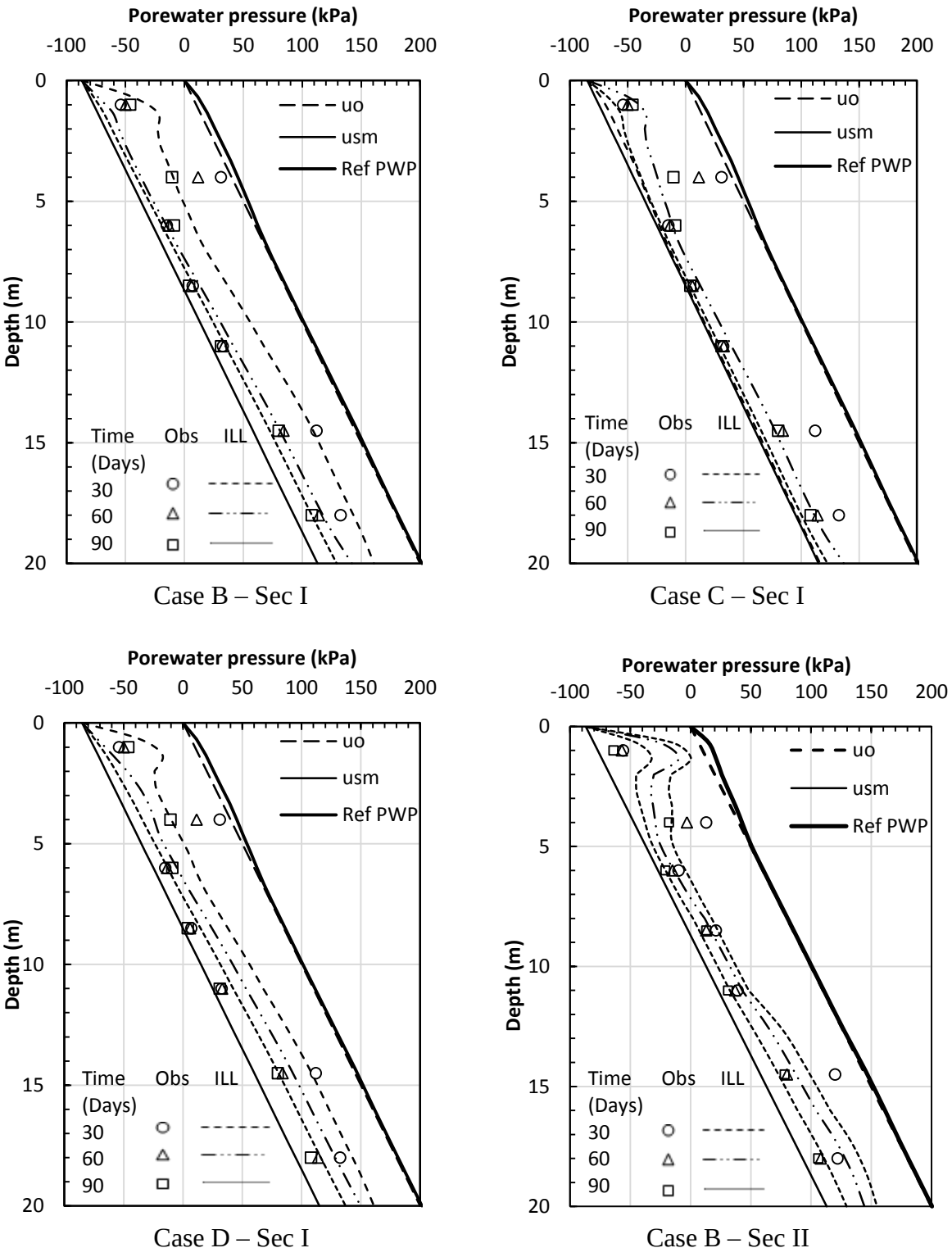

Figure 4.18: Observed and predicted porewater pressures at different times and at different depths for assumed loading conditions of Section I and Section II

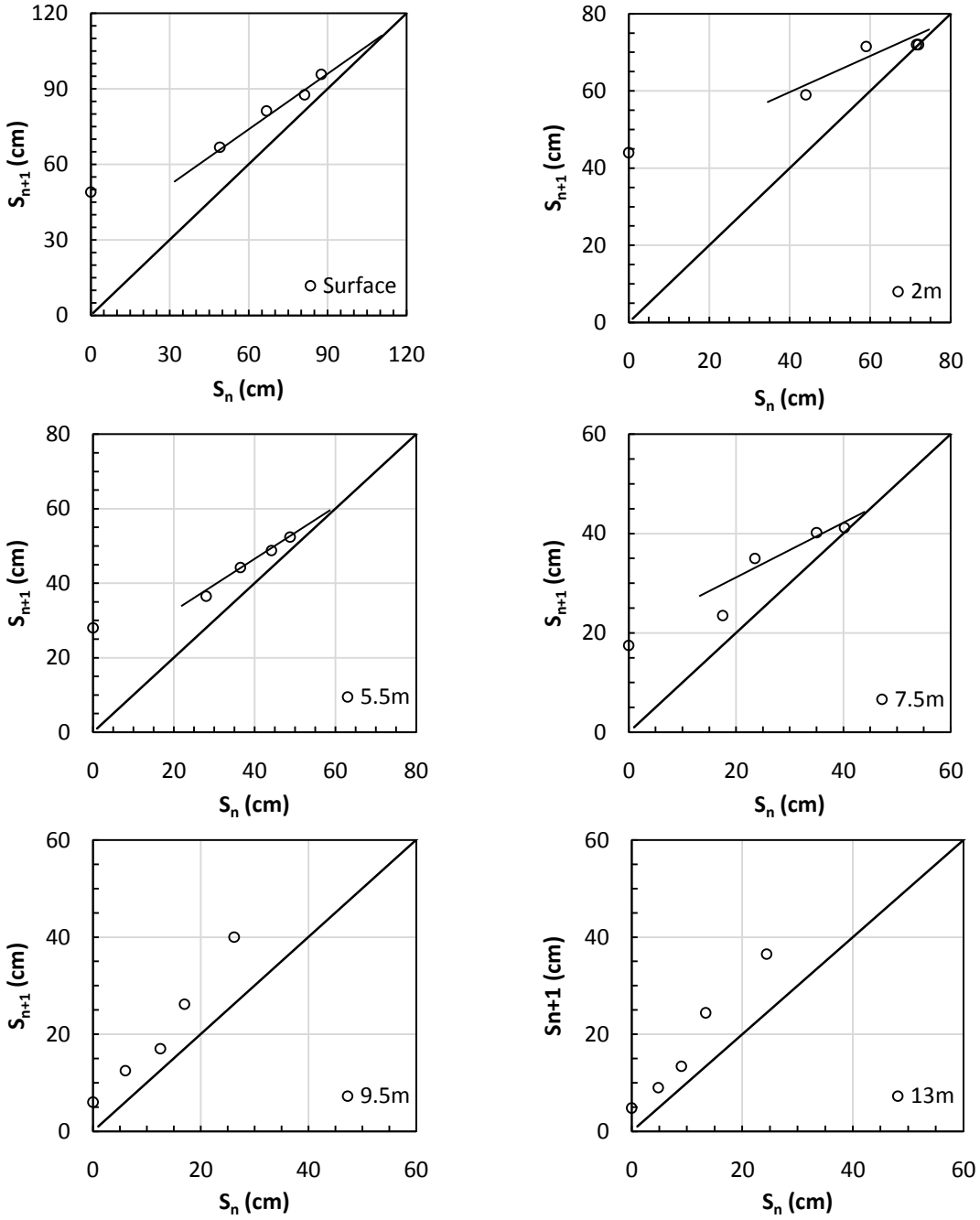

Figure 4.19: EOP settlements for surface and subsurface layers for Section I using the Asoaka Method

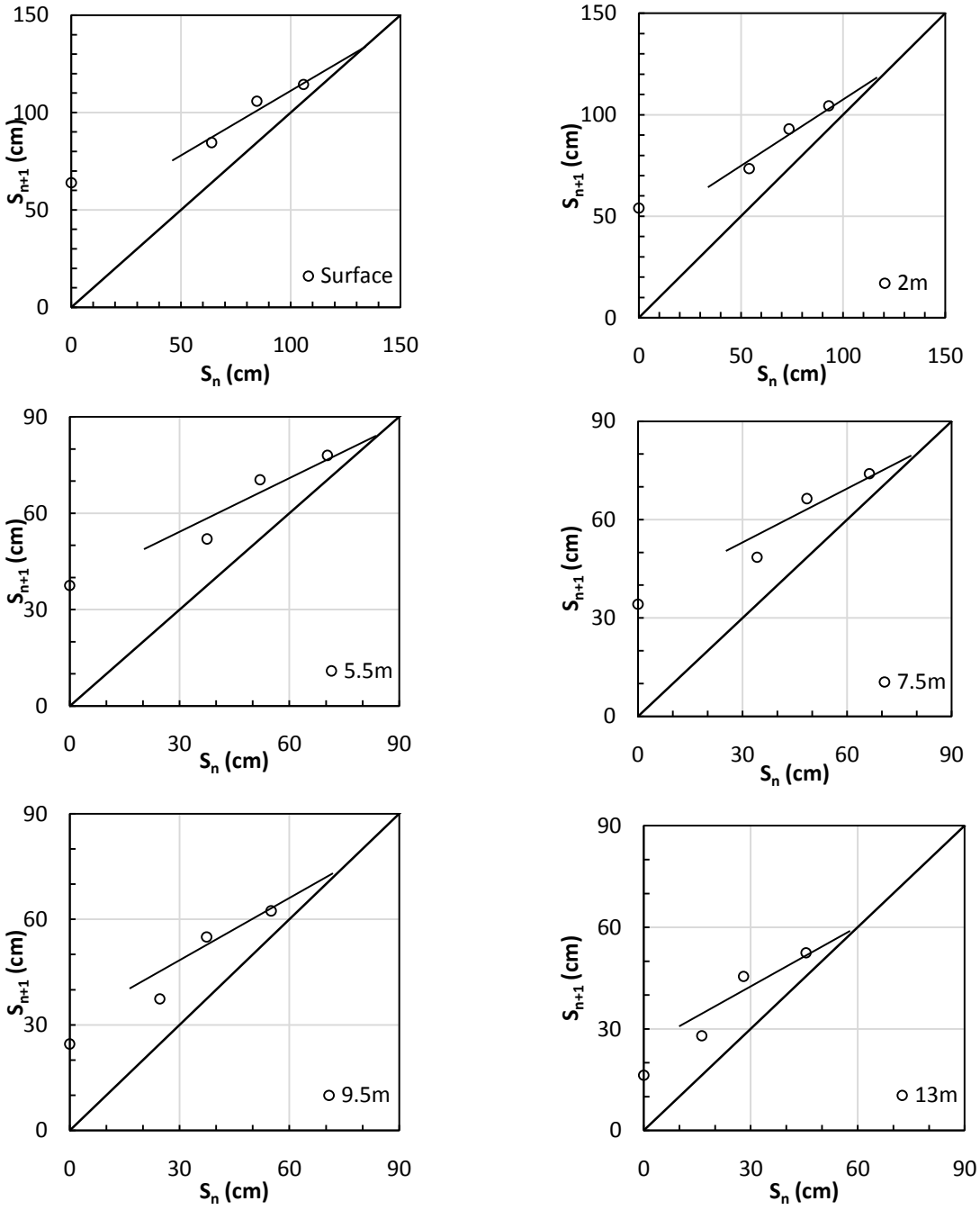

Figure 4.20: EOP settlements for surface and subsurface layers for Section II using the Asoaka Method

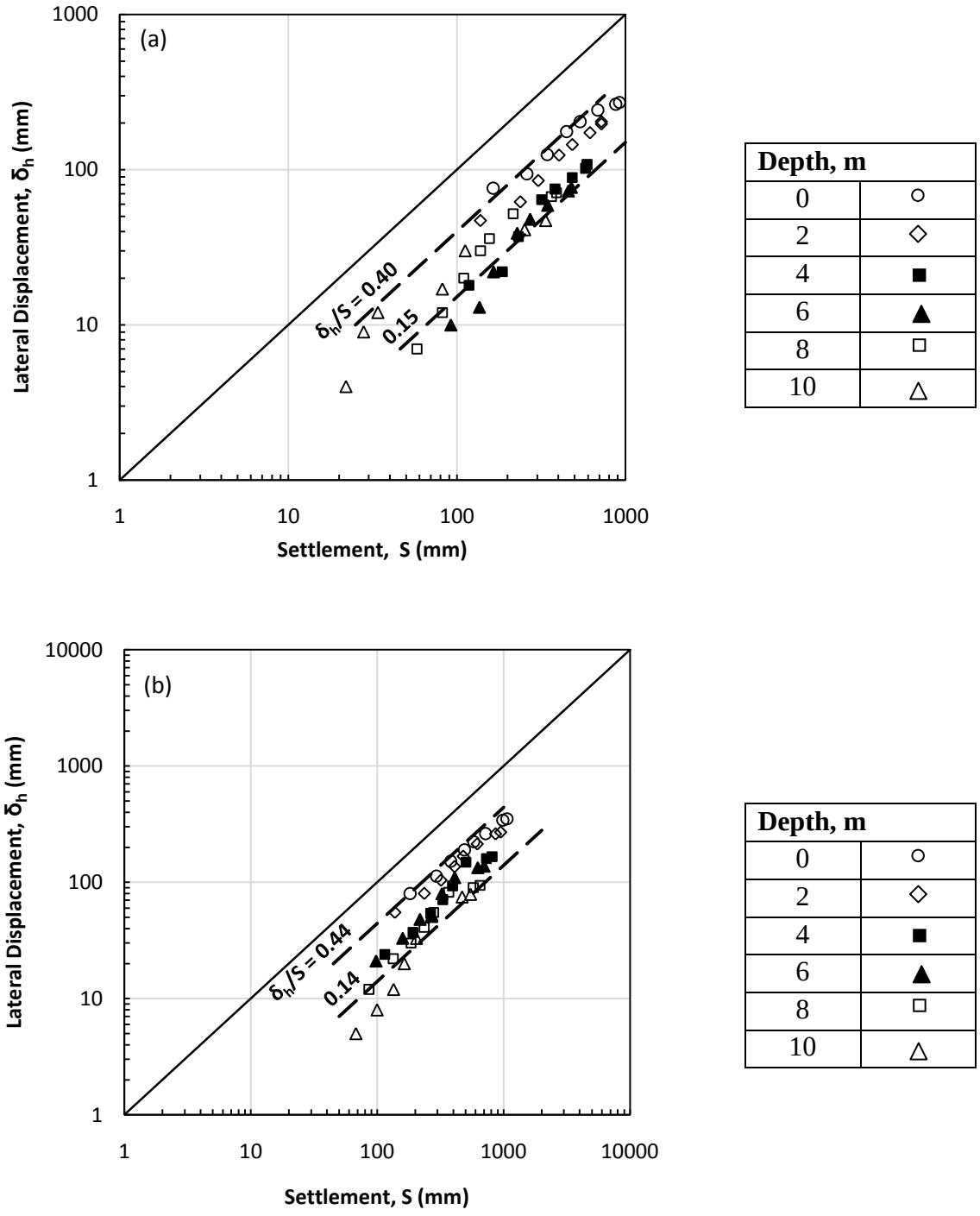

Figure 4.21: Lateral displacements at different depths plotted against settlements at respective depths for (a) Section I, and (b) Section II

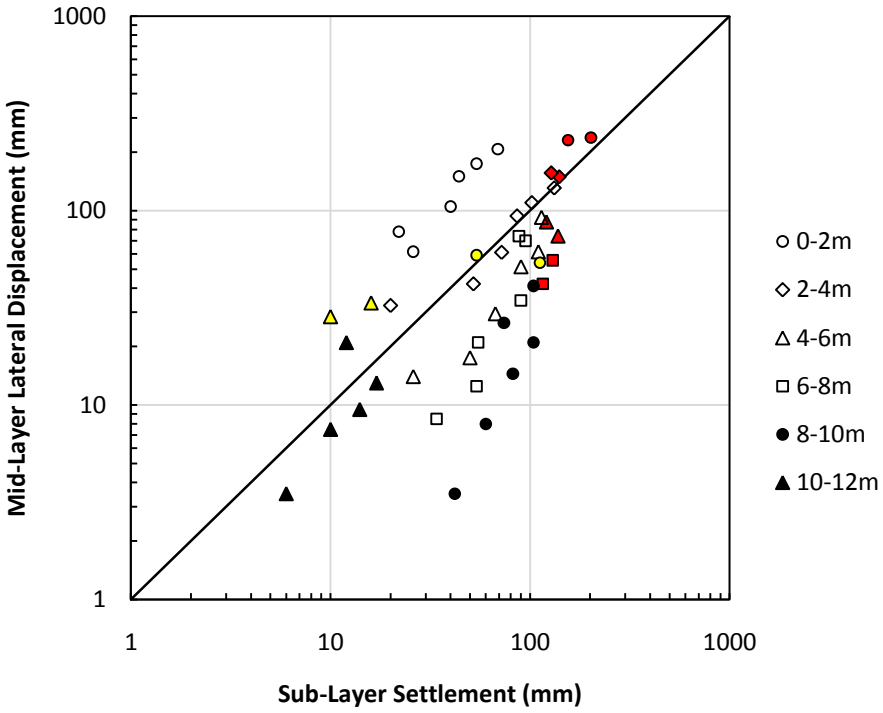

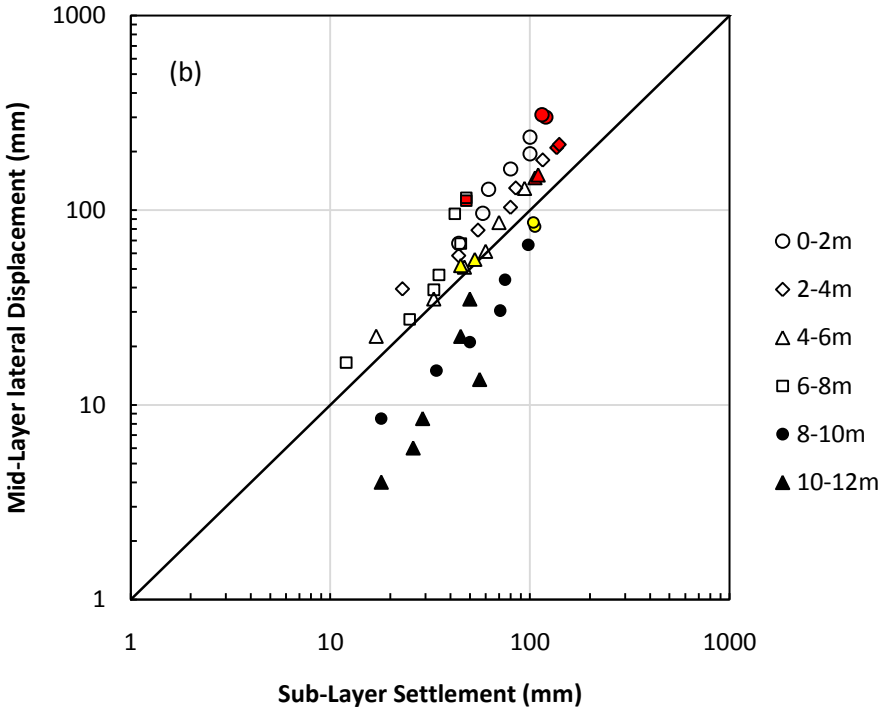

Figure 4.22: Mid-layer lateral displacements plotted against sub-layer settlements for (a) Section I, and (b) Section II

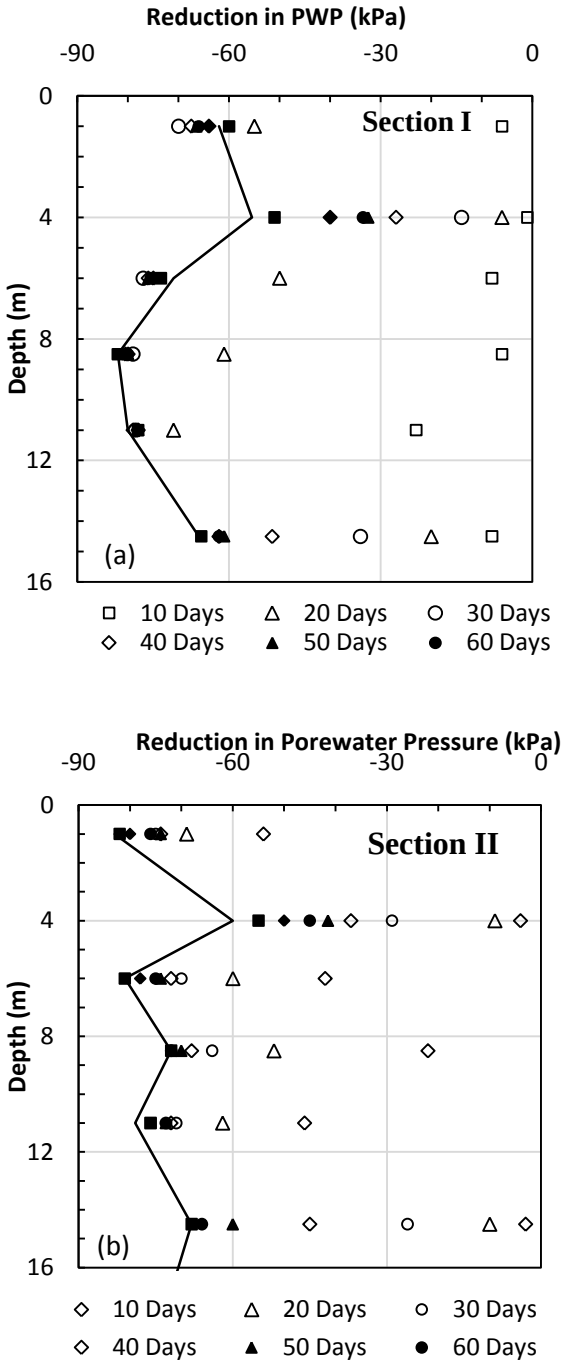

Figure 4.23: Vacuum pressure distribution in (a) Section I, and (b) Section II (data from Yan and Chu 2003)

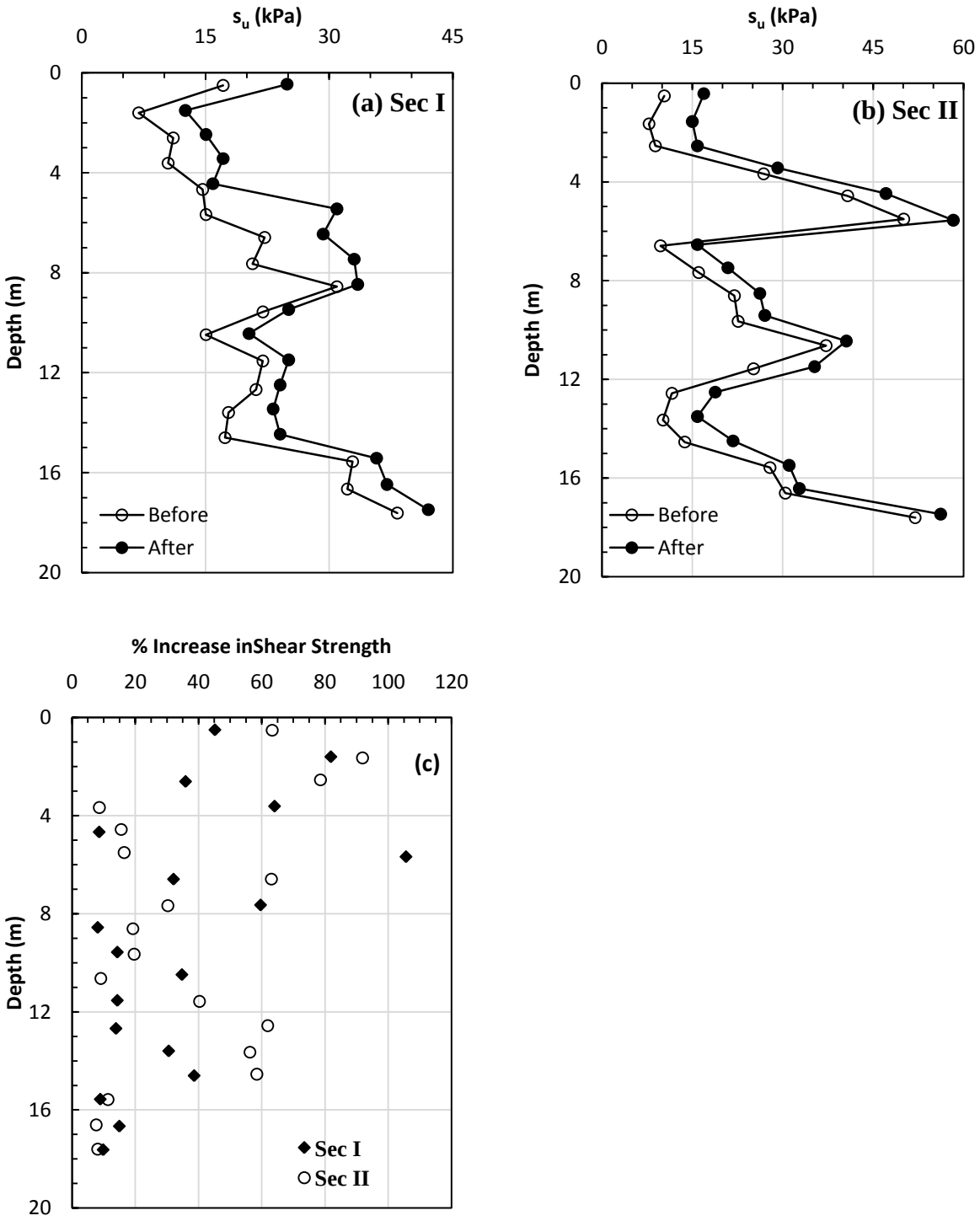

Figure 4.24: Increase in shear strength due to vacuum preloading (data from Yan and Chu 2003)

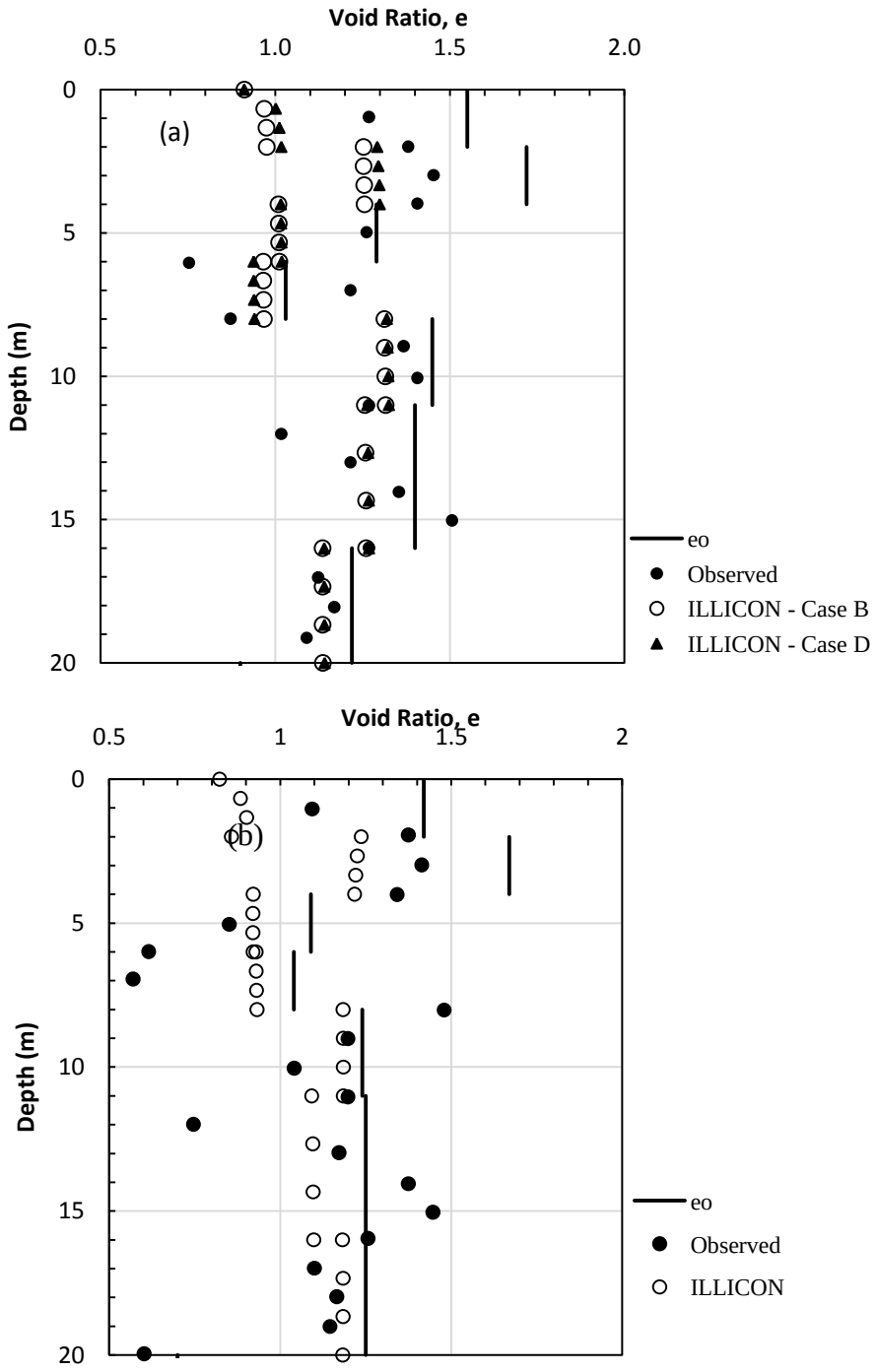

Figure 4.25: Comparison of measured and predicted distribution of void ratio with depth for (a) Section I, and (b) Section II

CHAPTER 5. VACUUM AND FILL PRELOADING OF SOFT GROUND, TOGETHER WITH PREFABRICATED VERTICAL DRAINS, FOR A STORAGE YARD AT PORT OF TIANJIN, CHINA

5.1 Introduction

Tianjin port is the largest man made port in China. It is located in the west of Bohai Gulf and on the north bank of the estuary of Haihe River (Yixiong, 1996a), approximately 170km southeast of Beijing. The port is mostly developed on dredged material reclaimed from sea bed in recent past. Construction of a new pier for expansion of Tianjin port included a storage yard which was to be constructed on a 3 to 4m thick, recently reclaimed clay layer underlain by 16 to 19m thick very soft seabed clay. The treatment area (7433m^2) was divided into three sections as shown in Fig. 5.1. A combination of vacuum and fill loading was used to apply the required preload. Vacuum was successfully maintained for the entire period of treatment (approximately six months) without any leakage. The only interruption in vacuum loading was due to a power failure in section I during 8/9th week of vacuum application.

The case history has been reported by Yan and Chu (2005), and has also been analyzed by Rujiakiatkamjorn et al. (2007). Section II, which was a well instrumented section and had an area of 3570m^2 (119m x 30m) is analyzed using the computer program ILLICON and the predictions are compared with field observations. The subsurface information for ILLICON analysis has been extracted from articles referred above. Empirical correlations have also been utilized to estimate parameters which were not reported.

5.2 Subsurface Conditions

The 22m thick compressible soil consists of four distinct layers. Fig. 5.2a presents the idealized soil profile which was similar in all three sections. The top 3.5m consists of dredged clay, recently reclaimed from the seabed. From 3.5m to 16m, soft clay layer consists of muddy clay and soft silt to silty clay layers. From 16 to 22m, a stiff silty clay layer is

present. The vertical distributions of various geotechnical properties are shown in Figs. 5.2b through 5.2e. It can be seen that the natural moisture content in the entire soil profile is either equal to or greater than the liquid limit. The void ratio varies between 1.0 and 1.8, except in the stiff silty clay layer where it is 0.70.

The position of ground water table is not specifically reported; however, the hydrostatic porewater pressure record (Fig. 8, Yan and Chu 2005) suggests that the groundwater table is located at a depth of 0.5m, and the same was used in the ILLICON analyses. The field vane and initial void ratio profiles indicate a desiccated crust with a thickness of 0.5m. Also, no pre-treatment was required before the installation of prefabricated vertical drains (PVDs) as has been required in other cases of dredged material in the Tianjin port area (Shang et al. 1998; Chu et al. 2000). Therefore, the assumption on location of groundwater table is considered reasonable. Rujiakiatkamjorn et al. (2007), however, for their analysis, have assumed water table at the ground surface. The seabed clay was still undergoing primary consolidation as a result of the placement of dredged materiall; hence, the excess porewater pressures observed at different depths are as shown in Fig. 5.3.

The compressible layer was divided into 9 sublayers for ILLICON analyses. The average soil properties used as input parameters for ILLICON analyses are shown with solid vertical lines on Fig. 5.2. The average properties were either directly used in the analysis or were used to estimate other properties which are required for the ILLICON analysis, but were not available in the literature that reported this case history.

5.3 EOP e - log σ'_v Relationships

ILLICON analysis requires an EOP e-log σ'_v relation for each layer. These relations for the treatment area are not available, and therefore, these were estimated based on the available data, empirical correlations and reasonable assumptions. In order to construct an EOP *e-log* σ'_v relation, information is required on initial void ratio, initial effective vertical stress, preconsolidation pressure and recompression and compression index. Preconsolidation pressure (σ'_p) was estimated both from field vane shear strength (empirical correlation between $s_{uo}(FV)/\sigma'_p$ and plasticity index, Terzaghi et al. 1996) and from the overconsolidation ratios suggested by Rujiakiatkamjorn et al. (2007). The values estimated from empirical relationship for top layers of soil were quiye high (probably due to unreliable field vane data), and, therefore, considered inconsistent with described consistency of soil

(dredged clay slurry). For the top layers, the σ'_p values estimated from overconsolidation ratios reported by Rujiakiatkamjorn et al. (2007) were used in the analyses. The value of compression index (C_c) beyond σ'_p, for various sublayers, was estimated using the empirical correlation between C_c and natural water content (w_o) as suggested by Terzaghi et al. (1996). A value of C_r/C_c = 0.1 was assumed for all sub layers. The values of compression index, preconsolidation pressure, and EOP *e-log* σ'_v relations for various sublayers are shown in Fig. 5.4.

5.4 Coefficient of Permeability

The *e-log* k_v relation is also an essential input information for the ILLICON analysis. As the permeability data are not reported in the literature, the initial permeability (k_{vo}) was estimated by using (1) empirical correlation suggested by Mesri et al. (1994), and (2) by computing coefficient of consolidation (c_v) and the coefficient of volume compressibility (m_v) based on the field data (as explained later). The values thus computed were compared with the values of k_{vo} reported by Rujiakiatkamjorn et al. (2007).

Assuming clay size fraction (*CF*) between 30 to 50%, k_{vo} values were computed using Eq. 5.1 (Mesri et al. 1994) and are shown in Table 5.1. A *CF* of 30% more closely represents the values reported by Rujiakiatkamjorn et al. (2007) for all layers except for dredged material.

$$k_{vo} = 6.5*10^{-11}\left[\frac{e_o/CF}{Ac+1}\right]^4 \tag{5.1}$$

where k_{vo} is the vertical permeability, e_o is the initial void ratio, *CF* is the clay size fraction, and A_c is the activity of soil.

The value of initial permeabily (k_{vo}) for various sublayers was also computed from the coefficient of consolidation (c_v) and the coefficient of volume compressibility (m_v) using Terzaghi's definition of c_v as given in Eq. 5.2 (Terzaghi et al. 1996).

$$c_v = \frac{1}{\gamma_w}\frac{k_v}{m_v} \tag{5.2}$$

The c_v for each sublayer was estimated from the empirical correlation between c_v and liquid limit proposed by Terzaghi et al. (1996), and m_v was computed from the change in effective stress ($\Delta\sigma'_v$) and the corresponding change in void ratio (Δe) for each sublayer. In this case also the computed values were in good agreement with the k_{vo} values reported by

Rujiakiatkamjorn et al. (2007) for all sublayers except for dredged material as shown in Table 5.1. Therefore, the computed value of k_{vo} was used for dredged material, whereas assuming that values reported by Rujiakiatkamjorn et al. (2007) were based on direct measurements of k_{vo}, were used for all other sublayers for the settlement analyses using ILLICON.

The decrease in permeability during consolidation was computed assuming a constant C_k between e_o and e_p (void ratio at the end of primary compression) which was determined from empirical correlation, $C_k = 0.5e_o$ (Tavenas et al. 1983; Mesri et al. 1994). Permeability anisotropy was not considered in the analysis, i.e. the ratio between horizontal and vertical permeability has been assumed as unity, as no data on k_h/k_v were available. The vertical profile of k_{vo}, C_k, and *e-log* k_v relations used in the analysis are shown in Fig. 5.5.

5.5 Prefabricated Vertical Drains (PVDs)

It has been previously assumed that PVDs perform without any well resistance when subjected to vacuum preloading. Hence, Yan and Chu (2005) have not mentioned any details regarding the type and properties of PVDs that were used in the project. Table 5.2 presents the PVD parameters reported by Rujiakiatkamjorn et al. (2007) as well as those assumed for the ILLICON analyses. It is interesting to note that the discharge capacity of PVDs used by Rujiakiatkamjorn et al. (2007) is sufficiently high for the drains to perform without any well resistance. Mesri and Lo (1991) reported that with a discharge factor [$D=q_w/(k_h*l_m^2)$] of 5, the drains can be assumed as freely draining; the discharge capacity of $100m^3$/yr. corresponds to a discharge factor of approximately 8 in this case. ILLICON analysis was carried out to evaluate the performance of PVDs as shown in Fig. 5.6. The radius of smear zone, r_s, was defined assuming $r_s/r_m = 2.4$, where r_m is the equivalent radius of the mandrel used to install PVDs. In the ILLICON analyses, the compressibility of the smear zone was defined by a constant C_c connecting (e_o, σ'_{vo}) to (e_p, σ'_{vf}), and the permeability of the smear zone remained the same as the vertical permeability of undisturbed soil because k_h/k_v was assumed as unity. It can be seen in Fig. 5.6a that beyond a discharge capacity of $50m^3$/yr., the drains are expected to perform without significant well resistance. Fig 5.6b shows that for the assumed loading condition (discussed subsequently in section 5.8 and shown in Fig. 5.9a), there is no increase in rate of settlement when the discharge capacity was increased from 54 to well over $100m^3$/yr. Moreover, the rate and magnitude of

settlement agree well with the field observations, which shows that PVDs performed without any well resistance.

5.6 Installation of Vacuum System

The vacuum consolidation system was installed in the following sequence:

- The ground surface was covered with a 0.3m thick sand blanket to serve as a drainage layer for PVDs and for housing of horizontal pipes for efficient distribution of vacuum pressure and collection of water.
- PVDs were installed to a depth of 20m in a square grid at spacing of 1m. The PVDs were installed using a steel mandrel which was continuously pushed into the soil using a static weight.
- Corrugated and perforated flexible pipes with a diameter of 100mm, wrapped in a filter fabric, were placed inside the sand blanket to link PVDs to vacuum pressure line.
- Three layers of thin (thickness not specified) PVC membranes were used to seal the area. The thin PVC membrane is susceptible to damage due to any sharp objects, debris or movement of animals etc. Moreover, the membrane can also have pin holes which may not be visible to naked eye but through which vacuum pressure can be lost. To safeguard against such eventualities, in China PVC membrane is often used in multiple layers.
- Vacuum pressure was then applied using jet pumps.

Note: *The authors have not mentioned about the construction of peripheral trench which is used to anchor PVC membranes and is an essential requirement for completing sealing of the area. However, the trench can be dug simultaneously with other activities and may not need separate allocation of time.*

5.7 Instrumentation

All three sections were instrumented for monitoring settlements; however, Section II was most comprehensively instrumented. The instrumentation for Section II included surface settlements plates, multilevel settlement gauges, inclinometers, porewater pressure transducers and standpipe piezometers. The plan and section location of various instruments is shown on Fig. 5.1 and Fig. 5.7, respectively.

5.8 Loading Sequence

The placement of 0.3m thick sand blanket for installation of PVDs and for application of vacuum loading induced a uniform pressure of 6kPa on the ground surface. The ground was first subjected to a vacuum pressure of more than 80kPa for a period of 4 to 8 weeks. It is important to note that a nominal vacuum pressure of 80kPa is reported by Yan and Chu (2005) and the same intensity is used by Rujiakiatkamjorn et al. (2007) for their analysis. However, the measurements in Fig. 4 of Yan and Chu (2005) indicate that in all sections, a vacuum in excess of 80kPa was successfully maintained throughout the pumping duration. For Section II, the average intensity of vacuum pressure was maintained at 87kPa and this value has been used in the ILLICON analyses. In all sections, vacuum pressure achieved its full intensity in 3 to 4 days. After 4 – 8 weeks of vacuum application, a silty clay fill with an average unit weight of 17.1kN/m^3 was placed in stages on top of the sealing membranes. The total fill height was 2.53, 3.50 and 2.84m in sections I, II and III respectively. The treatment began in section I and was followed by section II and then section III.

Loading schedule used in the ILLICON analyses is shown in Fig. 5.8a. Following was considered in constructing the loading schedule for each layer

- The time of loading started with the placement of 0.3m thick sand blanket which was considered as a strip load of 6kPa applied uniformly over the ground surface.
- The pretreatment excess porewater pressure as shown in Fig. 5.3 was considered to be equal to the vertical stress increase at the corresponding depth. This implies that at time t=0, an instantaneous load equal to the pretreatment excess porewater pressure was applied at respective depths for the analysis. For example, a load of 45kPa was applied at a depth of 14.5m at zero time. Vertical distribution of pretreatment excess porewater pressure taken into account in the loading schedule is shown in Fig. 5.9.
- Vacuum loading was considered to act as a wide fill, i.e. vacuum load was transferred with full intensity to the penetration depth of vertical drains. Following the application of vacuum, settlements were observed at a depth of 14.5m suggesting that vacuum was effective within the vertical drain for the

entire thickness of soft clay (including muddy clay and soft silt to silty clay). A period of 4 days was considered for vacuum to develop to its full intensity within the drainage system.

- Elastic stress distribution was assumed for sand blanket and applied fill load assuming uniform strip loading.
- PVDs and horizontal drainage system are installed in the ground using light weight machinery. A live load of 10kPa was assumed in the analysis to act for a duration of 2 weeks (Figure 5.8a).
- Vacuum load was applied 30 days after the placement of the sand blanket.

5.9 Settlements

The extracted/assumed parameters for ILLICON analyses are considered reasonable because of the following

- Based on field observations, ground surface EOP settlement predicted by the Asoaka method is around 1.96m as shown in Figure 5.10. This settlement, together with settlement before the commencement of field observation at the application of vacuum, predicts an EOP settlement of 2.27m. The settlement predicted by ILLICON analysis is 2.10m, which is a reasonable agreement.
- The degree of primary consolidation at the end of preloading (180 days of vacuum treatment) as reported by Yan and Chu (2005) is between 82% and 87% based on porewater pressure data and settlement data, respectively. The corresponding degree of primary consolidation predicted by ILLICON is 85%.

Surface settlements of 0.21, 0.31 and 0.25m were observed respectively, in Sections I, II, and III, after installation of PVDs and before application of the vacuum load. These settlements are attributed to the dissipation of the pretreatment excess porewater pressure, soil disturbance due to installation of PVDs, and machinery live load. Figure 5.8b shows the comparison of observed settlements and those predicted by ILLICON. It is important to note that the initial settlement of 0.31m was added to the observed surface settlements reported on Fig. 4 of Yan and Chu (2005) which started at the application of vacuum 30 days after the placement of drainage layer. Similarly, a time period of 30 days was added to each field observation time to make it comparable with the ILLICON predictions. It can be seen from

Fig. 5.8b that there is an excellent agreement between the observed and the predicted ground surface settlement. ILLICON predicts a surface settlement of 0.29m before the application of vacuum load, which is similar to the observed settlement of 0.31m. Figure 5.11 compares the observed and predicted subsurface settlements. Subsurface settlements predicted by ILLICON at 30 days were added, at the corresponding depths, to the observed subsurface settlements reported on Fig. 6b of Yan and Chu (2005). Figure 5.11 also shows excellent agreement between the observed and predicted settlements and reinforces the fact that a vacuum load acts in a similar way as a fill load. The vertical profiles of observed and predicted settlements at different times as shown in Fig. 5.12 also show a very good agreement between observed and predicted settlements at all depths at different times. Hence a combination of vacuum-fill preload can be modeled as a single fill load with equivalent intensity to estimate the settlement.

5.10 Porewater Pressure

Figures 5.13 and 5.14 show, respectively, the comparison of observed and predicted porewater pressures with respect to time at different depths, and with respect to depth at different times. The porewater pressures from ILLICON analysis were interpreted using Eq. 4.2. As in the case of settlement, the reported data has been reinterpreted considering the following:

- The observed data has been reported starting from the time of application of vacuum, whereas, the settlement analyses using ILLICON started from the placement of sand blanket. Therefore, to compare the observed data with ILLICON predictions, ILLICON time is taken as a reference and a period of 30 days is added to the field observations in Fig. 7 of Yan and Chu (2005).
- The reported data (Figs. 7 and 8 of Yan and Chu; 2005) give the observed reductions in porewater pressure with time considering the pretreatment excess porewater pressure as the reference line. This cannot be justified because part of these pretreatment excess porewater pressures dissipated as evidenced by the settlement observed before the application of vacuum load. Therefore, the reference porewater pressure for the comparison of observed and predicted settlements is taken as the total porewater pressure predicted by

ILLICON at 30 days (just before application of vacuum) for the respective depths.

It can be seen from Fig. 5.13 that there is generally a good agreement between the observed and predicted porewater pressures at all depths. The minor differences between in observed and predicted response can be attributed to the uncertainties in soil properties used in the analyses, especially in permeability data. The differences in distribution of observed and computed porewater pressure with depth (Fig. 5.14) at various times is because of the difference in the reference porewater pressures. Because Yan and Chu (2005) did not take into account the dissipation of pretreatment excess porewater pressure, their distribution of porewater pressures with depth, which is essentially parallel to the pretreatment excess porewater pressure line, is not considered reasonable. Moreover, the agreement in observed and predicted porewater pressure response with time at various depths confirms that the interpretation of porewater pressures with depth suggested by Yan and Chu (2005) cannot be justified.

5.11 Lateral Displacements

A vacuum load results in an inward lateral displacement as a result of consolidation and volume decrease (toward the center of loaded area), whereas a fill load generates outward movements (away from the center of loaded area) as a result of shear stresses generated in the soil. The relative magnitude of these movements depends upon the magnitudes as well as the sequence in which vacuum and fill loads are applied. As discussed earlier, the vacuum load of 87kPa was first applied for 4 – 8 weeks followed by a gradual application of fill load of 60kPa, as vacuum loading was continued. As a consequence, the inward ground movements were experienced for the duration for which only vacuum was acting on ground. However, as soon as the fill load was placed, the inward movements at the ground surface were counteracted by outward lateral deformation of soil. As a result, the net inward movements at the ground surface, at the end of preloading were less than the maximum inward movement under vacuum load alone as shown in Fig. 5.15. However, it can also be seen from Fig. 5.15 that the interaction between inward and outward lateral movements is different at different depths in both sections. In addition to differences in relative magnitudes and time rate of applied vacuum and fill preloads, it is important to realize that (1) vacuum pressure in soil may vary with time as well as with depth, and (2)

after initial outward deformation at the boundaries of loaded area, a fill load is also likely to contribute toward the inward movement with the progress of consolidation; therefore, no fixed relation can be expected between lateral displacements and settlements under a combined vacuum-fill preload. Hence it is reasonable to examine lateral displacements due to vacuum load acting alone, i.e. up to a time when fill load was added.

Figure 5.16 shows the lateral displacements plotted against settlements at different times and at different depths due to vacuum load only, for Sections I and II (data up to 39 days for Section I and 42 days for Section II). It can be seen from Fig. 5.16 that lateral displacements due to vacuum only are (1) maximum at ground surface and gradually decrease with depth, (2) linearly related to vertical settlements especially at shallow depths, and (3) at any time, 30 to 40% of settlements near the ground surface, and 10% of the settlements at greater depth. Mid-sublayer lateral displacements plotted against sublayer settlements are shown in Fig. 5.17. For section II, the mid-sublayer lateral displacement at surface and at shallow depths are generally greater than the sublayer settlements, however, at greater depths the sublayer settlements are greater. In section I, initially all sublayers (except sublayer at depth of 6 – 8m) experienced greater mid-sublayer lateral displacements than the corresponding sublayer settlements; however, with time settlements became more significant at greater depths as shown in Fig. 5.17a. This might be due to development of higher vacuum intensity at greater depth in earlier times as compared to the shallow depths; however, due to non-availability of porewater pressure records for Section I, it is difficult to draw a more meaningful interpretation.

5.12 Increase in Undrained Shear Strength

Field vane was used to measure the undrained shear strength before and after the ground improvement. An increase in vane undrained shear strength at all depths is reported for Sections II and III by Yan and Chu (2005). The ratio of shear strength after preloading to shear strength before preloading, $s_u(FV)/s_{uo}(FV)$, with depth is shown in Fig. 5.18a. The increase in shear strength expressed in terms of $s_u(FV)/s_{uo}(FV)$ is more or less constant with depth. For Section II, the maximum increase in undrained shear strength was observed at a depth of 17m, where the strength increased from 17kPa to 58kPa. For Section III, the maximum increase in undrained shear strength was observed at a depth of 2m, where the strength increased from 16 to 45kPa. Moreover, Fig. 5.18 does not suggest any particular

pattern for increase in shear strength with depth. Distribution of vacuum intensity with depth for section II at various times is shown in Fig 5.18b. The vacuum pressure distribution up to 40days (vacuum was acting alone during this period) shows that initially, higher vacuum intensity developed in deeper sublayers and hence a greater increase in shear strength is expected. However, as the shear strength is measured at the end of preloading operation, the increase in shear strength also includes the effects of fill preload; therefore, the effect of vacuum alone cannot be estimated. By the end of preloading operation (fill load included), the vacuum intensity was more or less constant with depth. It is therefore considered more reasonable to explain the increase in shear strength due to vacuum or combined vacuum-fill preloading in terms total load (consolidation pressure, σ'_{vc}) under which consolidation progresses at different depths.

5.13 Concluding Remarks

The ILLICON settlement analyses of this case history of combined vacuum-fill preload shows the following:

- Taking into account loading and consolidation resulting from pre-vacuum activities such as placement of sand blanket, installation of vertical drains, and machinery live load, etc. is essential for meaningful comparison of observations of settlement and porewater pressures.
- Vacuum may develop to full intensity at different rates at different depths; however, with time vacuum intensity in soil became constant with depth.
- The combined application of a vacuum-fill preload can be analyzed in a similar way as that of an equivalent fill load acting alone.
- Porewater pressures due a combined vacuum-fill preload can be interpreted with reasonable accuracy using Eq. 4.2.
- PVDs performed without any significant well resistance.
- Lateral displacements generally reduce with depth; moreover, lateral displacements were generally in the range of 10 – 40% of the vertical settlements at that depth. In addition to other factors, vacuum intensity at different depths is expected to be a major factor affecting lateral displacements.

- The increase in shear strength expressed in terms of $s_u(FV)/s_{uo}(FV)$ is independent of the depth. It is more reasonable to explain the increase in shear strength as a function of consolidation pressure.

5.14 Tables

Table 5.1: Initial vertical permeability computed using Eqs. 5.1 and 5.2

Layer #	Description	Iniitial Permeablity, k_{vo} (cm/s)				
		Computed, Eq. 5.1		Computed, Eq. 5.2	Reported[1]	ILLICON
		CF= 30%	CF=50%			
1	Dredged Slurry	2.02E-07	5.2E-08	2.7E-07	6.7E-08	3E-07
2	Muddy Clay	6.39E-07	1.5E-07	2.3E-07	1.3E-07	1.3E-07
3	Muddy Clay	1.84E-07	5E-08	1.3E-07	1.3E-07	1.3E-07
4	Soft Silt to Silty Clay	1.6E-07	4.8E-08	9.3E-08	6.7E-08	6.7E-08
5	Soft Silt to Silty Clay	3.96E-07	1.2E-07	8.0E-08	6.7E-08	6.7E-08
6	Soft Silt to Silty Clay	2.22E-07	6.4E-08	7.0E-08	6.7E-08	6.7E-08
7	Stiff Silty Clay	1.57E-07	3.7E-08	4.9E-08	1.7E-08	1.7E-08
8	Stiff Silty Clay	6.37E-08	1.2E-08	3.4E-08	1.7E-08	1.7E-08
9	Stiff Silty Clay	6.37E-08	1.2E-08	2.9E-08	1.7E-08	1.7E-08

[1]Reported by Rujiakiatkamjorn et al. (2007)

Table 5.2: PVD parameters used in ILLICON analysis

Section	100mm x 3mm	Rujiakiatkamjorn et al. (2007)
Discharge Capacity, q_w	100 m^3/year	
Dimension of Mandrel	120mm x 50mm	
Penetration Depth, l_m	20m	
Spacing	1.0m square grid	
r_s/r_m	2.4	Assumed
Time for Installation of drains	7 days	
r_s : Radius of smear zone r_m : Radius of mandrel		

5.15 Figures

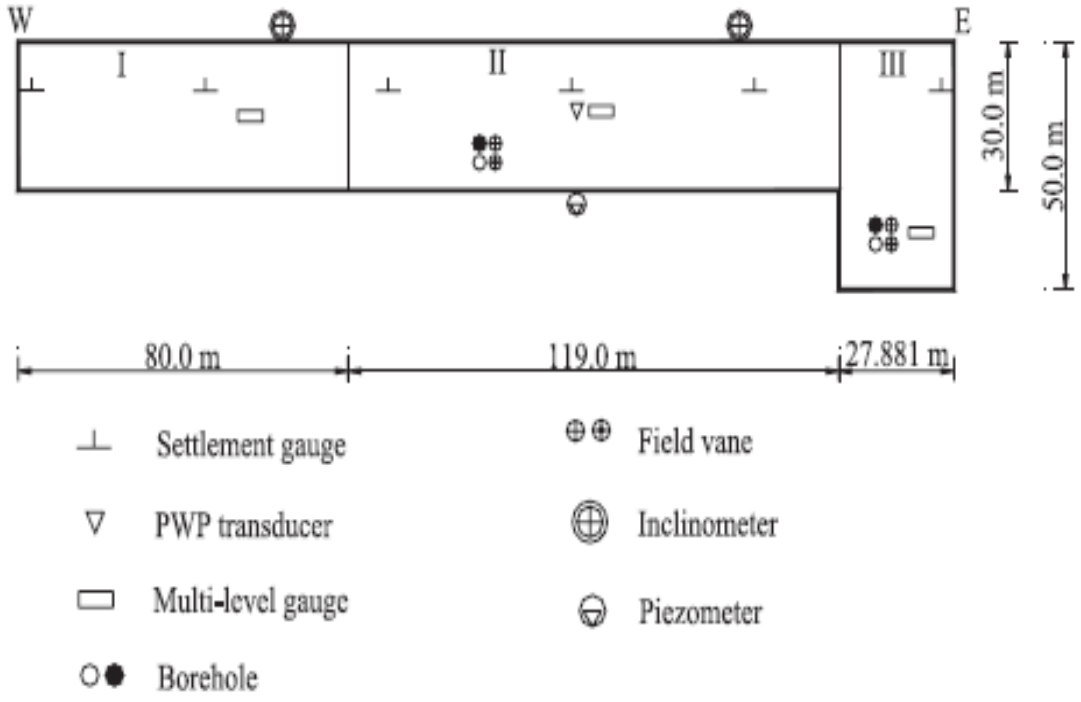

Figure 5.1: Plan view of treatment area with location of various instruments (after Yan and Chu 2005)

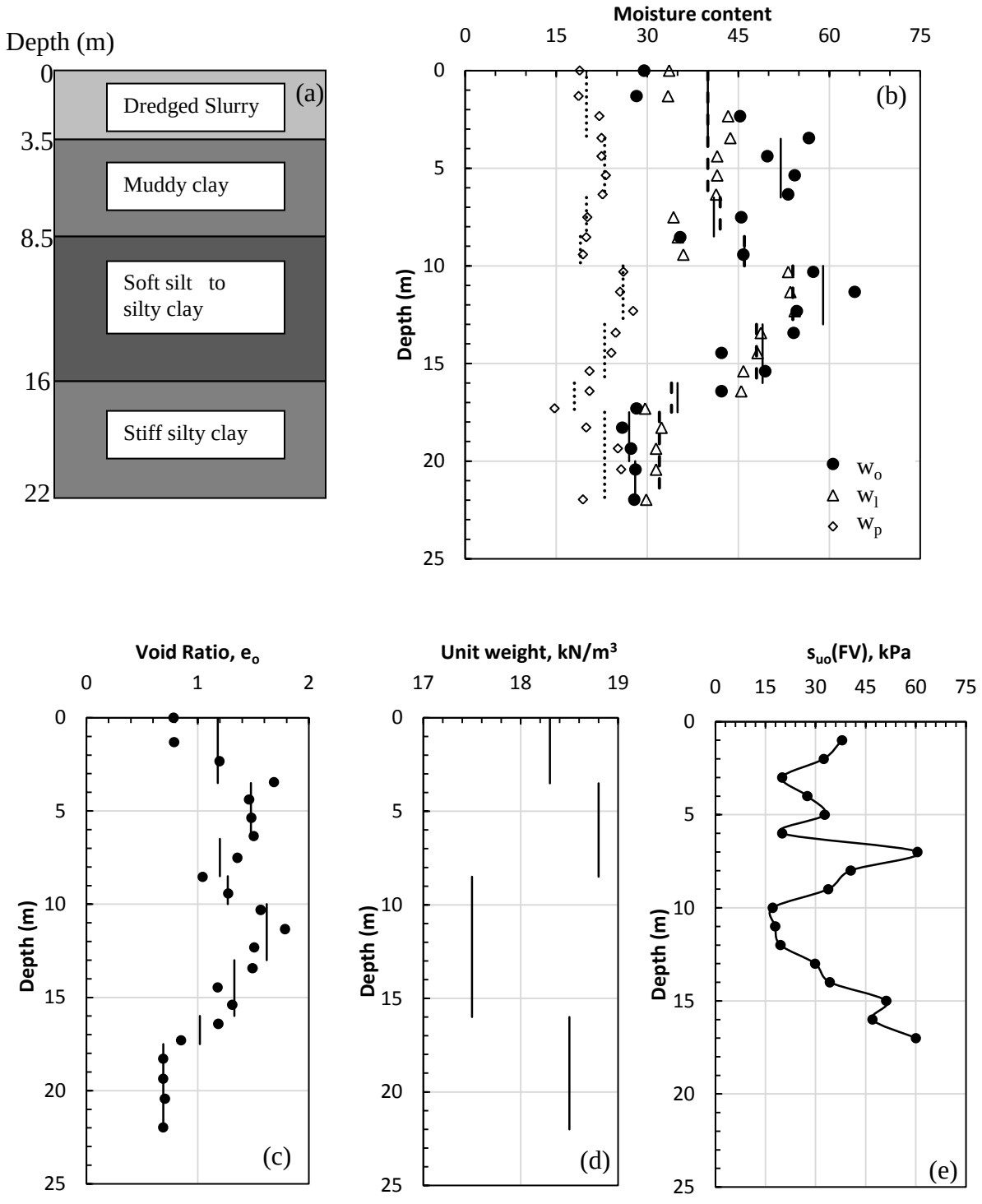

Figure 5.2: Generalized ground profile and distribution of geotechnical properties with depth

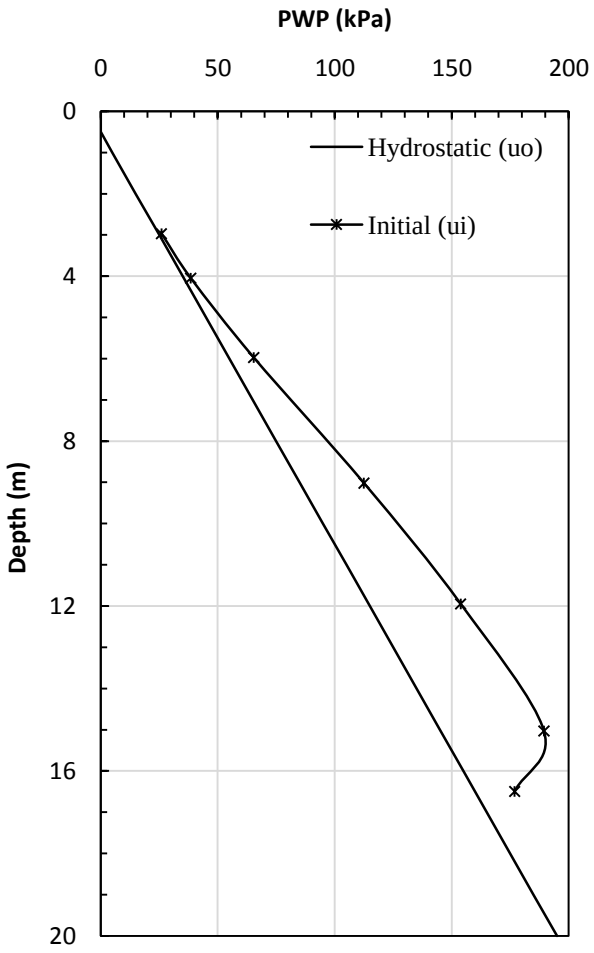

Figure 5.3: Porewater pressure before commencement of treatment

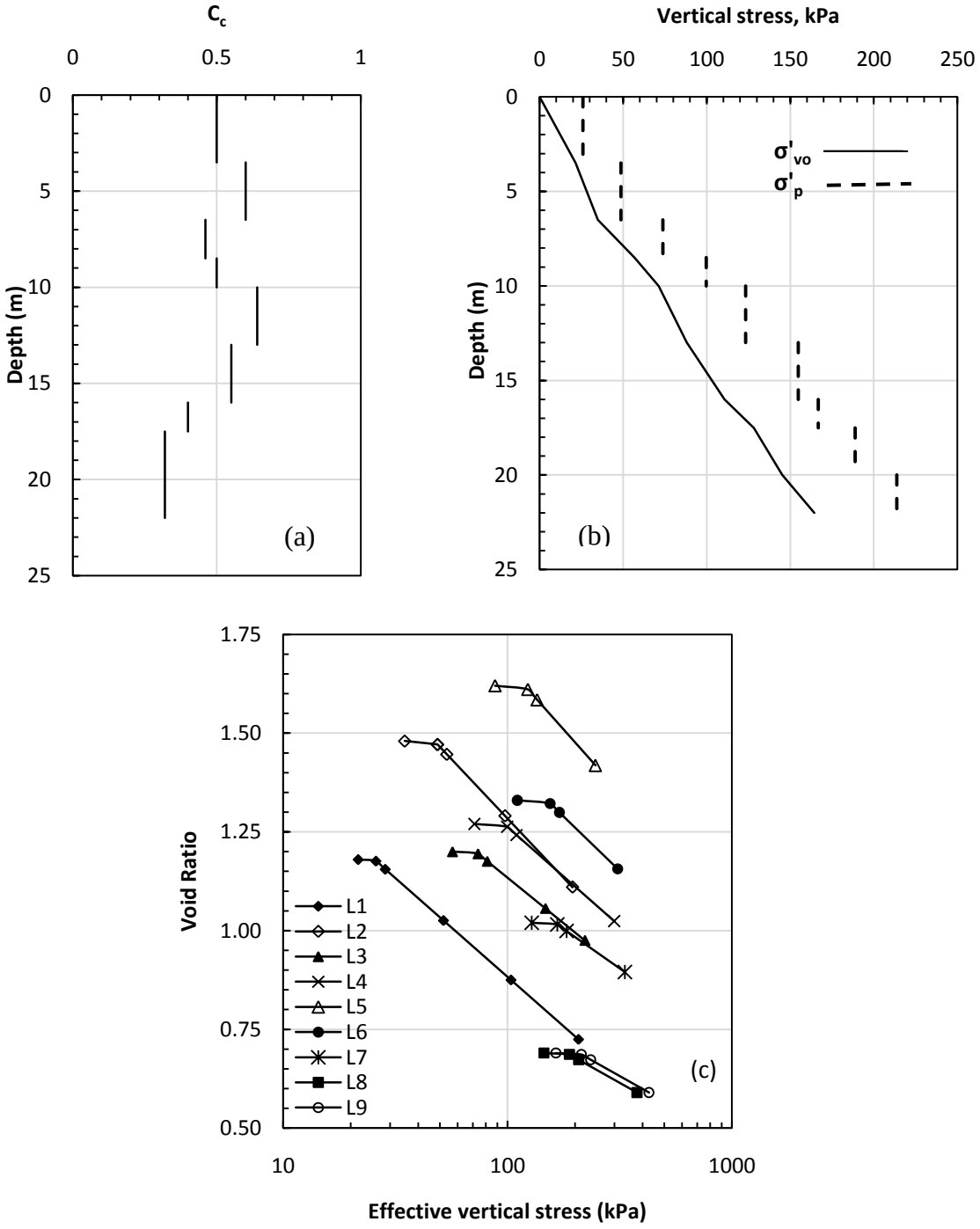

Figure 5.4: Vertical profile of (a) compression index, (b) preconsolidation pressure with depth, and (c) EOP e-log σ'_v relations for different sublayers

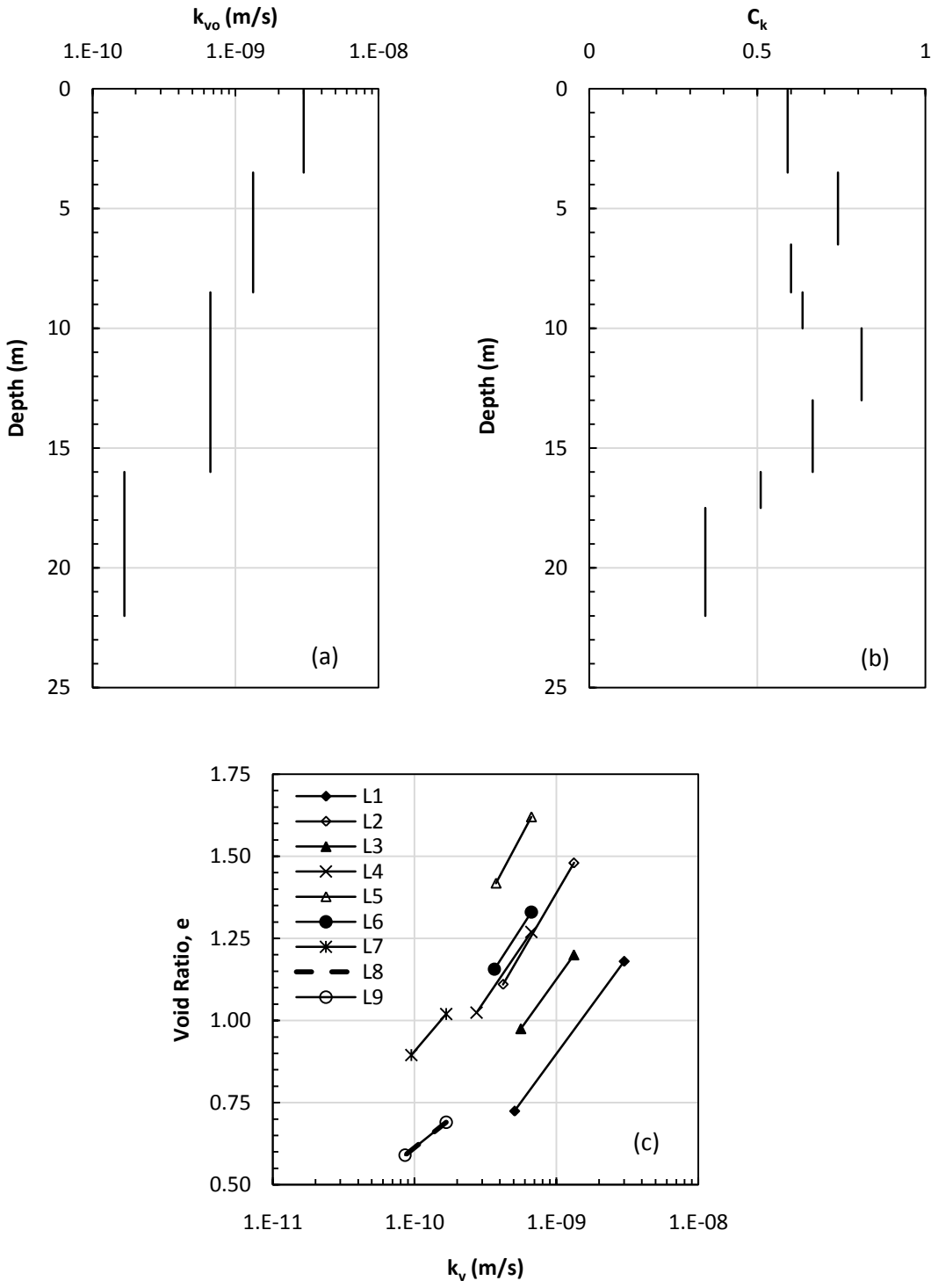

Figure 5.5: (a) k_{vo} profile (b) C_k profile and (c) e-log k_v relations for different sublayers

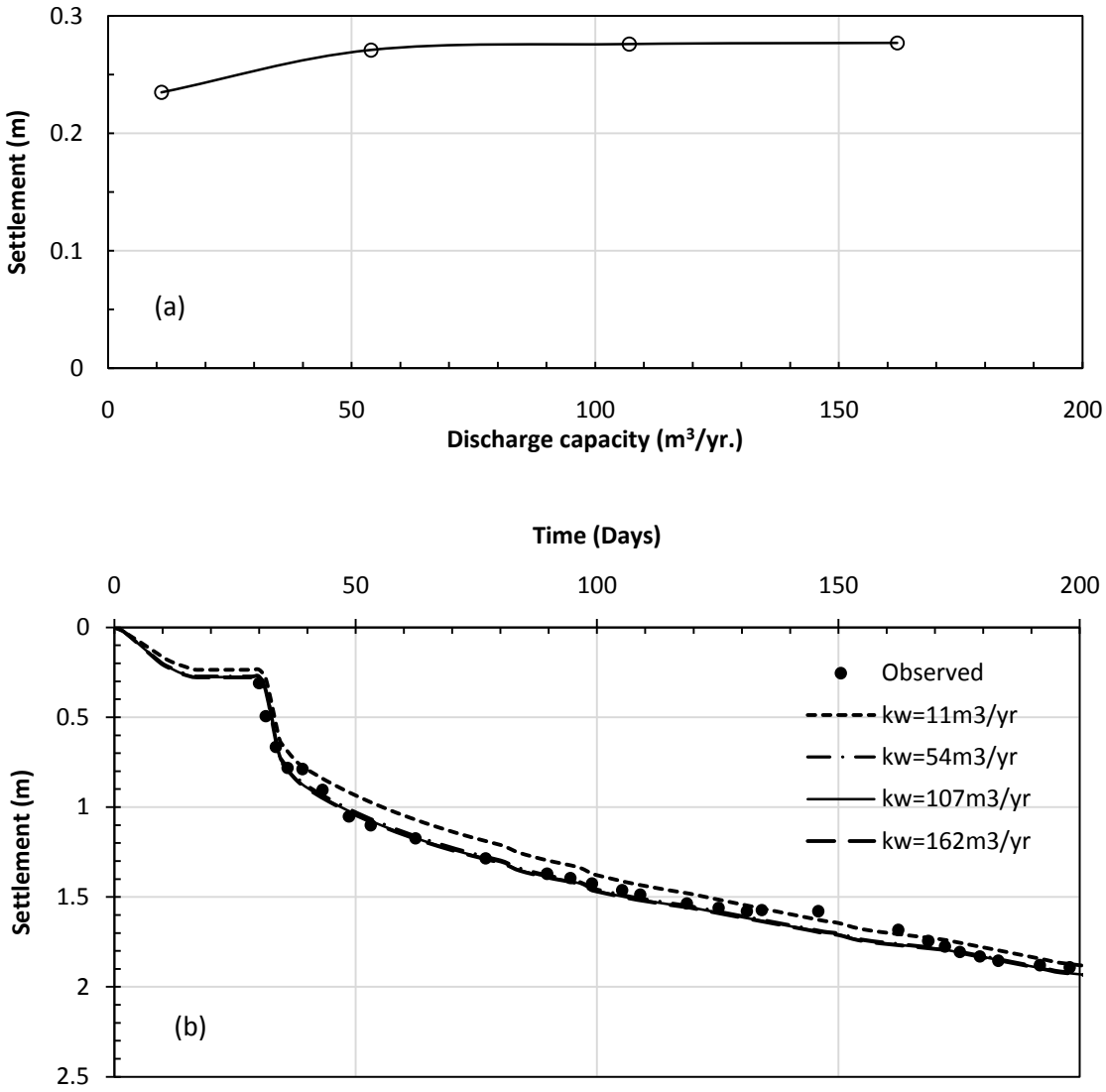

Figure 5.6: Settlement due to different discharge capacities of PVDs (a) before application of vacuum at 30 days, and (b) with time.

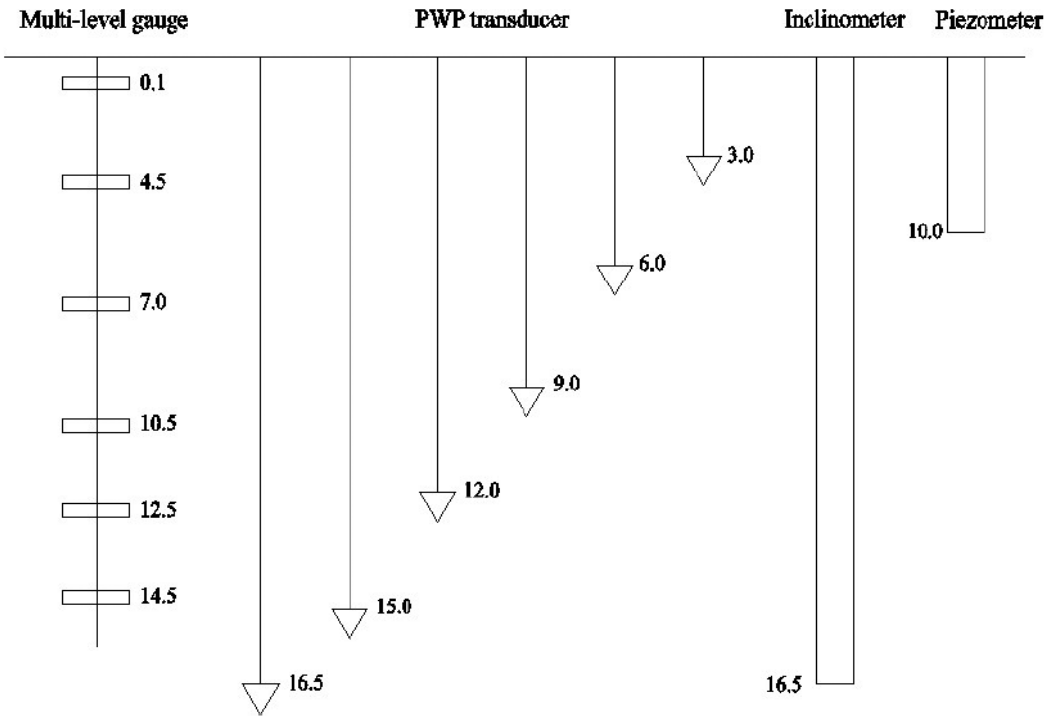

Figure 5.7: Location of various instruments (after Yan and Chu; 2005)

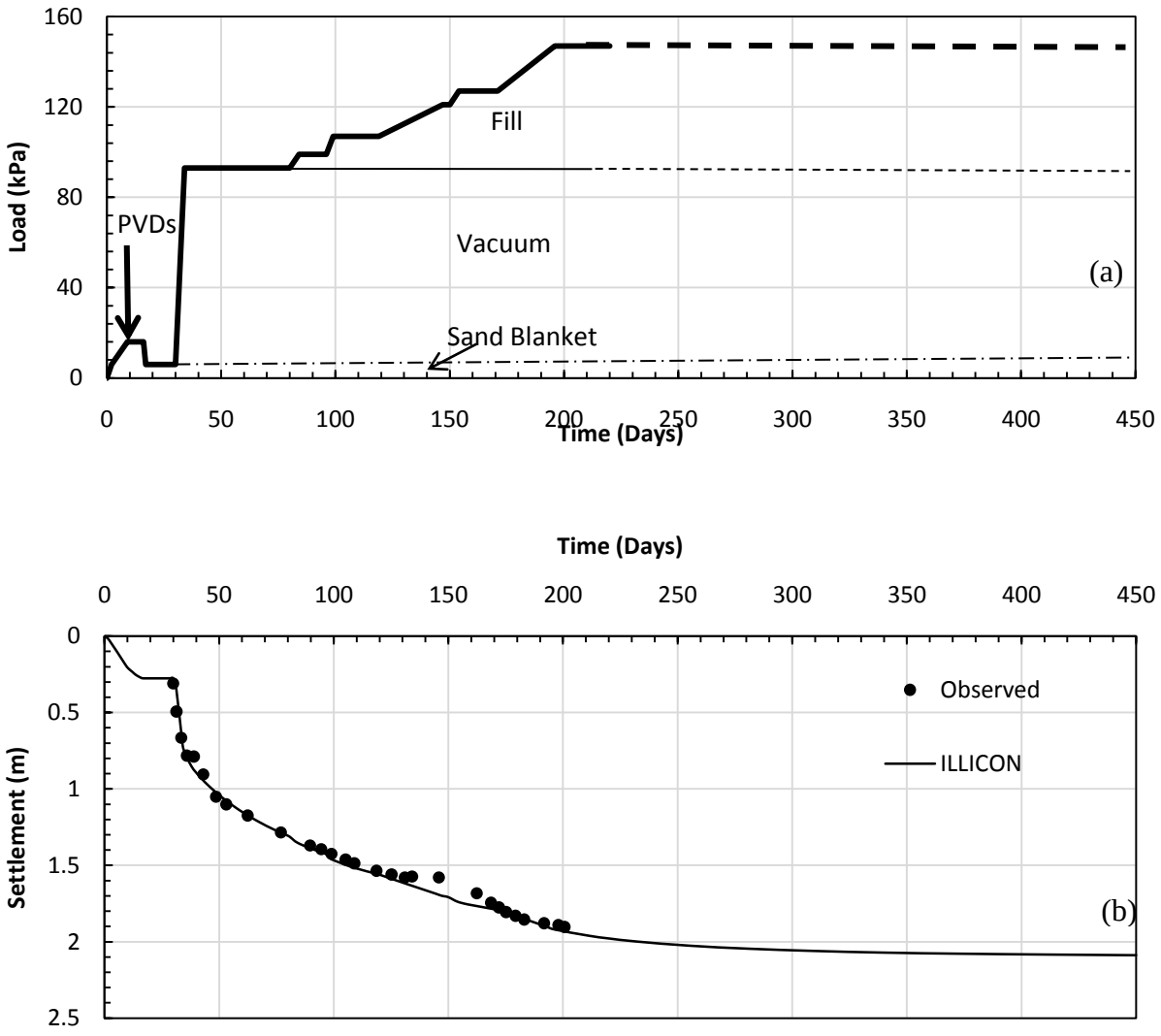

Figure 5.8: (a) Loading schedule, and (b) comparison of observed and predicted surface settlement

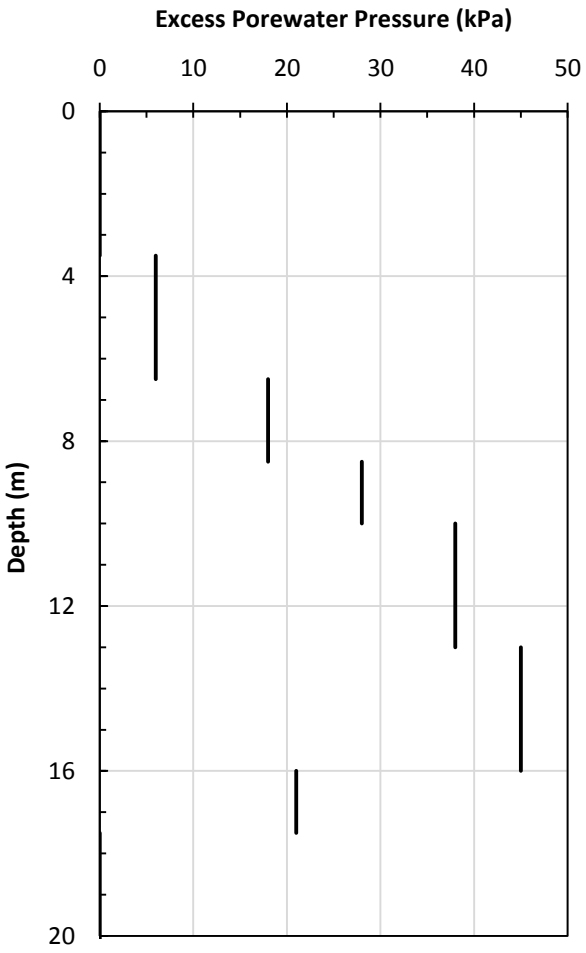

Figure 5.9: Vertical distribution of pretreatment excess porewater pressure assumed as load at time, t = 0, in the settlement analysis.

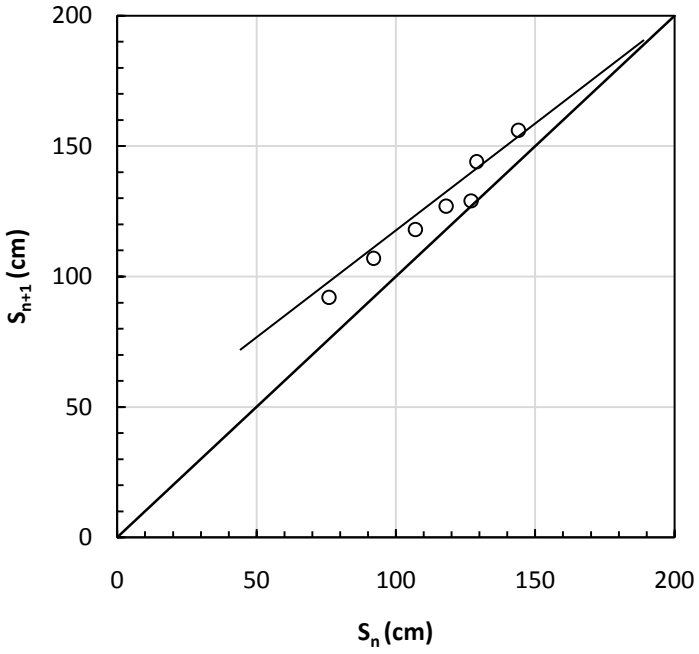

Figure 5.10: EOP settlement using the Asoaka method

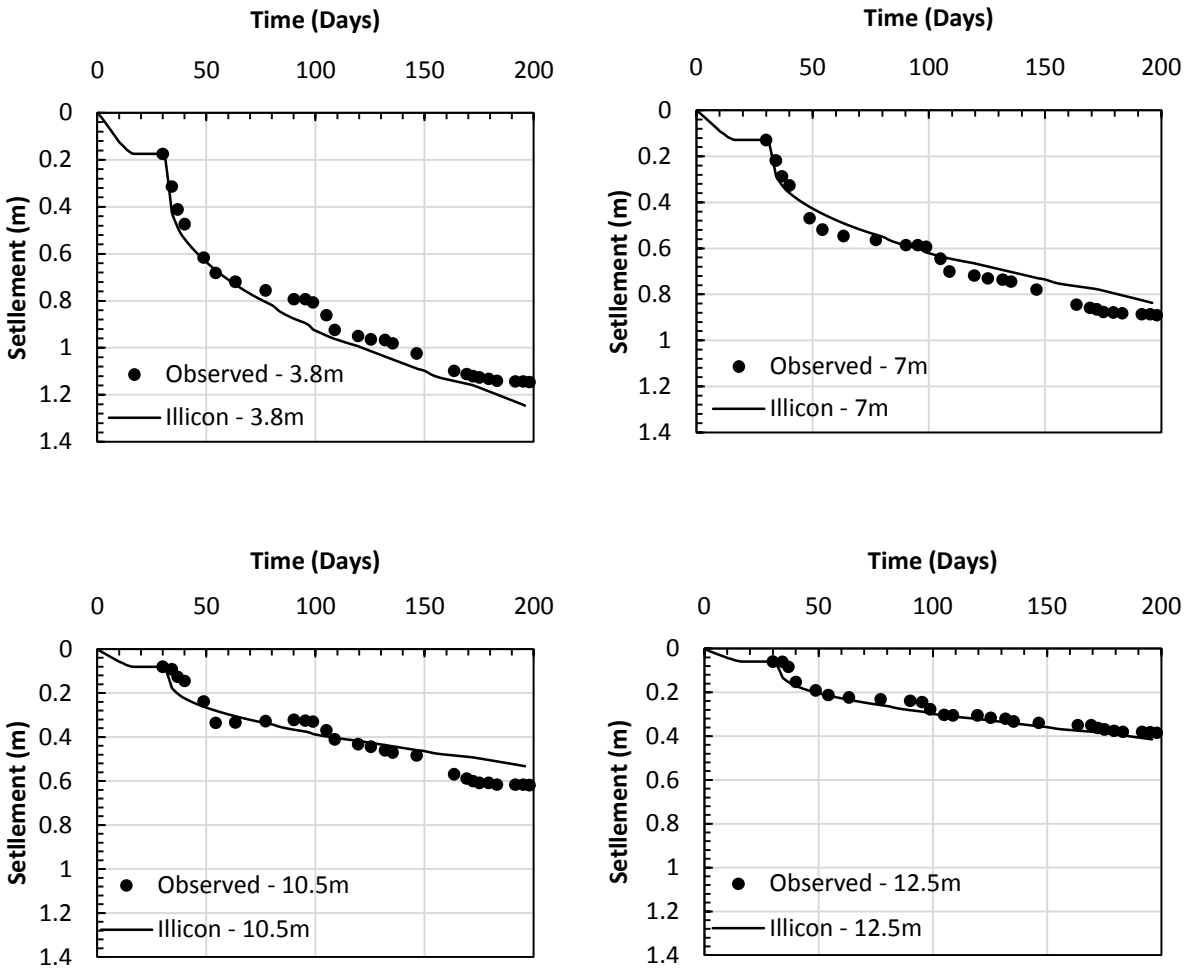

Figure 5.11: Comparison of observed and predicted subsurface settlements

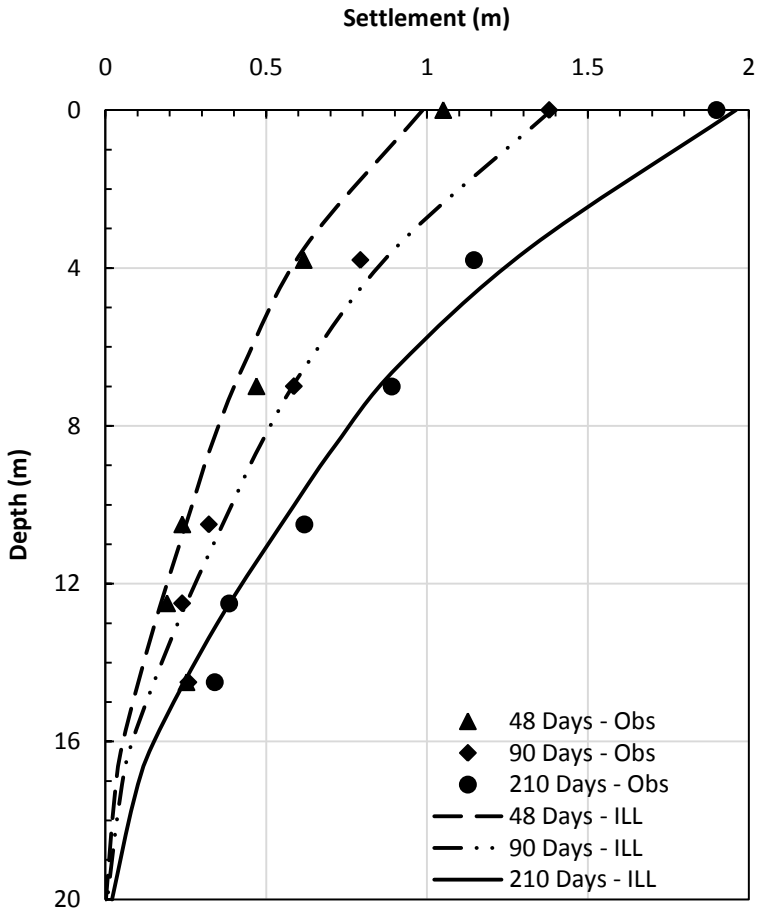

Figure 5.12: Comparison of observed and predicted settlements with depth at different times

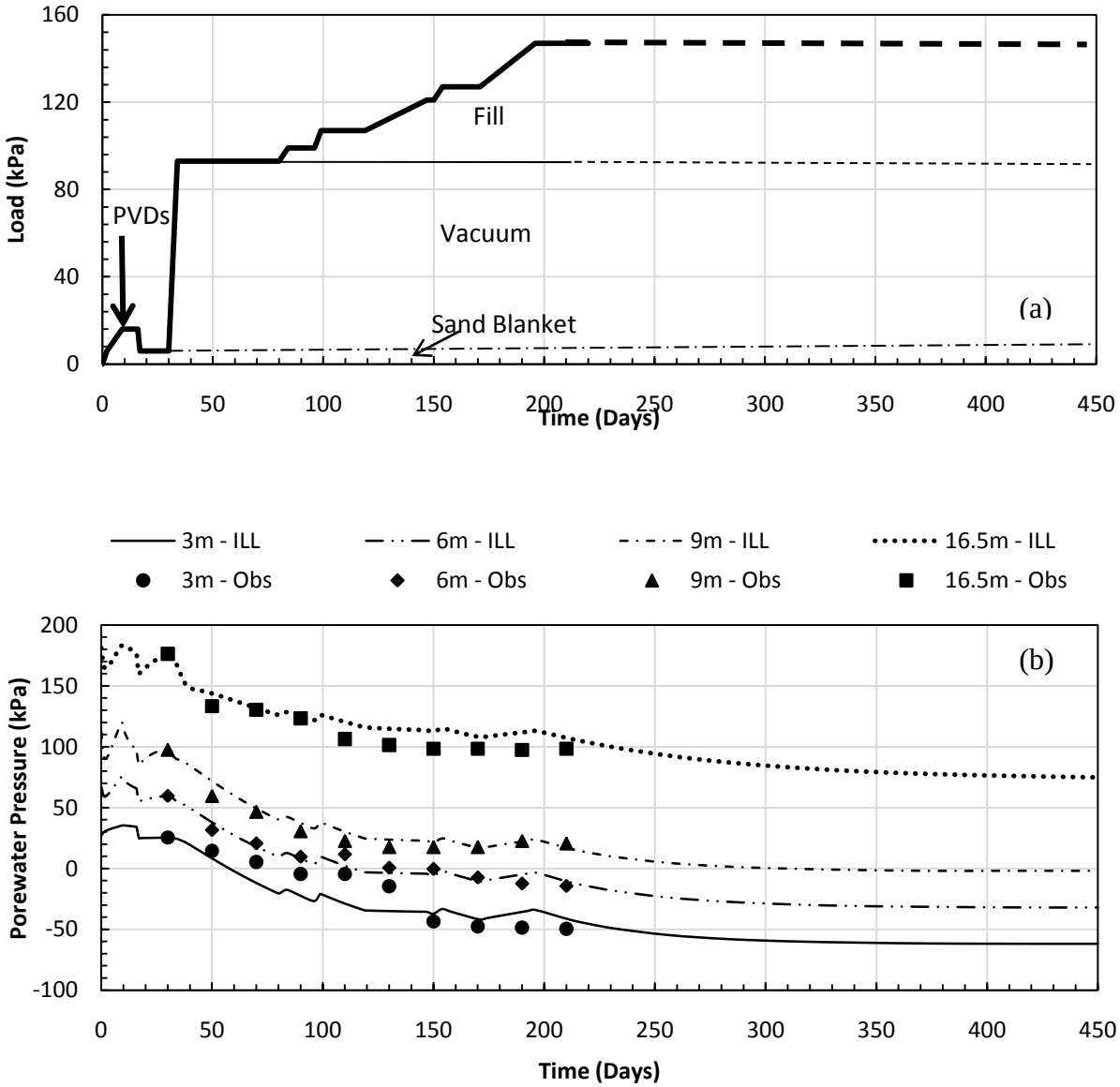

Figure 5.13: Comparison of observed and predicted porewater pressures with time at different depths

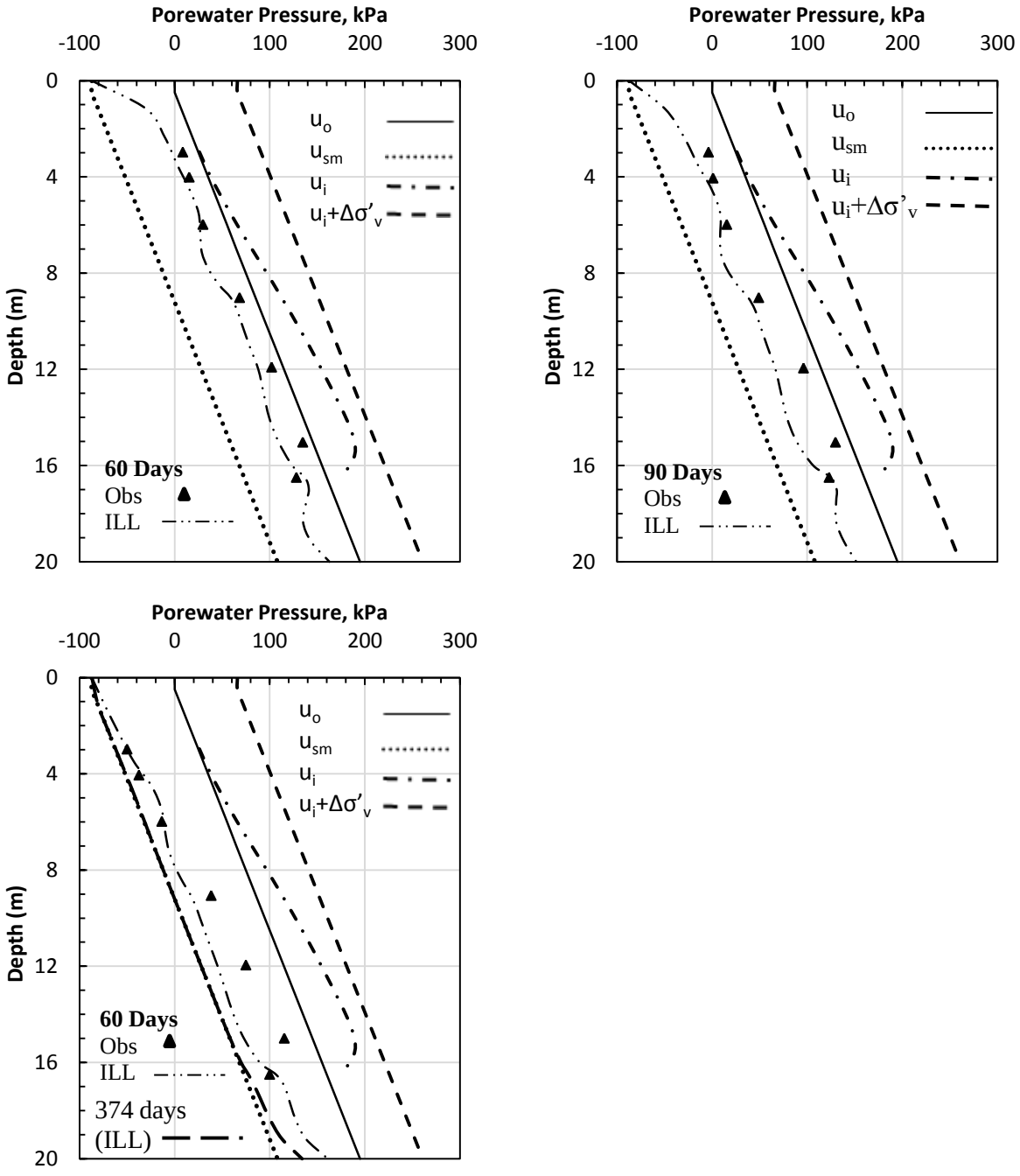

Figure 5.14: Comparison of observed and predicted porewater pressures with depth at different times

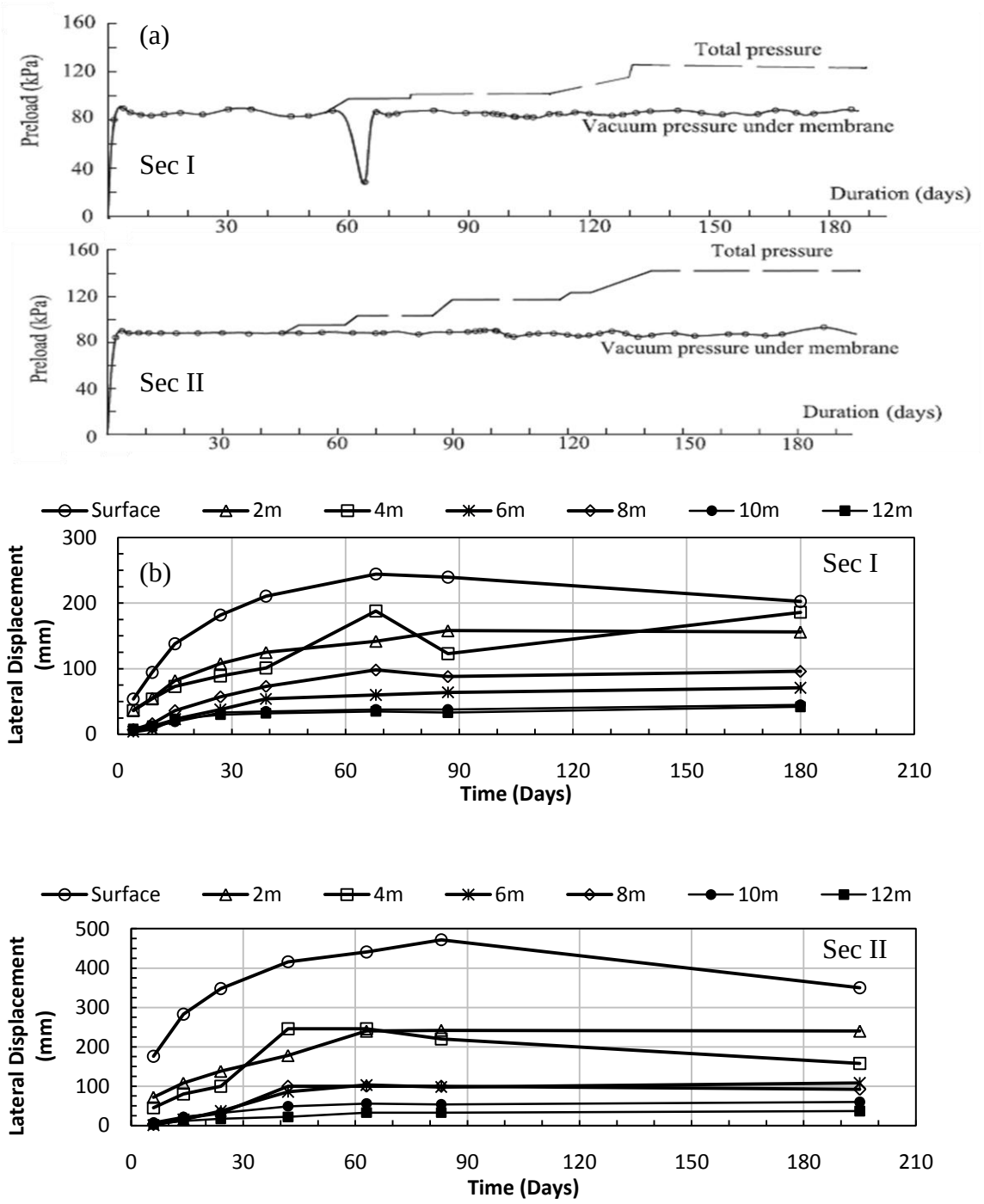

Figure 5.15: Lateral ground movements under combined vacuum and fill preloading (data from Chu and Yan 2005)

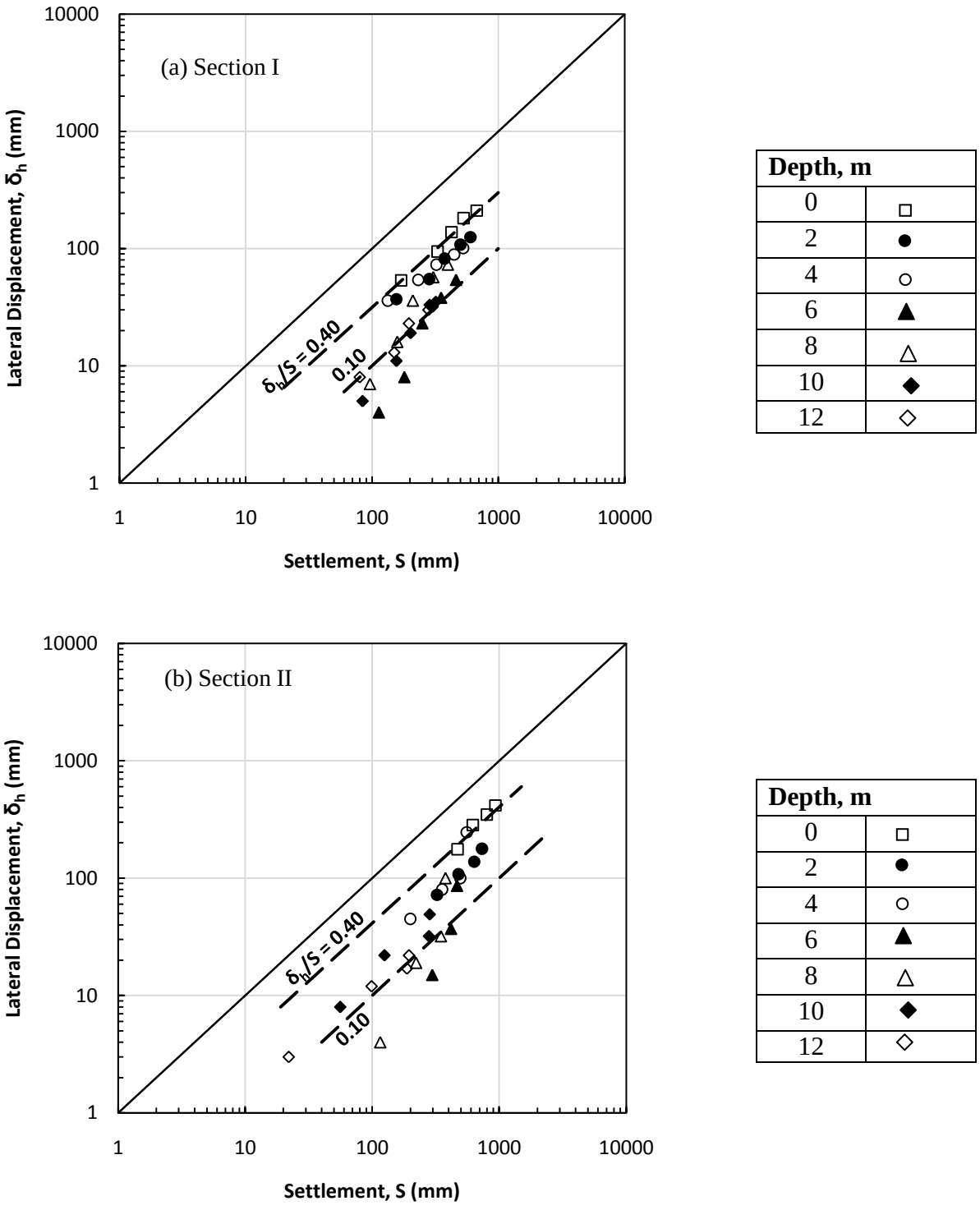

Figure 5.16: Lateral displacement at different depths plotted against settlement at different depths due to vacuum preloading only (data from Yan and Chu 2005)

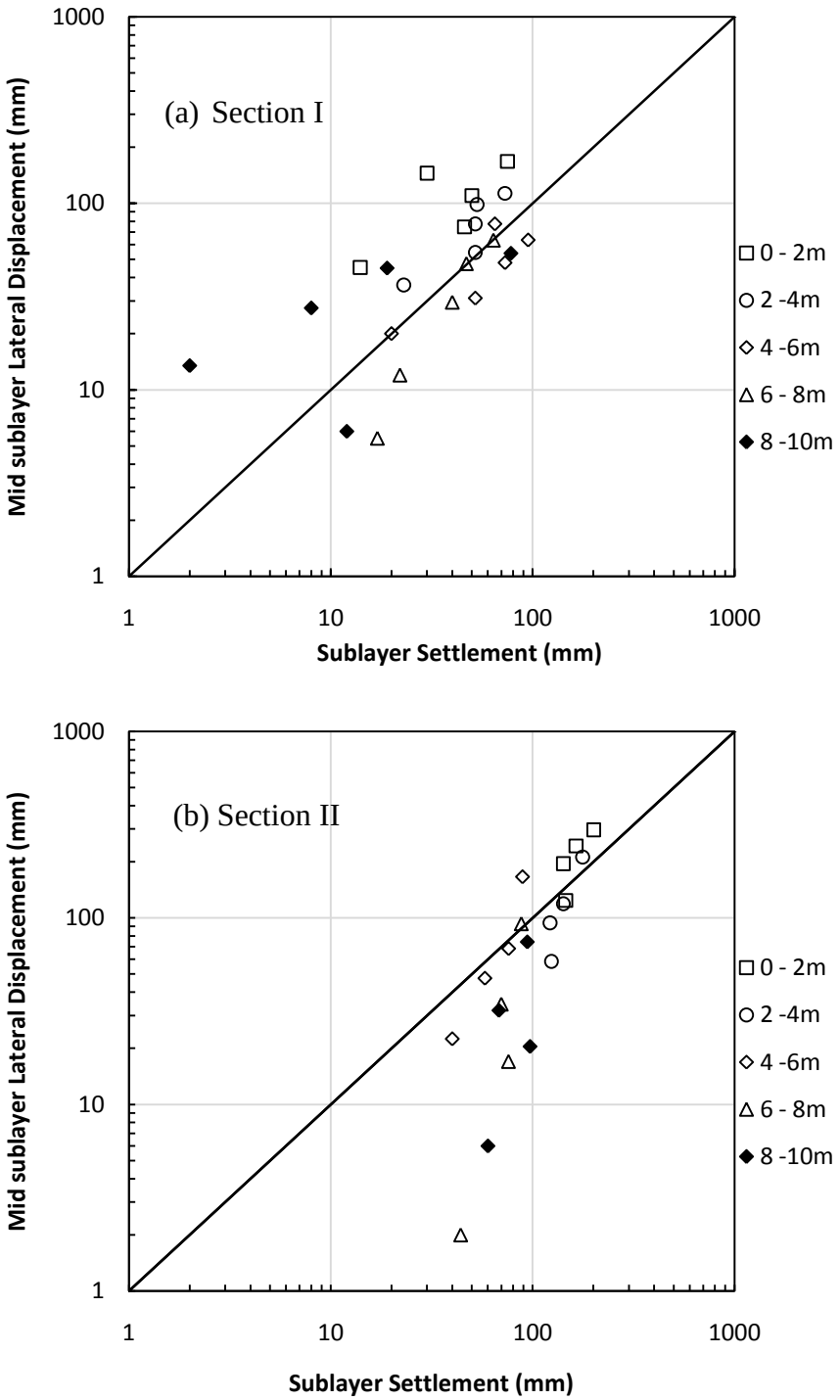

Figure 5.17: Mid-layer lateral displacement depths plotted against sublayer settlements at different depths due to vacuum preloading only (data from Yan and Chu 2005)

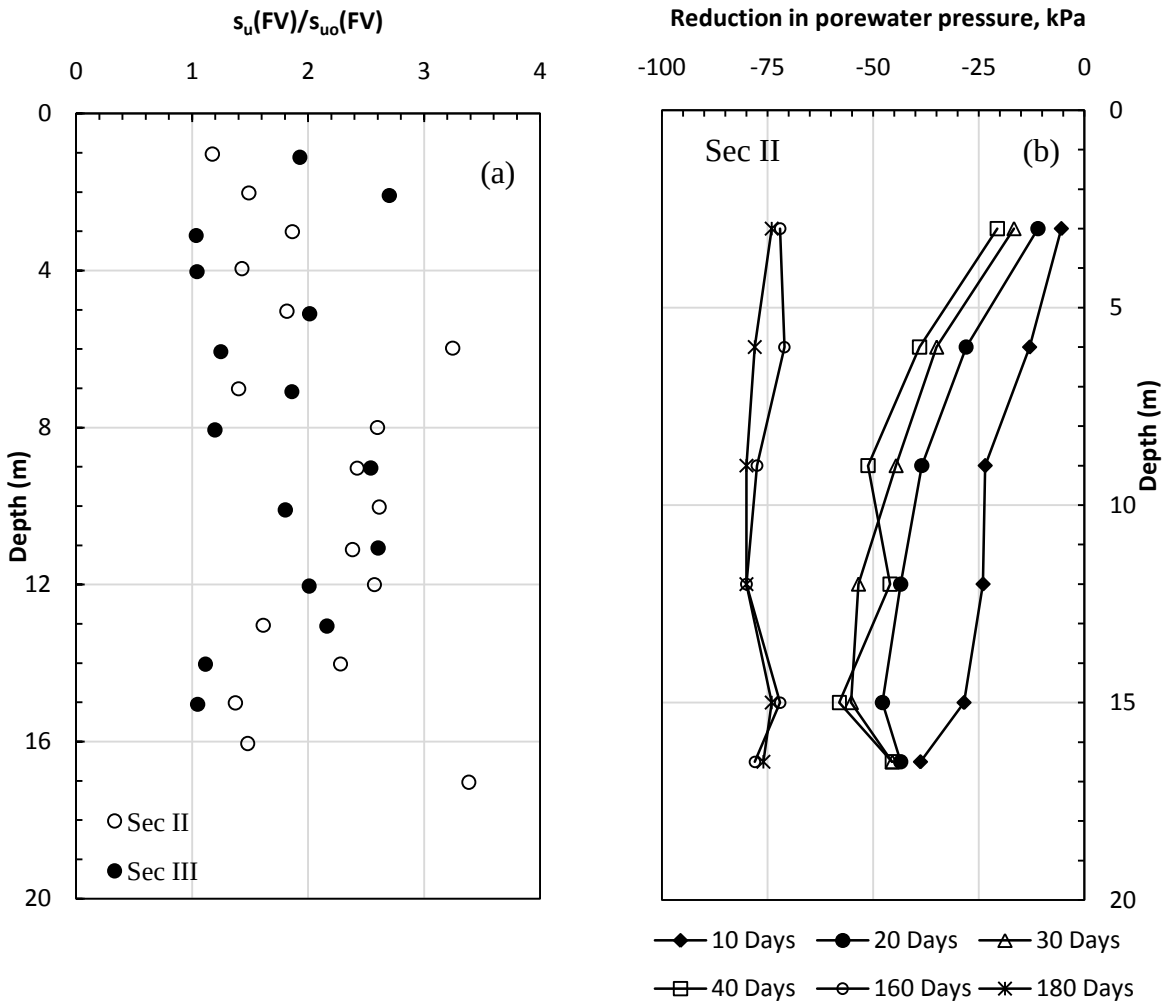

Figure 5.18: (a) Ratio of increase in vane shear strength for Section II and III, and (b) Observed reductions in porewater pressure with depth at different times for Section II (data from Yan and Chu 2005)

CHAPTER 6. COMBINED APPLICATION OF VACUUM AND FILL PRELOADING TOGETHER WITH VERTICAL DRAINS FOR SECOND BANGKOK INTERNATIONAL AIRPORT, THAILAND

6.1 Introduction

Second Bangkok international airport is located 30km east of Bangkok, Thailand. The plan for expansion of airport was originally conceived in 1960s, and in the following 30years, extensive geotechnical investigations were carried out in four major phases, i.e. 1972 - 1974, 1983 – 1984, 1992 and 1993 – 1995 (Moh and Lin 2003). Various ground improvement techniques including preloading with prefabricated vertical drains (PVDs), soil cement columns with cement stabilized mat and pile foundations were evaluated (Seah et al. 2006). Preloading with PVDs was adopted for ground improvement for runways and taxiways (Moh and Lin 2003).

Owing to shortage of sand as fill/preloading material, studies were carried to explore the use of vacuum to replace the conventional fill preloading. The field trial conducted in 1984 using vacuum together with non-displacement type sand drains (Woo et.al, 1989), trials conducted by Asian Institute of Technology (AIT) between 1993 and 1995 (Bergado et al. 1997, 1998, 2002; Bergado and Patawaran 2000) using prefabricated vertical drains (PVDs), and field test conducted by Cofra BV in 1996 (Saowapakpiboon et.al, 2008), where capped prefabricated vertical drains (CPVDs) were used in combination with vacuum and fill preloading, are reviewed and analyzed in this chapter.

6.2 Subsurface Conditions

6.2.1 General

The site for Second Bangkok International Airport is part of Chao Phraya plain which consists of deltaic, alluvial and sedimentary marine deposits (Chung et al. 2008). The subsoil consists of 1.5 – 2m thick weathered crust, underlain by a 10m thick very soft to soft

clay layer. A medium clay layer, approximately 4m thick, is underlying the soft clay layer. A stiff clay layer with SPT N values increasing from 10 to 40 is present to a depth of 24m (Woo et al. 1989; Bergado et al. 1997, 1998, 2002; Bergado and Patawaran 2000; Seah et al. 2006). Figure 6.1 shows the generalized profile along with the vertical profiles of geotechnical properties including unit weight, natural water content, Atterberg's Limits, Clay size fraction, and specific gravity of solids. It can be seen that in the soft clay layer, natural moisture content is generally more than 100% and the clay size fraction is more than 50% at all depths. Plasticity index is greater than 50% indicating a high plasticity soil. Specific gravity of solids and natural moisture contents were used to calculate the initial void ratio as shown in Fig. 6.2a. Figure 6.2b shows the vertical profile of field vane shear strength which is generally around 12kPa for soft clay layer.

6.2.2 Ground Water Conditions

Ground water table (GWT) was located at a depth of 0.5m to 1.0m below the ground surface according to Bergado et al. (1997, 2002), and 0.5m below the ground surface according to Saowapakpiboon et al. (2008). However, porewater pressure records reported by Bergado et al. (1997 and 1998) and Moh and Lin (2003) suggest that the water table was located at the ground surface. Indraratna et al. (2005) has also used GWT at the ground surface for their analysis.

Due to excessive withdrawal of water from the underlying aquifer, porewater pressures below 6 – 10m depth were lower than the hydrostatic pressure. This phenomenon was first noted in 1973 (Moh and Lin 2006). Figure 6.3 presents the data on porewater pressure distribution with depth from a number of studies as reported by Moh and Lin (2003). Bergado et al. (1998) observed a recharging effect of PVDs and reported that the porewater pressure after installation of PVDs and before application of vacuum was nearly hydrostatic, starting at ground surface as shown in Fig. 6.3b. Therefore, GWT is assumed at the ground surface and the initial distribution of porewater pressure is assumed to be equal to hydrostatic for the settlement analyses using the ILLICON.

6.2.3 Initial Vertical effective Stress (σ'_{vo}) and Preconsolidation Pressure (σ'_{p})

Figure 6.4a shows the vertical distribution of overconsolidation ratio (σ'_p/σ'_{vo}) reported in different studies. It can be seen that σ'_p/σ'_{vo} of 2.5 to 3 is generally reported for the crust and 1 to 1.3 for the soft clay layer. It was mentioned in Section 6.2.2 that due to

recharging effect of PVDs, the porewater pressure was nearly equal to hydrostatic, starting at ground surface, before the application of vacuum pressure; if true, this process would affect the σ'_p/σ'_{vo} of the soft clay layer. Therefore, σ'_p/σ'_{vo} was calculated based on the free field porewater pressure observations of 1994, new vertical effective stress condition (corresponding to hydrostatic ground water pressure) and s_{uo}(FV) profile reported by Bergado et al. (1997). A $s_{uo}(FV)/\sigma'_p = 0.30$, as recommended by STS and NGI (1992), was used to estimate σ'_p. It can be seen from Fig. 6.4a that the calculated values of σ'_p/σ'_{vo} used in the ILLICON analyses are near the upper bound of the σ'_p/σ'_{vo} data reported in the literature.

It is interesting to note that in the four case studies concerned with Bangkok clay considered here (Bergado et al. 1998, 2002; Rujiakiatkamjorn and Indraratna 2006; and Saowapakpiboon et al. 2008) the values of σ'_p/σ'_{vo} used in the settlement analysis are different from values determined from interpretation of laboratory and insitu tests. Table 6.1 presents a comparison of the values of σ'_p/σ'_{vo} determined from laboratory and insitu measurements and those used in the analysis of respective case histories concerning Bangkok Clay. It can be seen from the table that the reported σ'_p/σ'_{vo} values are significantly different from those used to back calculate the settlements and porewater pressure in the field. It is also interesting to note that Bergado et al. (1998) and Saowapakpiboon et al. (2008) have used σ'_p/σ'_{vo} values of less than 1 for some sublayers. No attempt has been made in any case to justify the use of σ'_p/σ'_{vo} values for settlement analyses different than those determined by laboratory and insitu tests. The computed values of σ'_{vo} along σ'_p used in the ILLICON analyses are shown in Fig. 6.4b.

6.2.4 Compressibility

Figure 6.5a shows the compressibility data for Bangkok clay reported in the literature. It can be seen that the compressibility ratios are generally high, indicating the highly compressible nature of the soft Bangkok clay. Solid vertical lines on Fig. 6.5a show the representative values used to calculate the C_c values in Fig. 6.5b for constructing EOP *e-log* σ'_v relations in Fig. 6.5c for the ILLICON analyses. The representative values of $C_c/(1+e_o)$ are generally near the upper bound of the reported data; however the back calculated C_c values lie within the values reported by STS/NGI (1992) based on a large

number of oedometer tests. A C_r/C_c = 0.2 (Bergado et al. 2002) and C_α/C_c = 0.045 (STS/NGI 1992) were used in the settlement analysis.

6.2.5 Permeability

Figure 6.6a shows the data on initial vertical permeability, k_{vo}, reported by STS/NGI (1992), Bergado et al. (1998), and Indraratna et al. (2005). The representative values used in ILLICON analysis are shown as solid lines on Fig. 6.6a. The decrease in permeability during consolidation was computed assuming a constant C_k which was determined by using $C_k = 0.45e_o$ as suggested by STS/NGI (1992) for soft Bangkok clay. STS/NGI (1992) reported that k_h/k_v for soft Bangkok ranges from 1 to 3 with an average value of about 1.7 for soft clay layer up to a depth of around 10m. Seah and Kolsant (2003) concluded that the soft Bangkok clay is isotropic in its natural state, i.e., k_h/k_v = 1.0. For the The permeability anisotropy was not considered settlement analyses using ILLICON. The vertical profile of k_{vo}, C_k and *e-log* k_v relations used in the settlement analyses are shown are shown in Fig. 6.6.

6.3 Vertical Drains

Sand drains were used during 1984 field trial to transmit vacuum to the compressible layer (Woo et al. 1989). In subsequent studies conducted by Asian Institute of Technology (AIT) and Cofra BV; PVDs and CPVDs, respectively, were used along with vacuum preloading. Table 6.2 summarizes vertical drain parameters used in different studies and those used in the present study. It can be seen from Table 6.2 that except for discharge capacity, the drain parameters reported in respective studies have not been changed in the present settlement analyses. To determine the performance of PVDs in the field, settlement analysis was carried out using a discharge capacity of $30m^3/yr$ (Bergado et al. 2002), which corresponds to negligible well resistance, and the results were compared with the field observations as shown in Fig. 6.7. It can be seen that the rate of surface settlement is over-predicted at this discharge capacity. ILLICON analyses, carried out at reduced discharge capacities, as shown in Fig. 6.7b, show that the predictions are in good agreement with the observed surface settlements at a discharge capacity of $1.5m^3/yr$. Therefore, this discharge capacity was used as reference in the subsequent analyses as described in following sections.

6.4 Instrumentation

Instruments including surface and subsurface settlement gauges, piezometers, and inclinometers to monitor, respectively, settlement, porewater pressure and lateral movements, used in different studies are as shown in Table 6.3.

6.5 Field Trial of Fill Preloading by Asian Institute of Technology, (AIT) Bangkok

6.5.1 General

During 1993 to 1995, AIT carried out full-scale field trials to evaluate the performance of PVDs to improve the geotechnical properties of subsoil at the proposed site of Second Bangkok International Airport (Moh and Lin 2003). Three test embankments, TS1, TS2, and TS3 with PVDs installed to a depth of 12m, at a spacing of 1.5, 1.2 and 1m, respectively, were constructed during the field study. All embankments were constructed with a base area of 40 x 40m, side slope of 1V:3H, and subjected to a fill preload of 75kPa (Bergado et al. 1997 and 2002). Test embankment TS3 is analyzed using computer program ILLICON and the predictions are compared with field observations. Subsurface conditions as well as PVDs details have been described in previous sections; additional details specific to this case study are described in the following sections.

6.5.2 Loading Schedule

Due to stability concerns, the construction of embankment was carried out in stages as shown in Fig. 6.7a. Fill construction commenced in April 1994 and was completed in 8.5 months. A 1m thick granular blanket was placed on the ground surface and then the fill (γ = 18kN/m^3) was raised to 4.2m in stages to apply a maximum surface load of 76kPa. The time of installation of PVDs is not specified in the literature, however, the settlement and porewater pressure response as well as the stability analysis presented by Bergado et al. (2002) suggest that PVDs were installed around 60 days after commencement of construction. Different other studies on Second Bangkok International Airport, also show that drains were invariably installed 60 days or more after placement of a sand blanket (Woo et al. 1989; Seah 2006). Therefore, a period of 60 days was assumed for the settlement analysis. Elastic stress distribution (rectangular loaded area) was used to calculate the increase in vertical stress.

6.5.3 Settlement

Bergado et al. (1997) estimated an end-of-primary (EOP) settlement of 1.68m under the embankment load. The surface settlement observed by the end of observation period (September 1996) was 1.86m; 10% more than the estimated EOP settlement. It was therefore concluded by Bergado et al. (1997) that the soil had completed its primary consolidation and was undergoing secondary compression. For the selected soil parameters, ILLICON procedure predicts an EOP settlement of 1.95, which suggests that the soil was still undergoing primary compression at the end of observation period. The Asoaka method was also used to predict EOP settlement based on field observations as shown in Fig. 6.8. The surface settlements under final stage of loading were used together with a time interval (ΔT) of 60 days. It can be seen that, the Asoaka method predicts an EOP settlement of 2.05m which is in close agreement with ILLICON prediction and also confirms that the soil was still undergoing primary compression at the last settlement observation.

Figures 6.9 and 6.10 show the comparison of surface and subsurface settlements observed in the field to those predicted by the ILLICON. There is a good agreement in observed and predicted settlements for shallow depths; however, at greater depths the agreement is not very good. There is a possibility of malfunctioning (or incorrect readings) of instruments as acknowledged by Bergado et al. (1997). For example, it can be seen from Fig. 5 of Bergado et al. (1997) that up to 300 days, the subsurface settlements at 6m depth are less than the settlements at 8m (theoretically not possible), thereafter, the subsurface settlements at this depth become almost equal to settlement at 4m depth, indicating a very small compression in the sublayer from 4 to 6m depth. Both of these observations clearly indicate an error in settlement recording at these depths; therefore the predictions by ILLICON are considered reasonable.

6.5.4 Porewater Pressure

Figure 6.11 compares the observed and predicted porewater pressures with time at different depths. It can be seen that the observations and predictions are in good agreement at depths of 6 and 8m; however, at shallow depths, i.e. 2 and 4m, the agreement is not very good. Similar to settlement data, porewater pressure data reported by Bergado et al. (1997) indicate possible errors in recording/interpretation of porewater pressures at some depths. For example, the total porewater pressure records at depths of 2m, 4m and 14m, dropped below

the respective hydrostatic levels, (as shown in Fig. 7 of Bergado et al. 1997) whereas at other depths, some excess porewater pressure existed by the end of observation period. It was mentioned in Section 6.2 that the negative drawdown in GWT was observed below 6m depth which becomes significant around 10m depth; therefore, total porewater pressure below hydrostatic pressure, at 2m and 4m depths may be due to reading or instrumental error or change in reference groundwater pressure. At 4m depth, the observations and predictions up to 250 days (end of construction) are in agreement; however, after this time the agreement is not very good probably due to instrumental/recording error or a change in referenceporewater pressure as stated earlier. The degree of consolidation at the end of observation period based on the Asoaka method is 90% which also indicates that there should be some excess porewater pressures in the soil mass. Therefore, the predictions by ILLICON are considered reasonable as these represent the field behavior more realistically.

6.6 Field Trial of Combined Vacuum and Fill Preloading by the Asian Institute of Technology (AIT) Bangkok

6.6.1 General

In addition to the three test embankments (TS1, TS2, and TS3), two more test embankments, TV1 and TV2 were also constructed where vacuum preloading was used in combination with reduced fill preload. The type, spacing and penetration depth of PVDs used in TV2 were same as those of TS3; therefore, analysis of TV2 was carried out in detail as presented in the following sections. Subsurface conditions described in Section 6.2 and PVD parameters listed in Table 6.2 have been used in the settlement analyses.

6.6.2 Loading Sequence

A 0.8m thick sand blanket was first placed on the ground surface through which PVDs were installed. Exact time schedule for installation of vertical drains and sealing of the area has not been reported in the literature; however, for the installation of PVDs and completing the sealing arrangements for the area, a period of 60 days after placement of sand blanket was assumed. A vacuum pressure of 70kPa was applied to the soil. Forty five days after application of vacuum pressure, embankment was gradually raised to 2.5m (45kPa, including the sand blanket) as shown in Fig. 6.12. Bergado et al. (1998) and Bergado and Patawaran (2000) concluded that only 35 – 40kPa vacuum pressure was available during the preloading, therefore, the following loading options were considered in the present analysis:

- ***Case I***. Consolidation progressed under an effective vacuum pressure of 35 – 40kPa and the applied fill load of 45kPa as shown in Fig. 6.12a. The vacuum intensity was assumed uniform with depth.
- ***Case II***. Consolidation progressed under applied fill preload only (Fig. 6.13a). This option was considered to assess the contribution of fill preload in the observed settlements.
- ***Case III***. Consolidation progressed under the applied fill preload and a variable vacuum intensity at different depths (based on porewater pressure measurements) which gradually increased to maximum of around 35 to 45kPa and then decreased to a minimum valuem of 10kPa with time as shown in Fig. 6.14a.

In all cases, elastic stress distribution (load over a rectangular area) was used for the applied fill load.

6.6.3 Settlements

Case I loading condition (Fig. 6.12a) over-predicts the field settlements by the end of vacuum preloading period (Fig. 6.12b) assumed to extend passed to 250 days; moreover, there is a trend of continuing settlement as compared to the observations which level off. It is important to note that case I loading condition (combined load of 80kPa; 45kPa fill load and 35kPa vacuum) predicts a surface settlement of 1.96m in 800 days, as shown in Fig. 6.15, which is similar to 1.95m predicted by ILLICON for TS3 which was subjected to fill load (75kPa) only. It can be inferred from Fig. 6.12 together with Fig. 6.15 that the actual load imposed by vacuum in TV2 decreased with time such that the rate of settlement came practically to a stop. As fill load for TV2 is known with certainty, it is most likely that the vacuum load significantly decreased, possibly approaching very small value by 150 days. Figure 6.13b (case II) shows that, fill alone contributes about 70% of the observed settlements, however; the initial rate of observed settlements is much higher than produced by fill alone. Thus case II loading condition shows that vacuum was initially developed to around 35 to 45kPa; however, with time decreased, possibly to very small value. Case III loading condition, which accounts for a variable vacuum intensity with depth and the reduction in vacuum intensity with time (based on the observed reductions in porewater pressures), predicts the surface settlement better as shown in Fig. 6.14.

Figure 6.16 compares the predicted subsurface settlements with the observed subsurface settlements at different depths for Case III loading condition. It can be seen that at all depths, there is a very good agreement between the observed and the predicted subsurface settlements, which shows that the assumptions made with respect to distribution of vacuum pressure with depth and with time are reasonable.

6.6.4 Porewater Pressure

Figure 6.17 shows the comparison between predicted and observed porewater pressures at different depths for case III loading condition. Equation 4.2 was used to interpret the porewater pressures from ILLICON analysis. It is important to note that the maximum value of vacuum pressure (u_{sm}) used in equation 4.2 was -60kPa for the surface, 3m, and 6m depths and -70kPa for 9 and 12m depths. There is a reasonable agreement between the observed and predicted porewater pressures at all depths except at 12m below the ground surface. The observations indicate a higher negative porewater pressure at 12m depth than what can be produced by the applied vacuum pressure (assuming no leakages in vacuum) alone. This can be explained in terms of the pretreatment porewater pressures which were lower than the hydrostatic porewater pressure. Porewater pressures at depths of 9 and 12m were re-interpreted assuming u_o profile of 1994, i.e. 75kPa at depth of 9m and 86kPa at depth of 12m, and u_{sm} of 60kPa, as shown in Fig. 6.18. It can be seen that there is a good agreement between the observed and predicted porewater pressures. It was mentioned in Section 6.2.4 that the porewater pressure profile before the application of vacuum pressure was nearly hydrostatic (Bergado et al. 1998); however, it appears from the analysis that there were fluctuations in the porewater pressures and the measured porewater pressure (just before application of vacuum) may only existed for a brief period of time and then the effect of drawdown reappeared. Because the fluctuation of porewater pressure would keep the soil in the recompression range, it is not likely to affect the settlement of the sublayers.

6.7 Field Trial of Vacuum-PVD System by COFRA

6.7.1 General

In a Vacuum-PVD system, capped prefabricated vertical drains (CPVDs) are used. CPVDs are conventional PVDs, covered with an impermeable cap, and connected directly to the vacuum pumps through a hose. A unique feature of this system is that the surface is not

covered with impermeable membrane; instead the insitu clay layer is used as sealant (details of the system are covered in Chapter 2).

The general soil profile and vertical distribution of geotechnical properties for the test section were similar to the previous sections and have been used as such in the settlement analysis using ILLICON with following modifications:

- The penetration depth of CPVDs in this test section was reduced to 10m and the drain spacing was reduced to 0.85m (Saowapakpiboon et al. 2008).
- Crust thickness was increased to 2m, and GWT was assumed 0.5m below the ground surface as reported by Saowapakpiboon et al. (2008).
- The division of compressible layer into various sublayers for the ILLICON analysis is shown in Fig. 6.19.

6.7.2 Loading Sequence

A discrepancy is observed in the literature in connection to this case history, regarding the time required for installation of PVDs. Cortlever et al. (undated) from COFRA, reports a period of 6months for installation of PVDs, whereas Saowapakpiboon et al. (2008) used a period of 2months in their analysis. As the drainage blanket was not used in this case and fill was constructed after application of vacuum pressure, this discrepancy is ignored in the ILLICON analysis and a period of 60 days is assumed for installation of vertical drains.

After installation of drains, a vacuum pressure of 50kPa was applied followed by construction of a 2.8m (45kPa) high embankment in stages as shown if Fig. 6.20a. After the completion of embankment, the applied vacuum was increased (-70 to -90kPa at the pump, which resulted in a vacuum pressure of -50 to -60kPa at the vertical drain). The following additional points were considered to construct a loading schedule for the settlement analysis.

- A period of 15 days was assumed between installation of vertical drains and application of vacuum pressure.
- As the top of CPVDs is sealed, vacuum pressure cannot be directly transmitted to the soil layer in contact with the capped portion of the prefabricated vertical drains. Therefore, (a) the crust was subjected to fill load only, and (b) as water can flow only in vertical direction through the crust and the sealing layer (top

0.5m of soft clay layer), for ILLICON analysis a k_h/k_v = 0.1 was assumed for these sublayers.

- Vacuum pressure was assumed constant with depth in the soft clay layer. For the sealing layer, applied vacuum was assumed at the interface of sublayer 2 and 3 (Fig. 6.19) and zero at the top of sealing layer. Similarly, at 0.5m below the tip of CPVDs, vacuum intensity was assumed to reduce to zero. The vertical distribution of assumed vacuum pressure is shown in Fig. 6.19. Figures 6.20a and 6.21a show the gradual development of vacuum with time and total load for different sublayers, shown on Fig. 6.19, considered in the settlement analysis.

6.7.3 Settlement

The observed surface settlements were quite non-uniform, ranging between 0.90 to 1.20m after about 100 days of vacuum application (Fig. 15 of Saowapakpiboon et al. 2008). Preliminary settlement analysis with ILLICON shows that the EOP settlement under the applied loads is 2.05 and 2.15m, respectively, for fill load of 45kPa together with vacuum pressure of 50kPa and 60kPa (Fig. 6.22). This is slightly more than the EOP settlement predicted by the Asoaka method (1.94m) corresponding to settlement plate EW4-ZB-01 indicating maximum settlement (Fig. 6.23); although the settlement observations corresponds to less than 50% degree of consolidation where the Asoaka method might underestimate the EOP settlement. The degree of consolidation at elapsed time of 170days (100 days after application of vacuum) as per the Asoaka method is around 62% which is less than 66 to 80% reported by Saowapakpiboon et al. (2008). However, it is important to note that Saowapakpiboon et al. (2008) reported degree of consolidation based on Asoaka method which is not considered reasonable. Figures 6.20 and 6.21 compare the observed and predicted surface settlements, for different discharge capacities of CPVDs, and for vacuum pressures of 60 and 50kPa, respectively. It appears from the predictions of Asoaka method and ILLICON analysis that consolidation in the field progressed under a vacuum pressure of 50kPa. It is also important to note that the CPVDs performed with a significant well resistance as the maximum and minimum surface settlements observed in the field, respectively, correspond to discharge capacities of 1.2 and 0.8m^3/yr. This is probably due to connecting each CPVD individually to the vacuum pumping system.

6.7.4 Porewater Pressure

The porewater pressure data for this case history have not been reported in the literature. The probable distribution of porewater pressure with time at different depths from an ILLICON analysis is shown in Fig. 6.24. Equation 4.2 was used to interpret the porewater pressure together with a vacuum pressure (u_{sm}) of 50kPa.

6.8 Application of Vacuum Preloading Together with Vertical Sand Drains

6.8.1 General

Vacuum preloading for the improvement of soft Bangkok clay was first studied in mid 1980s. The vacuum pressure was applied with the help of 0.26m diameter, non-displacement type sand drains. Vacuum was applied in a different way than the conventional system. Salient features of this system are described by Woo et al. (1989):

- A 60cm thick sand blanket was placed over the test section of 40x40m.
- Non displacement sand drains, 0.26m in diameter, were installed to a depth of 14.5m in triangular pattern, each sand drain covering an area of 3.5m^2.
- The top 1.3m of sand drains was sealed with cement-bentonite slurry.
- Two filters were placed inside each sand drain, at depths of 3m and 11m to transmit vacuum to the soft clay layer. Five subsidiary horizontal lines, each connected to approximately 92 sand drains via 8 manifolds, were linked with the vacuum pump through a main line.
- A control valve was attached to each manifold to regulate vacuum pressure in top and bottom filter as required. Specific details on connections between vacuum pump and sand drains have not been reported; however, it appears that the top and bottom filters in each sand drain were connected to different valves so as to apply vacuum to either of the filters independently.
- The vacuum pump had a capacity of 110m^3 of water and 130m^3 of air.

Vertical drain parameters as shown in Table 6.2 were used in the ILLICON settlement analysis. The soil parameters were kept the same as in sections 6.5 and 6.6 of this chapter; however, the extent of smear zone was reduced (Table 6.2) because non-displacement sand drains were used in this case.

6.8.2 Application of Vacuum

Vacuum was applied in the following way (Woo et al. 1989)

- The valve connected to the top filters were closed and vacuum was applied to lower filters. This lowered the water level in the sand drains to 6 to 8m below the ground surface.
- Air in the sand drains was pumped out through top filters, creating an under pressure in the sand drains.
- Top filters were then opened to the atmosphere to allow the water from the surrounding soil to flow into the sand drains.
- The process was repeated continuously to affect precompression.

A maximum pressure of 0.68bars (68kPa) was achieved during the operation; However, after about five weeks the process was stopped due to observed leakages in the vacuum. A plastic sheet was used to seal a small area (12x46m) covering 132 sand drains. Preloading operation was resumed and a vacuum pressure of 0.6 to 0.7bars (60 – 70kPa) was successfully maintained in the sealed area.

6.8.3 Loading Sequence

A 60cm thick sand blanket was placed on the ground surface through which sand drains were installed. As stated earlier, the vacuum pressure was discontinued 5 weeks after initial application to improve the sealing of the area (Fig. 9 of Woo et al. 1989); however, for ILLICON analysis, a uniform vacuum pressure of 60kPa was assumed to remain effective throughout the duration of treatment as shown in Fig. 6.25a. As the top of sand drains was sealed with bentonite slurry, vacuum pressure was applied to soil sublayers excluding the sealed prtion of the sand drains for reasons as discussed in Section 6.7.2.

6.8.4 Performance of Sand Drains

ILLICON analyses were carried out by varying the discharge capacity from $1.5m^3$/yr. to $15m^3$/yr. as shown in Fig. 6.25b. As no settlements are reported under the load of sand blanket, and due to installation of sand drains, ILLICON predictions have been adjusted by assuming zero settlements at 83 days (time of start of vacuum), to make the predictions comparable with field observations. It can be seen from Fig 6.25b that a discharge capacity of $8m^3$/yr. most closely predicts the observed surface settlements; whereas, an increase in discharge capacity beyond $8m^3$/yr. over-predicts the magnitude as well as rate of observed settlements. This shows that although sand drains also performed with well resistance; the

discharge capacity of sand drains was almost 5 to 6 times the discharge capacity of PVDs in the same soil conditions.

6.8.5 Settlement

Figure 6.26b compares the observed subsurface settlements to those predicted by ILLICON analysis for a discharge capacity of $8m^3/yr$. Because the loading sequence is simplified for the ILLICON analysis (ignoring the interruption and leakages in vacuum application); it is expected that there should be a difference in the observed and predicted settlements during the time when leakage was observed in the field and vacuum was stopped to seal the area. It can be seen from the Figs. 6.25b and 6.26b that the observed surface and subsurface settlements are less than the predicted settlements after the time period when leakage was observed and during which no vacuum was applied. However, the observations and predictions are in good agreement towards the end of treatment period. In the absence of more specific data, especially on porewater pressures at different times during vacuum application, the assumptions made for the loading schedule cannot be further verified; however, the agreement between observed and predicted settlements shows that the assumptions made are quite reasonable.

6.9 Concluding Remarks

Four cases of ground improvement in soft Bangkok clay have been analyzed. The following conclusion based on the analysis of these case histories,:

- The preconsolidation pressure of soft Bangkok clay is higher than what is reported in the literature. This is probably due to excessive withdrawal and subsequent recharging of ground water. The assumption that pretreatment porewater pressures are equal to hydrostatic porewater pressure seems reasonable as it predicted the settlements and porewater pressure reasonably well.
- It is evident from the settlement response of TS3 and TV2 that both the vacuum and fill preloading are essentially similar in nature. The acceleration in settlement due to application of vacuum is primarily related to the ability to achieve the desired vacuum intensity in a shorter time as compared to fill loading.

- Sufficient sealing arrangements are essential to successfully apply vacuum in the field. The settlement analysis of TV2 reveals that the vacuum initially developed to a higher level; however it could not be maintained throughout the duration of the treatment. It appears that the loss in vacuum intensity became significant as the fill was being constructed on top of the treatment area. Presence of high permeability layers (desiccated crust) warrants more specific measures, such as slurry cut off wall, to be considered while planning a vacuum preloading operation. It is also possible that the applied fill might have caused some damage to the sealing membrane which accelerated the loss of vacuum.
- Use of vacuum together with PVDs, CPVDs, and sand drains is feasible, however; it should be realized that the vertical drains may or may not be freely draining. In the case histories analyzed, there was significant well resistance in all the cases. It is shown that the discharge capacity, at which the PVDs actually performed in case of embankments TS3 and TV2, was significantly less than those reported in the literature. Moreover, CPVDs performed at even lower discharge capacity than the conventional PVDs. The direct application of vacuum pressure to each CPVD might result in a partial collapse and hence a reduction in the of cross sectional area; however, no data are available to support this argument. The non-displacement sand drains also displayed well resistance, however; in this case the discharge capacity of non-displacement type sand drains was about 5 to 6 times the discharge capacity of PVDs.
- It appears that the Vacuum-CPVD system results in a less uniform settlement than the conventional vacuum system; however more cases need be studied to verify this observation. The system also appears to have an inbuilt leakage as a substantial amount of applied vacuum at the pump does not reach the top of the drains. For example, in this case, almost 30 to 40% of the applied vacuum was lost in the system.
- The intensity of applied vacuum pressure may vary with depth as well as with time. It is important to correctly interpret the load induced by vacuum under which consolidation takes place in the field. Use of porewater pressure records is a reasonable way to interpret the vacuum load.

- Equation 4.2 can be used reliably to interpret the porewater pressure at any time and at any depth during the vacuum preloading operation.

6.10 Tables

Table 6.1: Reported and calculated values of OCR at different depths used in different studies and those used in ILLICON settlement analysis

Bergado et al. (1998)			**Bergado et al. (2002)**			**Rujiakiatkamjorn and Indraratna (2006)**			**Saowapakpiboon et al. (2008)**		**ILLICON**	
Depth (m)	Reported	Used in Analysis	Depth (m)	Reported	Used in Analysis	Depth (m)	Reported	Used in Analysis	Depth (m)	Used in Analysis	Depth (m)	Used in Analysis
0	2.50	11.50	1	2.50	5.13	1	2.50	5.27	1	2.22	0.75	5.00
0.5	2.50	6.59	3	1.30	2.42	5.25	1.60	1.35	3.5	0.72	1.75	3.81
1	2.50	1.65	5	1.30	1.61	9.5	1.40	1.28	7.5	0.69	3	2.66
2	2.00	1.33	7	1.30	1.42	12.25	1.30	1.29	11.5	0.99	5	1.81
3	1.80	1.15	9	1.20	1.60	14	1.20	1.09	14	1.08	7	1.39
8.5	1.20	1.37	11	1.20	1.60				16	3.40	9	1.59
10.5	1.20	1.00	14	-	1.69						11	1.43
13	1.20	0.92									14	1.56
18	-	0.92										

Table 6.2: Vertical drain parameters used in ILLICON analysis

Case History	**1984 study (Woo et al. 1989)**	**Fill -TS3 (Bergado et al. 1997)**	**Vacuum – Fill, TV2 (Bergado et al. 1998)**	**Vacuum –Fill (Saowapakpiboon et al. 2008)**	**ILLICON**
Spacing, (m)	2.0 x 1.75	1.0	1.0	0.85	No change
Pattern	Triangular	Triangular	Triangular	Triangular	No change
Type of Drains	Sand	PVD	PVD	CPVD	-
Section (mm)	0.26m dia	100 x 4	100 x 4	106 x 4	No change
Discharge Capacity (m^3/year)	-	30	50	-	1.5 to 0.8, 1.5 to 15[1]
Penetration Depth (m)	14.5	12	12	10	No change
r_s/r_m	-	-	-	-	2/1.4[1]
Time for Installation of drains (Days) [2]	60	60	60	60	No change

[1]Used for sand drains
[2]After placement of sand blanket

Table 6.3: Details of instruments used in different studies

Case History	Settlement Gauges		Piezometers	Vacuum Gauge	Inclinometers
	Surface	Subsurface			
1984 study (Woo et al. 1989)	x	x	Used but type not specified	x	x
Fill -TS3 (Bergado et al. 1997)	x	x	Pneumatic, hydraulic, and open stand pipe	-	x
Vacuum –Fill, TV2 (Bergado et al. 1998)	x	x	Observation well, stand pipe and electric	x	x
Vacuum –Fill (Saowapakpiboon et al. 2008)	x	-	Used but type not specified	x	-

x: Used

-: No information

6.11 Figures

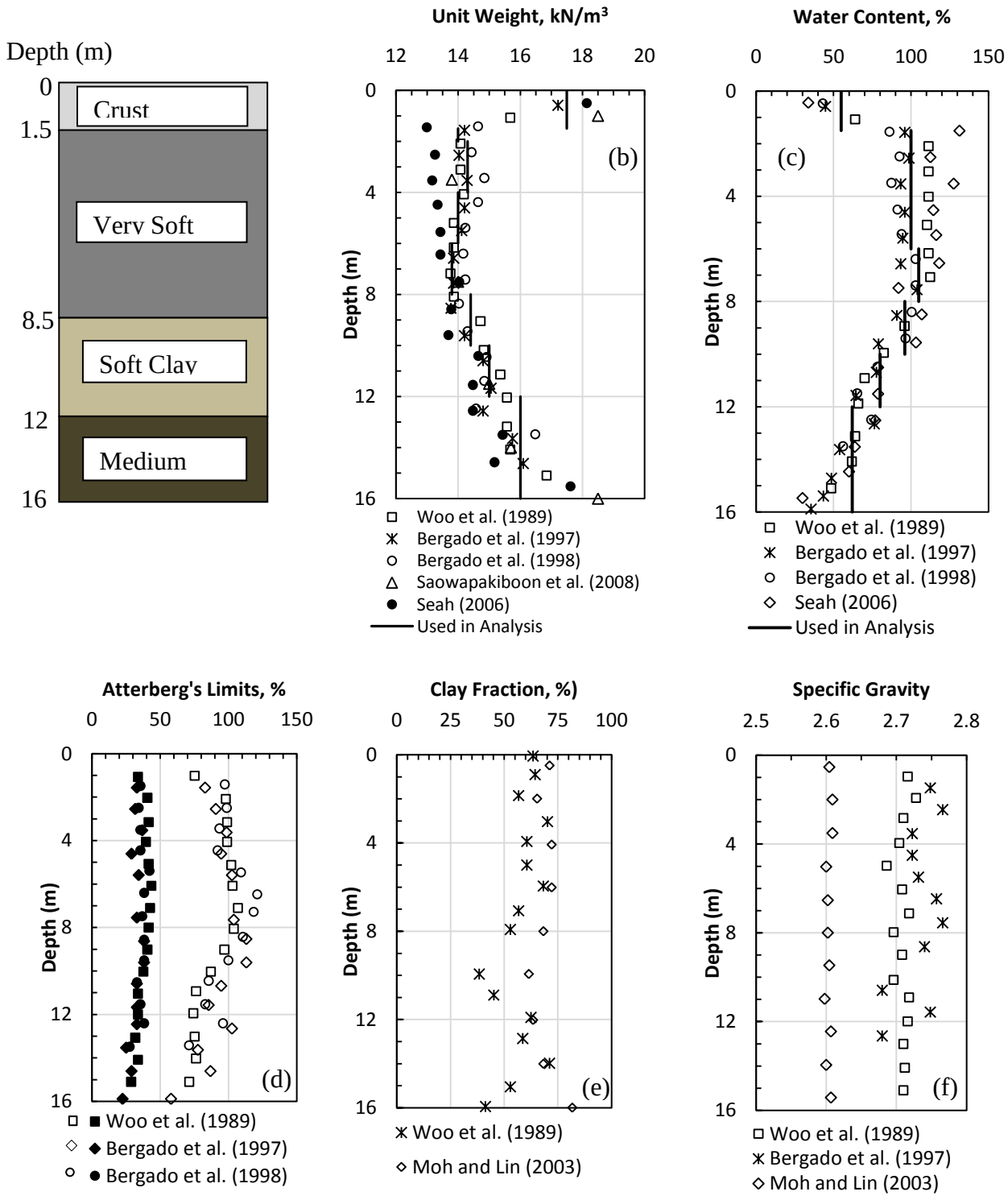

Figure 6.1: Generalized soil profile and vertical distribution of geotechnical properties

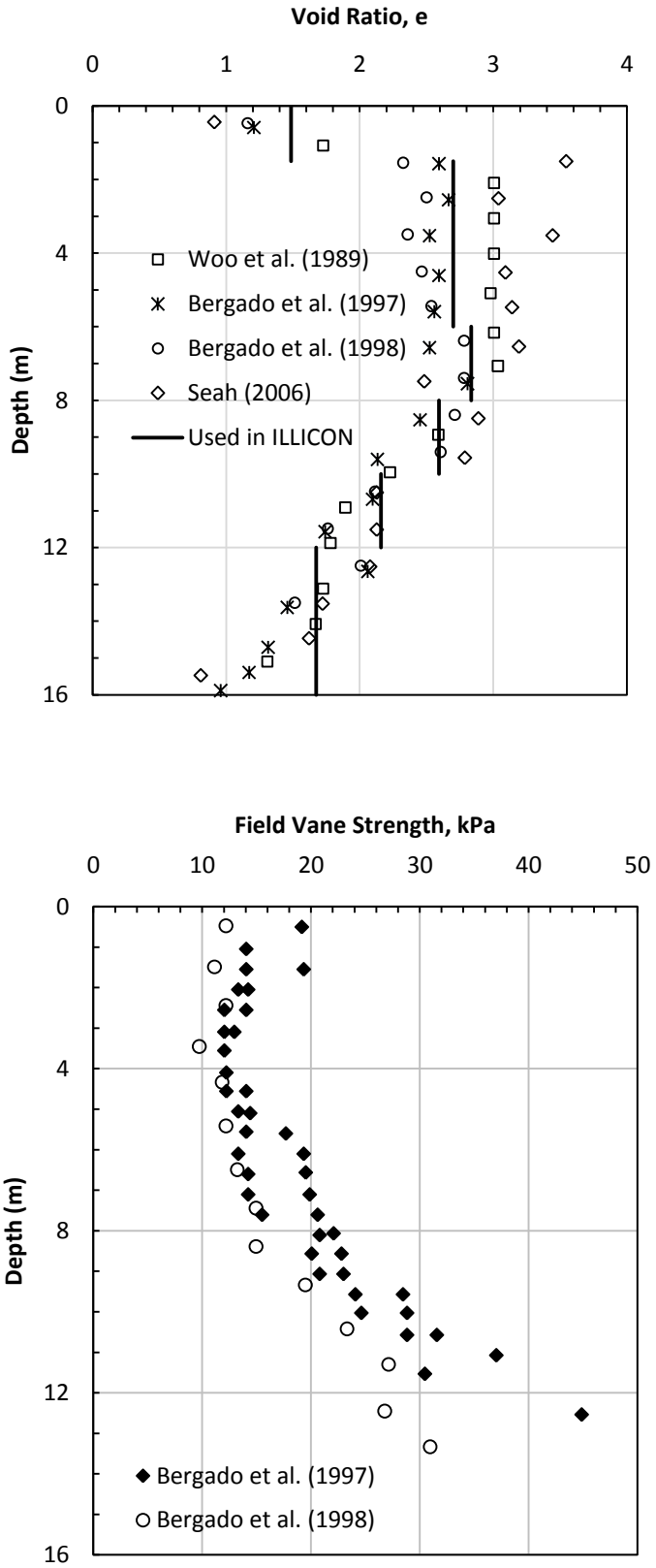

Figure 6.2: Vertical distribution of (a) void ratio and (b) field vane shear strength

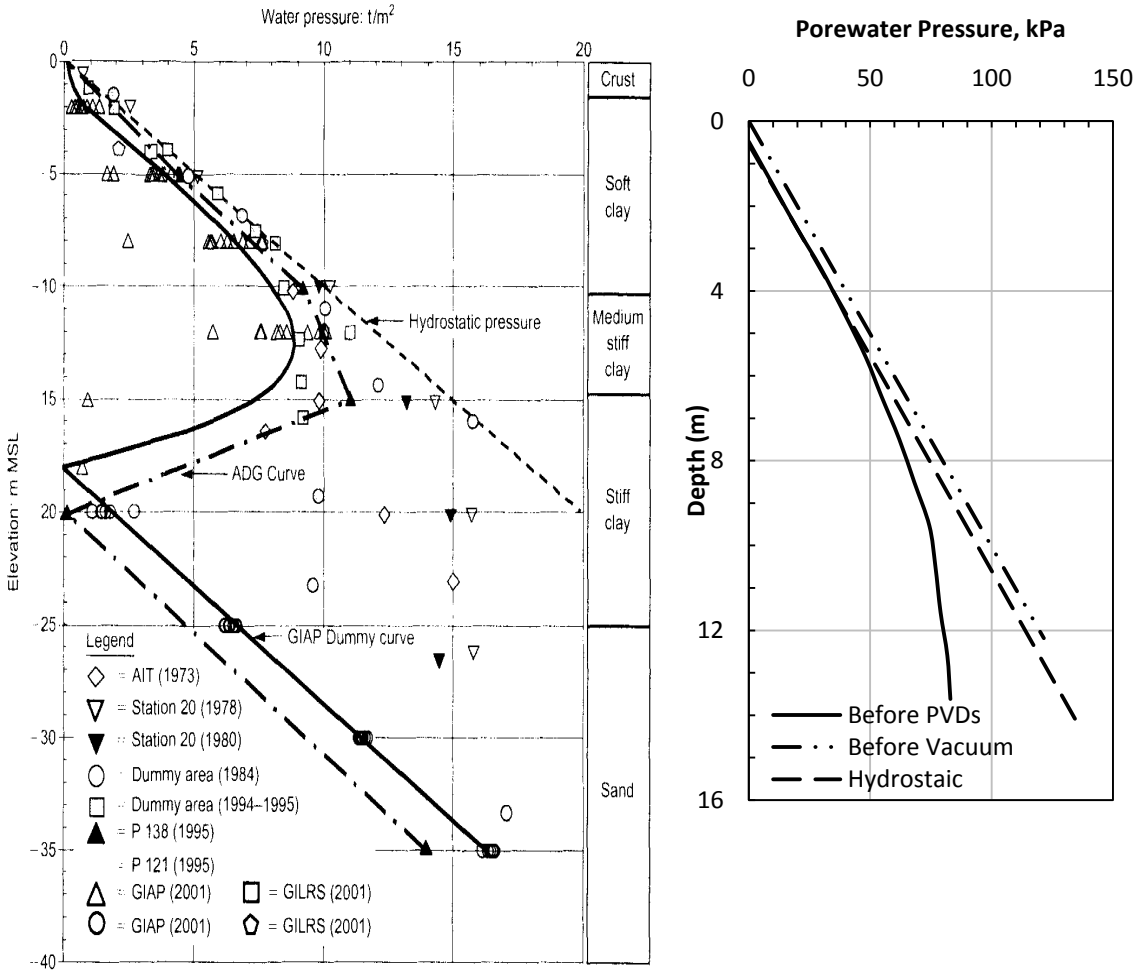

(a): After Moh and Lin (2003) (b): Data from Bergado et al. (1998)

Figure 6.3: Pretreatment porewater pressure and porewater pressure immediately before application of vacuum preload

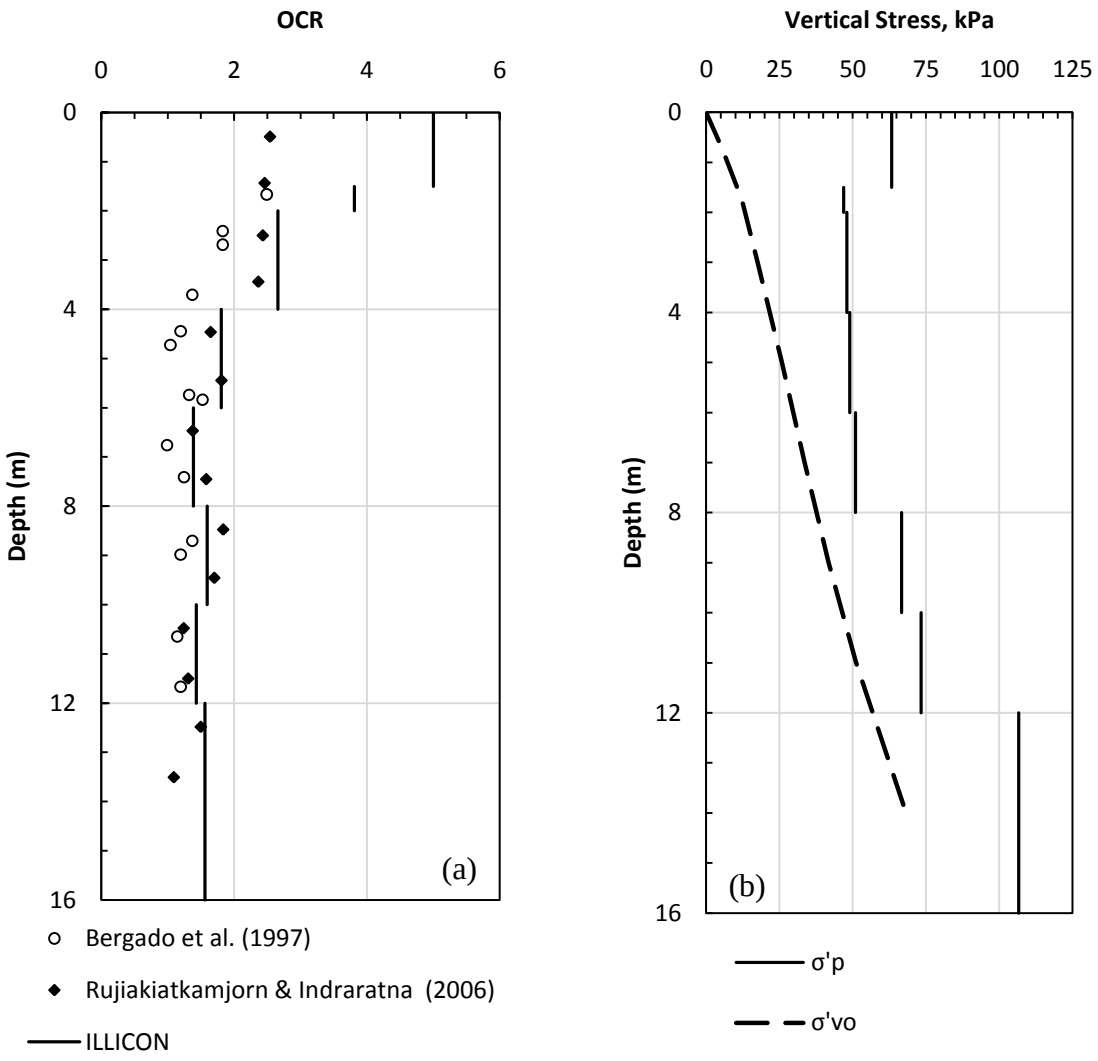

Figure 6.4: Vertical profile of (a) OCR and (b) initial effective vertical stress and preconsolidation pressure

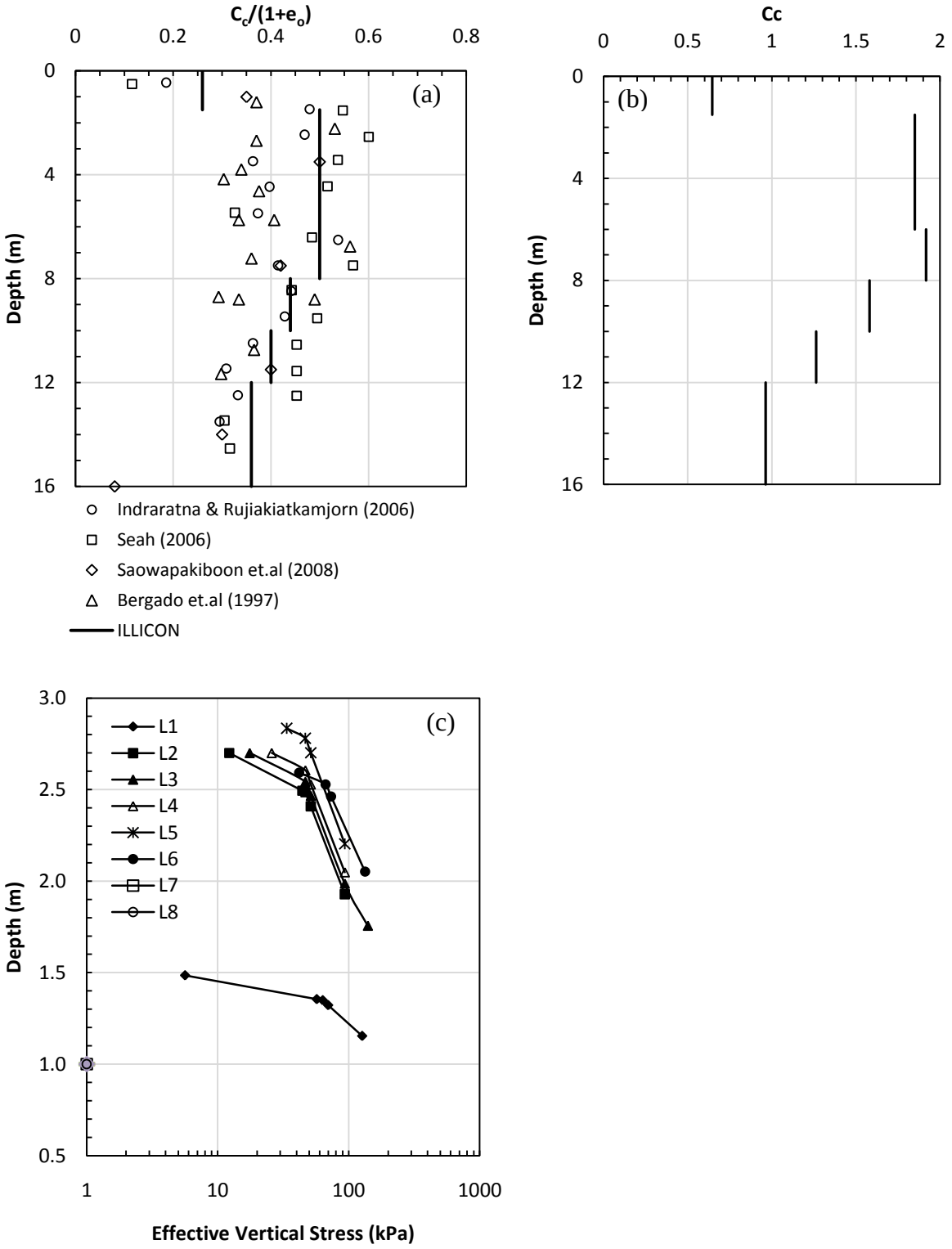

Figure 6.5: Vertical profile of (a) compression ratio, (b) compression index, and (c) EOP *e* - *log* σ'_v relations used in the ILLICON analysis

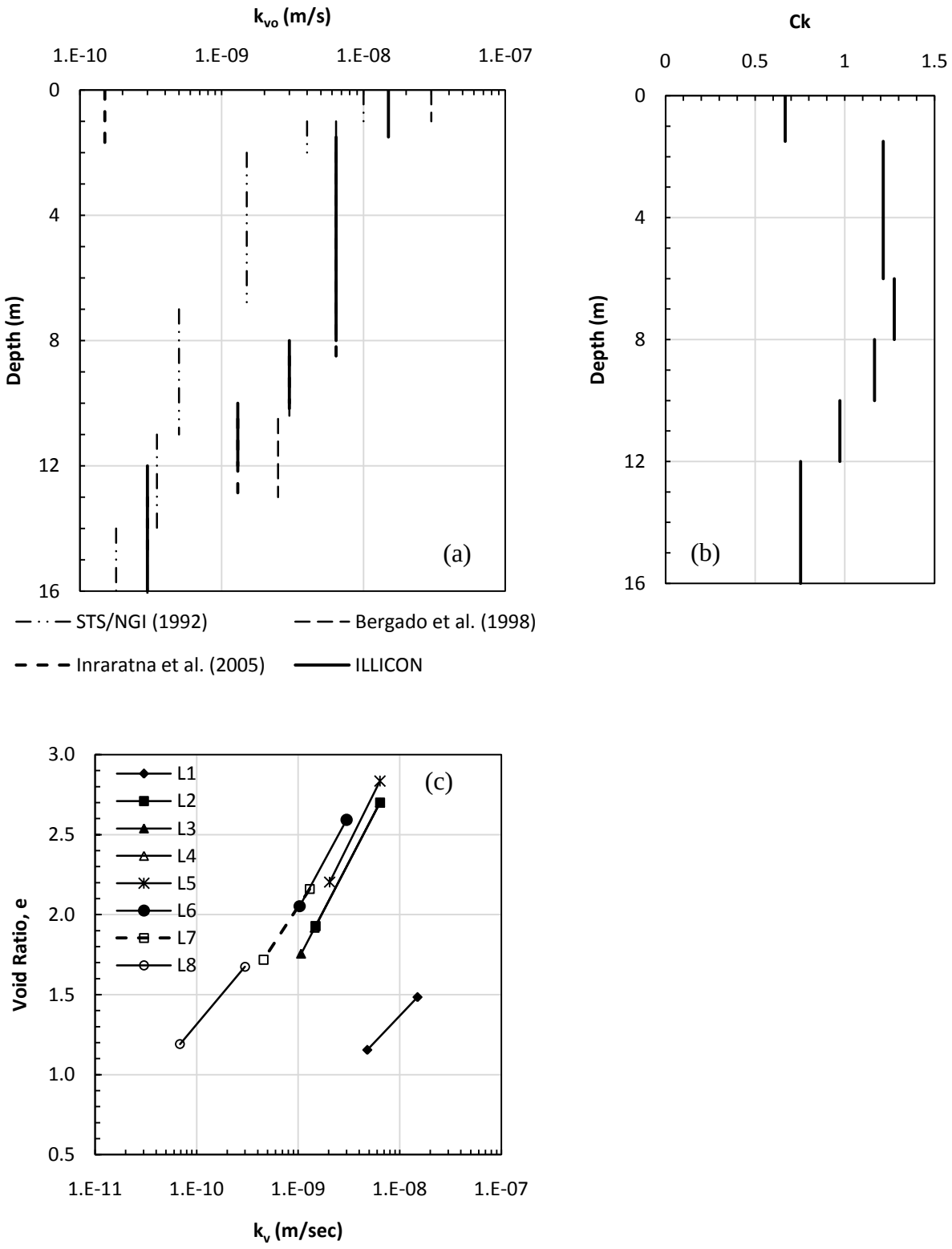

Figure 6.6: Vertical profile of (a) initial vertical permeability, (b) C_k and (c) *e - log* k_v relations used in the ILLICON analysis

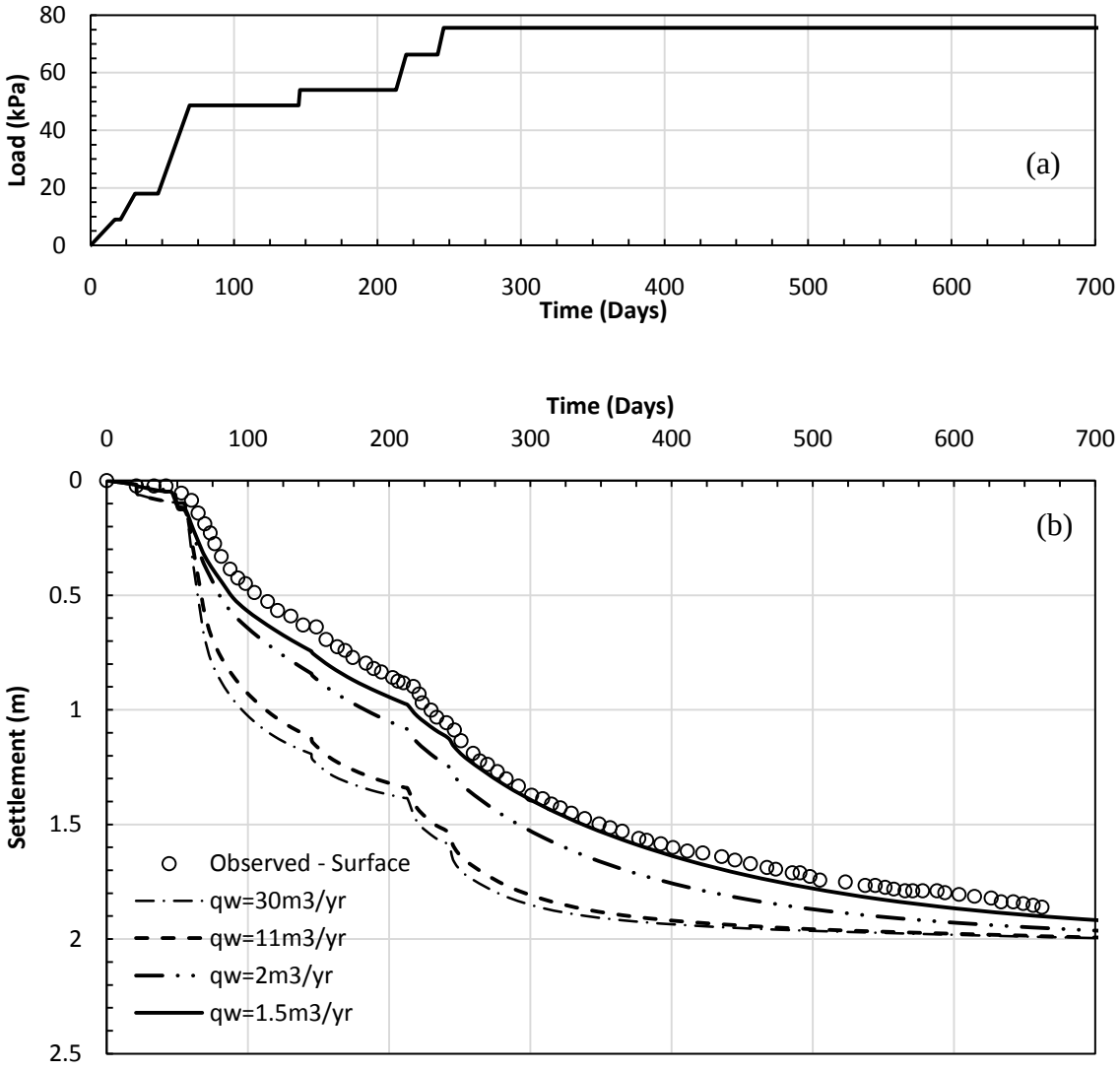

Figure 6.7: (a) Loading sequence, and (b) observed and predicted settlements for different discharge capacities for TS3 (field data from Bergado et al. 1997)

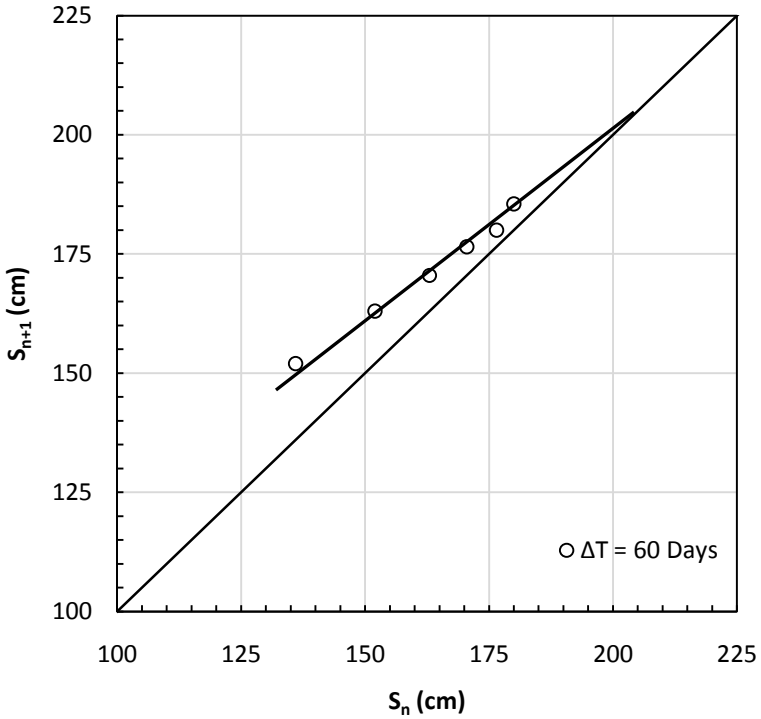

Figure 6.8: Asoaka method applied to observed surface settlements of TS3 (data from Bergado et al. 1997)

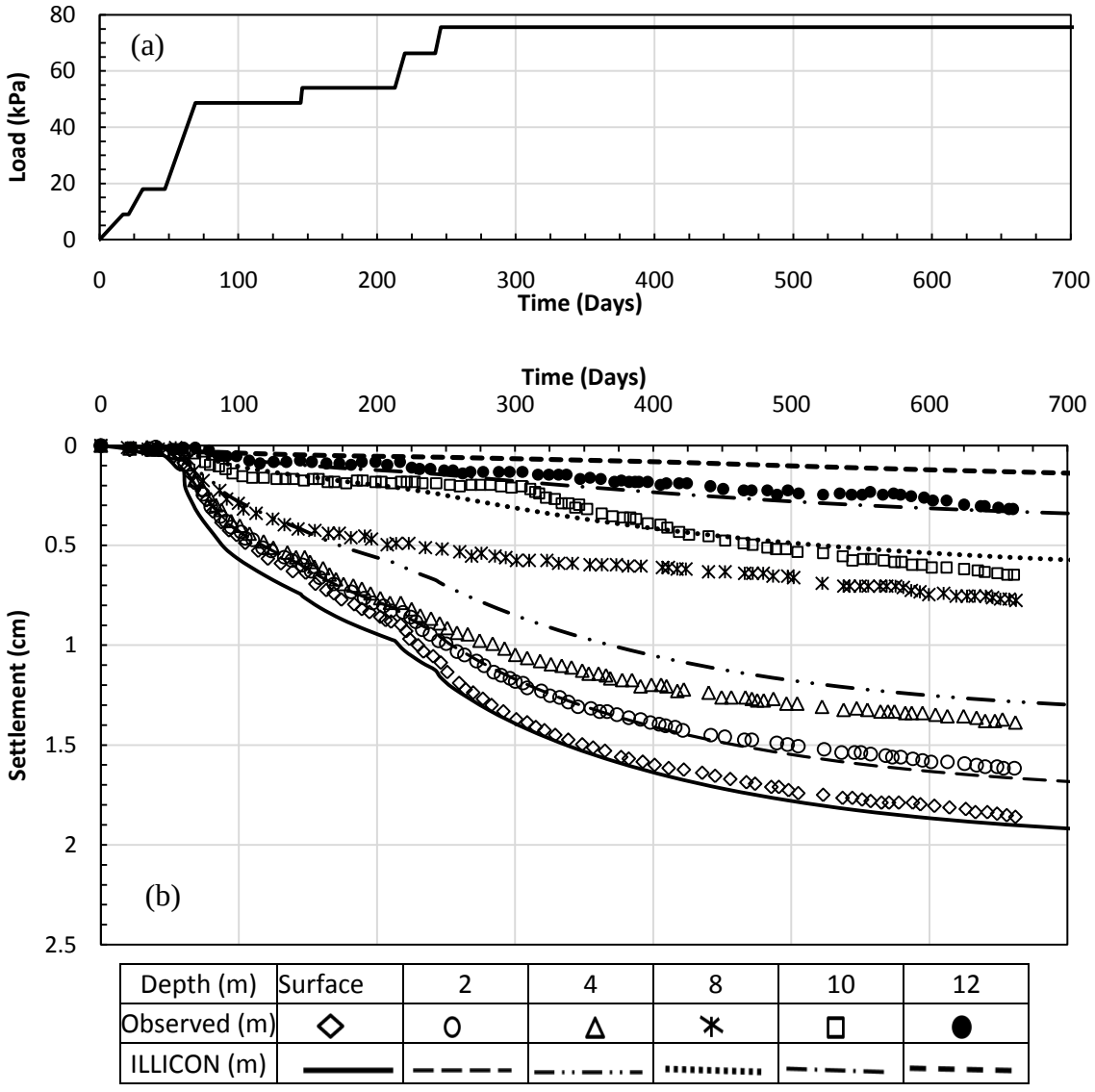

Figure 6.9: Observed and predicted subsurface settlements corresponding to a discharge capacity of 1.5m^3/yr. for TS3 (field data from Bergado et al. 1997)

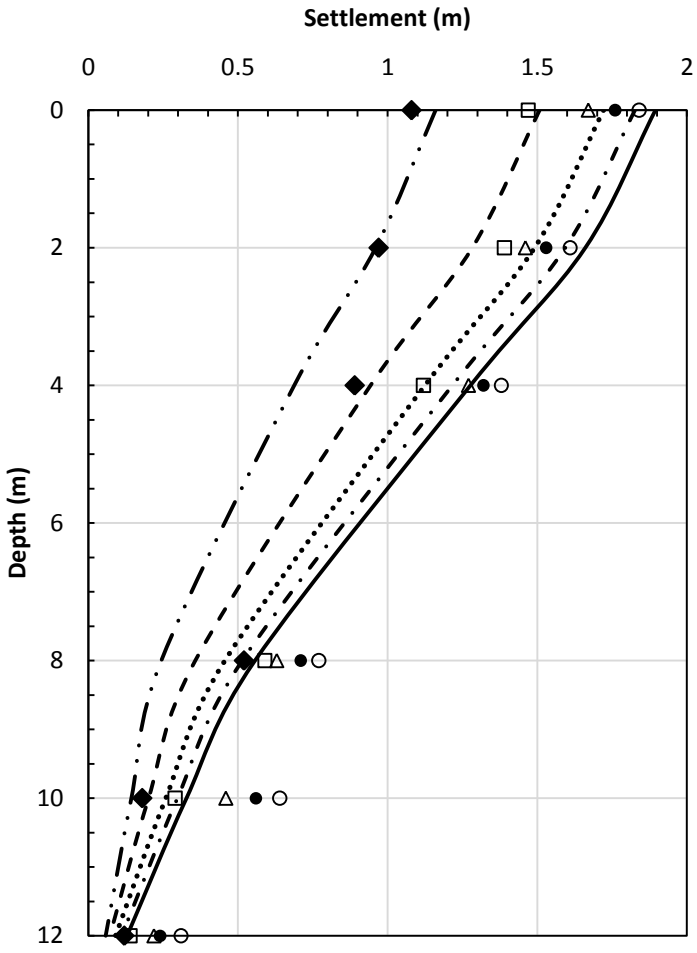

Time (Days)	246	340	453	548	650
Observed (m)	◆	□	△	●	○
ILLICON (m)	— · · — · · —	— — — —	.....	— · — · —	———

Figure 6.10: Vertical profile of observed and predicted subsurface settlements corresponding to discharge capacity of 1.5m^3/yr. for TS3 (field data from Bergado et al. 1997)

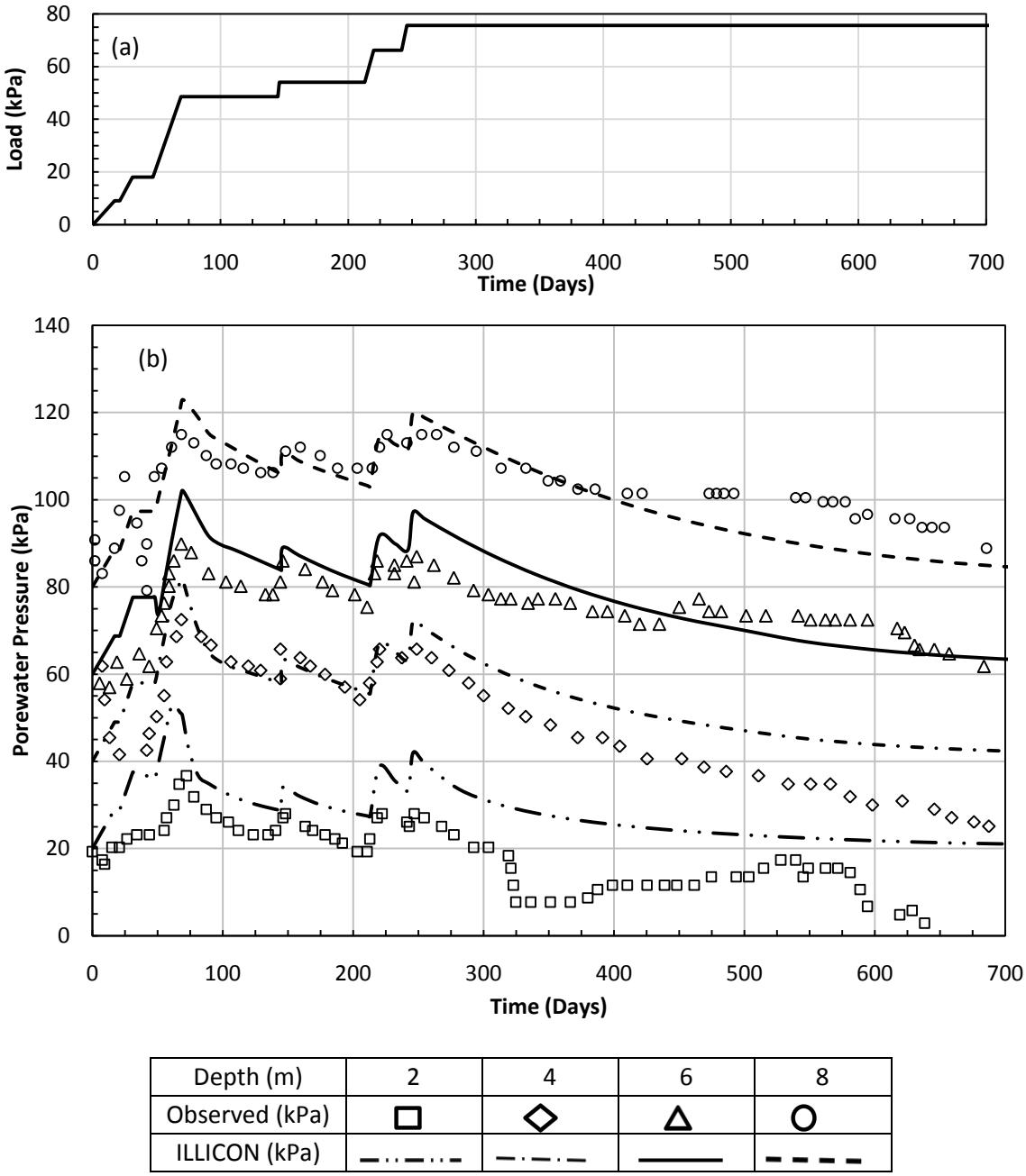

Figure 6.11: Observed and predicted porewater pressure distribution at different depths, corresponding to a discharge capacity of 1.5m^3/yr. for TS3 (field data from Bergado et al. 1997)

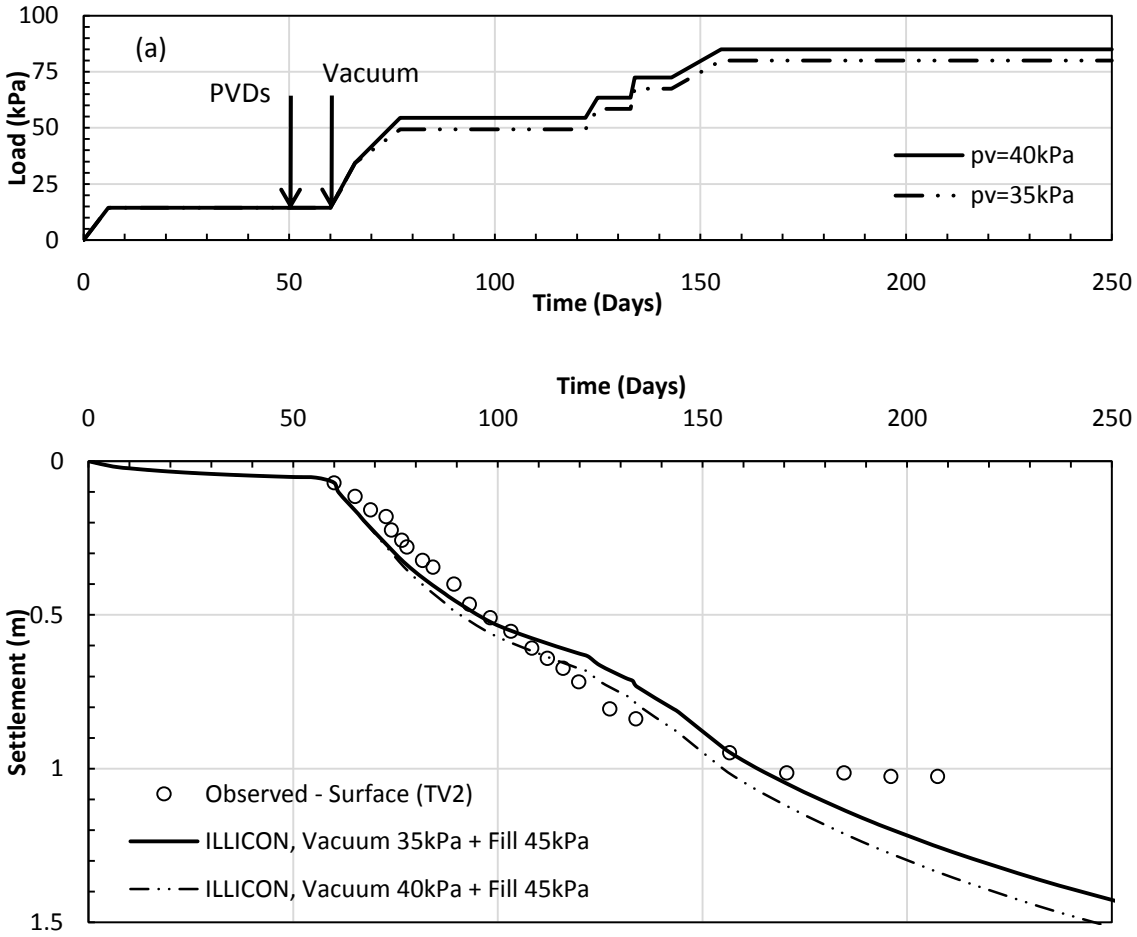

Figure 6.12: Observed and predicted surface settlements, assuming constant vacuum pressure passed 200 days, corresponding to a discharge capacity of 1.5m^3/yr. for TV2 (field data from Bergado et al. 1998)

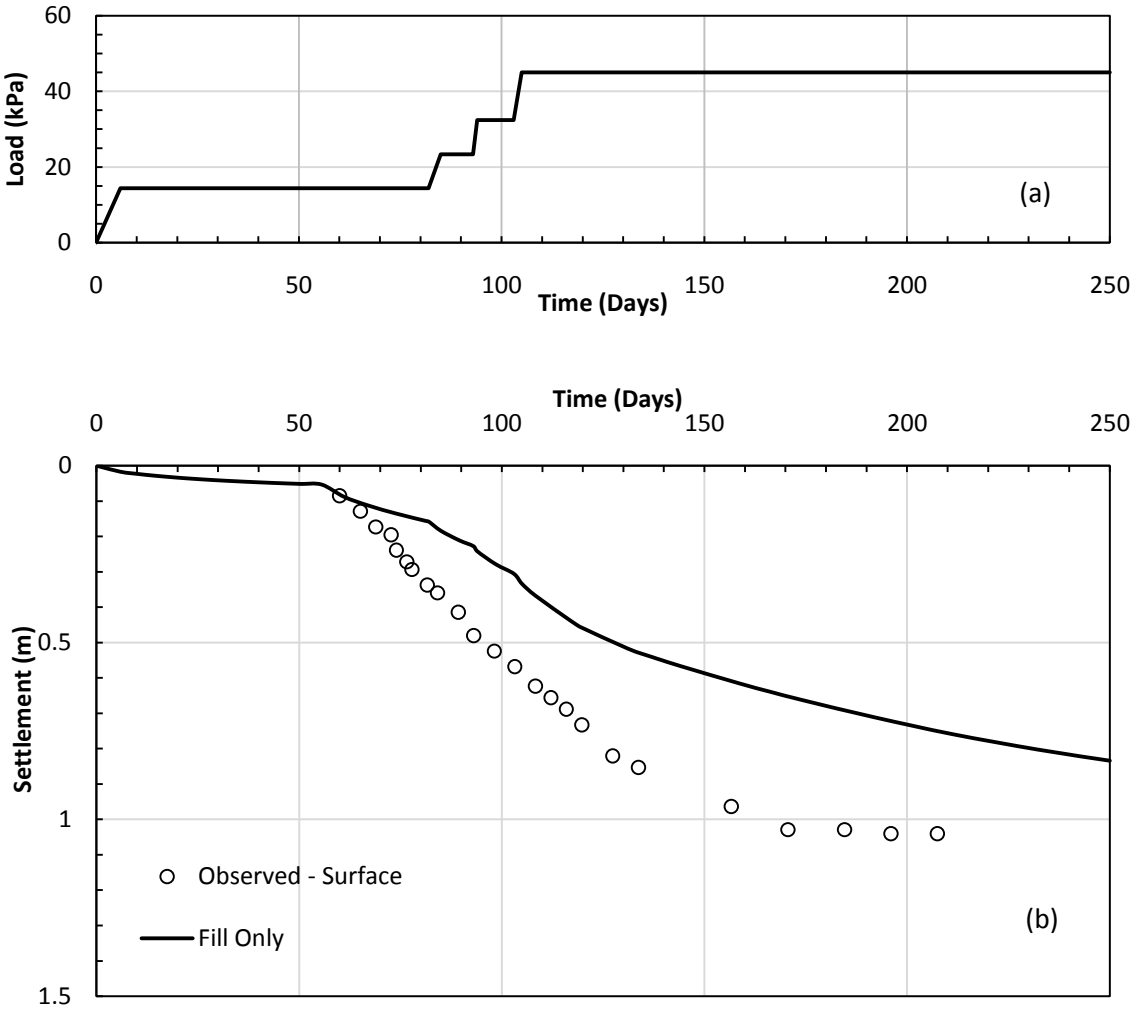

Figure 6.13: Predicted surface settlements under the action of fill load only, corresponding to a discharge capacity of 1.5m^3/yr for TV2 (field data from Bergado et al. 1998)

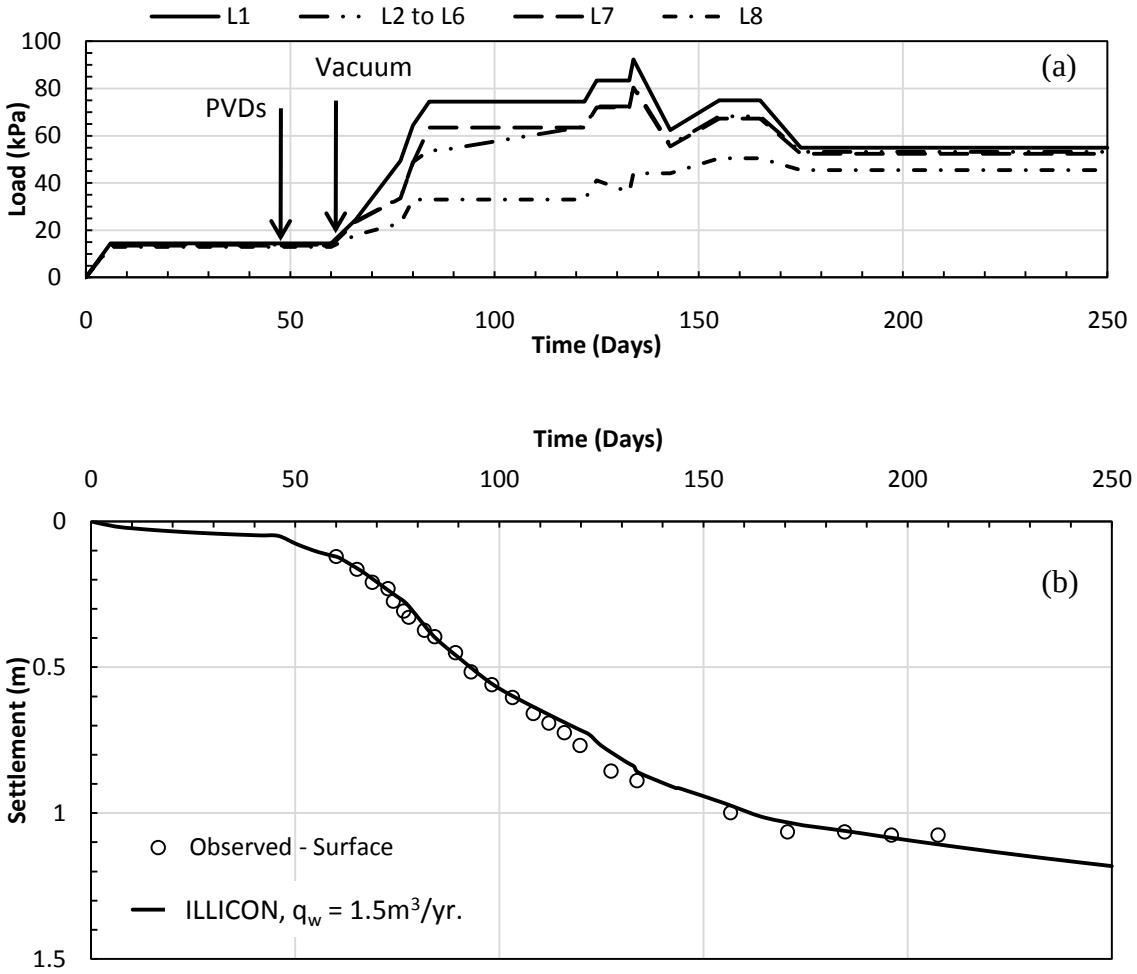

Figure 6.14: (a) Loading schedule considered for different sublayers, and (b) observed and predicted surface settlements corresponding to a discharge capacity of 1.5m^3/yr. for TV2 (field data from Bergado et al. 1998)

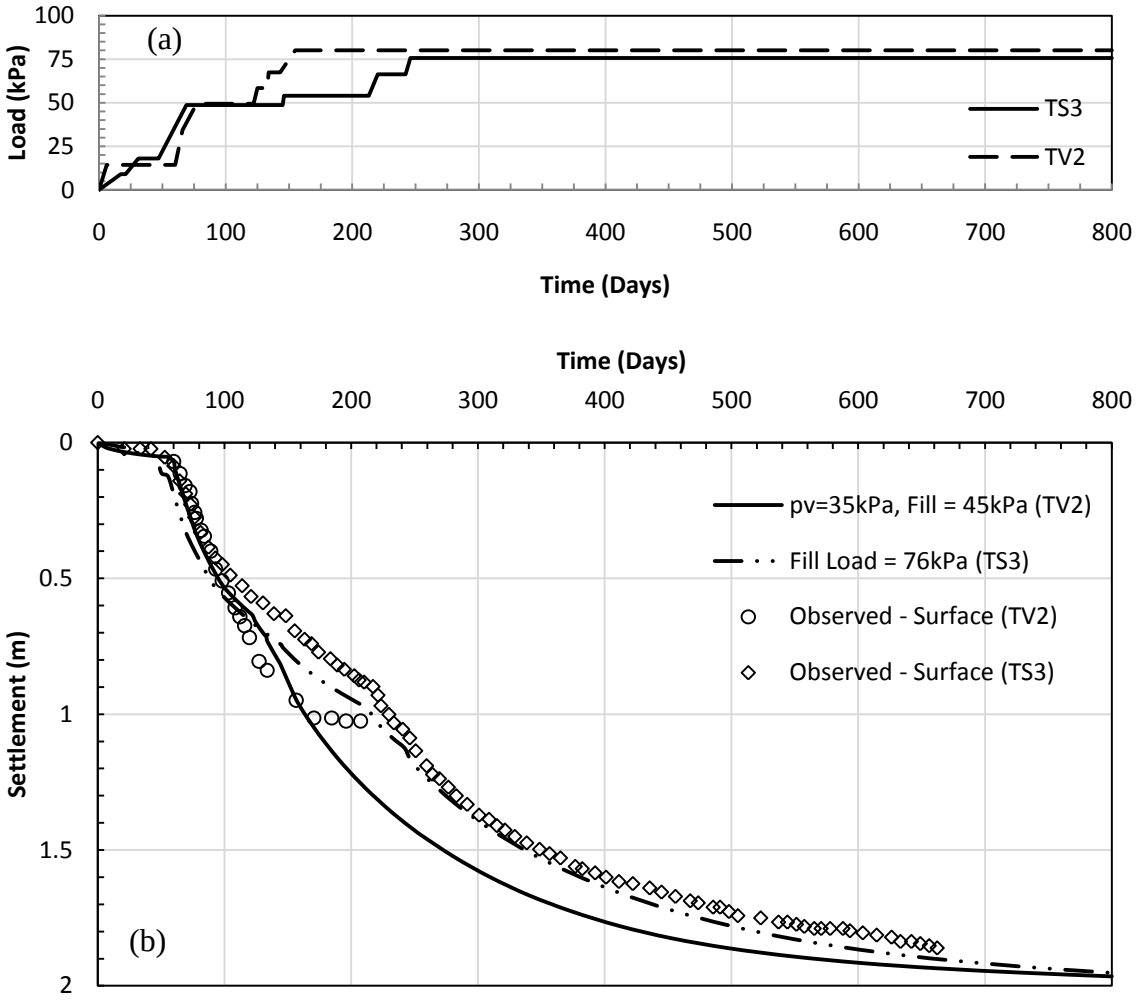

Figure 6.15: Comparison of ILLICON predictions for TS3 and TV2 along with the observed settlements

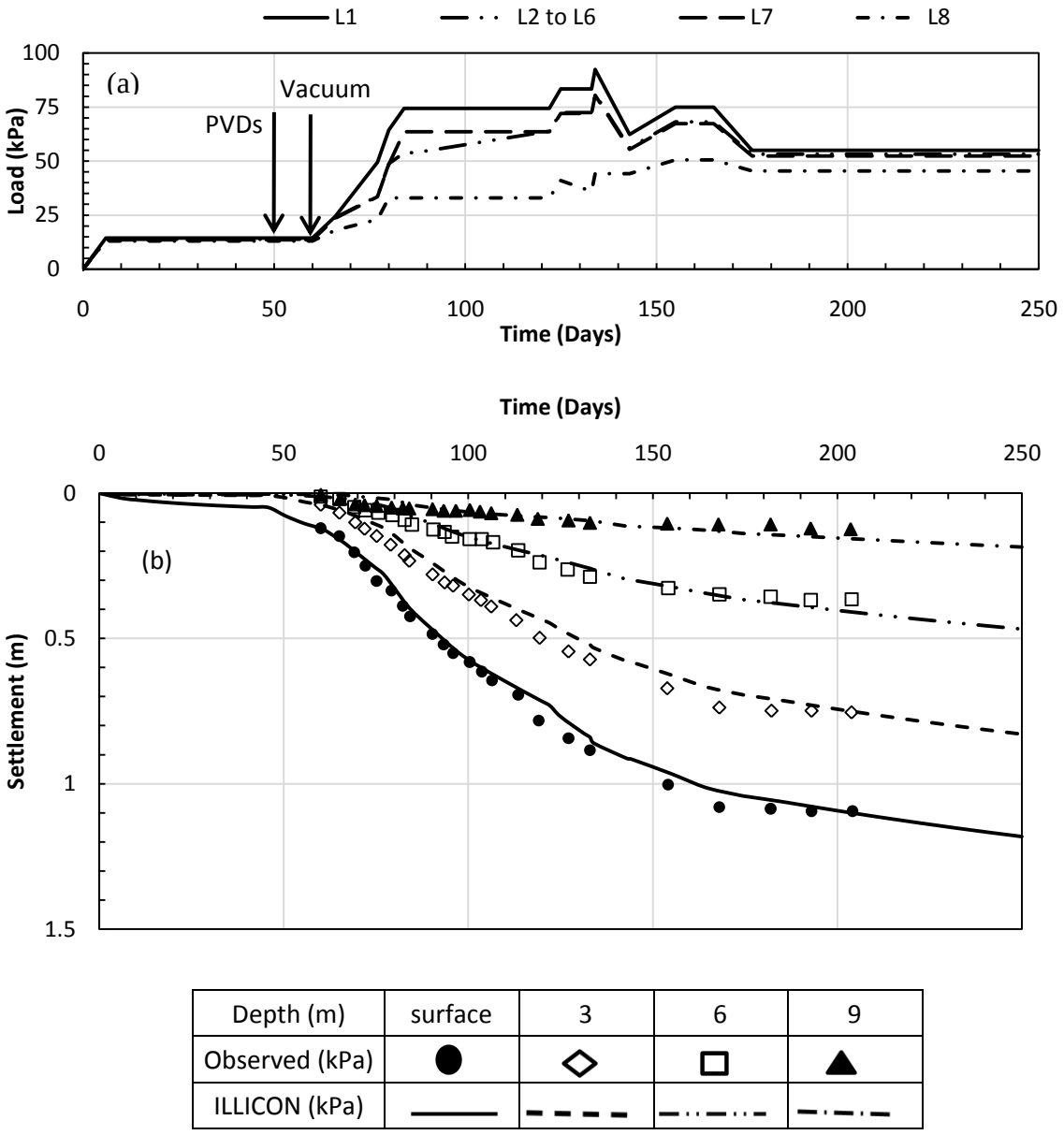

Figure 6.16: Observed and predicted subsurface settlements corresponding to a discharge capacity of 1.5m^3/yr. for TV2 – Case III (field data from Bergado et al. 1998)

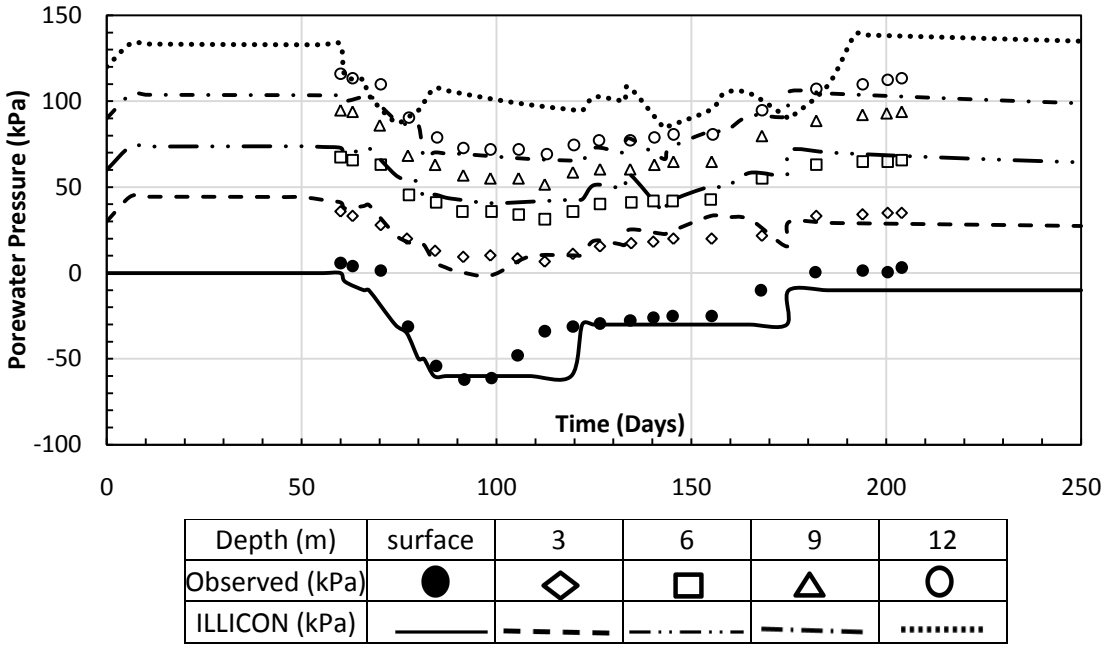

Figure 6.17: Observed and predicted porewater pressures at different depths, corresponding to a discharge capacity of 1.5m^3/yr. for TV2 (field data from Bergado et al. 1998)

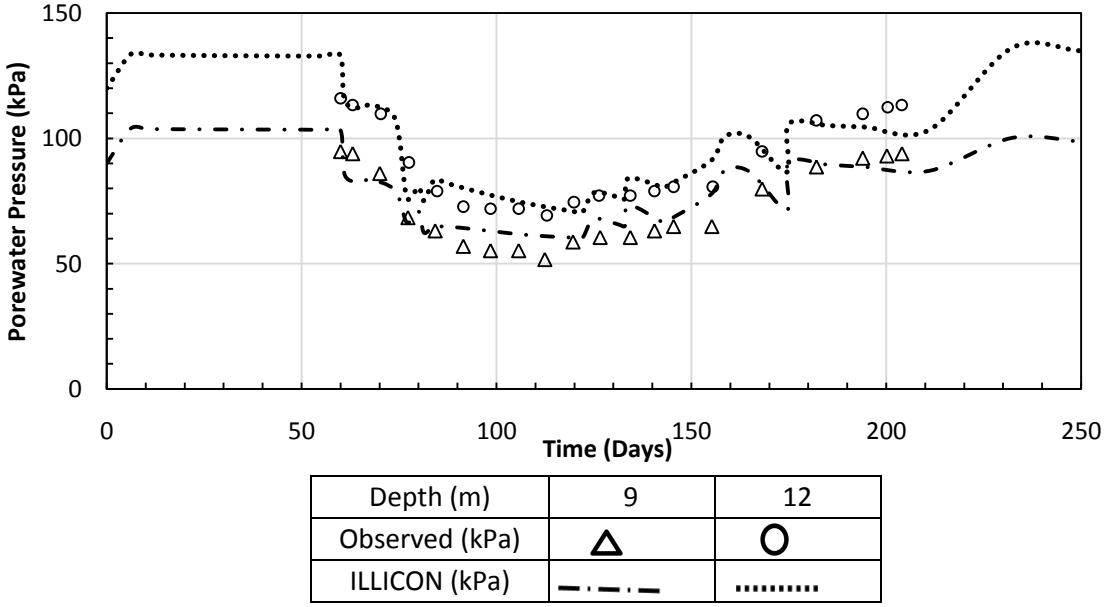

Figure 6.18: Observed and predicted porewater pressures at depths of 9m and 12m, corresponding to a discharge capacity of 1.5m^3/yr. and hydrostatic porewater pressures of 1994.

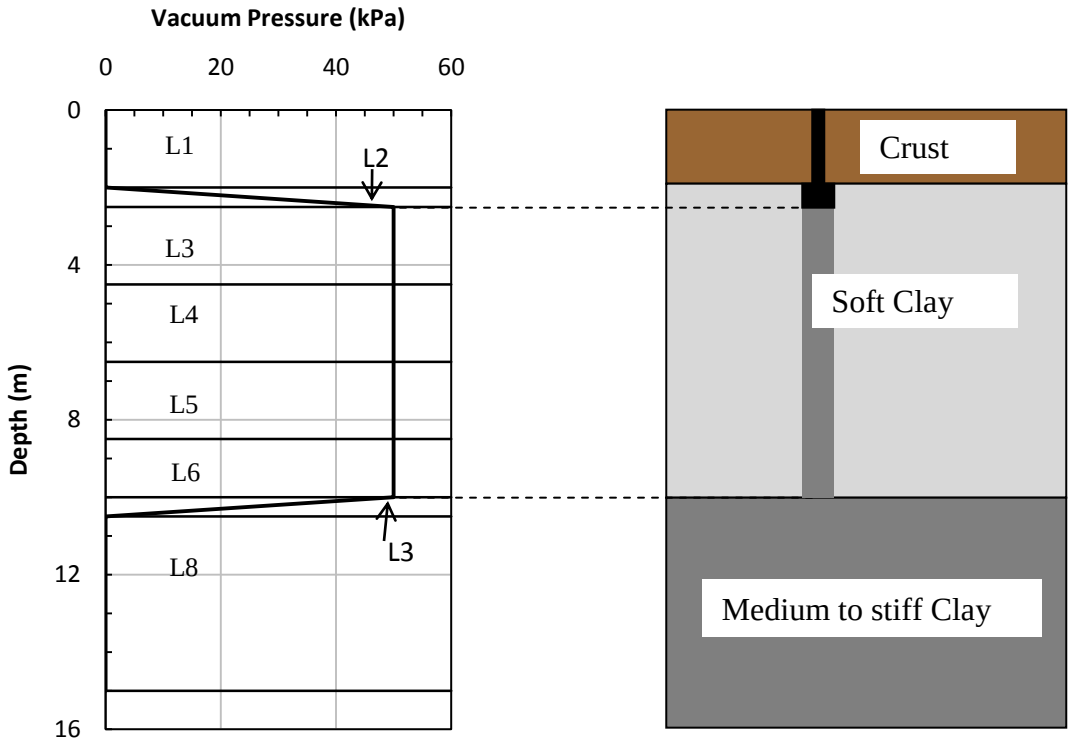

Figure 6.19: Vertical distribution of vacuum pressure applied to soft clay layer through CPVD and sublayers considered in ILLICON analyses

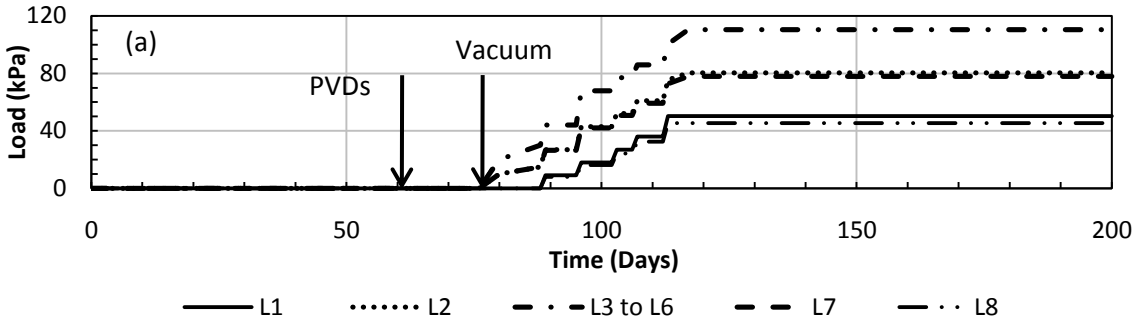

(a)

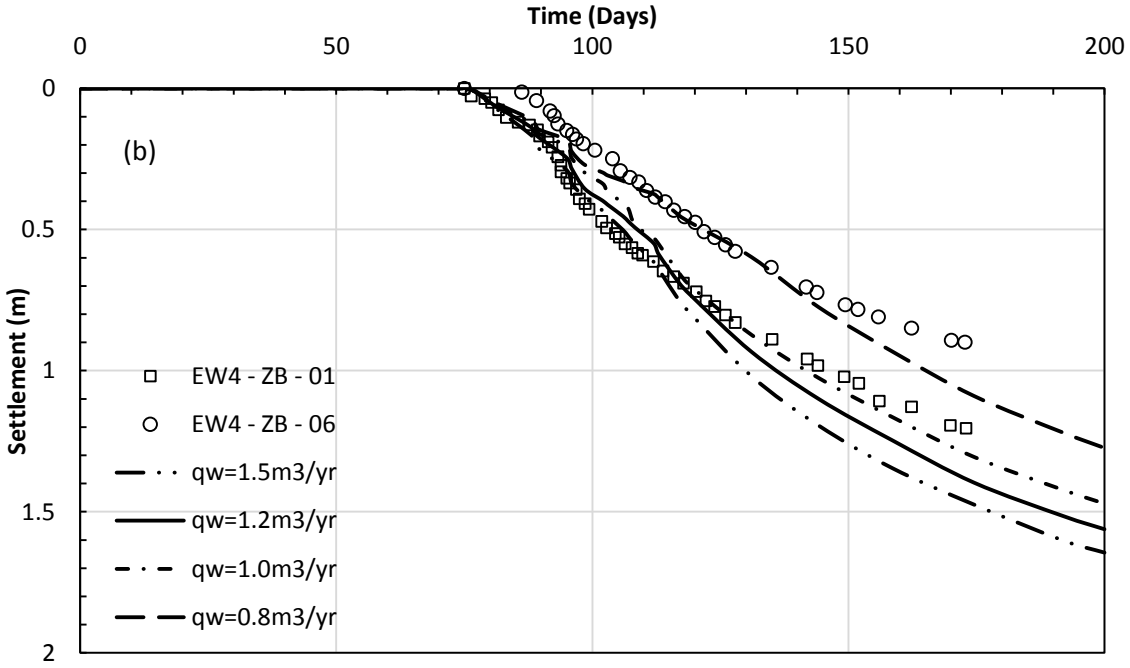

(b)

Figure 6.20: (a) Load applied to different sublayers, and (b) observed and predicted settlements for different discharge capacities corresponding to a maximum vacuum pressure of 60kPa (data from Saowapakpiboon et al. 2008)

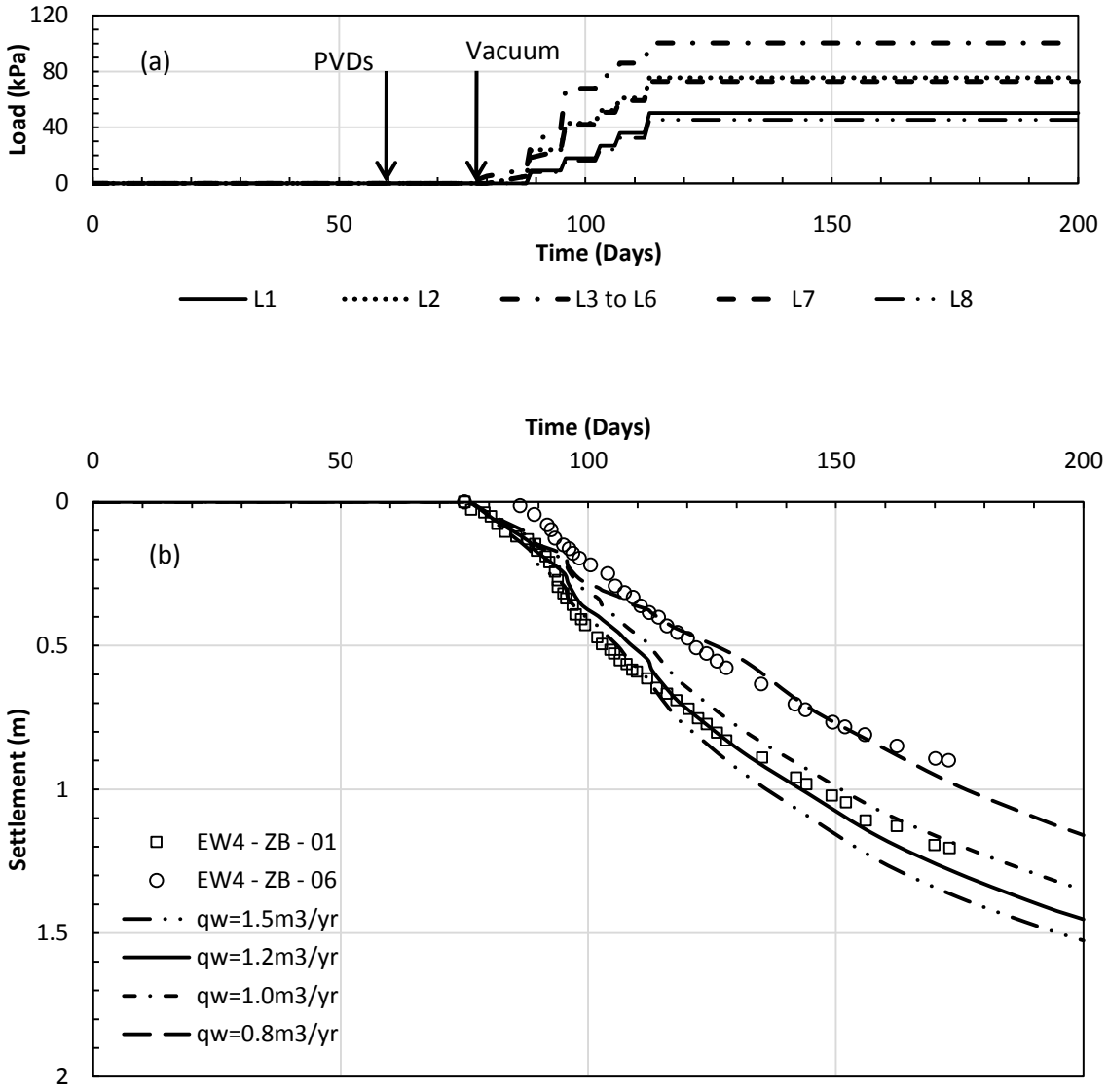

Figure 6.21: (a) Load applied to different sublayers, and (b) observed and predicted settlements for different discharge capacities corresponding to a maximum vacuum pressure of 50kPa (data from Saowapakpiboon et al. 2008)

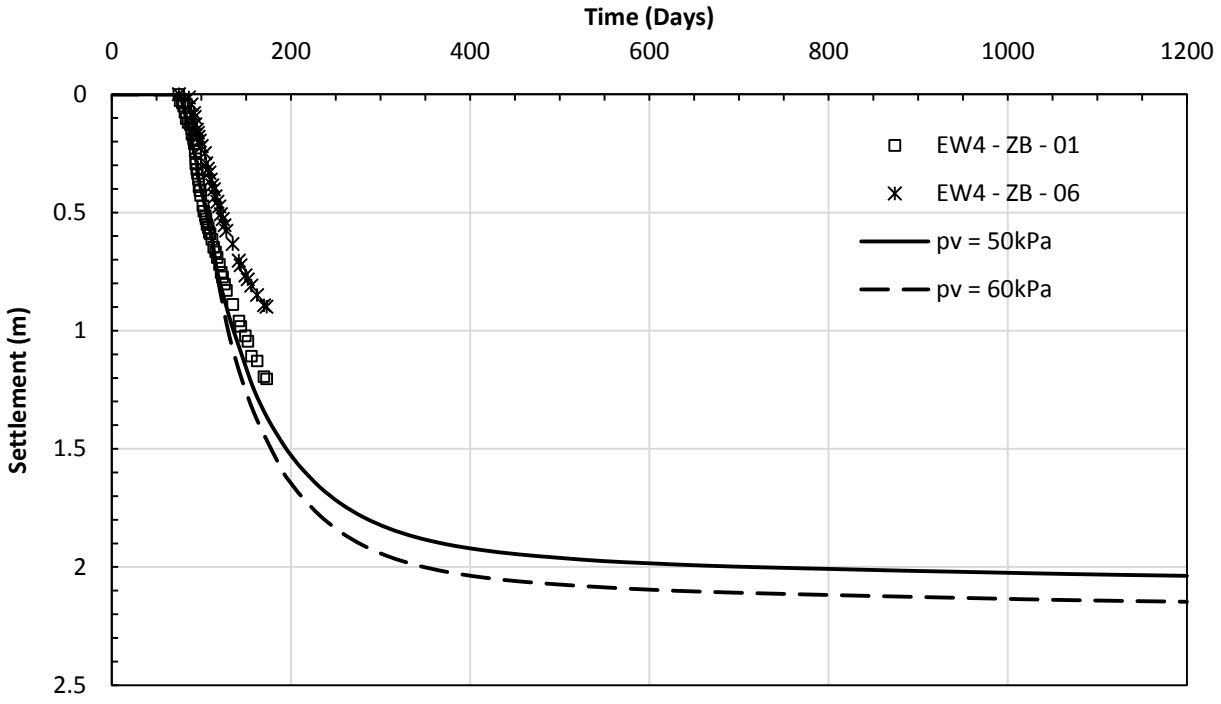

Figure 6.22: End-of-primary settlement corresponding to a vacuum pressure in the range of 50 to 60kPa for a discharge capacity of 1.5m^3/yr.

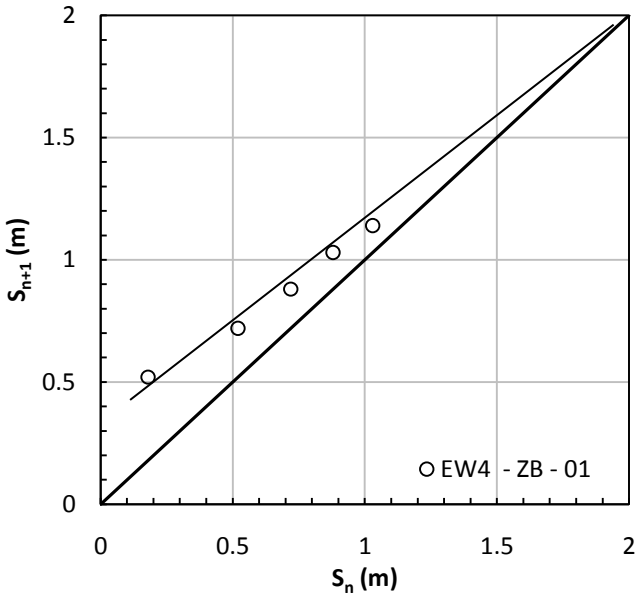

Figure 6.23: Asoaka method applied to predict EOP settlement (data from Saowapakpiboon et al. 2008)

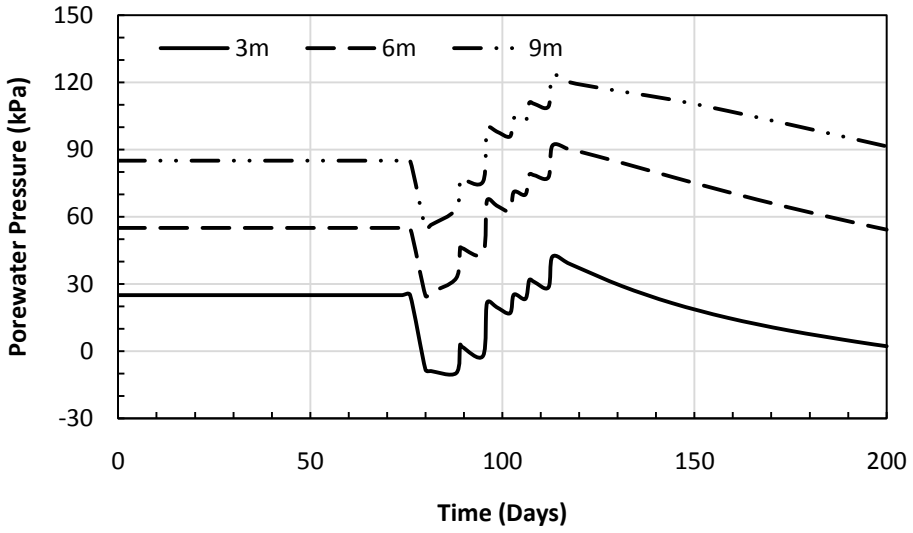

Figure 6.24: Predicted porewater pressure response at various depths

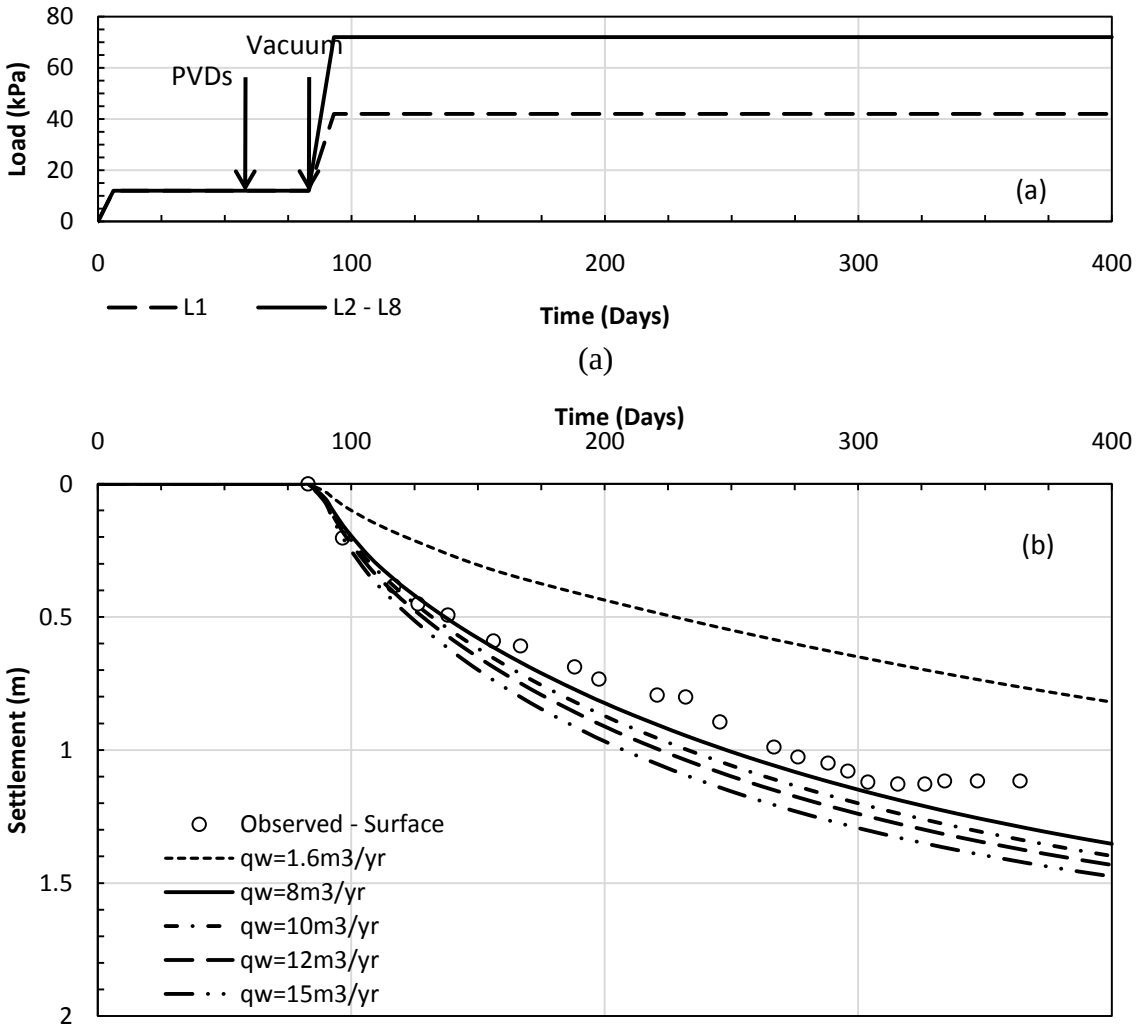

Figure 6.25: Observed and predicted settlements for different discharge capacities of sand drains (observed settlement data from Woo et al. 1989)

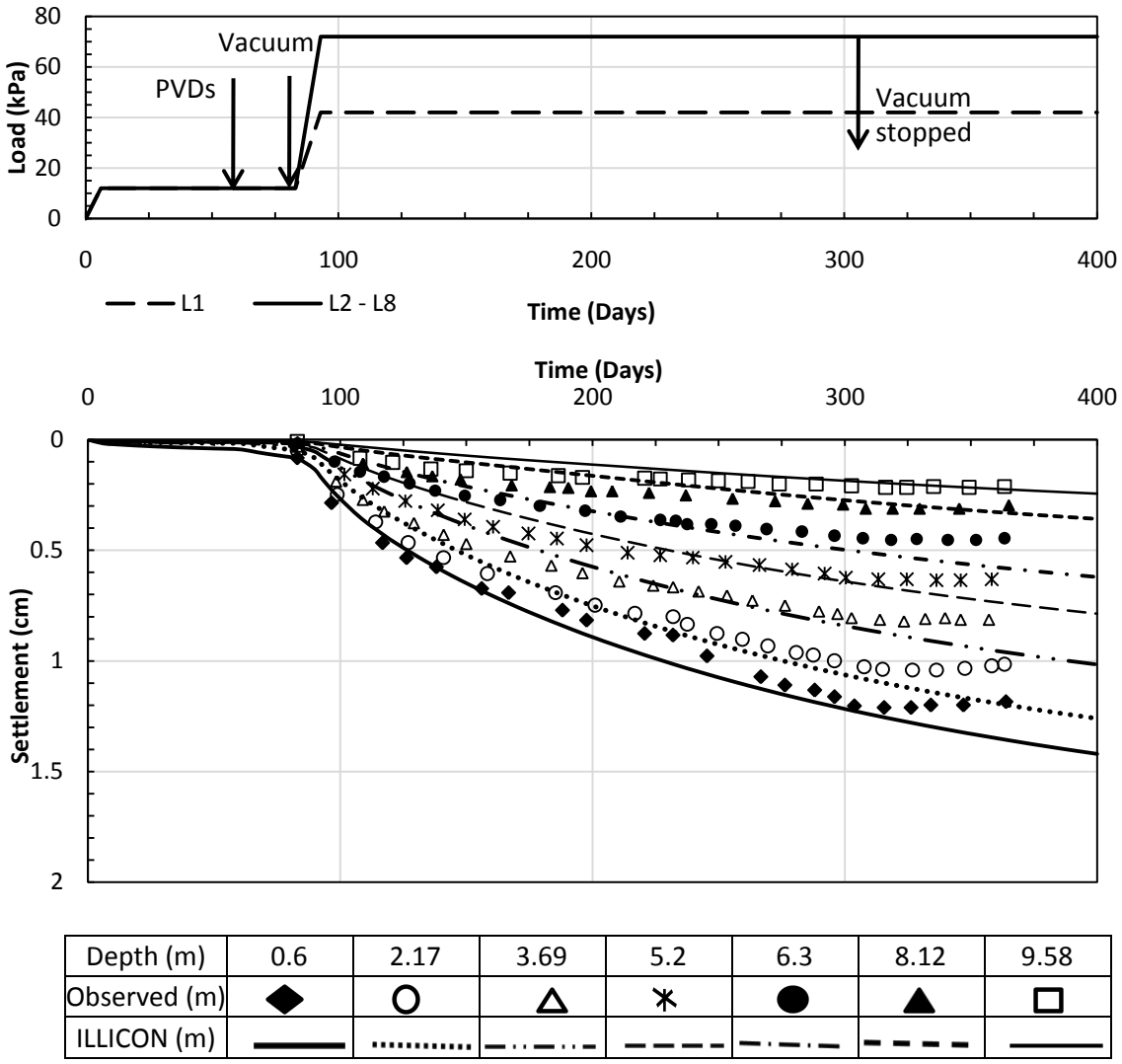

Figure 6.26: Observed and predicted subsurface settlements corresponding to a discharge capacity of $10m^3/yr$. (observed settlement data from Moh and Lin 2006)

CHAPTER 7. SOIL IMPROVEMENT FOR A ROAD CONSTRUCTION PROJECT IN JAPAN USING VACUUM TOGETHER WITH PREFABRICATED VERTICAL DRAINS

7.1 Introduction

Soil improvement, using vacuum as a preload together with PVDs was carried out in Saga, Japan. The improvement area was over a strip, with a length of 1000m and a width of 16 – 18m. The subsurface conditions were poor, and a 1m thick sand mat was constructed in order to carry out investigations and install PVDs in the ground. The improvement area was divided into six sections and an average vacuum pressure of 60kPa was successfully maintained in the sand blanket of all sections for a period of 80 - 110 days. Observed settlements under vacuum preloading ranged from 0.9 to 1.1m. Section 4 of the improvement area, is analyzed using the computer program ILLICON and the results are compared with the field observations of settlement and porewater pressure.

7.2 Subsurface Conditions

Ariake clay, found in Kyushu Island of Japan (Fig. 7.1), is characterized by high sensitivity and low shear strength. The natural water content of Ariake clay deposits varies between 100 to 150% (Hanzawa et al. 1990; Hong and Tsuchida 1999). Geologically, these deposits are classified as normally consolidated; however, the preconsolidation pressure is found to be greater than the present overburden (Hanzawa et al. 1990). Figure 7.2 presents the soil profile and vertical distribution of geotechnical properties as reported by Chai et al. (2006). Solid dots on Fig. 7.2 represent the reported values, whereas, the solid vertical lines represent average soil properties of each sublayer used in the ILLICON settlement analysis. It can be seen that the natural moisture content is generally in excess of liquid limit. The void ratio varies between 2.0 and 3.8.

Depth of ground water table (GWT), for the project site generally varies between 0.5m and 1.5m; however in Section 4, it was found to be located at the ground surface during the entire period of treatment (Chai et al. 2006). It is important to note that for evaluating settlements and porewater pressure response, Chai et al. (2006) assumed GWT to be located at ground surface, however, for calculation of initial effective vertical stress condition, the GWT was assumed 1m below the natural ground surface (Fig. 7.3b). Porewater pressure profile from piezocone tests and actual measurements of porewater pressure (Figs. 7 and 14 of Chai et al. 2006) confirms that the preconstruction GWT was located at the ground surface and the same has been used in the ILLICON analysis.

7.3 Compressibility and Permeability Characteristics

Figures 7.3a to 7.3c, respectively, show the initial effective vertical stresses (σ'_{vo}), preconsolidation pressure (σ'_{p}) used in ILLICON analyses, initial effective vertical stresses (σ'_{vo}), preconsolidation pressure (σ'_{p}) used by Chai et al. (2006) in their analysis, and values of compression index (C_c) reported by Chai et al. (2006). It can be seen that the reported values of C_c are quite high, indicating high compressibility of the soft ground. It was reported by Chai et al. (2006) that a settlement of 112mm was observed at a depth of 4.1m from the original ground surface, before the application of vacuum pressure, but after placement of drainage blanket and installation of vertical drains. A period of 182 days is assumed by Chai et al. (2006) between placement of sand blanket and application of vacuum pressure. Also the excess porewater pressure due to placement of sand blanket was completely dissipated before the commencement of vacuum preloading. Therefore, it is expected that, any back-analysis of the case history should approximately fulfill these two conditions, as well as the subsequent field observations. The values of C_c reported by Chai et al. (2006) along with σ'_{vo} and σ'_{p} together with $C_r/C_c = 0.1$ were used to construct the EOP *e-log*σ'_v relations as shown in Fig. 7.3d. These were used in ILLICON analysis to determine the settlement behavior under 1m thick sand blanket only, as shown in Fig. 7.4. It can be seen that under the load of sand blanket alone, the values of C_c reported by Chai et al. (2006) predict a higher settlement at the given depth, and porewater pressures that are completely dissipated within 182 days (before application of vacuum). It is also important to note that the values of C_c reported by Chai et al. (2006) predict a settlement equal to the observed value of 112mm even without installation of PVDs.

The values of C_c reported by Chai et al. (2006) were considered to be on the high side and therefore, alternative values of C_c were estimated empirically from the correlation between C_c and natural water content as proposed by Terzaghi et al. (1996) and shown by dashed lines on Fig. 7.3c. The new C_c and the corresponding EOP *e-log*σ'_v relations, as shown in Fig. 7.3e, were used in ILLICON analysis. It can be seen from Fig. 7.4 that the predicted and observed settlements are in closer agreement; moreover, ILLICON analysis predicts dissipation of 95% of the excess porewater pressure in 182 days which is in accordance with the field observations. It is also important to note that, most of the studies, in which compressibility characteristics of Ariake clays have been discussed, report significantly lower values of C_c as compared to those reported by Chai et al. (2006). For example, Kolsant (2006) quoted following relations from Japanese literature (Fujikawa and Takayama, 1980; Onitsuka, 1988)

$$C_c = 0.49\left(e_n - 0.49\right) \tag{7.1a}$$

$$C_c = 0.013\left(w_n - 10\right) \tag{7.1b}$$

Using Eq. 7.1, and the reported values of void ratio and natural water content; the C_c values were calculated and shown on Fig 7.3c. Additional data on C_c reported by Hino (2009) for a coastal road project in Saga lowlands (general area including project site) is also shown in Fig. 7.3c. It can be seen that the estimated values of C_c based on natural water content are the lower bound of the overall data, and therefore, these values of C_c as well as the values reported by Chai et al. (2006) are used in the subsequent analyses.

Chai and Miura (1999), based on their laboratory study on discharge capacity of PVDs and back analysis of test embankments, concluded that the permeability computed from the laboratory coefficient of consolidation (c_v), underestimates the actual field permeability. Therefore, the values of initial vertical permeability (k_{vo}) used by Chai et al. (2006) in their numerical model are twice the values estimated from the c_v of laboratory IL consolidation tests. Mesri et al. (1994) showed that the permeability representing field values can be reliably measured in the laboratory falling head or constant head permeability tests; however, the k_v computed from c_v may be equal or lower than the measured value. Considering the clay size fraction and plasticity index of Ariake clay, values of k_{vo} computed from the c_v of laboratory IL consolidation tests are considered to be reasonable estimates of

field permeability and are used in ILLICON analysis. A k_h/k_v ratio of 1.0 and reduction in permeability with $C_k = 0.5e_o$ is assumed in the ILLICON analysis. Figure 7.5 shows the vertical profiles of k_{vo}, C_k and $e - log\ k_v$ relations used in the ILLICON analysis.

7.4 Installation of Vacuum Consolidation System

The area was divided into six sections and each 167 x 17m section was treated separately. As reported earlier, a 1.0m thick sand blanket was placed on the soft clay layer to improve its bearing capacity. This sand blanket was used as a working platform to install PVDs to a depth of 10.0 to 11.5m from top of the sand blanket. In Section 4, the penetration depth of PVDs was 11.5m from the top of sand blanket or 10.5m from the natural ground surface (the gravelly sand layer was located 0.5m below the tip of PVDs). The PVDs were arranged in a square pattern at a spacing of 0.8m. The horizontal drainage was provided by placing 300mm wide and 4.5mm thick PVDs on top of the sand blanket. The horizontal drains were spaced at 0.8m to ensure efficient drainage. A 0.5mm thick PVC membrane, anchored into a 1.5m deep peripheral trench, was used to seal the area. Table 7.1 shows the PVD parameters used in the ILLICON analysis and those used by Chai et al. (2006). It can be seen that values of discharge capacity and permeability of the smear zone, different from those used by Chai et al. (2006) have been used in the present analysis as discussed in section 7.6.

7.5 Instrumentation

Surface settlement and vacuum pressure in drainage blanket and porewater pressure at several depths were monitored in all the sections; however, for Section 4, instrumentation was carried out in more detail. Figure 7.6 shows the plan and section of instrumentation used in Section 4. It can be seen in Fig. 7.6 that settlements were measured near the centre line, whereas the porewater pressures were measured near the edge of the treatment area. Additional piezometers were also installed outside the treatment area to monitor the influence of vacuum outside the treatment area.

7.6 Evaluation of Discharge Capacity of PVDs

Figure 7.7 shows the computed settlement at 182 days (just before application of vacuum pressure) for different discharge capacities of PVDs. It can be seen that beyond a discharge capacity of $10m^3$/yr PVDs are expected to drain freely. Chai et al. (2006) assumed a discharge capacity of $100m^3$/yr for the PVDs used in the project. With this discharge

capacity, PVDs are expected to perform without any well resistance; however, Fig. 7.7 indicates significant well resistance as the observed subsurface settlement at 4.1m, corresponds to a discharge capacity of $2m^3/yr$. Figure 7.8 compares the observed surface settlement after vacuum preloading with the values predicted by ILLICON assuming different discharge capacities. For the purpose of this comparison, a uniform vacuum intensity of 60kPa and estimated values of C_c were used. It is clear from this analysis that PVDs continued to perform with significant well resistance as the settlements after application of vacuum pressure correspond to a discharge capacity of around $2m^3/yr$. Therefore, further analyses by ILLICON were carried out using this discharge capacity.

7.7 Loading Sequence

Based on the data reported by Chai et al. (2006), following was considered/assumed for determining the loading sequence for the ILLICON analysis

- Sand blanket was assumed as a wide fill, applying a load of 18kPa to the full depth of compressible layer. A period of 30 days is assumed for the construction of sand blanket as reported by Chai et al. (2006).
- Figure 14 of Chai et al. (2006) shows that excess porewater pressures due to placement of sand blanket were almost completely dissipated at the time of application of vacuum. Therefore, it is assumed that sufficient time was available for PVDs to dissipate excess porewater pressure before the application of vacuum. Hence PVDs were assumed to be installed at most 120 days after beginning of treatment or at least 62 days before the application of vacuum.
- During actual field operation, vacuum was applied for 9 hours per day for 5 weeks; thereafter, the vacuum pumps were run for 24 hours per day till the end of treatment. There were two breaks in vacuum application due to power failure/holidays. As it is difficult to input these many loading/unloading points in the computer program, following two loading options were considered
    - ***Case IA - Vacuum Constant with Depth.*** Vacuum was assumed to develop gradually to its full intensity (60kPa) in 28 days as shown in Fig. 7.9a. Thereafter, vacuum intensity was assumed constant until the end of treatment. C_c values reported by Chai et al. (2006) were used in this case.

- ***Case IB - Vacuum Constant with Depth.*** Same as IA (Fig. 7.10a), however C_c values estimated from water content were used in this case.
- ***Case IIA – Reduced Vacuum Intensity.*** Vacuum was assumed to develop gradually to 25kPa in the clay layer (top 4m) and to 45kPa in remaining compressible layer as shown in Fig. 7.11a. C_c values reported by Chai et al. (2006) were used in this case.
- ***Case IIB – Vacuum Variable with Depth.*** Vacuum was assumed to develop gradually to 50kPa in clay layer (top 4m) and to 60kPa in remaining compressible layer as shown in Fig. 7.12a. C_c values estimated from water content were used in this case.

- For the bottom 0.5m thickness of compressible layer, where PVDs did not penetrate; an average vacuum pressure of 30kPa was assumed (60kPa at the top of the layer and zero at the bottom of the layer) for Case IA, Case IB and Case IIB, and 23kPa for Case IIA. In this layer also, vacuum was assumed to develop gradually to the assumed intensity.

7.8 Settlement

It was mentioned in section 7.7 that after about 210 days, a constant vacuum pressure with time was assumed in the ILLICON analysis to simplify the input loading condition. Therefore, it is expected that, the ILLICON predictions should follow only approximately the observed settlement, especially at times when vacuum pumps did not operate and rebound was observed in the field. Figures 7.9 through 7.12 compare the ILLICON predictions with the observed field settlements for the assumed loading conditions and C_c values. Case IA loading conditions (Fig. 7.9) predicts a surface settlement of 1.92m against an observed settlement of 1.5m (including settlement before application of vacuum) at a time corresponding to end of vacuum treatment. Moreover, the predicted settlement at the end of treatment corresponds to a degree of consolidation of 65%, whereas based on field observations, (Asoaka method, Fig. 7.13), degree of consolidation is estimated as 80%. There is a reasonably good agreement between the observed and the predicted settlements at all depths for Case IB, Case IIA and Case IIB loading conditions (Figs. 7.10, 7.11, and 7.12). Predictions of Case IB and Case IIB loading conditions are more realistic as these loading conditions show a difference between predicted and observed settlements at times when there

was an interruption in vacuum application; however, the observed settlements and predictions are again in good agreement toward the end of treatment period. This suggests that the assumptions made in connection with compressibility and distribution of vacuum pressure with time and with depth are reasonable.

7.9 Porewater Pressure

The data reported by Chai et al. (2006) show that porewater pressure as a function of time during vacuum preloading is more sensitive to changes in applied vacuum intensity than the settlements. At all depths, a reduction in porewater pressure was observed; however, the observed porewater pressure remained more constant with time at greater depths than those at the shallower depths. The maximum reduction in porewater pressure, observed at 4.2m and 7.5m depths was greater than that recorded at 2.5m depth below natural ground surface. This observation justifies the assumption made in case-II loading conditions. In this case, the vacuum intensity was higher at greater depths than at shallower depths; hence a linear decrease in vacuum intensity with depth as proposed by Indraratna et al. (2004 and 2007) and Chai et al. (2005a and b) is not justified. Figures 7.14, 7.15 and 7.16, respectively, compare the observed reductions in porewater pressure to those predicted by ILLICON for Case IB, Case IIA and Case IIB loading conditions. Equation 4.2, together with a vacuum pressure (u_{sm}) of 60kPa was used to interpret porewater pressure from ILLICON analysis. It can be seen that for both Case IB and Case IIB loading conditions (Figs. 7.14 and 7.16), porewater pressure response in the lower layer is predicted quiet accurately; however, in the top clay layer; the dissipation of excess porewater pressure in the field seems to progress quiet slowly. It appears that the actual permeability of this layer is lower or the developed vacuum intensity was smaller than that assumed in the analysis. As case IIB gives a closer agreement at depth of 2.5m, it is considered more representative loading condition than case IB. Assuming a vacuum pressure (u_{sm}) of 40kPa in the top clay layer improves the predictions as shown in Fig. 7.16. Figure 7.15 shows that for Case IIA loading condition, there is not enough dissipation of excess porewater pressures as observed in the field. This is possible if either or both of the reported C_c and k_{vo} values are on the high side. Thus, porewater pressure data also validate the assumption made in connection with the compressibility of Ariake clay. Figure 7.17 shows the vertical distribution of observed porewater pressure with depth at different times, and those predicted for Case IB and Case

IIB loading conditions. The comparison confirms that vacuum did not develop to its full intensity (60kPa) at shallow depths. Therefore Case IIB loading condition is considered to be the most representative of actual field conditions.

It was mentioned in Section 7.5 that additional piezometers were installed outside the treatment area. These piezometers were installed at depths of 2.5m and 7.5m from natural ground surface, 1.3m and 3.4m away from the edge of treatment area as shown in Fig. 7.6. Data obtained from these piezometers are shown in Fig. 7.18. It appears that the maximum reduction in porewater pressure reduces with depth as well as with distance from embankment area. It is also important to note that the maximum reduction was observed towards the end of treatment process which indicates that vacuum develops at a much slower rate outside the treatment area. However, as vacuum was applied in a discontinuous way with several stoppages, it is difficult to draw any meaningful conclusion from these data.

7.10 Lateral Displacements

Figure 7.19 shows the lateral displacement observed at different times and at different depths plotted against the settlement at the same depth. It can be seen that the lateral displacements at all depths were around 21% of the settlement. This is the lower bound value for the lateral displacement observed in other case histories of vacuum consolidation as discussed in Chapters 4 and 5. Figure 7.20 shows the mid-sublayer lateral displacements plotted against the sublayer settlements. The mid-sublayer lateral displacement at all depths is less than the corresponding sublayer settlement, which is generally not the case (see Figs. 4.22 and 5.17); i.e. for the surface layers, the mid-sublayer lateral displacement generally exceed sublayer settlement. The possible reasons could be (1) non-uniform distribution of vacuum; i.e. vacuum developed to a lower intensity at shallow depths, and (2) intermittent application and removal of vacuum especially during the first 50 days of loading.

7.11 Concluding Remarks

The analysis of this case history shows that:

- The values of compression index reported by Chai et al. (2006) are greater than the typical values reported in the literature for the Ariake clay deposit. The values reported by Chai et al. (2006) result in significantly larger EOP settlement than that predicted on the basis of field observations using the Asoaka method. Whereas, the estimated values of compression index, which lie

well within the reported data for Ariake clay, more closely represent the field behavior.

- The repeated removal and reapplication of vacuum had more profound effect on the observed porewater response as compared to the settlement response. Moreover, to model repeated vacuum applications for settlement analysis (ILLICON analysis in this case), it is reasonable to use an average vacuum constant with time over the period when vacuum was applied and removed.
- Vacuum developed to a lower intensity in the top clay layer and to a higher intensity in the silty clay layer. Thus the field observations do not support the concept of a linear reduction in vacuum intensity as proposed by Chai et al. (2005a, b and 2006).
- A drop in porewater was observed outside the treatment area especially at shallow depths over a period of about 70 days. Contrary to the treatment area, the porewater pressure drop outside the treatment area was greater near the top of the clay layer suggesting a 'leakage' of vacuum pressure through this layer.
- The PVDs performed with well resistance, well below the discharge capacity assumed by Chai et al. (2006) for their analysis.

7.12 Tables

Table 7.1: PVD parameters used in the settlement analysis

Parameter	Chai et al. (2006)	ILLICON Analysis
Equivalent Radius of drain (mm)	26.15	26.15
Drain Spacing (m)	0.8	0.8
Installation Pattern	Square	Square
Radius of soil, r_e (m)	0.452	0.452
Radius of smear zone, r_s (m)	$6*r_w$	$5.75*r_w$
Discharge capacity (m^3/yr)	100	2 - 9
k_h/k_s	10	-
k_h/k_v	-	1.0

7.13 Figures

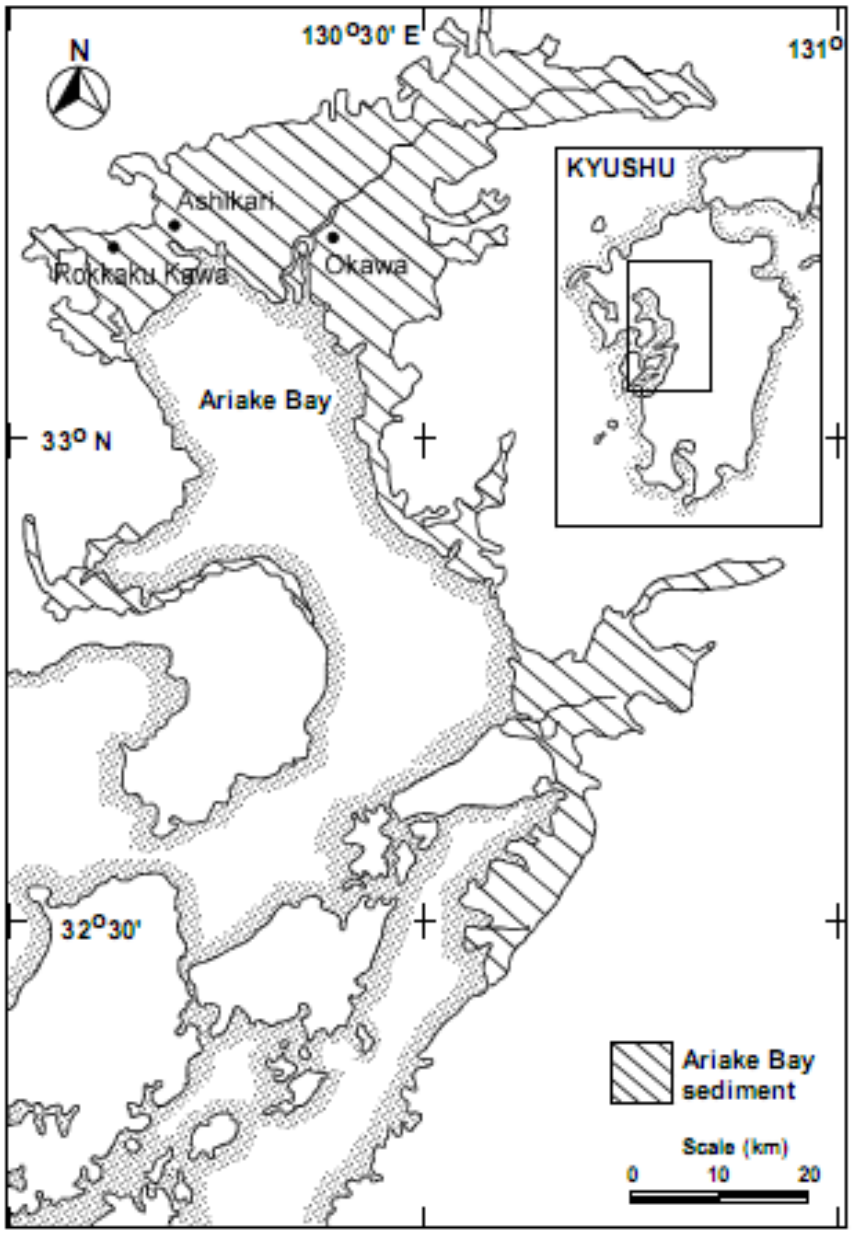

Figure 7.1: Occurrence of Ariake clay in Kyushu Island; Saga, Japan (After Kolsant, 2006)

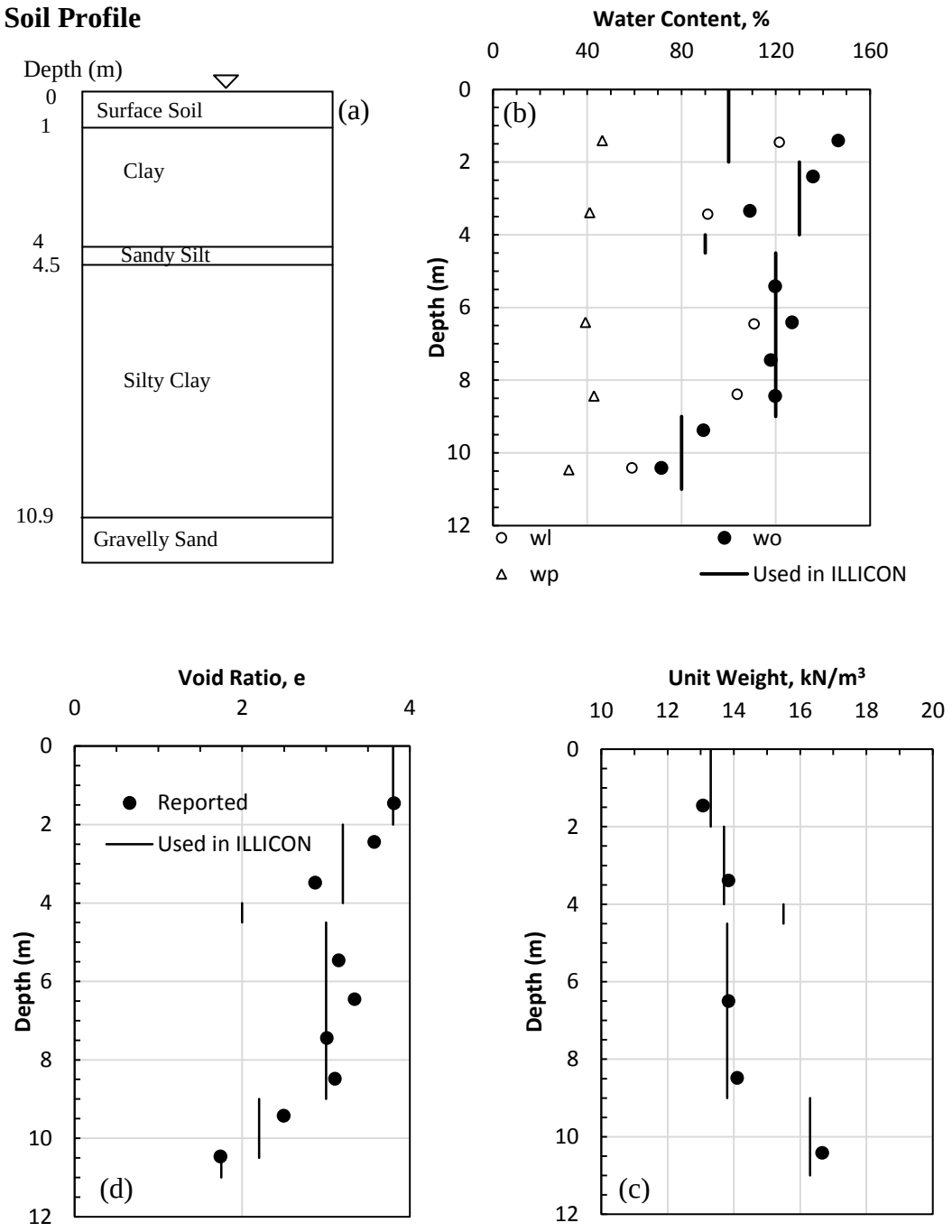

Figure 7.2: Generalized soil profile and vertical distribution of geotechnical properties (data from Chai et al.; 2006).

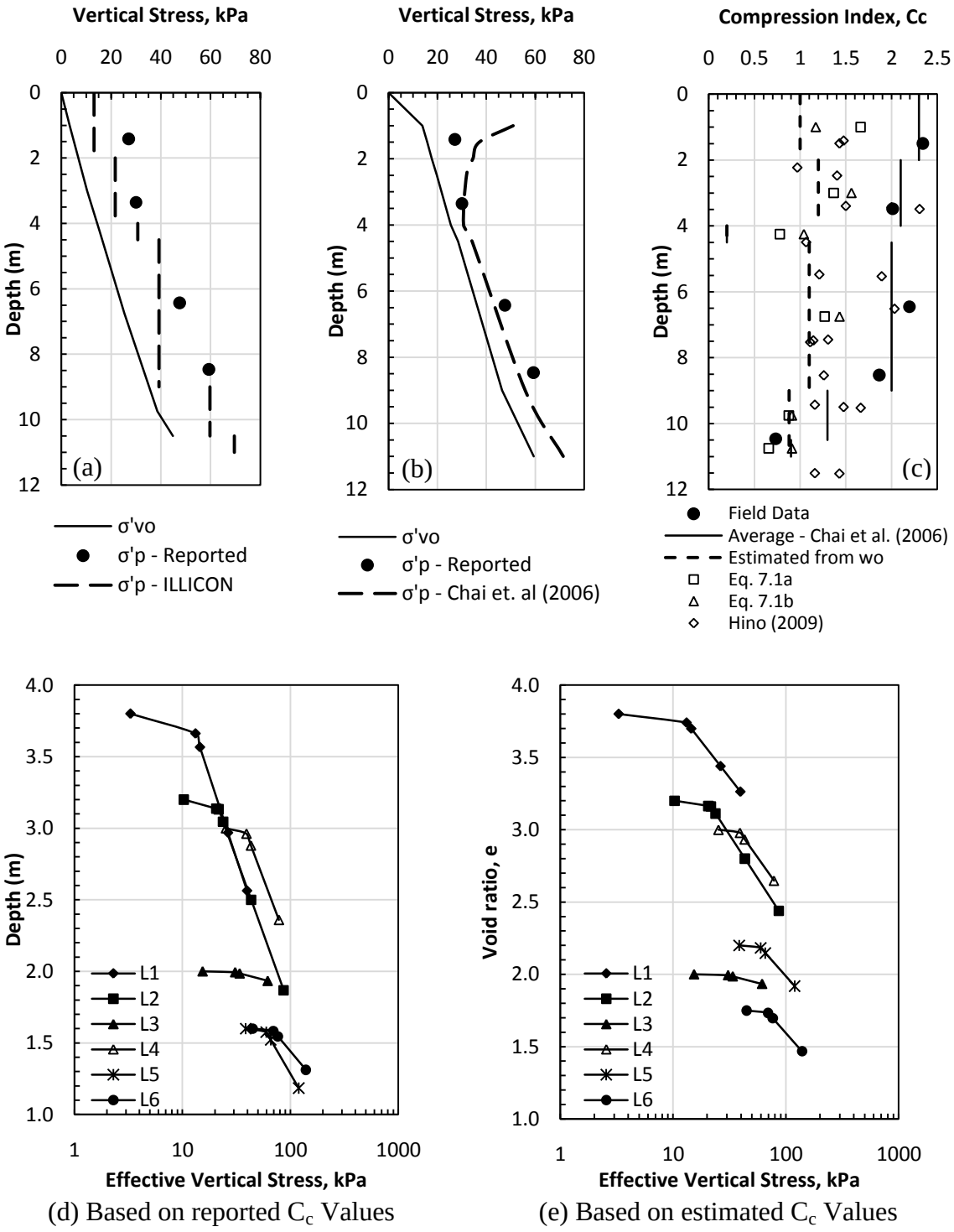

(d) Based on reported C_c Values (e) Based on estimated C_c Values

Figure 7.3: Vertical distribution of (a) initial effective stress and preconsolidation pressure, (b) reported and assumed compression index and (c) & (d) EOP *e-log σ'* relations, used in the analysis (data from Chai et al. 2006).

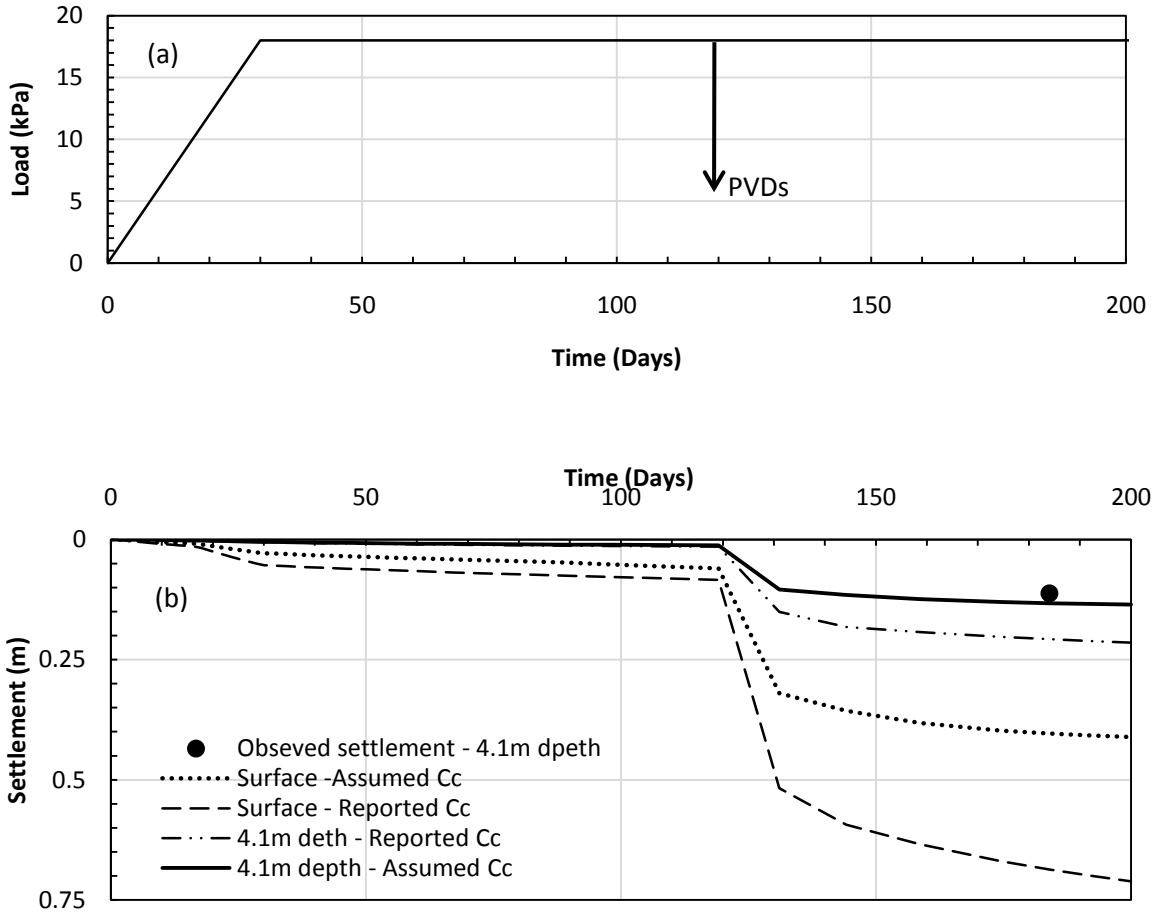

Figure 7.4: Surface and sub-surface settlements with time under 1m thick sand blanket for the reported and assumed compressibility index

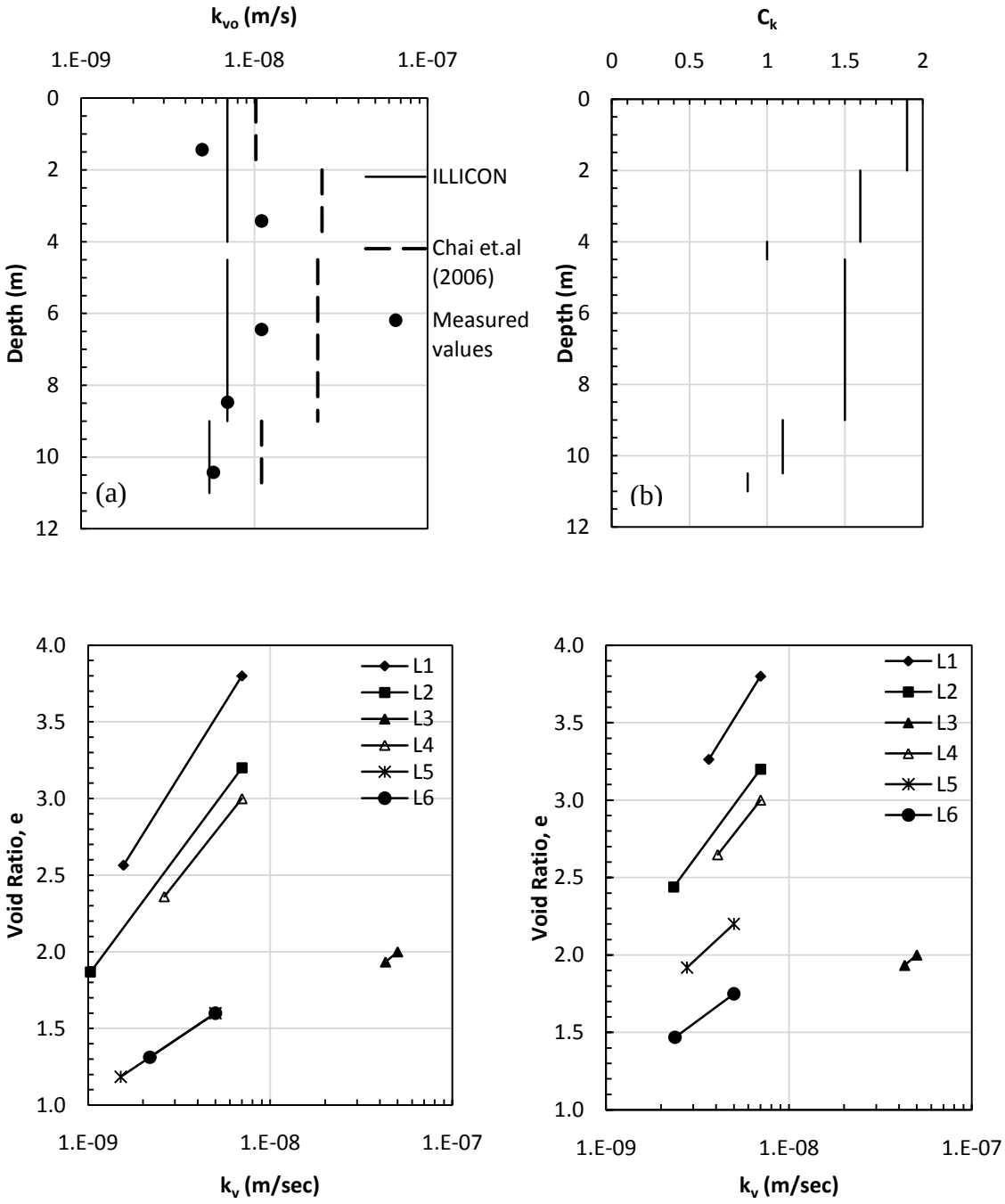

(c) Based on reported Cc Values (d) Based on estimated Cc Values

Figure 7.5: Vertical distribution of (a) initial vertical permeability, (b) C_k and (c) *e-log*k_v relation used in ILLICON analysis (data from Chai et al. 2006).

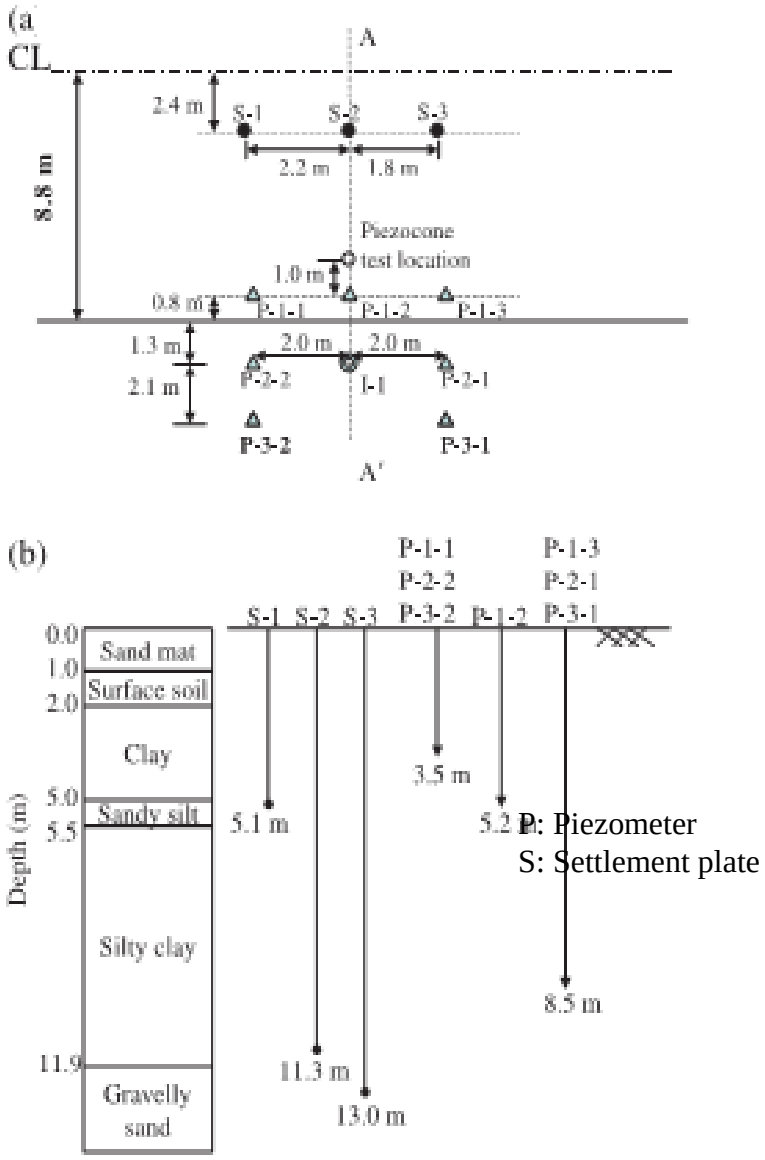

Figure 7.6: Plan and section of instrumentation at Section 4 (after Chai et al. 2006)

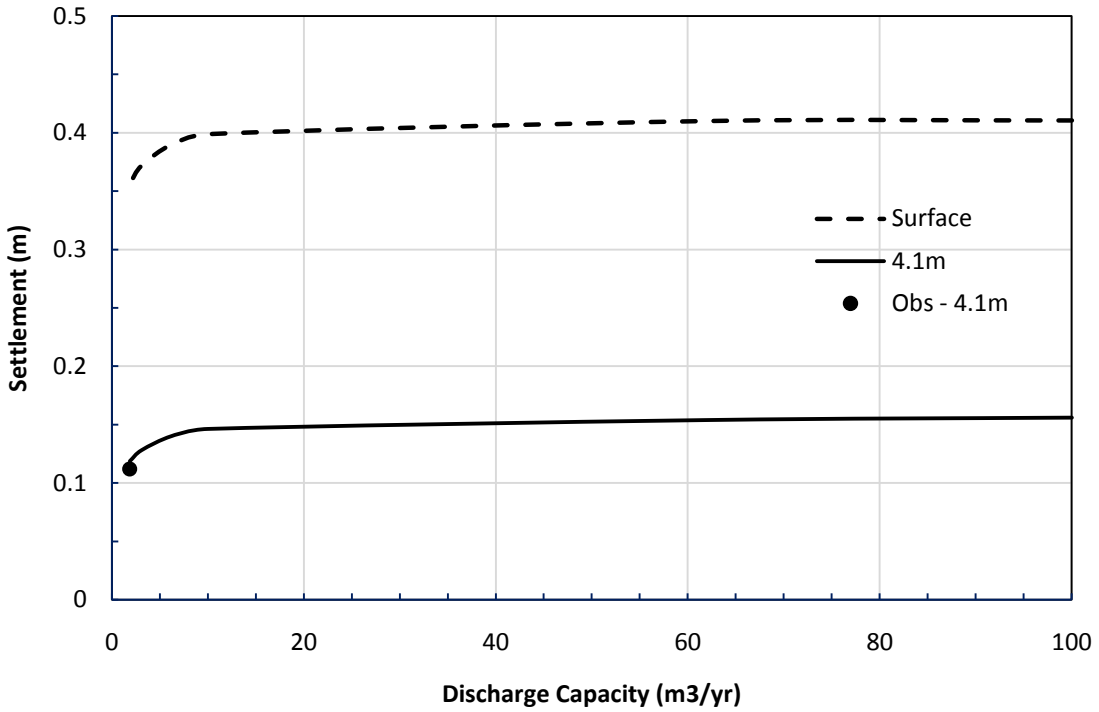

Figure 7.7: Settlement at 182 days due to sand blanket for different discharge capacities of PVDs

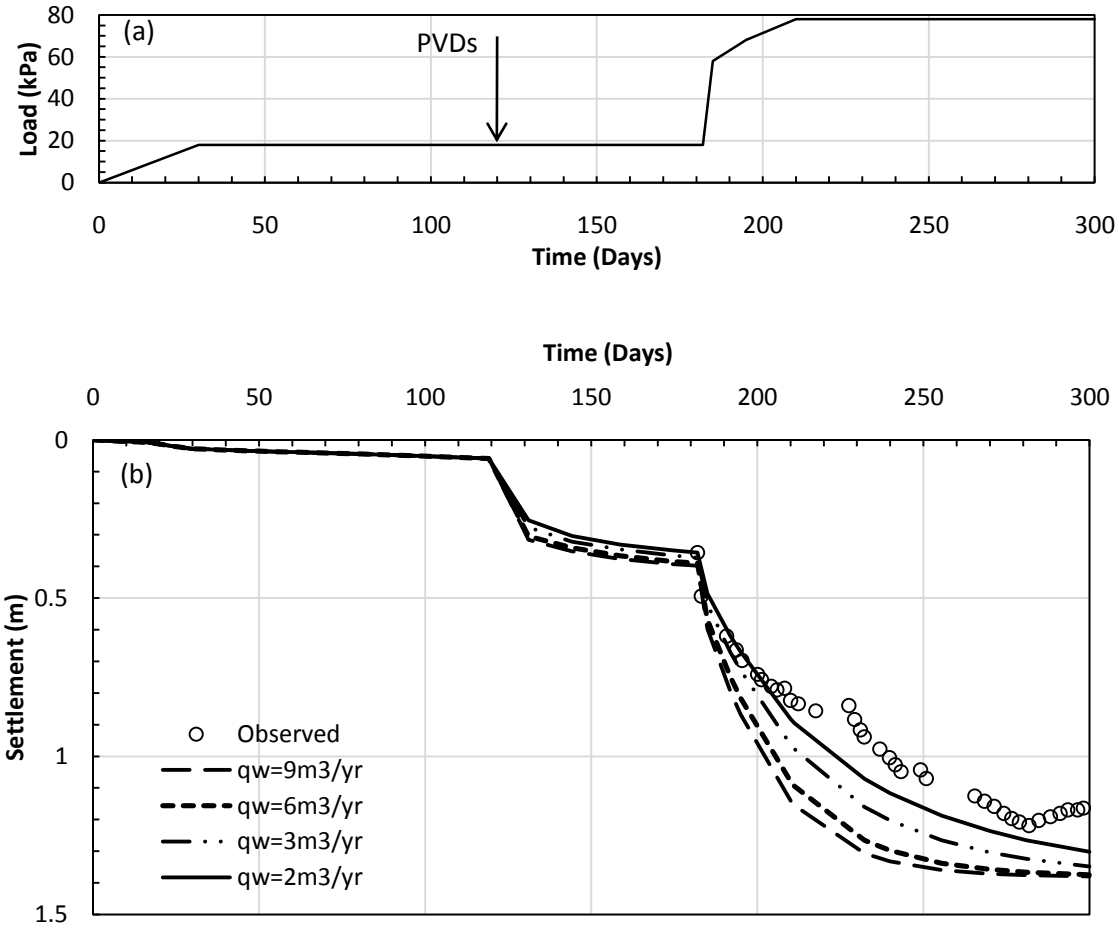

Figure 7.8: Settlement predictions for different discharge capacities of PVDs

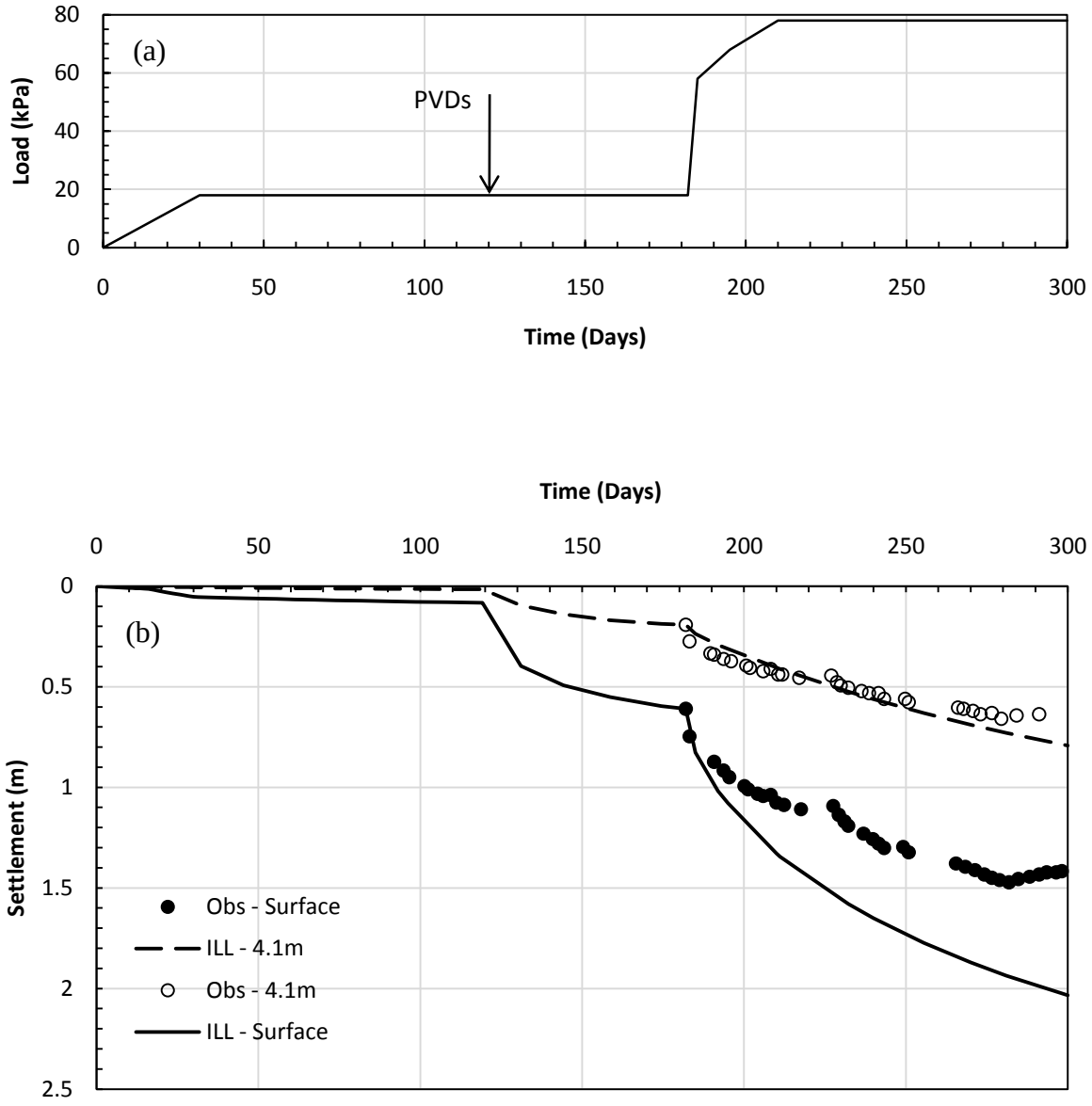

Figure 7.9: Observed and predicted surface and subsurface settlements due to a constant vacuum pressure of 60kPa and reported values of compressibility (Case – IA)

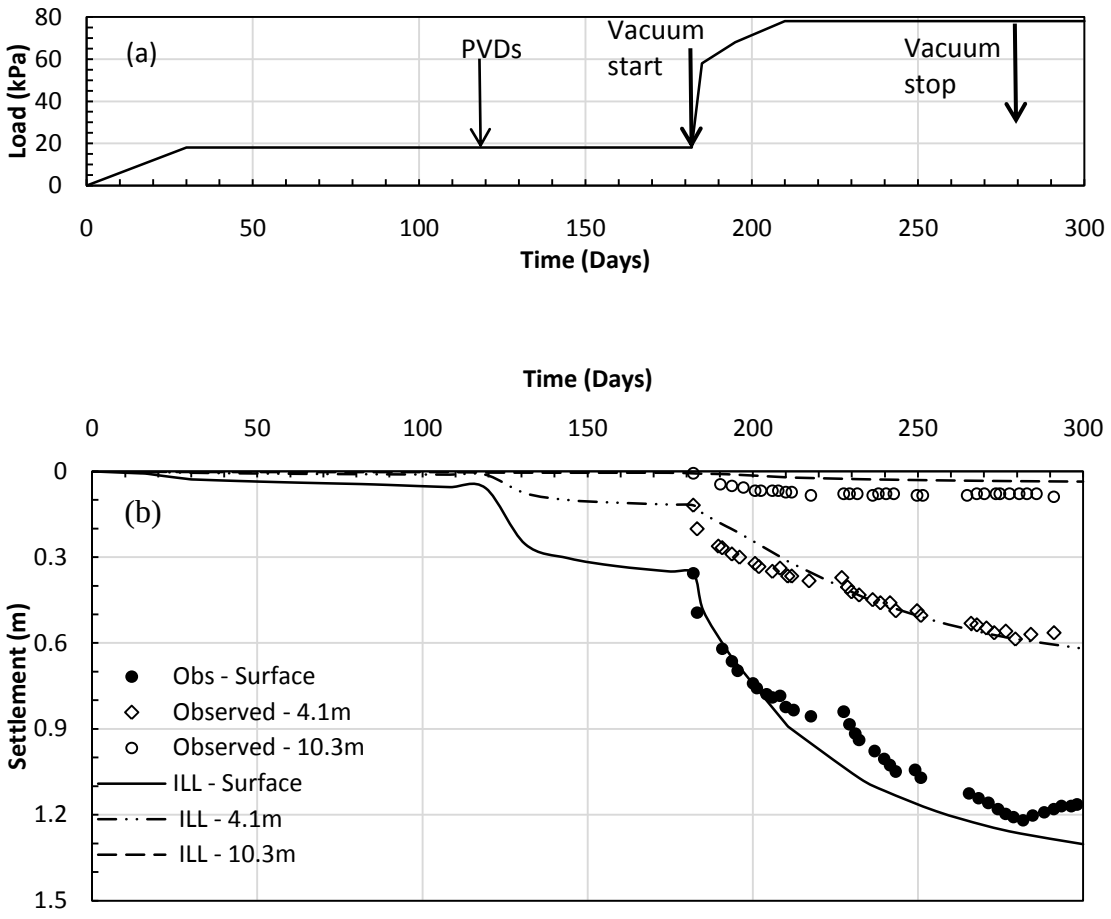

Figure 7.10: Observed and predicted surface and subsurface settlements due to a constant vacuum pressure of 60kPa and assumed values of compressibility (Case – IB)

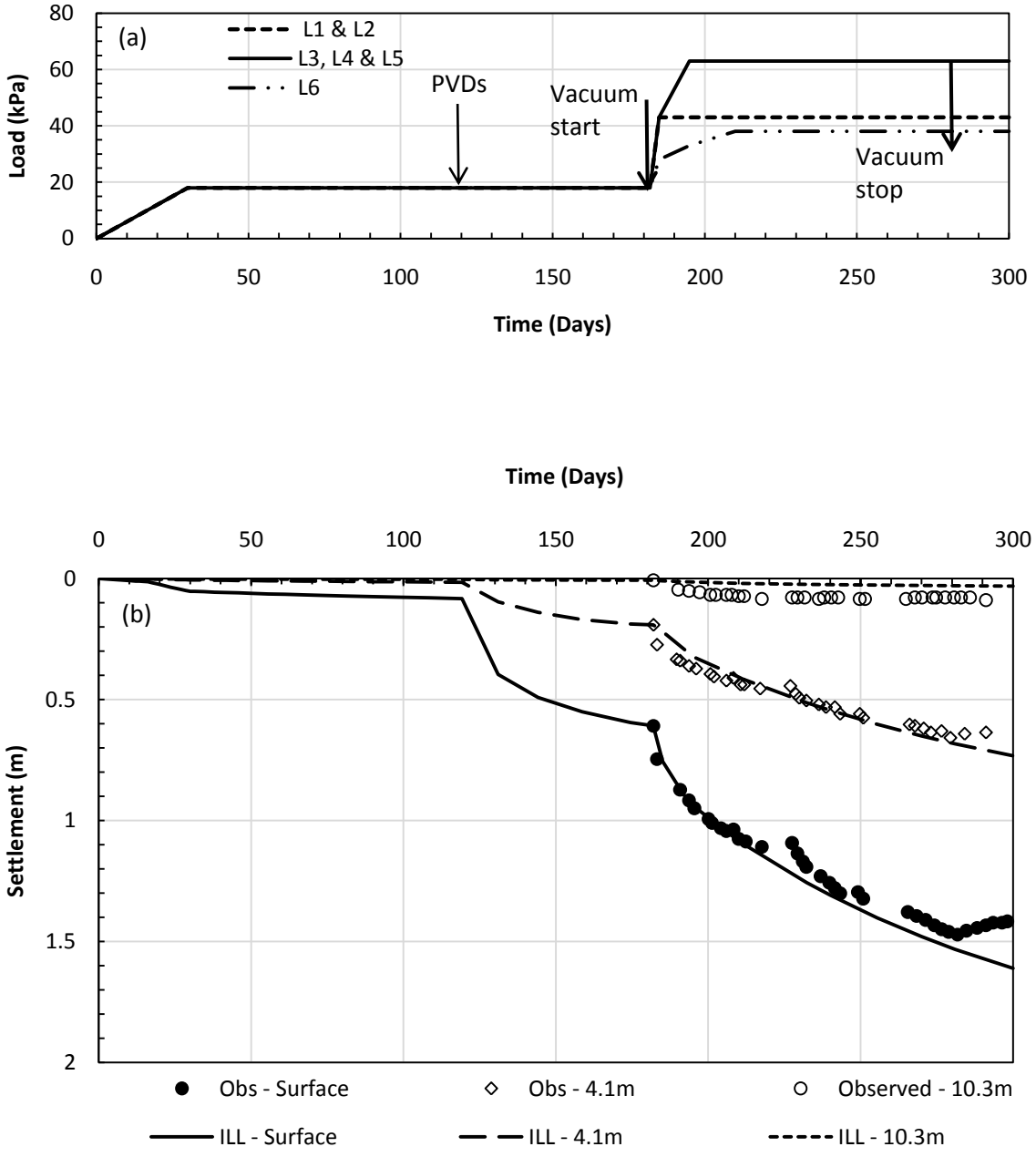

Figure 7.11: Observed and predicted surface and subsurface settlements due to a constant vacuum pressure of 60kPa and reported values of compressibility (Case – IIA)

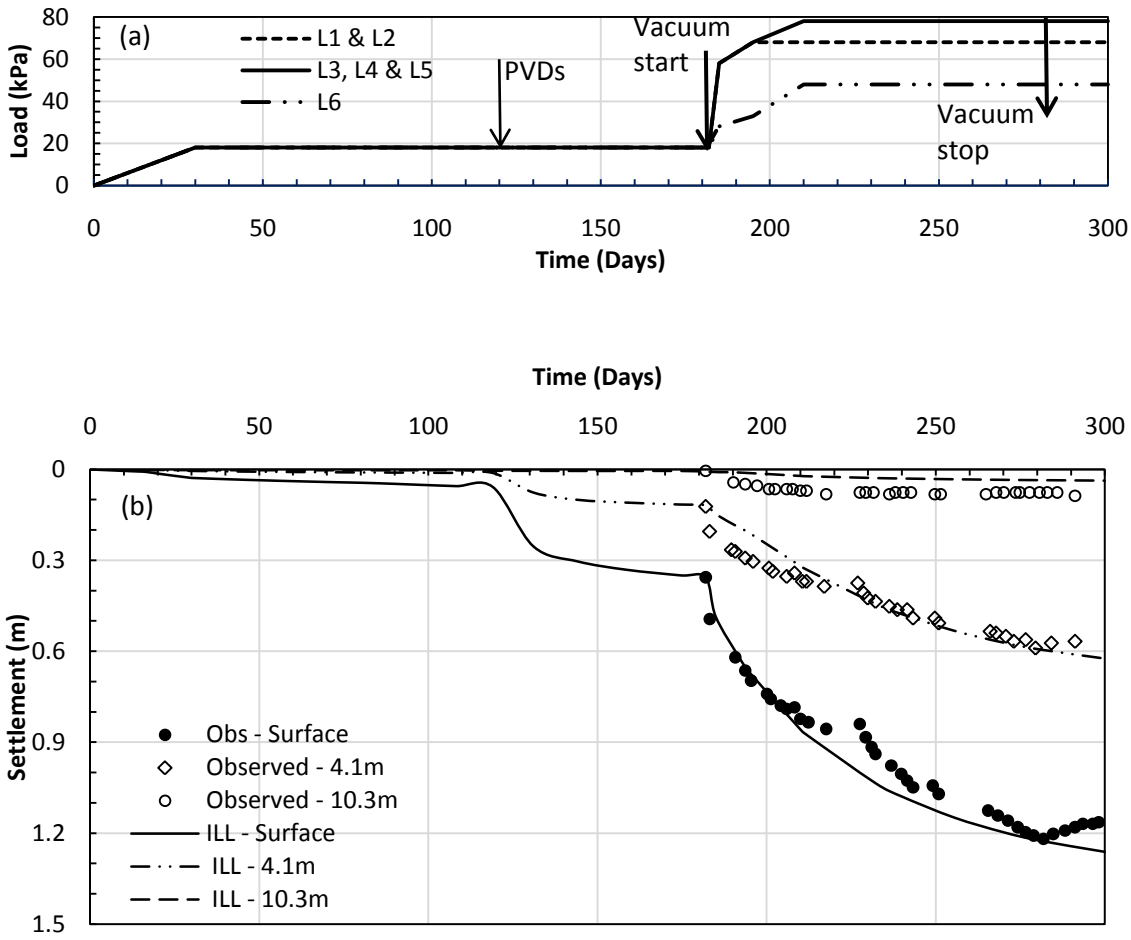

Figure 7.12: Observed and predicted surface and subsurface settlements due to variable vacuum pressure at different depths and assumed values of compressibility (Case – IIB)

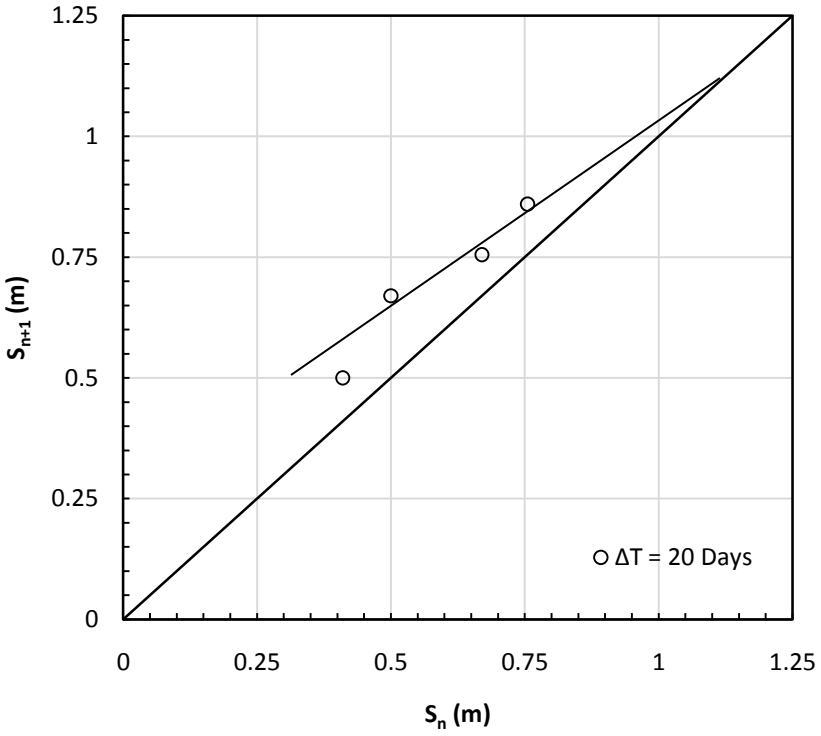

Figure 7.13: Asoaka Method applied to observed surface settlements

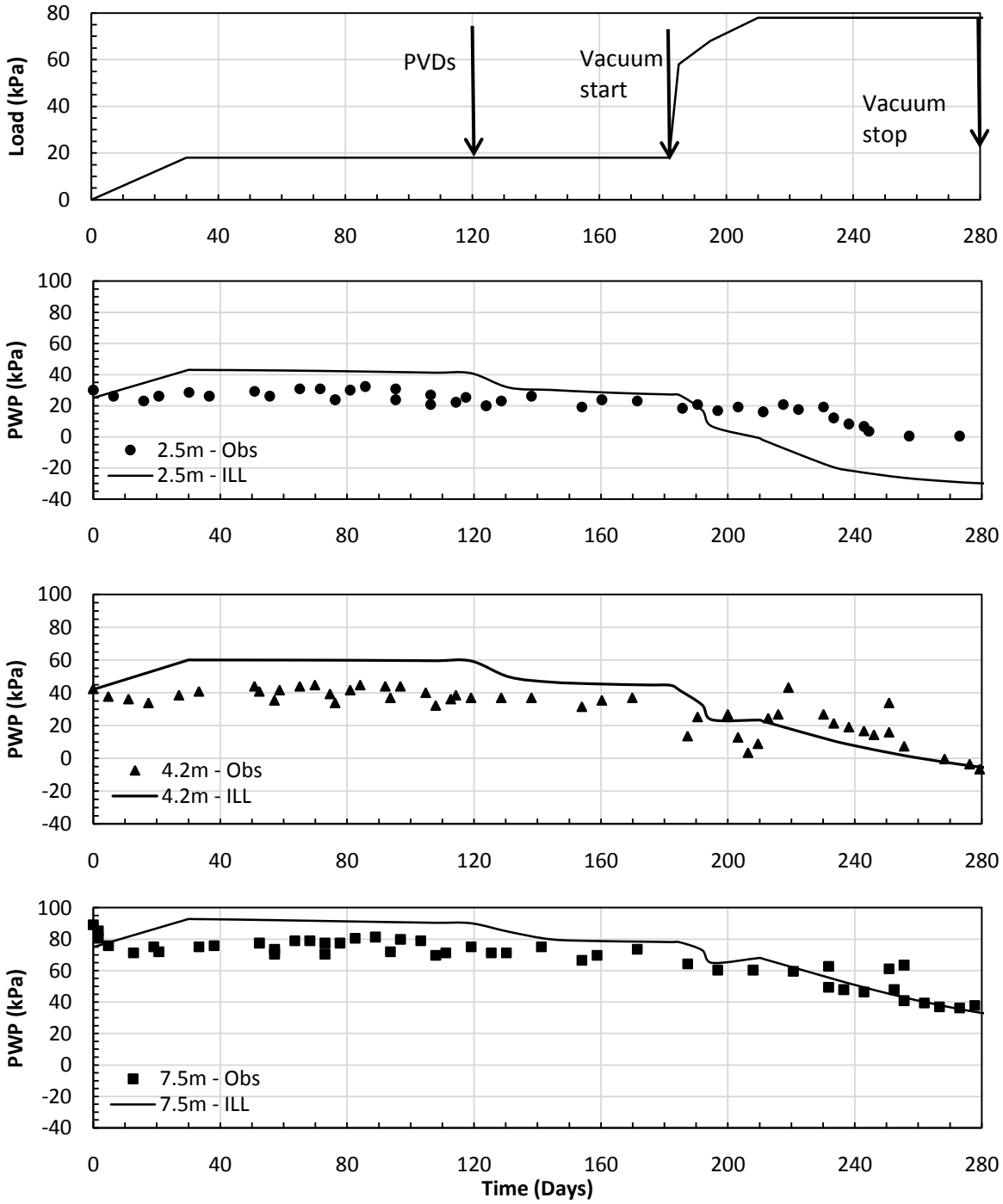

Figure 7.14: Observed porewater pressure at different depths compared to those predicted for Case IB loading condition

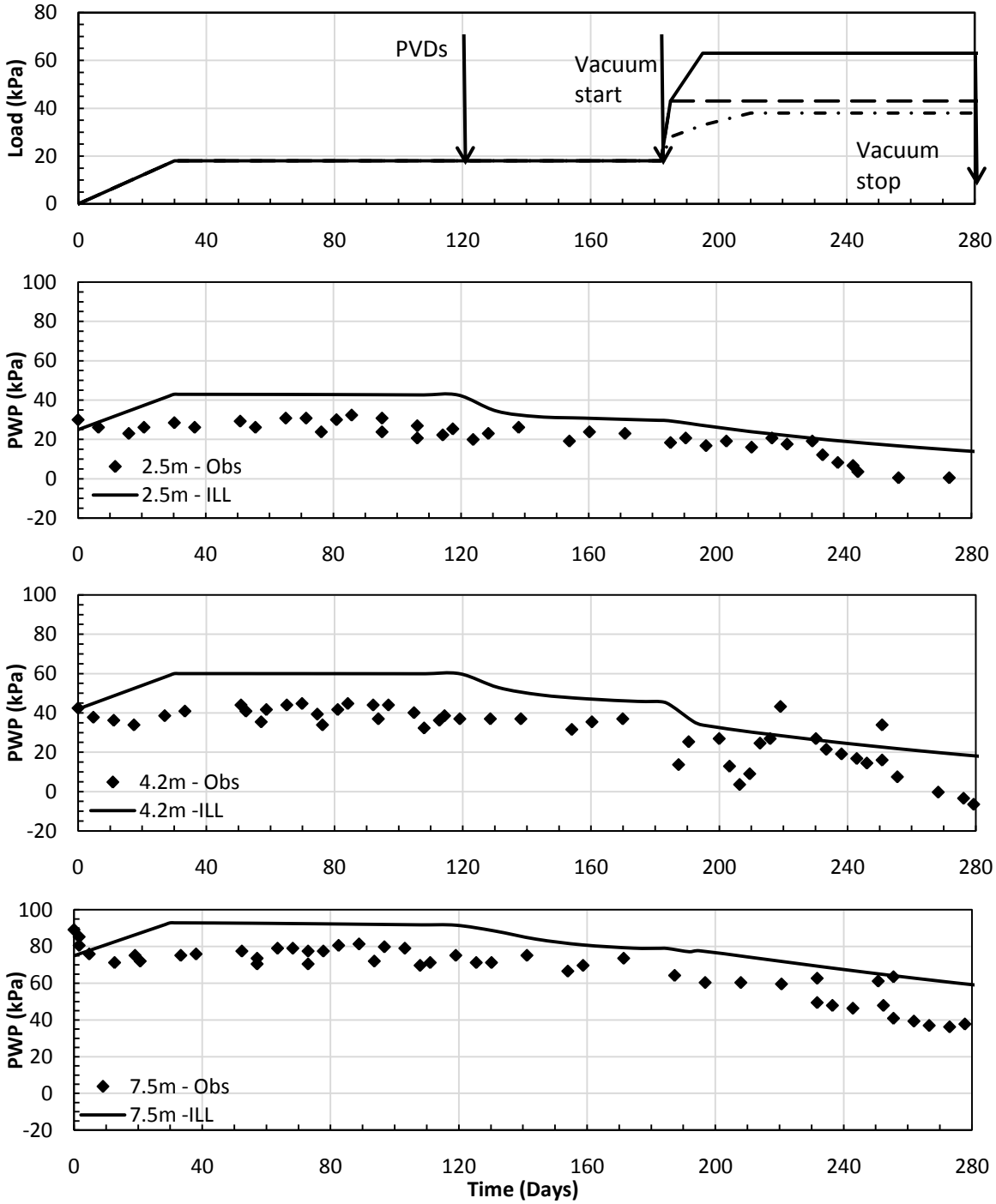

Figure 7.15: Observed porewater pressure at different depths compared to those predicted for Case IIA loading condition.

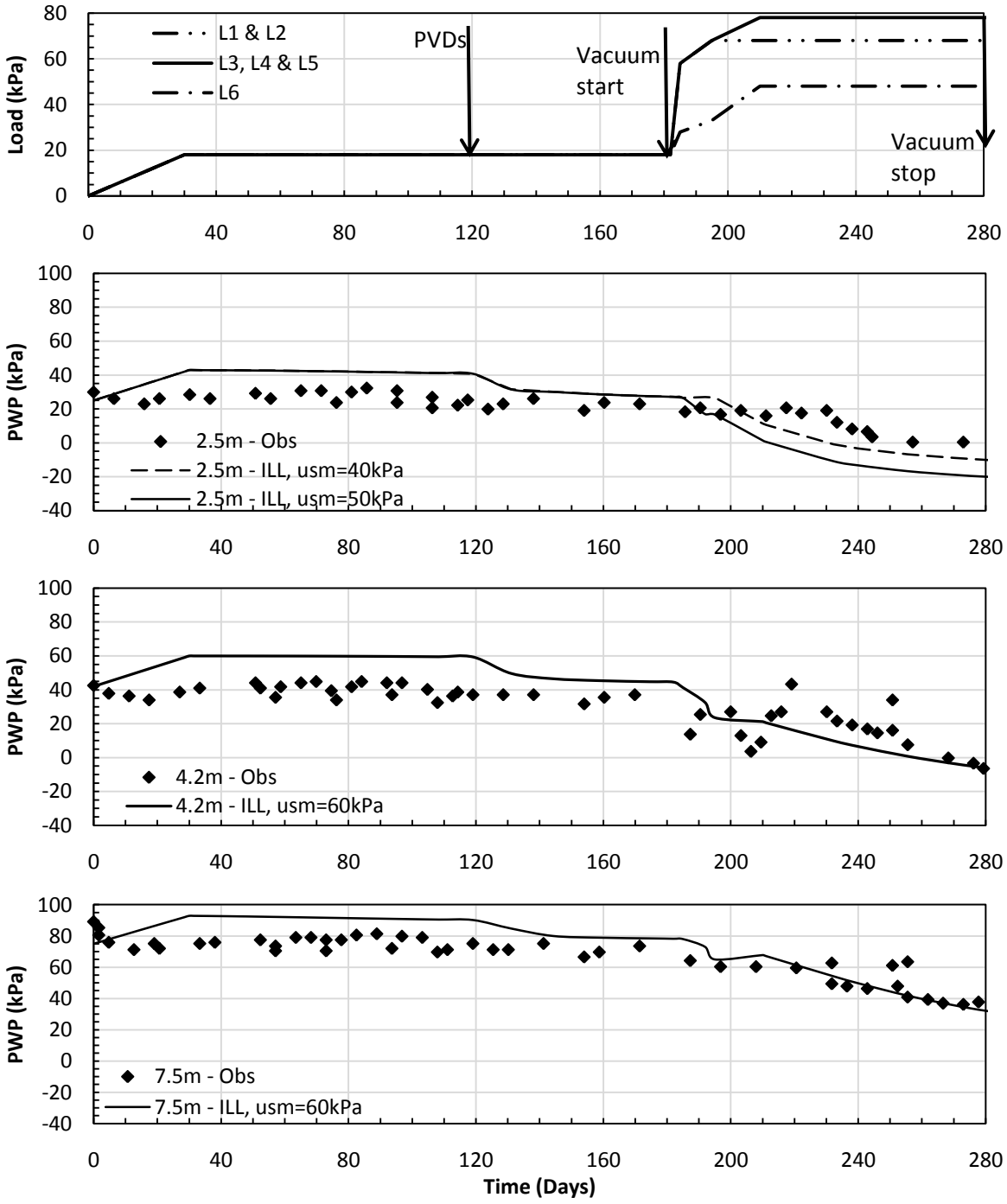

Figure 7.16: Observed porewater pressure at different depths compared to those predicted for Case IIB loading condition.

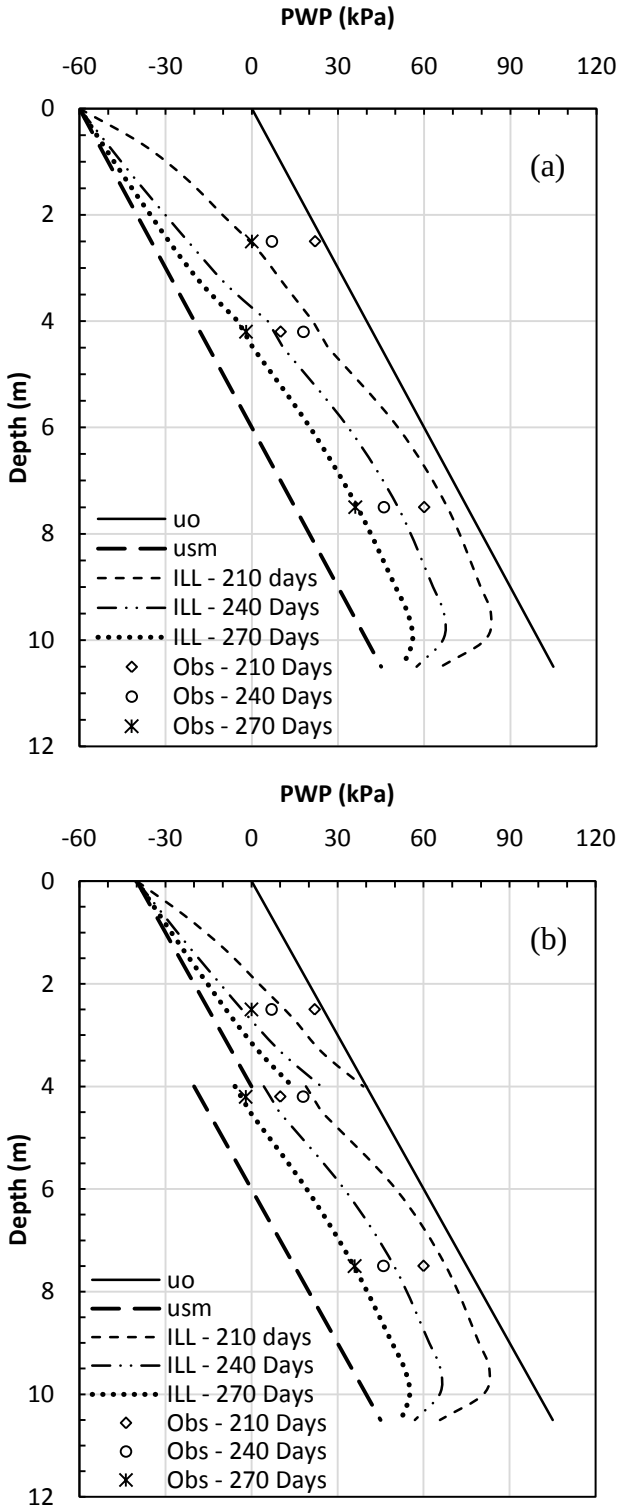

Figure 7.17: Observed and predicted porewater pressure with depth at different times (a) Case – IB and (b) Case – IIB. (vacuum was applied at 182 days)

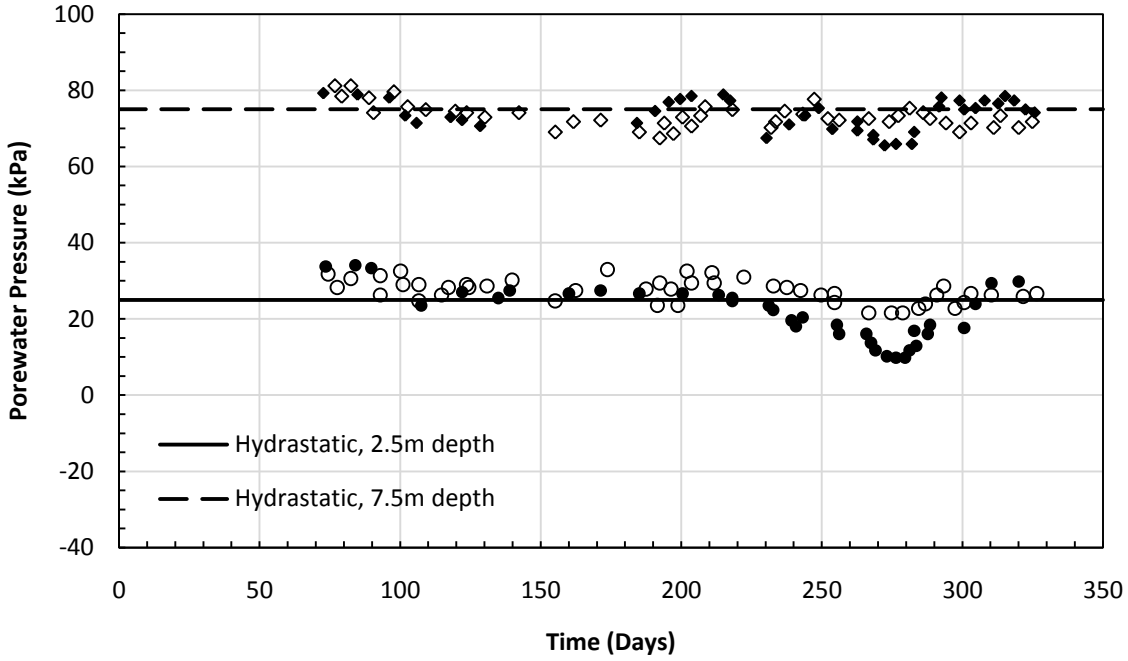

Piezometer	Depth, m	Distance from edge, m
● P-2-1	2.5	1.3
◆ P-2-2	7.5	1.3
○ P-3-1	2.5	3.4
◇ P-3-2	7.5	3.4

Figure 7.18: Observed porewater pressures outside the treatment area at different depths and at different distance from edge of treatment area (redrawn from Chai e.al, 2006)

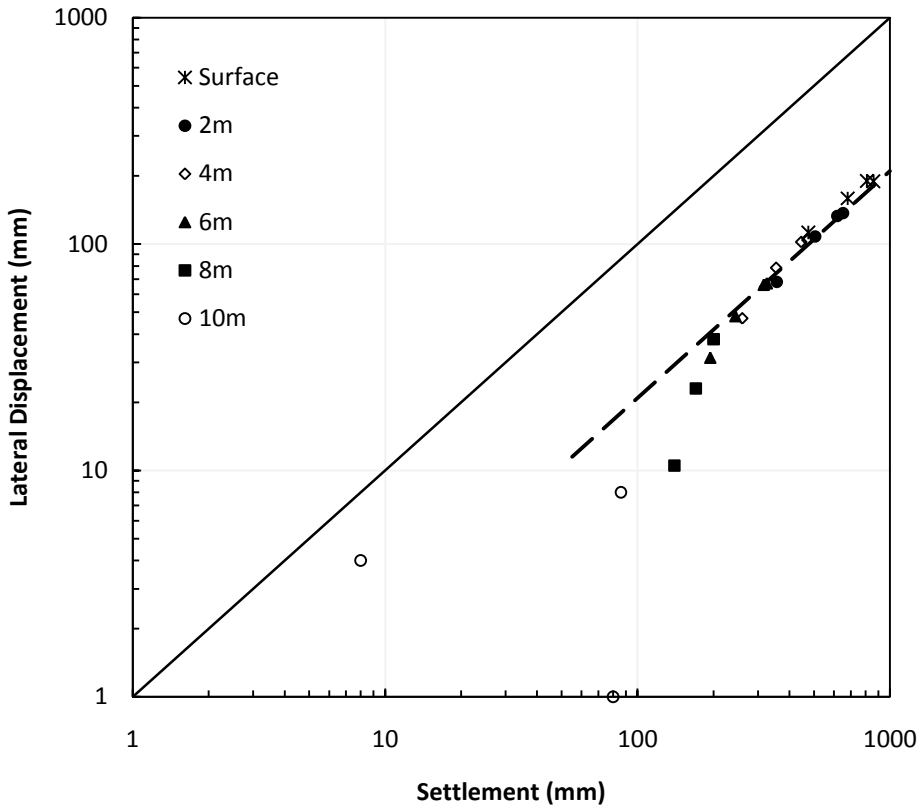

Figure 7.19: Lateral displacements at different depths plotted against the corresponding settlements (data from Chai et al. 2006)

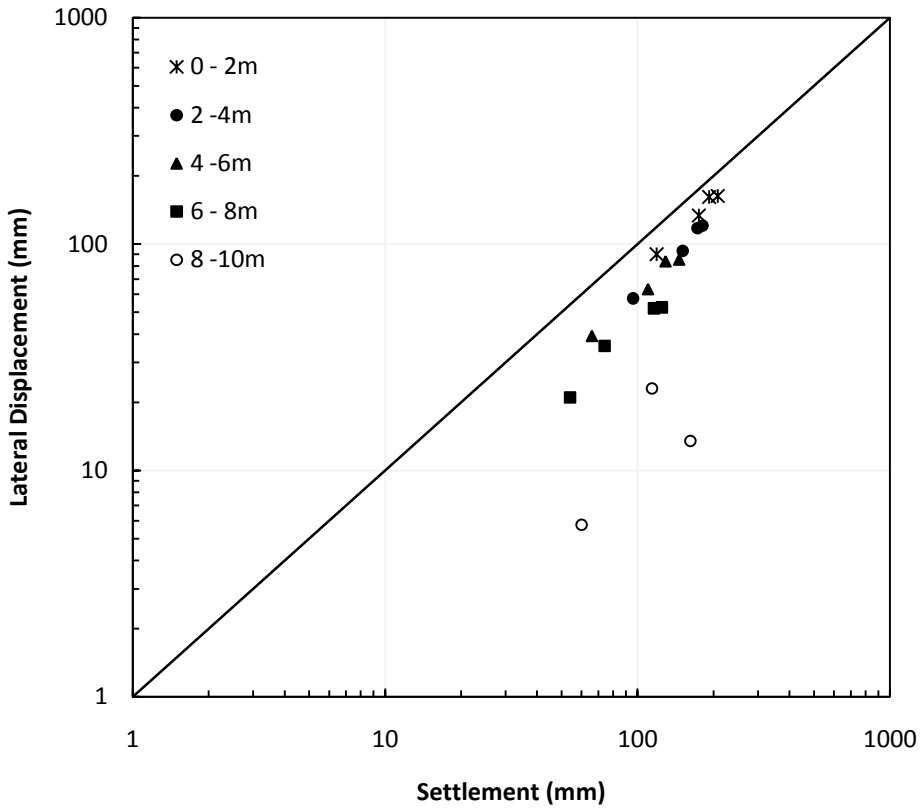

Figure 7.20: Mid-layer lateral displacements plotted against sublayer settlements (data from Chai et al. 2006)

CHAPTER 8. SOIL IMPROVEMENT FOR EAST PIER PROJECT USING VACUUM PRELOADING TOGETHER WITH PREFABRICATED VERTICAL DRAINS

8.1 General

Port of Tianjin, China, is mostly developed on the largest reclaimed land. Development of east pier of this port required improvement of an area of 480,000m^2 for construction of warehouses, roads and stacking yards etc. The design loads varied between 50 and 87kPa (Yixiong, 1996b; Shang et.al 1998). Owing to shortage of suitable fill material, vacuum preloading was chosen as the treatment method to improve the subsurface conditions. In areas of high design loads (>80kPa), vacuum preloading was used together with fill preloading.

The improvement area was divided in six sub-areas which were further divided into 72 sections, as shown in Fig. 8.1. Depending on the design load, each of the 72 sections was individually subjected to either vacuum or a vacuum-fill preload. The computer program ILLICON is used to carry out settlement analysis and the results are compared with the field observations.

8.2 Subsurface Conditions

The land reclamation in the area began in 1939 with stone dumping at the estuary of Haihe River to form an enclosure for land reclamation. Up to 1945, 1.76km^2 of land was reclaimed using dredged material from harbor and channel basins. From 1951 to 1979, another 10.70km^2 of land was reclaimed in two different phases (Yixiong, 1996a). Further reclamation work at the project site was carried out in two stages from April 1982 to October 1986. In first stage, from April 1982 to June 1984, hydraulic fill was placed to an elevation of +3.5 CD (datum) between the first set of cofferdams. From November 1984 to October 1986

(second stage), hydraulic fill was raised to an elevation of +6.5m CD between the second series of cofferdams (Choa 1989, 1990). The hydraulic fill was placed on a 17 to 30m thick soft layer which consisted of layers of peat, organic clay, silty clay and silt (Choa 1989, 1990; Yixiong 1996b; Shang et al. 1998), as shown in Fig. 8.2. At the pilot testing sites (both for vacuum-fill and fill preloads), the 20m thick compressible layer consisted of a 4.2m thick hydraulic fill, which was underlain by layers of muck, mucky loam, muck, and mucky clay, having thicknesses of 3.5, 4, 3 and 5m, respectively (Yixiong, 1996b; Shang et al. 1998), as shown in Fig. 8.3. It is important to point out that Choa (1989, 1990) has described the sub-soils as silty clay and clay with interlacing of silts and organic content, however, the thicknesses of various sublayers and the distribution of geotechnical properties are similar to those reported by Yixiong (1996b) and Shang et al. (1998); therefore, the sublayer thicknesses and description are adopted from Yixiong (1996b). Vertical profiles of soil properties including Atterbergs' limits, natural water content, natural void ratio, unit weight and initial undrained shear strength are also shown in Fig. 8.3. The solid vertical lines on Fig. 8.3 show the average value reported by Yixiong (1996b) and Shang et al. (1998) and are used as such in the ILLICON settlement analysis; whereas the data points on Fig. 8.3 show the measured values for both area 44 (vacuum-fill) and area S-2 (fill), preloading test sections, as reported by Yixiong (1996b) and Shang et al. (1998). It can be seen from Fig. 8.3 that the natural water content generally exceeds the liquid limit at all depths, especially in the hydraulic fill, where it is approximately 1.5 times the liquid limit. The void ratio of the deposit varies between 1.0 and 1.6 and the unit weight varies between 16 and 19kN/m^3.

It can be seen from Fig. 8.3e that the initial vane shear strength in the hydraulic fill was generally less than 5kPa. The original sea bed clay was also quite soft, with an average undrained strength of 10 - 20kPa up to a depth of 15m.. It is reported that it was not possible to work on the existing ground surface without improving the bearing capacity to allow movement of men and material. Therefore, the ground surface was pretreated using two layers of twig mats, 40cm of hill cut fill and 30cm of medium sand to provide a working platform (Choa 1989, 1990; Yixiong 1996b; Shang et al. 1998). A rest period of 6 to 12 months was allowed between pretreatment and commencement of actual preloading operation for soil to gain sufficient strength (Yixiong 1996b).

Position of ground water has not been specified in the literature; however, it can be seen from the porewater pressure records (Choa 1989) that the water table coincides with the ground surface. Figure 8.4 shows the pretreatment porewater pressures at two vacuum-fill test sites, which also show that both the hydraulic fill and the original sea bed clay were still undergoing primary compression at the time of treatment.

Settlement analysis using computer program ILLICON was carried out for the vacuum-fill preloading section in control tower area (Fig. 9 of Choa 1990), vacuum-fill pilot testing area (Fig. 8 of Choa 1990) and fill preloading pilot test section (Fig. 7 of Choa 1990), and the results are compared with the field measurements. The compressible layer was divided into 6 layers, with average soil properties as shown with solid vertical lines on Fig. 8.3. These properties were either directly used as an input, or were used to compute other input parameters required for the ILLICON analysis. As the vertical drains were terminated well within the mucky clay, partially penetrating vertical drain was assumed for the settlement analysis.

8.3 Compressibility and Permeability Characteristics

Choa (1989, 1990) reported a range of compression index (0.35 to 0.50 for silty clay and 0.05 and 0.15 for clayey silt); however data on compressibility of specific sublayers with depth is not reported in the literature. Therefore, the compression index for different sublayers was estimated based on the empirical correlation between compression index (C_c) and natural water content (w_o) proposed by Terzaghi et al. (1996). It can be seen from Fig. 8.5a that the reported values of compression index for clayey silt are on the low side as compared to those estimated empirically; however, the estimated values are more comparable to the compression index reported for silty clay. The preconsolidation pressure (σ'_p) was also estimated based on empirical correlation between $s_u(FV)/\sigma'_p$ and plasticity index, I_p, (Terzaghi et .al. 1996) as shown in Fig 8.5b. The estimated values of C_c and σ'_p together with e_o, C_r (assumed $C_r/C_c = 0.1$), *and* σ'_{vo} were used to construct EOP$e - log\sigma'_v$ relations for each sublayer in both the test sections as shown in Fig. 8.5c.

The reported values of coefficient of consolidation (c_v) together with coefficient of volume compressibility (m_v) were used to estimate the initial value of permeability as under:

$$k_v = c_v * m_v * \gamma_w$$

$$m_v = \frac{\Delta e}{\Delta \sigma_v^{'}}$$

The value of Δe for each sublayer was estimated from the individual sublayer settlement and the estimated consolidation pressure. The computed values of k_{vo} compare well with values for other cases of vacuum preloading with similar soil profile in Tianjin Port (Fig. 8.6b). The reduction in vertical permeability was estimated using $C_k = 0.5*e_o$ (Tavenas et al. 1983). The ratio between horizontal and vertical permeability was taken as unity. Vertical profiles of c_v, k_{vo}, C_k, and e - $logk_v$ relations used in the ILLICON analysis are shown in Fig 8.6.

8.4 Instrumentation

Sub-areas 12, 13, 44 and S-2 (Fig. 8.1) were monitored with vacuum pressure gauges, settlement plates, multilevel settlement gauges, electric piezometers, stand pipe piezometers and inclinometers; respectively, used to measure vacuum pressure, surface settlements, subsurface settlements, porewater pressures and lateral displacements (Choa 1990; Shang et al. 1998). Although extensive instrument and monitoring was carried out during the preloading operation, a very limited amount of information is reported in the literature. For example, subsurface settlements with time, lateral displacements with depth at different times, porewater pressure with time, settlement and lateral displacement data due to vacuum preloading only, etc are not reported in the literature. Choa (1989, 1990) has reported surface settlement for pilot test sections using fill and combined vacuum-fill preloading and porewater pressure data for vacuum-fill preloading sections only which are analyzed in subsequent sections.

8.5 Prefabricated Vertical Drains

A total of about 290000, plastic board type prefabricated vertical drains (PVDs), embedded to depth of 16 to 20m were installed in the treatment area (Yixiong 1996b). In some cases where soil layer was thick, 25m long PVDs were also used (Shang et al. 1998). Different machines including gantry type, floating type, crawler type and double mandrel installing machines were used to install the drains. Vibro-driving method was used to install the PVDs. Installation of PVDs was completed in 1.5 years (Yixiong 1996b). Table 8.1 summarizes the PVD parameters used in the ILLICON analysis.

8.6 Loading Sequence

Sections I and II (Fig. 8.1) were treated with vacuum preloading (80kPa) only; whereas, sections III to VI were treated with combination of vacuum (80kPa) and Fill (17kPa) preloads. Following was considered in constructing loading schedule for ILLICON analysis:

- The initial excess porewater pressure observed at different depths was taken as an additional applied load at zero time (t=0).
- Table 8.2 summarizes dates for various activities in the treatment area. It can be seen that the pretreatment of soil was completed in April 1987 and soil improvement works began after a lapse of two months. The initial porewater pressures measured approximately 6.5 months after the completion of pretreatment were found in excess of hydrostatic porewater pressure. As the initial excess porewater pressures included the porewater pressure resulting from the placement of pretreatment fill; the load applied due to pretreatment fill is not considered in the subsequent loading.

8.6.1 Vacuum-Fill Preloading in Control Tower Area (Choa 1989, 1990)

There is a discrepancy in the reported data with regard to the commencement of vacuum preloading operation. Figure 9 of Choa (1990) shows that vacuum preloading commenced during the last week of November, 1987; whereas Fig. 11 of Choa (1990) suggests that the vacuum preloading commenced on December 26, 1987 as shown in Table 2. It is also important to note that Fig. 9 of Choa (1990) shows that vacuum initially developed to 27kPa and remained at this level for almost a month, however there were no settlements observed under this load. This is possible only if the compressible sublayer remained within recompression range after application of this load (27kPa). However, it can be inferred from Fig. 8.5 that the addition of 27kPa of load is likely to take all the sublayers into the compression range; therefore, the information given in Fig. 11 of Choa (1990) is considered more reasonable. Hence a period of 55days is assumed between installation of PVDs and the application of vacuum preload (Table 8.2). A fill load of 17kPa was added 150 days after commencement of vacuum preloading. To analyze the settlement and porewater pressure response in Control Tower area (CTA), following loading options were considered:

8.6.1.1 Option I – CTA

Vacuum was assumed to gradually develop to a uniform intensity of 91kPa (Choa 1990) throughout the compressible layer (to the depth of penetration of PVDs) as shown in Fig. 8.7a. The difference in magnitude of load for various sublayers is because of the existence of pretreatment porewater pressures. The discharge capacity of PVDs was investigated in the range of $2m^3$/yr. to $790m^3$/yr. (Choa 1990).

8.6.1.2 Option II - CTA

Vacuum was assumed to gradually develop to different intensities at different depths, based on the observed reduction in porewater pressure, as shown in Fig. 8.7b. The discharge capacity of PVDs was investigated in the range of $2m^3$/yr to $11m^3$/yr.

8.6.2 Vacuum-Fill Preloading in Pilot Test Area (Choa 1989, 1990)

For the vacuum-fill pilot test area (VFTA), vacuum was applied 25 days after measurement of initial excess porewater pressures as shown in Table 8.2. In this area, vacuum developed quickly to approximately 85kPa; however, it remained unstable for almost 90 days, fluctuating around a mean value of 60kPa (Fig. 8 of Choa, 1990). Thereafter, it increased to 95kPa and remained constant for the remaining period of treatment. A 17kPa fill load was added after 115 days of vacuum preloading. Similar to Control Tower testing area, two loading options were considered:

8.6.2.1 Option I –VFTA

Vacuum was assumed to develop gradually to a uniform intensity of 60kPa and then to 95kPa as shown in Fig. 8.7c (the observed fluctuations in vacuum pressure were ignored in the analysis). The discharge capacity of PVDs was investigated in the range of $2m^3$/yr to $790m^3$/yr.

8.6.2.2 Option II –VFTA

Based on the porewater pressure records vacuum was assumed to develop gradually to different intensities at different depths as shown in Fig. 8.7d. The discharge capacity of PVDs was investigated in the range of $2m^3$/yr to $11m^3$/yr.

8.6.3 Fill Preloading Pilot Test Area (Choa 1989, 1990)

The initial excess porewater pressure record for fill preloading area has not been reported in the literature. Choa (1990) reported that during the reclamation process, the

discharge points for hydraulic fill were located at the south end of the project site; therefore, the concentration of clay particles increased from South to North. It can be seen from Fig. 8.1 that the test site for fill preloading area (S-2) is located at the North of vacuum-fill pilot test site (area 44); therefore, it is highly unlikely that the pretreatment excess porewater pressures did not exist at the fill preloading test site. In fact, due to increased clay content, the pretreatment porewater pressures at this site are likely to be slightly higher, or at least equal the vacuum-fill pilot test site. Therefore, in addition to time dependent loading (Fig. 7 of Choa, 1990), a pretreatment porewater pressure profile, similar to vacuum-fill test site was assumed to exist at the time of fill construction as shown in Fig 8.7e.

8.7 Results and Discussion

8.7.1 Settlement and Porewater Pressure

Figure 8.8 shows the distribution of pretreatment surface settlements observed before the application of vacuum or fill preloads. It can be seen from the Fig. 8.8 that the observed pretreatment surface settlement in the pilot test areas ranged between 0.8 - 1.0m. It was mentioned in the Section 2 that both the original sea bed clay and the hydraulic fill were undergoing primary compression at the time of the commencement of preloading operation; therefore, part of the pretreatment settlements can be associated with the settlements occurring during the rest period (6.5 months) while part the settlement could be due to remolding of soil due to installation of PVDs and subsequent dissipation of associated porewater pressure before the commencement of preloading. Hence it is likely that the soil parameters used in the ILLICON analysis do not correctly represent the subsurface conditions prior to the settlement reported in Fig. 8.8.

8.7.2 Control Tower Area

Figures 8.9 and 8.10 respectively compare the observed and the predicted settlements for different assumed discharge capacities of PVDs for option I–CTA and option II-CTA. It can be seen that the discharge capacity of 790m^3/yr. reported in the literature (Choa 1990; Yixiong 1996b) over predicts the rate of settlements even for option II-CTA, which accounts for a reduced vacuum pressure. Figure 8.9 shows a good agreement between the observed and the predicted settlements for a discharge capacity corresponding to 2m^3/yr; whereas, Fig. 8.10 suggests that the PVDs performed at a discharge capacity between 5 and 11m^3/yr. It can also be seen from Figs. 8.9 and 8.10 that the settlement induced before the

application of vacuum was almost identical for discharge capacities of 11 and 790m^3/yr. This indicates that in the recompression range, the minimum discharge capacity required for PVDs to function without significant well resistance was around 11m^3/yr.

Figures 8.11 and 8.12 compare the observed and the predicted porewater pressure response for the loading options considered in the settlement analyses. The porewater pressure response plotted in Figs. 8.11 and 8.12 corresponds to a discharge capacity of 2, 5.5, 11 and 790m^3/yr. It can be seen that for Option II–CTA, a discharge capacity of 11m^3/yr predicts the porewater pressure response in a much better way as compared to Option I-CTA with a discharge capacity of 2m^3/yr. Figures 8.9 to 8.13 suggest that (a) as a result of vertical variation in permeability of subsoil, vacuum did not develop uniformly in the compressible layer and (b) PVDs performed without any significant well resistance at a discharge capacity of 11m^3/yr.

8.7.3 Vacuum-Fill Pilot Test Area

Observed and predicted settlement response for Vacuum-Fill pilot test area for the loading options considered is shown in Figs. 8.13 and 8.14. Similar to control tower area, the agreement in observed and predicted settlement corresponds respectively to a discharge capacity of 2m^3/yr and 5.5 to 11m^3/yr for option I-VFTA (constant vacuum intensity) and option II-VTFA (variable vacuum intensity).

The observed and predicted porewater pressure response corresponding to different discharge capacities is shown in Figs. 8.15 and 8.16. It can be seen that the porewater pressure response corresponding to an assumed discharge capacity of 11m^3/yr. for option I-VFTA presents the best agreement with the observed porewater with depth (Fig. 8.15c); however, this option over-predicts the rate and magnitude of settlement and therefore, is not considered reasonable. There is generally a good agreement between observed and predicted porewater pressure response for a discharge capacity of 11m^3/yr for option II-VFTA except at the depths of 5 and 14m (Fig. 8.16c). As the settlement for option II-VFTA is also in good agreement for a discharge capacity of 11m^3/yr., it is considered more realistic to represent actual field conditions by a discharge capacity of 11m^3/yr. It was mentioned in Section 8.6.2 that vacuum remained unstable during the first 90 days of application; however, for settlement analyses, it was assumed to gradually develop to 60kPa in this period without any

fluctuations. The minor variations in observed and predicted porewater pressure responses can be attributed to the fluctuating vacuum pressure.

8.7.4 Fill Preloading Pilot Test Area

The observed and predicted settlement response for fill preloading pilot test area is shown in Fig. 8.17. It can be seen that in this case also, the discharge capacity of 790m^3/yr. reported in the literature over-predicts the rate of settlement, whereas, there is a good agreement between the observed and predicted settlement corresponding to a discharge capacity of 11m^3/yr. The assumption on existence of an initial excess porewater pressure also appears to be quite reasonable and represents the field behavior well. In the absence of more specific data pertaining to this section, i.e. porewater pressure response and time rate of subsurface settlements, it is not possible to further validate the assumptions made for the settlement analysis of fill preloading test area.

8.7.5 Increase in Shear Strength

The increase in vane shear strength due to vacuum, vacuum-fill and fill preloading reported by Yixiong (1996b) is shown in Fig. 8.18a. An increase in undrained vane shear strength was observed for all three types of preloads. Figure 8.18b shows the ratio of strength increase at the end of treatment period for all three types of loading conditions. It can be seen from Fig. 8.18b that $s_u(FV)/s_{uo}(FV)$ is independent of type of load. Moreover, $s_u(FV)/s_{uo}(FV)$ decreases with depth irrespective of the type of load, which indicates that the increase in shear strength may also depend upon the initial state of stresses including effective stress and preconsolidation pressure. Figure 8.19 shows the ratio of increase in shear strength due all three type of loads plotted against initial shear strength. It can be seen from Fig. 8.19 that the ratio of increase in shear strength depends upon the initial shear strength, i.e., irrespective of the type of load, the ratio of increase in strength is maximum for sublayers with low initial shear strength as compared to those with relatively high initial shear strength. It is also important to note that $s_u(FV)/s_{uo}(FV)$ due to vacuum, vacuum-fill and fill preloads generally plot around the same line; which suggests that for a lower initial shear strength, fill preload would have resulted in a similar strength increase. Therefore, it is more reasonable to evaluate the increase in shear strength as a function initial shear strength and the preconsolidation pressure.

8.8 Concluding Remarks

The settlement analysis shows that:

- The combined vacuum-fill preload acts in a similar way as that of a conventional fill preload. Therefore, existing consolidation theories and settlement analysis procedures can be effectively used to explain soil behavior under vacuum or vacuum-fill preloading, and predict settlement, porewater pressure and increase in undrained shear strength.
- The plastic board type PVD performed without any significant well resistance; however, the minimum discharge capacity ($11 m^3/yr.$) required for the PVDs to perform without well resistance was significantly less than the discharge capacity ($790 m^3/yr.$) reported in the literature.
- In all cases, the best agreement between the observed and predicted settlement and porewater pressure response corresponds to a discharge capacity of $11 m^3/yr.$ Hence the PVDs perform independently of the type of applied load.
- The distribution of vacuum pressure, which as a result of stratigrafic variations, may not be constant with depth, should be accounted for in the settlement analysis. Estimating vacuum intensity at a given depth by using the observed reduction in porewater pressure with depth is a reasonable method.
- Incorporating pretreatment excess porewater pressure into loading schedule (at t=0) is a reasonable assumption which helps in explaining the settlement and porewater pressure response due to vacuum/fill preloading.
- The increase in shear strength due to either type of loads is similar and can be satisfactorily predicted by using the empirical correlation suggested by Terzaghi et al. (1996).

8.9 Tables

Table 8.1: Vertical drain parameters

Parameter	Reported	ILLICON
Spacing, (m)	1.3	No change
Pattern	Square	No change
Type of Drains	PVD, plastic board type	-
Section (mm)	100*4	No change
Discharge Capacity (m^3/year)	790	2 to 790
Penetration Depth (m)	16 – 20, upto 25	20
r_s/r_m	-	2
Time for Installation of drains (Days)	-	20 to 30
r_s: Radius of smear zone r_m: Radius of smear zone		

Table 8.2: Time line for various activities

Activity	Date	Remarks
Completion of Pretreatment	Apr 1987	Choa (1990)
Commencement of soil improvement (Installation of PVDs/Instrumentation)	June 15, 1987	Choa (1990) & Shang et. al (1998)
Vacuum-Fill Preloading in Control Tower Area (Choa, 1989 & 1990)		
Measurement of porewater pressure		
a. Initial	Nov 01, 1987	Before application of vacuum
b. 110 days after Vacuum	Apr 15, 1988	
c. Vacuum applied on	Dec 26, 1987	Vacuum applied after 55 days of initial measurements ; from a & b
Vacuum-Fill Preloading in Pilot Testing Area (Choa, 1989 & 1990)		
Measurement of porewater pressure		
a. Initial	Nov 02, 1987	Before application of vacuum
b. 110 days after Vacuum	Mar 15, 1988	
c. 180 days after Vacuum	May 30, 1988	
d. Vacuum applied on	Nov 27, 1988	Vacuum applied after 25 days of initial measurements ; from a & b

Fill Preloading in Pilot Testing Area (Choa, 1989 & 1990)

Loading Stage	From	To	Total Height of Fill (m)
First	Nov 7, 1987	Nov 15, 1987	0.6
Second	Nov 22, 1987	Nov 30, 1987	1.27
Third	Dec 26, 1987	Feb 2, 1988	3.63
Fourth	Feb 14, 1988	Feb 24, 1988	5.55

8.10 Figures

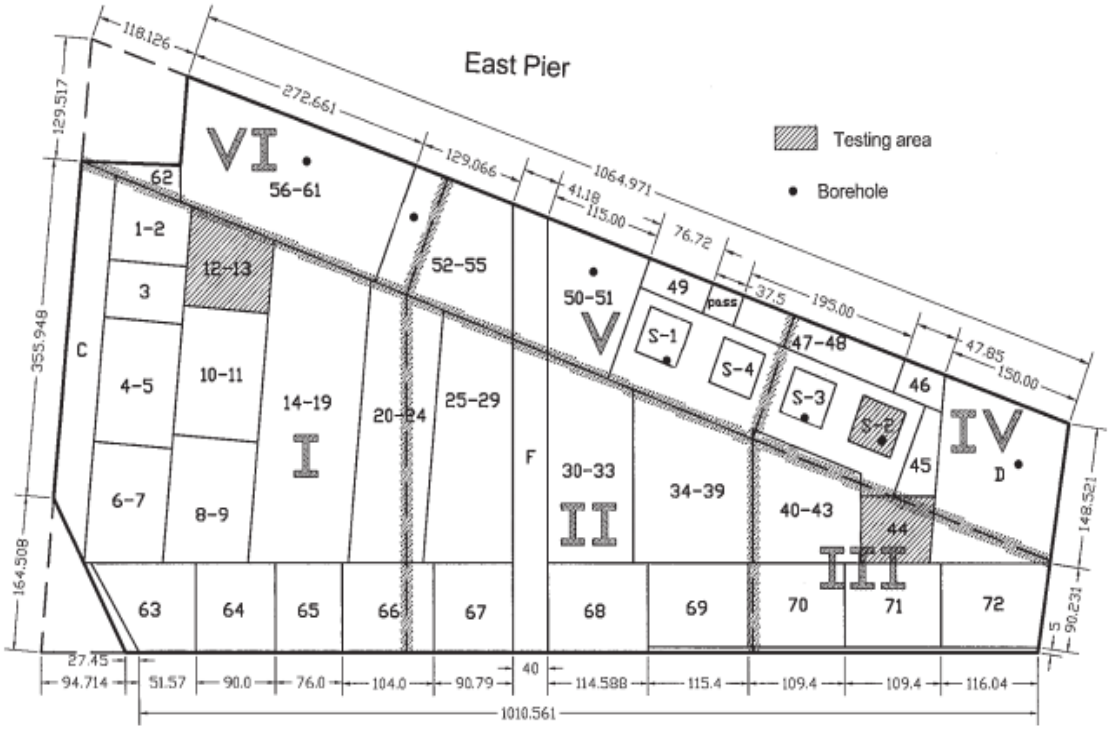

Figure 8.1: Layout and distribution of treatment area into sub-areas and sections (after Shang et al. 1998)

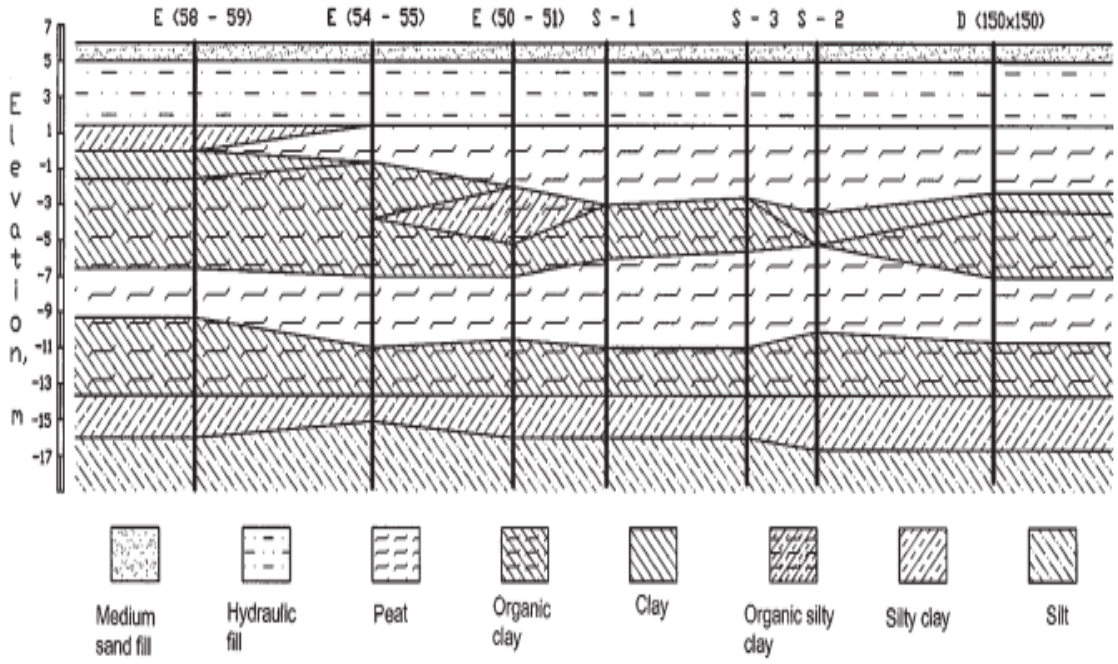

Figure 8.2: Generalized soil profile in East Pier area (after Shang et al. 1998)

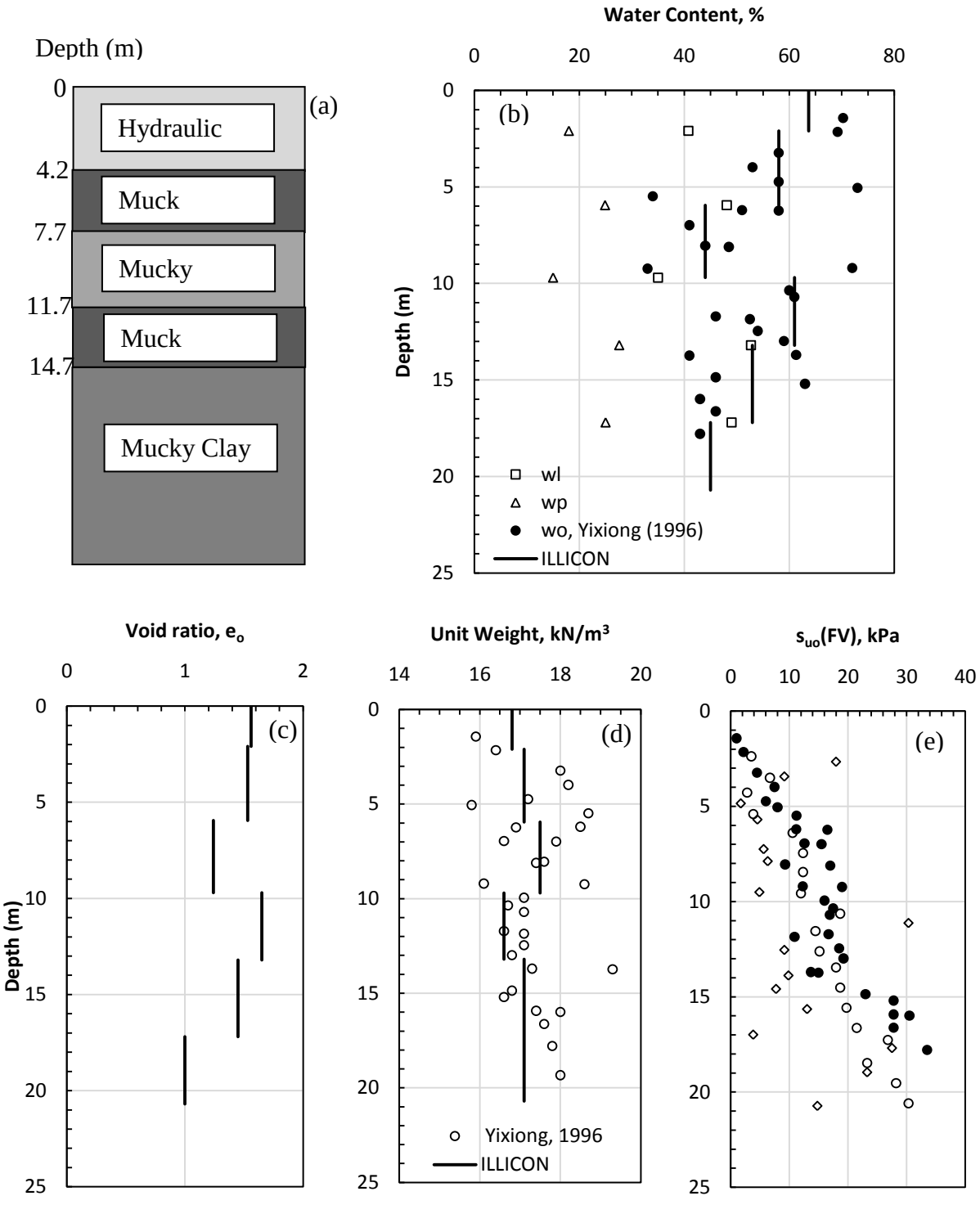

Figure 8.3: Generalized soil profile and vertical profile of various geotechnical properties

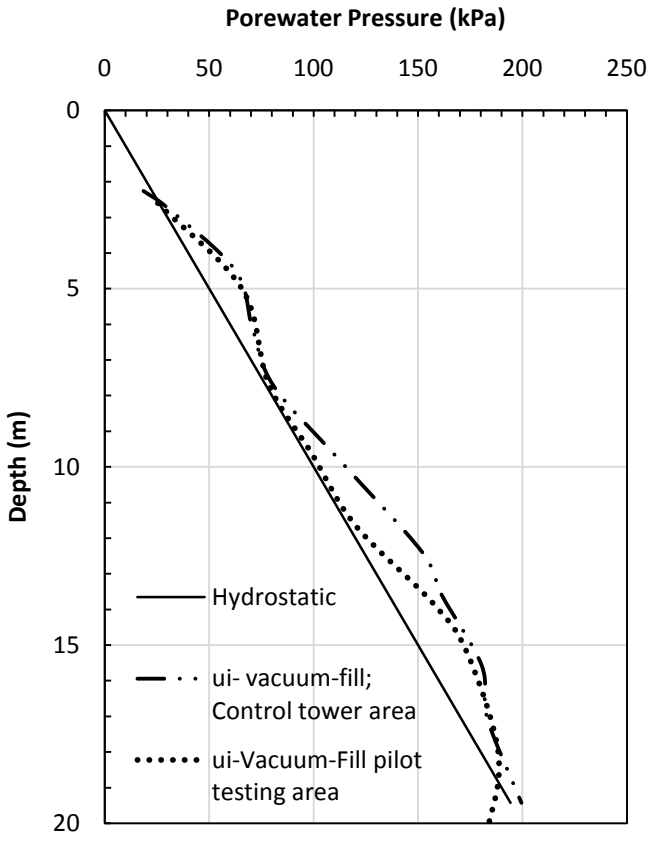

Figure 8.4: Pretreatment porewater pressure in vacuum-fill testing sites

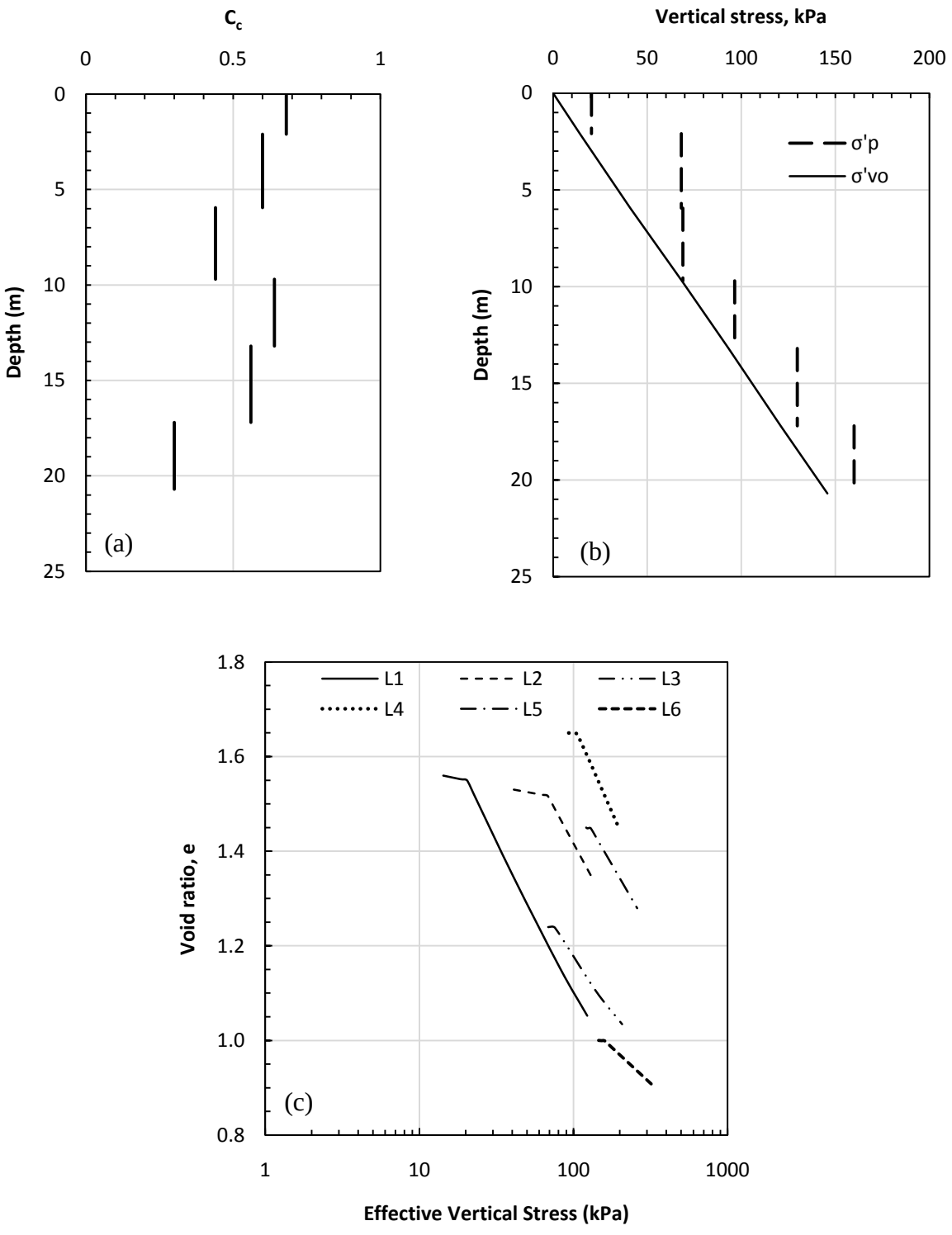

Figure 8.5: Vertical profile of (a) compression index, (b) initial effective stress and preconsolidation pressure, and (c) EOPe -logσ'_v relations for different sublayers

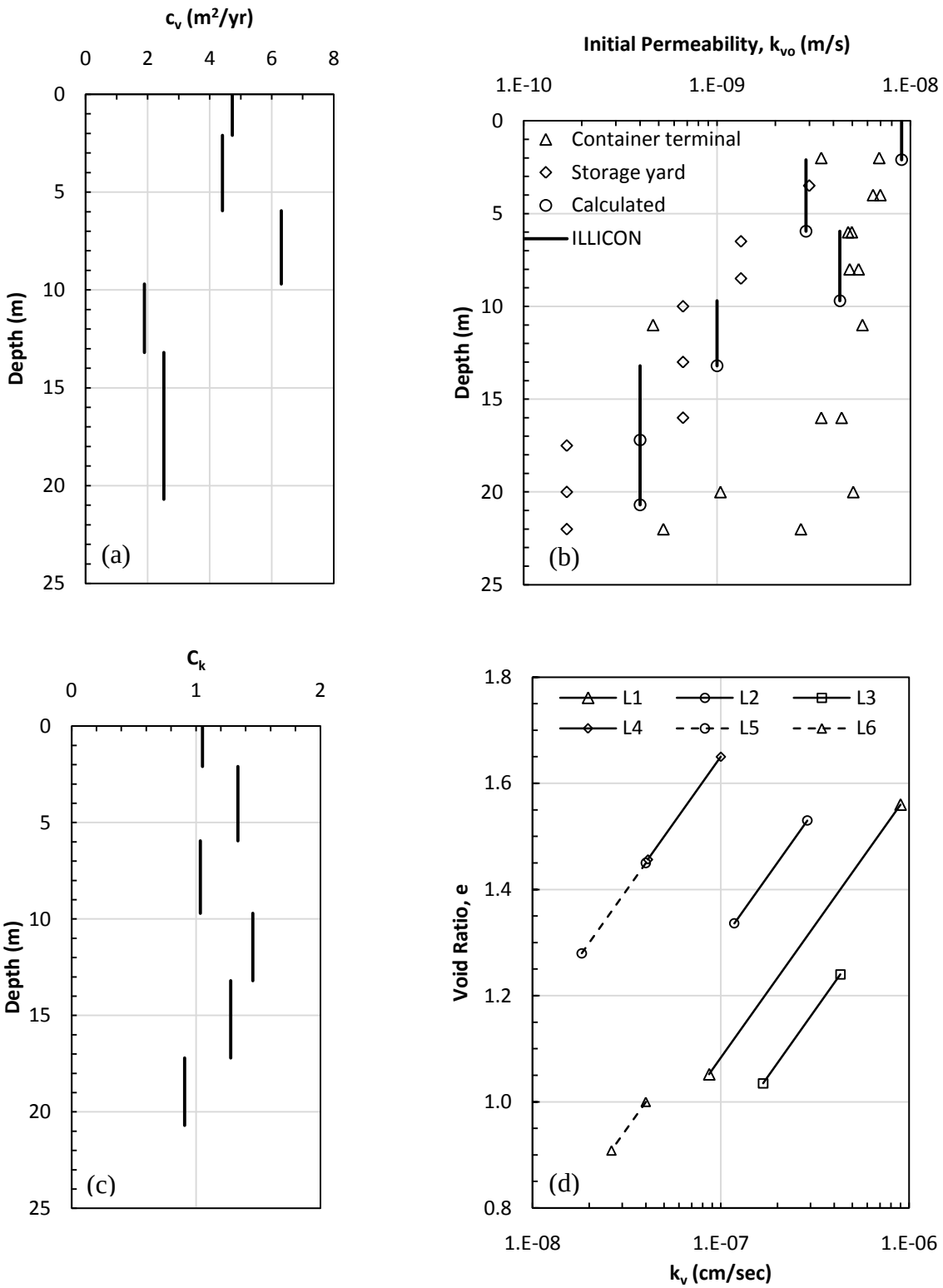

Figure 8.6: Vertical profile of (a) coefficient of consolidation, (b) initial vertical permeability, (c) C_k, and (c) e -logk_v relations for different sublayers

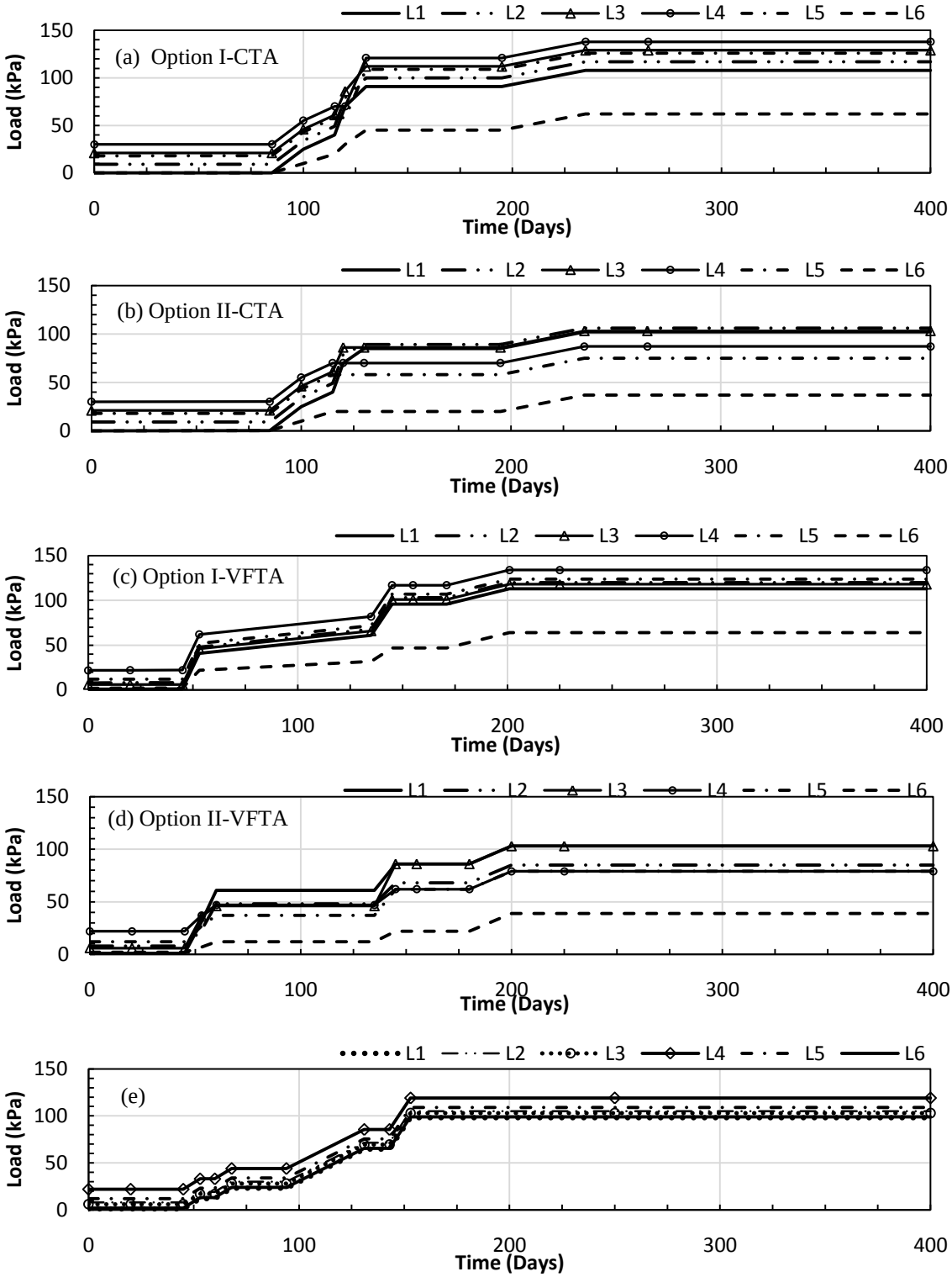

Figure 8.7: Loading options considered for the settlement analysis of (a & b) control tower area (c & d) vacuum-fill pilot testing area and (e) fill pilot testing area

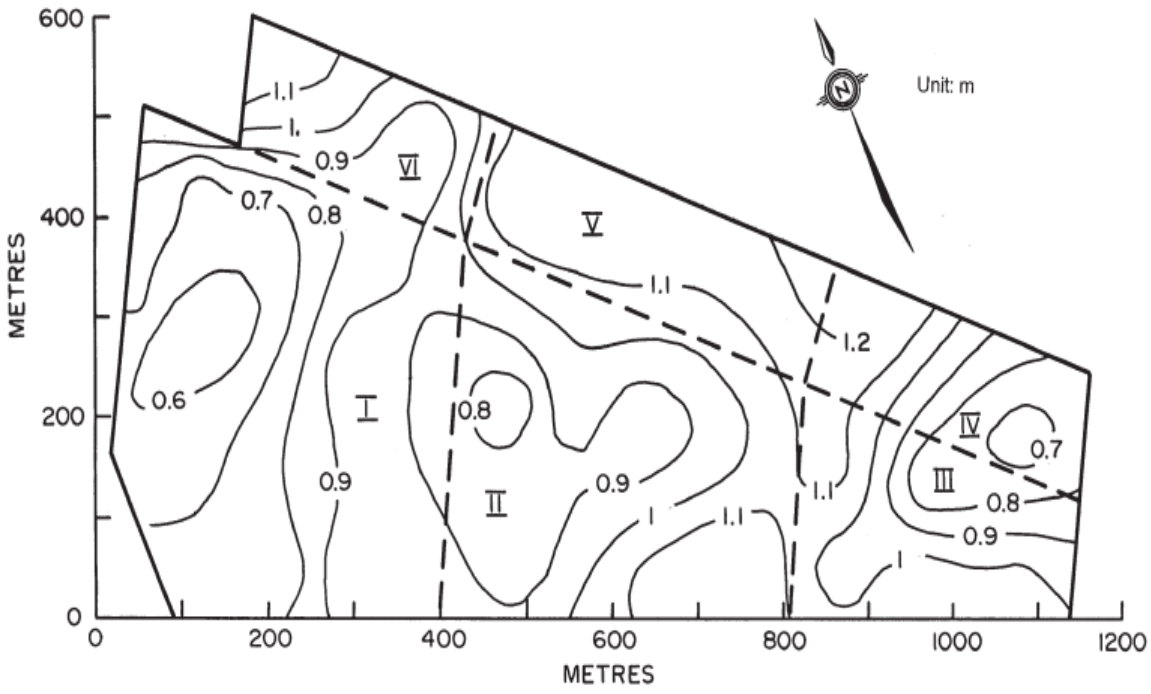

Figure 8.8: Settlement contours before application of preload (after Shang et al. 1998)

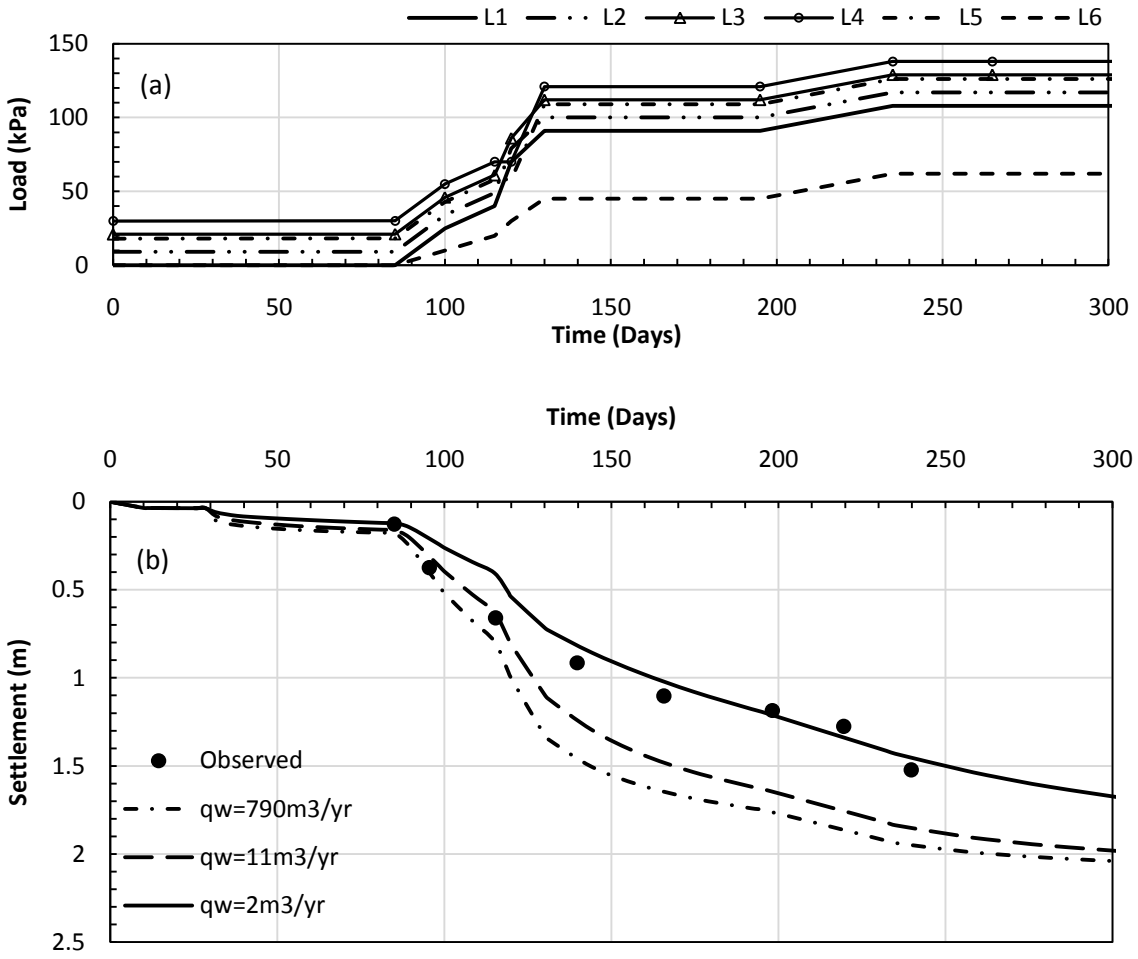

Figure 8.9: Observed and predicted settlements in control tower area for loading option I-CTA

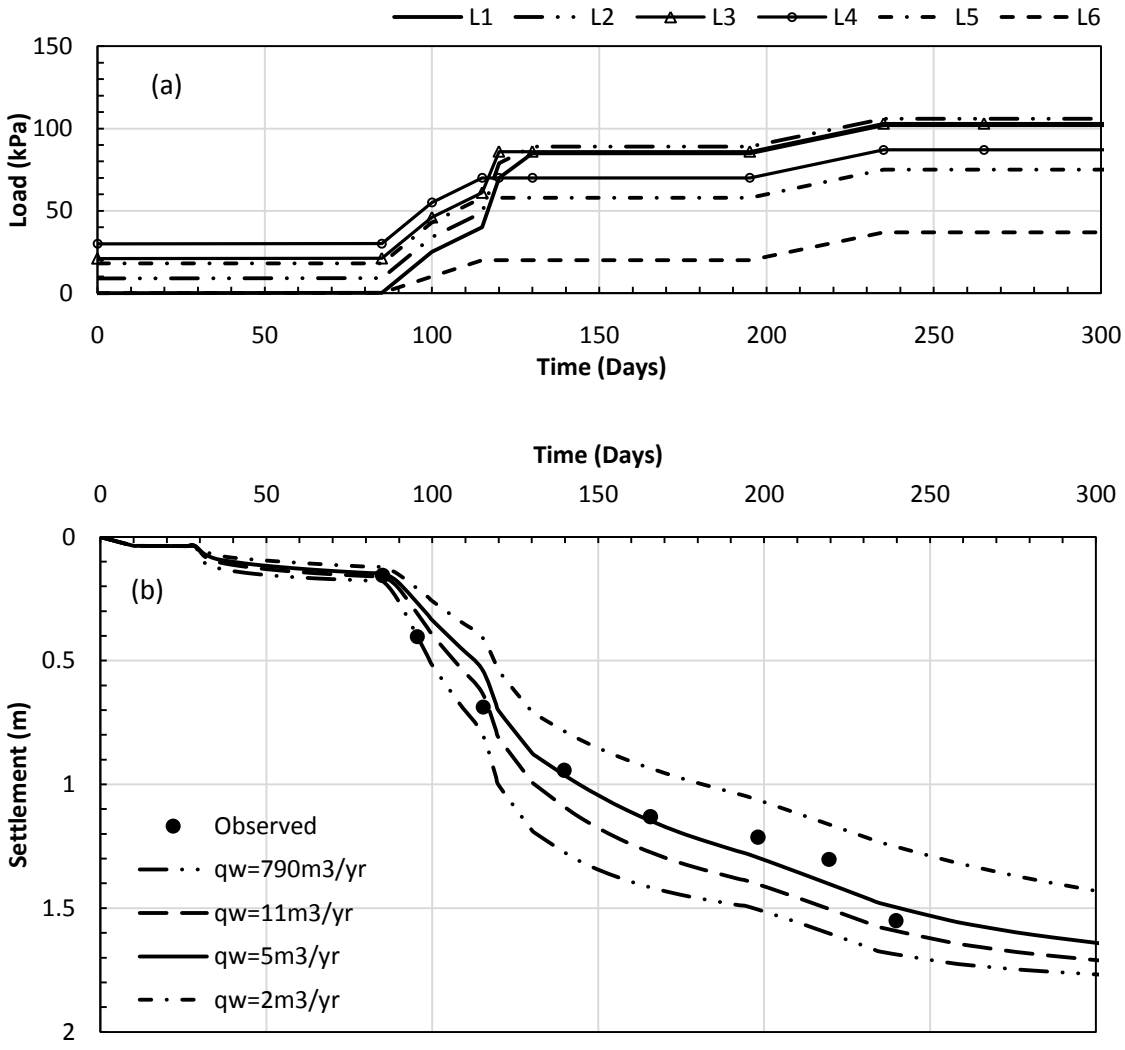

Figure 8.10: Observed and predicted settlements in control tower area for loading option II-CTA

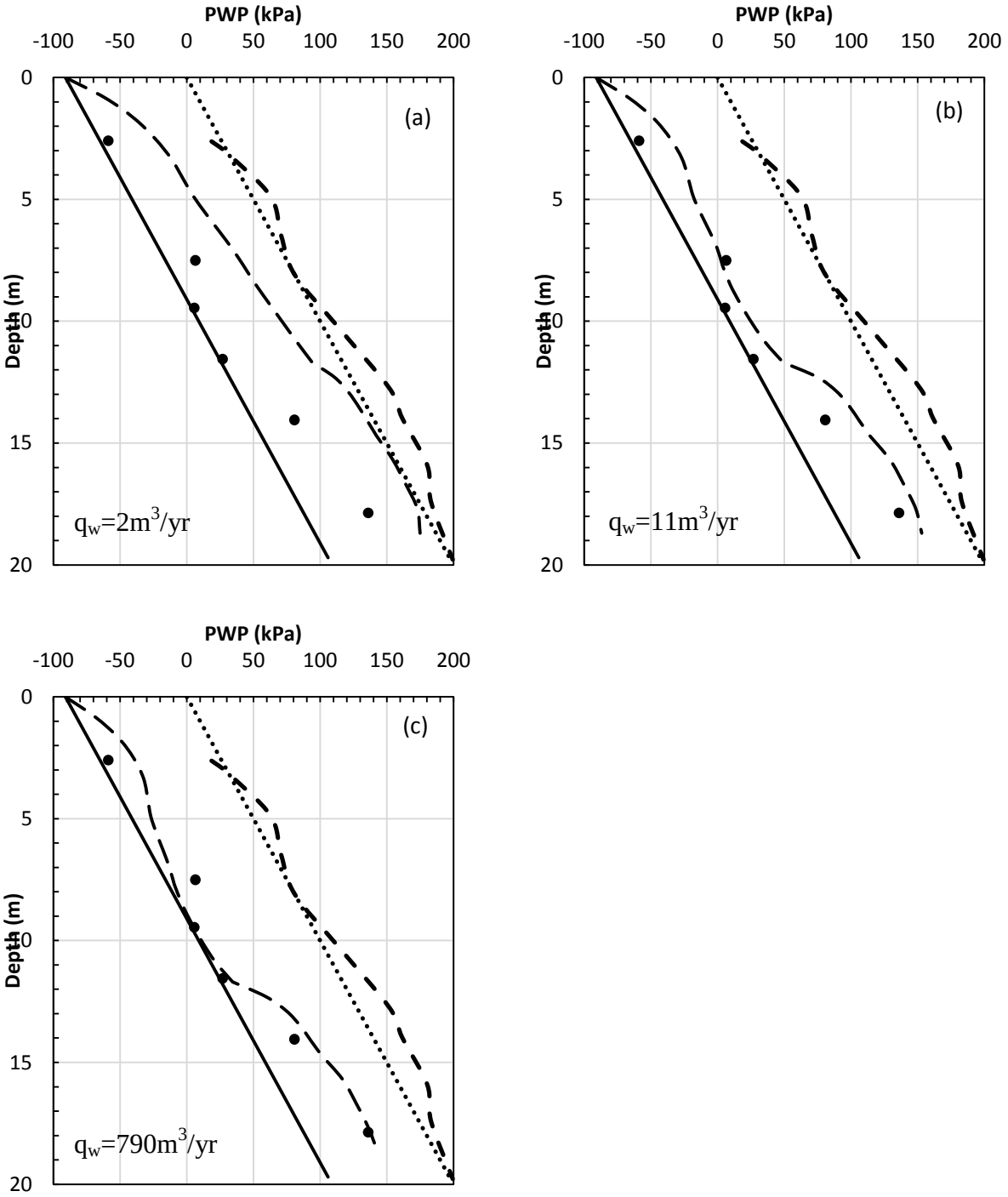

u_o (kPa)	u_i (kPa)	u_{sm} (kpa)	110 Days	
			Observed	ILLICON
.....	- - - -	———	●	— — —

Figure 8.11: Observed and predicted porewater pressure with depth in control tower area for loading option I-CTA

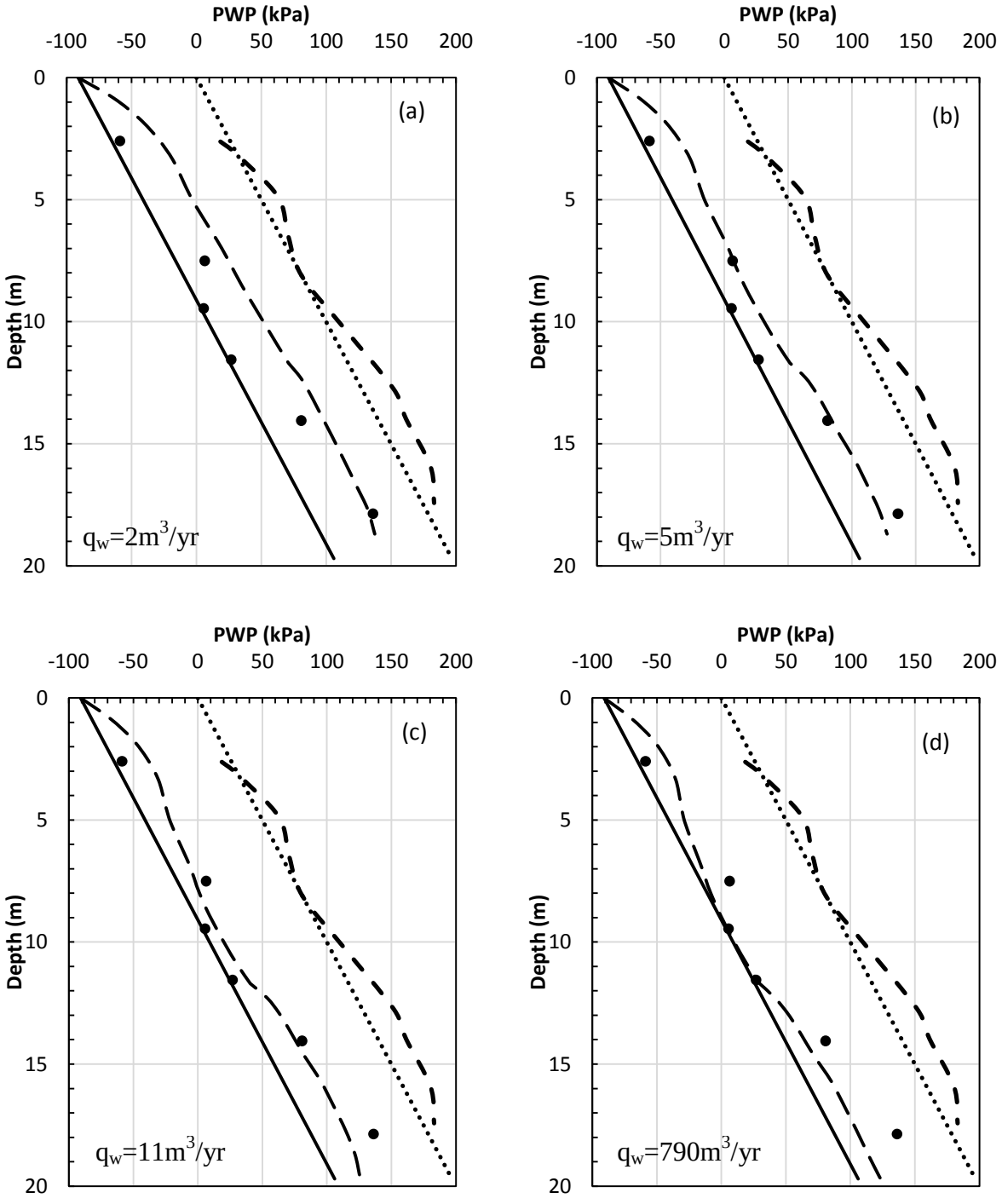

u_o (kPa)	u_i (kPa)	u_{sm} (kpa)	110 Days	
			Observed	ILLICON
.....	- - - -	———	●	— — —

Figure 8.12: Observed and predicted porewater pressure with depth in control tower area for loading option II-CTA

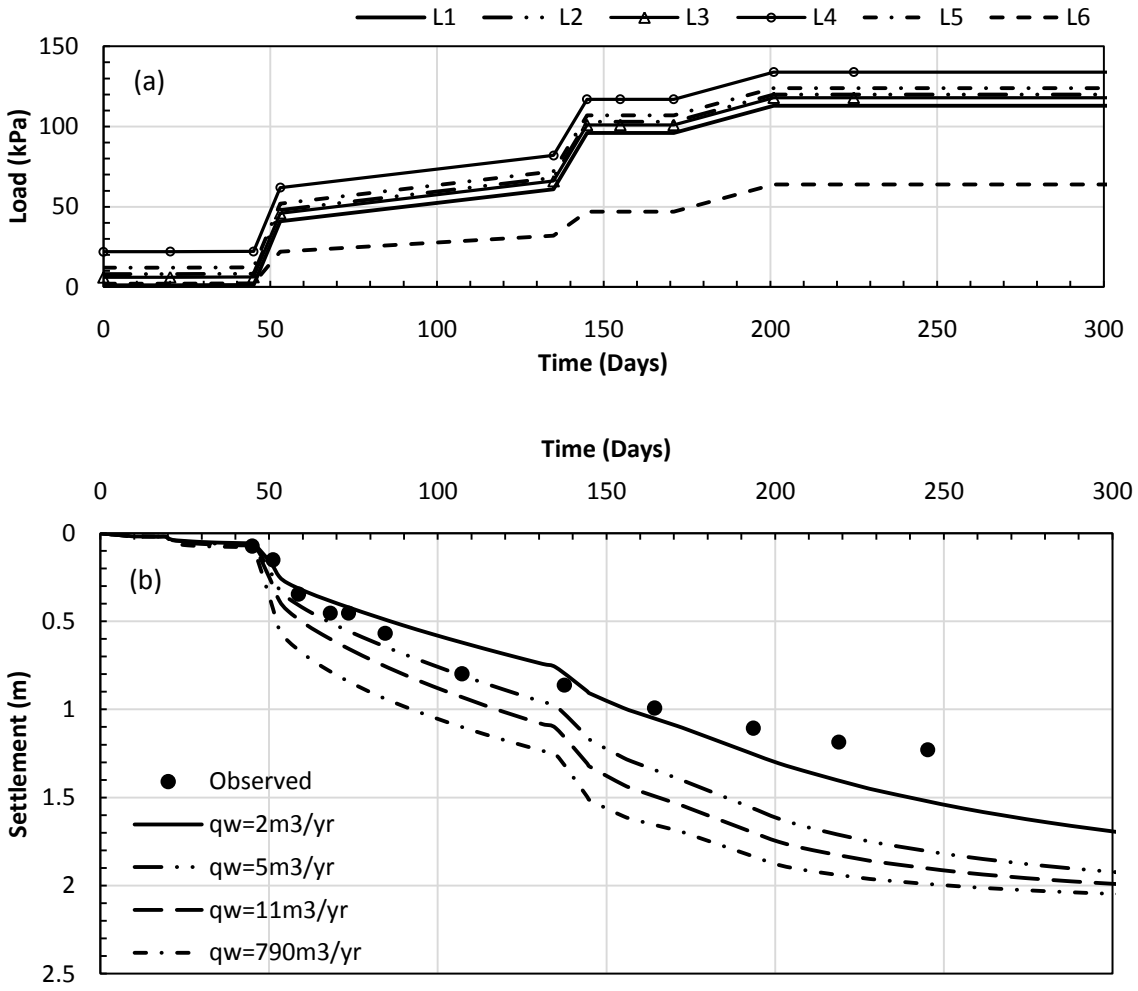

Figure 8.13: Observed and predicted settlement in vacuum-fill pilot testing area for loading option I-VFTA

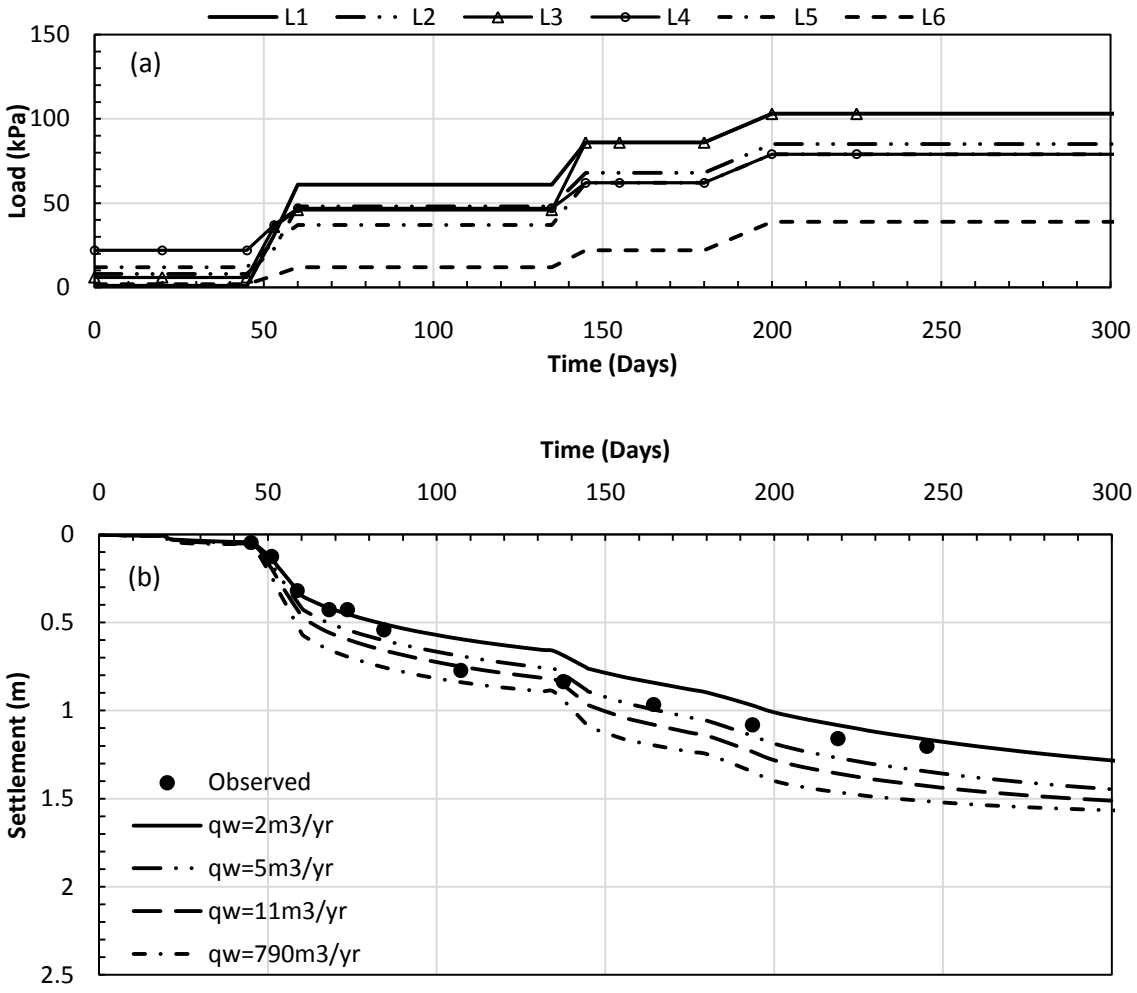

Figure 8.14: Observed and predicted settlement in vacuum-fill pilot testing area for loading option II-VFTA

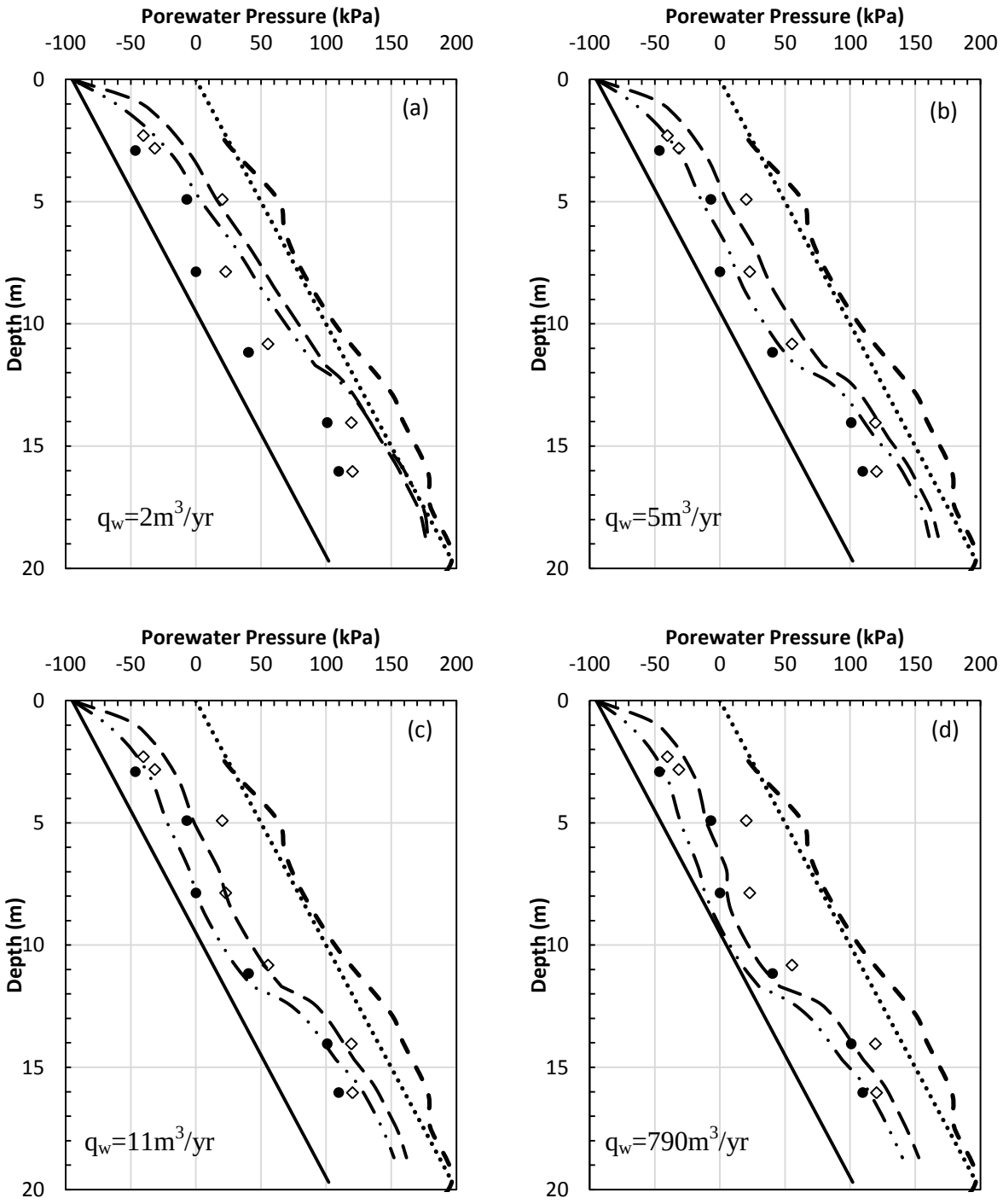

u_o (kPa)	u_i (kPa)	u_{sm} (kpa)	110 Days		180Days	
			Observed	ILLICON	Observed	ILLICON
·····	- - - -	———	◇	— — —	●	— · · —

Figure 8.15: Observed and predicted porewater pressure with depth in v acuum-fill pilot testing area for loading option I-VFTA

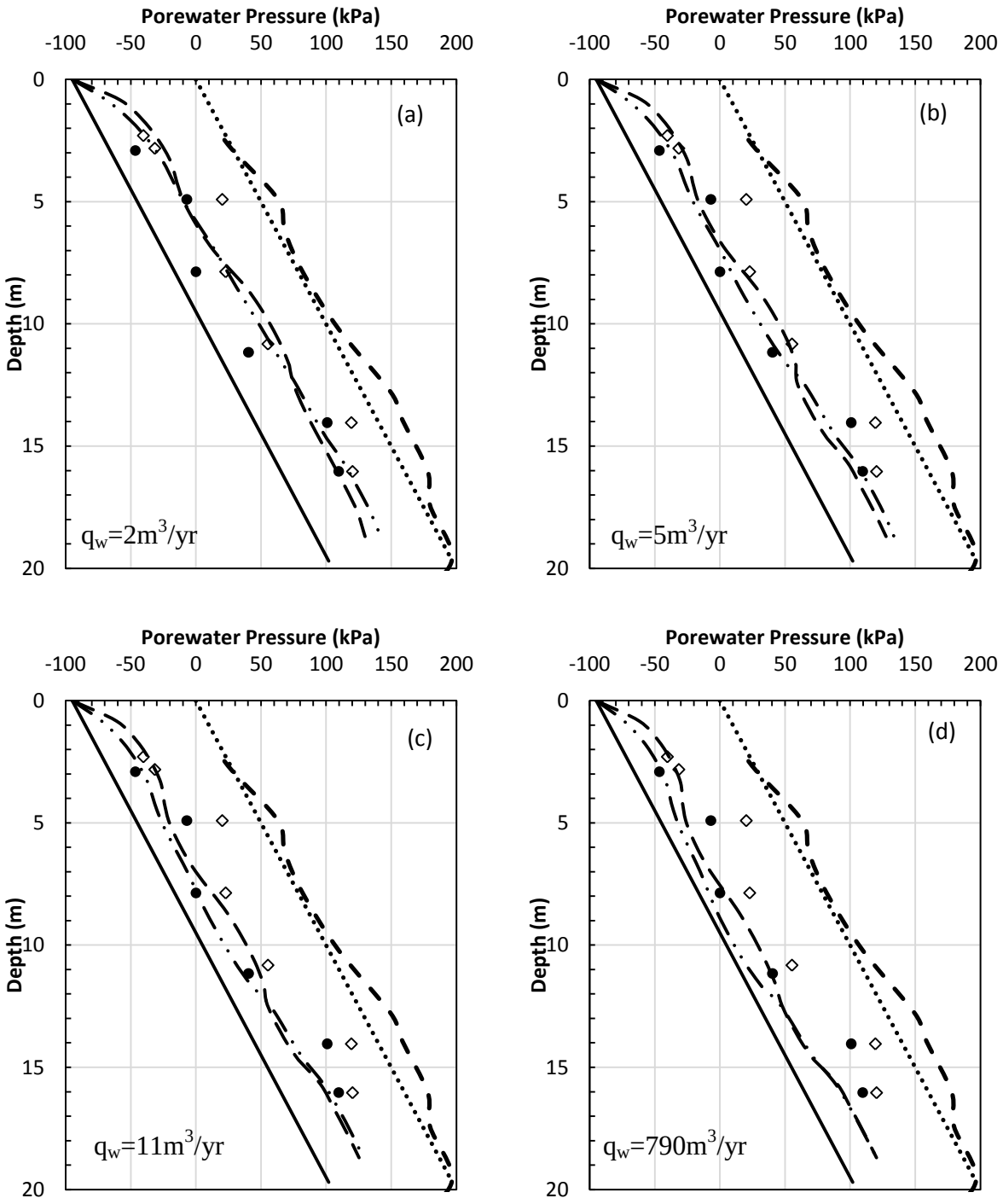

u_o (kPa)	u_i (kPa)	u_{sm} (kpa)	110 Days		180Days	
			Observed	ILLICON	Observed	ILLICON
·····	- - - -	———	◇	— — —	●	— · · —

Figure 8.16: Observed and predicted porewater pressure with depth in vacuum-fill pilot testing area for loading option II-VFTA

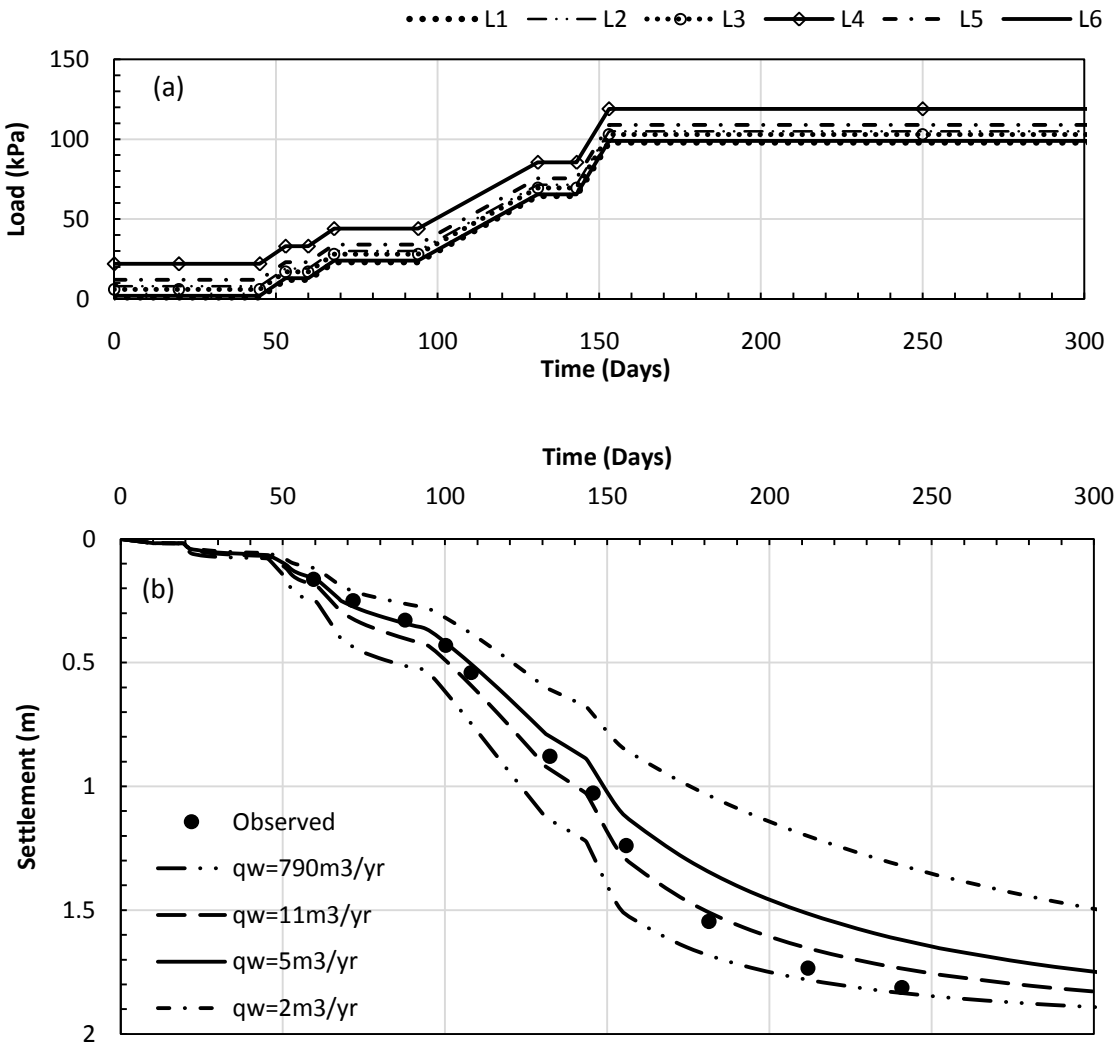

Figure 8.17: Observed and predicted settlements for ill preloading pilot testing area

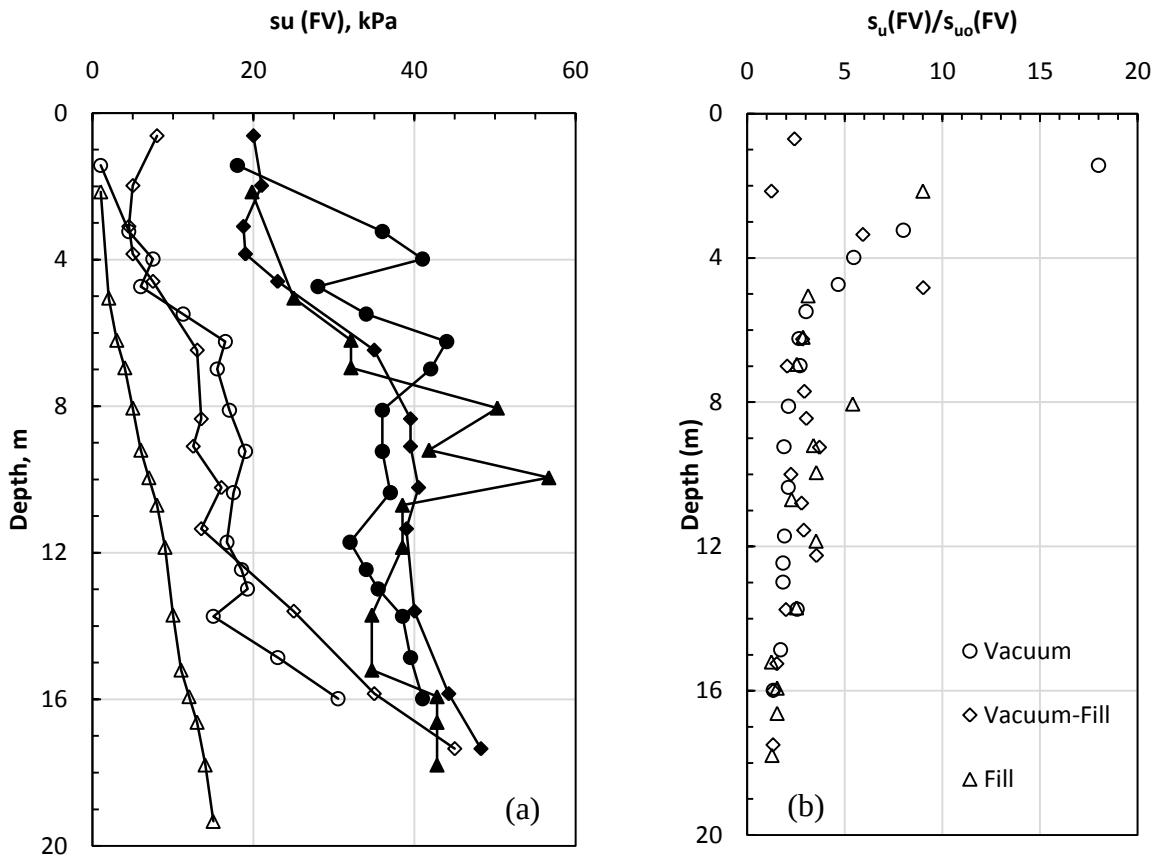

	Vacuum	Vacuum-Fill	Fill
Before Treatment			
After Treatment			

Figure 8.18: (a) Increase in field vane shear strength due to preloading, and (b) ratio of increase in shear strength at different depths (data from Yixiong 1996b).

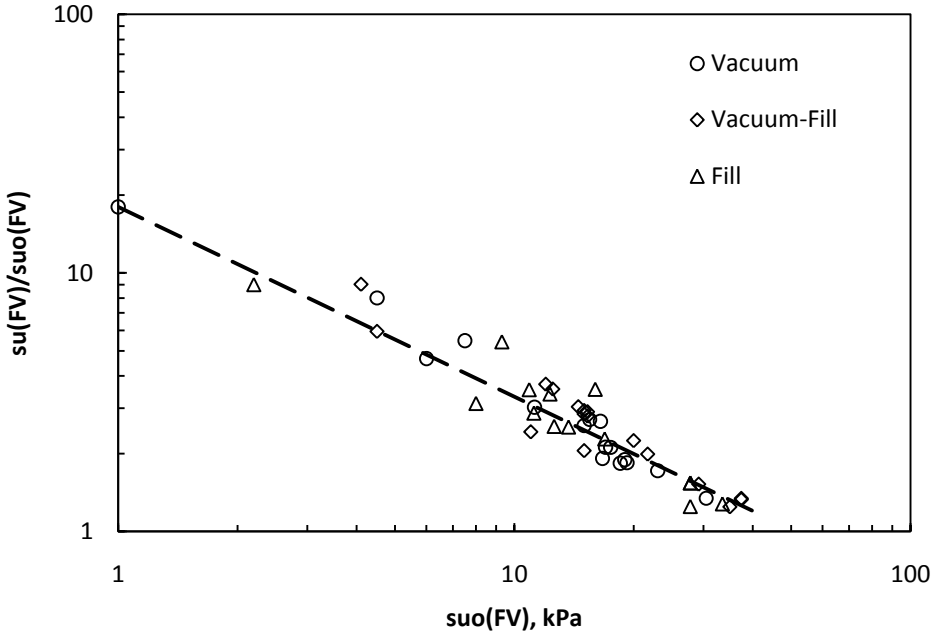

Figure 8.19: Ratio of increase in shear strength plotted against initial shear strength due to different type of loads

CHAPTER 9. CHARACTERISTICS OF VACUUM CONSOLIDATION

9.1 Introduction

Although vacuum consolidation has been effectively used during the last two decades for precompression of soft ground, different opinions exist regarding its exact mechanism and characteristics. Some engineers and researchers believe that preloading with vacuum is principally similar to fill preloading and therefore the magnitude and rate of settlement can be evaluated by simply replacing the applied vacuum load with an equivalent fill preload (Ter-Martirosyan and Cherkasova 1983; Woo et al. 1989; Mohamedelhassan and Shang 2002). On the other hand, some engineers and researchers claim that the rate of settlement with vacuum preloading is faster while the magnitude of settlement may be less than that by the equivalent fill preload (Masse et al. 2001; Indraratna et al. 2004; Chai et al. 2005a, b; Rujiakiatkamjorn et al. 2007, etc). In the following sections, an effort is made to clarify the mechanism involved in vacuum consolidation. Different laboratory studies and field trials, carried out to explain the characteristics of vacuum consolidation are reviewed in this chapter.

9.2 Nature of Loading and Depth of Improvement

There is a consensus among the researchers that vacuum pressure induces an isotropic load in the soil mass (Qian et al. 1992; Masse et al. 2001). It is important to realize that the isotropic nature of loading is only possible by the use of vertical drains, i.e. the applied vacuum pressure propagates down to the depth of compressible layer through materials of high permeability (granular filter and vertical drains), and therefore generates an equal all round pressure within the soil mass. In the absence of vertical drains, the applied vacuum can only act as a load applied to the ground surface (Chen and Bao 1983). It is also widely believed that vacuum pressure is transmitted within the vertical drains down to the

depth of compressible layer with full intensity and therefore there is no practical limit on the depth of improvement that can be achieved by vacuum preloading (Masse et al. 2001; Chu and Yan, 2006). Some of the recent studies (Indraratna et al. 2004; Chai et al. 2005a, b and 2009; Rujiakiatkamjorn et al. 2007; Qiu et al. 2007), however, suggest that the vacuum intensity reduces with depth; however, there is no disagreement on the isotropic nature of loading.

9.3 Distribution of Vacuum Pressure along PVDs

The assumption on distribution of vacuum pressure with depth has a direct influence on design of preloading as well as on the back-analysis of case histories. Assuming a vacuum intensity constant with depth justifies the use of vacuum as a wide fill. On the other hand, assuming a reduction in vacuum intensity suggests a practical limit on the depth of improvement using vacuum as a preload. A limiting depth of improvement is not supported by the field evidence, and more importantly, it is not proposed as a general approach.

Indraratna et al. (2004) and Rujiakiatkamjorn et al. (2007) suggest a linear decrease in vacuum intensity with depth. Their recommendation is based on a laboratory study (Rujiakiatkamjorn, 2005) in which series of tests were carried out within 450mm diameter and 900mm height (D/L_o = 0.5) Teflon lined confining cylinder, on reconstituted clay specimens, provided with a PVD at the centre. The consolidation was carried out under; (1) a vertical load of 30kPa (SP1); (2) vacuum pressure of 20kPa applied to top of specimen (VP1); (3) vacuum pressure of 40kPa (VP2); (4) vertical load of 30kPa combined with vacuum pressure of 20kPa (SV1) and (5) vertical load of 30kPa combined with vacuum pressure of 40kPa (SV2). The reconstituted specimens were prepared from slurry having water content above the liquid limit of the soil and one-dimensionally consolidated under 20kPa while drainage was allowed from only top of the specimen (Rujiakiatkamjorn, 2005). Figure 9.1 shows the schematic diagram of test apparatus used in the study. The vertical load was applied by an air jack through a rigid piston and the vacuum load was applied through a hole in the rigid piston.

Figure 9.2 shows the locations at which the porewater pressure was measured during respective tests. Transducers T1, T2 and T3 were initially placed at the soil-PVD interface and were subsequently moved 70mm away from PVD as shown in Fig. 9.2. Figure 9.3 gives the measured distribution of porewater pressure at the PVD-soil interface during

initial stages of tests SP1, VP1, SP2 and VP2 (description of SP2 with unknown vertical pressure is not reported by Rujiakiatkamjorn, 2005). The results of VP1 and VP2 are consistent and show approximately 15% drop in vacuum pressure between the top and bottom transducers (or 20% in 0.9m). This is a very significant drop and leads to a conclusion that there should be a limiting depth up to which vacuum consolidation will be effective (e.g. only 4 to 5m by extrapolation of this study). It is also interesting to note that there was no loss in vacuum intensity up to T1 (top transducer), which shows that vacuum intensity was constant at least up to this depth. Although vacuum is transmitted through materials of high permeability, it needs some time to develop uniformly to its full intensity. Shang et al. (1998) and Tang and Shang (2000) reported an average period of 15 days for vacuum to develop to its full intensity in the field. It appears that the measurement of porewater pressure at the PVD-soil interface might have been made just after the application of load (after which transducers were moved to new location) before vacuum could achieve equilibrium in the PVD, and therefore, a systematic decrease in the vacuum intensity was observed. Porewater pressure response of SP1 ($\Delta\sigma_v$ = 30kPa) and SP2 ($\Delta\sigma_v$ = unknown) are also on Fig. 9.3. The porewater pressure for SP is expected to be positive in the soil mass and zero at the PVD-soil interface; whereas, the measured porewater pressure response for SP1 and SP2 are shown negative on Fig. 9.3. It is interesting to note that Fig. 4.11 of Rujiakiatkamjorn (2005) shows the porewater pressure for SP1 starting with +30kPa and gradually dissipating to zero with time. More importantly, the porewater pressure for vertical loads (SP1 and SP2) are also decreasing with depth indicating a reduction in the intensity of applied vertical load as well, which has not been explained by the author. It is also important to point out that there was no drop in vacuum intensity from top of the specimen to a depth of 110mm (840mm from bottom of specimen), which reinforces the idea that transducers (T1, T2 and T3) were moved to their new locations without allowing sufficient time for vacuum to achieve equilibrium.

It was mentioned earlier that the transducers T1, T2 and T3 were moved 70mm away (approximate extent of smear zone) from the vertical drain face to monitor porewater pressure response at this location. The measured porewater pressures at different radial distance from PVDs and at different distances from the bottom of oedometer were obtained from Figs. 4.11 to 4.15 of Rujiakiatkamjorn (2005) and are plotted in Figs. 9.4 and 9.5.

Figure 9.4 shows the vertical distribution of measured porewater pressure for test series SP1, VP1 and VP2, at radial distances of 70mm and 140mm from the face of PVD. It can be seen that for VP1, there is generally a constant vacuum intensity all along the length of drain. Moreover, the pattern of porewater pressure distribution for VP1 is quite similar to that of SP1, which shows that under ideal conditions, vacuum will propagate with full applied intensity to the depth of penetration of drains. Moreover, Fig. 9.4 also clearly reflects that there is no difference in consolidation due vacuum and fill preloading. Test series VP2 show some drop in vacuum intensity with depth toward the end of consolidation process, however, it should be noted that in an earlier time frame, the vacuum intensity was more at greater depth than at shallower depth (i.e. porewater pressure distribution for 1 Day in Fig. 9.4c and d). This may be due to some localized phenomenon like excessive smearing of soil due to movement of the transducer to new location during the test. Figure 9.5 shows the porewater pressure distribution response in specimens subjected to combined application of vacuum and fill loads. It can be seen that the porewater pressure distribution is following the same pattern as in case of individual vacuum or fill load. This confirms that there is no inherent loss in vacuum intensity with depth, along the length of vertical drains, and more importantly, soil behavior under vacuum or a combined vacuum-fill preload can be interpretted in terms of existing consolidation theories. It is interesting to note that Rujiakiatkamjorn et al. (2007) proposed a linear reduction in vacuum intensity with depth while describing their numerical model for vacuum consolidation; however, they used a constant vacuum pressure distribution with depth while analyzing a case history of combined vacuum-fill preloading.

For top and bottom permeable boundaries in the field, Chai et al. (2005a and b) also propose a reduction in vacuum intensity with depth; however, for only permeable top and impermeable bottom, a constant vacuum intensity with depth is assumed. The model proposed by Chai et al. (2005a and b) is discussed in detail in Sections 9.4 and 9.6.

Field applications of vacuum preloading, which show that clay deposits thicker than 40m have been treated successfully using vacuum as a preload (Masse et al. 2001), do not support the idea of reduction in vacuum intensity with depth. The observed reductions in porewater pressure in soil as a function of depth suggest no fixed pattern for the development of vacuum intensity with depth. Analyses of field data reported in various case histories

suggest that consolidation at different depths may or may not progress under a uniform vacuum intensity in soil. It may be possible that consolidation progresses under a higher vacuum intensity at greater depths and a smaller vacuum intensity at shallower depths (similar to dissipation of excess porewater pressure in a multi layer system subjected to fill loading). Figures 9.6 and 9.7 show the observed reduction in porewater pressure (vacuum pressure) for two different case histories of vacuum preloading. Figure 9.6 shows that vacuum developed at different rate and to a different intensity at different depths. In Section I in Fig. 9.6, after 90 days, vacuum developed to a maximum of 55kPa and 85kPa at depths of 4m and 11m, respectively. Thus, during the preloading period (90 days), neither constant, nor a linearly decreasing vacuum intensity in the soil, with depth would be a reasonable assumption in this case. Yan and Chu (2005) reported a case history of combined vacuum and fill preloading (discussed in detail in Chapter 5), where the soil was first subjected to a vacuum preload for 40 days, and then fill load was added to it. The overall duration of vacuum-fill preloading was 180 days. Figure 9.7 presents the data on observed reductions of porewater pressure with depth at different times. Interestingly, a linear increase in vacuum intensity with depth can be observed up to a time when vacuum was acting alone, however toward the end of preloading operation, vacuum intensity is quite constant with depth.

The analysis of laboratory studies and actual case histories of vacuum preloading indicates that under ideal conditions, vacuum intensity in soil remains constant with depth and with time; however, it may develop to different intensities at different depths. Data from case histories also show that it is possible for vacuum to quickly develop to a higher value at great depth and to a lower value at shallow depth; therefore, the assumption of linear reduction in vacuum intensity with depth is not considered reasonable.

9.4 Settlements due to Vacuum Preloading

It was pointed out in the beginning of this chapter that there is a difference of opinion with regard to relative magnitude and rate of settlement induced by vacuum preload as compared to an equivalent fill preload. Field trials and laboratory studies are available that appear to support the contradicting arguments; therefore, it is important to critically examine the available literature to establish whether a vacuum preload results in a similar or different settlement response.

Figure 9.8 compares the settlement induced by vacuum preloading and an equivalent fill preload, during a study carried out to improve soft Bangkok clay (Woo et al. 1989). It can be seen from Fig 9.8a that the two loading methods yielded exactly the same settlement at the centre of the loaded area; however, the overall maximum settlement due to fill preloading is slightly higher than the overall maximum settlement induced by vacuum preloading. This minor difference can be disregarded as severe leakages in vacuum were observed during initial phase of vacuum application, which were reduced by use of plastic membrane (detailed analysis of case history is presented in Chapter 6). Ye et al. (1983) reported a field trial of vacuum consolidation where larger subsurface settlements were observed due to vacuum preloading as compared to those of an equivalent fill load. In this case, the loaded area was small (11m x 24m) and therefore, due to elastic stress distribution, the deeper layers in fill preloading section experienced less load and thus settled less as compared to vacuum preloading test section. Thus minor differences in observed settlement behavior may be attributed to site specific conditions instead of a fundamental difference in mechanism of consolidation. It is also important to note from Fig. 9.8a that (a) settlement induced by vacuum was more uniform than the equivalent fill preload, and (b) a peripheral area of 5 – 10m around the test section also experienced settlement as a result of vacuum preloading (Woo et al. 1989). Figure 9.8b shows settlement at different depths expressed in terms of surface settlements under respective loading conditions. It can be seen that irrespective of the type of load, consolidation progressed in a similar way.

Mohamedelhassan and Shang (2002) and Mahfouz et al. (2005) concluded from their respective laboratory studies that under similar loading conditions, both vacuum and an equivalent fill preload generate similar settlement profiles. Results of experimental study conducted by Mohamedelhassan (2002) on 70mm diameter and 25mm high, oedometer specimens, without provision of a central drain, are shown in Fig. 9.9. The study was conducted on reconstituted specimens, prepared at a water content of 100 to 150%. The specimens were placed in the consolidation ring in layers; each layer gently compacted with a thin rod to remove any air from the specimen. It is evident from the figure that, under similar loading conditions, both vacuum and equivalent fill preload generate a similar settlement response. It is also interesting to note that the combined application of vacuum and fill loads resulted in an increase in rate and magnitude of settlement. The results of this

laboratory study clearly show that the principal of superposition is valid and justifies use of available consolidation theories for designing the preloading projects involving vacuum as a preload. Thus, ILLICON which makes realistic assumptions on compressibility and permeability of the soft ground and on characteristics of vertical drains, and incorporates time-dependent loading, can be used effectively to predict the settlement response of soft soils under applied vacuum preload.

Chai et al. (2005a, b) relates the magnitude of settlement with the prevailing coefficient of lateral pressure, K, condition in the soil deposit. If the value of K is such that it inhibits the inward lateral movement, (i.e. $K=K_o$), then according to Chai et al. (2005a, b) the settlement induced by vacuum preload will be the same as that produced by fill preload. However, if inward lateral movements take place, then the magnitude of settlement with vacuum preloading will be less than that of an equivalent fill preload. Results of laboratory studies conducted by Chai et al. (2005b) are shown in Fig. 9.10. It can be seen from Fig. 9.10a that the settlement response of a normally consolidated sample with zero initial vertical stress ($\sigma'_v = 0$) subjected to the applied vacuum is less than the settlement of a specimen that was subjected to a vertical load of same magnitude as the vacuum. Figure 9.10c shows that a soil specimen initially consolidated to 80kPa, responded in a similar fashion to both the fill and vacuum loading. Figure 9.10b shows an intermediate condition between 9.10a and 9.10c, in which the soil specimen was preconsolidated to 40kPa and then subjected to a vacuum pressure of 80kPa; i.e., the settlement induced by vacuum pressure is less than the equivalent vertical load; however, the difference in magnitude of settlements is less than that of Fig. 9.10a. As there appears to be a systematic reduction in settlement with increasing preconsolidation pressure, it was concluded that the inward lateral displacements due to vacuum preload resulted in smaller vertical settlements. It was also reported that a gap developed between the soil sample and consolidation ring, for samples that were subjected to zero or smaller effective vertical stress. The formation of this gap was attributed to isotropic nature of vacuum loading; however, it must be realized that the laboratory study was conducted on conventional oedometer specimens, 60mm diameter and 20mm height, without any provisions of vertical drains. In the absence of vertical drains, the applied vacuum can only act as an equivalent vertical load applied on the surface, i.e., acting in one direction only and therefore the isotropic loading condition cannot be achieved.

According to the uniqueness of EOP e – log σ'_v concept (Mesri and Choi 1985, Mesri et al. 1995), the end of primary settlement for a given load should be same irrespective of the drainage boundary conditions. Therefore, after a given elapsed time, if less settlement is observed under vacuum preloading as compared to an equivalent vertical load, the specimen under vacuum could still be undergoing primary consolidation. Contrary to this, Fig. 9.10 shows that all the specimens, under vacuum load and under vertical load had completed their primary compression and also had undergone some secondary compression, indicating that specimens with smaller pre-vacuum consolidation pressure were subjected to smaller loads. It was shown in Section 9.3 that under identical conditions, the vertical distribution of vacuum pressure is same as the vertical distribution of a fill load, and therefore the induced settlements should also be similar under both types of loading conditions. It appears that for small pre-vacuum consolidation pressure, part of the vacuum was lost due to formation of gap between the ring and the soil specimen, thus causing a reduction in the effective stress generated by the application of vacuum. For softer soil specimen, the gap is expected to form quickly, thus incurring a greater loss on the applied vacuum and therefore, resulting in a less settlement. Thus, the differences in measured settlement for fill load and vacuum pressure for initial effective vertical stress of 0 and 40kPa in Figs. 9.10a and 9.10b result from the shortcomings of the laboratory oedometer test (formation of gap), and are therefore misleading in connection to the behavior expected in the field. Also these effects, if any, only occur at the boundaries of the area subjected to vacuum loading.

In the present study, the computer program ILLICON was used to evaluate the possibility of modeling applied vacuum load as an equivalent fill preload for predicting the settlement under a vacuum preload or a combined vacuum-fill preload. It is important to point out that for most case histories in the literature, data on time rate of ground settlement due to vacuum preloading, is reported from the time of application of vacuum; whereas, only the magnitude of settlement, observed prior to application of vacuum is reported. Moreover, the subsurface investigation is usually carried out much prior to actual preloading operation. For example, in Fig. 9.11 (STS/NGI 1992) significant settlements took place before the application of the main fill preload. These factors must be taken into account in settlement analyses and in comparison of predicted and observed settlements. Therefore, whenever it

was necessary, sufficient time was allowed in the ILLICON analysis for the soil to undergo the initial settlements resulting from the placement of surface drainage layer etc., observed before the first application of vacuum pressure. The results of surface settlements of three sections from two different case histories of vacuum and combined vacuum-fill preloading are shown in Fig. 9.12 (detailed analyses of case histories are presented in Chapters 4 and 5). It can be seen from Fig. 9.12 that (1) the applied vacuum can be modeled as an equivalent fill preload, (2) the principal of superposition can be used effectively for prediction of settlements under combined vacuum-fill preloading by replacing the applied vacuum with an equivalent fill load, and (3) there is no difference in soil behavior due to vacuum or fill preload. The apparent acceleration in settlements due to vacuum preload is primarily related to (1) the ability of vacuum to become fully effective relatively quickly as compared to equivalent fill preload, and (2) probable increase in permeability due to removal of air (Ye et al. 1983). Similarly, in some cases the differences in magnitude of settlements can be explained in terms of fluctuations of water table due to vacuum preloading. Ye et al. (1983) reported lowering of water table by 1m during vacuum preloading and as a consequence settlement due to vacuum preloading was more than the equivalent fill preload; on the other hand, the upward movement of ground water table would reduce the effective stresses and therefore, less settlements are expected.

9.5 Porewater Pressure Generation and Dissipation

Porewater pressure generation and dissipation with vacuum preloading is different from the conventional fill preloading. A fill preload generates positive porewater pressure within a soil mass; thus a gradual increase in effective stress is experienced with the dissipation of the excess porewater pressure. On the other hand a vacuum preload gradually generates negative porewater pressure which also results in a gradual increase in effective stress. Mohamedelhassan and Shang (2002) showed that, similar to settlement, excess porewater pressure in a soil mass, subjected to a vacuum or a combined vacuum-fill preload, can also be evaluated using the principal of superposition as shown in Fig. 9.13. However, as the vacuum actually results in negative porewater pressure, care must be exercised to properly define and interpret the porewater pressure at any given time and at any depth. Therefore, it is imperative that when vacuum is treated as a positive fill load, the positive porewater pressure response generated by any settlement analysis is converted to the actual

porewater pressure in the field which may be positive or negative under the action of vacuum or a combined vacuum-fill preload. While analyzing the case histories using the computer program ILLICON, it was found convenient to work with an excess porewater pressure, *u''*, the initial value of which for a vacuum plus fill preload is:

$$u_i'' = |u_{sm}| + \Delta\sigma_v \tag{9.1}$$

where, u_{sm} is the maximum vacuum-induced decrease in porewater pressure and the $\Delta\sigma_v$ is the embankment-induced increase in total vertical stress. The actual porewater pressure at any depth and any time is calculated by:

$$u = u_o - |u_{sm}| + u'' \tag{9.2}$$

where u_o is the initial in-situ (preconstruction, e.g. hydrostatic) porewater pressure. The value of *u''* at a given depth and time is calculated using ILLICON.

The excess porewater pressure, *u'* at any time during vacuum consolidation can be defined as:

$$u' = -|u_{sm}| + u'' \tag{9.3}$$

Consider a soft clay deposit with thickness H, having a permeable top and an impermeable bottom subjected to a vacuum pressure, -u_{sm} at the surface. Then using the Terzaghi theory of consolidation together with an initial excess porewater pressure equal to a positive u_{sm}, applied at the surface of clay deposit, u'' at any time and at any depth z, can be computed by:

$$u'' = \sum_{m=0}^{\infty} \frac{2u_{sm}}{M} Sin\left(\frac{Mz}{H}\right) \exp(-M^2 T) \tag{9.4}$$

where $$M = \frac{\pi(2m+1)}{2} \qquad and \qquad T = \frac{c_v t}{H^2}$$

Substituting Eq. 9.4 in Eq. 9.3, we get

$$u' = -u_{sm} + \sum_{m=0}^{\infty} \frac{2u_{sm}}{M} Sin\left(\frac{Mz}{H}\right) \exp(-M^2 T)$$

or $$u' = -u_{sm}\left[1 - \sum_{m=0}^{\infty} \frac{2u_{sm}}{M} Sin\left(\frac{Mz}{H}\right) \exp(-M^2 T)\right] \tag{9.5}$$

Using Eq. 9.5 together with a u_{sm} = 80kPa, c_v = 1m^2/yr and a 4m thick compressible deposit, porewater pressure corresponding to different degrees of consolidation, at different depths, are computed as shown in Fig. 9.14a. The excess porewater pressure distribution due to an equivalent fill preload (u') is also shown in Fig. 9.14b. It can be seen that the porewater pressure isochrones under both type of loading are similar, but in opposite sense, i.e., the excess porewater pressure due to a vacuum preload is initially zero, and gradually approaches the applied vacuum; whereas in case of a fill load, the excess porewater pressure instantly reaches the maximum value (applied load) and gradually dissipates to zero with time.

Figure 9.15a shows the idealized distribution of excess porewater pressure (u'') at the mid depth of a 10m thick, normally consolidated soil deposit, freely draining from top only, subjected to a combined vacuum-fill preload of 100kPa (20kPa fill and 80kPa vacuum), with fully penetrating vertical drains spaced at 1m in a square pattern. Settlement analysis using computer program ILLICON was carried out assuming the applied vacuum as a fill load. Using Eqs. 9.2, 9.3 and Fig 9.15a, the value of excess porewater pressure (u') and total porewater pressure (u) during vacuum preloading, at any time and at any depth can be estimated. For the mid depth, computed values of u' and u with radial distance from the drain at different times are shown in Figs. 9.15b and 9.15c. For example, after 10 days, at a radial distance of 0.3m from centre of PVD, u'' = 83kPa. Therefore, assuming u_o = 50kPa and using Eqs. 9.2 and 9.3,

$$u = 50 - 80 + 83 = 53\text{kPa},$$

and

$$u' = -80 + 83 = 3\text{kPa}$$

Figure 9.16 presents the results of laboratory study (Rujiakiatkamjorn 2005) in which porewater pressures was measured at different radial distance from the PVD as described in Section 9.3. It is important to note that full intensity of applied vacuum was assumed to develop within the PVD at zero time. Unfortunately, porewater pressures were not measured at the maximum radial distance (225mm in this case); however the trend shown is generally the same as in Fig. 9.15. For VP1 and VP2, which were loaded by vacuum only, the porewater pressure approached the applied vacuum pressure; whereas, for combined loading tests SV1 and SV2, the porewater pressure started positive and approached the applied vacuum.

Hence, the total porewater pressure at any time and at any depth, during a vacuum or vacuum-fill preloading operation can be computed by using the following two steps:

- Compute excess porewater pressure, u'' at the desired time and depth by assuming the applied load given by Eq. 9.1.
- Compute actual porewater pressure or excess porewater pressure under vacuum or vacuum-fill preloading, respectively, using Eq. 9.2. or Eq. 9.3.

Figure 9.17 compares the porewater pressure, observed during treatment of foundation soil for a storage yard in China (Yan and Chu 2005), and the predicted response obtained using ILLICON and Eq. 9.2. It can be seen from the figure that the results of proposed method for porewater pressure interpretation are in good agreement with the observed porewater pressures at different times and at different depths.

9.6 Lateral Displacements

Contrary to the fill preloading, which causes an outward movement (away from under the loaded area) of the soil mass, the vacuum induced consolidation generates inward lateral movements (toward the loaded area). The inward movement of the ground surface can cause tension cracks in the surrounding ground, and may therefore be detrimental to the structures located adjacent to the treatment area. For land reclamation projects, however, these cracks do not pose a serious problem as these projects are mostly located away from urban centers.

9.6.1 Area of Influence

It is of interest to know the extent of area, surrounding the treatment zone, which is affected due to vacuum preloading. Figure 9.18 presents the lateral displacements measured at the ground surface during a test study carried out in Japan by Hazama Corporation (Dam et al. 2007). The ground comprised of 8m thick reclaimed layer (6m silty clay and 2m sand) underlain by a 30m thick layer of Ariake clay (a soft clay deposit in Japan). The study was carried out on an area of 20x20m and the PVDs were penetrated to a depth of 27m. Consolidation progressed under an effective vacuum pressure of 50kPa (Dam et al. 2007); however, the total settlements and duration of preloading are not reported. It can be noted from the figure that the lateral displacements were affected in a radius of 30 to 40m; however, the maximum displacements were observed at a distance of 10m from the edge of treated area. Moreover, with reference to the edge of the treated area, greater inward

displacements can be observed outside the treatment area as compared to the inside. For example, the recorded inward displacement at the ground surface, 3m outside the treated area is 18cm, whereas, it is only 6cm at a similar distance from the edge inside the treated area. It is also important to realize that the presence of a 2m thick sand layer inclusion can result in transmitting the vacuum in horizontal direction to a significant distance. It is probably due to the presence of sand layer that an effective vacuum pressure of 80kPa could not be maintained. The leakage of vacuum through a permeable seam may develop some under-pressure outside the treatment area and cause settlements. Gao (2004) also reported significant ground settlements (30 to 40cm) at a peripheral width of 50m around the treatment area while conducting a pilot study for improvement of high permeability ($k_v = 10^{-3}$ to 10^{-5}cm/s) soils using vacuum consolidation. A total of 67.4cm of settlement was affected under a vacuum pressure of 80kPa within the treatment area in 83days. Considering the relative magnitudes of settlements within and outside the treatment area, it is likely that vacuum was transmitted outside the treatment area, created an under-pressure and affected consolidation. It is also important to note that in both cases, where vacuum preloading affected adjacent ground to a large distance (40 to 50m), high permeability soils were present. Qiu et al. (2007) reported measured reductions of 50kPa, 47kPa, and 43kPa respectively, at 1m inside, 2m outside and 5m outside the treatment area, in a sandy-silt layer located at a depth of 9.6m to 11.6m from the ground surface. Chai et al. (2006) also reported significant reductions in porewater pressures outside the treatment area (see Fig. 7.18). Interestingly, a 0.50m thick sandy silt layer was present at a depth of 4 to 5m below the ground surface through which leakage could occur. This shows that the applied vacuum can propagate to a significant distance outside the treatment area in the presence of a high permeability layer. Thus in these cases, the lateral deformations may not be entirely due to the vacuum preloading of treated area.

In cases, where any leakage in the vacuum intensity is not likely, the extent of surrounding area, affected by vacuum consolidation is not specifically reported. For example, Chu et al. (2000) reported formation of tension cracks 10m away from the edge of vacuum treatted area (20000/30000m^2). Mahfouz et al. (2007) and Vinh and Imai (2001) reported cracks appearing at some distance away from the edge of vacuum treatment area, however,

the exact distance from edge was not reported. In all the above cases, the average vacuum pressure of 80kPa was used during the preloading operation.

9.6.2 Review of Available Models to Predict Lateral Displacements

When a fill load is applied on the ground surface, it generates shear stresses within the soil mass, and as a result the soil tends to deform outward. Therefore, in certain situations, the load is applied in stages to allow consolidation of the soil and to avoid excessive deformations or a bearing capacity failure. On the other hand, a vacuum preload is applied not only to the ground surface but also applied directly to the deeper ground through the vertical drains and therefore, it induces an isotropic load within the soil mass. Due to isotropic loading condition, no shear stresses are generated within the soil mass and therefore, there is no risk of failure. Experience has shown that maximum lateral displacements occur, respectively, on the ground surface or at some depth below the ground surface, due to vacuum or fill preloading.

Chai et al. (2005a and b) and Dam et al. (2007) have tried to relate the lateral ground movements observed during vacuum preloading to the lateral earth pressure. A brief summary of their studies is as following:

9.6.2.1 Chai et al. (2005a and b)

Chai et al. (2005a and b) propose an elaborate procedure involving an earth pressure coefficient defined as:

$$K = \frac{\Delta\sigma_{vac}}{\Delta\sigma_{vac} + \sigma'_{vo}} \tag{9.6}$$

and conclude that for $K \leq K_o$ there will be no inward lateral displacement for vacuum preloading. According to Eq. 9.6, K is expected to increase with depth implying a decrease in lateral displacement with depth.

Figure 9.19 shows the result of application of the model proposed by Chai et al. (2005) to two case histories of vacuum preloading. In both cases for constant vacuum intensity and for both values of β (which is used to estimate value of K), the surface lateral displacements are grossly over-predicted. It is interesting to note that, for the oil storage station, both the values of β, under-predict the field observations for Section II from elevation of +5.0 to -5.0m, however; there is a reasonable agreement with field observation for Section I. Also, the lateral displacements below elevation of -5.0m agree well assuming

β=0.67 for Section II and β=1.0 for Section I. It is important to point out that both the sections had similar soil properties and were subjected to similar loading (Chu et al. 2000) and therefore, a similar response is expected, however; the field response is quite different in both cases which suggests contribution of factors, other than lateral earth pressure alone. Similar observations can be made on the predictions of lateral displacement for the Yaoqiang airport case history. It is important to point out that Tang and Shang (2000) reported an applied vacuum intensity of 80kPa, however, Fig 9.19b shows that the maximum vacuum intensity was taken as 65kPa and further reduced to 52kPa with depth (without any justification). The average drawdown of porewater pressure reported by Tang and Shang (2000) is 50kPa near the surface increasing linearly to 55kPa at a depth of 14m for the entire treatment area. For pilot test area, Fig. 13 of Tang and Shang (2000) show 65kPa, 42kPa, 36kPa and 62kPa, respectively, at depths of 2m, 8m, 10m, and 14m. Therefore, the assumption on vacuum pressure made by Chai et al. (2005b) is not supported by the field evidence. Moreover, a 120cm thick and 4.5m deep clay slurry wall was constructed around the treatment area to prevent leakage of vacuum (Tang and Shang, 2000), which is likely to have some restraining effects on the lateral soil movements. The effect of slurry wall on lateral ground movement has not been discussed in the solution.

It appears from the analysis of case histories that lateral displacements are not entirely dependent on the lateral earth pressure in the soil mass, and therefore, cannot be fully explained in terms of active or at-rest earth pressure conditions.

9.6.2.2 Dam et al. (2007)

Dam et al. (2007) related lateral displacements to earth pressure in an active rupture zone and extension zone outside the treatment boundary (Figs. 9.20 and 9.21). They compared predictions based on their approach to field measurements of lateral displacements for soft ground subjected to vacuum consolidation. The most complete observation of surface lateral displacement was available for Hazama Case A.

Hazama Corp. conducted a field project starting in 1990's to investigate effectiveness of vacuum treatment (Mutsomoto et al. 1998; Dam et al. 2007). An embankment over an area of 20m x 20m was constructed with 0.3m sand mat, through which 27m long vertical drains were installed. The soft ground profile is shown in Fig. 9.18. Measurements during vacuum consolidation indicated an applied vacuum pressure of 50kPa.

Surface and subsurface lateral displacements at various distances from embankment edge were measured. The surface lateral displacements are shown in Fig. 9.18, together with a prediction based on Dam et al. (2007) approach. It can be seen from Fig. 9.18 that the maximum displacements are predicted near the boundary of treatment area, whereas the measured maximum displacements were 10m away from the boundary. Also the magnitude of measured lateral displacement is almost half of the predicted magnitude. Moreover, the application of proposed approach to other case histories of vacuum consolidation (Table 2 of Dam et al. 2007) suggests no direct relation between the width of treatment area and the extension zone. For example, the extension zones are 16.7m, 32.6m and 46.2m, respectively, for loaded areas of 54m, 200m, and 20m. Therefore, the approach proposed by Dam et al. (2007) is not considered reasonable for predicting the lateral displacements.

9.6.3 Proposed Approach to Predict Lateral Displacements due to Vacuum Preloading

It is interesting to note that the interpretation of horizontal displacements proposed by both Chai et al. (2005a and b) and Dam et al. (2007) involve parameters that are related to the consolidation behavior of soil. Chung (2009) also consider compression index (along with thickness of soft layer and intensity of applied vacuum) to be the most important factor affecting lateral displacements. The Asoaka method, which is a graphical procedure used to predict end of primary settlement based on field observations (Mesri and Huvaj 2009), is applied to lateral ground displacement data observed during three projects where vacuum was used as a preload, as shown in Fig. 9.22. It can be seen that the Asoaka method is equally applicable for predicting lateral ground movements. Therefore, it is reasonable to assume that lateral displacement behavior due to vacuum preloading can be explained and predicted in terms of consolidation behavior of soft soils. It may be convenient to explain the lateral displacements with depth in terms of a horizontal preconsolidation pressure, σ'_{ph}, which may be assumed to be related to σ'_p in a similar way as the effective horizontal stress is related to effective vertical stress (Mesri and Castro, 1987)

$$\sigma'_{ph} = K_o \sigma'_p \tag{9.7}$$

Equation 9.7 explains why larger lateral displacements are observed near the ground surface as compared to those at the greater depth. Although vacuum is applied with same intensity all along the depth of the compressible layer, in the absence of desiccated

crust, the value of σ'_{ph} increases with depth, thus increasing the recompression range. Therefore, the $\sigma'_{hf} - \sigma'_{ph}$, under which compression takes place at beyond σ'_{ph}, reduces with depth, and the lateral displacements also reduce with depth. For example, consider a 10m thick, uniform clay deposit with average value of submerged unit weight = 6kN/m^3, K_o = 0.5 and OCR = 1.2, treated with a vacuum pressure of 80kPa. The initial effective stress in horizontal direction for top 2m sublayer is 3kPa and that for the bottom 2m sublayer of the deposit is 27kPa, and the corresponding σ'_{ph} is 3.6kPa and 32.4kPa, respectively. Hence the lateral displacements are affected under a $\sigma'_{hf} - \sigma'_{ph}$ of 76.4kPa and 47.6kPa, respectively, in the top and bottom sublayers of the deposit. For the assumed case, lateral displacements were computed at the mid depth of 2m thick sublayers, by substituting vertical stresses with horizontal stresses in Eq. 16.8 of Terzaghi et al. (1996) as shown in Fig. 9.23. A compression ratio of 0.33 and an effective vacuum pressure of (a) 80kPa, (b) 60kPa, and (c) 40kPa, up to 2m outside the edge of treatment area, were assumed for the calculations. It is clear from the Fig. 9.23 that the lateral displacements will reduce with depth even for a constant vacuum pressure distribution with depth. As uniform soil deposits are rarely encountered in the field, the distribution of lateral displacements may vary with depth (based on preconsolidation pressure, compressibility, permeability of sublayers, and K_o etc). Moreover, non-uniform distribution of vacuum pressure in soil, and settlements outside the treatment area along with aforementioned factors interact in a complex way to influence the magnitude of lateral displacements at a given time and at a given depth. Therefore, it is considered more appropriate to develop an empirical procedure based on the observed field behavior to predict lateral displacements due to vacuum preloading.

Data on lateral displacements and vertical settlements, obtained from 10 different case histories, are shown in Figures 9.24 to 9.28. Figure 9.24 shows the lateral displacement at ground surface plotted against ground surface settlement, at different times. It can be seen that the lateral displacements, at any time, fall within a range of 20% to 50% of the surface settlements with an average value of around 36%. Thus the lateral displacement, at any time during the vacuum preloading operation, may be predicted with a reasonable accuracy with reference to the surface settlement at that time. For 2m thick sublayers, mid-sublayer lateral displacement are plotted against sublayer settlement as shown in Fig. 9.25. It can be seen that for the top two, 2m thick sublayers, the mid-sublayer lateral displacements are generally

greater than sublayer settlements. With increasing depth however; lateral displacements decrease in comparison to sublayer settlements and beyond 6m depth, the sublayer lateral displacements are significantly smaller than sublayer settlements. Figure 9.26 shows the lateral displacements at different depth normalized with respect to lateral displacement at the ground surface for ten different case histories of vacuum consolidation. In all these case histories, either vacuum was used alone or data are taken up to a point, where vacuum was acting alone as a preload. Figures 9.25 and 9.26 show a similarity with distribution of lateral displacements suggested in Fig. 9.23, which is based on the assumptions that the lateral displacements due to vacuum preloading are due to consolidation movements. This reinforces the idea that lateral displacements due to vacuum preloading are primarily due to consolidation movements, however, these are influenced by other factors including stratification, non-uniform vacuum pressure distribution and K_o conditions, etc.

Table 9.1 shows data on maximum lateral displacements and depth where zero or negligible lateral displacement was observed; along with the penetration depth of PVDs and size of treatment area. It can be seen that there is no direct relation between the magnitude of lateral displacements, size of treatment area and penetration depth of PVDs. For a given L/H_o ratio, (where H_o is the initial thickness of compressible layer/depth of penetration of vertical drains) there is a significant difference in magnitude of lateral displacements at the surface of treatment area (e.g. Storage yard, sections I and II). Similarly, for similar magnitude of lateral displacements, there is a difference in L/H_o ratio (e.g. Oil storage station sec I-N and section II). It can also be seen from Table 9.1 that in most cases, the lateral displacements become zero (or close to zero) at a depth, significantly less than the penetration depth of PVDs (60% to 80% from Table 9.1). Moreover, there is no direct relation between the observed lateral displacements, depth of penetration of PVDs, and width or half width of treatment area. Therefore, it is not reasonable to relate lateral displacements to one or two major factors, especially with width or half width of the treatment area.

Figure 9.27 presents the data on lateral displacements and observed reductions in porewater pressure with depth at various times for sections I and II of a case history of vacuum preloading (improvement of subsoil for road leading to container terminal; discussed in detail in Chapter 4). It can be seen from Fig. 9.27 that the lateral displacements in Section II, where the applied vacuum pressure developed gradually to maximum and remained more

or less uniform with depth, are significantly greater than lateral displacements in Section I, where vacuum gradually developed to maximum and then reduced to around 60kPa near the surface and below 12m depth. Therefore, vacuum pressure can be regarded as a key factor affecting the lateral displacements, along with other soil parameters such as preconsolidation pressure, compressibility and permeability etc.

Maximum lateral displacements at different depths (from different case histories shown in Fig. 9.26) normalized with respect to surface lateral displacements are shown in Figs. 9.28a and 9.28b. Figure 9.28a shows the normalized lateral displacements with depth, whereas Fig. 9.28b shows the normalized lateral displacement with normalized depth (depth normalized with respect to thickness of compressible layer, H_o). The data points which lie outside the maximum curve on Fig. 9.28a (shown with open circles) appears to be unusual, however, it is pointed out that a 28m thick soil deposit including 17m thick reclaimed layer, characterized with high pretreatment excess porewater pressures (Chai et al. 2008) was improved using vacuum preloading. Normalizing the depth with respect to the treatment depth (Fig. 9.28b), however, shows that these data do not represent an unusual soil behavior. As expected, the trend of reduction in lateral displacement with depth, shown in Fig. 9.28 is also similar to Fig. 9.23.

An empirical procedure is suggested to predict the lateral displacement at any time and at any depth during the vacuum preloading operation as under:

- Compute the magnitude and time rate of surface settlement due to vacuum preloading.
- Compute the lateral displacement at the ground surface, at the desired time using $\delta_{hs}/S_s = 0.36$ (Fig. 9.24). The average value may be used for design; however upper ($\delta_{hs}/S_s = 0.50$) and lower ($\delta_{hs}/S_s = 0.20$) bound values may also be estimated to completely define the anticipated displacements at the ground surface, especially during back analysis of a case history.
- Using Fig. 9.28b, compute the lateral displacement at different times at the desired depth. In this case also average upper and lower bound values may be used.

9.6.4 Application of Proposed Method to Case Histories

9.6.4.1 Zhuhai Power Station - China

Vacuum preloading together with fill load was used to improve subsurface conditions for construction of a power station in Zhuhai, China. The improvement area (110,000m^2) subsoil consisted of 3m of hydraulic fill underlain by 19m of soft clay deposit. A brief account of the case history is given below.

The ground surface was pretreated with two layers of bamboo-splint mat, 50cm thick layer of hill cut and a 40cm thick layer of medium-coarse sand (Yixiong, 1996b). The sand layer also acted as the working platform through which PVDs were installed to a depth of 20m, in a square grid of 1.0m spacing. Vacuum pumping started on 15 December, 1994, reached 80kPa in 14 days, and continued for 149 days. Seventy five days after application of the vacuum, a fill load of 40kPa was added during about 8 days.

The observed ground surface settlement near the center of the treated area, due to vacuum preloading only, at 15, 35 and 73 days, respectively, were 0.40m, 0.70m and 0.81m. These settlements were used to estimate the lateral displacements at the ground surface and at different depths using Figs. 9.24 and 9.28b as shown in Fig. 9.29. The average curves from Figs. 9.24 ($\delta_{hs}/S_s = 0.36$) and 9.28b were used respectively, to predict surface and subsurface lateral displacements at different times. There is generally a good agreement between the observed and predicted lateral displacements for 35 and 73 days, however; for 15 days, the lateral displacements are under-predicted near the ground surface. Using upper bound curve on Fig 9.24 ($\delta_{hs}/S_s = 0.50$) to predict the surface lateral displacements at 15 days show a good agreement between the prediction and observation. Hence, the lateral displacements at different times and at different depths can be predicted with reasonable accuracy.

9.6.4.2 Yaoqiang Airport - China

An area of 2600x60m, for a runway site at Yaoqiang airport, China, was required to be improved. The surface soil was 3.0m thick silty sand underlain by layers of silty clay (2m), silt (2.5m) and soft clay (4.0m). It was decided to use vacuum preloading to improve the soft soil layers. To avoid loss of vacuum through the top layer, a 120cm thick and 4.5m deep clay slurry wall was constructed around the treatment area, using deep soil mixing (Tang and Shang, 2000).

PVDs were installed to a depth of 12m, in a square grid of 1.3m spacing. Vacuum pumping started on July 1, 1989, reached 80kPa on July 14, 1989 and remained stable for the remaining duration of the treatment (Tang and Shang, 2000). The observed settlement due to vacuum preloading in the pilot test area (60x40m) was 32.6cm, which was used to calculate the surface lateral displacement using the average curve (δ_{hs}/S_s = 0.36) from Fig. 9.24. The average and lower-bound curves from Fig. 9.28b were used to predict the lateral displacements as shown in Fig. 9.30. It can be seen from Fig. 9.30 that the average curve over-predicts the lateral displacements; however, there is a very good agreement between the observed and the predicted lateral displacements at all depths for minimum curve. Lateral displacements, normalized with respect to depth, predicted by Chai et al. (2005b) for the same case history are also shown on Fig. 9.30. It can be seen that despite Chai et al. (2005b) accounting for a reduction in vacuum intensity to 65kPa at the surface (80kPa vacuum was applied and maintained during treatment) and further reducing it to 52kPa at 16m depth (PVDs were installed to a depth of 12m only), and using a strain reduction factor, β=0.67, the lateral displacements are over-predicted near the ground surface. Thus the approach proposed in the present study is considered more suitable for prediction of lateral displacements in the field.

9.7 Performance of Vertical Drains during Vacuum Preloading

Vertical drains, an essential component of any vacuum consolidation system, are used to transmit vacuum to the compressible layer and to convey water out of the soil. Unfortunately, the performance of vertical drains under vacuum load has not been studied extensively; it is rather assumed that vertical drains perform without any well resistance when used together with vacuum preloading. It is probably due to this reason that most engineers and researchers either do not report the discharge capacity of vertical drains (Chu et al. 2000; Masse et al. 2001; Yan and Chu, 2003, and 2005; etc.), or associate a discharge capacity, high enough such that drains are expected to perform without any significant well resistance (Yixiong 1996b; Bergado et al. 1998; Indraratna et al. 2004; Chai et al. 2006; Rujiakiatkamjorn et al. 2007; etc.). Most of the laboratory studies carried out to study soil behavior under vacuum preloading were conducted on conventional oedometer size specimens without the use of vertical drains (Mohamedelhassan 2002; Chai et al. 2005a, b and 2009; Mahfouz et al. 2005; Chung 2009). The study carried out by Bamunawita (2004)

and Rujiakiatkamjorn (2005), however, used a central PVD as discussed in Sections 9.3 and 9.5. Factors like, increase in confining/lateral pressure, bending of drain, clogging of filter/core of PVD, reduction in horizontal permeability due to consolidation and alteration in filter fabric due to chemical action, are equally applicable to vacuum preloading as in fill preloading. Additionally, the direct exposure of a PVD to vacuum pressure may result in partial collapse of the PVD, thereby reducing its cross-sectional area. Hence, it is important to critically examine the performance of vertical drains under vacuum preloading.

Mesri and Lo (1991) introduced a discharge factor, D, defined as:

$$D = \frac{q_w}{k_h * l_m^2} \tag{9.8}$$

where q_w is the discharge capacity of vertical drain, k_h is the horizontal permeability of the soil deposit and l_m is the length water has to travel within the drain. They also suggested that for a discharge factor of 5, the drains are expected to perform with negligible well resistance. Thus the minimum discharge capacity, $q_{w(min)}$ required to perform without well resistance can be estimated by:

$$q_{w(\min)} = 5 * k_h * l_m^2 \tag{9.9}$$

Table 9.2 shows the case histories which were analyzed using the computer program ILLICON. The minimum discharge capacity was estimated using Eq. 9.9 in cases involving Bangkok clay. In other cases, averaging horizontal permeability to obtain k_h was not considered reasonable due to significant variation in soil properties, therefore, ILLICON analysis was used to estimate the $q_{w(min)}$. It is expected that increase in discharge capacity of vertical drains will result in increasing the rate of settlement up to a point where drains starts to perform without any well resistance. Any increase in discharge capacity beyond this point will not increase the rate of settlement as shown in Fig. 9.31. Figure 9.32 compares the mobilized discharge capacities, $q_{w(mob)}$, with $q_{w(min)}$ for different case histories listed in Table 9.2. It can be seen from Fig. 9.32 and Table 9.2 that the vertical drains, irrespective of their type, generally performed with significant well resistance. It is also important to note that PVDs used for improvement of soft Bangkok clay performed with same efficiency under fill and combined fill vacuum preloading; however, the CPVDs, which are individually connected with the vacuum pump, performed with higher well resistance in the same soil

conditions. It is therefore unreasonable to assume vertical drains to be draining freely under vacuum preloading.

9.8 Increase in Shear Strength due to Vacuum Preloading

One of the purposes of preloading is to increase the shear strength of soft soil deposits. Most engineers and researchers (Shang et al. 1998; Chu et al. 2000; Tang and Shang 2000; Yan and Chu 2003 & 2005; etc.) have reported a significant increase in undrained shear strength at the end of vacuum preloading operation; however, limited attempts have been made to explain the influence of vacuum preloading on the undrained shear strength of soil. The undrained shear strength after vacuum preloading is commonly measured by field vane test; however, laboratory tests and CPTs have also been carried out to evaluate the undrained shear strength before and after treatment.

Dam et al. (2007) suggests that the increase in shear strength due to vacuum preloading is more significant as compared to that by an equivalent fill preload, especially at shallow depths. According to Dam et al (2007) for a soil deposit with $K_o = 0.50$, the increase in shear strength near the ground surface due to vacuum preloading can be 1.5 times more than that by an equivalent fill preload. Qian et al. (1992) suggests that the increase in undrained shear strength can be estimated by using the relation between undrained shear strength and overconsolidation ratio; however, their proposed approach was not explained in detail.

Leong et al. (2000) conducted a laboratory study to compare the effects of vacuum and fill preloading on the undrained shear strength of undisturbed soil specimens from Kallang marine clay formation in Singapore. The oedometer was used for fill preloading, whereas a pressure plate apparatus was used to simulate vacuum preloading. At different consolidation pressures or assumed pressure plate vacuum, the specimens were taken out and undrained shear strength was measured using a laboratory miniature vane device. Assuming a possible desaturation of soil due to vacuum preloading, it was concluded by the authors that the shear strength increase due to fill preloading is more significant than an equivalent vacuum preloading. However, it should be realized that; (1) the assumption of soil getting unsaturated during vacuum preloading is neither supported by field evidence nor by other laboratory studies, (2) the mechanism of generating negative porewater pressure in a pressure plate apparatus is different from the application of vacuum to a saturated soil either in the

laboratory or in the field. In the field, the negative porewater pressure is applied through the drainage blanket and vertical drains and it reaches the entire depth of treatment. The pressure plate apparatus is not a suitable apparatus to simulate vacuum preloading, and (3) the successful applications of vacuum preloading in the field (Ye et al. 1983; Choa 1989, Qian et al. 1992) referenced by the Leng et al. (2000). show an increase in undrained shear strength comparable to that induced by fill preloading, which is not explained by the authors. Therefore, the conclusion of Leong et al. (2000) in connection to comparison of increase in shear strength produced by fill preloading and vacuum preloading is not considered to be reasonable.

Mahfouz et al. (2005) carried out a laboratory study to investigate the characteristics of vacuum consolidation using a triaxial device. The study was conducted on 100mm diameter, 200mm high, undisturbed specimens from a soft soil deposit of Wenzhou, China. The undisturbed specimens were obtained from a depth of 9 to 11m, by means of a 100mm diameter, thin tube sampler with overcoring device. The three specimens tested, were subjected to (1) a vacuum pressure of 80kPa, (2) a fill of 80kPa, and (3) 80kPa of combined vacuum-fill load (40+40). Unconfined compressive strength of the specimens subjected to vacuum and fill preloads increased respectively, from 20.1kPa and 23.2kPa to 39.2kPa and 47.2kPa. The increase in unconfined compressive strength due to vacuum and fill preloading was almost identical (1.95 times for vacuum and 2.03 times for fill load). However, the specimen that was subjected to a combined vacuum-fill loading, displayed a greater increase in unconfined compressive strength (2.54 times) as compared to the other two specimens. Therefore, Mahfouz et al. (2005) concluded that vacuum and fill loads influence the shear strength in a similar way; however, a combination of vacuum and fill loading is likely to have more beneficial effects on engineering properties of soil being treated. It is important to note that the 100mm diameter, undisturbed specimens used in the study, were obtained from a thin wall sampler of same diameter, i.e., samples were only trimmed to the required height and the diameter was kept constant. As there is a likelihood of increased degree of disturbance along the length of sampling tube from top to bottom, due to smearing/remolding of soil at the soil-sampler interface, it is possible that the specimens trimmed (to a height of 200mm) from different sections of the sampling tube likely had different degrees of disturbance and therefore, the differences in the test results is expected. Moreover, the

undisturbed specimens, which were obtained from a depth of 9 to 11m (sampling depth of individual specimens not reported) are likely to have different initial effective vertical stress (54kPa and 66kPa, respectively, for 9 and 11m) and consequently, different preconsolidation pressure for a given overconsolidation ratio. The greater increase in shear strength due to a combined vacuum-fill load may also be due to different initial conditions of the specimen being tested. It can be seen from the porewater pressure dissipation curves (Fig. 9.33) that the porewater pressure dissipation is quite similar for specimens loaded with vacuum and fill loads. However, for the combined vacuum-fill load, the dissipation curve is significantly different, indicating a difference in the initial condition of the specimens. As the specimens subjected to vacuum and fill loading responded in a similar way, it is not reasonable to expect a different response from a specimen subjected to combined vacuum-fill load. Instead, the increase in undrained shear strength is independent of the type of load and the differences in test results may be attributed to different initial conditions of the specimens.

Although the increase in undrained shear strength near the ground surface is more significant in few of the reported cases of vacuum preloading (Yixiong 1996b; Shang et al. 1998; Dam et al. 2007 etc), in many cases, a more significant increase in shear strength was observed in deeper layers as compared to the surface layers. It was shown in Chapters 4 and 5 that maximum increase in the shear strength ratio was observed at different depths in different sections of the improvement area. Tang and Shang (2000) and Shinsha et al. (1991) also reported cases of vacuum preloading where the shear strength increase was more significant at depth as compared to near surface. Figure 9.34 shows the shear strength of waste slurry improved using vacuum preloading with horizontal drains (Shinsha et al. 1991). It can be seen from Fig. 9.34 that there is a more significant increase in shear strength at depth as compared to increase near the ground surface. Therefore, the increase in shear strength is not entirely dependent upon the depth; instead it is more reasonable to relate gain in shear strength to the soil parameters such as initial strength, initial effective stress and preconsolidation pressure.

Before analyzing the shear strength data due to vacuum or a combined vacuum-fill load, it is important to understand the mechanism of shear strength increase due to fill preload only. It is well known that for soft soil deposits, the ratio of vane shear strength to

preconsolidation pressure [$s_{uo}(FV)/\sigma'_p$] remains constant in the compression range; i.e., for $(\sigma'_{vo} + \Delta\sigma_v) \geq \sigma'_p$ (Terzaghi et al. 1996):

$$\frac{s_{uo}(FV)}{\sigma'_p} = \frac{s_u(FV)}{\sigma'_{vc}} \tag{9.10}$$

where, $s_{uo}(FV)$ is the initial vane shear strength, $s_u(FV)$ is the vane field shear strength after preloading, σ'_p is the preconsolidation pressure, and σ'_{vc} is the consolidation pressure. Equation 9.10 can be rewritten as:

$$\frac{s_u(FV)}{s_{uo}(FV)} = \frac{s_{uo}(FV)}{\sigma'_p}\frac{1}{s_{uo}(FV)}(\sigma'_{vo} + \Delta\sigma'_v) \tag{9.11a}$$

or $$s_u(FV) = \frac{s_{uo}(FV)}{\sigma'_p}(\sigma'_{vo} + \Delta\sigma'_v) \tag{9.11b}$$

Equation 9.11 shows that $s_u(FV)/s_{uo}(FV)$ is a function of $s_{uo}(FV)/\sigma'_p$, σ'_{vo}, $\Delta\sigma'_v$ and that the shear strength after preloading can be estimated by using the ratio $s_{uo}(FV)/\sigma'_p$ and consolidation pressure.

A parametric study was carried out by assuming a soil deposit with (1) σ'_p/σ'_{vo} values of 1.0, 1.2, 1.4, and 1.6, (2) $s_{uo}(FV)/\sigma'_p$ values of 0.20, 0.25 and 0.30, (3) fill loads of 20, 40, 60, 80, and 160kPa, constant with depth and (4) σ'_{vo} between 5 to 100kPa. For a given value of σ'_p/σ'_{vo}, σ'_{vo} and $\Delta\sigma'_v$, the $s_{uo}(FV)$ and $s_u(FV)$ were calculated using the $s_{uo}(FV)/\sigma'_p$ ratio. Sample calculations for $s_{uo}(FV)/\sigma'_p$=0.3 and $\Delta\sigma'_v$ = 80kPa are shown in Table 9.3. The ratio of strength increase was computed using Eq. 9.11b and the results are shown in Fig. 9.35. The solid line on Fig. 9.35 corresponds to a $\Delta\sigma'_v$ of 80kPa which represents a typical increase that can be achieved in the field with vacuum, whereas the dashed lines represents the upper and lower bound values of increase in effective vertical stress due to combined vacuum-fill load or a reduced vacuum load due to leakage. Figure 9.35 shows that:

- For a given $\Delta\sigma'_v$, the increase in shear strength is relatively independent of σ'_p/σ'_{vo} for all $s_{uo}(FV)/\sigma'_p$ ratios considered in the analysis, especially for high $\Delta\sigma'_v$.
- For a given $\Delta\sigma'_v$, the increase in strength is more pronounced for very soft soils, i.e., small $s_{uo}(FV)$. The ratio of strength increase decreases with increasing $s_{uo}(FV)$. This indicates that in the absence of a desiccated crust, the strength

increase is more significant at shallow depths (lower values of σ'_{vo}) as compared to deeper sublayers.

- For all ratios of $s_{uo}(FV)/\sigma'_p$, a small $\Delta\sigma'_v$ may result in a high strength ratio for small values of $s_{uo}(FV)$ as compared to high $\Delta\sigma'_v$ acting on a soil with high $s_{uo}(FV)$. For example, for a σ'_p/σ'_{vo} value of 1.6 and $s_{uo}(FV)/\sigma'_p$=0.25, the $s_u(FV)/s_{uo}(FV)$ is 3.5 and 2.0, respectively, for $s_{uo}(FV)$ of 2kPa and 20kPa.
- For a given $s_{uo}(FV)$, a high $s_{uo}(FV)/\sigma'_p$ ratio results in a higher $s_u(FV)/s_{uo}(FV)$.

Data on pre-treatment and post-treatment field vane shear strength, obtained from 18 different sections of 11 different case histories (5 cases of vacuum preloading, 2 cases of fill preloading and 4 cases of combined vacuum-fill preloading) are shown in Fig. 9.36. Figure 9.37 shows the result of strength improvement at different depths (data from Fig. 9.36). It can be seen from these figures that irrespective of depth, the increase in undrained shear strength for layers with low initial strength (s_{uo}<10kPa) is more significant as compared to soil layer with high initial shear strength (s_{uo}>20kPa). The field data shown in Figs. 9.36 and 9.37 also show that with increase in $s_{uo}(FV)$ and increasing depth (σ'_{vo}), the increase in undrained shear strength become less significant; which is consistent with the trend shown in Fig. 9.35. More importantly, the increase in shear strength appears to be independent of the type of load.

The ratio of strength increase is plotted against the initial shear strength as shown in Fig. 9.38 along with the average, upper and lower bound values from Fig. 9.35. It is important to point out that in most of the cases of vacuum preloading, an average vacuum pressure of 80kPa is reported in the literature; however the actual consolidation pressure may vary with depth in certain cases as shown in Chapters 4 to 8. It can be seen from Fig. 9.38 that most of the data for vacuum and fill preloading plot around the average line representing an 80kPa of fill load; whereas, the data for combined vacuum-fill load, which corresponds to a consolidation pressure higher than 80kPa, mostly plot above the average line. The scatter in the data can be explained by considering the following:

- Data for vacuum or combined vacuum-fill preloading which plot respectively, above the average and upper bound lines can be attributed to the existence of pretreatment excess porewater pressures. Therefore, the actual increase in

effective vertical stress exceeds the externally applied stress, and hence a greater increase in strength is expected.

- Data which are plotting below the average line can be explained by considering the following; (1) the removal of load (vacuum or combined vacuum-fill) before reaching the EOP compression, and (2) due to 'leakages' in vacuum, the consolidation progressed under a reduced load as shown in analysis of case histories (Chapters 4 to 8).

The agreement between the field data from vacuum and combined vacuum-fill preloading case histories and the theoretically developed limits for fill preloading shows that the strength increase due to preloading is independent of the type of load applied. The reason vacuum appears to be more efficient near the ground surface is because of its ability to be applied with full intensity to very soft ground relatively quickly; whereas, an equivalent fill load is applied in stages to avoid stability problems. It can be seen from Fig. 9.38 that the number of cases where vacuum or a combination of vacuum-fill preloading was used to improve soils having $s_{uo} < 5$kPa, are more than the cases where fill load was used. However, when used, the improvement affected by fill preload is quiet similar to that of vacuum preload.

The increase in undrained shear strength due to vacuum preloading can therefore be predicted using the existing empirical procedures/correlations. Figure 9.39 shows the relation between initial vane strength normalized with respect to preconsolidation pressure [$s_{uo}(FV)/\sigma'_p$] and vane strength at the end of vacuum preloading normalized with respect to consolidation pressure [$s_u(FV)/\sigma'_{vc}$]. The data in the figure show some scatter; however, it should be realized that in addition to variation in vacuum intensity at different depths, the vacuum preload was removed before reaching the end-of-primary compression. It is reasonable to assume that if the soil was allowed to complete primary compression under a vacuum intensity constant with depth, the strength to consolidation pressure ratio [$s_u(FV)/\sigma'_{vc}$] will improve resulting in a less scatter. It is also important to point out that in most of the analyzed case histories, specific data on preconsolidation pressure at various depths was not available and therefore, best possible assumptions were made. The availability of more specific data on preconsolidation pressure may also be helpful in reducing the scatter in Fig. 9.39.

Figure 9.40 shows the increase in shear strength predicted using Eq. 9.11 for vacuum-fill, fill and vacuum test sections for East Pier Project in China (Chapter 8). It can be seen that there is a reasonable agreement between the observed and predicted strengths using Eq. 9.11. The minor difference in prediction and field measurements can be attributed to the uncertainties in (1) loading conditions especially for fill test section, (2) consolidation pressure, and (3) degree of consolidation of individual sublayers. It is interesting to note that the vacuum loading test section, which could not be analyzed due to non-availability of data, shows a very good agreement between the measured and predicted shear strength (Fig. 9.40c). Figure 9.40 shows that Eq. 9.11 together with $s_u(FV)/\sigma'p$ ratio can be reliably used to predict the increase in field vane shear strength due to vacuum, fill or vacuum-fill loads.

9.9 Ground Water Fluctuations during Vacuum Preloading

Position of groundwater table (GWT) and its possible fluctuation can affect the consolidation process. Conflicting views exist with regard to movement of GWT during vacuum preloading. The available literature does not explicitly discuss the movement of GWT during vacuum treatment; however, the porewater pressure measurements suggest an upward movement of groundwater table (Bergado et al. 1997; Chu et al. 2000). The addition of 1.5m thick primary fill under the sealing membrane (after installation of VTPs) to "maintain non-submerged action" in the Menard vacuum consolidation technique (see Section 2.5.2), indicates a tendency for upward movement of GWT during the process of consolidation. In certain cases of vacuum preloading, the treatment area is isolated from the adjoining ground by providing a cutoff (such as slurry wall) to avoid loss of vacuum pressure. In such a case, the flow of water from the adjoining area is restricted and may therefore result in a temporary lowering of GWT. However, case histories of vacuum consolidation where deep cutoffs were provided do not report any lowering of GWT due to provision of cutoffs (Tang and Shang 2000; Masse et al. 2001; Berthier et al. 2009). Chung (2009) has summarized the work of a number of Chinese engineers and researchers and has concluded that a constant water table best describes the ground water condition during vacuum preloading operation.

Qiu et al. (2007) conducted a laboratory study to show that the fluid flow under vacuum pressure may be (1) a single phase water flow, (2) a two-phase air water flow, and (3) a single phase air flow. The schematic layout of laboratory study is shown in Fig. 9.41.

Seven vacuum gauges (G1 – G7) were used to measure vacuum pressure distribution at locations shown in Fig. 9.41. Three glass bottles were used to serve, respectively, as air-water separating bottle (AWSB), water-storing bottle (SWB), and water-supplying bottle (WSB). Table 9.4 shows the tests carried out during the study. Test 1, during which all valves were closed showed no movement of water when subjected to vacuum pressure. This is an expected result as water moves out of the soil mass if subjected to atmospheric pressure; which is ensured in the field by using a flexible membrane to seal the area. Closed valves and rigid glass bottles cannot transmit the atmospheric pressure to the water and hence there is no movement of water. Vacuum pressure measurements at different gauges during Test 2 (single phase water flow) are shown in Table 9.5. Based on the experimental results, Qiu et al. (2007) concluded that (1) vacuum preloading causes a drop of GWT which enlarges the unsaturated zone and hence results in a two phase (air-water) flow, (2) the vacuum pressure cannot be uniformly distributed, and (3) the treatment area cannot be sealed and need not to be airtight during vacuum preloading. Following factors need critical evaluation to examine the validity of the study carried out by Qiu et al. (2007):

- It was shown in Section 9.3 (based on the field data and laboratory studies incorporating vacuum preloading) that under ideal conditions, vacuum intensity remains constant with depth; however, vacuum may develop to different intensities at different depths in field conditions involving stratified soil. Thus, there is no limit on the theoretical depth of improvement when vacuum is used for preloading. Qiu et al. (2007) propose a reduction in vacuum with depth (11kPa/m from their laboratory study) which restricts the depth of improvement, and therefore, it is not supported with field evidence.
- According to Qiu et al. (2007), the vacuum reduces with depth at fixed gradient and therefore, the effectiveness of vacuum should reduce with depth causing a smaller reduction in porewater pressure with depth; however, the case history reported by Qiu et al. (2007) does not support this argument. The observed reduction in porewater pressure was about 60kPa at a depth of 20.60m (elevation; -16m) below the original ground surface (Fig. 7 of Qiu et al. 2007); whereas the maximum reductions observed at depths of 5.60m and 7.60m were

28kPa and 40kPa, respectively. This shows that a fixed gradient cannot be assigned to vacuum pressure applied/developed in the soil mass.

- The average vacuum gradient of 11kPa/m for single phase water flow (test 2) should be the same in the segment DC of the pipe. However, the gradients between G7 – G6, G6 – G5 and G5 – G4 were neither the same nor suggest any regular pattern as shown in Table 9.5. This indicates a variable density (water and air) of flowing fluid, possibly due to leakages which allowed the air to enter into the system.
- The reasons for vacuum loss between G1 and G2 are not explained by the authors.
- More importantly, the experimental setup of Qiu et al. (2007) does not simulate the actual filed conditions. In the field, the vacuum pressure is applied using vertical drains, water moves through the soil and vertical drains, and atmospheric pressure is transferred to consolidating soil through use of a flexible membrane. Therefore, the results of experiments by Qiu et al. (2007) cannot be extrapolated to the field conditions.

Therefore, it is reasonable to assume that the position of ground water table is not affected during the vacuum preloading.

9.10 Cost of Vacuum Preloading

There appears to be a consensus that the unit cost for implementing a vacuum consolidation is less than that of the conventional fill preloading. While evaluating 'enhanced consolidation (with vacuum)' for dredged material at a confined disposal facility at Newark Bay, vacuum consolidation was accessed to be cheapest method with a unit cost of $9.50 per cubic meter of soft ground as opposed to $11.00 for 'accelerated (with PVDs) consolidation' (Sandiford et al. 1996). Although detailed cost analyses have not been reported, however, the approximate cost for vacuum consolidation appears to be two-third (Ye et al. 1983) to one-third (Yixiong 1996b) as compared to that of an equivalent fill preload.

The cost effectiveness of vacuum consolidation can be expressed in two different ways; i.e., direct savings and indirect savings. Direct savings are affected due to low unit cost of the vacuum consolidation over the conventional fill preloading as stated above; whereas, indirect saving results from the early completion of project as a result of more rapid

application and rapid removal of vacuum load. The relative cost of vacuum preloading and conventional fill preloading vary according to site conditions, cost of availability of quality fill material, cost for power/electricity and labor charges etc. Considering cost of fill material, including transportation, as the main factor, a study carried out by Simon and Rodriguez (1996) indicated that the cost of vacuum preloading and conventional fill preloading will break even if the cost of fill material were $5 per cubic yard of treated soil; however, with increasing cost of fill material, especially in countries like Japan, Singapore and Hong Kong, the scarcity of fill material makes the vacuum consolidation an attractive alternative. Indirect savings are in the form of additional income as a result of early completion of the project. Simon and Rodriguez (1996) also showed that the anticipated additional income due to early completion of a toll way could exceed 3million dollars based on an estimated traffic of 45000 vehicles per day at a toll rate of $0.25 per vehicle.

9.11 Concluding Remarks

A brief review of this chapter is as following:

- Vacuum pressure induces isotropic load and therefore absence of shear stresses avoids instability during construction. Thus a vacuum preload can be applied in a single step which enables subsequent more quick construction of fill (if necessary) and reduces the overall duration of preloading operation.
- There is no difference in soil behavior due to vacuum, fill, or vacuum-fill preloads. With proper interpretation of field observations, existing consolidation theories can be used to predict settlement and porewater pressure response as well the increase in undrained shear strength. Thus there is no need of developing new or modifying existing theories to incorporate the effects of vacuum pressure.
- Due to complex interaction of soil parameters and possible variation in vacuum intensity with depth and time, an empirical approach is considered more reasonable to predict lateral displacements due to vacuum preloading. The proposed method can be used to estimate the lateral displacements with depth and time with reasonable accuracy.

- Vacuum consolidation offers a cost effective solution for improvement of soft soil deposits especially in areas where quality fill material is not available in sufficient quantities.

9.12 Tables

Table 9.1: Lateral displacement data for different case histories of vacuum preloading

Case History	Prefabricated Vertical Drains		Maximum Lateral Displacement (mm)	Zero Lateral Displacement		Treatment Area (m x m)	L/H_o (L=half width)	Remarks
	Penetration Depth, H_o (m)	Spacing (m)		Depth (m)	z/H_o			
Container Terminal - China								
• Section I	20	1	277	14	0.7	175 x 51	1.275	
• Section II	20	1	351	14	0.7	189.5 x 51	1.275	
Nansha Terminal - China	22	1	250	15/16	0.73	235 x 120	2.72	
Oil Storage Station - China								
• Section I (N)	20	1	320	13	0.65	30000m^2	3.4	136m wide
• Section I (S)	20	1	460	15	0.75			
• Section II	20	1	320	13	0.65	20000m^2	2.95	118m wide
Yamaguchi – Japan	27	1.2	2550	27	1	250 x 44	0.81	CPVDs
Saga – Japan	10.5	0.8	186	10	0.95	146 x 18	0.85	
Storage Yard - China								Combined Vacuum – Fill Preloading
• Section I	20	1	242	16	0.8	80 x 30	0.75	
• Section II	20	1	475	16	0.8	119 x 30	0.75	
Soda-Ash Tailings	8	1.2	320	8.5	1.06	45 x 45	2.81	
Sanriku Ota Test Embankment - Japan	13	-	240	8	0.62	13 x 54	0.5	
Field Trial – Korea								
• Section A	10	-	38	>8	>0.8	30 x 10	0.5	
• Section B	10		53	>8	>0.8	30 x 10	0.5	

Table 9.2: Comparison of $q_{w(min)}$ and $q_{w(mob)}$ for different case histories

S.No	Case History	Drain Length, l_m (m)	k_h (cm/s)	q_w (m^3/yr)		
				Minimum	Mobilized	Reported
1	Storage Yard – Vacuum preloading with PVDs	20.0	-[@]	100	100	100
2	Saga road project – Vacuum preloading with PVDs	10.5	-[@]	50	2	100
3	Container terminal, Sec I – Vacuum-Fill preloading with PVDs	20.0	-[@]	60	5	-
4	Container terminal, Sec II - Combined loading with PVDs	20.0	-[@]	60	11	-
5	Bangkok Airport, Vacuum preloading with Sand drains	14.5	$5*10^{-7}$	104	10	-
6	Bangkok Airport, combined loading with PVDs (TV2)	12	$5*10^{-7}$	70	1.5	50
7	Bangkok Airport, Fill preloading with PVDs (TS3)	12	$5*10^{-7}$	70	1.5	30
8	Bangkok Airport, combined loading with CPVDs	10	$5*10^{-7}$	50	0.8 -1.0	-
9	East Peir Project; Vacuum, Vacuum-Fill, and Fill preloading with PVDs	20	-[@]	11	11	790
[@] Minimum discharge capacity estimated by ILLICON analysis using permeabilities of individual sublayers						

Table 9.3: Increase in shear strength at different depths due to stress increment, $\Delta\sigma_v$ = 80kPa for a soil deposit with constant $s_{uo}(FV)/\sigma'p = 0.3$

	σ'_{vo} (kPa)	σ'_p (kPa)	σ'_{vf} (kPa)	$s_{uo}(FV)$ kPa	$s_u(FV)$ kPa	$s_u(FV)/s_{uo}(FV)$
σ'_p/σ'_{vo}=1	10	10	90	3	27	9.00
	20	20	100	6	30	5.00
	30	30	110	9	33	3.67
	40	40	120	12	36	3.00
	50	50	130	15	39	2.60
	75	75	155	22.5	46.5	2.07
	100	100	180	30	54	1.80
σ'_p/σ'_{vo}=1 .2	10	12	90	3.6	27	7.50
	20	24	100	7.2	30	4.17
	30	36	110	10.8	33	3.06
	40	48	120	14.4	36	2.50
	50	60	130	18	39	2.17
	75	90	155	27	46.5	1.72
	100	120	180	36	54	1.50
σ'_p/σ'_{vo}=1.4	10	14	90	4.2	27	6.43
	20	28	100	8.4	30	3.57
	30	42	110	12.6	33	2.62
	40	56	120	16.8	36	2.14
	50	70	130	21	39	1.86
	75	105	155	31.5	46.5	1.48
	100	140	180	42	54	1.29
σ'_p/σ'_{vo}=1.6	10	16	90	4.8	27	5.63
	20	32	100	9.6	30	3.13
	30	48	110	14.4	33	2.29
	40	64	120	19.2	36	1.88
	50	80	130	24	39	1.63
	75	120	155	36	46.5	1.29
	100	160	180	48	54	1.13

Table 9.4: Tests conducted with corresponding flow pattern under vacuum pressure (after Qiu et al. 2007)

Series No.	Test No.	State of Valve			Flow Pattern
		V1	V2	V3	
I	1	Close	Close	Close	Single-phase air flow
I	2	Close	Open	Open	Single-phase water flow
II	3	Open	Close	Close	Air-water two-phase flow
II	4	Open	Open	Open	Air-water two-phase flow

Table 9.5: Test results for test 2, series I for single-phase water flow (data from Qiu et al. 2007)

G1	G2	G7	G6	G5	G4	G3	Δp1 (G1-G3)kPa	Δp2 kPa/m	$\Delta p_{(G7-G6)}/\Delta h$ kPa/m	$\Delta p_{(G6-G5)}/\Delta h$ kPa/m	$\Delta p_{(G5-G4)}/\Delta h$ kPa/m
90	85	66	52	44	34	23	67	12.80	14.00	8.00	20.00
80	78	64	49	40	32	22	58	12.80	15.00	9.00	16.00
70	68	59	44	36	28	20	50	12.40	15.00	8.00	16.00
60	54	52	36	30	24	16	44	11.20	16.00	6.00	12.00
40	39	41	28	22	18	12	28	9.20	13.00	6.00	8.00
30	29	40	24	19	18	10	20	8.80	16.00	5.00	2.00
20	19	28	15	11	9	4	16	7.60	13.00	4.00	4.00
							Average	10.69	14.57	6.57	11.14

9.13 Figures

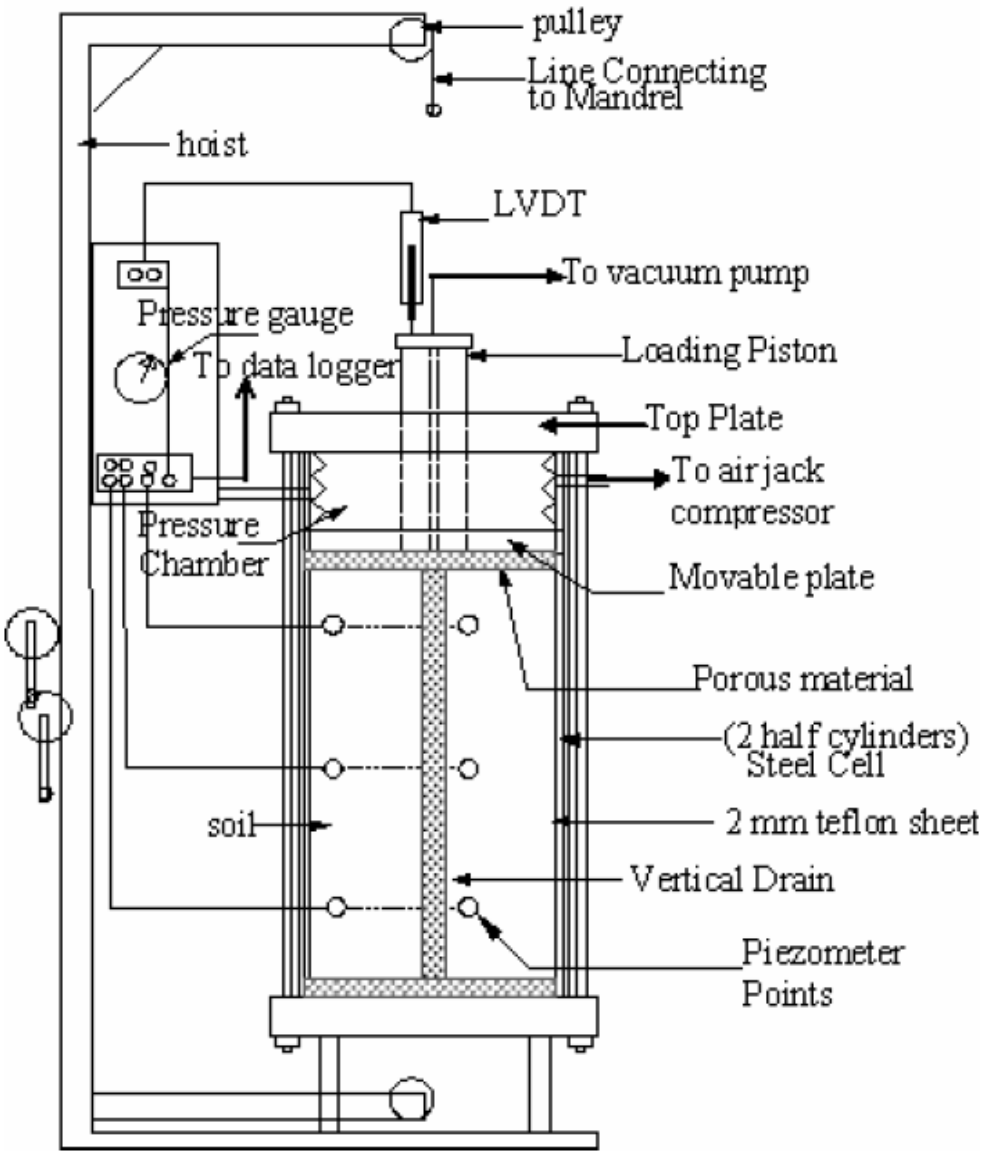

Figure 9.1: Schematic Diagram of large scale oedometer (after Rujiakiatkamjorn, 2005)

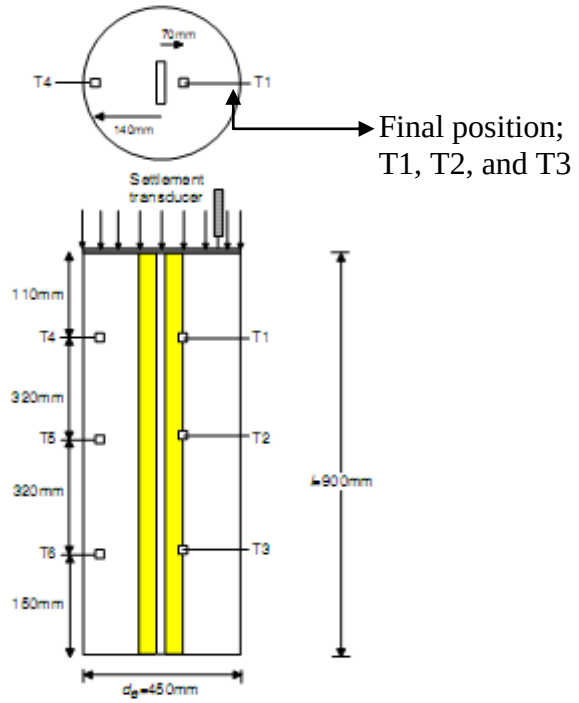

Figure 9.2: Location of transducers for measurement of porewater pressure during consolidation (after Rujiakiatkamjorn, 2005)

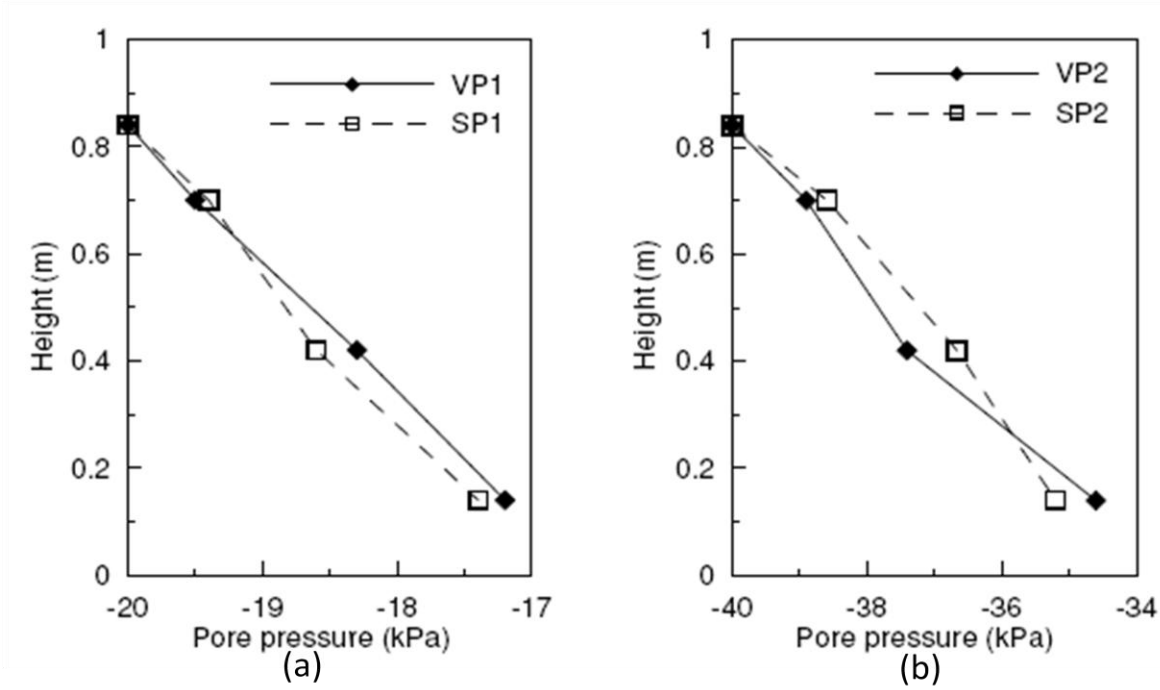

Figure 9.3: Measured porewater pressure with depth at PVD-soil interface in a large oedometer (after Rujiakiatkamjorn, 2005)

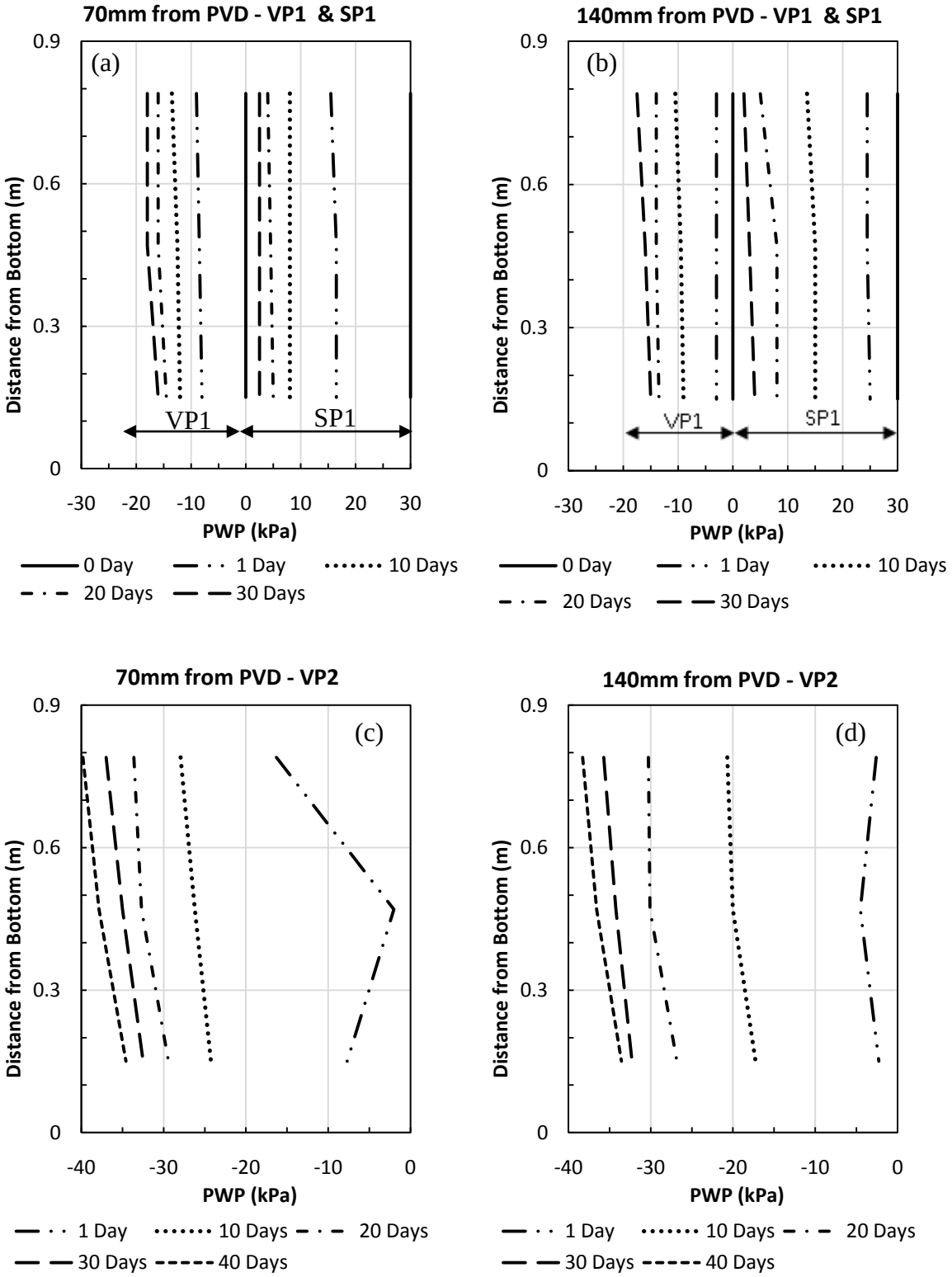

Figure 9.4: Variation in vacuum intensity with depth at different radial distances from PVD for (a & b) VP1 and SP1, and (c & d) VP2 (data from Rujiakiatkamjorn, 2005)

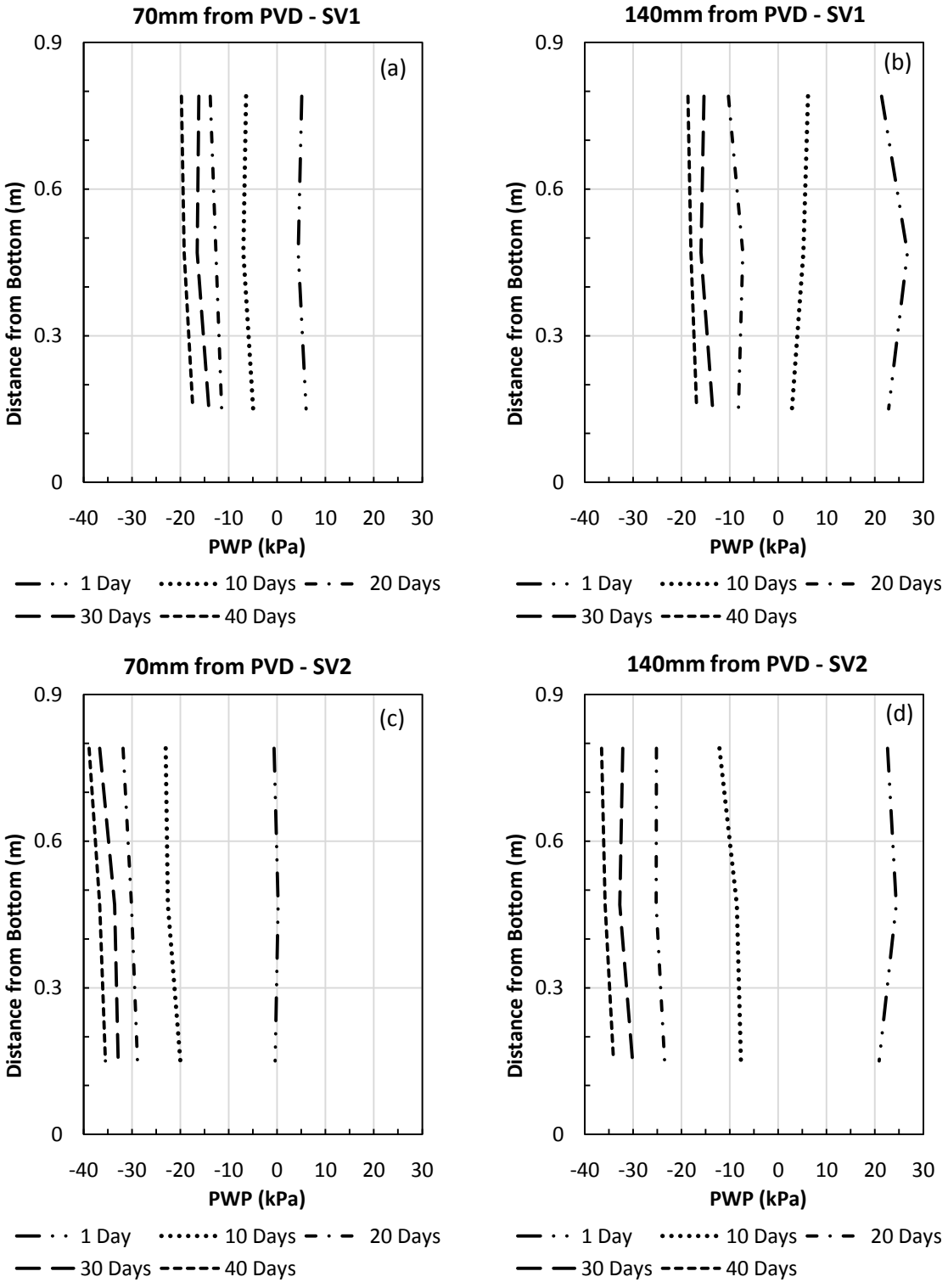

Figure 9.5: Variation in vacuum intensity with depth at different radial distances from PVD for (a & b) SV1, and (c & d) SV2 (data from Rujiakiatkamjorn, 2005)

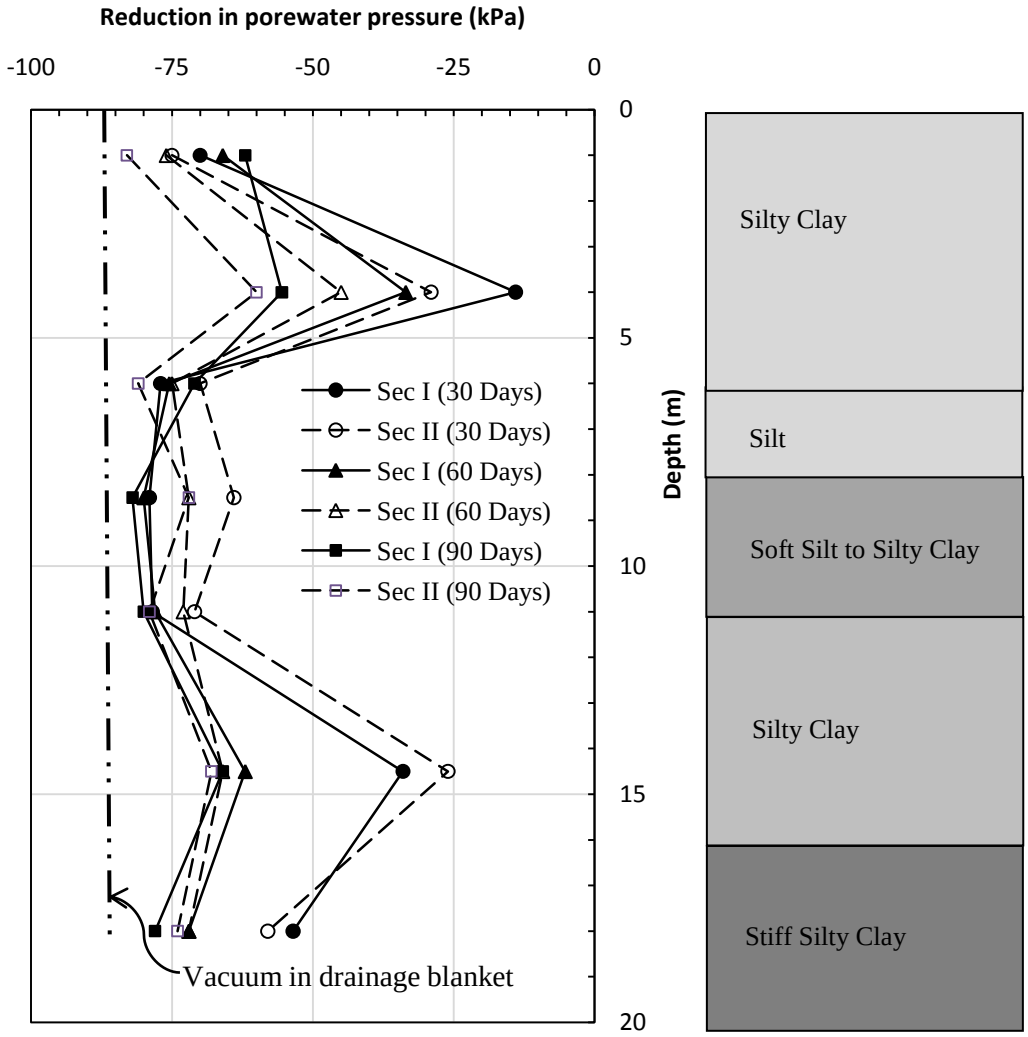

Figure 9.6: Measured reduction in porewater pressure during a vacuum preloading project in China (data from Yan and Chu, 2003)

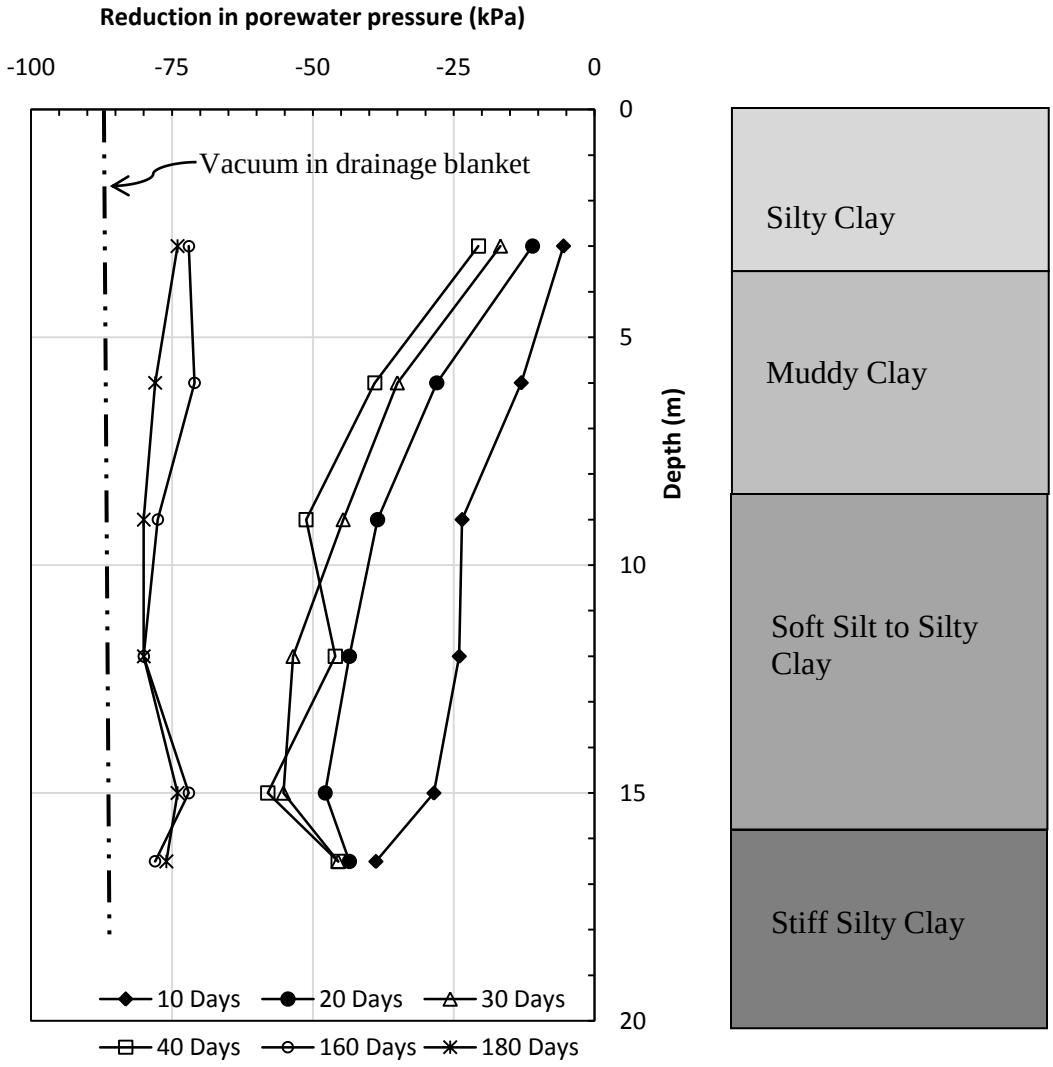

Figure 9.7: Measured reduction in porewater pressure during a combined vacuum-fill preloading project in China (data from Yan and Chu, 2005)

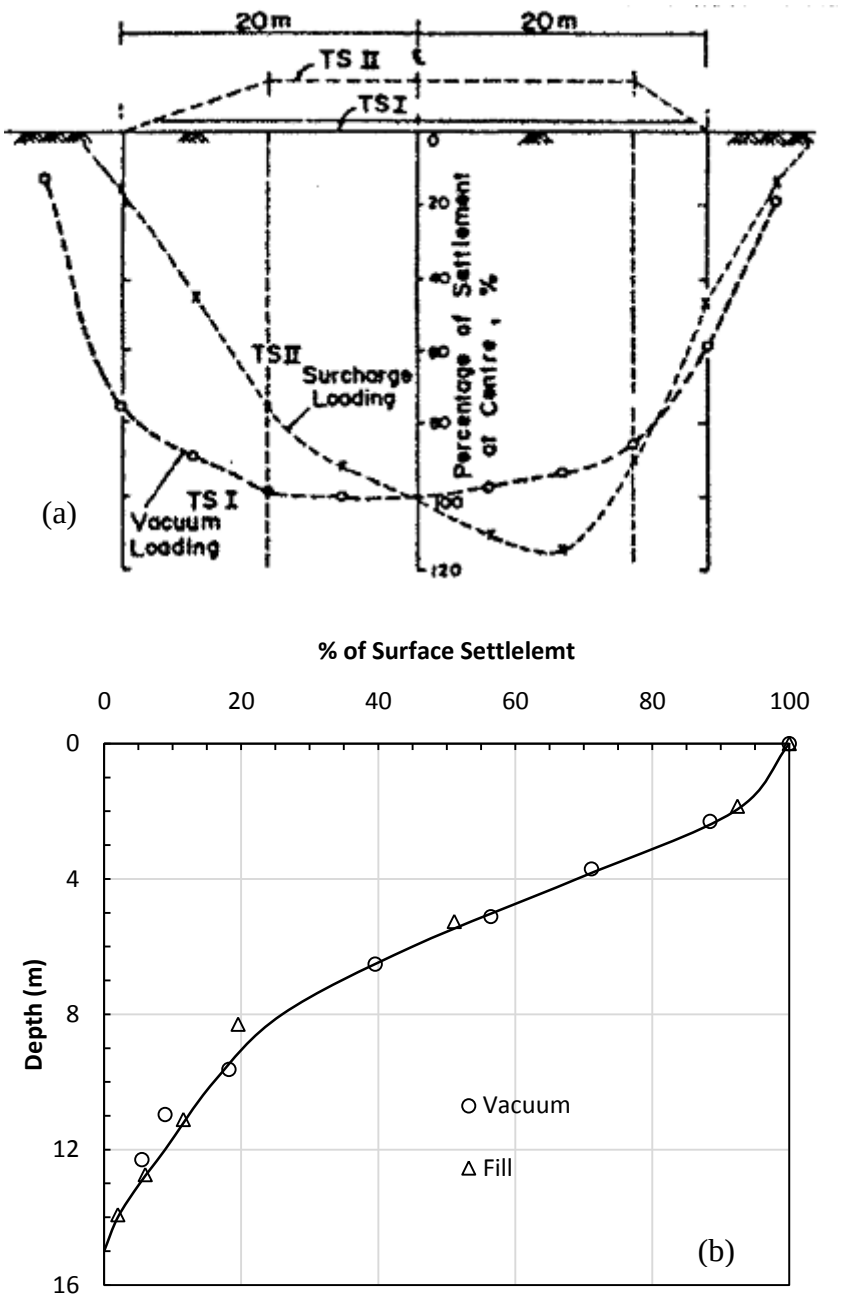

Figure 9.8: (a) Settlements induced by vacuum and equivalent fill preload and (b) settlement with depth expressed in terms of percent of surface settlement (after Woo et al. 1989)

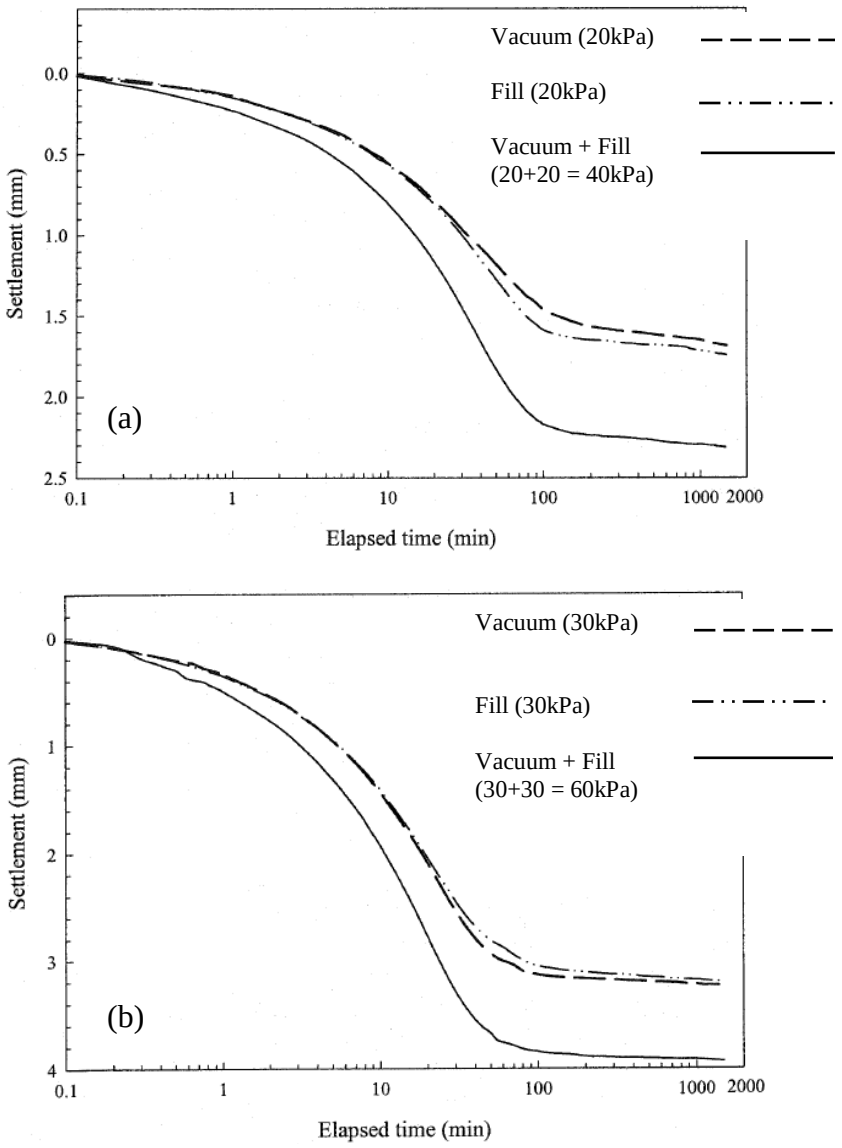

Figure 9.9: Laboratory measurement of settlement due to vacuum, fill and vacuum-fill loading (after Mohamedalhassan, 2002)

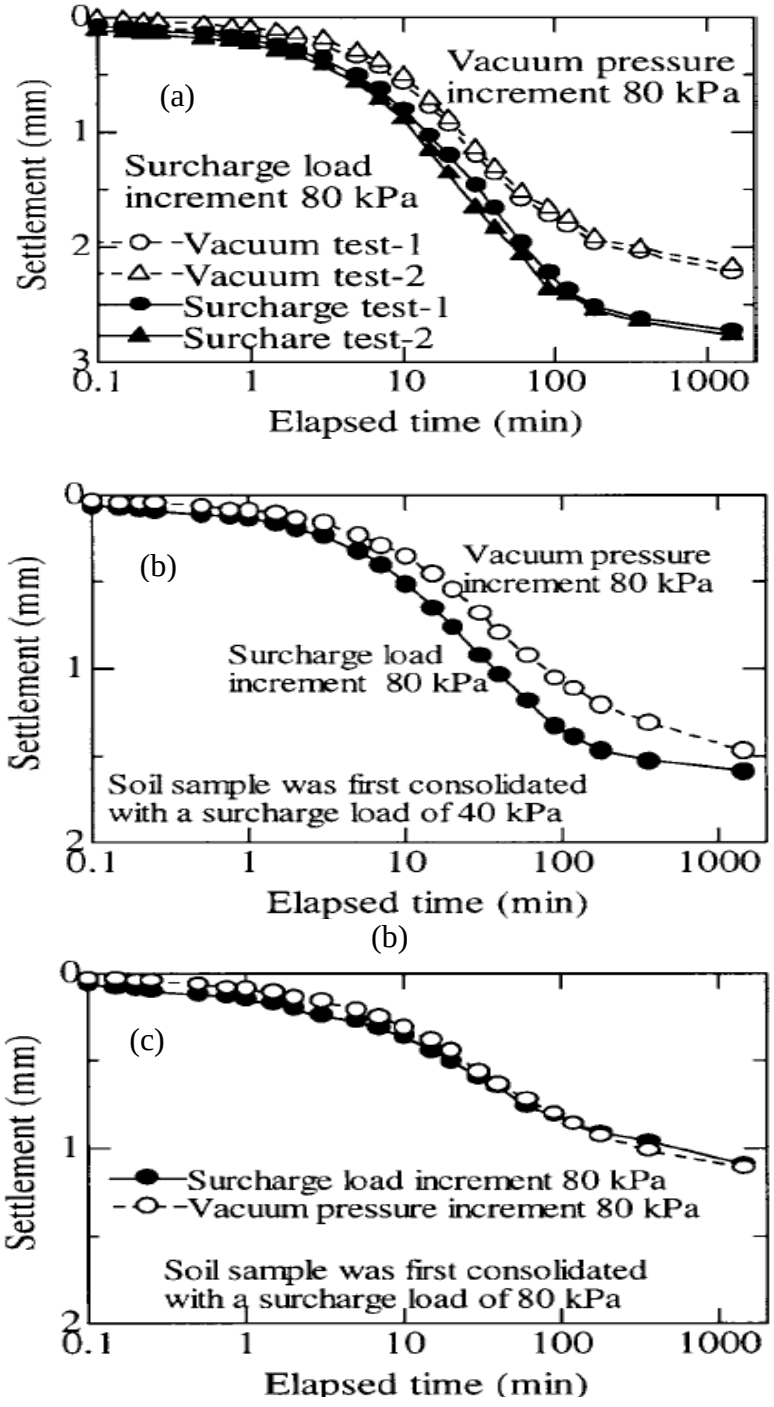

Figure 9.10: Laboratory measurement of settlements due to vacuum and fill loads for specimens with different preconsolidation pressures (after Chai et al. 2005b)

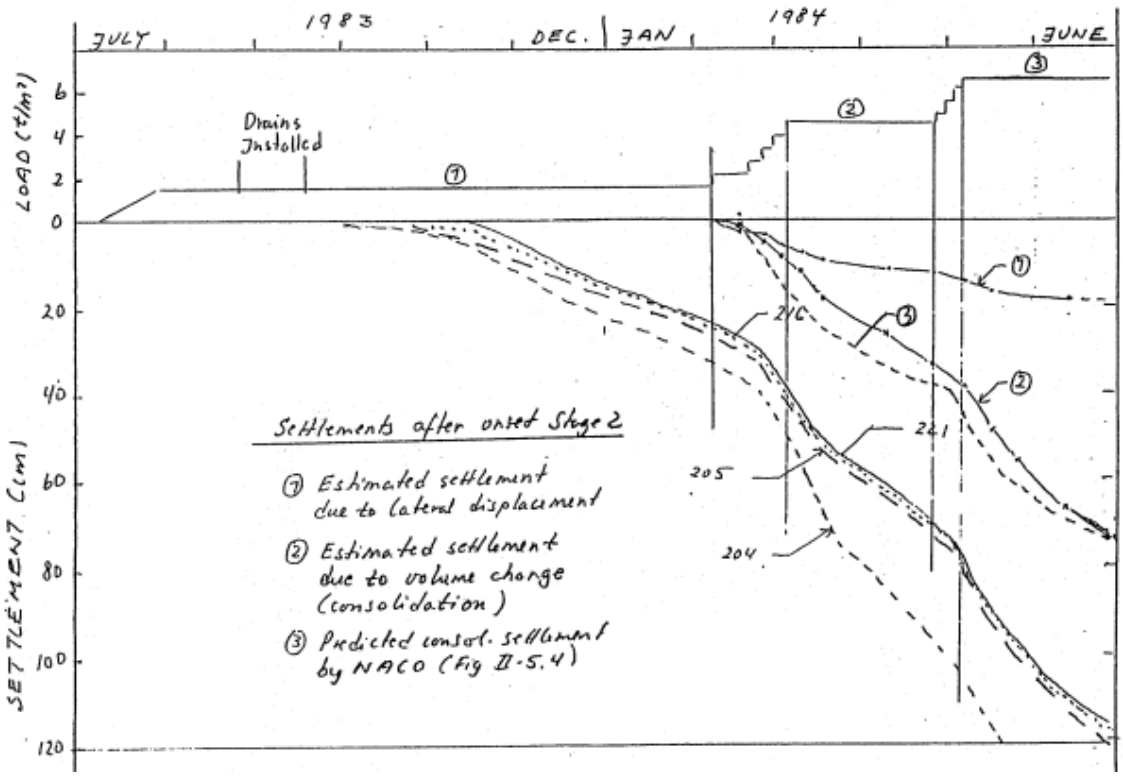

Figure 9.11: Contribution of settlement due to placement of drainage blanket and installation of vertical drains in overall settlement due to fill preloading (after STS/NGI 1992)

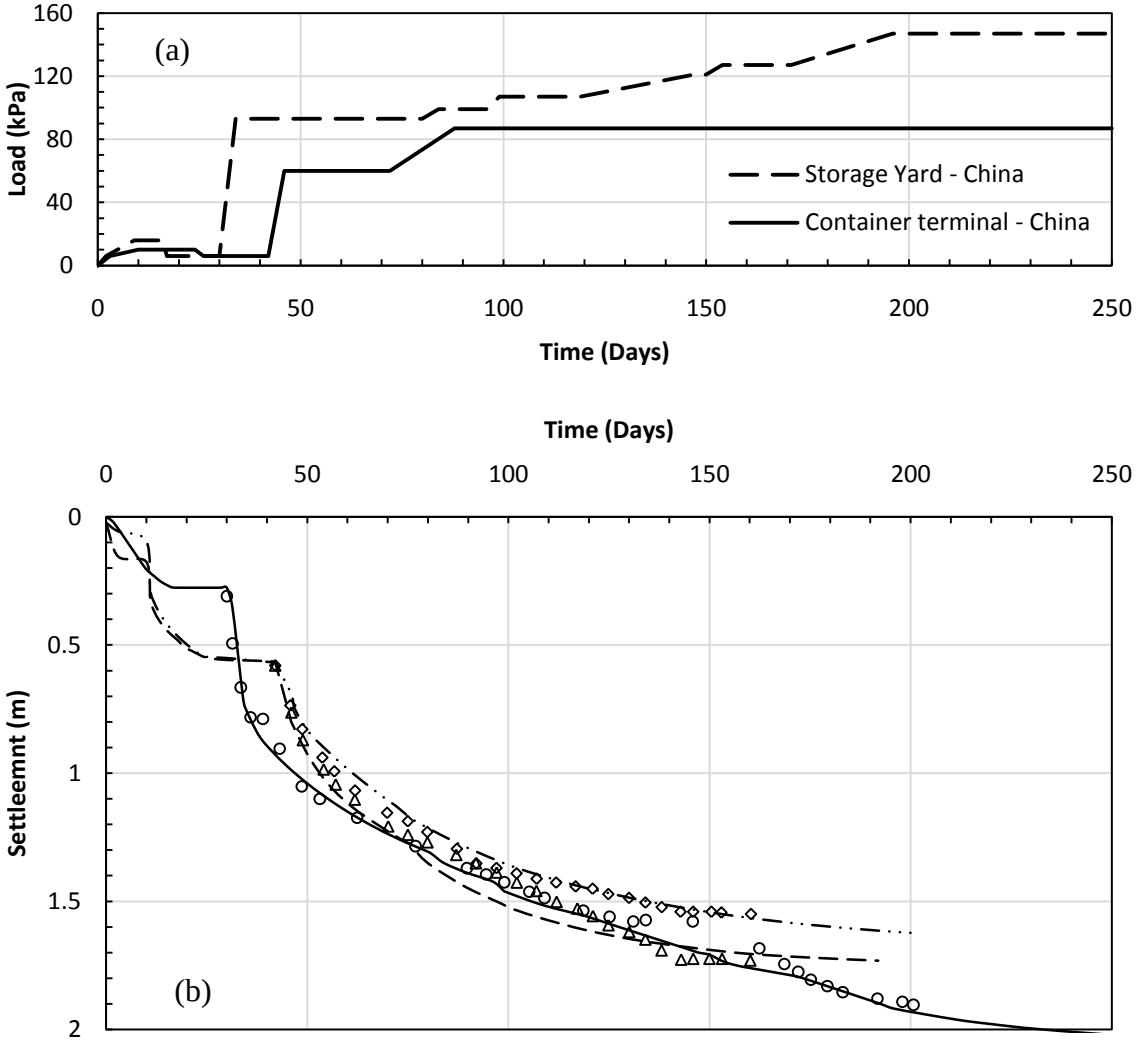

Case History	Observed Settlement	ILLICON Prediction
Storage yard – China	○	———
Container terminal – Sec I	◇	—·—·—
Container terminal – Sec II	△	- - - - -

Figure 9.12: (a) Loading Schedule, (b) Comparison of field settlement with those predicted by ILLICON assuming applied vacuum as an embankment load (field data from Yan and Chu 2003 and 2005)

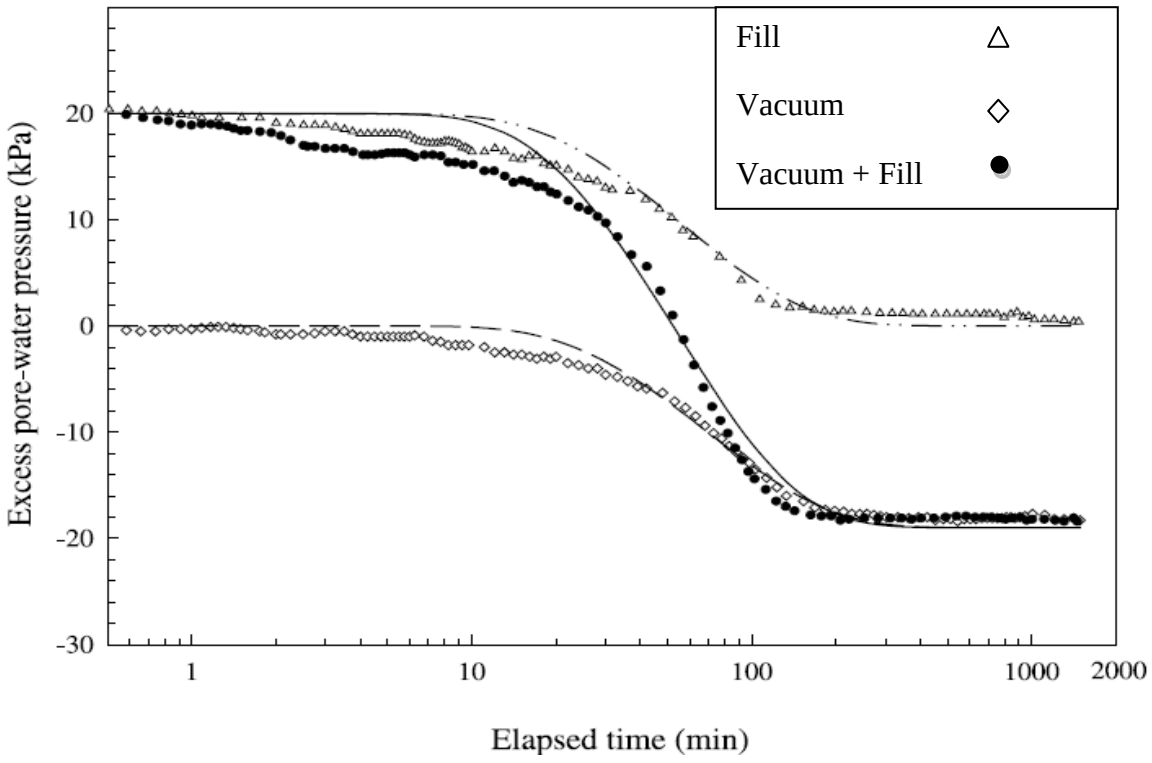

Figure 9.13: Laboratory measurement of porewater pressure due to vacuum, fill and vacuum-fill loading (after Mohamedalhassan, 2002)

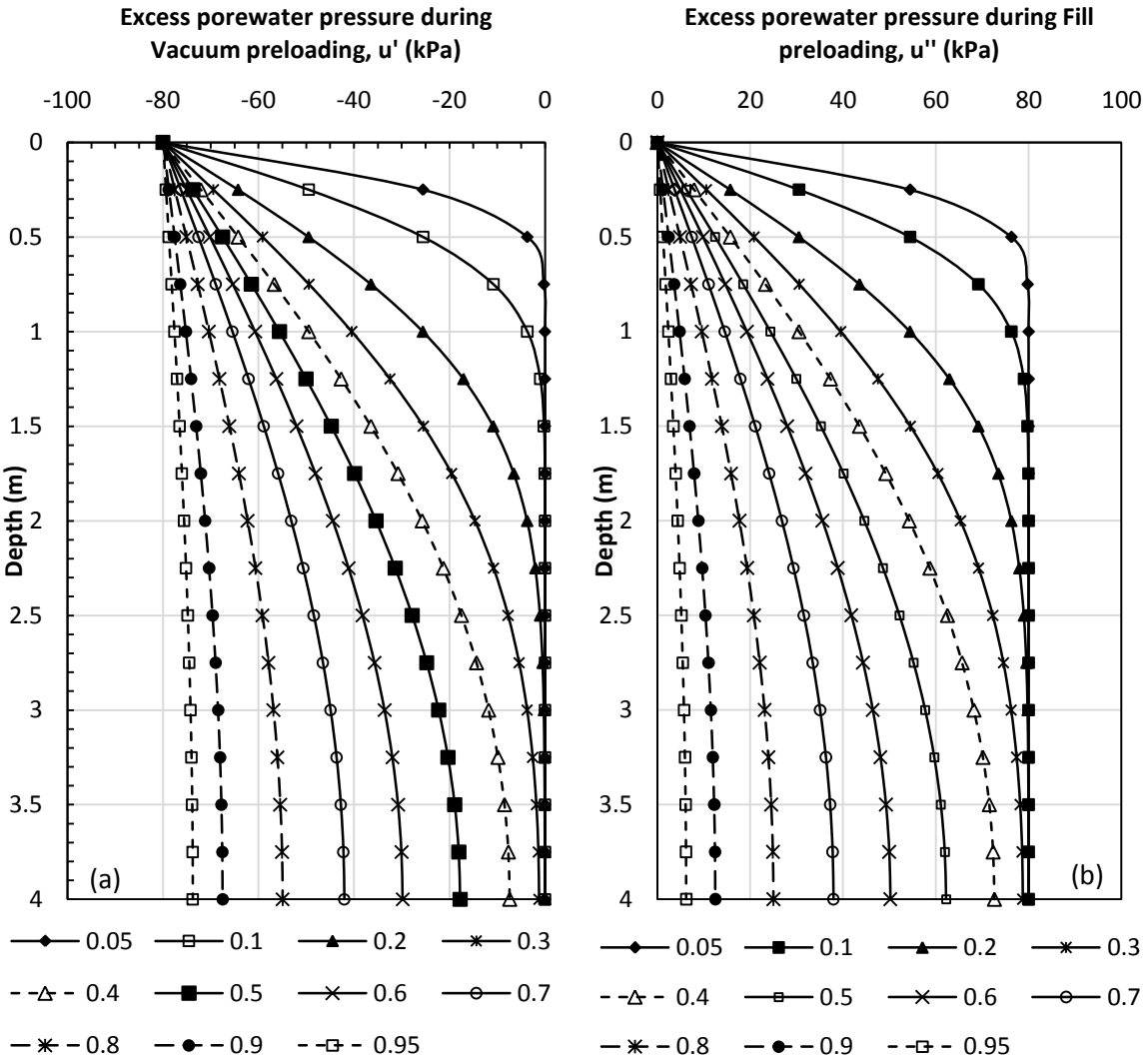

Figure 9.14: Excess porewater pressure distribution with depth corresponding to different degree of consolidation for (a) vacuum preload applied at the ground surface, and (b) fill preload applied at the ground surface

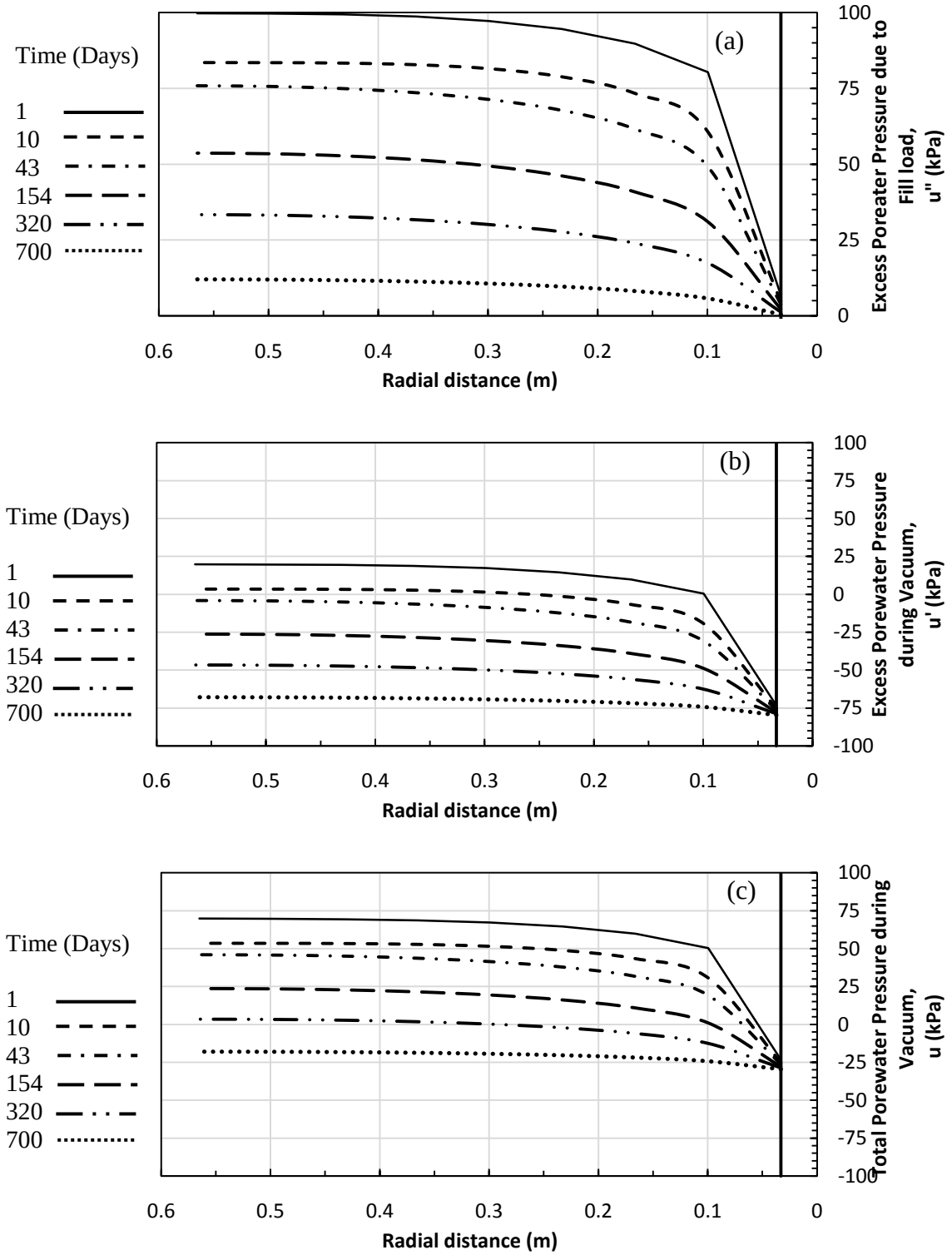

Figure 9.15: Porewater pressure at different times for a given depth (a) assuming vacuum as fill preload, (b) excess porewater pressure during vacuum preloading, and (c) total porewater pressure during vacuum preloading.

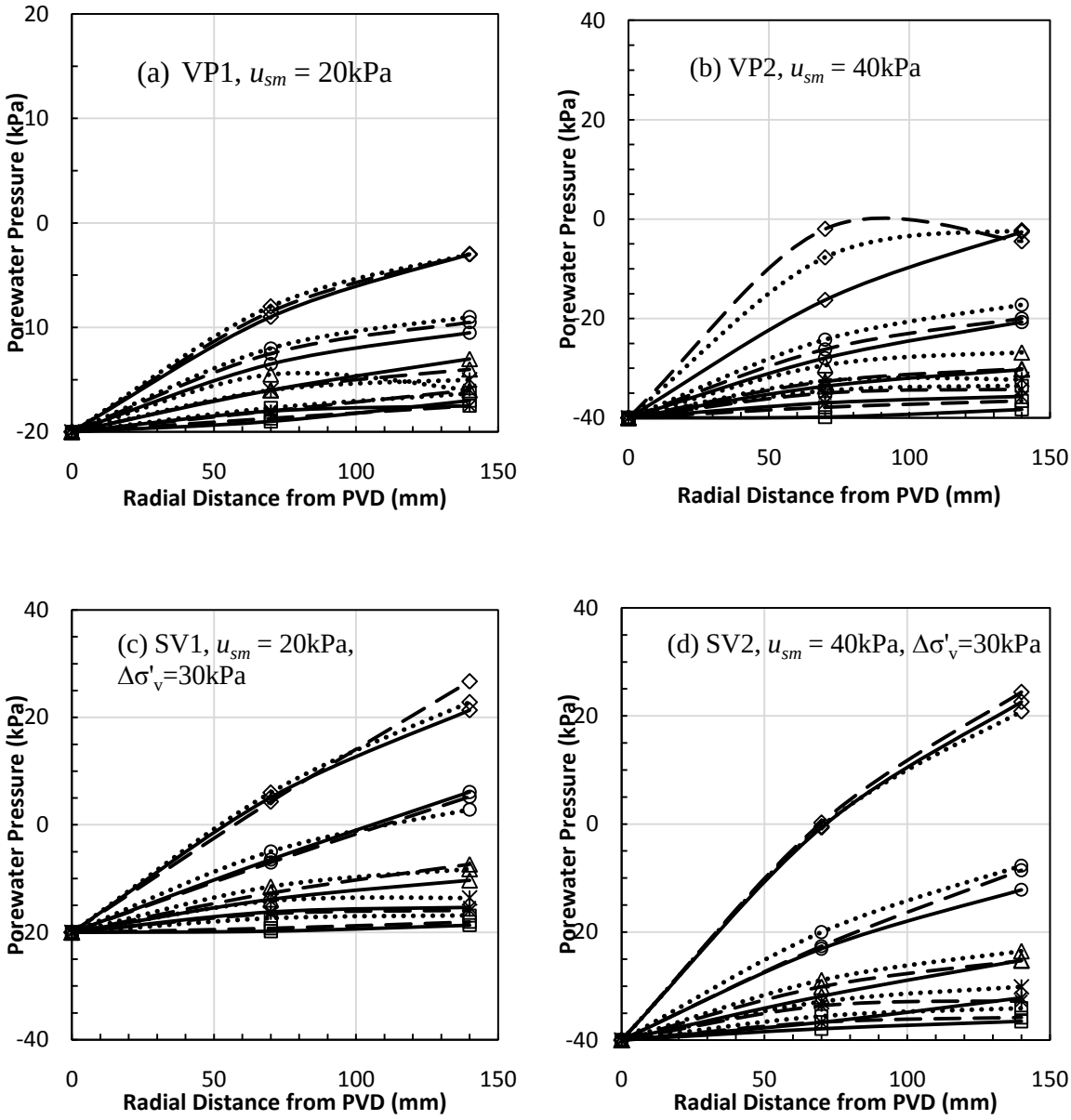

Distance From Bottom of Oedometer		Time (Days)				
		1	10	20	30	40
0.79m	———	◇	○	△	✳	□
0.47m	– – – –					
0.15m	.....					

Figure 9.16: Measured porewater pressure at different depths and times, at different radial distance from PVD under vacuum and combined vacuum-fill preloading (data from Rujiakiatkamjorn, 2005)

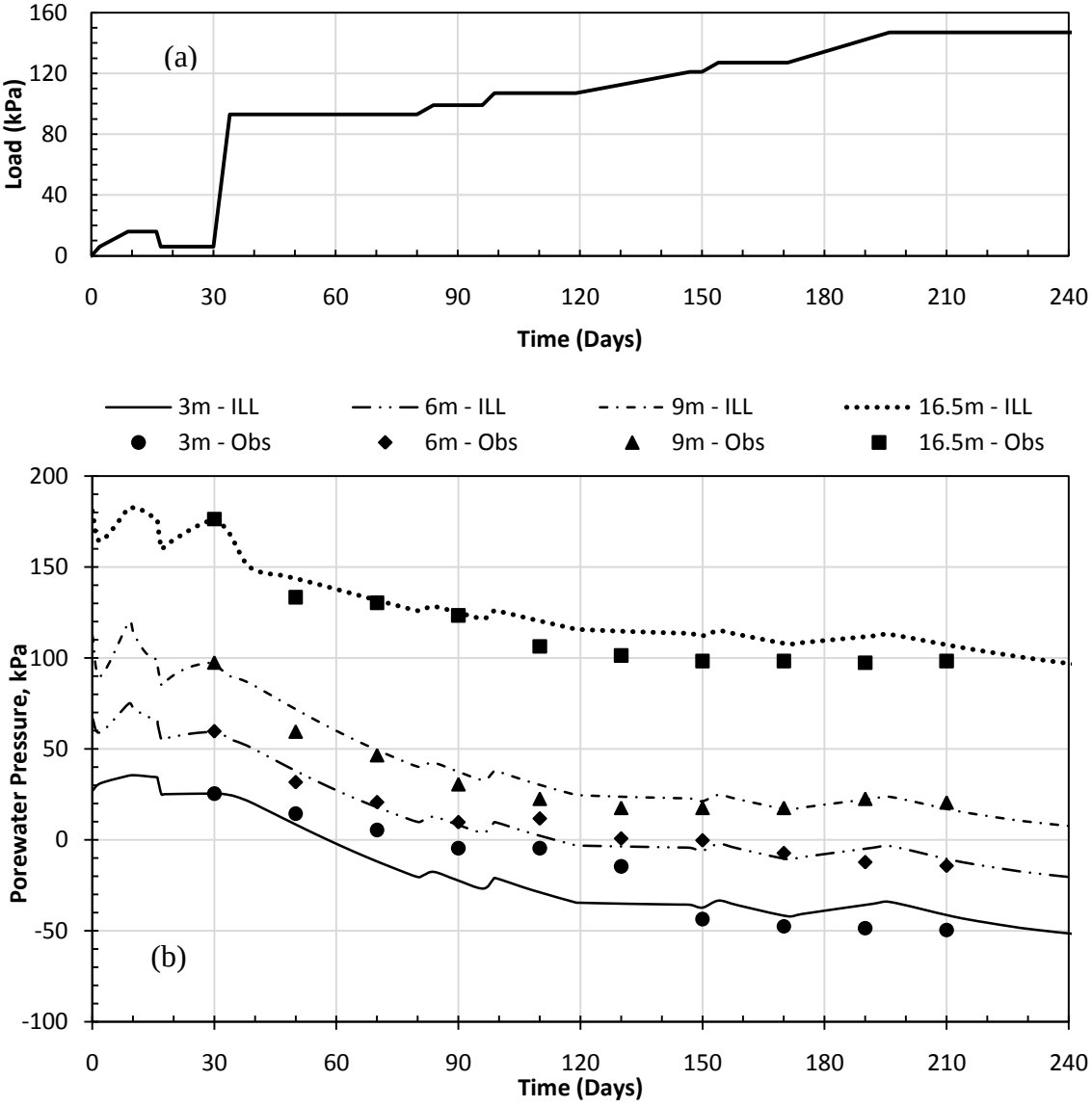

Figure 9.17: Comparison of porewater pressure measured in the field with those predicted by ILLICON assuming applied vacuum as an embankment load (field data from Yan and Chu 2003 and 2005)

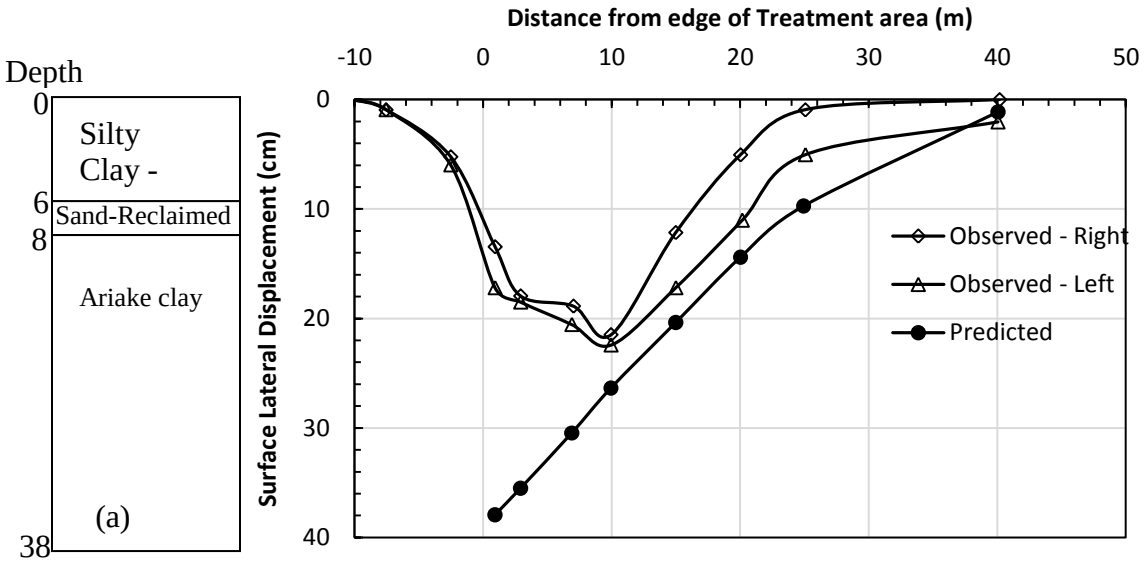

Figure 9.18: (a) The soil profile, and (b) lateral displacements measured at ground surface (redrawn from Dam et al. 2007)

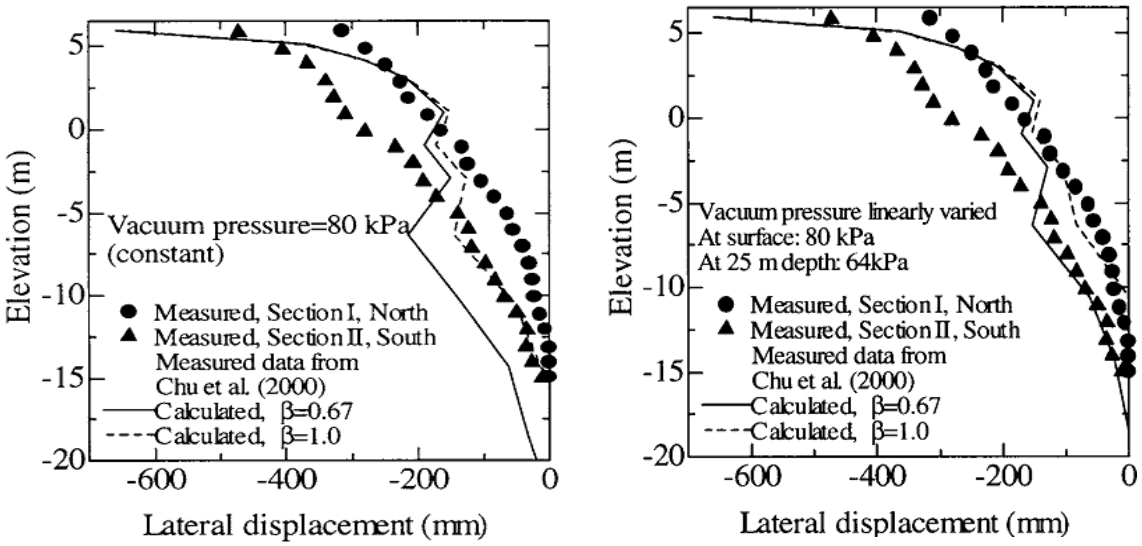

(a) Oil Storage Station

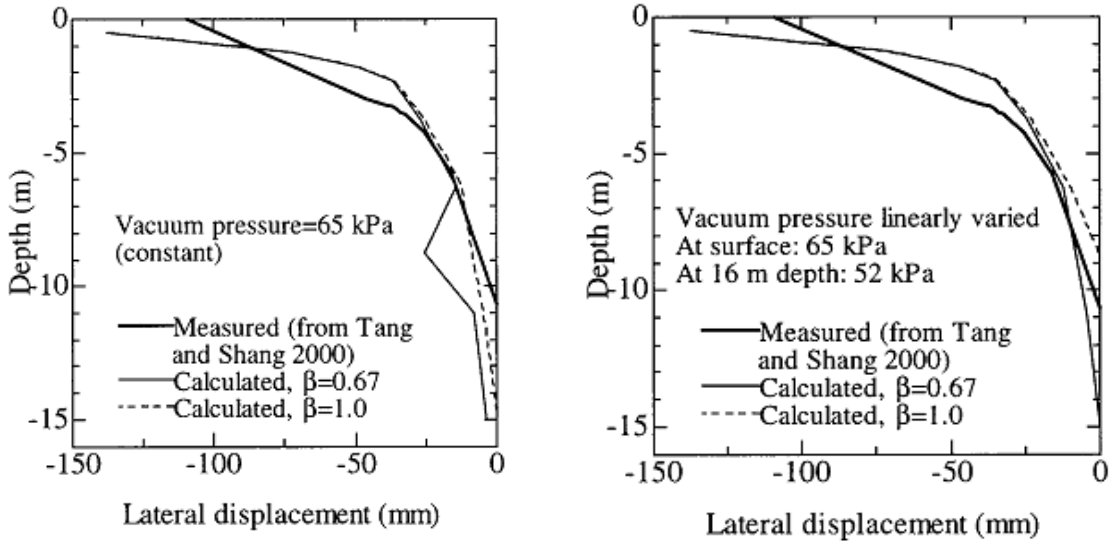

(b) Yaoqiang airport

Figure 9.19: Comparison of observed and predicted lateral displacement for different vacuum intensities and different values of β (reproduced from Chai et al. 2005)

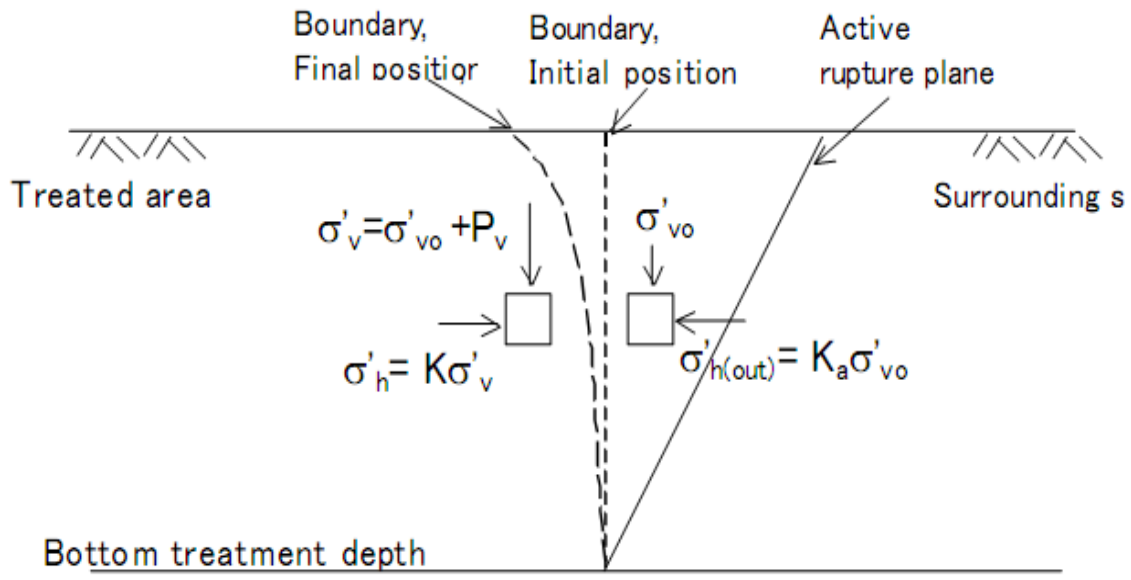

Figure 9.20: Assumed lateral stress condition inside and outside the treatment area during vacuum preloading (after Dam et al. 2007)

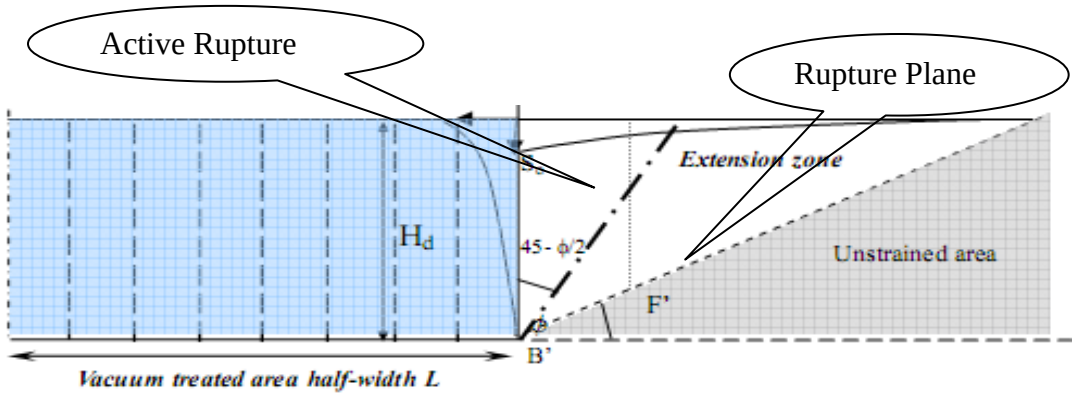

Figure 9.21: Extent of extension zone, active rupture zone and location of rupture plane (after Dam et al. 2007)

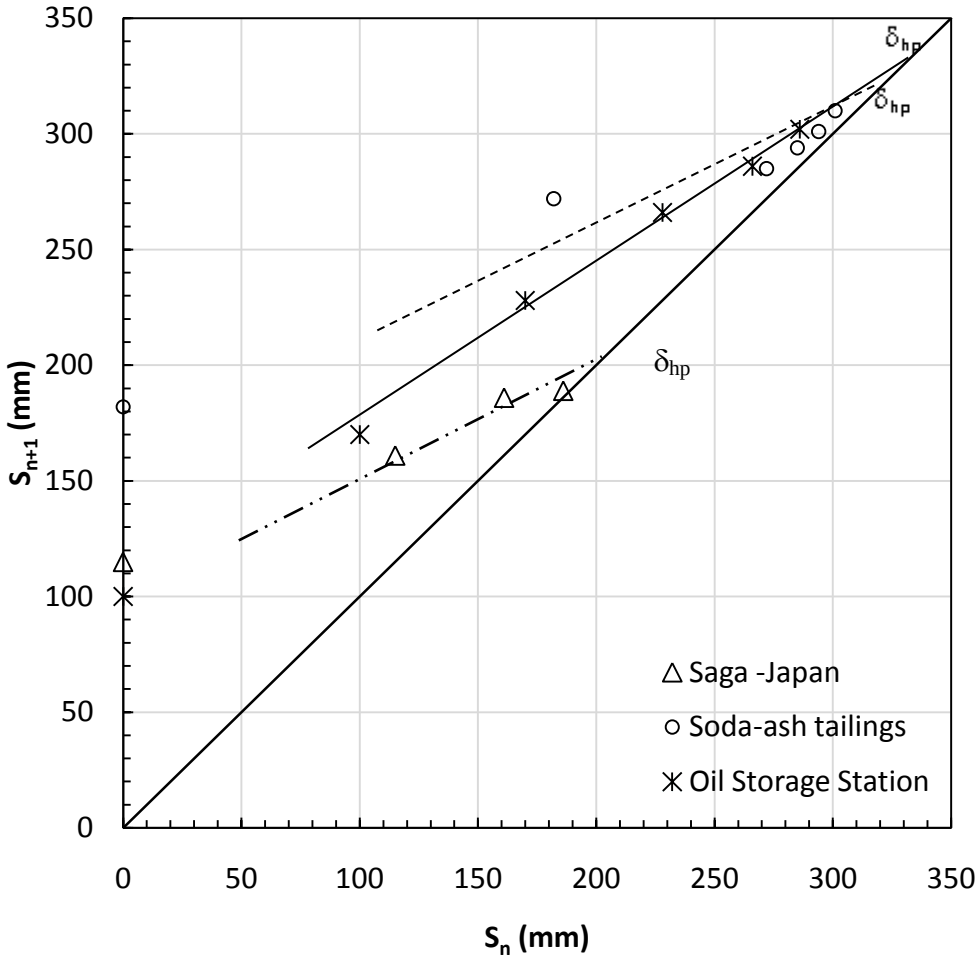

Figure 9.22: Application of the Asoaka method to predict lateral displacements (data from Shang and Zhang, 1999; Chu et al. 2000 and Chai et al. 2006)

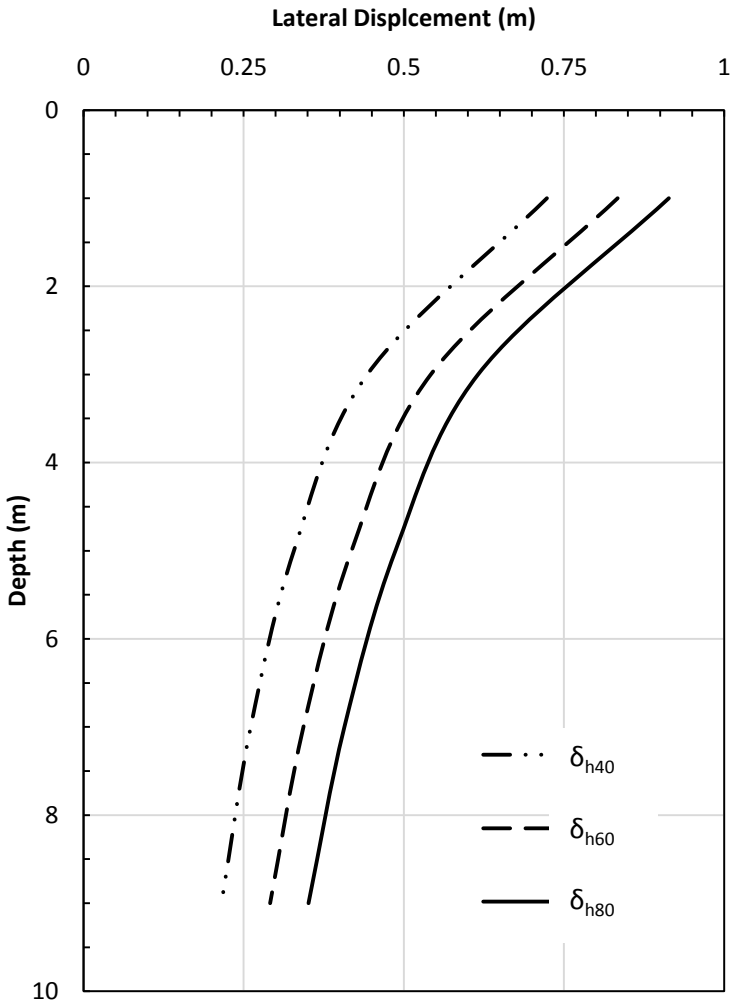

Figure 9.23: Lateral displacements at boundary of the treatment area due to consolidation movements only, under vacuum pressure of 40, 60 and 80kPa.

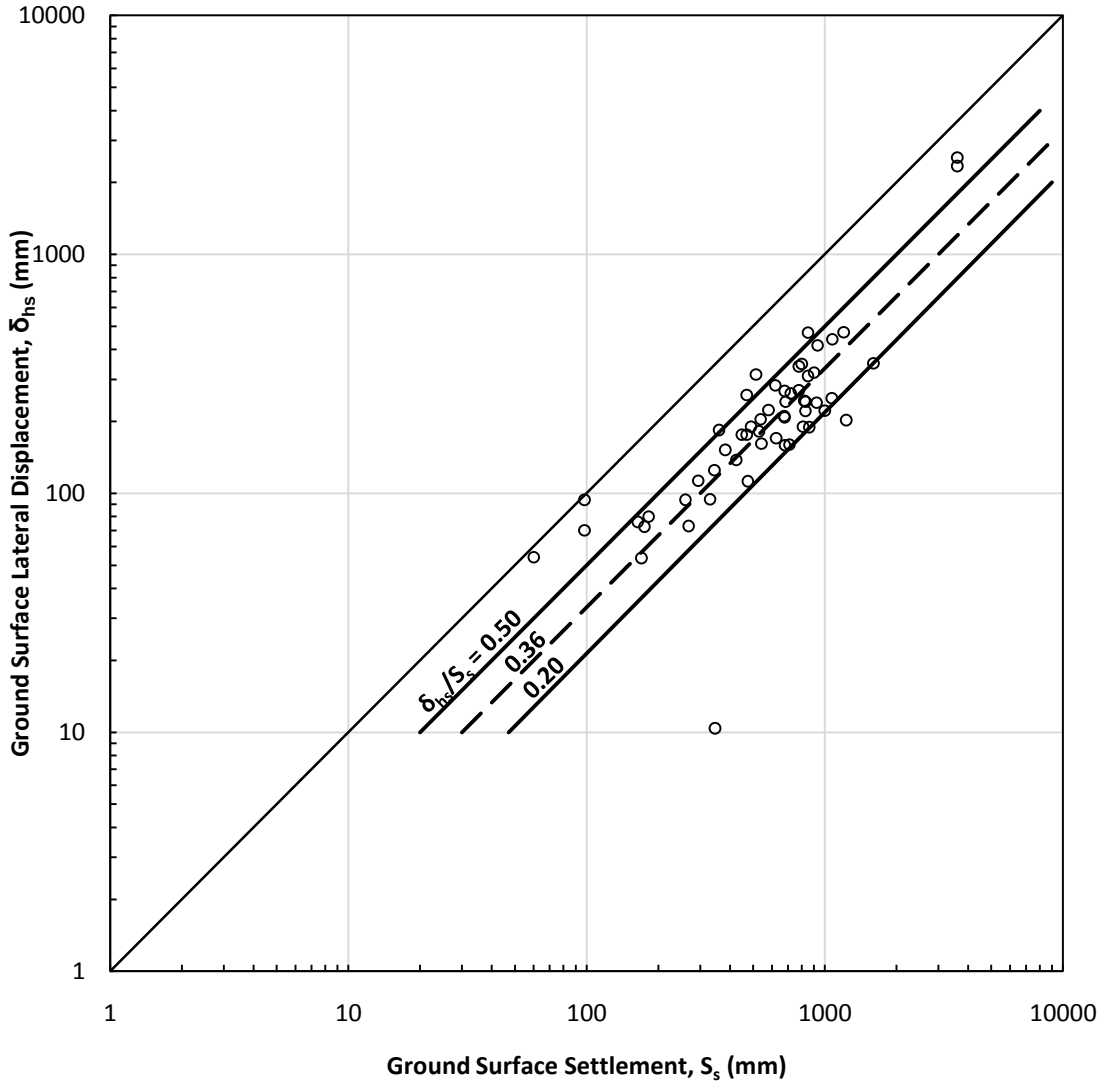

Figure 9.24: Ground surface lateral displacements, δ_{hs}, plotted against ground surface settlements, S_s at various times (data from 9 case histories)

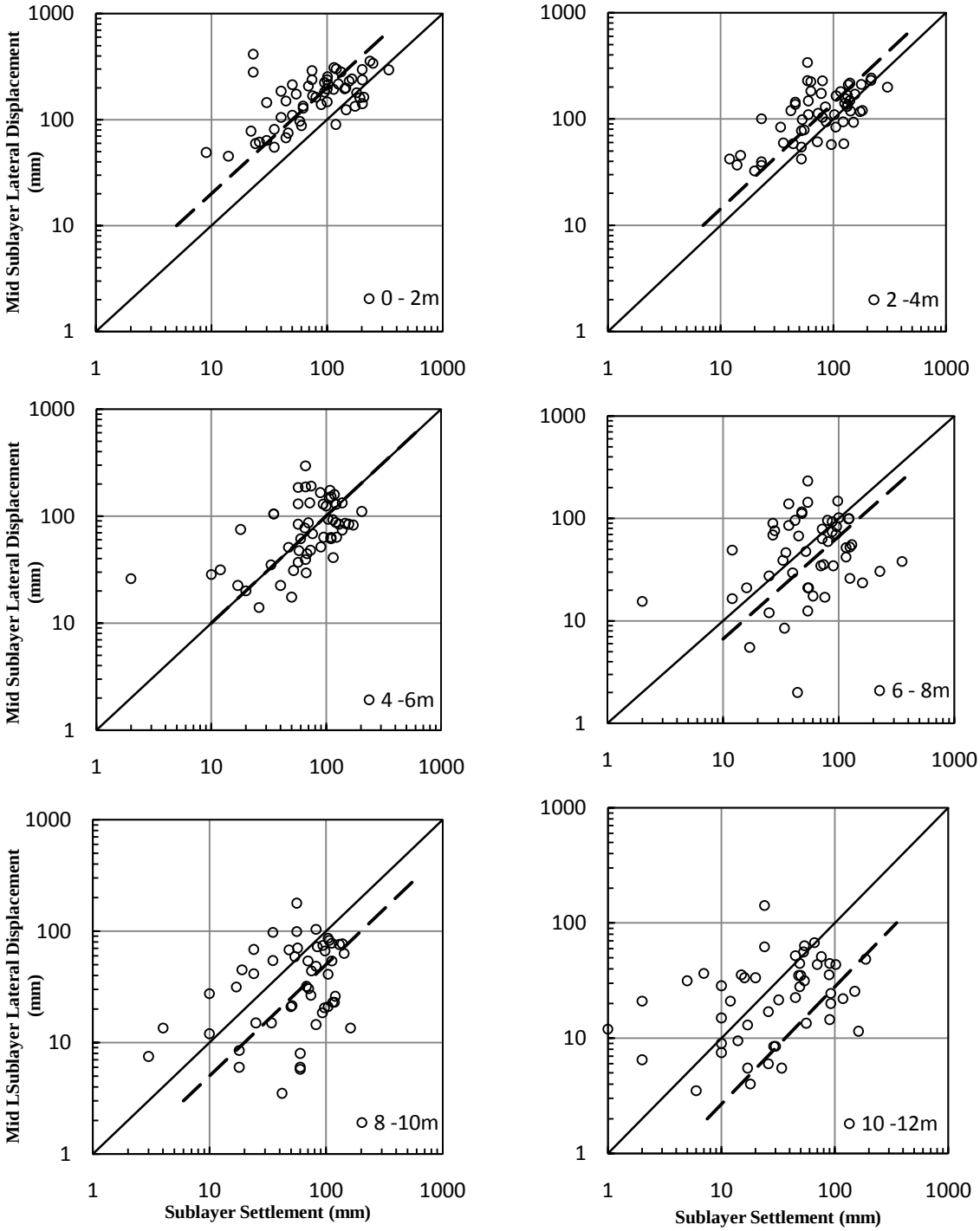

Figure 9.25: Mid sublayer lateral displacement plotted against sublayer settlement (data from 9 case histories)

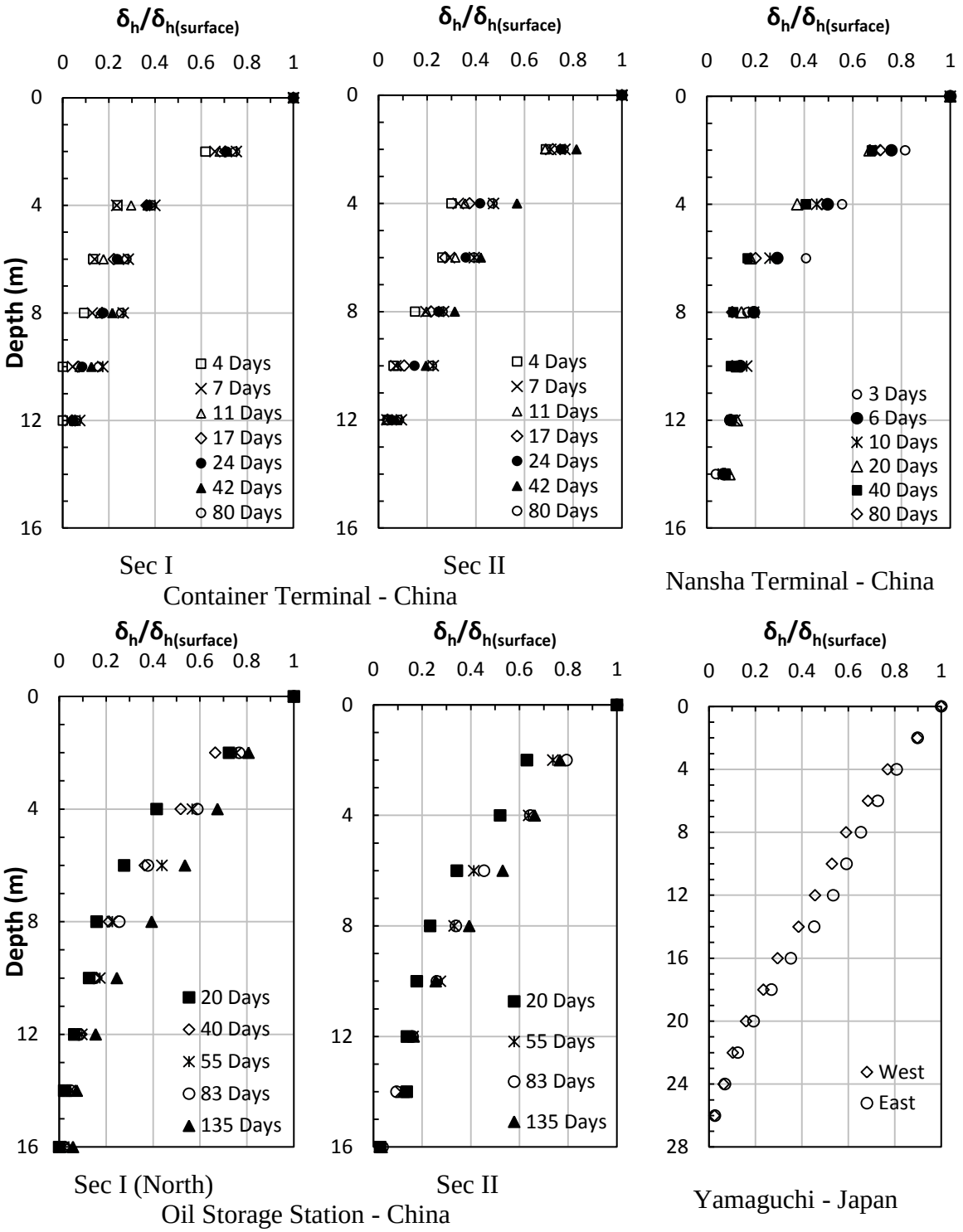

Figure 9.26: Normalized lateral displacements at different depths and at different times (Data from 9 case histories)

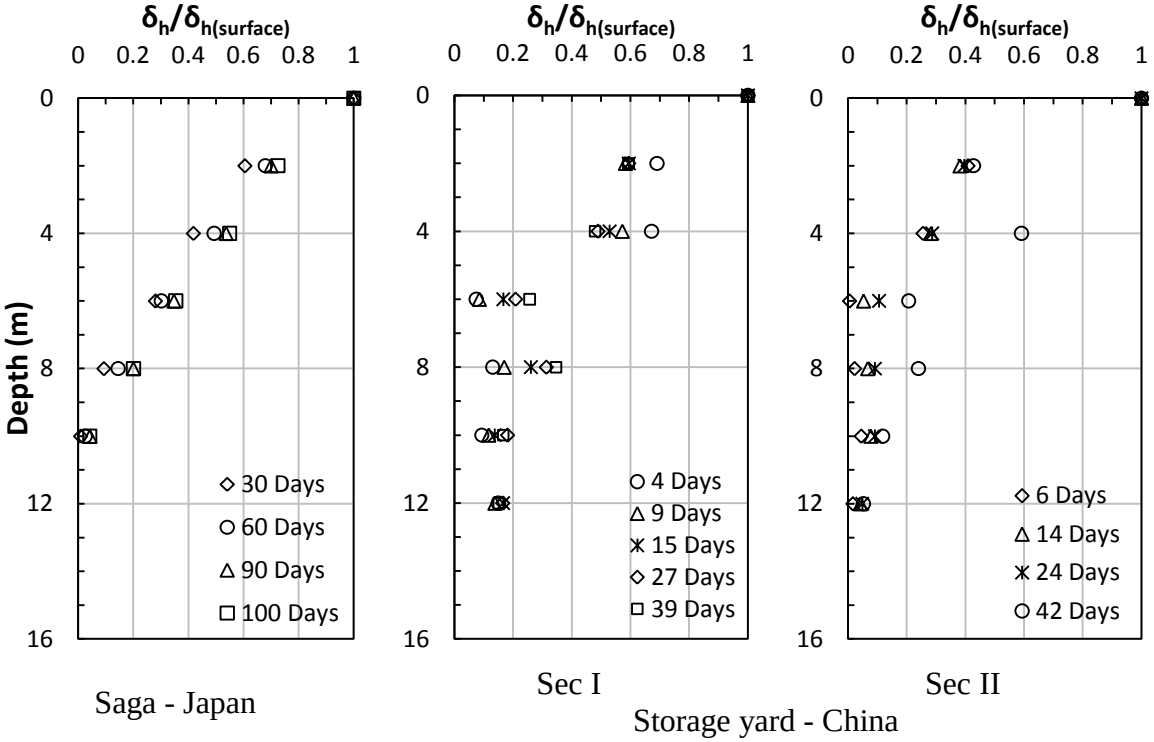

Saga - Japan

Sec I

Sec II

Storage yard - China

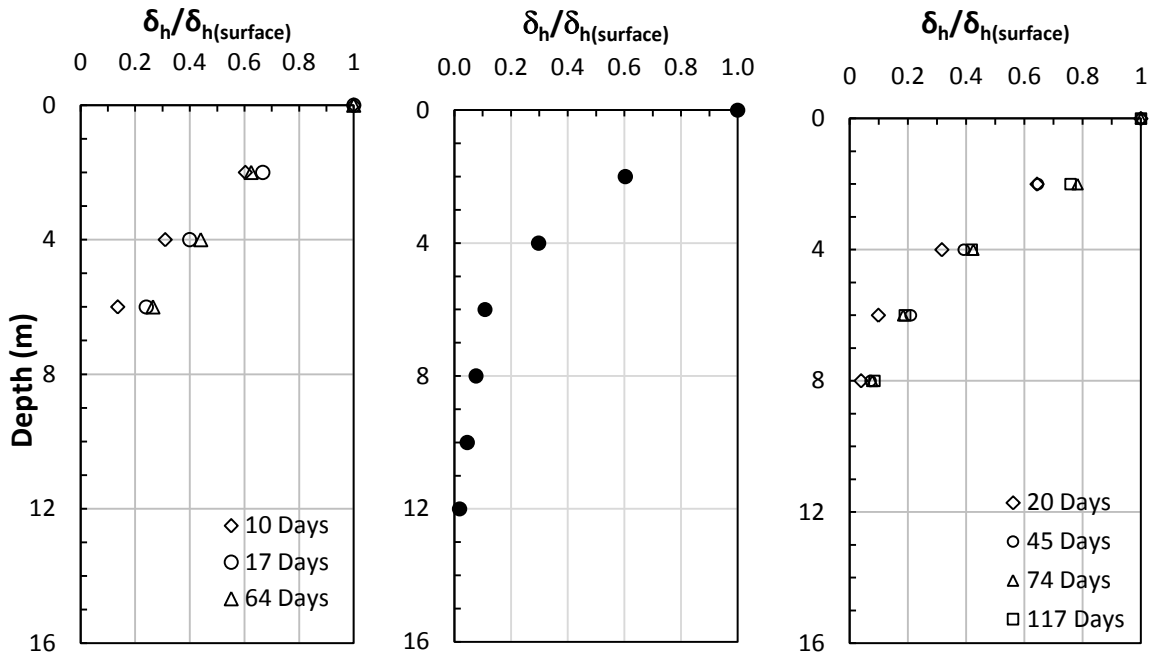

Soda-ash Tailings - China

Sanriku Ota test embankment - Japan

Field trial - Korea

Figure 9.26: Continued

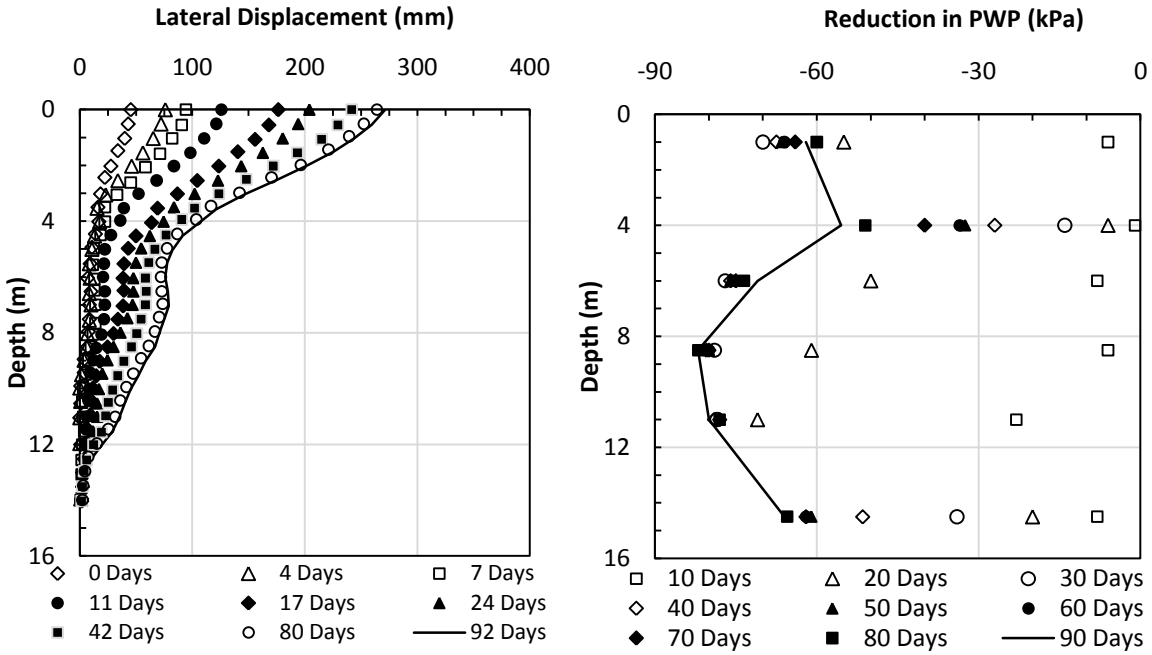

a. Section I

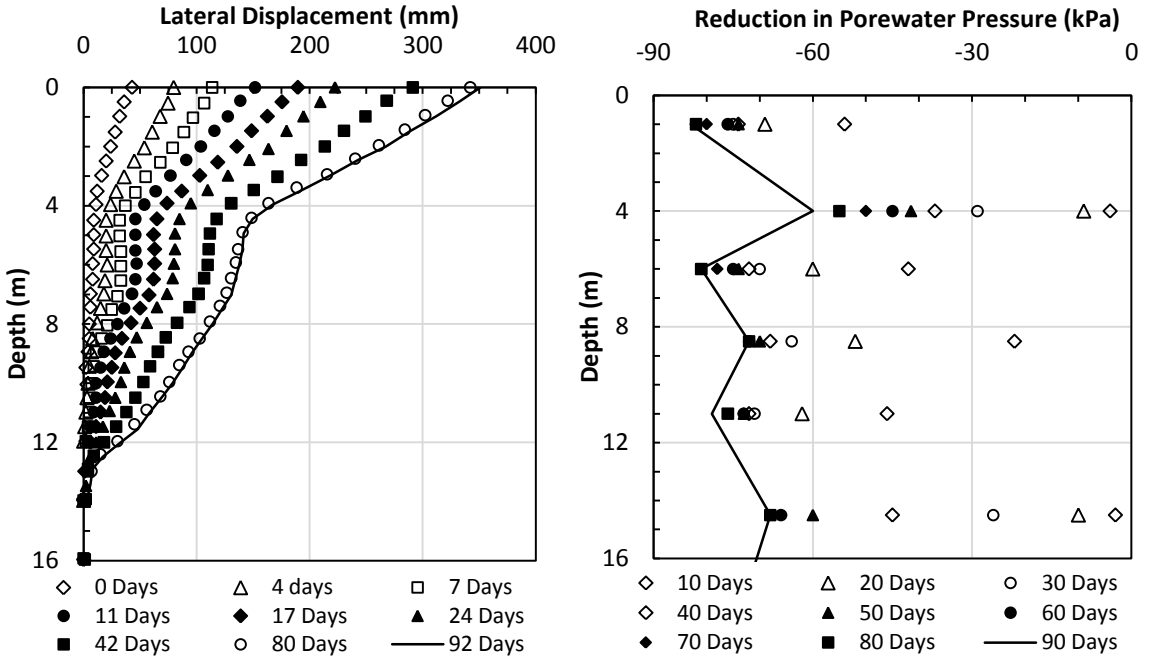

b. Section II

Figure 9.27: Observed lateral displacements and reductions in porewater pressure with depth at different times, due to vacuum preloading in (a) Section I and (b) Section II (data from Yan and Chu, 2003).

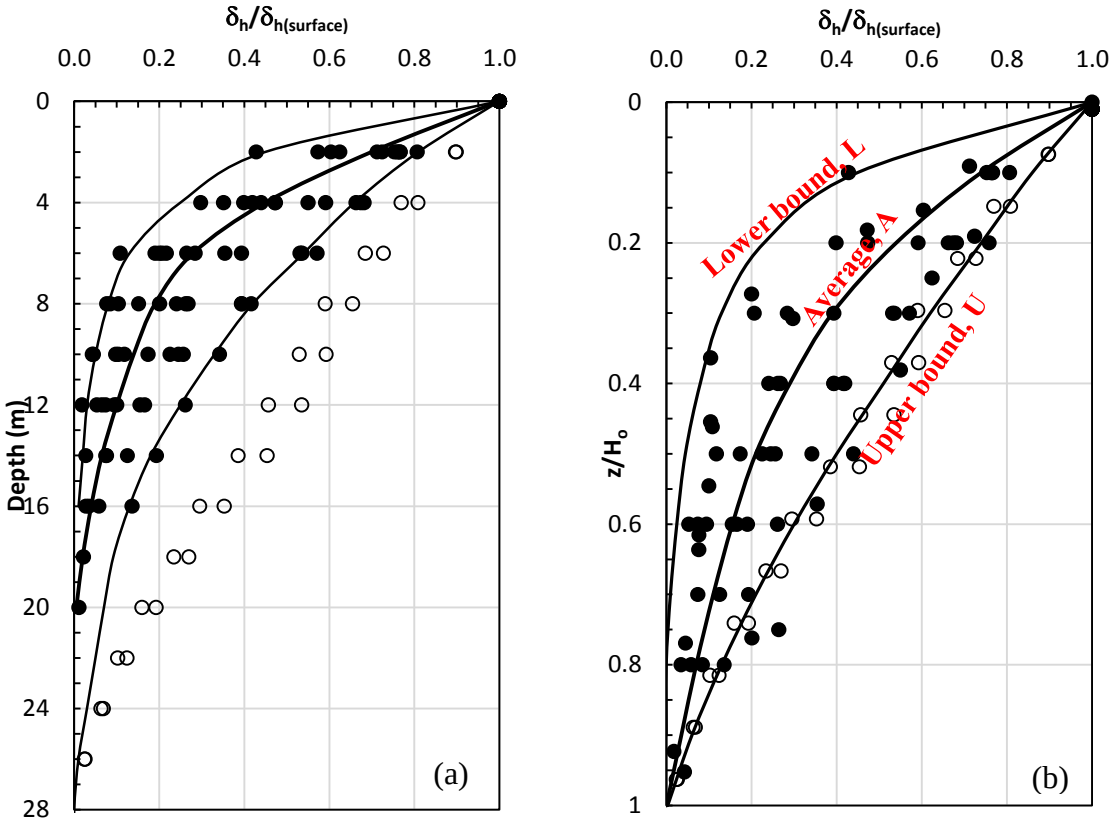

Figure 9.28: Normalized lateral displacements (a) with depth and at different times, and (b) with normalized depth (z/H_o) at different times (Data from 9 case histories).

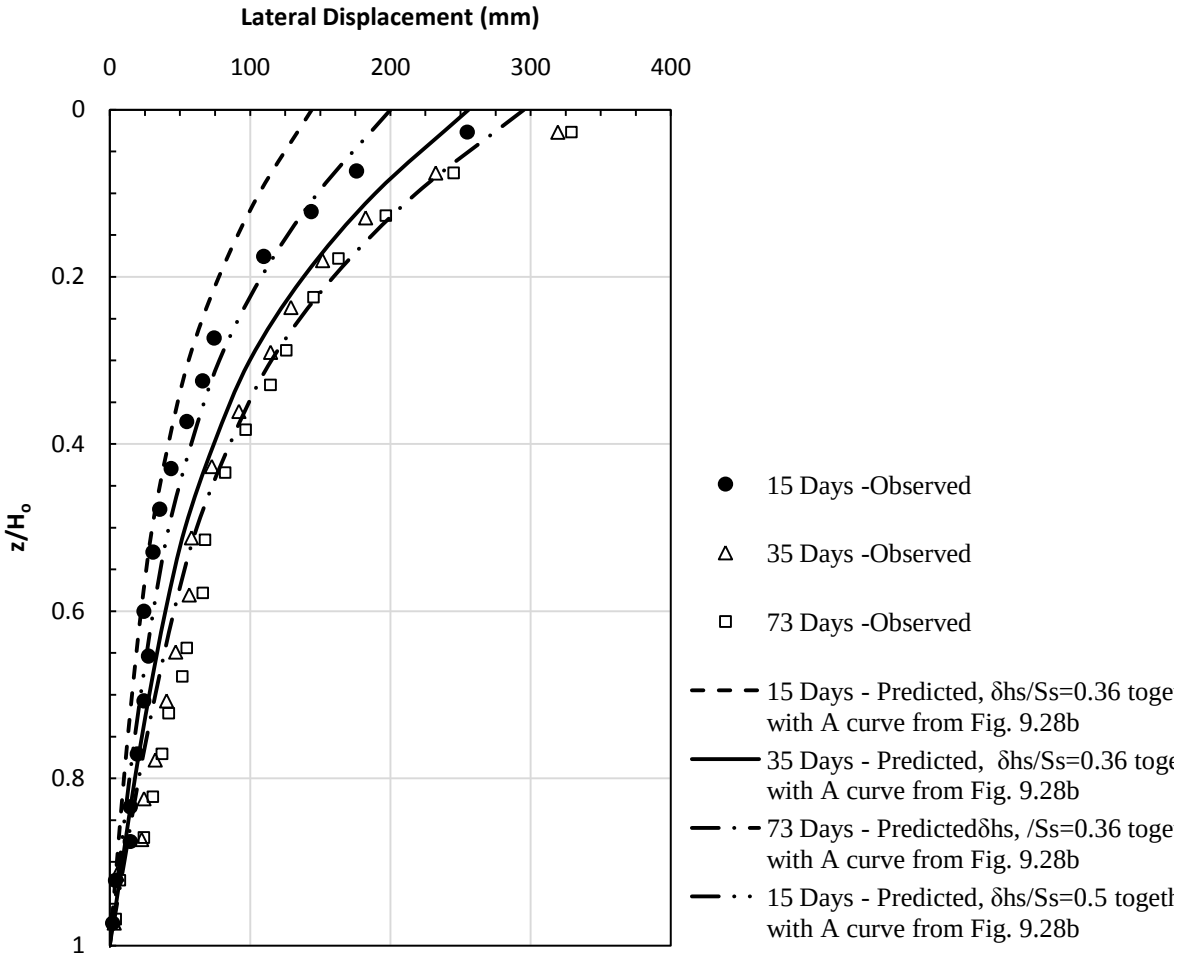

Figure 9.29: Comparison of observed and predicted lateral displacements at different times and at different depths for Zhuhai power station (data from Yixiong, 1996b).

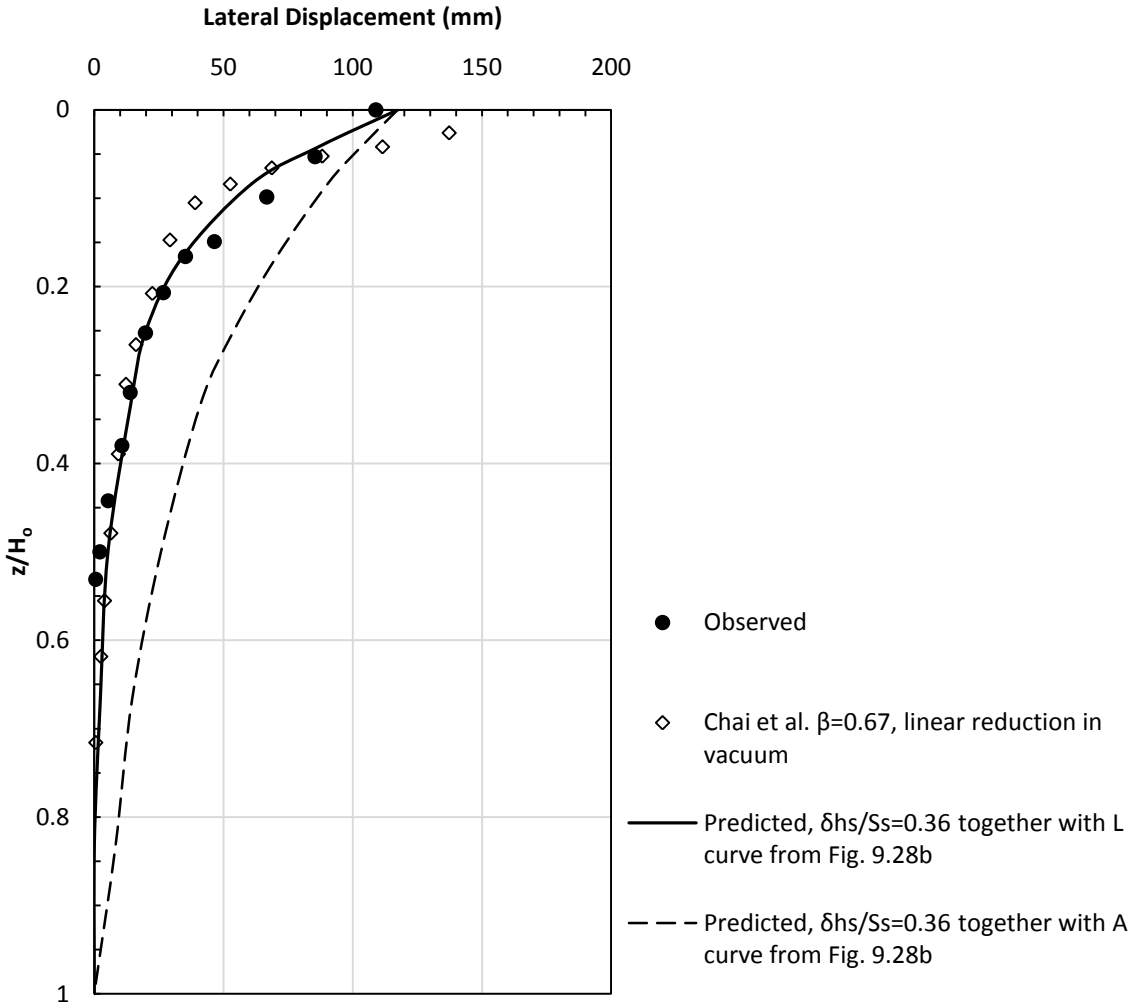

Figure 9.30: Comparison of observed and predicted lateral displacements for Yaoqiang airport runway site (data from Tang and Shang, 2000).

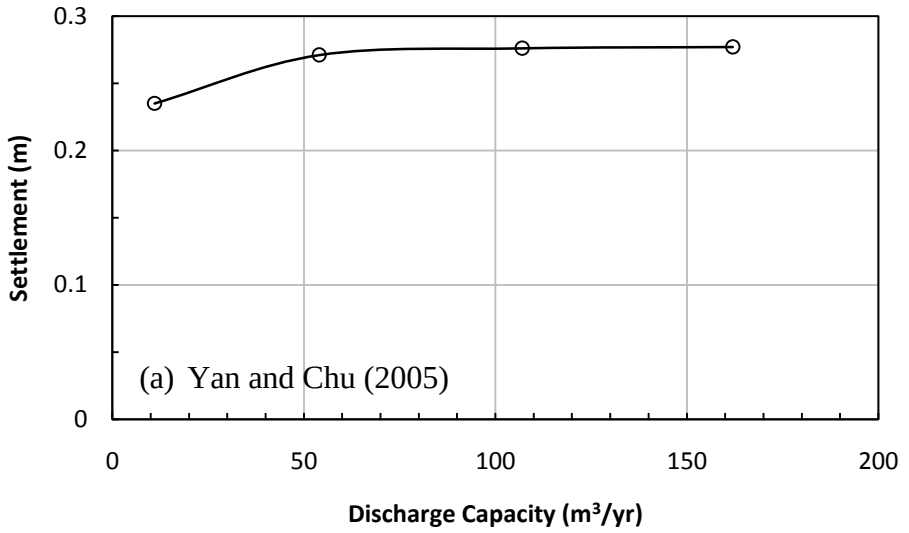

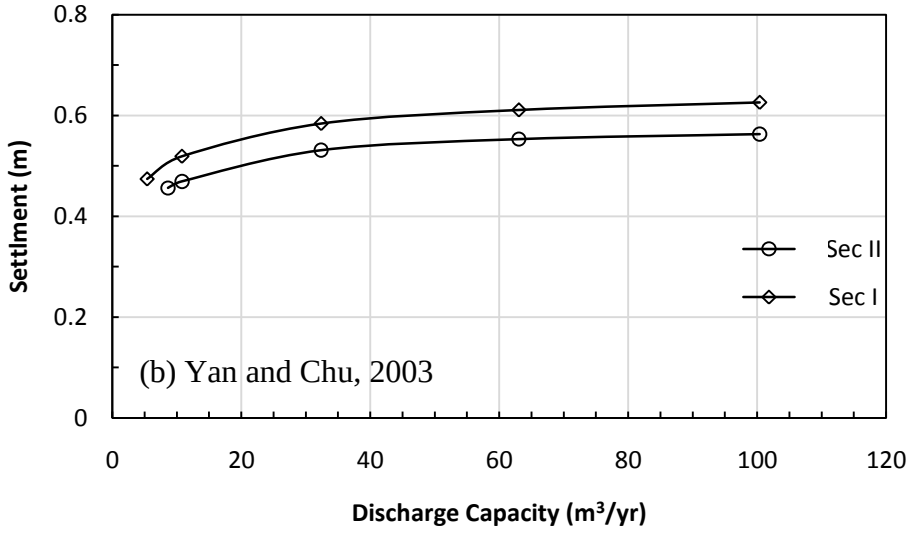

Figure 9.31: Evaluation of minimum discharge capacity of vertical drains for two case histories of vacuum and vacuum-fill preloading using ILLICON

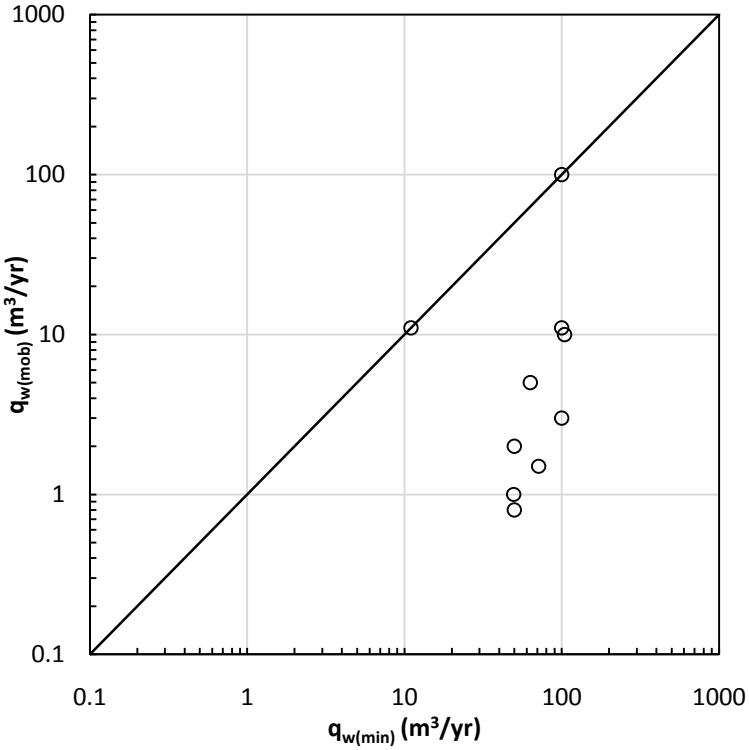

Figure 9.32: Comparison of minimum and mobilized discharge capacities for different case histories

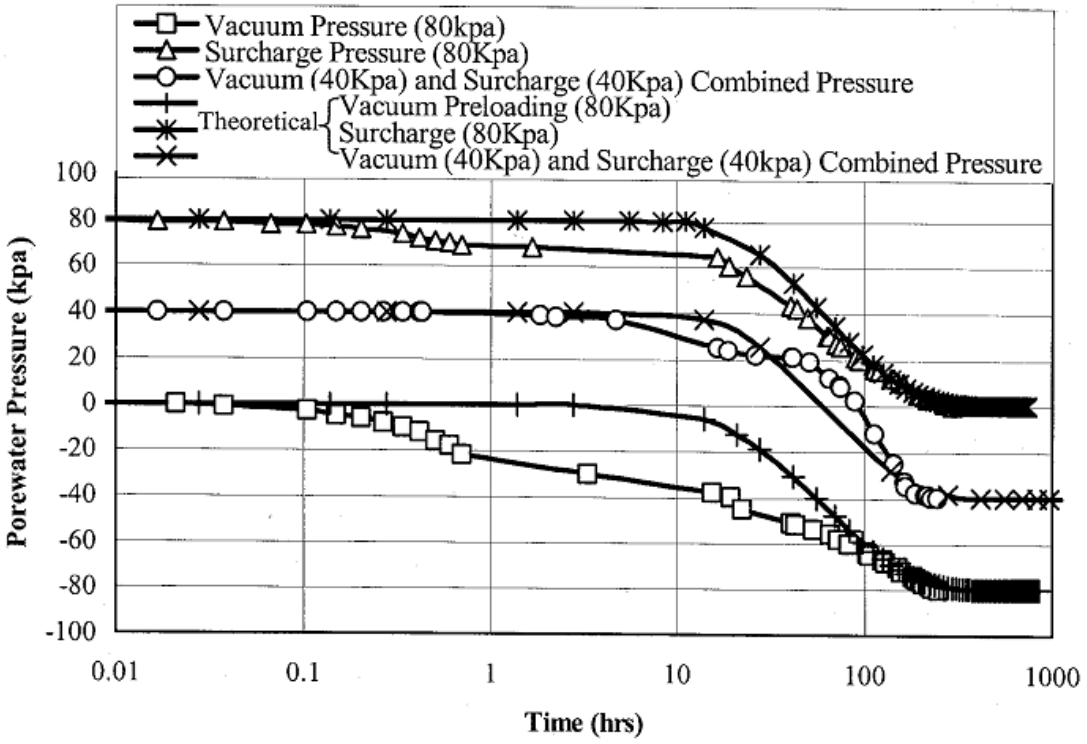

Figure 9.33: Porewater pressure dissipation for specimens subjected to vacuum, fill, and combined vacuum-fill loads (after Mahfouz et al. 2005)

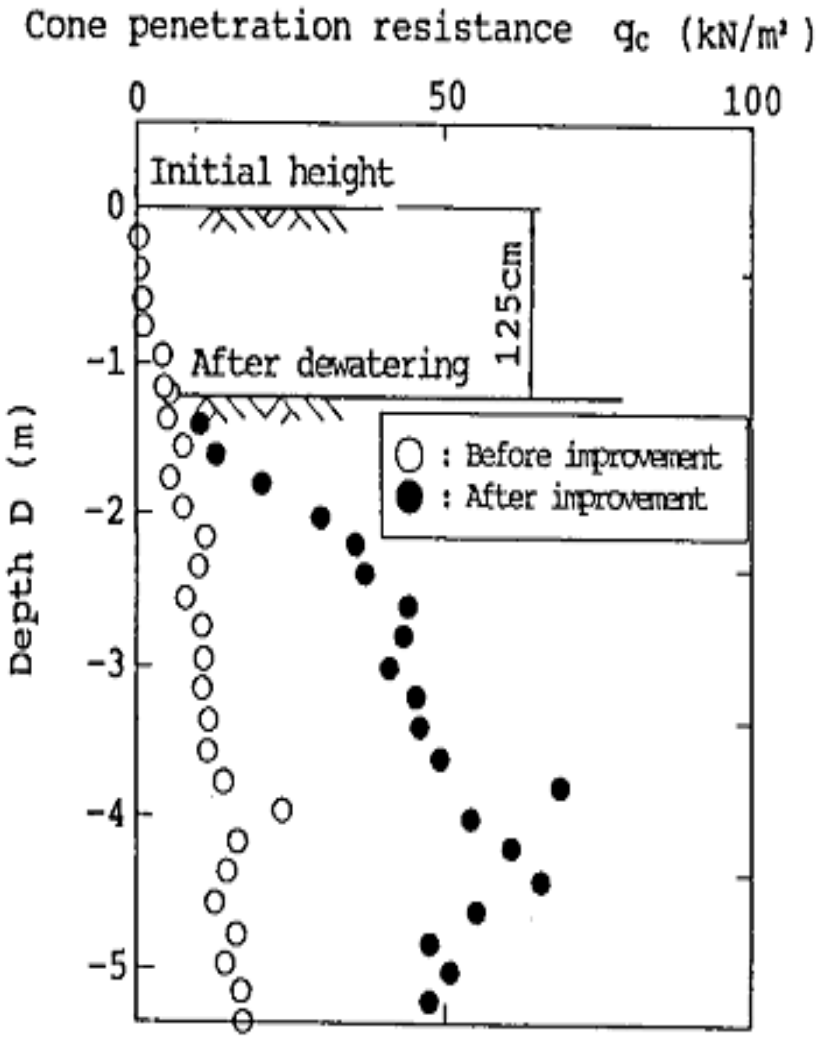

Figure 9.34: Improvement in shear strength of a sea bed clay due to vacuum preloading (after Shinsha et al. 1991)

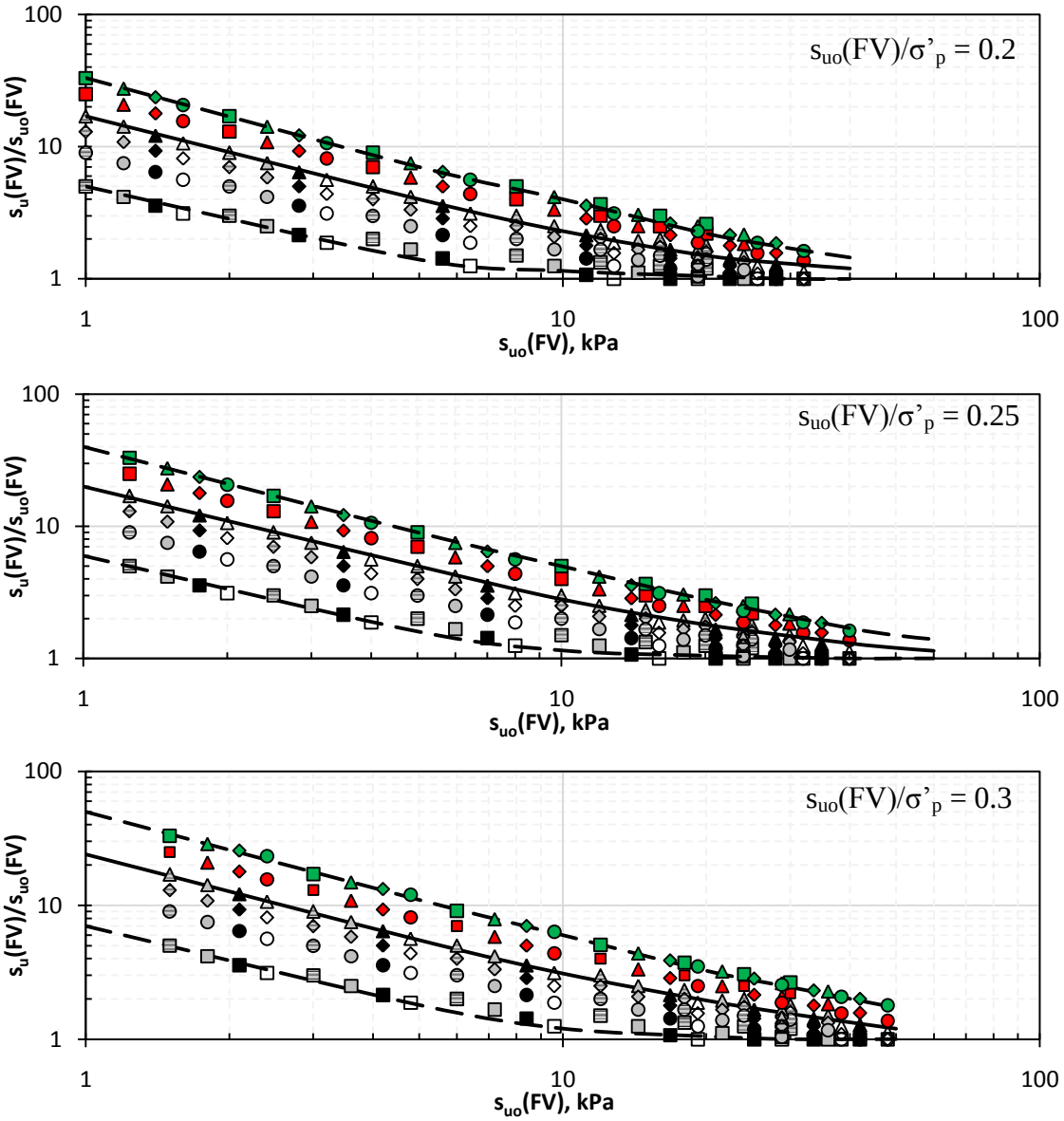

σ'_p / σ'_{vo}	$\Delta\sigma'_v$ (kPa)					
	20	40	60	80	120	160
1						
1.2						
1.4						
1.6						

Figure 9.35: Theoretical increase in vane shear strength plotted against initial vane strength for a soil deposit with $s_{uo}(FV)/\sigma'_p = 0.3$ and $\Delta\sigma_v$ =80kPa, for different values of σ'_p/σ'_{vo}.

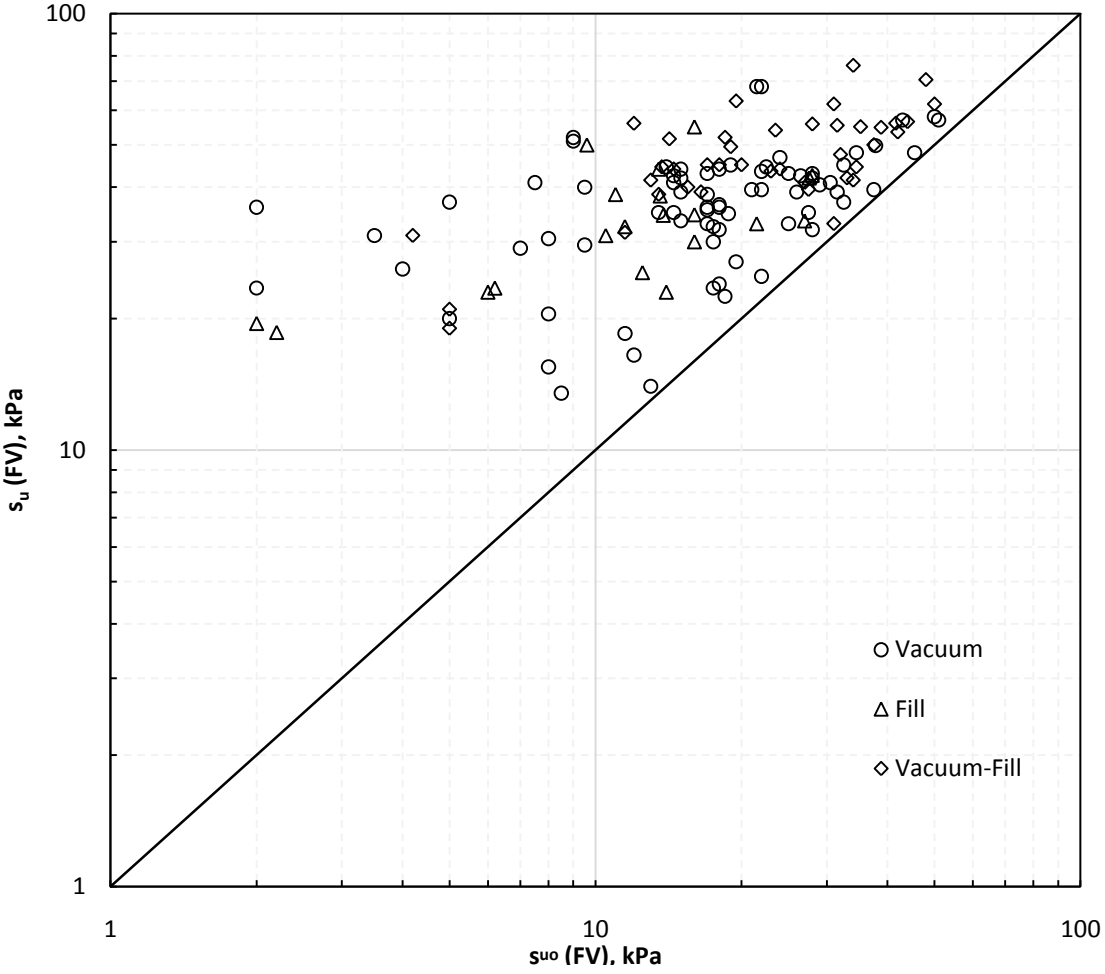

Figure 9.36: Field vane shear strength before and after improvement (data from 11 case histories)

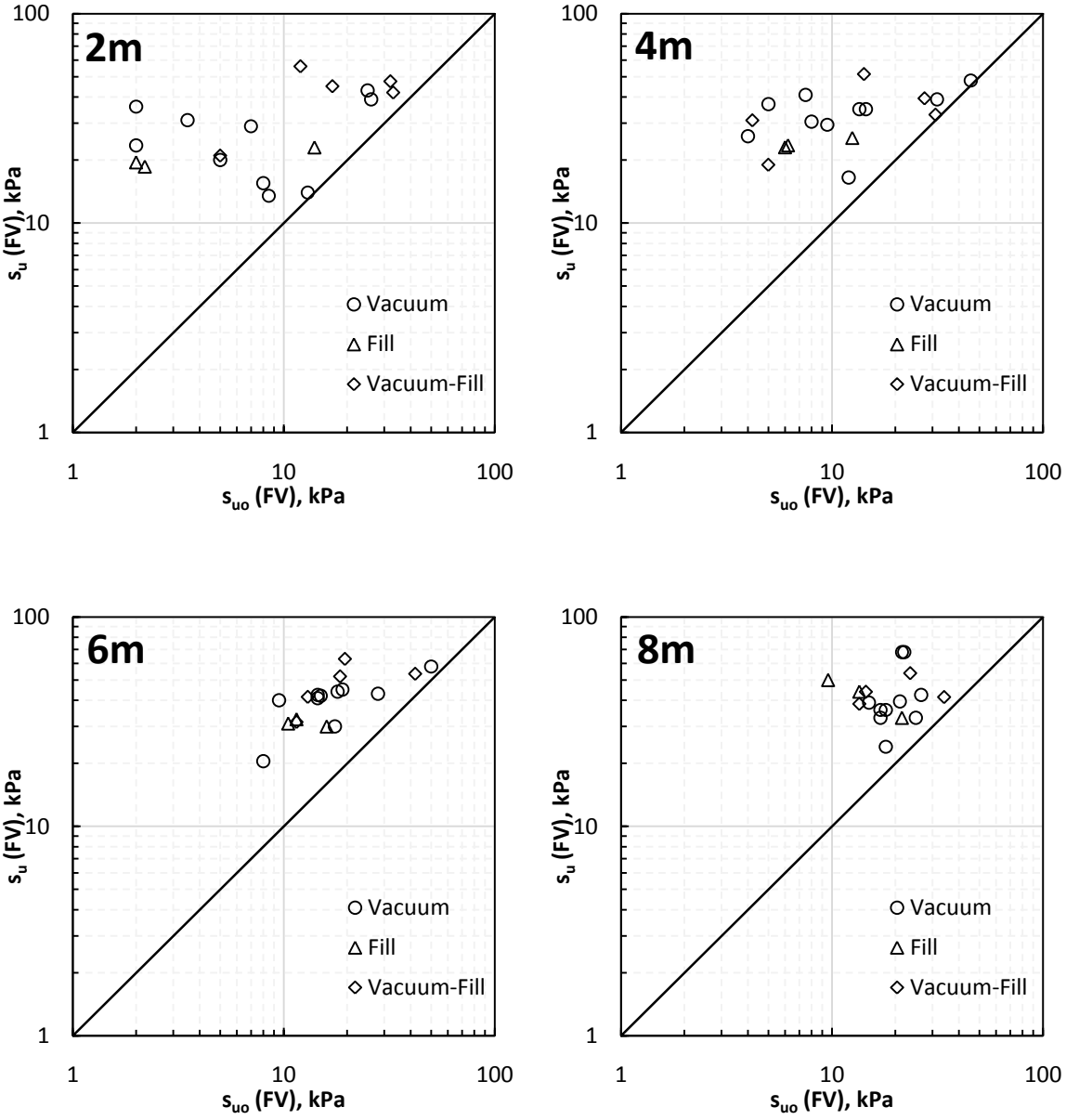

Figure 9.37: Field vane shear strength before and after improvement at different depths (data from 11 case histories)

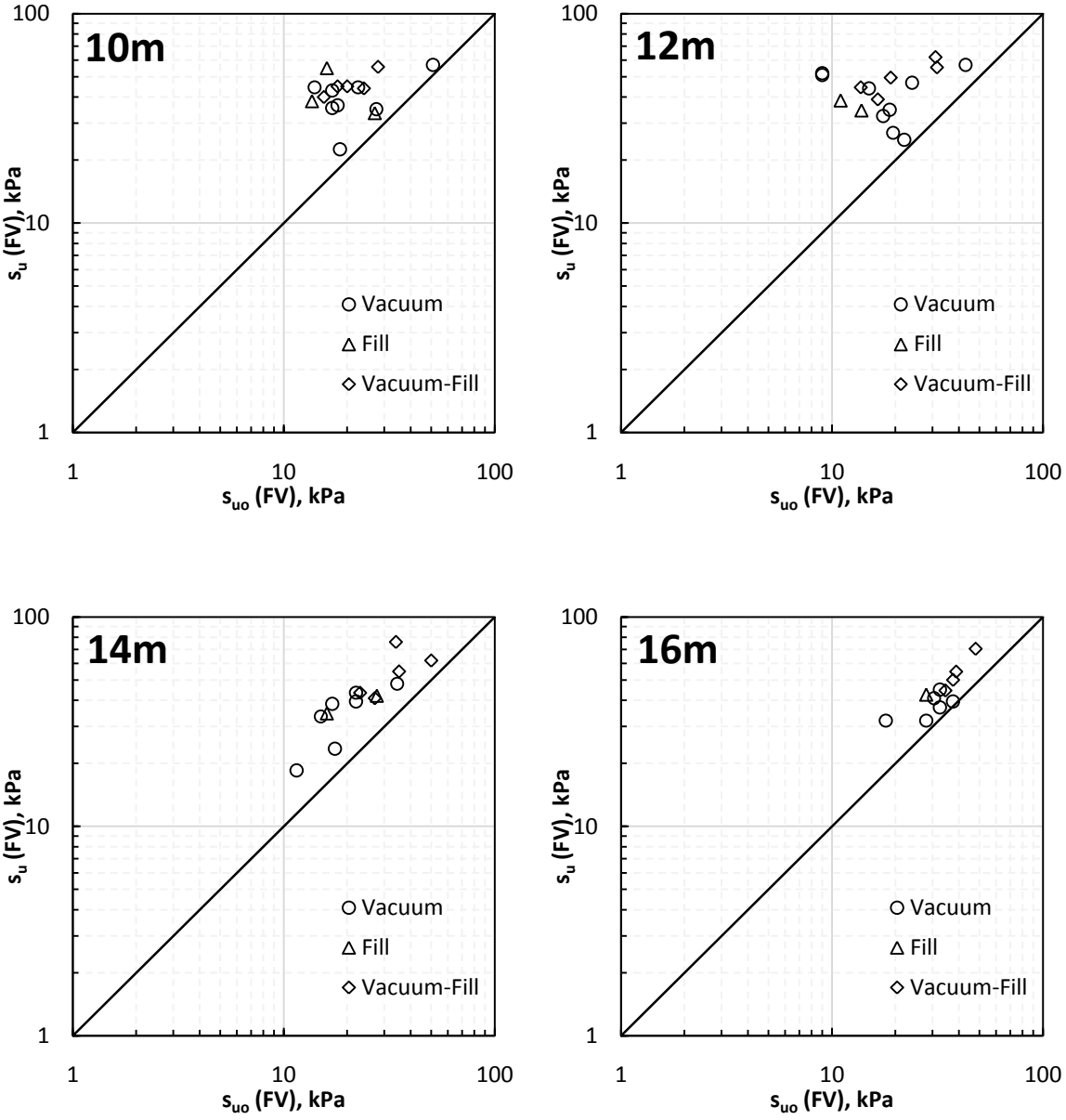

Figure 9.37: Continued

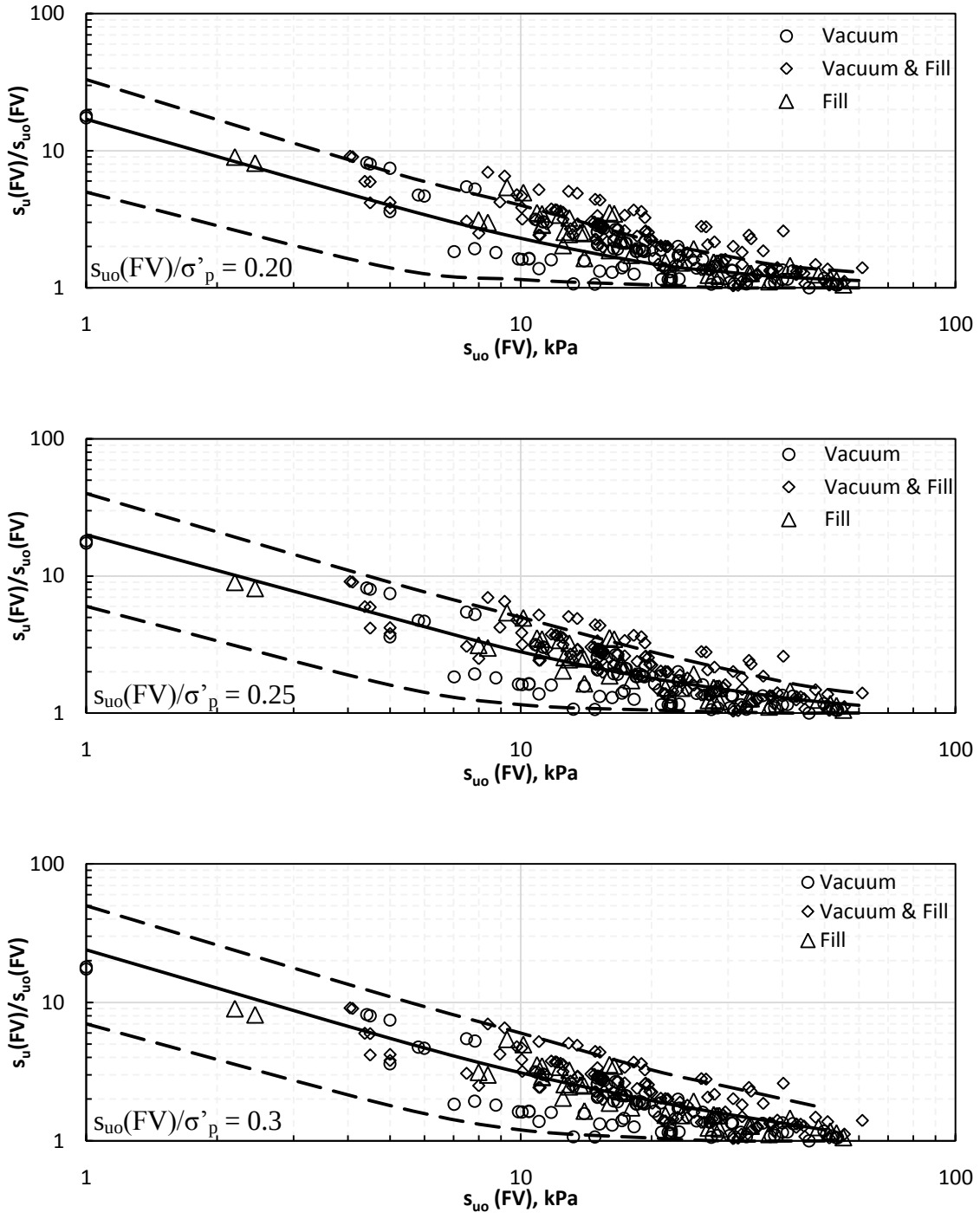

Figure 9.38: Ratio of increase in vane shear strength plotted against initial vane shear strength together with average, upper and lower bound lines from Fig. 9.35 (data from 11 case histories)

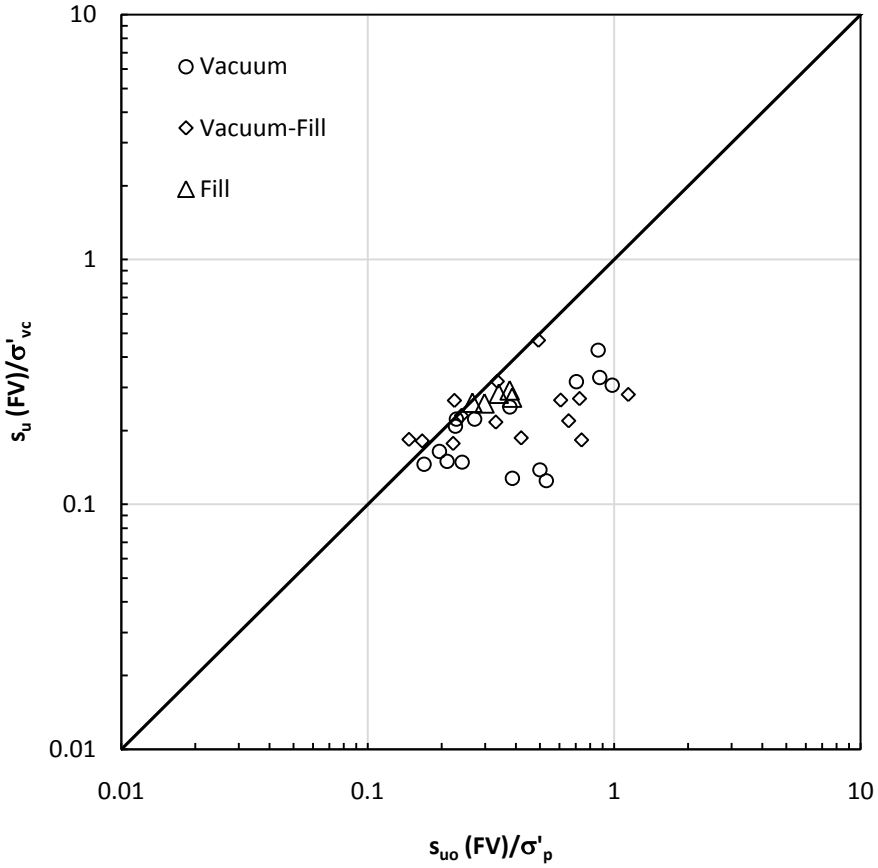

Figure 9.39: Vane strength after treatment normalized with respect to consolidation pressure plotted against initial vane strength normalized with respect to preconsolidation pressure

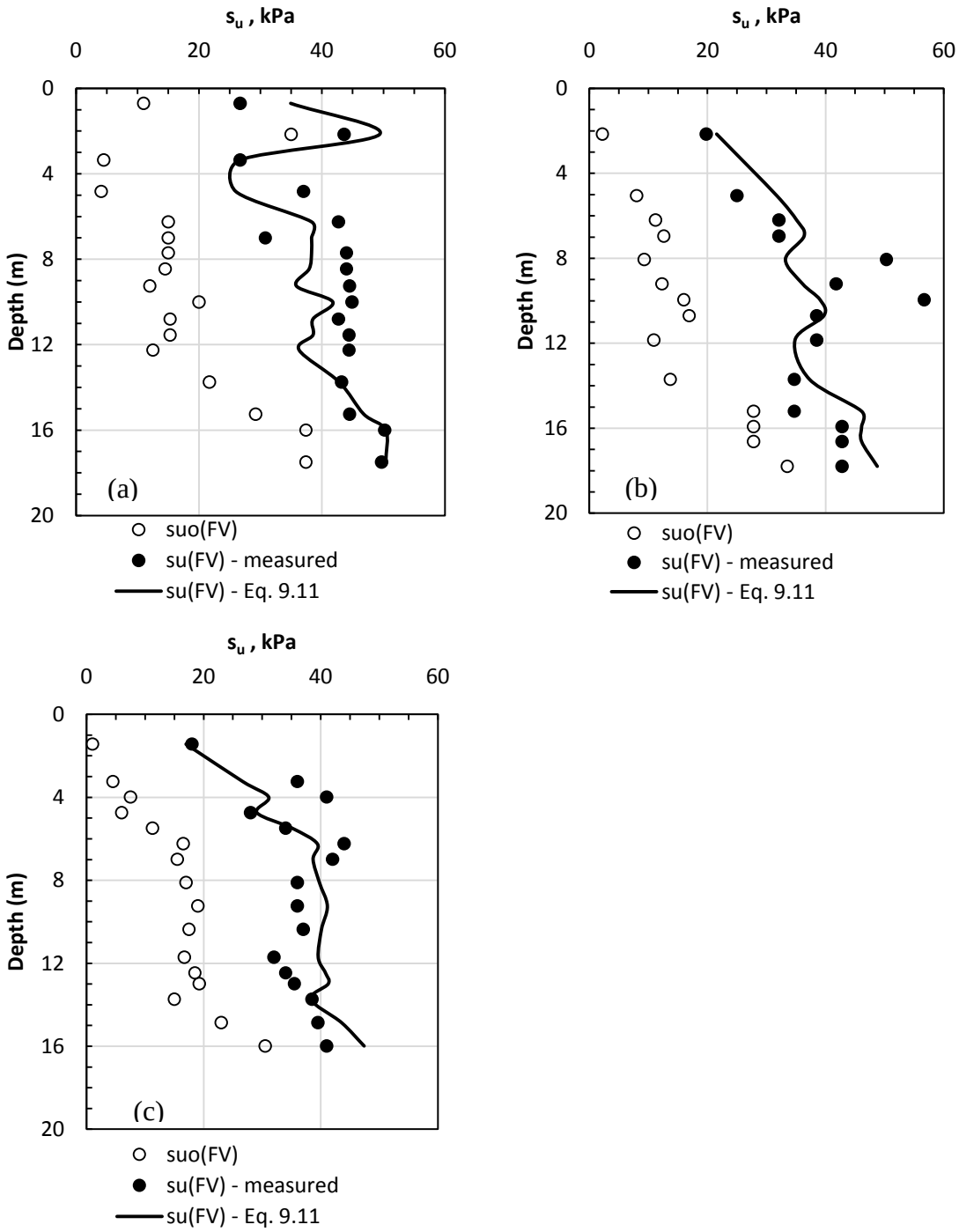

Figure 9.40: Measured and predicted increase in vane strength for (a) vacuum-fill load, (b) fill load, and (c) vacuum load (data from Yixiong 1996b and Shang et al. 1998).

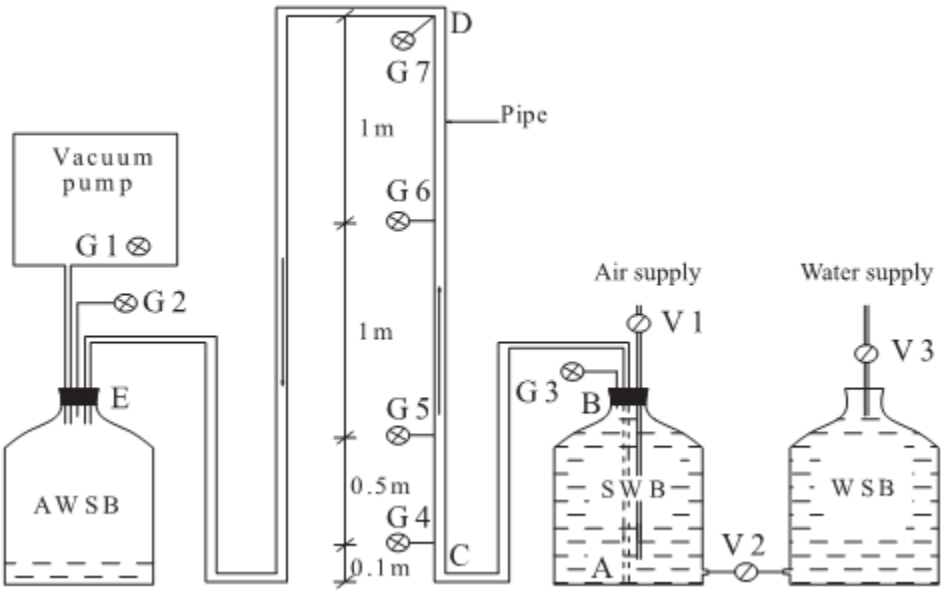

Figure 9.41: Experimental setup for measurement of single and two-phase flow (after Qiu et al. (2007).

CHAPTER 10. DESIGN EXAMPLES

10.1 Introduction

It is always desirable to complete the preloading operation within minimum possible time to proceed with construction at the site; however, poor subsurface conditions and stability issues often govern the rate of ground treatment, including preloading. Therefore, a fill load is often placed in stages to safeguard against excessive deformations and bearing capacity failure. As the vacuum load increases the effective stress without imposing shear stresses (as explained in Chapters 2 and 9), it can be applied with full intensity in a single stage. This not only reduces the time of preloading but also helps in quick construction of fill load when a preload in excess of 80kPa is required for precompression. A number of case histories have been reported in the literature where the use of vacuum enabled speedy subsequent construction of fill to a height which otherwise could not have been achieved with fill preload alone (Masse et al. 2001; Dam et al. 2007; Wang and Law 2007; Indraratna et al. 2009 etc.). However, it must be realized that the increase in effective stress due to vacuum is not instantaneous, instead the applied vacuum usually become effective within the drainage system in about 7 to 15 days and then it is gradually transmitted to the soil with time. It is therefore necessary to evaluate the increase in effective stress and associated increase in undrained shear strength with time, due to vacuum preload, so as to add the subsequent fill load without endangering the stability. A simple procedure based on case histories of vacuum, vacuum-fill consolidation is proposed for the design of preloading.

10.2 Proposed Design Procedure

A preloading effort is usually based on the anticipated structure loads to be subsequently applied to the ground, geotechnical properties of soil deposit to be improved, post construction settlement criterion and the time available for preloading. Because the proposed procedure is based on actual case histories, the above variables including spacing of vertical drains are directly adopted from the relevant case histories and therefore, are not discussed in detail in the present study. Following procedure is proposed for design of preloading with or without incorporating vacuum as a load:

10.2.1 Step I

Determine the geotechnical properties including compressibility and permeability characteristics of the soil being treated. This is usually done by carrying out soil investigations including insitu and laboratory testing. For the purpose of back-analysis, the required data were extracted from the associated literature and the missing data were estimated using empirical procedures as described in Chapters 3 to 8.

10.2.2 Step II

Estimate the settlement under the design load (take into account the post construction settlement criterion) to determine the preloading effort required. If the preloading effort required is less than 80kPa, vacuum can be used alone; however, for higher preloads, the additional load is provided by adding an embankment fill.

10.2.3 Step III

Carry out stability analysis to ascertain the present factor of safety and the preload that can be applied without causing instability (computer program XSTABL has been used in the present study for stability analysis). As the preload applied is temporary, a minimum factor of safety of slightly higher than unity is considered sufficient during the preloading operation. Because vacuum does not create instability, preliminary stability analysis is not required if vacuum is used alone or as a first stage preload; however, stability analyses would be required for subsequent fill loading stages.

10.2.4 Step IV

Estimate the degree of consolidation at various times for different spacing of vertical drains. Decide on the drain spacing keeping in view the average degree of

consolidation ($\bar{U}$) achieved in a particular time as well as any time restrictions for completion of the project. In the present study, computer program ILLICON was used to estimate the average degree of consolidation at different times; whereas, the drain spacing has been adopted from actual case histories.

10.2.5 Step V

Compute the increase in undrained shear strength using Eq. 10.1 (Terzaghi et al. 1996):

$$s_u(mob) = 0.22 * \sigma'_{vc} \tag{10.1}$$

where, σ'_{vc} is the sum of σ'_{vo} and the increase in effective stress corresponding to the average degree of consolidation at that time. For example, if 30kPa fill preload was applied in the first stage and the next stage preload is to be added after $\bar{U}$ = 60%, the increase in effective stress would be 18kPa (0.6*30). The stability analysis is carried out with undrained shear strength computed from Eq. 10.1 to determine the additional load that can be applied for a factor of safety of unity. Note that if for any sublayer, $\sigma'_{vc} \leq \sigma'_{p}$, use $s_{uo}(mob) = 0.22*\sigma'_{p}$ in the analysis.

10.2.6 Step VI

Repeat steps IV and V till the designed height of embankment is achieved.

10.3 Design Example I - Ballina Bypass, Australia

10.3.1 General

Vacuum consolidation in combination with fill preloading was used to improve subsoil for a highway construction near Ballina, Australia. The soft layer was up to 40m thick and consisted primarily of highly compressible saturated marine clays (Indraratna et al. 2009). At the project site, the compressible layer had a thickness of 1m to 25m (Kelly and Wong, 2009). Due to variable thickness of the soft layer, different preloading effort was required in different sections of the treatment area. In addition to vacuum intensity of 70kPa, a fill load of 80 to 180kPa was required to induce the desired precompression in different sections. In the following sections, vacuum-fill preloading of one of the sections is described and the proposed procedure is compared with the actual embankment construction in the field.

10.3.2 Design Parameters

The thickness of compressible layer in the selected section was 25m (Indraratna et al. 2009). The vertical profile of various soil properties is shown in Fig. 10.1. Figures 10.2 and 10.3, respectively, show the compressibility and permeability characteristics of the soft soil. The vertical profile of natural water content (w_o) shown in Fig. 10.1b suggests that the vertical profile of initial void ratio may be slightly different than what is shown in Fig. 10.1c; however, to remain consistent, the soil properties and other related data obtained from Indraratna et al. (2009), Kelly et al. (2008), and Kelly and Wong (2009) have been used as such in the ILLICON analyses. Whenever required, methods described in Chapters 3 to 8 were used to compute/estimate the input data required for the analyses but not reported in the associated literature. Figure 10.4 shows the results of preliminary settlement analyses carried out using computer program ILLICON. It is important to point out that Indraratna et al. (2009) and Kelly and Wong (2009), respectively, reported a period of 100 days and 114 days between the commencement of preloading operation (placement of sand blanket) and application of vacuum. For the preliminary settlement analysis, loading schedule and measured settlements were adopted from Indraratna et al. (2009). It can be seen from Fig. 10.4 that (1) for the adopted parameters ILLICON prediction is reasonable, and (2) the vertical drains (vacuum transmission pipes in this case) performed with significant well resistance.

A preload of 250kPa was required to induce the desired precompression. A vacuum load of 70kPa was accounted for in the design and the remaining load was to be applied by constructing a 9m high embankment over the treatment area. Actual records, however, show that a vacuum load of 75kPa was applied and fill was constructed to a height of 8.5m (Indraratna et al. 2009; Kelly and Wong 2009) and therefore, the same has been used in the present analyses.

Vacuum transmission pipes (VTPs) with a diameter of 34mm were installed to a depth of 23.7m, in a square grid of 1m (Indraratna et al. 2009). It was shown in Section 9.7 that the vertical drains under vacuum preloading perform in a similar way as in case of fill preloading, i.e., irrespective of the type of load, the vertical drains may or may not be freely draining during any preloading operation. In this case the discharge capacity of

VTPs is estimated to be between 2 to 3m^3/yr. (Fig. 10.4). The analyses of other case histories of vacuum consolidation showed that the vertical drains generally performed with a discharge capacity of 1.5 to 11m^3/yr. (Fig. 9.32). Therefore, it is considered unreasonable to base the design of preloading by assuming the VTPs to be freely draining. The degree of consolidation was examined by using discharge capacities of 3 and 10m^3/yr.

10.3.3 Design of Preloading

The initial activities including thickness of sand blanket (1.5m thick in this case), time of installation of drains, and time of application of vacuum preloading etc., were adopted from Kelly and Wong (2009). A preliminary stability analysis using computer program XSTABL (Sharma 1996) showed that the factor of safety immediately after placing of the sand blanket was 1.02, which improved during 114 days required for installation of VTPs and vacuum system, to 1.08 before the application of vacuum. A vacuum pressure of 75kPa was applied in the second stage of loading (assuming sand blanket as the first stage of loading) which reached its full intensity in about 15 days (Fig. 10.4a). The results of ILLICON analyses for discharge capacities of 3m^3/yr. and 10m^3/yr., are shown respectively, in Figs 10.5 and 10.6. The effect of discharge capacity of vertical drains on the rate of fill construction is quite obvious from these figures. For example, after application of vacuum, a degree of consolidation (U_t) of 40% is achieved in 200 days for a discharge capacity of 3m^3/yr. (Fig. 10.5b), whereas, the same degree of consolidation is achieved in 145 days for a discharge capacity of 10m^3/yr. (Fig. 10.6b). The corresponding increase in undrained shear strength predicted using Eq. 10.1 resulted in improvement of factor of safety to 2.52; hence, for a higher discharge capacity of vertical drains, the additional fill load can be applied relatively quickly. Similarly, the progress of consolidation for the assumed discharge capacities is different for all stages of preloading; thus the fill can be constructed to desired height(8.5m in this case), respectively, in 210 days and 320 days for discharge capacity of 10m^3/yr. and 3m^3/yr. It is important to note that a discharge capacity of 10m^3/yr., which allows a faster rate of fill construction, closely predicts the construction schedule that was actually followed in the field (Fig. 10.6a); however, the measured settlements are is good agreement with those

predicted using a discharge capacity of $3m^3$/yr., which suggests a mobilized discharge capacity of $3m^3$/yr (Fig. 10.5c). Note that the removal of vacuum load in the field after an elapsed time of 382 days is not accounted for in the design of preloading; therefore, the settlements corresponding to discharge capacity of $3m^3$/yr. exceed the measured settlements towards the end of preloading operation. It appears that the factor of safety during actual fill construction might have dropped below unity as the fill was constructed at a rate which is higher than the rate which corresponds to a minimum factor of safety of unity.

It was shown in Chapter 5 that lateral displacements due to a combined vacuum-fill load counteract each other; however, the order of application and relative magnitude of applied vacuum and fill preloads should be considered. Figure 10.7 shows the vertical distribution of lateral displacements from two case histories of vacuum-fill preloading. It is important to point out that DGI Menard carried out ground improvement in these two cases as well as the Ballina Bypass, and the sequence of activities followed in these two cases were generally the same as in case of Ballina bypass. The magnitude of applied fill was significantly greater than the applied vacuum and the compressible layer was more than 20m thick in all three cases. It is therefore, reasonable to expect a similar trend in lateral displacements in all three cases. Figure 10.7a shows the lateral displacements resulting from a combined application of vacuum-fill preload during ground improvement for a sewage treatment plant (Song et al. 2004). It can be seen from Fig. 10.7a that the initial outward movements due to fill preload (sand blanket) alone were counteracted by application of vacuum and the net lateral movement near the ground surface was inward. As the fill load was increased, the lateral movement near the ground surface remained inward and kept on increasing even when the applied fill load (6.32m; 125kPa) exceeded the applied vacuum of 80kPa. However, below 2 to 3m depth, net outward movements were observed. The termination of vacuum resulted in a sudden increase in lateral displacements below 5m depth, however, the surface lateral movements remained more or less constant. Similarly, Fig. 10.7b shows the vertical distribution of lateral displacements at different times, for a highway construction project in France (Masse et al. 2001). In this case vacuum was used in combination with 7 to 9m

(140 – 180kPa) of fill preload. It can be seen that in this case also, the lateral displacements near the ground surface remained inward despite the fact that the magnitude of fill preload was more than the applied vacuum. Therefore, it is reasonable to expect net inward lateral movements near the ground surface during a combined vacuum-fill preloading.

For Ballina bypass project, the sequence of construction was same as in above mentioned two cases, i.e., placement of a sand blanket, installation of vertical drains, application of vacuum preload, and construction of fill. The fill construction began 17 days after commencement of vacuum (Kelly and Wong 2008). Figure 10.8a shows the vertical distribution of measured lateral displacements at various locations as reported by Indraratna et al. (2009); whereas Fig. 10.8b shows the lateral displacements at different times for inclinometer, I3. The layout of treatment area and locations of various inclinometers (Fig. 1 of Kelly et al. 2008) suggest that the data from inclinometers I4 are representative of the subarea being analyzed in Section 10.3; however, data from inclinometers, I1 (fill load alone, 10 to 12m thick compressible layer), and I2 (5 to 7m thick compressible layer), are also included in Fig. 10.8a to study the overall trend of lateral displacement during the application of vacuum-fill preload. As expected, the vertical profile of lateral displacement at I3 (Fig. 10.8b) shows that the initial lateral movements were inward; however, with the introduction of fill load, the lateral movements due to vacuum are not counteracted and the net outward movements near the ground surface as well as at depth were observed. Unfortunately, data on lateral displacements at different times for I4 are not available; however, the available data suggests that the lateral movements were primarily due to fill load (the trend of lateral movements at all sections is similar to I1 where only fill load was used). This indicates that the fill load was applied rapidly without allowing sufficient time for soil to consolidate and gain strength under vacuum (or under subsequent stages of fill loading). A probable reason for following a rapid rate of construction could be incorrect estimation of discharge capacity of vertical drains which are normally assumed to be freely draining under vacuum preloading. Hence, it is absolutely important to base the design of

preloading on a realistic discharge capacity of vertical drains that can be achieved in the field.

In section A of the treatment area, where the thickness of compressible layer was 7m, fill load could not be applied beyond 80kPa (4m) when vacuum was not used (Indraratna et al. 2009). Figure 10.9 shows the compares the proposed (q_w = 10m^3/yr) and actual fill preloading construction schedule followed in the fiels as well as the proposed and the actual construction schedules for vacuum-fill preloading. It can be seen that by using vacuum as a first stage load, 140kPa (7m) fill load, in addition to sand blanket, could be applied in about 100 days after application of vacuum; whereas, without vacuum, only 20kPa (1.5m) fill load, in addition to sand blanket, could be applied in 100 days. Moreover, with use of vacuum, the preloading operation was completed in less than two years; whereas, without vacuum the desired preload (245kPa in this case) could not be applied in the same duration. Hence, the use of vacuum as a first stage load reduces the overall duration of preloading operation.

10.4 Design Example II – East Pier Project, China

10.4.1 General

Improvement of subsoil for development of East Pier in Port of Tianjin, China is one of the earliest large scale application of vacuum preloading. An area of about 486,000m^2 was improved using vacuum and vacuum-fill preloading. As the case history is described in detail in Chapter 8, all the relevant data required for ILLICON analyses as well as stability analyses were obtained from Chapter 8; therefore, only the additional considerations for stability analysis and design of preloading for vacuum-fill and fill preloads are described in the following sections.

10.4.2 Design Parameters

The soil parameters for the design of preloading have been adopted from Chapter 8. A preload of 50 to 87kPa was required in different sections to induce the desired precompression. To provide a preload of 50kPa, vacuum was used alone; whereas, to provide a preload of 87kPa, vacuum was used in combination with a fill load of 17kPa. PVDs were installed up to a depth of 20m in a square grid of 1m. It was shown in Chapter 8 that PVDs performed without significant well resistance at a discharge

capacity of $11m^3$/yr., therefore, this discharge capacity has been used in ILLICON analyses to predict degree of consolidation at different times. It is important to point out that the proposed design of preloading was carried out after the installation of PVDs, i.e., for ILLICON analyses, drains were assumed to be installed in one day only due to reasons described in Section 10.4.3.

10.4.3 Considerations for Stability Analysis

Yixiong (1996b) reported an initial vane shear strength, s_{uo}(FV) of 1 and 2kPa, respectively, for the surface layers in vacuum and fill pilot test sections; whereas, Shang et al. (1998) reported an average s_{uo}(FV) of 4.5kPa for the entire treatment area. It was mentioned in Chapter 8 that due to extremely low bearing capacity, ground surface was pretreated with two layers of twig mat and 0.7m (14kPa) of hill cut and sand fill. Moreover, a period of more than six months was allowed between the pretreatment and beginning of preloading activities. It was also shown in Chapter 8 that a significant portion of pretreatment excess porewater pressures had dissipated after installation of vertical drains and before commencement of vacuum preloading, which should have improved the undrained shear strength. Therefore, the s_{uo}(FV) reported by Shang et al. (1998) is considered reasonable and is used in the preliminary stability analysis. Because the pretreatment fill adds to the effective stress of the compressible layer, it was considered as a separate layer, with a friction angle of 40^o (sand and hill cut) in the stability analysis. The stability analysis was carried out by assuming the sand/hill cut layer as drained, while the remaining sublayers were assumed as undrained in the analysis. The plasticity index reported by Shang et al. (1998) was between 20 to 25, therefore, initial vane shear strengths were used as such in the stability analysis without applying any correction.

10.4.4 Design of Preloading

Design of preloading is carried out for (1) A preload of 97kPa provided by vacuum (80kPa) in combination with fill load (17kPa), and (2) a preload of 97kPa provided by fill load alone. Preliminary stability analysis indicated that a 1.5m high fill (26kPa) can be constructed in first stage without endangering stability (Fig. 10.10); whereas, the vacuum can be applied in a single stage without any stability concerns. The

results of stability and ILLICON analyses for vacuum-fill and fill preloading are shown in Fig. 10.10. It can be seen that use of vacuum as a first stage load enabled the placing of second stage load much quickly as compared to fill load used as the first stage. Because in this case, the preload required was 97kPa, preload with vacuum-fill load could be applied with full intensity in less than 25 days after the commencement of vacuum preloading. On the other hand, the fill load is required to be constructed in four stages over a period of 140 days. As a consequence, the settlement induced by vacuum-fill preload occurred at a faster rate as compared to that of a fill preload. It is important to note that the difference in rate and magnitude of settlement induced by vacuum-fill and fill load is very pronounced in the beginning of the preloading operation; however, this difference reduces with time and becomes insignificant near the end-of-primary settlement. Therefore, the apparent difference in rate and magnitude of settlement at any time due to either types of loads can only be attributed to the ability of that load to be applied with full intensity in a given time.

Figures 10.11 and 10.12, respectively, compare the proposed preloading design with the actual construction schedules followed in the field for fill and vacuum-fill preloading. It can be seen from Fig. 10.9 that the proposed and the actual construction schedule as well as the observed and predicted settlements are in good agreement; the minor difference observed at the beginning of preloading is attributed to the assumptions made on initial undrained shear strength as discussed in Section 10.4.3. It is important to note that the vertical drains performed without significant well resistance (as discussed in Chapter 8) which reinforces the importance of incorporating the correct discharge capacity in the design of preloading.

Figure 10.12 shows that the proposed loading schedule, which is based on a uniform distribution of vacuum pressure with depth over-predicts the rate and magnitude of observed settlements in the field. The actual loading schedule shows that the applied vacuum of 65kPa could not be maintained within the sand blanket and vertical drains during the first 100 days of application, although after 100 days, the vacuum intensity maintained in the drainage blanket around 95kPa. The fill construction in this case was probably delayed because of the unstable imposed vacuum. It is important to note that

although the initial rate of settlement with vacuum (under ideal conditions; Fig 10.12b) is faster than the initial rate of settlement under fill preloading (Fig. 10.11b), the end-of-primary settlement in both cases is achieved in almost the same time. This suggests that the rate of settlement is dependent on the rate of application of load and not the type of load. It should also be noted that the total load reported for vacuum-fill preload (112kPa) exceeds the fill preload (97kPa); whereas, the observed settlements were significantly less suggesting a non-uniform distribution of vacuum pressure with depth (as discussed in detail in Chapter 8). Therefore, it may be necessary to monitor the porewater pressure in soil during preloading operation for effective execution.

10.5 Concluding Remarks

Application of proposed design procedure to two case histories shows that:

- The discharge capacity of vertical drains is an important variable (among other factors) which significantly influences the degree of consolidation achieved in a particular time, and therefore, governs the rate of application of preload. Hence it is not reasonable to assume that the PVDs will always perform without any well resistance. In the case of Ballina Bypass (design example 1), the field construction schedule shows that the preloading design was apparently based on an assumed higher discharge capacity than the actual capacity yielded by the drains. Therefore, it is not prudent to base the design of preloading by assuming the PVDs to be draining freely; similarly, assuming a lower bound value for discharge capacity may result in prolonging the duration of preloading, and thus may be uneconomical. It is therefore important to carefully select the design discharge capacity for preloading effort.
- It takes some time for the vacuum to be fully effective within the drainage system (drainage blanket and vertical drains); furthermore, the distribution of vacuum pressure in soil may or may not be constant with depth, which can potentially delay the application of additional fill load required. For design example I, vacuum developed to full intensity in 15 days; whereas, for design example II, as a result of possible ‘leakage’ etc, it took 100 days

for vacuum to stabilize in the drainage system. As a consequence, the fill load (which could have been added after 20 days), was added after 100 days of vacuum application.

- Under ideal conditions, distribution of vacuum pressure, in the vertical drains, is uniform with depth; however, in the field, vacuum may or may not develop uniformly in the soil at all depths. As the loss of vacuum at different depths may not be predicted in advance, it is reasonable to base the design of preloading on a uniform distribution of vacuum pressure in the vertical drains with depth. However, in case of anticipated loss of vacuum pressure through any permeable layers, the design intensity of vacuum may be reduced to account for the leakages.
- The rate of settlement induced by any preload is independent of type of load; instead it depends upon the rate of application of load. It is the ability of vacuum to be applied relatively quickly, as compared to an equivalent fill preload, which results in an increased rate of settlement.
- For a preloading effort of 80kPa or less, vacuum alone can provide the desired preload. In such a case, vacuum preload can be applied in a single stage without any stability concerns. For a preloading effort of greater than 80kPa, the use of vacuum as a first stage load allows the embankment to be constructed quickly which significantly reduces the overall duration of the preloading operation.
- The close agreement between the proposed and actual construction schedules shows that the basis for design for vacuum, fill or a combined vacuum-fill preloading are the same; therefore, there is no requirement for separate design considerations for vacuum or fill preloads.

10.6 Figures

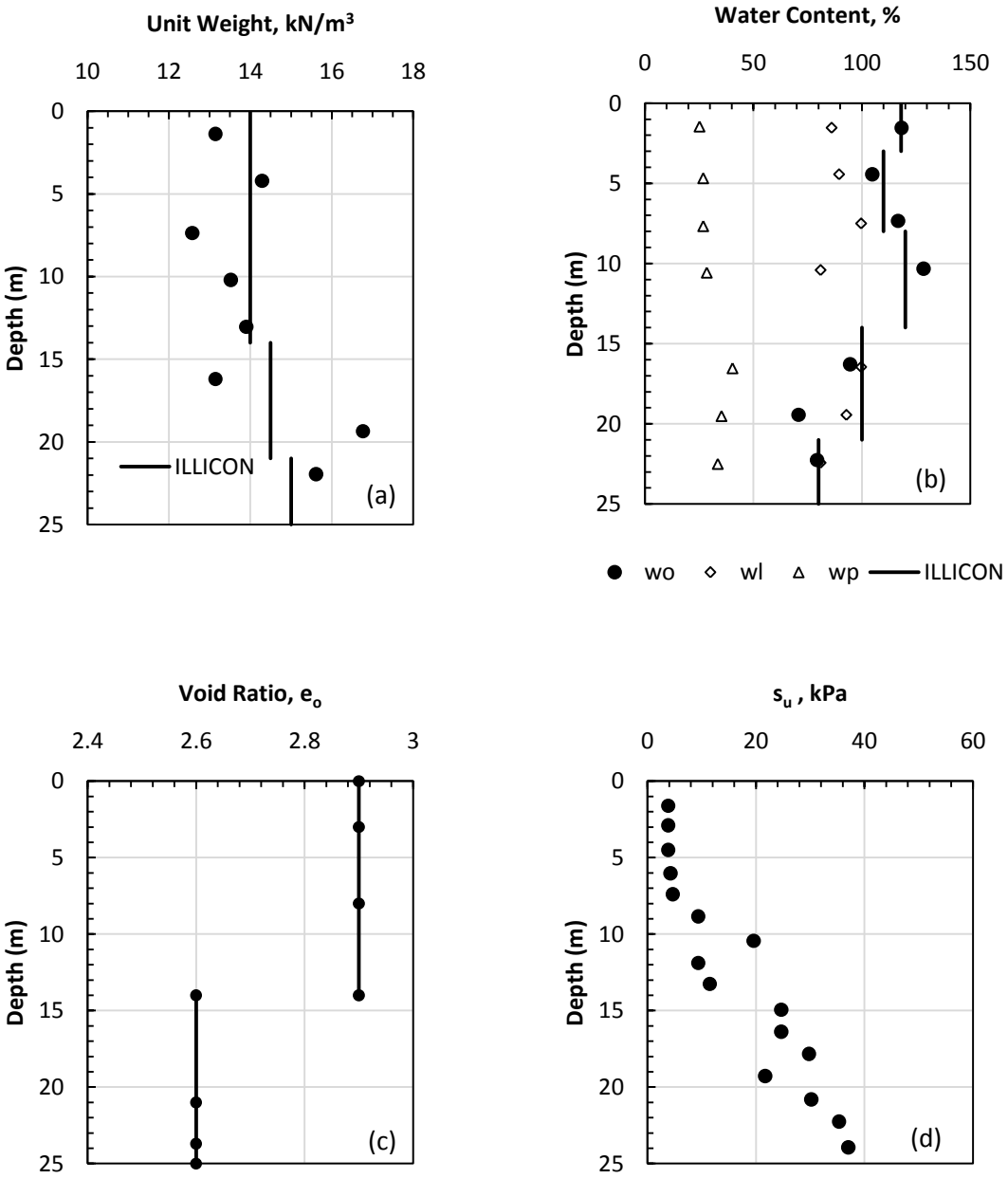

Figure 10.1: Vertical profile of soil properties (data from Indraratna et al. 2009)

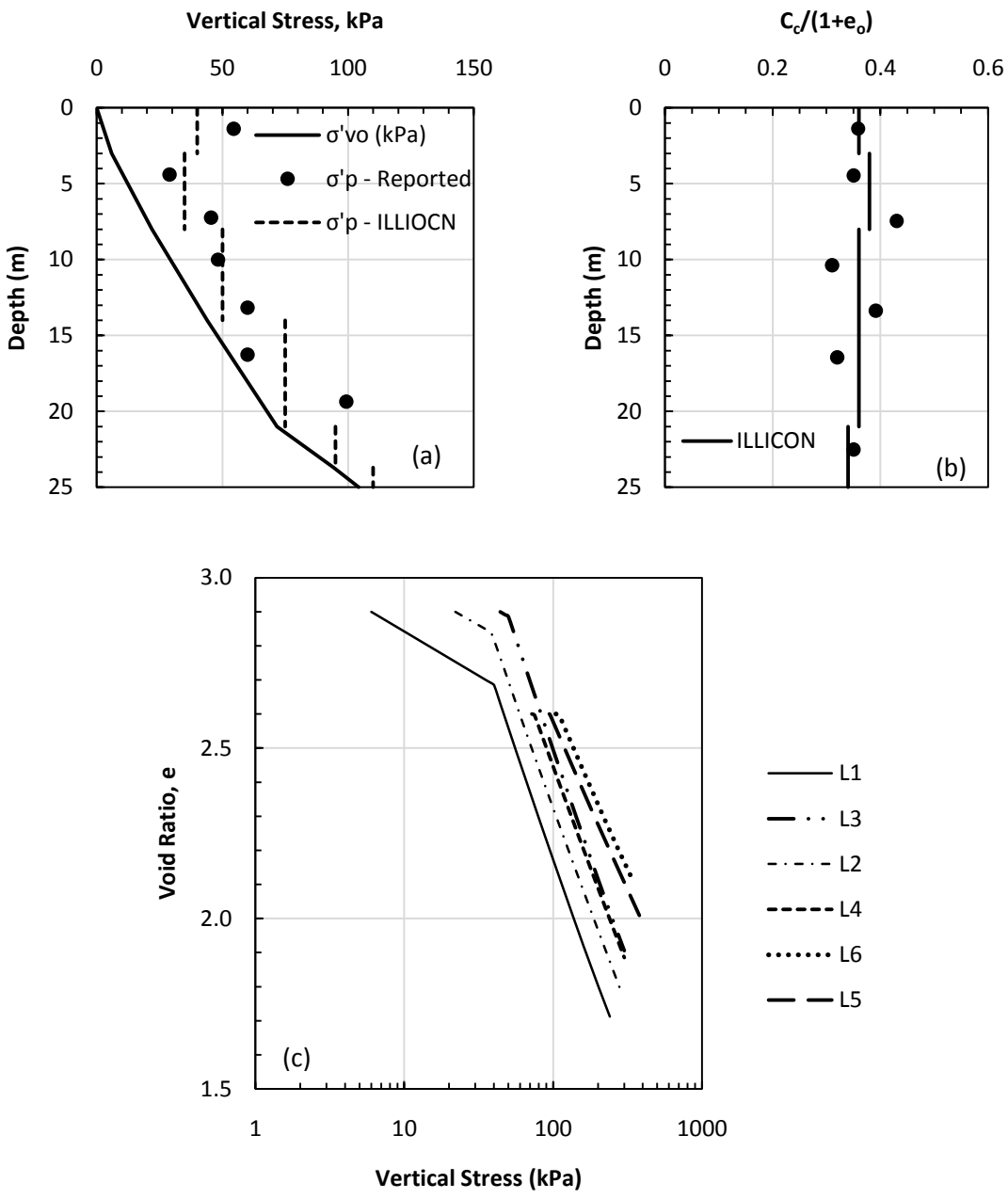

Figure 10.2: Vertical profile of (a) initial effective stress and preconsolidation pressure, (b) compressibility ratios, and (c) EOP e – logσ'_v relations for different sublayers

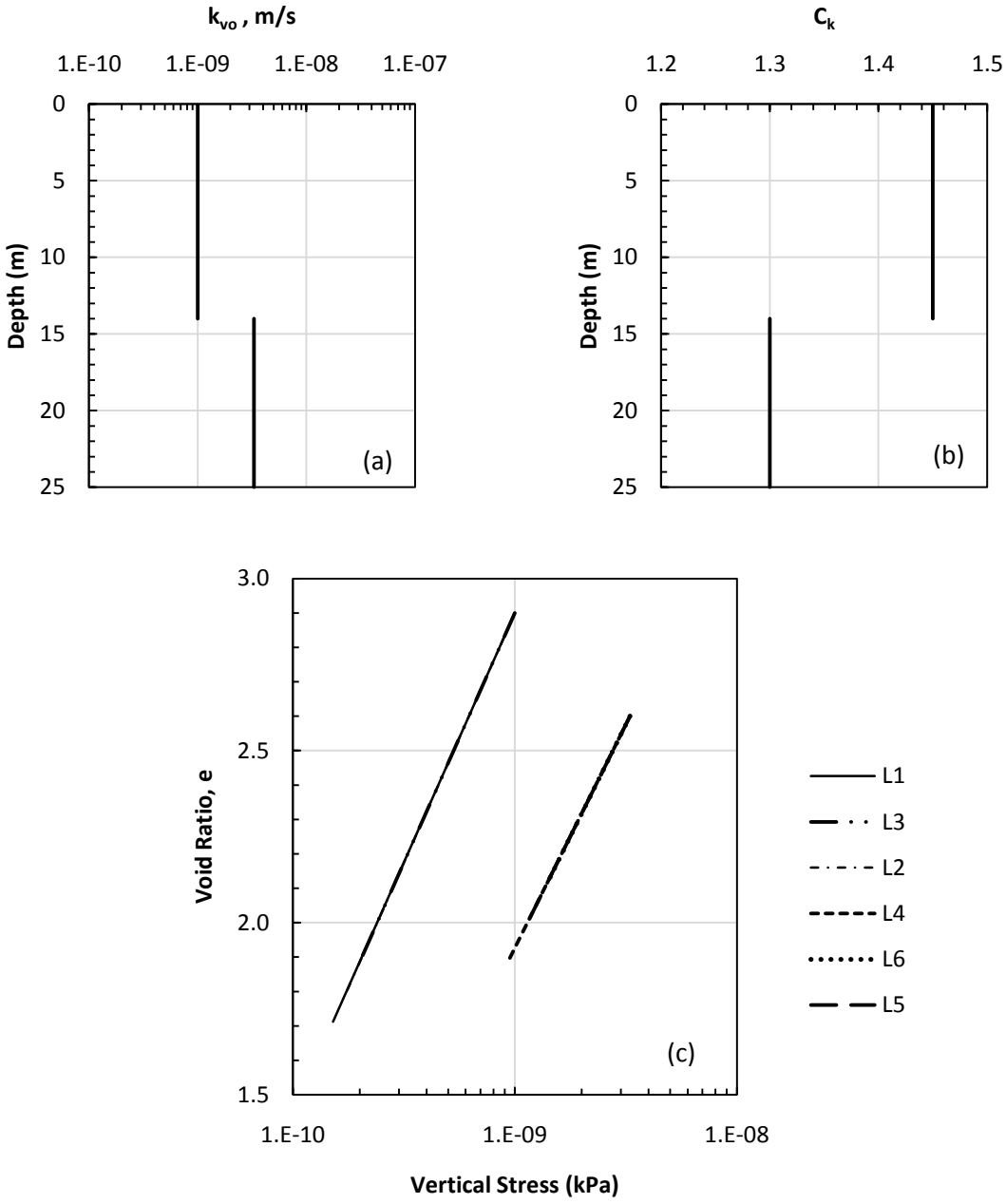

Figure 10.3: Vertical profile of (a) initial vertical permeability, (b) C_k, and (c) e – logk_v relations for different sublayers

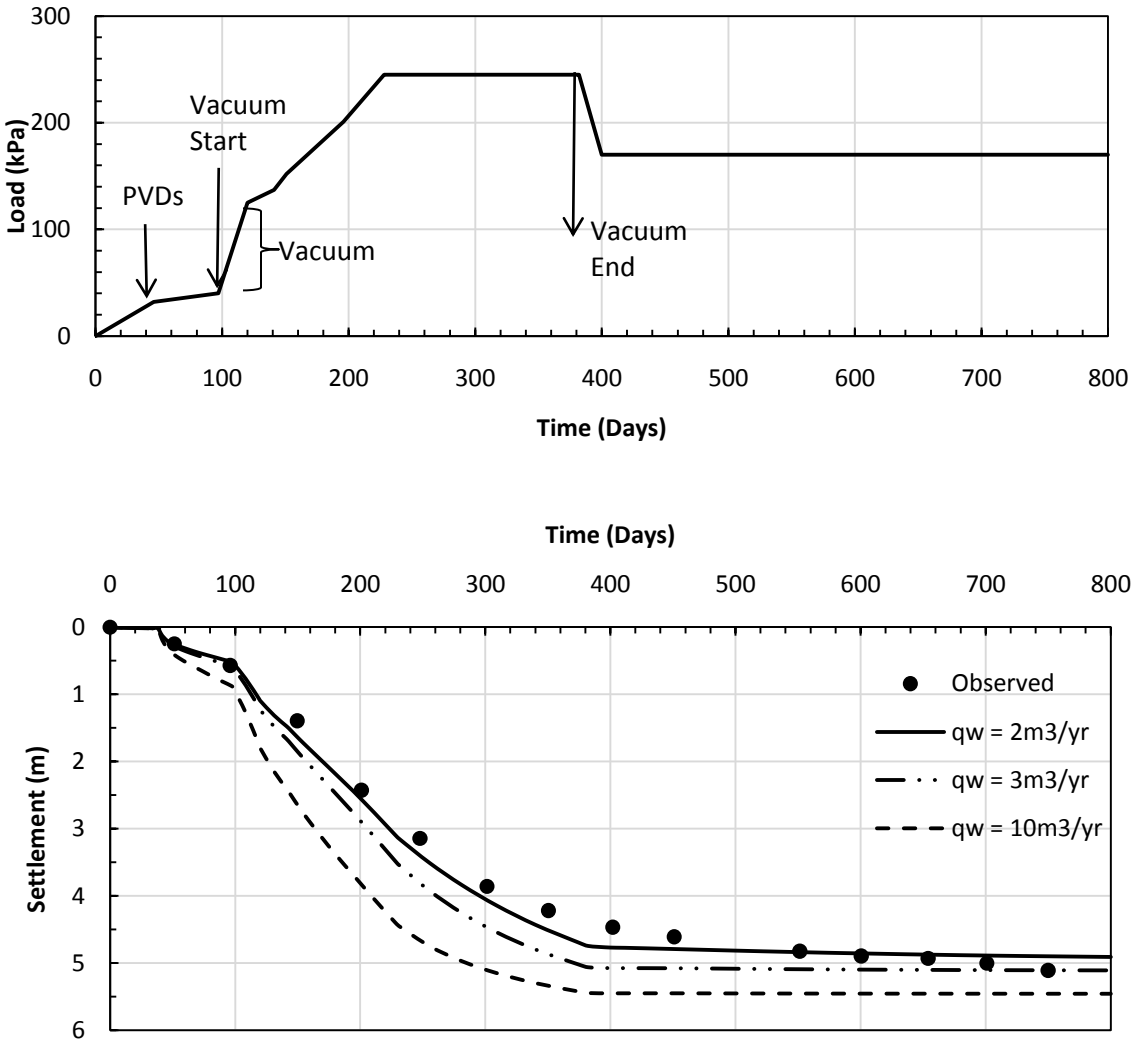

Figure 10.4: (a) Loading schedule, and (b) observed and predicted settlements (data from Indraratna et al. 2009)

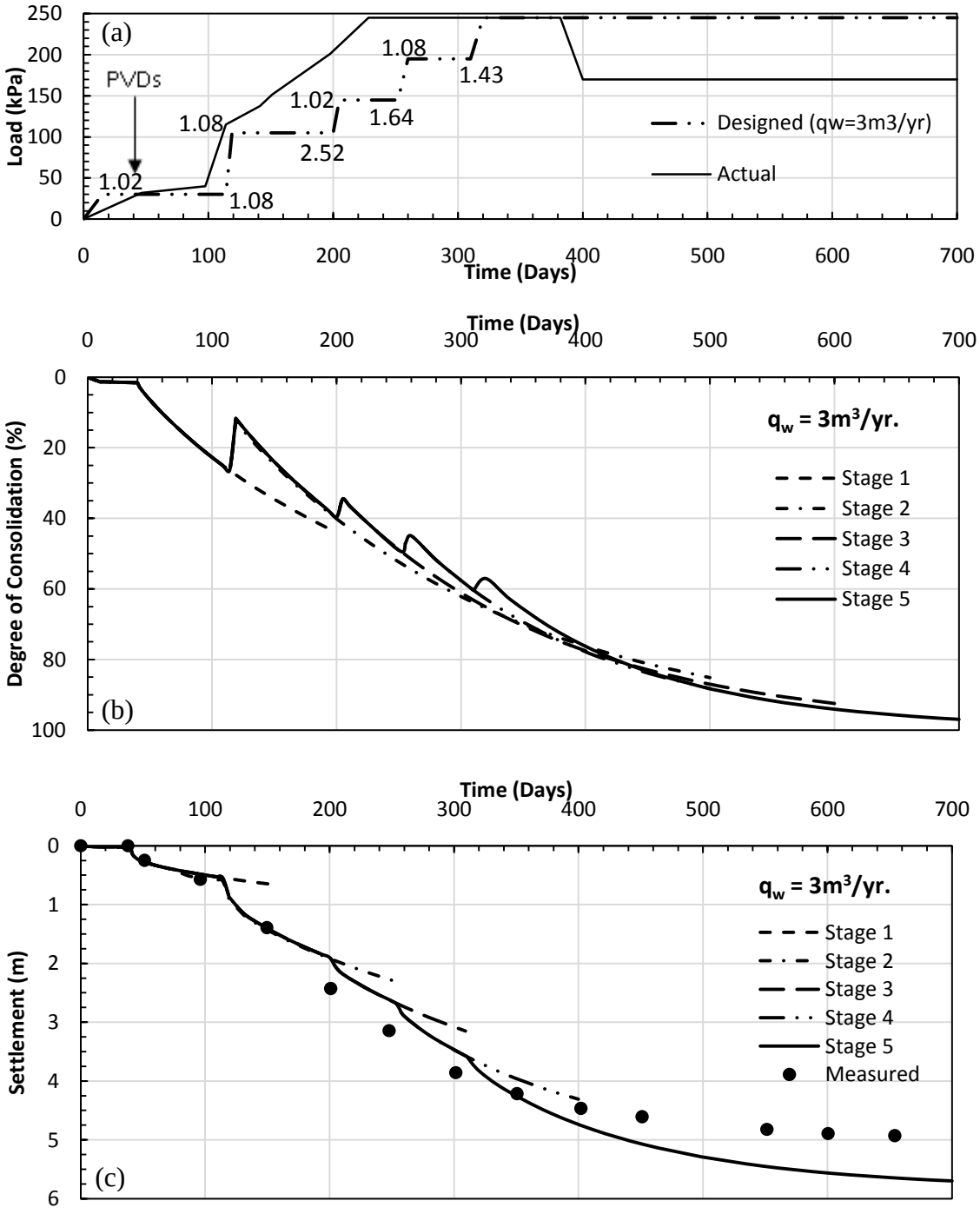

Figure 10.5: ILLICON analyses and stability analyses for an assumed discharge capacity of $3m^3/yr.$, (a) actual and proposed construction schedules for together with computed factors of safety at different times for different loading stages (b) degree of consolidation at different times during different loading stages, and (c) settlement at different times during different loading stages

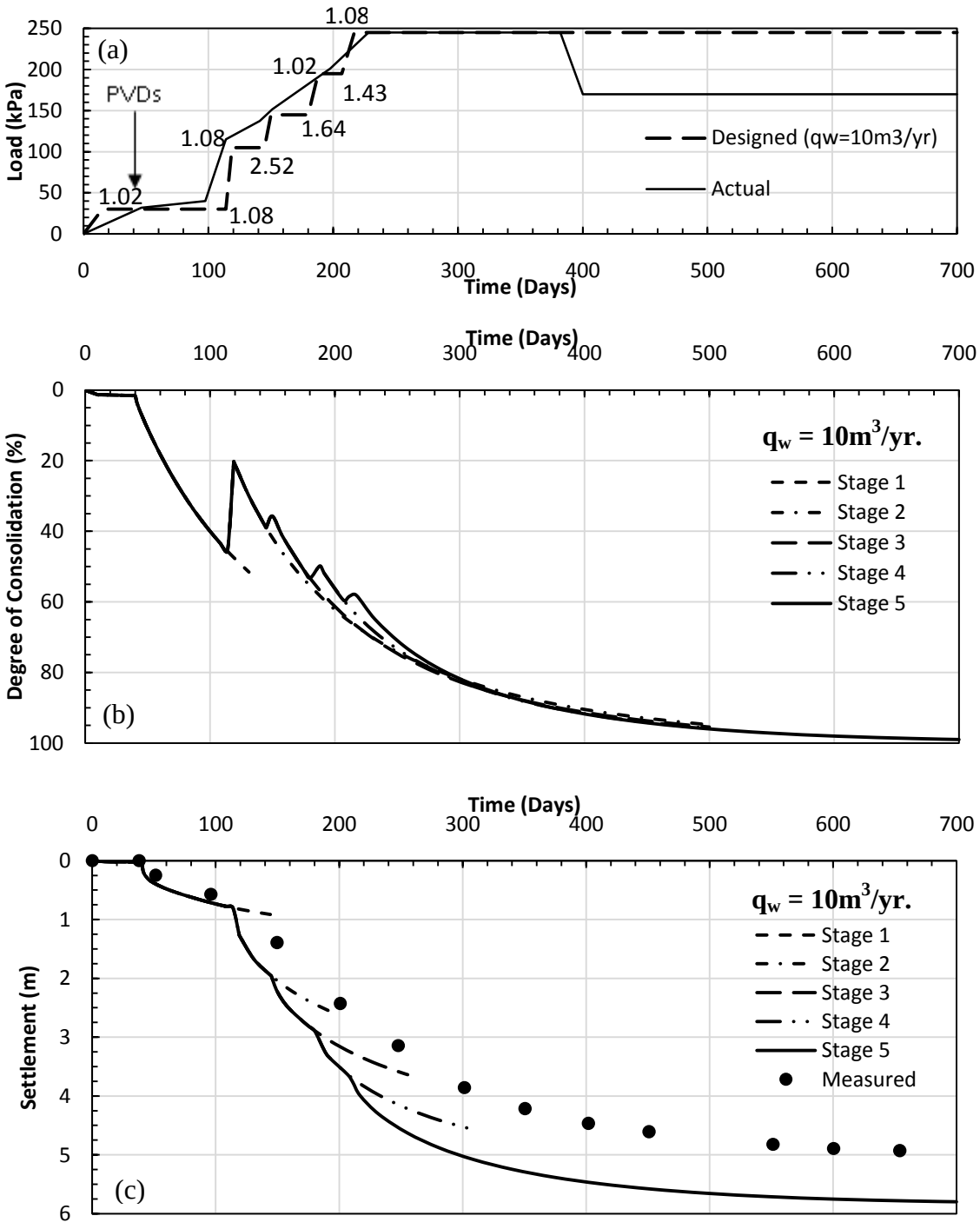

Figure 10.6: ILLICON analyses and stability analyses for an assumed discharge capacity of $10m^3/yr.$, (a) actual and proposed construction schedules for together with computed factors of safety at different times for different loading stages (b) degree of consolidation at different times during different loading stages, and (c) settlement at different times during different loading stages

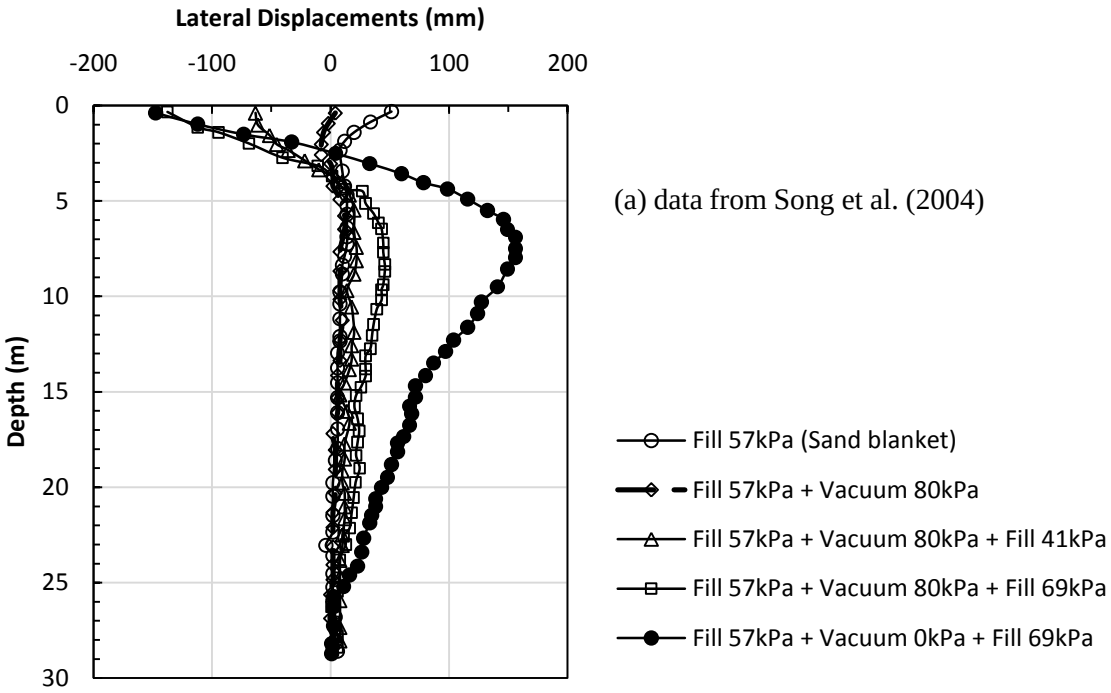

(a) data from Song et al. (2004)

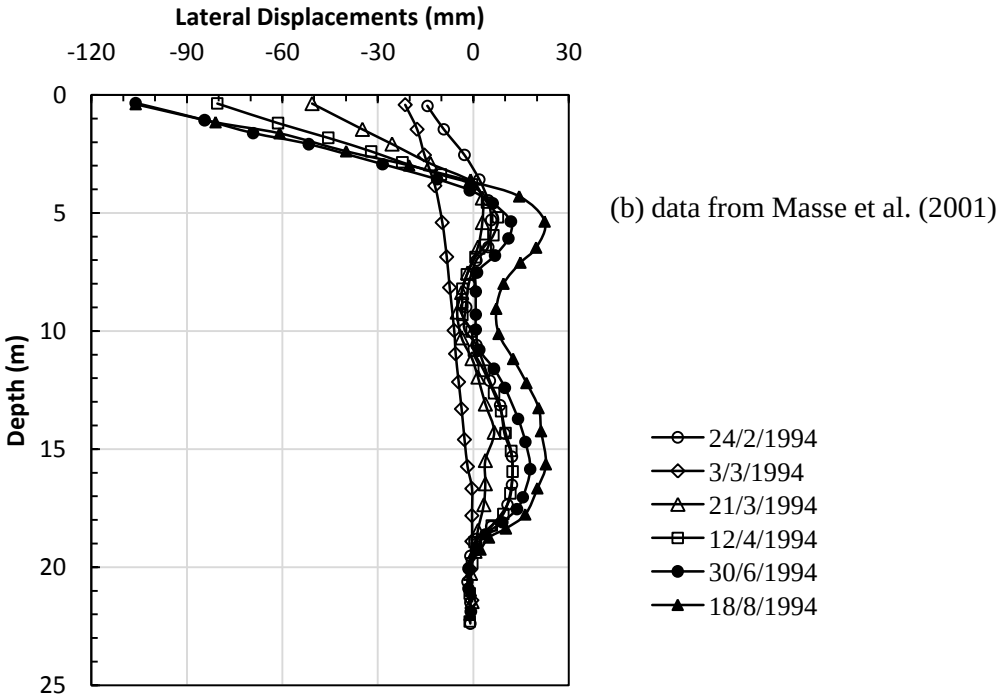

(b) data from Masse et al. (2001)

Figure 10.7: Lateral displacements due to combined vacuum-fill preloading at (a) Sewage treatment plant, South Korea, and (b) highway construction in France

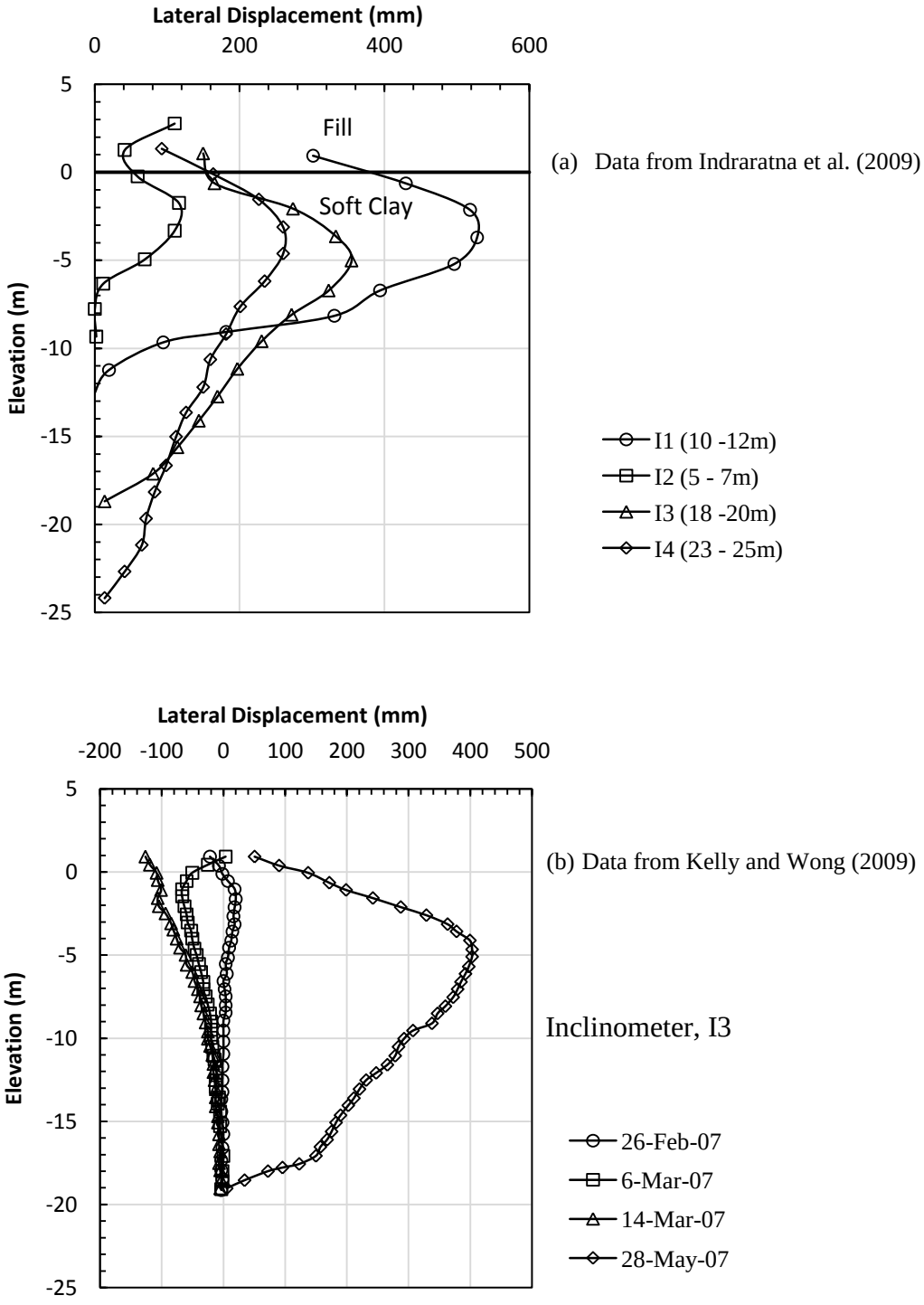

Figure 10.8: Lateral displacements observed due to combined vacuum-fill preloading at Ballina bypass, (a) Inclinometers at different sections, and (b) Inclinometer, I3

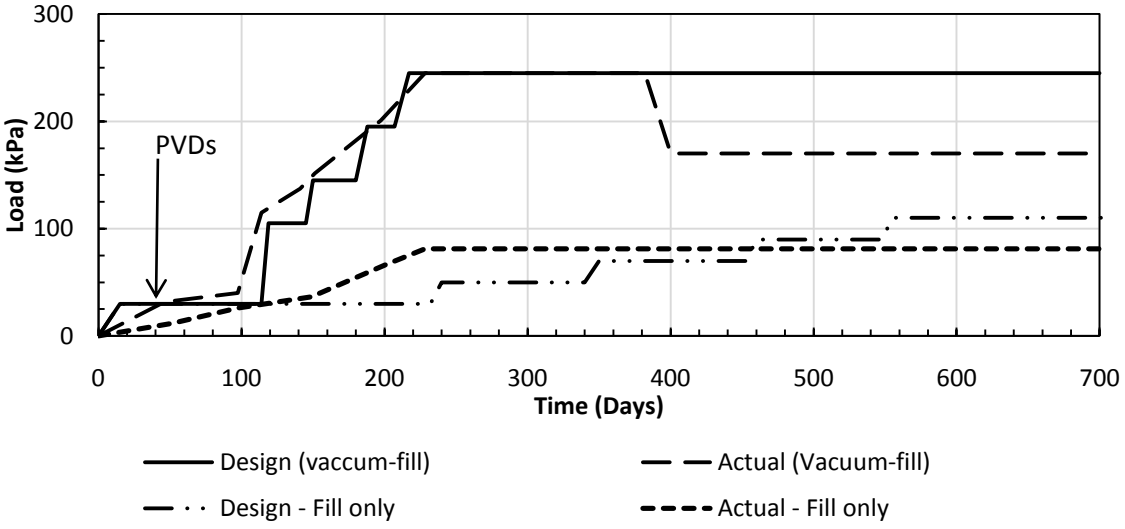

Figure 10.9: Effect of vacuum on rate of application of fill load

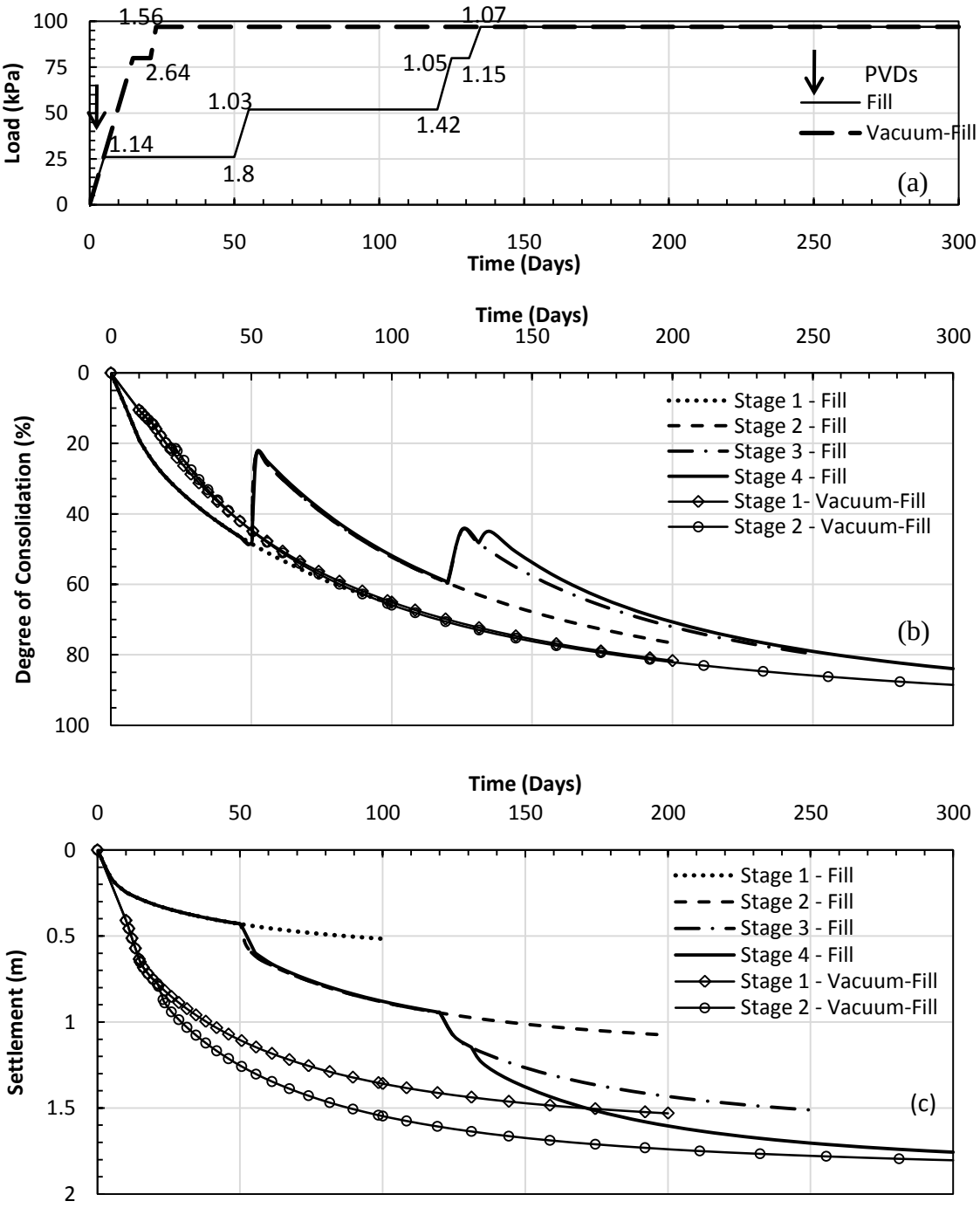

Figure 10.10: (a) Proposed construction schedules for vacuum-fill and fill preloading corresponding to a discharge capacity of 11m^3/yr., along with computed factors of safety at different times for different loading stages (b) degree of consolidation at different times during different loading stages, and (c) settlement at different times during different loading stages

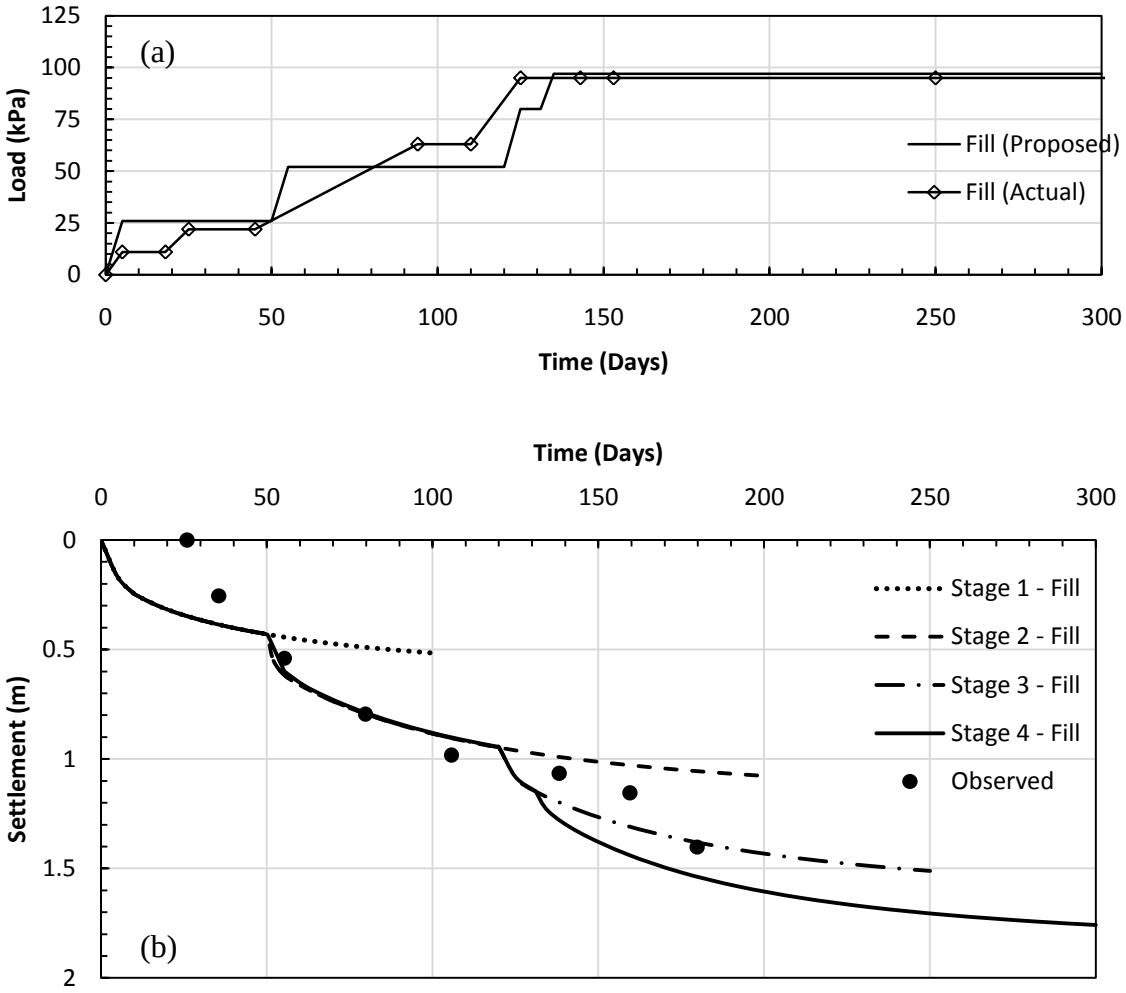

Figure 10.11: (a) Actual and proposed loading schedule for fill preload of 97kPa, and (b) comparison of observed and predicted settlement (Field data from Choa 1989)

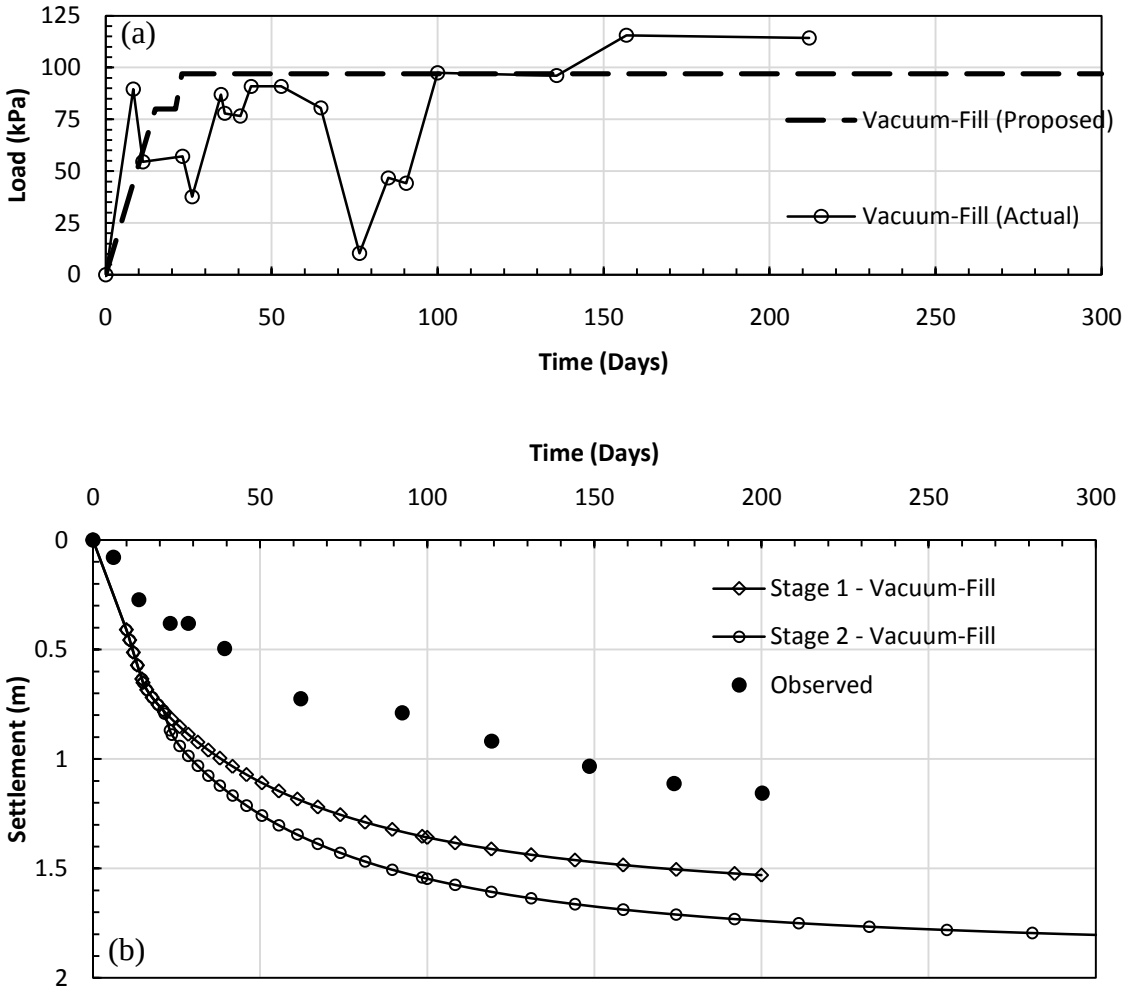

Figure 10.12: (a) Actual and proposed loading schedule for vacuum-fill preload of 97kPa, and (b) comparison of observed and predicted settlement (Field data from Choa 1989)

CHAPTER 11. CONCLUSIONS

11.1 Conclusions

The settlement analysis of case histories of vacuum and vacuum-fill preloading, interpretation of field data on lateral displacements and shear strength, and evaluation of laboratory studies on vacuum consolidation lead to the following conclusions:

11.1.1 General

- Precompression of soft soil deposits using vacuum as preload is becoming increasingly popular throughout the world. Contrary to fill preloading, where the increase in effective stress is achieved by increasing the total stress, the increase in effective stress during a vacuum preloading operation is achieved by reducing the porewater pressure within the soil mass. Thus, in a combined application of vacuum-fill preload, the total stress in the soil mass increases by an amount equal to the applied fill load, whereas, at the end-of-primary consolidation, the effective stress increases by an amount equal to the absolute sum of applied vacuum and fill loads.
- Since its inception, vacuum consolidation has been continuously studied throughout the world to develop an efficient method for its practical execution; however, limited success was achieved in thirty years following Kjellman's proposal in 1952. The advent of robust materials including prefabricated vertical drains, sealing membranes, and vacuum pump technology facilitated the development of Kjellman's method into a practically viable tool by mid 1980s. Since then the method has been used extensively in different parts of the world and a number of innovative

techniques have been developed to apply vacuum to the compressible layer. However, all the techniques are essentially based on the same basic concepts proposed by Kjellman in 1952. Unfortunately, sufficient details with respect to technology and equipment used for implementation of vacuum consolidation in the field have not been reported in the literature.

11.1.2 Components of Vacuum Consolidation System

Any vacuum consolidation system must have (1) a sealing mechanism to avoid loss of vacuum, (2) a source to generate vacuum, (3) a medium through which the vacuum is applied to the compressible layer, (4) a medium to collect and dispose-off the discharged water. A vacuum pump is used to generate the vacuum pressure which is transmitted to the compressible layer through an elaborate drainage system (usually consisting of a drainage blanket and a network of horizontal and vertical drains); the drainage system also collects and disposes off the water. Depending upon the technique used, sealing of the area may be completed in a number of ways; e.g., laying of an impermeable membrane on the surface and extending it at the boundary of the treatment area to slightly below the ground water table, or using the top portion of insitu clay layer as an impermeable blanket, etc. The presence of a high permeability layer at an intermediate depth necessitates more specific measures to seal and isolate the treatment area from its surroundings. Use of slurry walls to cut off a high permeability layer is an effective way to complete the sealing of the treatment area.

11.1.3 Nature of Loading and Depth of Improvement

As the applied vacuum propagates down the compressible ground through the vertical drains, it induces an isotropic load in the soil mass; hence, no shear stresses are generated within the soil mass. Thus, a vacuum load can be applied with full intensity (usually 80kPa) in a single stage without any stability concerns, whereas, the equivalent fill load is applied in stages to avoid excessive deformations or a bearing capacity failure. For the same reason (propagation of vacuum through the vertical drains), there is no theoretical limit for depth of improvement using vacuum as a preload; i.e., vacuum propagates down and remains effective in the entire depth up to which vertical drains are installed.

11.1.4 Vacuum Intensity

- Theoretically, a maximum vacuum pressure of 100kPa can be applied to the compressible layer; however, a vacuum pressure of 80kPa is regarded as the practical upper limit which can be developed and sutained in the field for the desired duration of preloading.
- Vacuum consolidation systems in which the vertical drains are not directly connected with the vacuum pumps (e.g. vacuum consolidation systems with PVDs and membranes) can generate and sustain a higher vacuum pressure as compared to the vacuum consolidation systems in which individual vertical drains are directly connected with the vacuum pump system (e.g. membrane-less vacuum consolidation systems with CPVDs). An average vacuum intensity of 80kPa (>90kPa in few cases) is reported for vacuum consolidation systems with sealing membranes, whereas an average vacuum intensity of 50kPa to 60kPa is reported for membrane-less systems. Moreover, the settlements produced by membrane-less systems are less uniform as compared to those produced by systems with sealing membranes. Thus, membrane-less systems are less efficient as compared to systems with sealing membranes.
- Following arguments can be made to explain relatively low efficiency of membrane-less systems with CPVDs, (1) the direct exposure of individual CPVDs to vacuum suction may result in a partial collapse which can potentially reduce the cross sectional area of vertical drain and may also create a gap between the cap and the drain through which leakage can occur, (2) the gap between the CPVDs and walls of the hole left open after withdrawl of mandrel is backfilled by clay slurry to avoid loss of vacuum; if this operation is not executed carefully, a link may be established between the permeable layer and CPVDs through which leakage can occur, and (3) a flexible membrane is absolutely necessary for atmospheric pressure to be transferred to the soil. In a system with sealing membrane, the drainage layer is confined within the membrane and is totally isolated from its

surroundings; therefore, as soon as the vacuum is generated below the membrane, the atmospheric pressure starts acting on top of the membrane and the drainage layer confined within the membrane starts experiencing that pressure, thus the complete thickness of compressible layer including drainage layer is subjected to atmospheric pressure. On the other hand, in a membrane-less system, CPVDs are penetrated into the compressible layer after bypassing the top permeable layer and a part of compressible layer (used as a seal), hence atmospheric pressure is not felt on the ground surface and a part of the compressible layer, and therefore, the efficiency is lower. However, no data are reported to further examine and verify these arguments.

11.1.5 Vacuum Pressure Distribution

- Under ideal conditions (assuming no leakages), the vacuum pressure distribution is constant with depth, i.e., the applied vacuum develops with same intensity in the drainage system up to the penetration depth of vertical drains; however, depending upon the stratification and relative permeability and compressibility characteristics of different sublayers, time rate of development of vacuum in the soft layer may vary at different depths.
- In actual field conditions, it takes some time for the vacuum to develop to the applied intensity within the drainage system. Typically, 5 to 15 days are required for vacuum in the drainage system to reach the applied intensity; therefore, it is not reasonable to assume that the vacuum can be applied instantaneously in the field. Moreover, vacuum intensity in the soil may vary with depth as well as with time; i.e., vacuum may develop to different intensities at different depths or it may develop relatively quickly to a higher value which cannot be maintained at the same level for the desired duration of preloading. The loss of vacuum intensity in soil with depth or time or both can be attributed to improper sealing of the area or an internal leakage through certain sublayers located at depth. In case of internal leakage (leakage through a sublayer), the vacuum may not develop to full intensity

in the sublayers adjacent to the sublayer through which leakages are affected. Reduction in porewater pressures at a significant distance outside the treatment area is an indicator of leakage of vacuum from within the treatment area.

- Field records show that the reduction in porewater pressures may be smaller at shallow depths and higher at greater depth, which imply that consolidation in the field may progress under different vacuum intensities at different depths. Thus, the assumption that vacuum intensity is maximum at the ground surface and decrease linearly with depth is not a valid assumption.
- The applied vacuum can propagate to a significant distance outside the treatment area in the presence of a high permeability layer. In one case porewater pressure reductions of 50kPa, 47kPa, and 43kPa, respectively, were measured at 1m inside, 2m outside and 5m outside the treatment area, in a sandy-silt layer located at a depth of 9.6m to 11.6m from the ground surface. In cases, where 'leakage' in vacuum to outside the treatment area is unlikely, the extent of surrounding area affected by vacuum consolidation is has not been specifically reported.

11.1.6 Settlement due to Vacuum Preloading

- Under identical loading conditions, the rate and magnitude of settlement induced by a vacuum preload is equal to the rate and magnitude of settlement induced by an equivalent fill preload. The accelerated settlements due to vacuum preloading operations (observed in some field cases) are primarily related to the ability to apply vacuum relatively quickly as compared to time required to place an equivalent fill preload (which in many cases is applied in stages due to stability concerns). Hence, the rate of settlement is independent of the type of load, instead, it depends on the rate of application of load.
- Soil behavior under vacuum or combined vacuum-fill preload can be fully explained using existing consolidation theories and computer programs;

therefore, there is no need for developing a new consolidation theory or a separate design procedure for cases involving vacuum as a preload. For the settlement analysis, the applied vacuum can be modeled as a fill load and the principle of superposition can be used to simulate combined vacuum-fill preloads. In such a case (modeling vacuum as a fill load), the settlement predictions depict the anticipated settlement response and can be used as such for evaluation or incorporation into the design.

- For back-analysis of a vacuum or vacuum-fill preloading case history, it is reasonable to estimate the consolidation pressures at different depths and at different times from the observed reductions in porewater pressure with depth and with time. The possibility of variable vacuum intensity (with depth and with time) is more realistic as opposed to an assumed linear reduction in vacuum intensity with depth.
- The ability of computer program ILLICON to model time-dependent increase or decrease in load makes it specially useful for settlement predictions for cases involving vacuum as a preload.

11.1.7 Interpretation of Porewater Pressure

Contrary to fill preloading, the excess porewater pressures generated by a vacuum preload are negative. Moreover, the location of maximum excess porewater pressure due to a vacuum or a fill preload is also different; i.e., the maximum excess porewater pressure due to a fill preload (positive) occurs at the mid distance between two adjacent vertical drains (or at the circumference of the zone of influence of vertical drain), whereas, the maximum excess porewater pressure (negative) due to vacuum is generated at the soil-drain interface. Thus, there is no "partial cancellation" of positive and negative porewater pressures due to a combined vacuum-fill load as envisaged by some engineers.

Under ideal conditions, at the end-of-primary consolidation the porewater pressure at all depths should reduce by an amount equal to the magnitude of applied vacuum provided the vacuum load remains effective at least till the end-of-primary compression. This is true even if the magnitude of applied fill load is much more than the

magnitude of applied vacuum in case of a combined vacuum-fill preload. Thus, at the end-of-primary (EOP) compression, the reduction in porewater pressures at all depths should be equal to the applied vacuum intensity from a given reference porewater pressure.

Similar to settlement analysis, porewater pressures due to vacuum and vacuum-fill preloads can also be interpreted using existing consolidation theories and computer programs by modeling the applied vacuum as a fill load (using principle of superposition for combined loads); however, in this case it is necessary to convert the positive excess porewater pressure response to a porewater pressure which may be positive or negative at a given depth and at a given time. The method suggested in the present study (Eq. 4.2) is found suitable for interpreting the porewater pressure response due to vacuum and combined vacuum-fill loads.

11.1.8 Performance of Vertical Drains

Vertical drains are an essential component of any vacuum consolidation system and perform the dual function of transmitting vacuum to the soft layer as well as carrying the discharged water to drainage blanket for further disposal. The present study shows that the vertical drains may or may not be freely draining during vacuum consolidation. In fact, the number of cases where vertical drains displayed significant well resistance are more than the number of cases where no well resistance was observed. Therefore, the common practice of assuming freely draining vertical drains or associating a high discharge capacity with vertical drains is not considered reasonable. Design of a preloading effort based on unrealistic (too high) discharge capacity may result in high lateral movements as shown in Chapter 10.

11.1.9 Lateral Displacements

Soft ground subjected to vacuum preloading experiences inward lateral movements, which are maximum at the ground surface and reduce with depth; whereas the lateral movements due to a fill preload are outward and maximum is generally at some depth below the ground surface. Thus, in a combined vacuum-fill preloading, the lateral ground movements due to either type of loads tend to counteract each other.

Lateral displacements due to vacuum preload are predominantly due to consolidation movements, however, the contribution of other soil parameters cannot be ignored. Due to complex interaction of different soil parameters, time-dependent loading, uncertainties in vacuum pressure distribution with depth and with time and extent of area influenced by vacuum outside the treatment zone, it is more reasonable to develop an empirical model based on the observed soil behavior to predict the lateral displacements during vacuum preloading. The empirical procedure proposed in the present study is found suitable and may be used to predict vertical profile of lateral displacements at any time during vacuum preloading.

11.1.10 Increase in Undrained Shear Strength

Similar to settlements, the increase in undrained shear strength due to vacuum or a combined vacuum-fill preloading can be fully explained in terms of the increase in shear strength due to an equivalent fill preload. Moreover, $s_u(FV)/s_{uo}(FV)$ is expected to decrease with depth irrespective of the type of load. Therefore, it is not reasonable to expect a greater increase in undrained shear strength due to vacuum or a combined action of vacuum-fill preload as compared to that resulting from an equivalent fill preload. The argument that increase in undrained shear strength due to vacuum preloading is higher near the ground surface is not supported by field observations and therefore, it is not considered reasonable.

The apparent discrepancies in observed increase in undrained shear strength can be explained by considering the initial shear strength, consolidation pressure and degree of consolidation achieved in a particular time. The $s_{uo}(FV)/\sigma'_p$, which remains constant in the compression range, together with σ'_p/σ'_{vo} can be used to predict the increase in undrained shear strength for a known consolidation pressure.

Because it is possible to apply vacuum relatively quickly, the initial rate of increase in effective stress is higher for vacuum preloading as compared to that of a fill preload. Thus, the undrained shear strength increases at a rapid rate which allows more rapid construction of fill load (if the preload is greater than 80kPa). Therefore, use of vacuum as a first stage preload can substantially reduce the overall duration of preloading.

In soft soils with very low initial strength, high compressibility, and low permeability, the increase in undrained shear strength during a particular stage of loading may be insufficient as only a very small fill load increments ($\Delta\sigma'_v$) can be added at a time. Moreover, the time required to affect the increase in undrained shear strength is generally large. Hence, it may not be possible to improve the properties of such soil deposit with use of fill load alone.

11.1.11 Ground Water Fluctuations

A constant ground water table best represents the ground water table during vacuum preloading, although, the lowering as well as upward movement of water table have been reported in the literature. The pumping equipment can handle both water and air, therefore, presence of air (if any) does not impede the progress of consolidation.

11.1.12 Design of Preloading

The computer program ILLICON to predict the increase in effective stress at a given time, and the empirical corelation $s_u(mob) = 0.22\sigma'_{vc}$, to predict the increase in undrained shear strength together with a program for stability analysis to predict factor of safety at different times during different prlaoding stages can be used with confidence for design of preloading.

The application of proposed design procedure to case histories of vacuum-fill as well as fill preloading shows that there is no difference between the design of preloading due to either type of loads. However, it is absolutely important to base the design of preloading on realistic discharge capacity of vertical drains. A factor of safety slightly higher than unity is sufficient for the design of preloading.

REFERENCES

Asoaka, A. (1978). "Observational procedure of settlement prediction" Soils and Foundations, 18, No. 4, 87 - 101

Bamunawita, C. (2004). "Soft clay Foundation improvement via prefabricated vertical drains and vacuum preloading" PhD Thesis. University of Wollongong, Australia

Bergado, D.T., Balasubramaniam., A.S., Fanin., R.J., Anderson., L.R., and Holtz., R.D. (1997). "Full scale test of prefabricated vertical drain (PVD) on soft Bangkok clay and subsiding environment" Ground Improvement Ground Reinforcement Ground Treatment, ASCE GSP 69, 372 - 393

Bergado, D.T., Chai., J.C., Miura., N., and Balasubramaniam., A.S. (1998) "PVD improvement of soft Bangkok clay with combined vacuum and reduced sand embankment preloading" Geotechnical Engineering Journal, SEAGC, 29 (1), 95 - 122

Bergado, D.T. and Patawaran, M.A.B. (2000). "Recent developments of ground improvement with PVD on soft Bangkok clay" Proc. International seminar on Geotechnics in Kochi, Japan.

Bergado, D.T., Balasubramaniam, A.S., Fannin, R.J. and Holtz, R.D. (2002). "PVD in soft Bangkok clay; A case study of New Bangkok International Airport Project". Can. Geotechnique, J 39, 304 – 315

Berthier, D., Boyle., P., Ameratunga, J., Bok, C.D., and Vincent, P. (2009). A successful trial of vacuum consolidation at the port of Brisbane" Coasts and Ports Conference, Wellington, New Zealand

Bo, M.W., Jian, C., Kong, L.B., and Choa, V. (2003). "Soil Improvement – Prefabricated Vertical Drains Techniques" Thomas Learning, Singapore

Chai, J.C., and Miura, N. (1999) "Investigations of factors affecting vertical drain behavior" Journal of Geotechnical and Geoenvironmental Engineering, ASCE, 216 - 226

Chai, J.C., Hayashi, S. and Carter, J.P. (2005). "Characteristics of Vacuum consolidation"

Chai, J.C., Carter, J.P. and Hayashi, S. (2005). "Ground deformation induced by vacuum consolidation" Journal of Geotechnical and Geoenvironmental Engineering, ASCE. 1552 - 1561

Chai, J.C., Carter, J.P. and Hayashi, S. (2006). "Vacuum consolidation and its combination with embankment loading". Can. Geotechnique, J 43, 985 -996

Chai, J. Miura, N. and Bergado, D.T. (2008). "Preloading clayey deposit by vacuum pressure with cap-drain: analyses versus performance". Geotextiles and Geomembranes 26, 220–230

Chai, J.C., Matsunaga, K., Sakai, A., and Hayashi, S. (2009). "Comparison of vacuum consolidation with surcharge load induced consolidation of a two-layer system" Geotechnique 59 (7), 637 - 641

Chen, H. and Bao, X.C. (1983). "Analysis of soil consolidation stress under the action of negative pressure". 8th ICSME, Helsinki. 591 - 596

Choa, V. (1989). "Drains and vacuum preloading pilot test". 1347 - 1350

Choa, V. (1990). "Soil improvement works at Tianjin east pier project". 10th Southeast Asian Geotechnical Conference, Taipei. 47 – 52

Choi, Y.K. (1982) "Consolidation behavior of natural clays" PhD Thesis, University of Illinois at Urbana-Champaign

Chu, J., Yan, S.W. and Yang, H (2000). "Soil improvement by the vacuum preloading method for an oil storage station". Geotechnique 50, No. 6, 625 - 632

Chu, J. and Yan, S.W. (2005). "Estimation of Degree of Consolidation for Vacuum Preloading Projects". International journal of geomechanics. ASCE

Chu, J. and Yan, S.W. (2005). "Application of the vacuum consolidation method in soil improvement projects".

Chu, J. and Yan, S.W. and Zheng, Y.R. (2006). "Three soil improvement methods and their application to road construction". Ground Improvement, 10, No. 3, 103 - 112

Chu, J. and Yan, S.W. (2006). "Effective depth of vacuum preloading". Lowland Technology International, Vol. 8, N0 2, 1 - 8

Chu, J., Yan, S.W., and Indraratna. B. (2008). "Vacuum preloading techniques – Recent developments and applications". http:// ro.uow.edu.au/engpapers/420

Chung, T.C., Chang, J.F., Hu, I.C. and Chen, J.R. (2008) "Geotechnical site characterization for Suvarnabhumi Airport" Proceedings of 3rd International Conference on Site Characterization, Taipei, Taiwan. Taylor and Francis, London

Chung, S.T. (2009). "Engineering behaviour of Hong Kong marine clay during vacuum preloading". PhD thesis, University of Hong Kong

Cognon, J.M., Juran, I. and Thevanayagam, S. (1994). "Vacuum consolidation technology – Principles and field experience". International workshop on technology transfer for vacuum induced consolidation: Engineering and practice, Los Angeles, 201 – 212

Cortlever, N.G. (2006). "PVD ground improvement with vacuum preloading at Suvarnabhumi Airport" Proceedings of the Institution of civil Engineers. 37 (3)

Dam, L.T.K., Sandabanta, I. and Kimura, M. (2006). "Vacuum consolidation method – Worldwide practice and the latest improvement in Japan".

Dam, L.T.K., Sandabanta, I., Matsumoto, K., and Kimura, M. (2007). "Consideration of ground deformation characteristics in vacuum consolidation and application for design"

Gao, C. (2004). "Vacuum preloading method for improving soft soils of higher permeability". Ground Improvement 8, No. 3, 101 -107

Halton, G.R., Loughney, R.W. and Winter, E. (1965). "Vacuum stabilization of subsoil beneath runway extension at Philadelphia International Airport". Proc., 6th ICSMFE, Montreal, QC, vol 2, 61 – 65

Hammer, D.P. (1981). "Evaluation of under-drainage techniques for the densification of fine grained dredged material" Final Report, USACE Vicksburg

Hanzawa, H., Fukaya, T., and Suzuki, K. (1990). "Evaluation of engineering properties of an Araike clay" Soils and Foundations, 30 (4), 11 - 24

Harvey, J.A.F. (1997). "Vacuum drainage to accelerate submarine consolidation at Chek Lap Kok, Hong Kong".

Hayashi, H., Nishikawa, J. and Sawai.K, (2004). "Improvement Effect of Vacuum Consolidation and Prefabricated Vertical Drain in Peat Ground"

Hino (2009). “The Ariake sea coastal road project in Saga lowlands: Properties of soft foundation and use of dredged clayey soil as an embankment material” Special lecture, Institute of Lowland Technology, Saga University

Holtz, R.D. and Wager, O. (1975). “Preloading by vacuum; current prospects” Committee on embankment and slopes

Holtz, R.D., and Kovacs, W.D. (1981). “An Introduction to Geotechnical Engineering” Prentice Hall, ISBN: 0134843940

Holtz., R.D. (1987). “Preloading with Prefabricated vertical strip drains” Geotextiles and Geomembranes, 6, 109 - 131

Hong, H.P. and Shang, J.Q. (1998). “Probabilistic analysis of consolidation with prefabricated vertical drains for soil improvement”. Can. Geotech. J. 35: 666–677

Hong, Z. and Tsuchida, T. (1999). “On compression characteristics of Ariake Clays” Can. Geotech. J 36, 807 - 814

Ihm, C.W. and Masse, F. (2002). “Successful application of Menard Vacuum Consolidation method to Nakdong River soft clay in Kimhae, South Korea”. Menard Co. Ltd

Impe, W.F.V., Mieghem, J.V., Vandycke, S., and Impe, P.O.V. (2001). “Under water vacuum consolidation of dredged silt – A case history” Proceedings of 3rd International Conference on Soft soil Engineering, Hong Kong, 499 - 506

Indraratna. B, Bamunawita, C. and Khabbaz, H. (2004). “Numerical modeling of vacuum preloading and field applications”. Can. Geotech. J. 41: 1098 - 1110

Indraratna. B, Sathananthan, I., Bamunawita, C. and Balasubramanium, A.S. (2005). “Theoretical and numerical perspectives of field observations for the design and performance evaluation of embankment constructed on soft marine clay” University of Wollongong

Indraratna, B. and Rujiakiatkamjorn, C. (2008). “Effects of partially penetrating prefabricated vertical drains and loading patterns on vacuum consolidation”. GeoCongress: Geosustainability and Geohazard mitigation

Indraratna, B. (2008). “Recent advancements in the use of PVDs in soft soils”. University of Wollongong

Indraratna, B., Rujiakiatkamjorn, C., and Chu, J. (2007). “Soft clay stabilization with geosynthetic vertical drains beneath road and railway embankments: a critical review of analytical solutions and numerical analysis”. University of Wollongong

Indraratna, B., Rujikiatkamjorn, C., McIntosh, G., Balasubramaniam, A.S. (2007). “Vacuum consolidation effects on lateral yield of soft clays as applied to road and railway embankment” Proc. International symposium on Geotechnical Engineering, Ground improvement, Bangkok, Thailand, 31 - 62

Indraratna, B, Redana, I.W., and Balasubramanium, A.S. (1999). “Settlement predictions of embankment stabilized with PVDs at Second Bangkok International Airport” Barends et al. © Balkema, Rotterdam, ISBN: 9058090477

Indraratna, B., Rujiakiatkamjorn, C., Kelly, R., and Buys, N. (2009). “Soft soil foundation improved by vacuum and surcharge preloading at Ballina Bypass, Australia” Ground improvement technologies and case histories, Geotechnical society of Singapore, 95 - 105

Jang, Y.S., Park, C.S., Park, J.Y., and Kim, S.S. (undated). “A study on consolidation behavior of dredged clay with horizontal drains”

Johnson, J.S., Cunny, W.R., Perry, E.B., and Devay, L. (1977). “State-of-the-Art applicability of conventional densification techniques to increase disposal area storage capacity” Final Report USACE, Vicksburg

Karslud, K., Gregersen, O., Nerland, O. and Sparrevik, P. (2007). “Vacuum consolidation of seabed clay – A full scale experiment”. The Norwegian Geotechnical Institute, Norway

Kelly, R., Small, J. and Wong, P. (2008). “Construction of an embankment using vacuum consolidation and surcharge”. GeoCongress: Geosustainability and Geohazard mitigation. 578 – 585

Kelly, R.B. and Wong, P.K. (2009). “An embankment constructed using vacuum consolidation” Australian Geomechanics Journal, 44 (2), 55 - 64

Kim, S.S., Ahn, D.W., Kim, K.N., Kang, B.Y., Han, S.J., and Kim, Y.Y. (2009) “Field application and numerical analysis of suction vertical drain method” Proceeding

17th International Conference on Soil Mechanics and Geotechnical Engineering, 2151 - 2154

Kjellman. (1952). “Consolidation of clay soil by means of Atmospheric pressure”. Proc., Conference on soil stabilization, MIT, 258 – 263

Kolsant, S. (2006). Influence of storage conditions on geotechnical properties of Ariake clay on its chemical stabilization” PhD Thesis, Saga University Graduate School of Science and Engineering, Japan

Liu, H., Mahfouz, A. H. and Yonghui, C. (2004). “Ground improvement of sea embankment by vacuum preloading methods with PVDs”. Journal of Southeast University (English edition), Vol.20, No.1

Li, H.L., Wang, Q., Wang, N.X., and Wang, J.P. (2009). “Vacuum dewatering and horizontal drainage blankets: a method of layered soil reclamation” Bull. Eng. Geol. Environ. 68, 277 - 285

Leong, E.C., Soemitro, R.A.A. and Rahardjo, H. (2000). “Soil improvement by surcharge and vacuum preloading”. Geotechnique 50, No. 5, 601 - 605

Lo. D.O.K. (1991). “Soil improvement by vertical drains”. PhD thesis, University of Illinois at Urbana-Champaign

Mahfouz, A.H.A. (2005). “Study of combined vacuum-surcharge preloading mechanism for ground improvement” PhD Thesis, Ho Hai University, China

Mahfouz, A. H., Liu, H. L., Gao, Y. and Liu, J.C. (2005). “Vacuum and surcharge combined axi-symmetric consolidation of soft clayey soils”. Journal of Southeast Asian Geotechnical Society. 25 - 33

Mahfouz, A. H., Long, L.H., Yufeng, G., Jie, P. and Tongchun, L. (2007). “ Vacuum preloading and PVDs application for soft soil improvement; A case study: Hangzhou highway project – China”. International Conference for Enhancing Scientific Research: Innovation and Development.

Mahfouz, A. H., Liu, H. L., Sakr, M. A. and Shalaby, S. I. (2007). “New technique of ground improvement by using vacuum preloading method with PVDs”. 12th ICSGE, Cairo – Egypt.

Mahfouz, A. H., Sakr, M.A. and Yufeng, G. (2009). " Microstructural Study of soft clayey soil under consolidation by vacuum preloading method". Geomechanics and Geoengineering, vol. 2, No. 2, 97 -108

Masse, F., Spaulding, C.A., Wong, I.C. and Varaksin, S (2001). "Vacuum consolidation a review of 12 years of successful development" Geo-Odyssey - ASCE/Virginia Tech - Blacksburg, Va Usa

Mesri., G., and Rokhsar., A. (1974) "Theory of Consolidation for Clays". J. Geotech. Eng., ASCE, 100, No. 8, 889-904

Mesri, G. and Choi Y.K. (1985a) "Settlements analysis of embankments on soft clays". J. Geotech. Eng., ASCE 111, No.4. 441-464

Mesri., G., and Lo. D.O.K. (1987). "Subsoil investigation: The weakest link in the analysis of test fills" Proceedings of Peck symposium

Mesri., G., Choi, Y.K., and Lo. D.O.K. (1988) "Manual for the ILLICON Computer Program – One dimensional settlement analysis with or without vertical drains" University of Illinois at Urbana-Champaign (Unpublished)

Mesri, G., and Castro, A. (1987). "The C_α/C_c concept and Ko during secondary compression" Journal of Geotechnical Engineering, ASCE, 112 (3), 230 - 247

Mesri, G. and Lo, D.O.K. (1991). "Field performance of prefabricated vertical drains". Geo-Coast, 231 – 236

Mesri, G., Feng, T.W., Ali, S., and Hayat, T.M. (1994). Permeability characteristics of soft soils" Proceedings XIII ICSMFE

Mesri, G. Lo, D.O.K., and Feng, T.W. (1994) "Settlement of embankments on soft clays". Proc. Settlement '94, ASCE Specialty Conf. Geotech. Special Publication No. 40, 1, 8 - 76

Mesri, G. and Huvaj, S.N. (2009). "The Asoaka method revisited". Proc. 17th International Conference on Soil Mechanics and Geotechnical Engineering, Alexandria, Egypt (Accepted for publication)

Mieghem, J.V., Aerts, F., Thues, G.J.L., Vlieger, H.D. and Vadycke, S. (1999). "Building on soft soils". Terra et Aqua – No. 75. 3 – 15

Mitchell, J.K. (1996) “Fundamentals of soil behavior” 2nd edition, John Wiley and Sons, New York

Mohamedelhassan, E. (2002). “Soil improvement using electrokinetic and vacuum techniques”. PhD thesis, University of Western Ontario, London Ontario Canada.

Mohamedelhassan, E. and Shang, J.Q. (2002). “Vacuum and surcharge combined one dimensional consolidation of clay soils”. Can. Geotechnique, J 39, 1126 -1138

Moh, Z.C. and Lin, P.C. (2003). “From cobra swamp to international airport: ground improvement at Suvarnabhumi International Airport, Thailand” Ground Improvement, 7, No. 2, 87 - 102

Moh, Z.C. and Lin, P.C. (2006) “Geotechnical history of the development of the Suvarnabhumi International Airport” Journal of South-East Asian Geotechnical Society 37 (3) 143 - 170

Mutsomoto, K., Ohno, M., Nakakuma, K., Shima, H., Ichikawa, H., and Imai, G. (1998). ”Study on applicability of vacuum consolidation method for deep soft clay ground” Proceedings International symposium on Lowland Technology, Saga university, 287 - 294

Qiu, Q.C., Mo, H.H. and Dong, Z.L. (2007). “Vacuum pressure distribution and pore pressure variation in ground improvement by vacuum preloading”. Can. Geotechnique, J 44, 1433 – 1445

Qian, J.H., Zhao, W.B., Cheung, Y.K. and Lee, P.K.K. (1992). “The theory and practice of vacuum preloading”. Computers and Geotechnics, 13, 103 - 118

Rollings, M.P. (1996). “Dredged material disposal, storage and management” International Workshop on Technology Transfer for Vacuum-Induced Consolidation: Engineering and Practice, Los Angeles, California, 13 – 29

Rujikiatkamjorn. C. (2005). “Analytical and numerical modeling of soft clay foundation improvement via prefabricated vertical drains and vacuum preloading”. PhD thesis, University of Wollongong, Australia

Rujikiatkamjorn. C. and Indraratna. B. (2006). “Performance and prediction of soft clay behavior under vacuum conditions”. University of Wollongong

Rujikiatkamjorn. C. and Indraratna, B. (2005). “Soft ground improvement by vacuum assisted preloading”. University of Wollongong

Rujikiatkamjorn. C. and Indraratna, B. (2007). “Analysis of Radial Vacuum-Assisted Consolidation Using 3D Finite Element Method”. University of Wollongong

Rujikiatkamjorn. C., Indraratna. B. and Chu, J. (2007). “Numerical modeling of soft soil stabilized by vertical drains combining surcharge and vacuum preloading for a storage yard”. Can. Geotech, J 44, 326 – 342

Rujikiatkamjorn. C. and Indraratna. B. (2007). “Soft ground improvement by vacuum assisted preloading” University of Wollongong

Sandiford, R.E., Ludewig, N. and Dunlop, P. (1996). “Evaluation of enhanced consolidation for dredged material disposal Newark bay confined disposal facility”. International Workshop on Technology Transfer for Vacuum-Induced Consolidation: Engineering and Practice, Los Angeles, California, 31 - 37

Saowapakpiboon, J., Bergado, D.T., Chai, J.C., Kovittayanon, N. and Zwart, T.P. (2008). “Vacuum –PVD combination with embankment loading consolidation in soft Bangkok clay: A case study of the Suvarnabhumi airport project”. Proc. Of the 4th Asian Regional Conference on Geosynthetics, Shanghai – China. 440 - 449

Seah, T.H. (2006). “Design and construction of ground improvement works at Suvarnabhumi Airport” Journal of South-East Asian Geotechnical Society 37, 171 - 188

Seah, T.H. and Kolsant, S. (2003). “Anisotropic consolidation behavior of of soft Bangkok clay”. Geotechnical Testing Journal, ASTM, Vol. 26. No.3, 1 - 11

Shang J.Q., Tang, M. and Miao, Z. (1998). “Vacuum preloading consolidation of reclaimed land: a case study”. Can. Geotechnique, J 35, 740 – 749

Shang. J.Q. and Zhang, J. (1999). “Vacuum consolidation of soda-ash tailings”. Ground Improvement 3, No.1, 169 – 177

Shinsha, H., Watari, Y., and Kurumada, Y. (1991). “Improvement of very soft ground by vacuum consolidation using horizontal drains” Geo Coast, 387 - 392

Shinsha, H. (1996) “Improvement of very soft ground by vacuum consolidation using horizontal drains” International Workshop on Technology Transfer for Vacuum-

Induced Consolidation: Engineering and Practice, Los Angeles, California, 169 - 179

Sharma, S. (1996). ``XSTABL: An integrated slope stability analysis program for personal computers." Reference manual, Version 5, Interactive Software Designs, Inc., Moscow, Idaho, 213 p.

Simon, P.S. and Rodriguez, Y. (1996). "Surcharge preloading: The vacuum consolidation process versus wick Drains". International Workshop on Technology Transfer for Vacuum-Induced Consolidation: Engineering and Practice, Los Angeles, California. 191 - 199

Song, Y.S. and Kim, T.H. (2004). "Improvement of estuarine marine clays for coastal reclamation using vacuum-applied consolidation method". Ocean Engineering, 31, 1999 – 2010

Spaulding, C. and Porbaha, A. (2004). "Embankment construction on marshland using vacuum consolidation technology".

STS and NGI (1992). "Independent soil engineering study for Second Bangkok International Airport implementation program" Final report, Volume I

Tang, M. and Shang, J.Q. (2000). "Vacuum preloading consolidation of Yaoqiang airport runway". Geotchnique 50, No. 6, 613 – 623

Thevanayagam, S., Kavazanjian, E. Jr., Jacob, A. and Juran, I. (1994). "Prospects of vacuum-assisted consolidation for ground improvement of coastal and offshore fills". Geotechnical special publication No. 45. ASCE, 90 - 105

Thevanayagam, S. (1997). "Vacuum-assisted consolidation of coastal and offshore dredge fills". Geotechnical special publication No. 65. ASCE, 67 - 86

Ter-martirosyan, Z.G. and Cherkasova, L.I. (1983). "theoretical basis for compaction of water-saturated soils by vacuum". 8th ICSME, Helsinki. 695 -696

Terzaghi. K., Peck, R.B. and Mesri, G. (1996). "Soil Mechanics in Engineering Practice". 3rd Edition, John Wiley and sons

Varaksin, S. and Herve, A.B.T. (2005). "Theory and practical application of vacuum consolidation at the site of Camau power plant in Vietnam".

Vinh, L.B. and Imai, G. (2001). “An analysis of deformation of soft ground improved by PVD with vacuum preloading”. Proceedings 36th National conference, Japan, 36, 1059 - 1060

Yan, S.W., and Chu, J. (2003). “Soil improvement for a road using the vacuum preloading method”. Ground Improvement, 7, No.4, 165 – 172

Yan, S.W. and Chu, J. (2005). “Soil improvement for a storage yard using the combined vacuum and fill preloading method”. Canadian Geotechnique, J 42, 1094 – 1104

Yan, S.W., Xiaowei, F. and Chu, J. (2009). “Mechanism of using vacuum preloading method in improving soft clay layers”. US-China workshop on Ground Improvement Technologies

Ye, M.B., Lu, S.Y. and Tang, Y.S. (1983). “Packed sand drain-Atmospheric preloading for strengthening soft foundation”. 8th ICSME, Helsinki. 717 – 720

Yee, K. and Wee, T.T. (2001) “Vacuum consolidation for soft soils” Conspectus Journal, Housing Development Board Singapore

Yee, K., Jullienne, D., Masse, F. and Varaksin, S. (2002) “Performance of road embankment on vacuum consolidated soft clay in Bangkok” 4th International Conference on Ground Improvement Techniques

Yee, K., Aun, O.T., and Hui, T.W. (2004). “Vacuum consolidation technology for soft soil treatment: Principles and field experiences” Malaysian Geotechnical Conference, Kaulalampur, Malaysia

Yixiong, L. (1996a). “Application and experience of vacuum preloading method”. International Workshop on Technology Transfer for Vacuum-Induced Consolidation: Engineering and Practice, Los Angeles, California, 47 – 69

Yixiong, L. (1996b). “Vacuum preloading method to improve soft soils and case histories”. International Workshop on Technology Transfer for Vacuum-Induced Consolidation: Engineering and Practice, Los Angeles, California, 71 - 135

Yoneya, H., Shiina, T. and Shinsha, H. (2003). “Improvement of soft ground applying vacuum consolidation method by expecting upper clay layer as sealing-up material”. Soft Ground Engineering in Coastal Areas, ISBN 90 5809 613 0. 275 - 283

Wang, B. T. and Law, K. T. (2007). “Building an embankment with simultaneous vacuum loading”. Soft Soil Engineering, Taylor & Francis Group, London, ISBN 13 978-0-415-42280-2

Woo, S. M., Moh, Z. C., Van Weele, A.F., Chotivittayathanin, R and Trangkarahart, T. (1989). “Preconsolidation of soft Bangkok clay by vacuum loading combined with non-displacement sand drains”. Proc. XII ICSMFE 2, 1431 - 1434

Zhu, S.L. and Miao, Z.H. (2002). “Recent development and improvement of vacuum preloading method for improving soft soil”. Ground Improvement, 6, No.2, 79 – 83

APPENDIX

INPUT FILE FOR COMPUTER PROGRAM IILICON

The input file for the computer program ILLICON is to be written as a '.txt' file using notepad application. The sample input file is as following:

CASENAME
Storage Yard
NUMLAYS (NUMBER OF LAYERS)
9
NUMCOLU (NUMBER OF COLUMNS)
8
NUMCOLS (NUMBER OF COLUMNS-SMEAR ZONE)
3
RAD_DRA (RADIUS OF THE DRAIN) [METERS]
0.033
RAD_SOI (RADIUS OF THE SOIL) [METERS]
0.565
RAD_SME (RADIUS OF THE SMEAR ZONE) [METERS]
0.13
CONSLIM (LIMIT OF CONSOLIDATION) [%]
101
PRNT_ST (PRINT START TIME)
10
PRNT_FC (PRINT FACTOR)
1.1
NUMDLAY (NUMBER OF DRAIN LAYERS)
8
UPPERBC (0=DRAINED, 1=UNDRAINED)
0
LOWERBC (0=DRAINED, 1=UNDRAINED)
1
TIM_DRA (TIME [DAYS] WHEN DRAINS WERE INSTALLED)
7
I_F_DRA (GRADIENT CORR. FACTOR, DRAIN)
1.57
I_F_SME (GRADIENT CORR. FACTOR, SMEAR)
1.67
K_DRAIN (DRAIN PERMEABILITY)
0.05
LOADING SCHEDULE (NUMPTS/ LOADS(LAY=1,NUMLAY))

18
0 2 9 16 17 30 34 80 84 96 99 119
147 150 154 171 196 220
0 6 16 16 6 6 93 93 99 99 107 107
121 121 127 127 147 147
6 5.82 21.52 21.52 5.82 11.82 98.82 98.82 104.64 104.64 112.4 112.4
125.98 125.98 131.8 131.8 151.2 151.2
18 5.64 33.04 33.04 5.64 23.64 110.64 110.64 116.28 116.28 123.8 123.8
136.96 136.96 142.6 142.6 161.4 161.4
28 5.4 42.4 42.4 5.4 33.4 120.4 120.4 125.8 125.8 133 133
145.6 145.6 151 151 169 169
38 5.16 51.76 51.76 5.16 43.16 130.16 130.16 135.32 135.32 142.2 142.2
154.24 154.24 159.4 159.4 176.6 176.6
45 4.92 58.12 58.12 4.92 49.92 136.92 136.92 141.84 141.84 148.4 148.4
159.88 159.88 164.8 164.8 181.2 181.2
21 4.5 33 33 4.5 25.5 112.5 112.5 117 117 123 123
133.5 133.5 138 138 153 153
0 4.2 11.2 11.2 4.2 4.2 91.2 91.2 95.4 95.4 101 101
110.8 110.8 115 115 129 129
0 3.9 10.4 10.4 3.9 3.9 90.9 90.9 94.8 94.8 100 100
109.1 109.1 113 113 126 126
LAY_PARAMETERS
LAY_PRO (H, P0, KHKV, ALPHA, ALPHAS, CS, NUMROW)
3.5 21.6 1 0.04 0 0 4
3 34.8 1 0.04 0 0 4
2 56.8 1 0.04 0 0 4
1.5 71.225 1 0.04 0 0 4
3 88.1 1 0.04 0 0 4
3 110.6 1 0.04 0 0 4
1.5 128.225 1 0.04 0 0 4
2.5 145.225 1 0.04 0 0 4
2 164.35 1 0.04 0 0 4
E_LOGKV NUMPTV(LAY)/ VOIDV(POINT,LAY) VPERM(POINT, LAY)
2
1.18 0.0000003
0.724 5.07085E-08
2
1.48 0.000000133
1.110 4.20578E-08
2
1.20 0.000000133
0.975 5.61465E-08
2
1.27 6.67E-08

1.024 2.73485E-08
2
1.62 6.67E-08
1.418 3.75603E-08
2
1.33 6.67E-08
1.156 3.65652E-08
2
1.02 1.67E-08
0.895 9.499E-09
2
0.69 1.67E-08
0.590 8.56903E-09
2
0.69 1.67E-08
0.590 8.56903E-09
E_LOGPS NUMPTS(LAYER)/ ELOGPU(POINT,LAY) STRES(POINT, LAY)
2
1.180 21.6
0.724 207.4
2
1.480 34.8
1.110 194.9
2
1.200 56.8
0.975 221.5
2
1.270 71.2
1.024 299.1
2
1.620 88.1
1.418 246.7
2
1.330 110.6
1.156 309.7
2
1.020 128.2
0.895 333.4
2
0.690 145.2
0.590 377.6
2
0.690 164.4
0.590 427.3

E_LOGPU NUMPTS(LAYER)/ ELOGPU(POINT,LAY) STRES(POINT, LAY)
6
1.180 21.6
1.176 25.9
1.155 28.5
1.026 51.8
0.875 103.7
0.724 207.4
5
1.480 34.8
1.471 48.7
1.446 53.6
1.291 97.4
1.110 194.9
5
1.200 56.8
1.195 73.8
1.176 81.2
1.056 147.7
0.975 221.5
4
1.270 71.2
1.263 99.7
1.242 109.7
1.024 299.1
4
1.620 88.1
1.611 123.3
1.584 135.7
1.418 246.7
4
1.330 110.6
1.322 154.8
1.299 170.3
1.156 309.7
4
1.020 128.2
1.015 166.7
0.999 183.4
0.895 333.4
4
0.690 145.2
0.686 188.8
0.673 207.7

0.590 377.6
4
0.690 164.4
0.686 213.7
0.673 235.0
0.590 427.3
ENDDATA